Evaluation of New Ferritic Steels by Computational Modeling and Synchrotron Radiation

Mike Santella, John Shingledecker, and Bob Swindeman

Metals & Ceramics Division

Oak Ridge National Laboratory

May 11, 2005

19th Annual Conference on Fossil Energy Materials

Knoxville, TN

Two advanced ferritic steels will be discussed

1. SAVE12
   - Fe-9Cr-3Co-3W-0.1Ta-0.1Nd-Nb-V
   - Issues relate to specifying tempering and post weld heat treatment temperatures
2. Japanese experimental steel
   - Fe-9Cr-3Co-3W-Nb-V-High B-Low N
   - Issues relate to suppression of Type IV cracking of weldments

Phase diagrams are fundamental roadmaps needed for alloy development, processing, heat treating

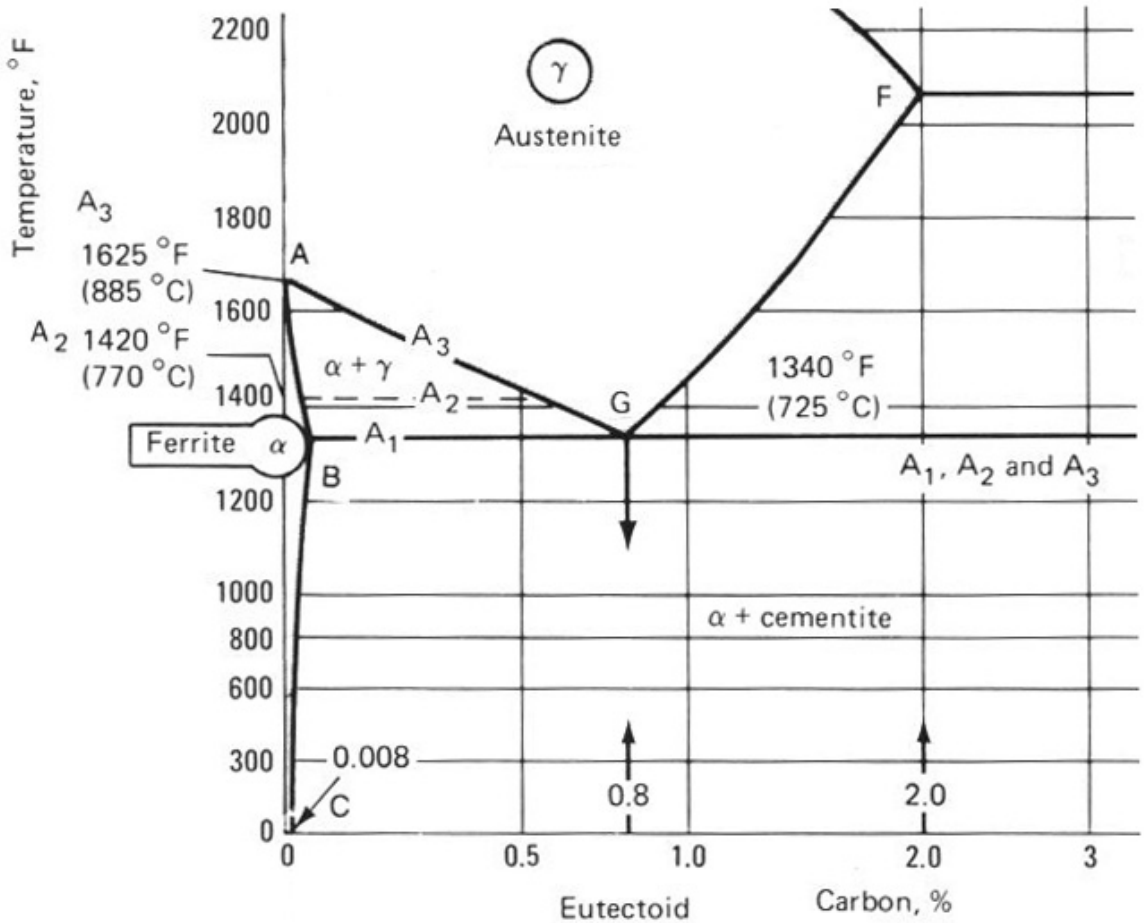

Thermal or dilation arrests is one way to identify critical transformation temperatures

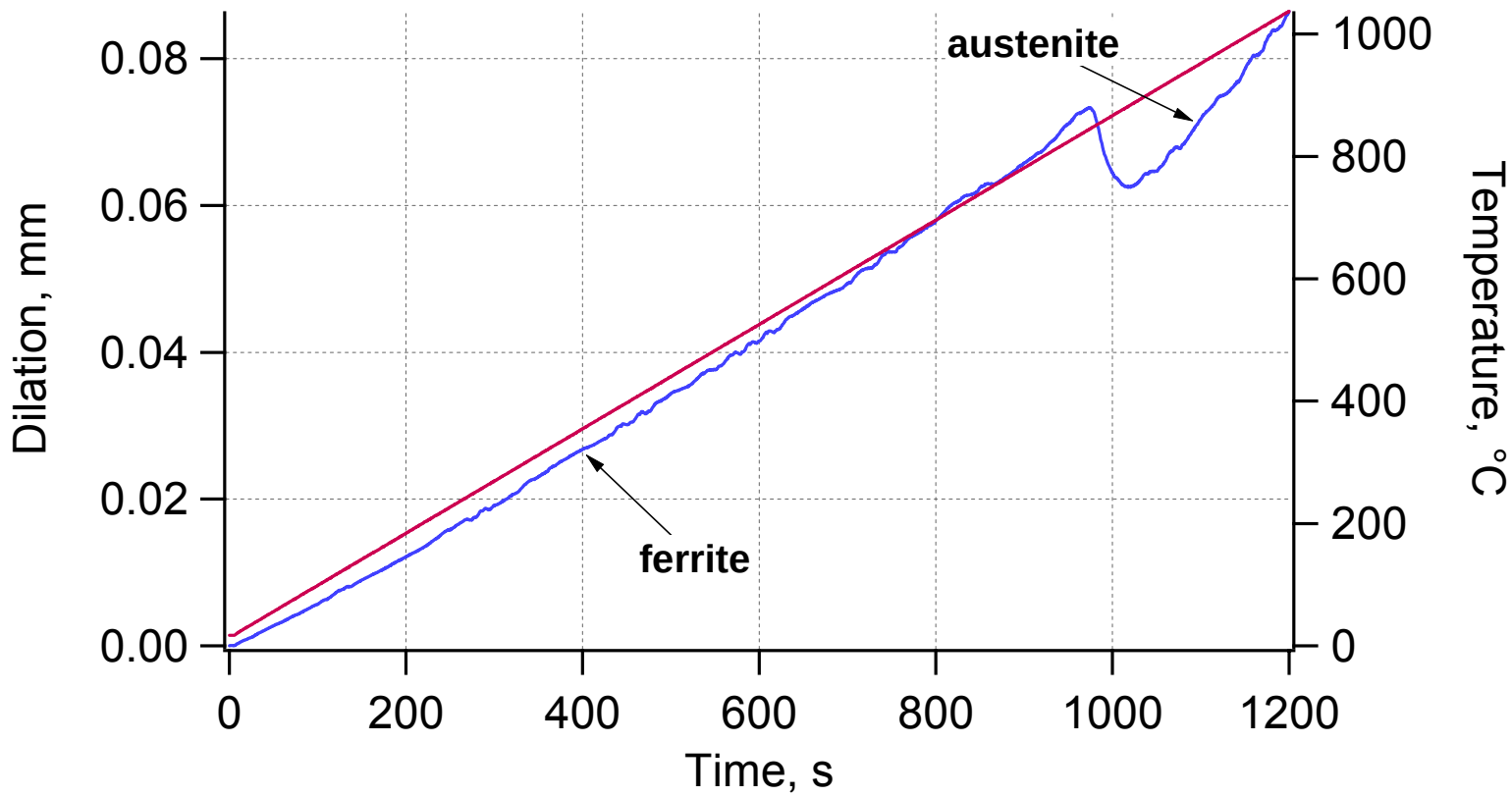

- Data for 9Cr steel heated at 20°C/min

Alloying influences arrest temperatures

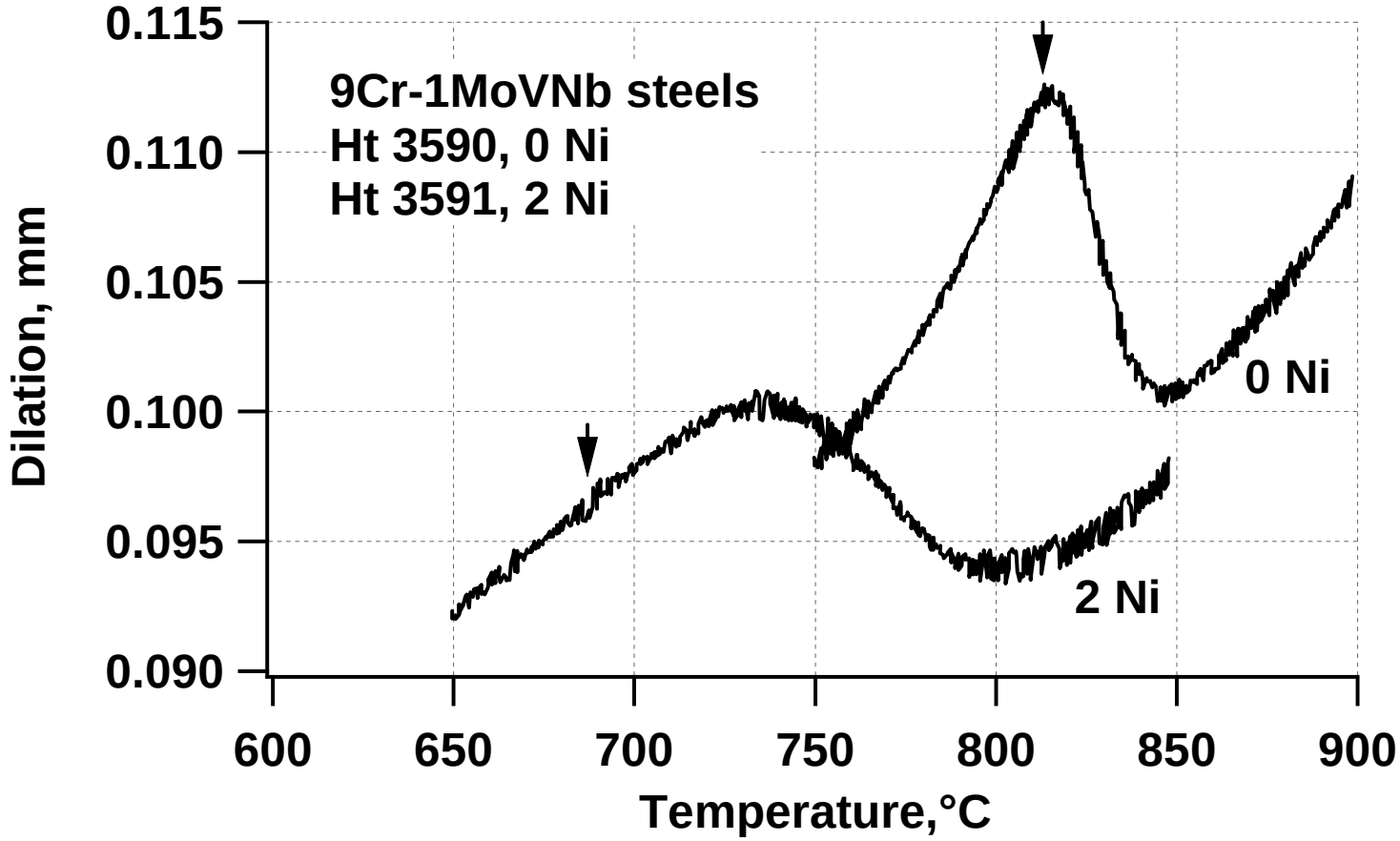

- Phase stability & transformation behavior depend on chemistry

Heating rate influences arrest temperatures

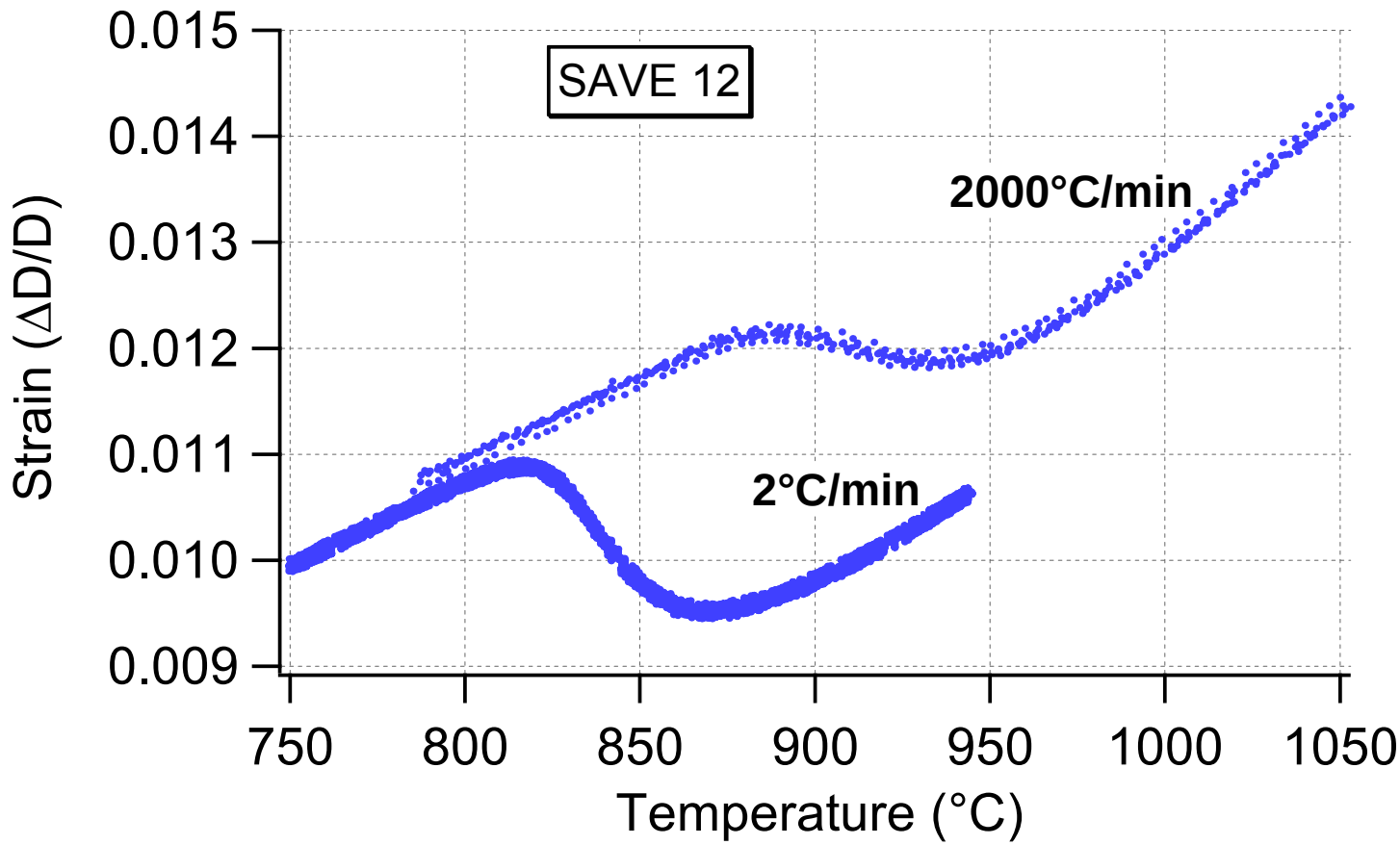

Which $\alpha \Rightarrow \gamma$ transformation temperature, A_{C1}, is the correct one?

A_{C1} approaches A_1 as dT/dt decreases

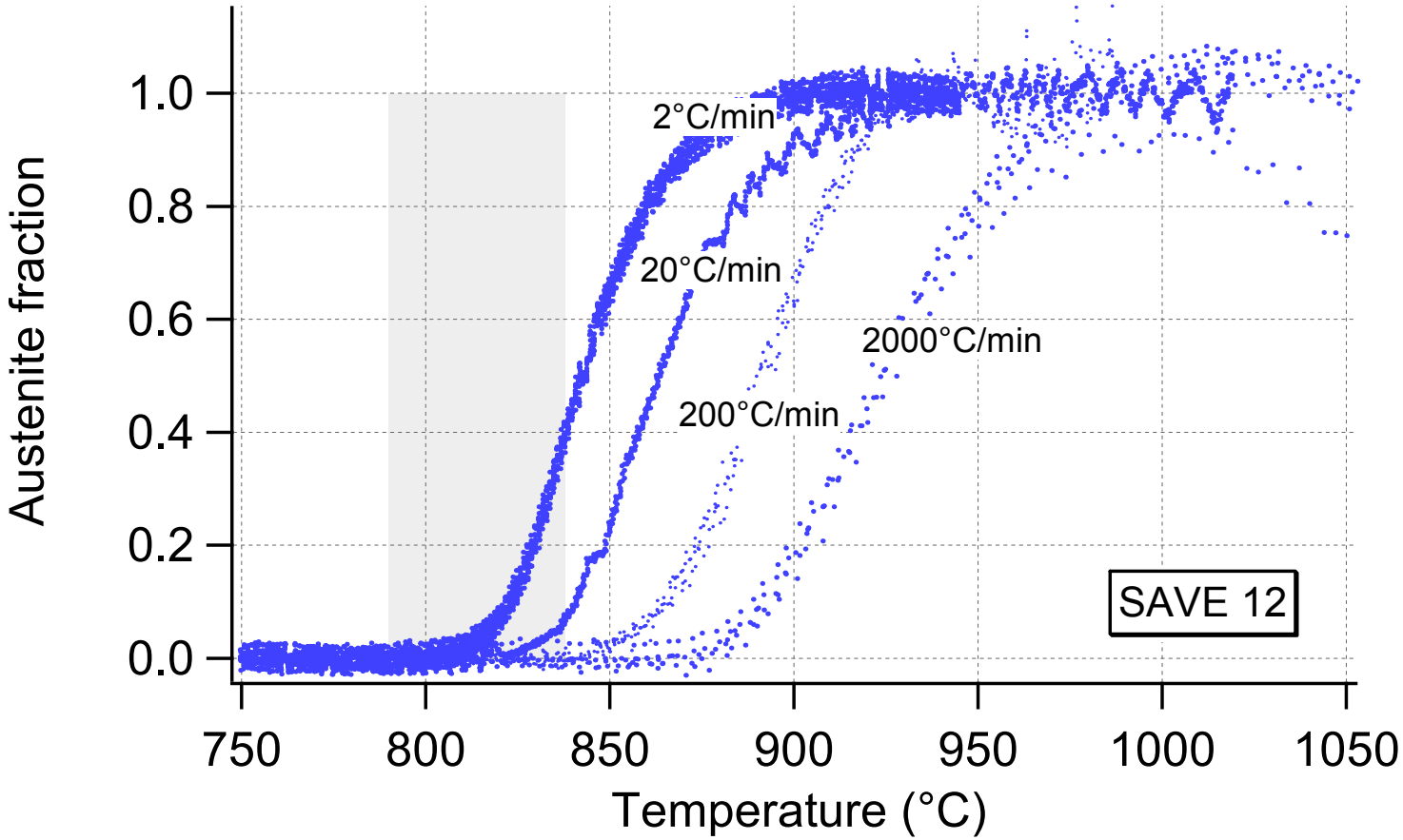

Shading represents $\alpha + \gamma$ range according to equilibrium thermodynamics

Transformation temperatures can be estimated with Computational Thermodynamics

- CT is a powerful tool for thermodynamic calculations in multicomponent (> 3) systems
- Calculations are based on thermodynamic databases produced by an expert evaluation of experimental data
- Models and parameters for the models have been developed for all types of phases (solid solution, compounds, carbides, oxides, etc)
  - G described as *f*(composition, temperature, etc)
  - Minimum G yields equilibrium; can add constraints

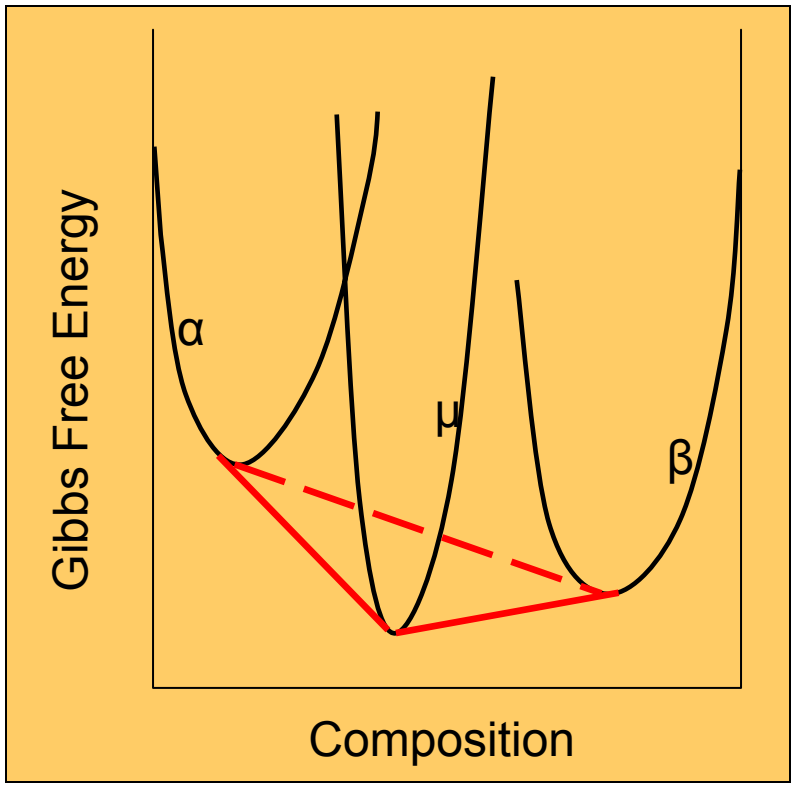

Computational thermodynamics were used to estimate A_1 variation with SAVE12 composition

- 2142 individual alloy compositions were evaluated
- Equilibrium calculations included Fe + 10 alloy elements
- Calculation permitted formation of carbides including M(C,N), $M_{23}C_6$, M_6C, etc.

	Element amounts, wt%									
	C	Co	Mn	N	Cr	Nb	Si	Ta	V	W
Min	0.05	2.0	0.0	0.00	8.5	0.00	0.0	0.00	0.00	2.0
Max	0.15	6.5	1.0	0.10	12.5	0.15	0.8	0.25	0.50	4.0

Neural Net analysis was used to make the thermodynamic predictions easily accessible

- A functional dependence of A_1 on composition was established using neural net analysis
- Neural net can be run on any PC to predict A_1
- No need to be a thermo "expert" or materials engineer/scientist

Press here

Neural net closely represents ThermoCalc results

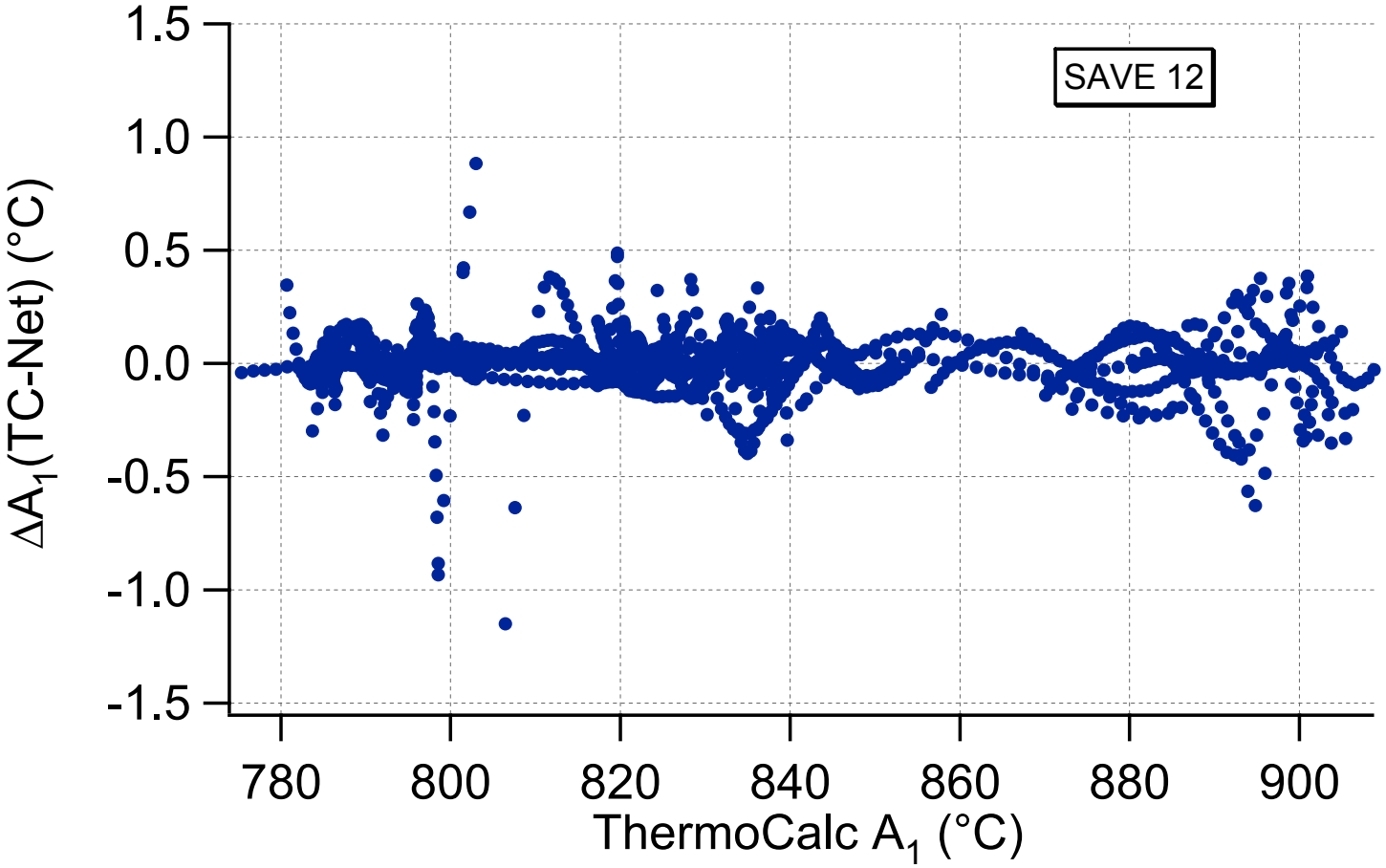

- 2142 A_1 calculations for SAVE12 steel

Newer 9Cr steels have improved creep strength and they resist Type IV cracking of welds

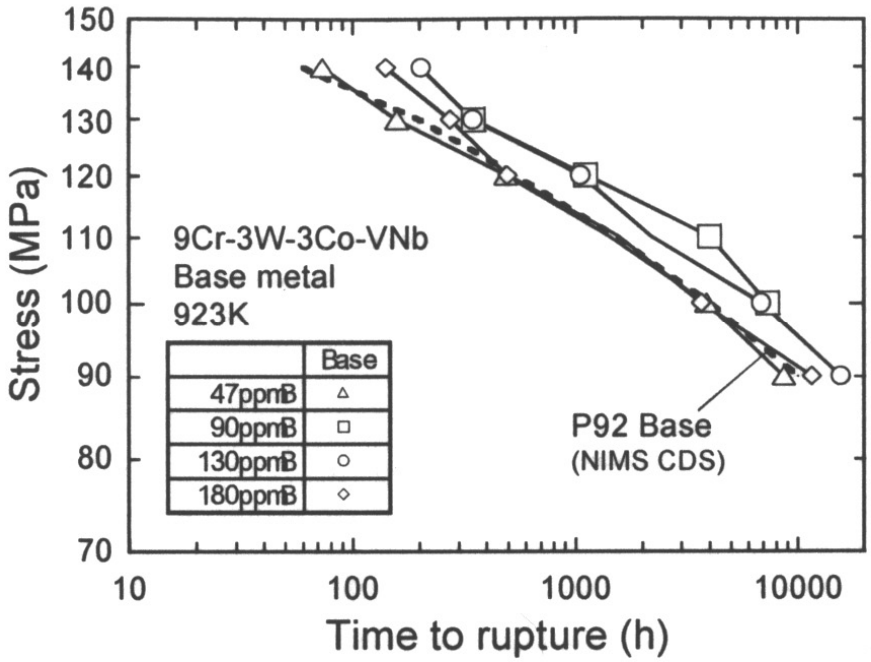

- Type IV cracking is due to weakened microstructures in HAZs
- Results from F. Abe et al., National Institute for Materials Science, Japan

HAZ behavior of new steel is significantly different from more conventional 9Cr steel

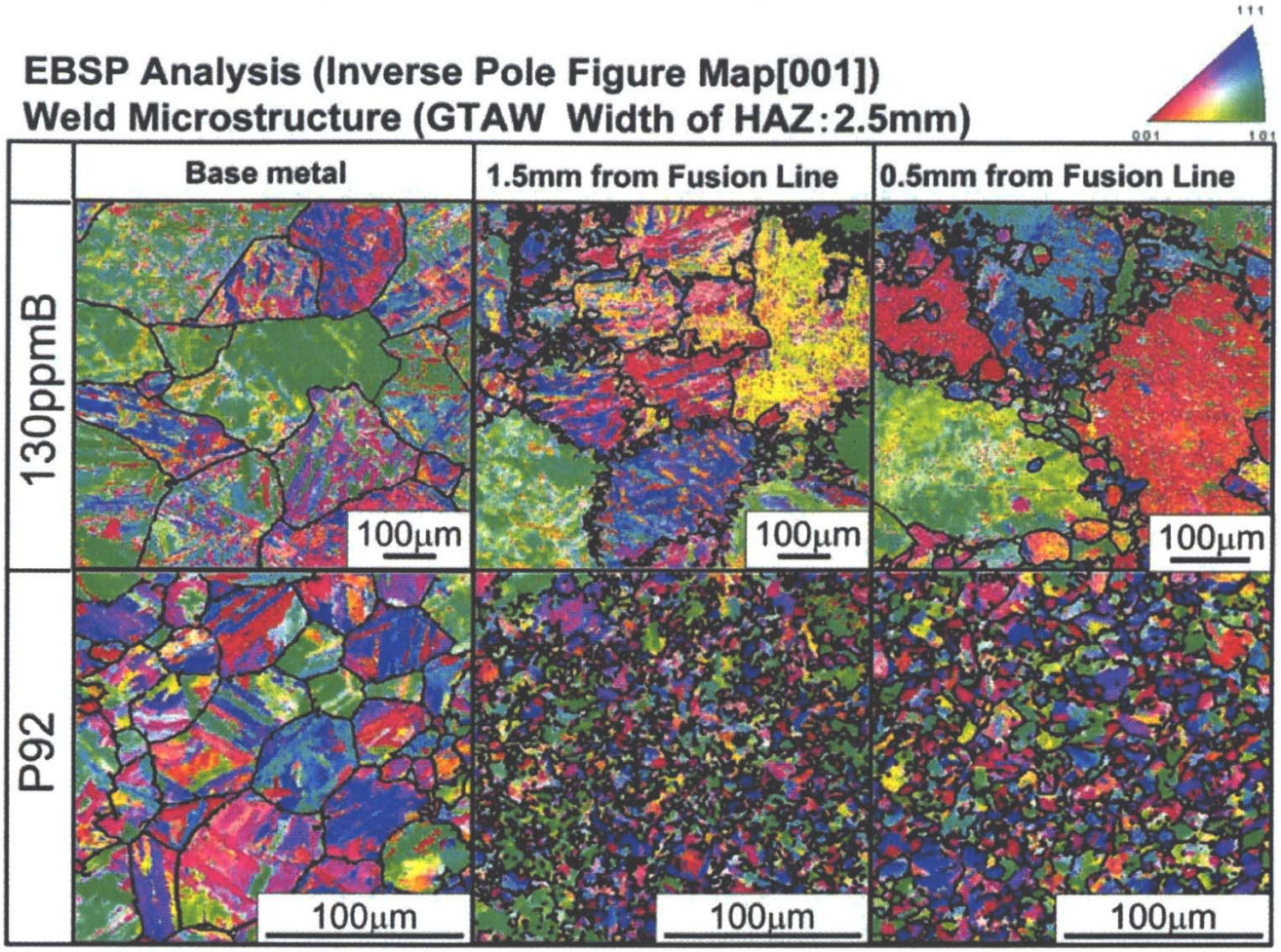

Two explanations are proposed for the unique behavior of the NIMS steels

1. Austenite memory effect
   - With retained austenite, heating to Ts above A_1 regenerates the original γ grains
2. Martensitic reversed transformation
   - Boron may suppress nucleation of γ in HAZs during welding

Previous ORNL work used APS diffraction experiments to verify that austenite was being retained in 9Cr steel welds

- *NIMS expressed interest in collaborating on a set of diffraction experiments with NIMS steel & P92*

Transformation behavior is being examined using the Advanced Photon Source

- The Advanced Photon Source (APS) at Argonne National Laboratory is a national synchrotron-radiation light source research facility funded by the U.S. Department of Energy, Office of Science, Office of Basic Energy Sciences.
- High-brilliance x-ray beams are used for forefront basic and applied research
- Researchers obtain beam time by submitting peer-reviewed beam time proposals.

http://www.aps.anl.gov/

Uniqueness of APS is flux and brilliance

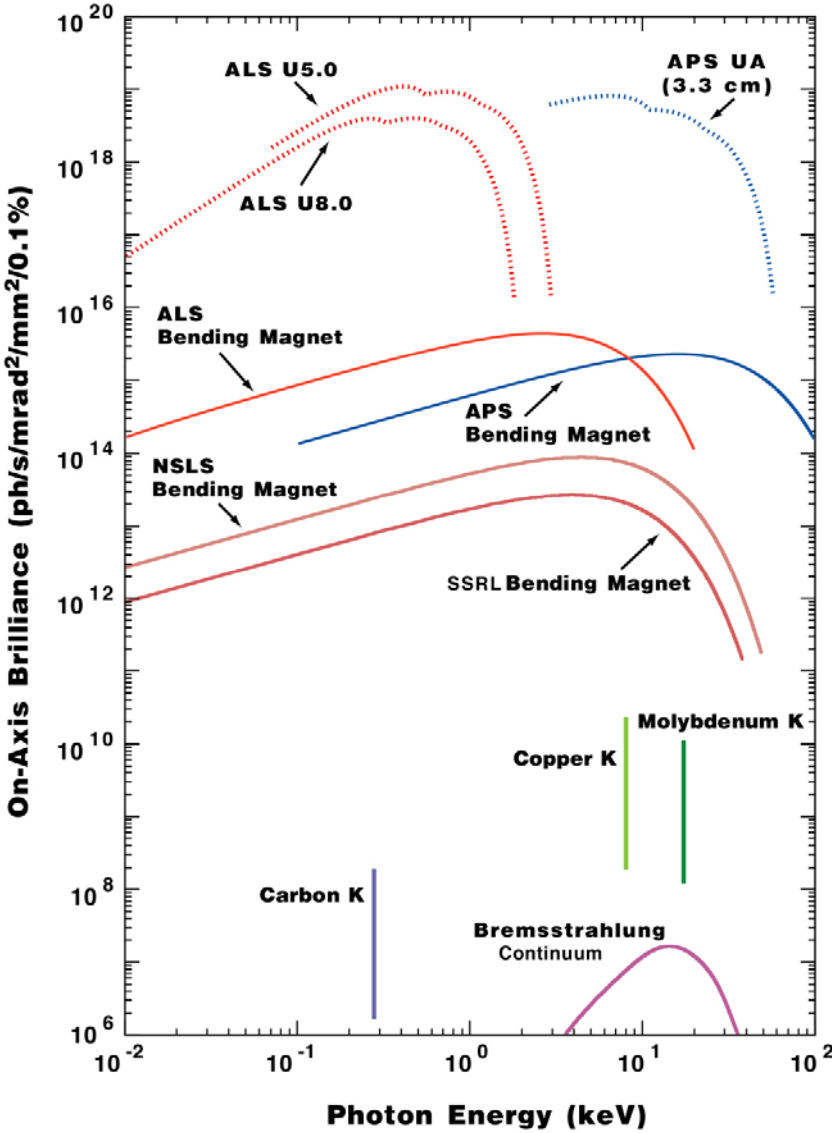

- Flux is number of photons per second
- Brilliance is a measure of the intensity and directionality of the x-rays
- Flux + brilliance = 1 second/diffraction pattern

Ferrite/austenite transformation was tracked through HAZ heating cycles

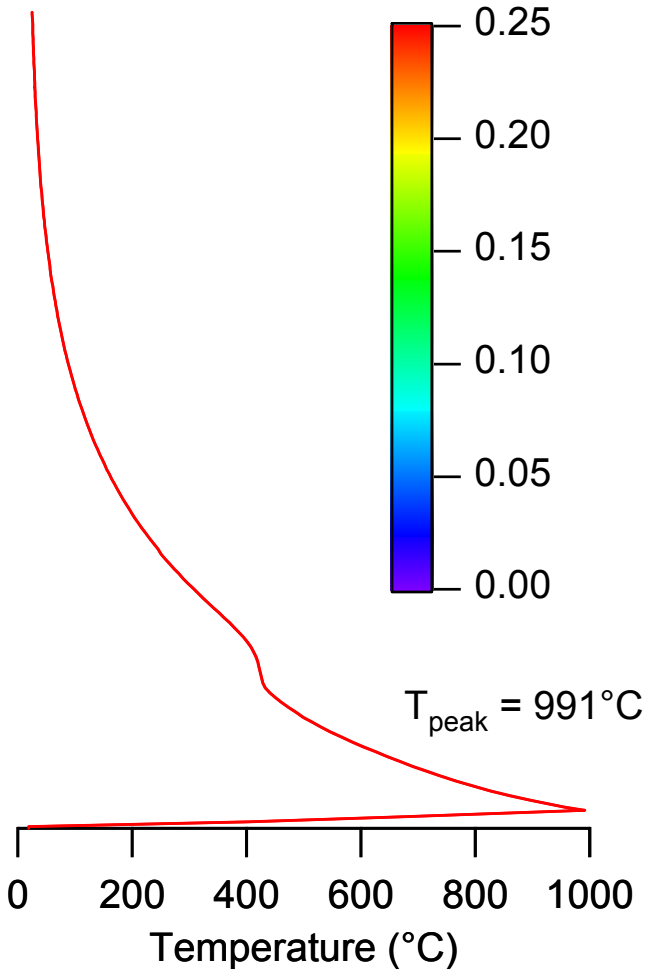

- NIMS 130B steel

Examination of diffraction spectra confirm that austenite can be retained at RT

- NIMS 130B steel

Evaluation of New Ferritic Steels by Computational Modeling and Synchrotron Radiation

Highlights:

- Using computational thermodynamics tools to assist manufacturers in specifying critical temperature limits for tempering and post weld heat treatments
  - Making thermodynamic analysis information accessible, available
- Using advanced tools – like APS – to better understand new high strength ferritic steels
  - Collaboration with NIMS

The Babcock & Wilcox Company

Generating Powerful Solutions℠

Update on the Coal Ash Corrosion Resistant Materials Testing Program

Evaluation of the First Two Sections and Status of the Third

19th Annual Conference on Fossil Energy Materials

By Dennis K. McDonald and Edward S. Robitz

Knoxville, Tennessee May 9-11, 2005

Presented by: Dennis K. McDonald

© 2004 The Babcock & Wilcox Company. All rights reserved.

Project Funding

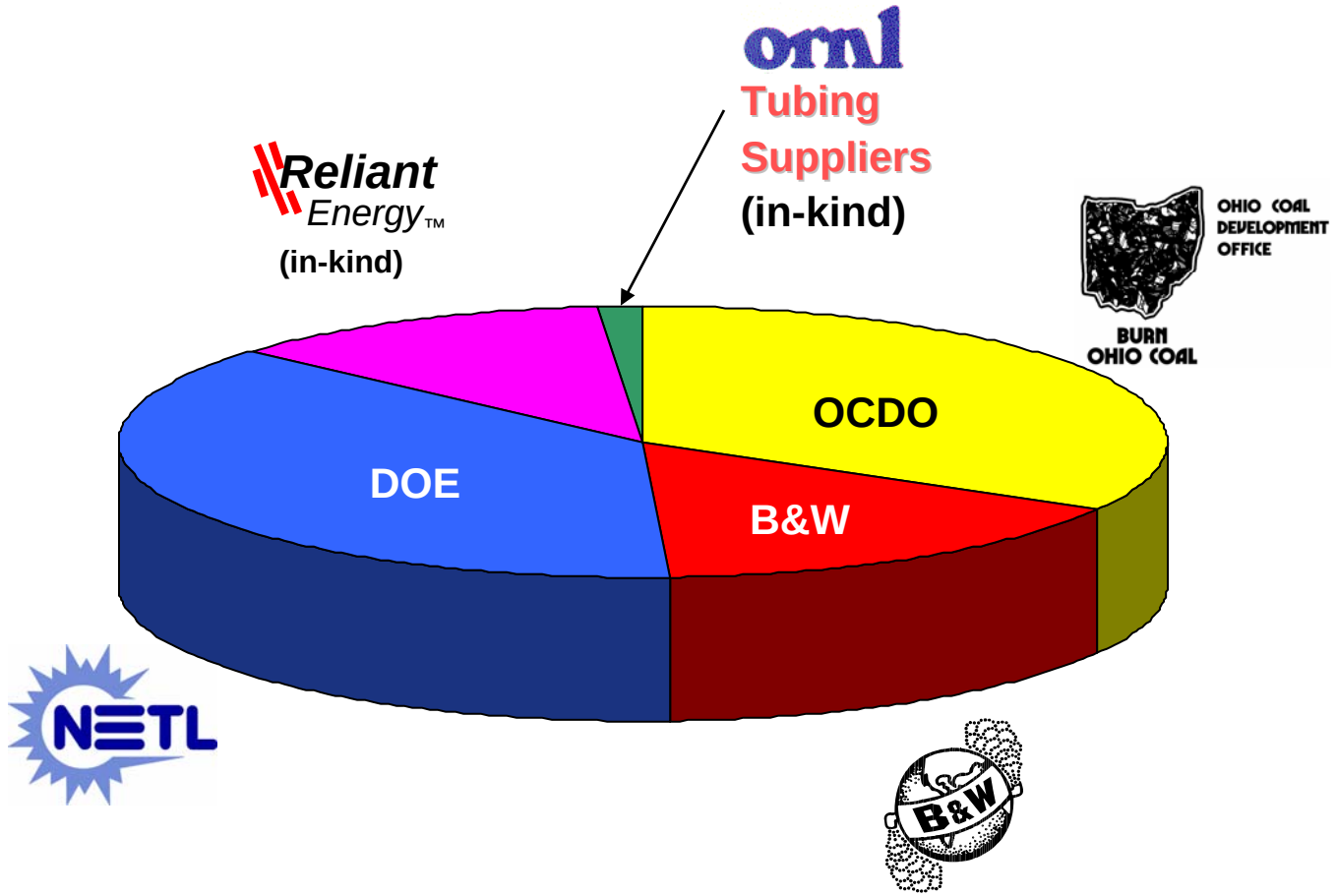

Total Project Cost = $1,864,603

© 2004 The Babcock & Wilcox Company. All rights reserved.

Materials Advancement is Necessary

1. ***Increasing price and volatility of natural gas, continuing concerns about nuclear power, especially waste disposal, and a strong need to rely less on foreign energy sources, indicates coal will continue to provide a major portion of our energy needs for decades to come.***

2. ***The greatest challenge to coal is mitigating its impact on the environment. Today this means SOx, NOx, mercury and PM2.5 and in the future this may also include CO_2.***

© 2004 The Babcock & Wilcox Company. All rights reserved.

Materials Advancement is Necessary

3. ***Advanced coal technologies such as IGCC are still decades away from commercial reliability and competitive cost and it is apparent that PC plants will dominate the current wave of new generation and perhaps even the next wave as a result of major advancements in emissions control technologies.***

4. ***Efficiency is not only good economics but sound environmental strategy.***

5. ***Efficiency is driven by steam temperature which is limited by materials.***

© 2004 The Babcock & Wilcox Company. All rights reserved.

Steam Temperature and Pressure vs Efficiency

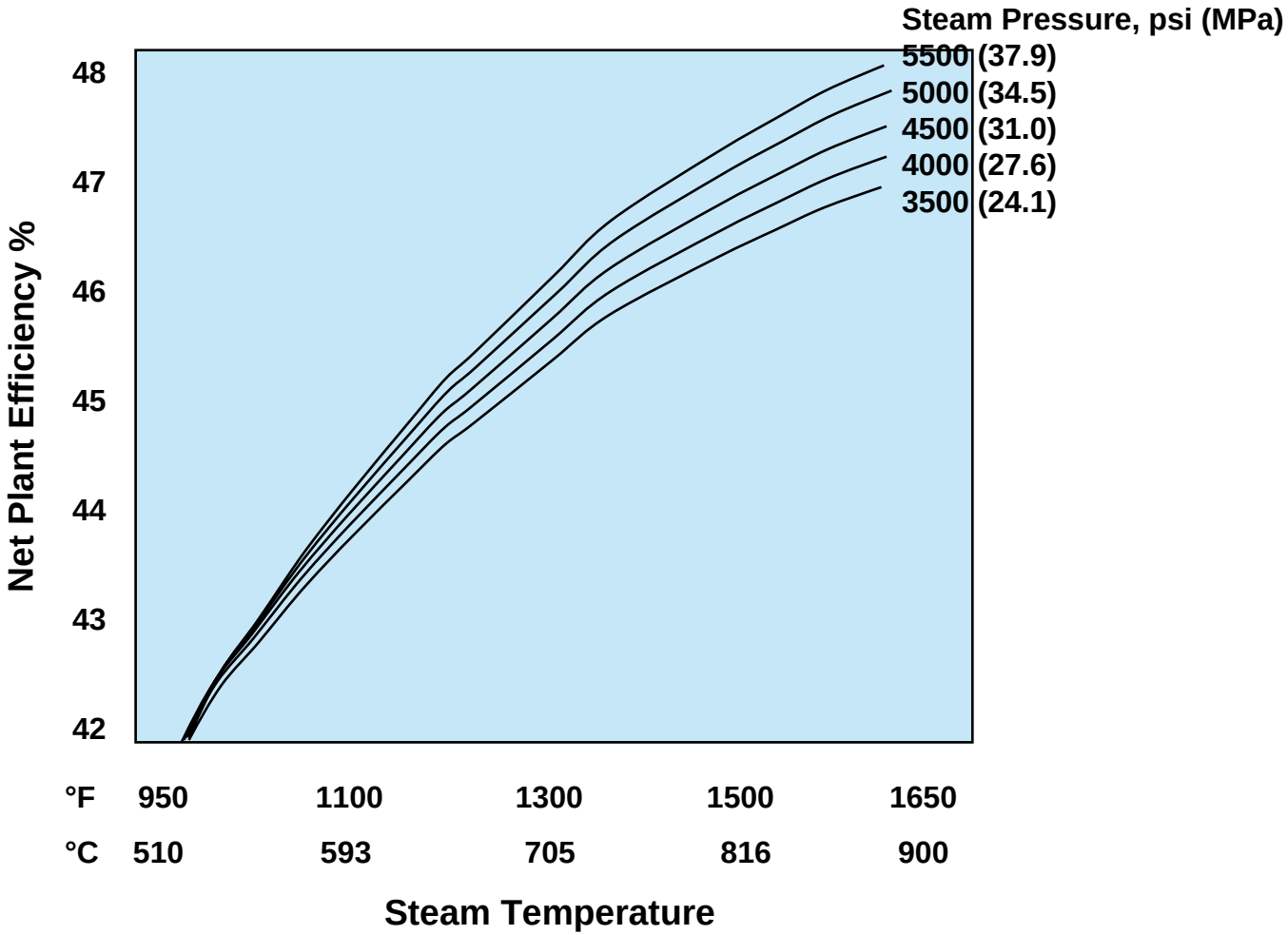

Data from NETL

DKM 2004 .5

© 2004 The Babcock & Wilcox Company. All rights reserved.

Need for the Program

- ***Materials are the key barrier to advancing steam temperatures***
- ***Coal-ash corrosion from <u>high sulfur coal</u> has not been adequately addressed for design***
- ***Manufacturing issues are also critical***

© 2004 The Babcock & Wilcox Company. All rights reserved.

Coal-Ash Corrosion Rate vs. Temperature

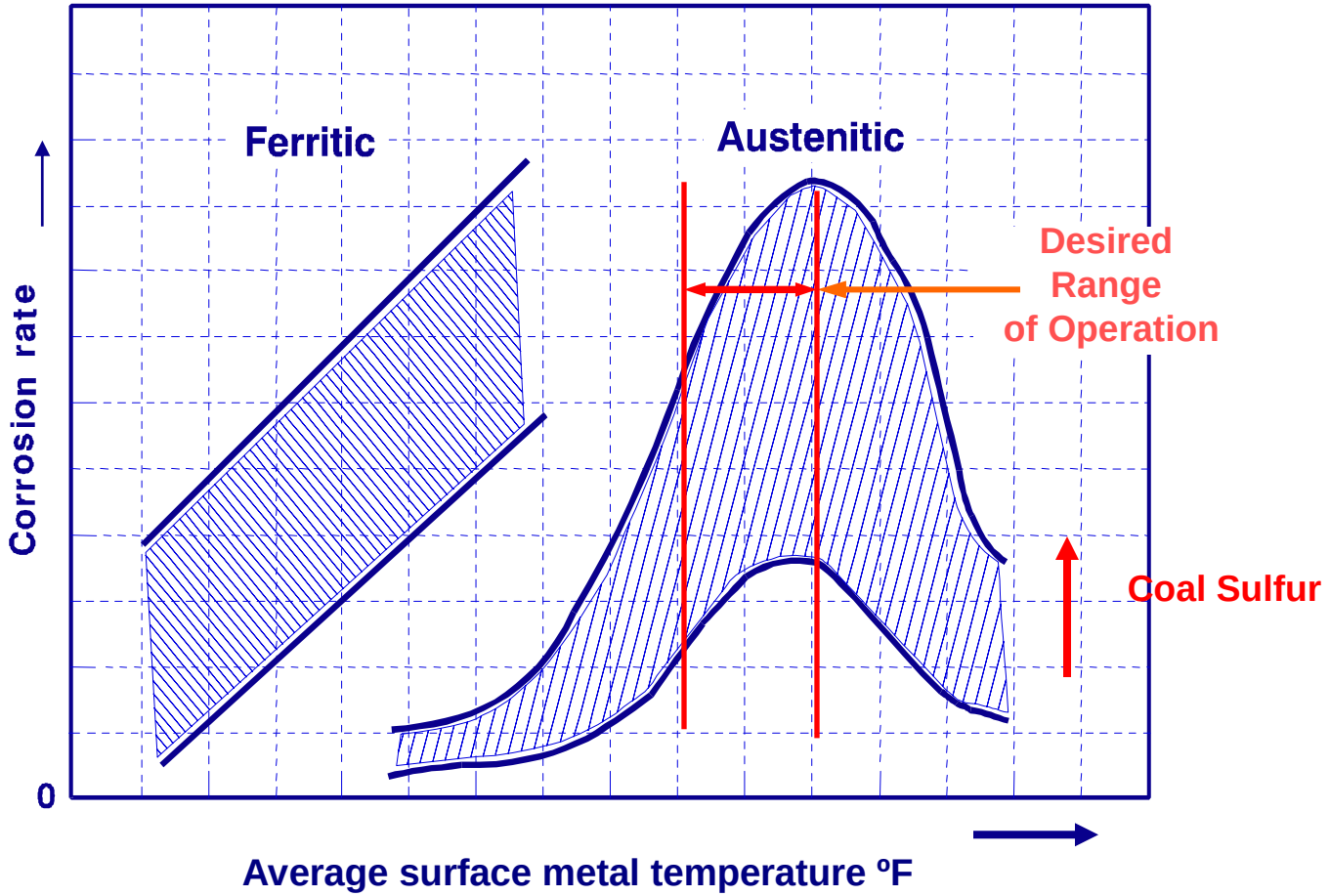

© 2004 The Babcock & Wilcox Company. All rights reserved.

DOE/B&W Coal Ash Corrosion Resistant Materials Testing Program

- ***Project began in 1998***
- ***Host is Reliant Energy's Niles Plant, Niles, Ohio***
- ***Coal contains 3.0-3.5% sulfur***
- ***110 MWe cyclone fired B&W boiler***
- ***Sections located with superheater at furnace exit (highest gas temperatures)***

© 2004 The Babcock & Wilcox Company. All rights reserved.

Coal Ash Corrosion Resistant Materials Testing Program

Objectives

- Evaluate the corrosion performance of newly developed superheater/ reheater materials for advanced supercritical boilers at surface temperature equivalent to 1100ºF (593ºC)
- Select materials resistant to fireside coal-ash corrosion
- Generate long-term corrosion data from field testing

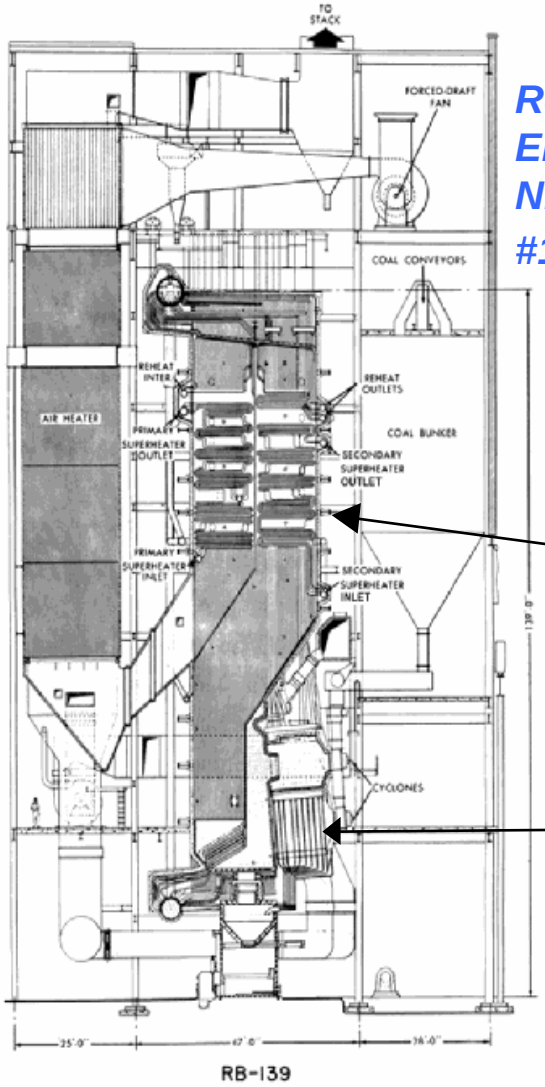

Reliant Energy's Niles Unit #1 Boiler

Location of Test Sections

Cyclone Burners

DKM 2004 .9

© 2004 The Babcock & Wilcox Company. All rights reserved.

Test System Arrangement

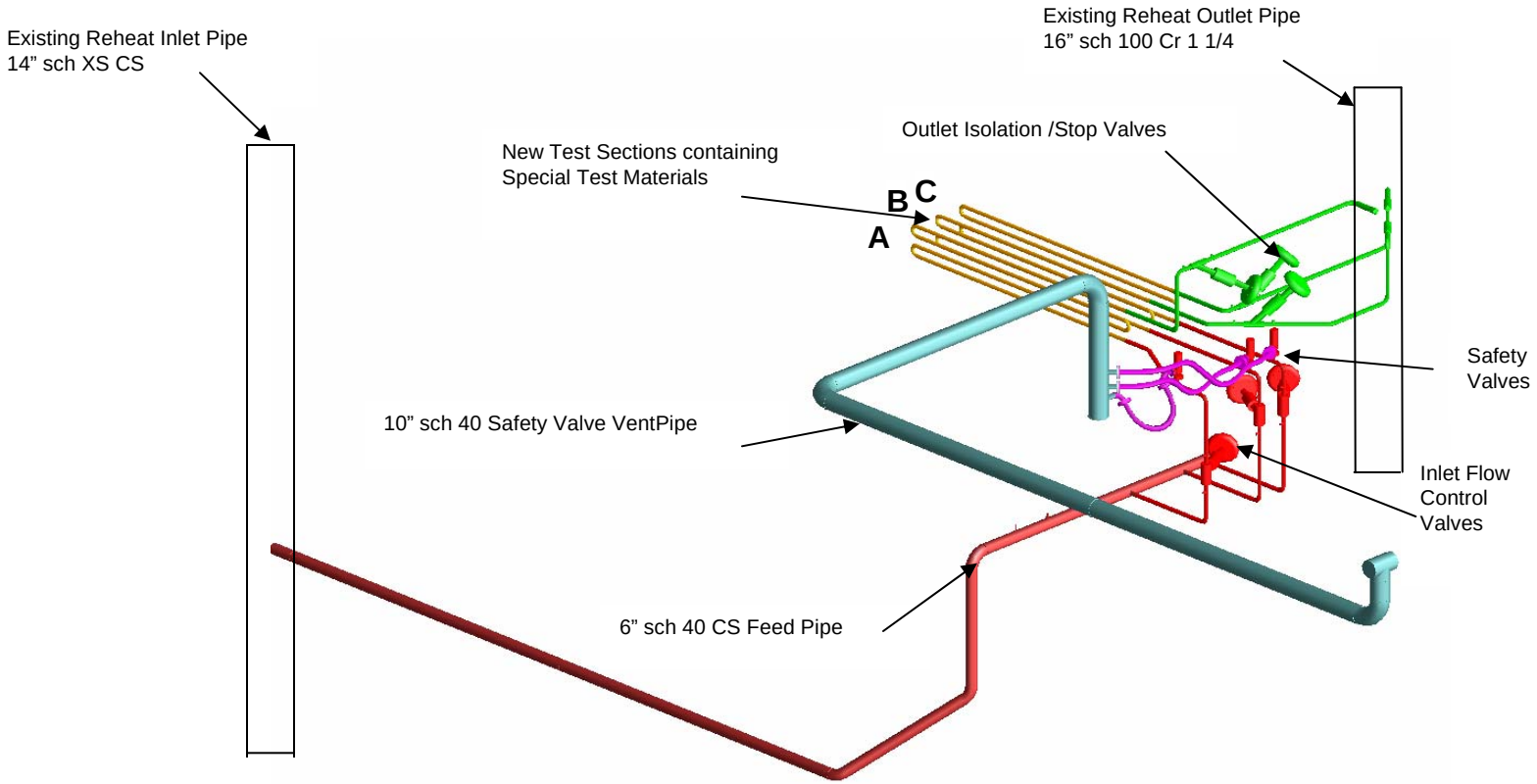

© 2004 The Babcock & Wilcox Company. All rights reserved.

Arrangement of Materials

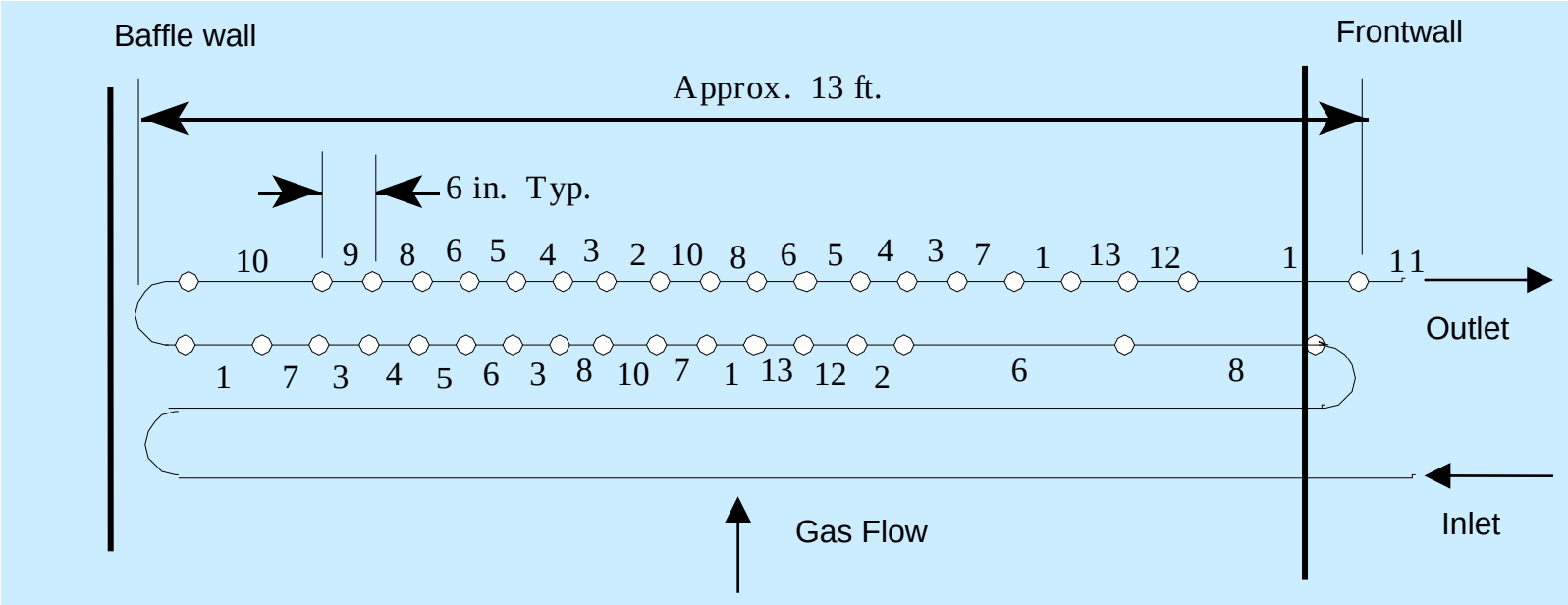

© 2004 The Babcock & Wilcox Company. All rights reserved.

Selected Test Materials

Mat'l #	MATERIAL	SUPPLIER	ASME RECOGNIZED	SIMILAR MATERIAL
1	Incoclad - Core is Incoloy 800H	INCO	Yes	SB407-UNS N08800
2	Thermie	ORNL	No	Inconel 617
3	HR3C – SA213TP310HCbN	Sumitomo	Yes	
4	Ta Modified 310	ORNL	No	SA213TP310H or SA213TP310HCbN
5	800 Modified	ORNL	No	Incoloy 800H
6	Save25	Sumitomo	No	SA213TP310H or SA213TP310HCbN
7	HR120	Haynes	No	SA213TP310H
8	NF709	Nippon Steel	No	SA213TP310H or SA213TP310HCbN
9	Fe3Al-2Cr/304H	ORNL	Yes	Core is SA213TP304H
10	TP347HFG – SA213TP347HFG	Sumitomo	Yes	
11	Transition Piece SA213TP304H	B&W – West Point	Yes	
12	690 clad 800HT weld metal INCO 52	INCO	Yes	Incoloy 800H
13	671 clad 800HT weld metal INCO 72	INCO	Yes	Incoloy 800H
14	SA213TP310H	B&W – West Point	Yes	

© 2004 The Babcock & Wilcox Company. All rights reserved.

Fabrication at B&W's Research Center

Orbital Tungsten Arc - rotating tube

- **Alloy 625 filler metal**
- **116 welds**
- **6 inch long specimens**
- **All bored to same ID**
- **Each specimen measured, marked and recorded for future evaluation**

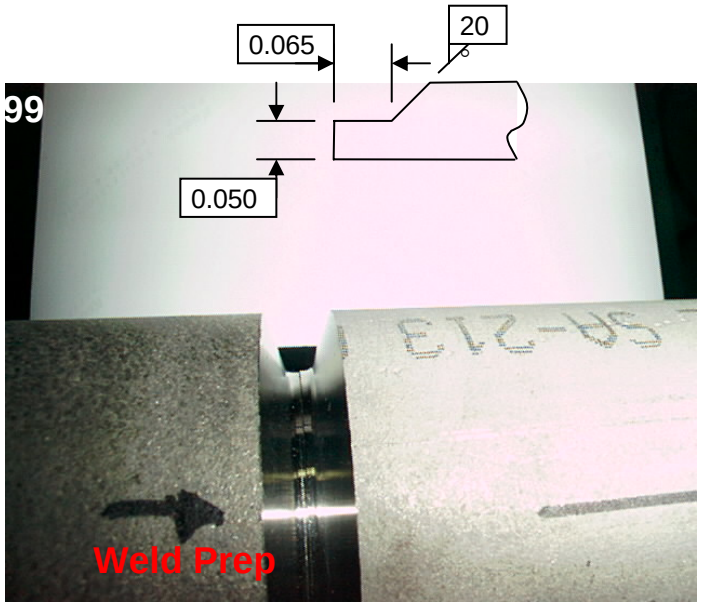

© 2004 The Babcock & Wilcox Company. All rights reserved.

Project Status

- *Design initiated November 1998*
- *Installation completed May 1999*

- *Startup Completed mid June 1999, steam temperature set at 1000ºF, raised to 1050ºF in July, minor controls tuning July to September, steam temperature raised to 1075ºF in November.*
- *Continuous Data Acquisition (4 min avgs.), remotely monitored daily from B&W offices throughout the program.*

© 2004 The Babcock & Wilcox Company. All rights reserved.

Project Status

- ***Several visual inspections in 2000 and 2001, corrosion evident, SAVE25 material nearly corroded through (some SAVE25 specimens replaced November 2001).***

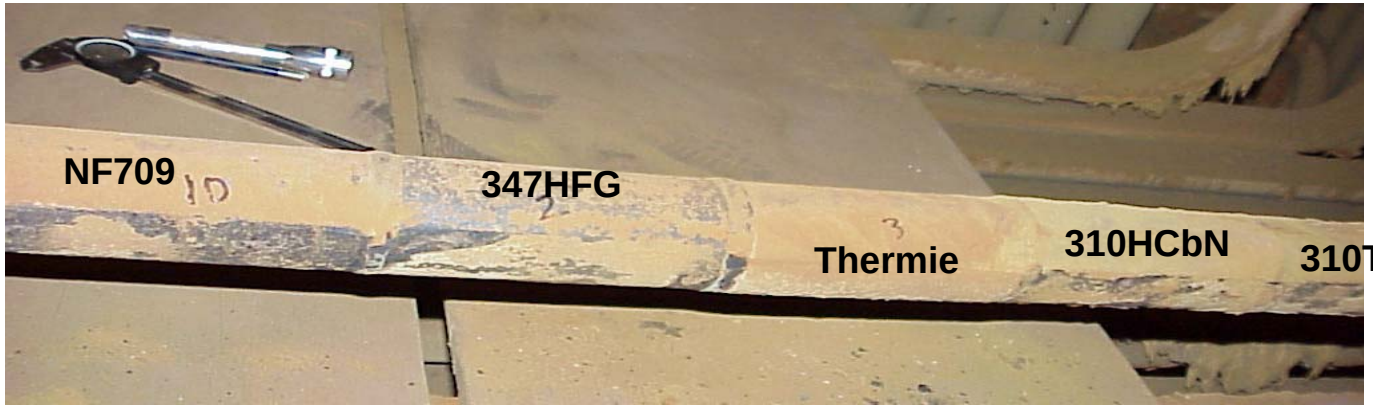

- ***First section "A" removed in November 2001; analysis, evaluation and report completed October 31, 2002.***

© 2004 The Babcock & Wilcox Company. All rights reserved.

Project Status

- ***Additional visual inspections in 2002 and 2003, additional SAVE25 specimens replaced in June 2002.***
- ***Second section "C" removed in August 2003.***

© 2004 The Babcock & Wilcox Company. All rights reserved.

Project Status

- ***Third section "B" was removed with section "C", repaired and re-installed in the "C" location in November 2003***
- ***Third section "B" removed in April 2005 and is being evaluated.***

© 2004 The Babcock & Wilcox Company. All rights reserved.

Evaluation Methods

- *Time/temperature data was correlated*
- *Section appearance was photographed and close- ups taken from top, bottom and side.*
- *Tube was sectioned (saw) for evaluation.*
- *Samples were sent to a third-party laboratory for chemical analysis and results compared with initial chemistry.*
- *Dimension rings removed from the middle of each sample, grit blasted and photographed to show the extent and type of attack occurring below the deposit/scale.*
- *The rings were dimensioned and compared at eight predetermined circumferential locations with initial dimensions to quantify the wall thickness losses at each position.*

© 2004 The Babcock & Wilcox Company. All rights reserved.

Evaluation Methods

- ***A full cross-section ring was polished and etched for each sample and examined using SEM and optical microscopy.***

- ***One sample from each material was selected (most metal lost) for detailed assessment of the microstructures of both the external and internal interfaces.***

© 2004 The Babcock & Wilcox Company. All rights reserved.

Evaluation

Daily Average Surface Metal Temperatures (ºF) for hottest sample

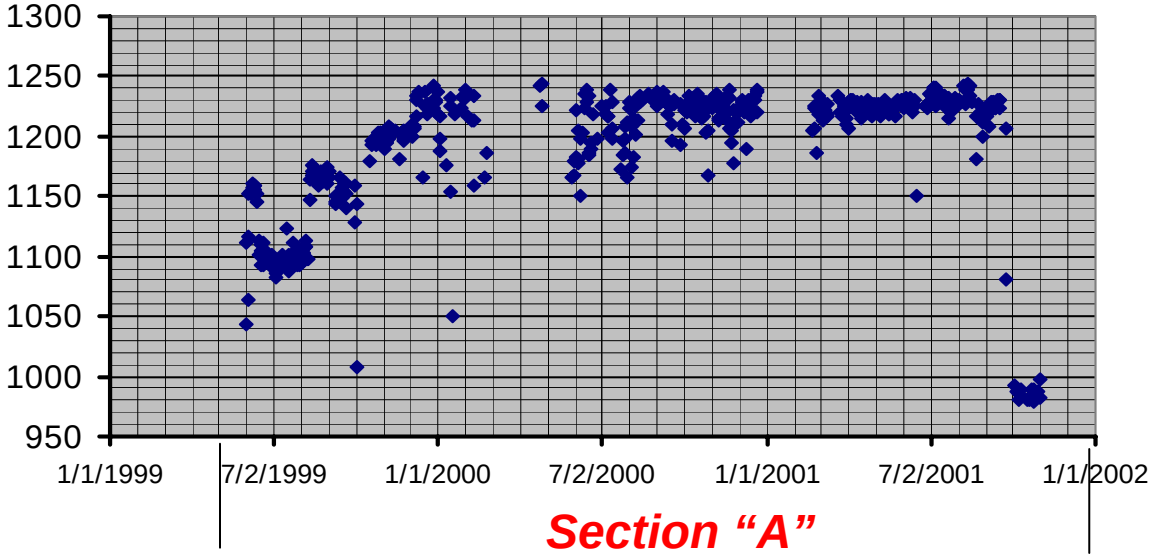

Section "A"

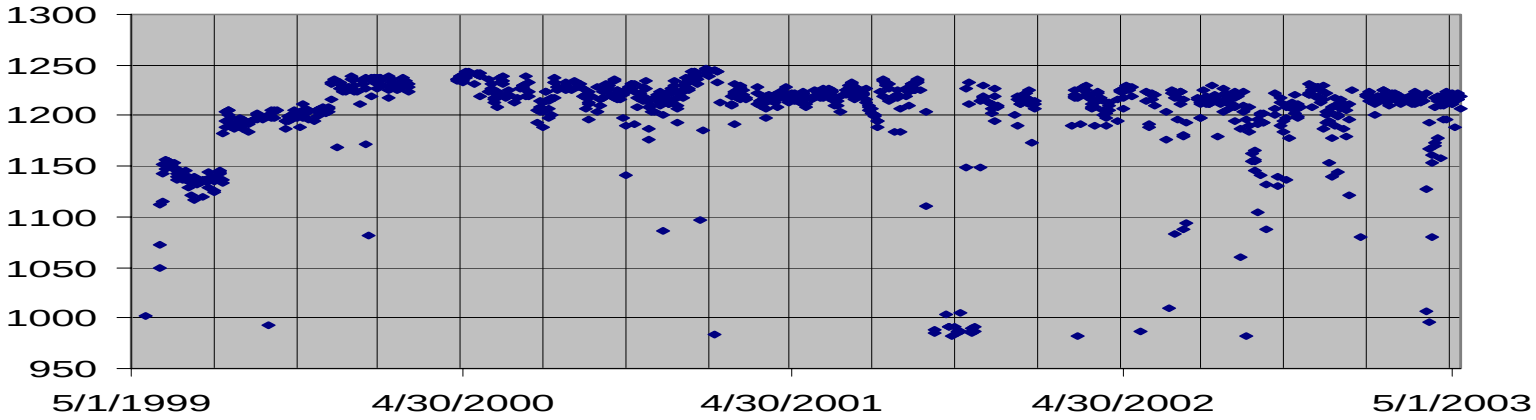

Section "C"

© 2004 The Babcock & Wilcox Company. All rights reserved.

SAVE 25 Performance

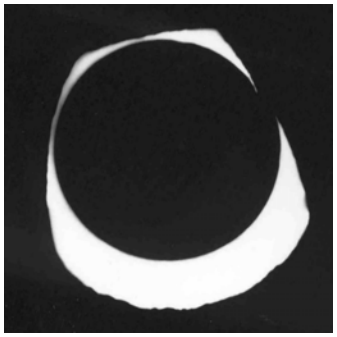

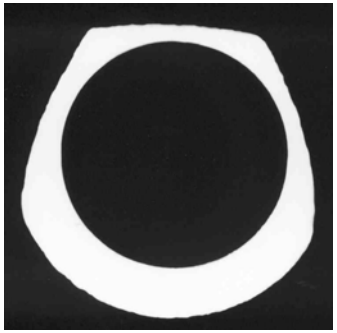

Average Surface Metal Temperature -	**1180 F**	**1096 F**	**1058 F**
Wastage Rate -	**>259 mils/yr**	**148 mils/yr**	**56 mils/yr**
Date Removed -	**Nov. 2001**	**Jun. 2002**	**August 2003**

© 2004 The Babcock & Wilcox Company. All rights reserved.

Results - Section "A"

Wastage Rate as a Function of Position in Test Section

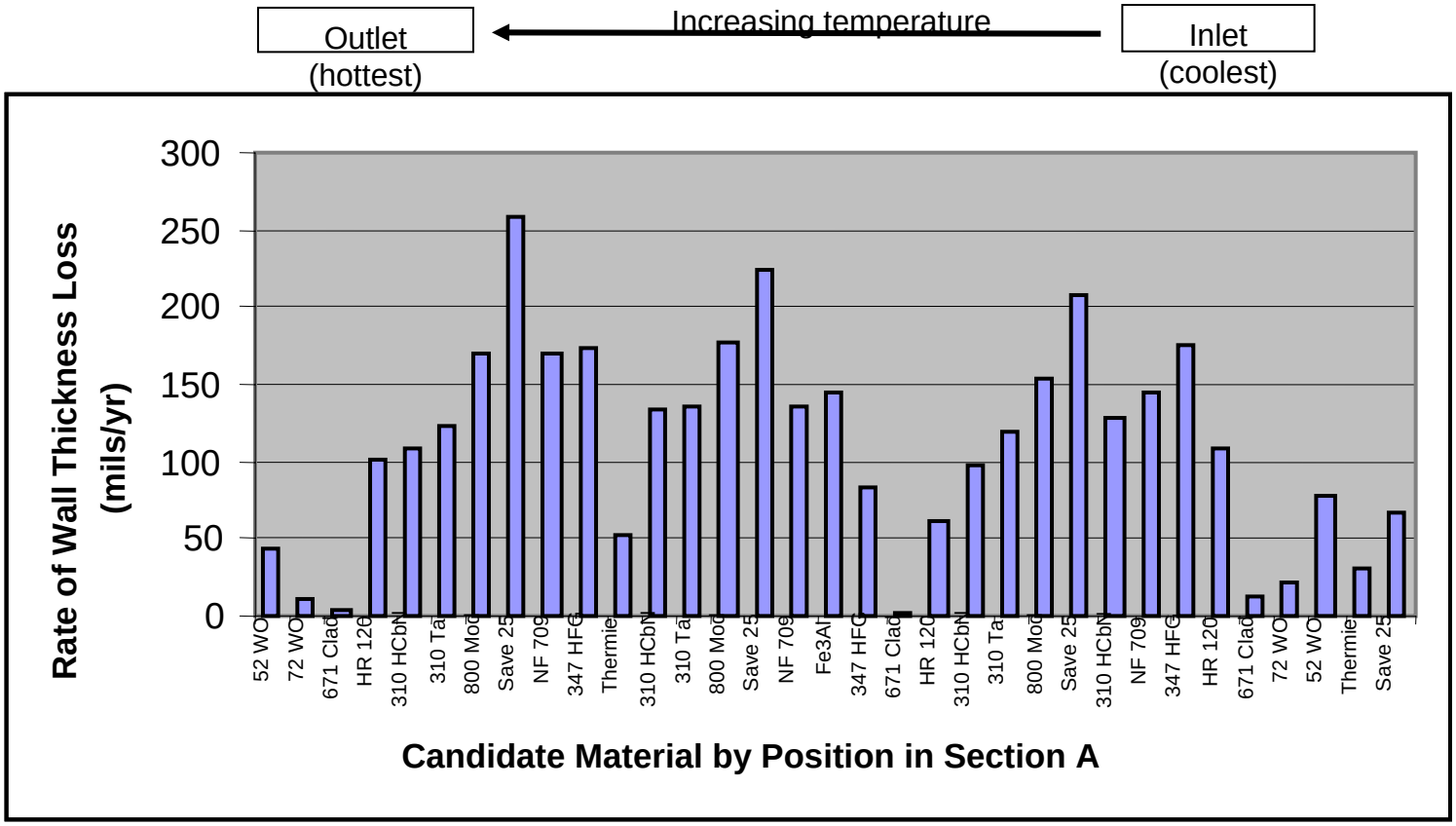

© 2004 The Babcock & Wilcox Company. All rights reserved.

Results - Section "C"

Wastage Rate as a Function of Position in Test Section

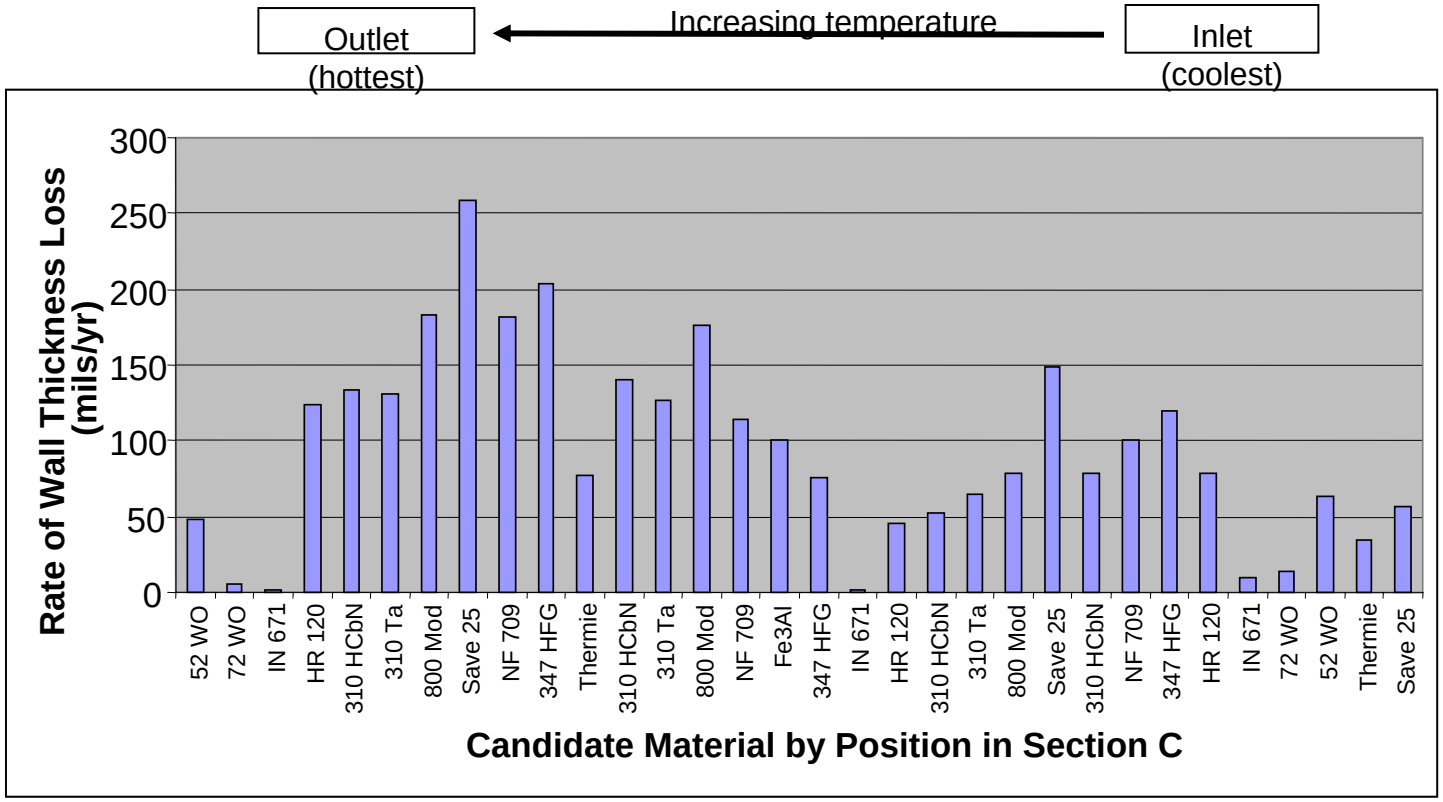

© 2004 The Babcock & Wilcox Company. All rights reserved.

Results - Section "A"

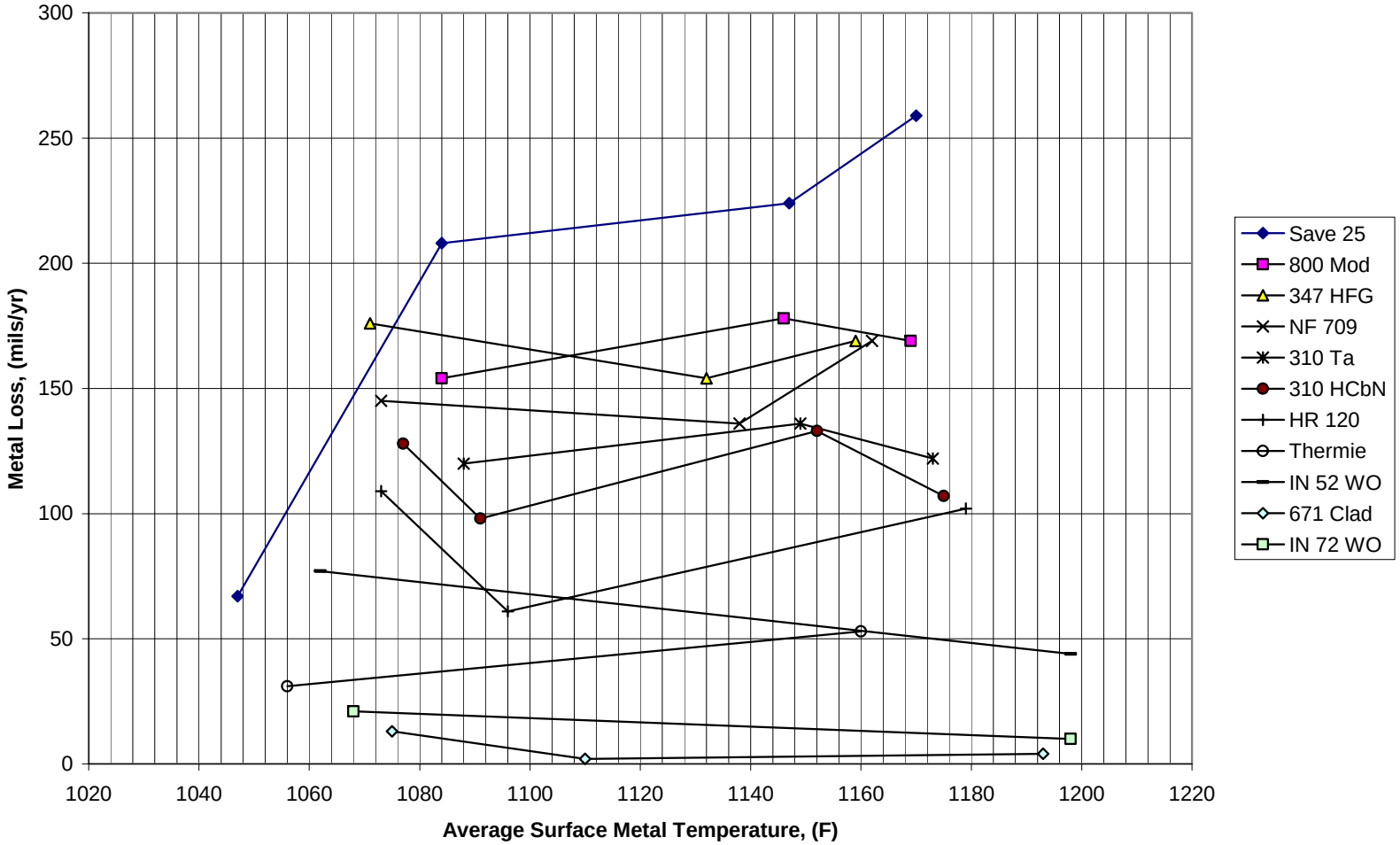

Wastage as a Function of Average Surface Metal Temperature

© 2004 The Babcock & Wilcox Company. All rights reserved.

Results - Section "C"

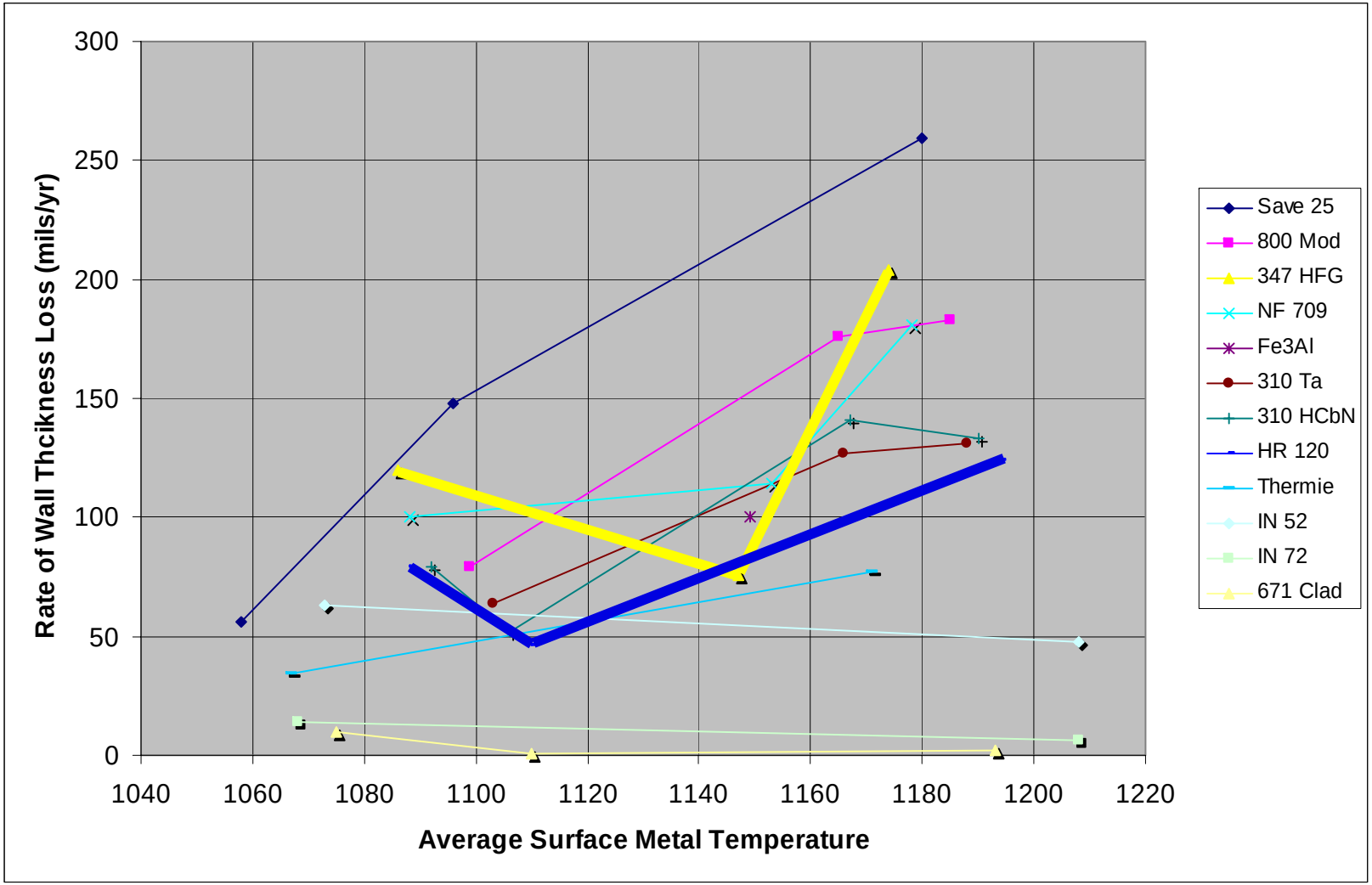

Wastage as a Function of Average Surface Metal Temperature

© 2004 The Babcock & Wilcox Company. All rights reserved.

Possible Location Effect

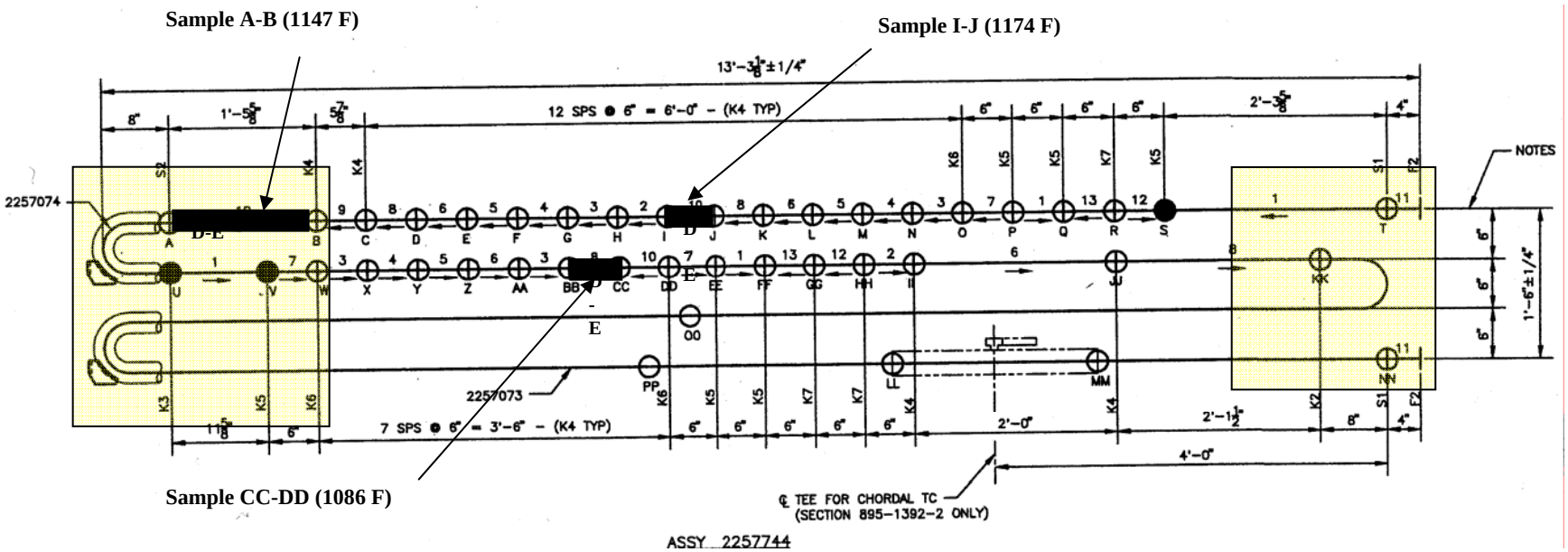

Position of 347 HFG Tube Samples

© 2004 The Babcock & Wilcox Company. All rights reserved.

Results - Sections "A" and "C"

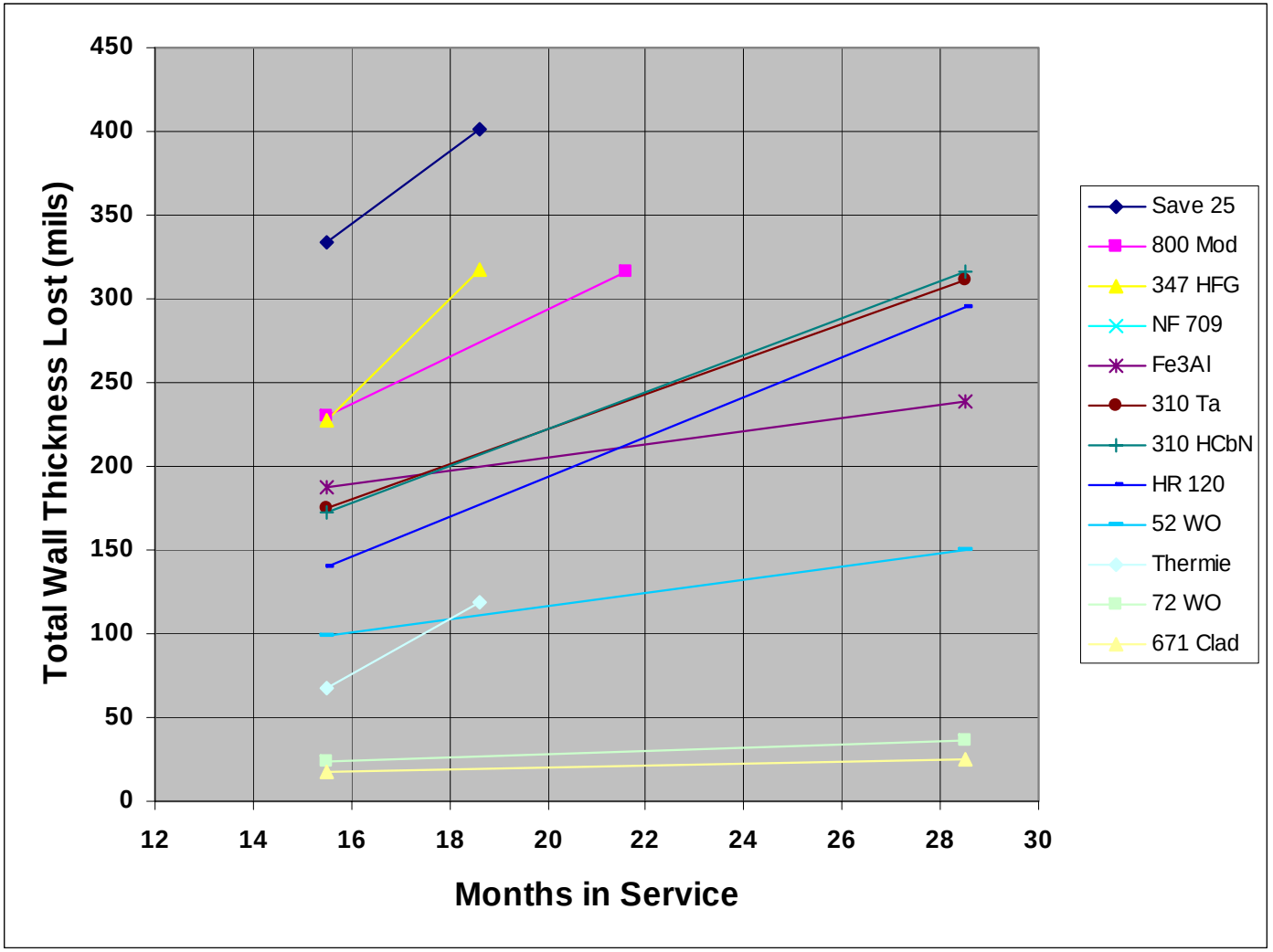

Metal Loss versus Time (Section A and C)

© 2004 The Babcock & Wilcox Company. All rights reserved.

Results - Sections "A" and "C"

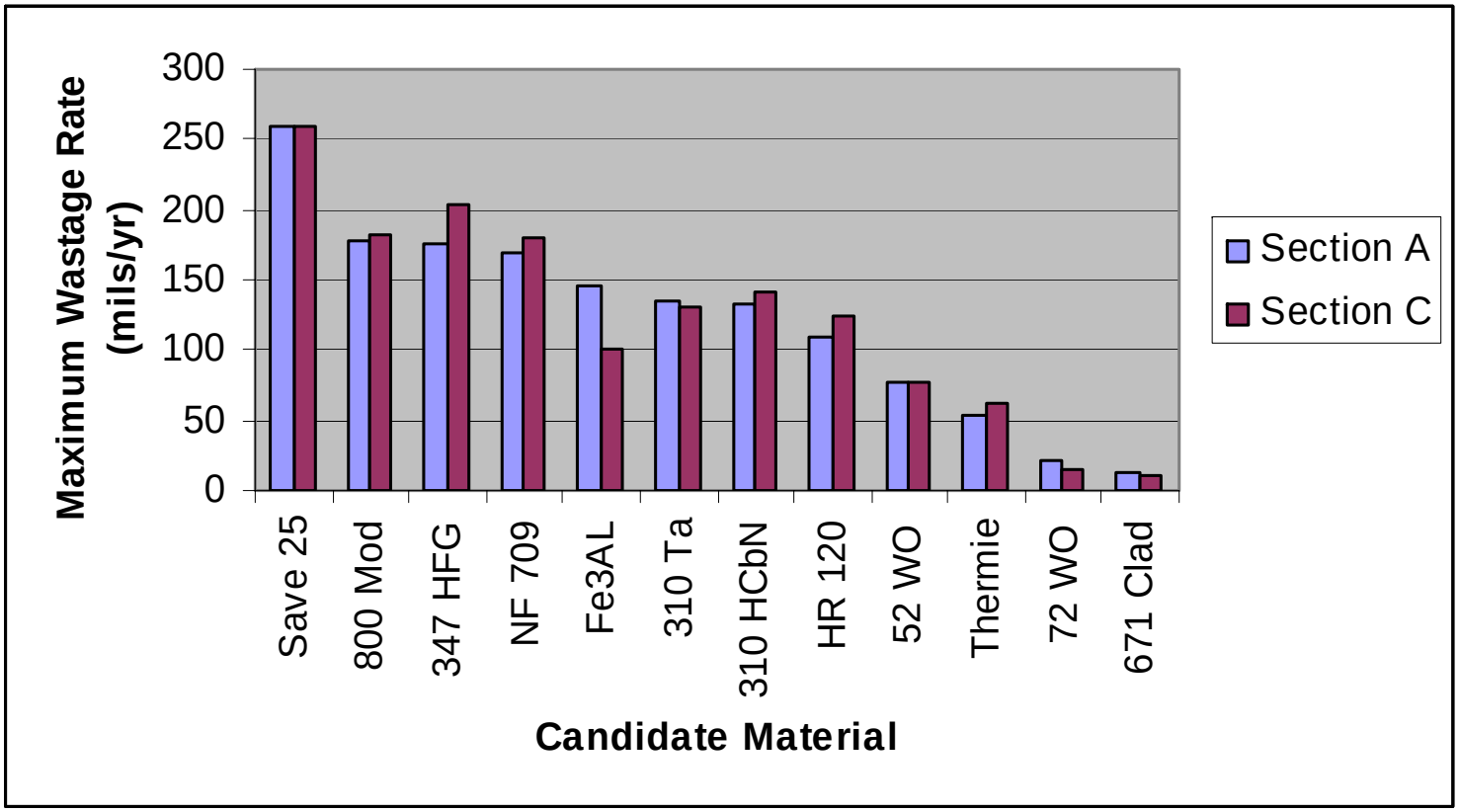

Materials performed very similarly in both Sections "A" and "C"

© 2004 The Babcock & Wilcox Company. All rights reserved.

Results - Sections "A" and "C"

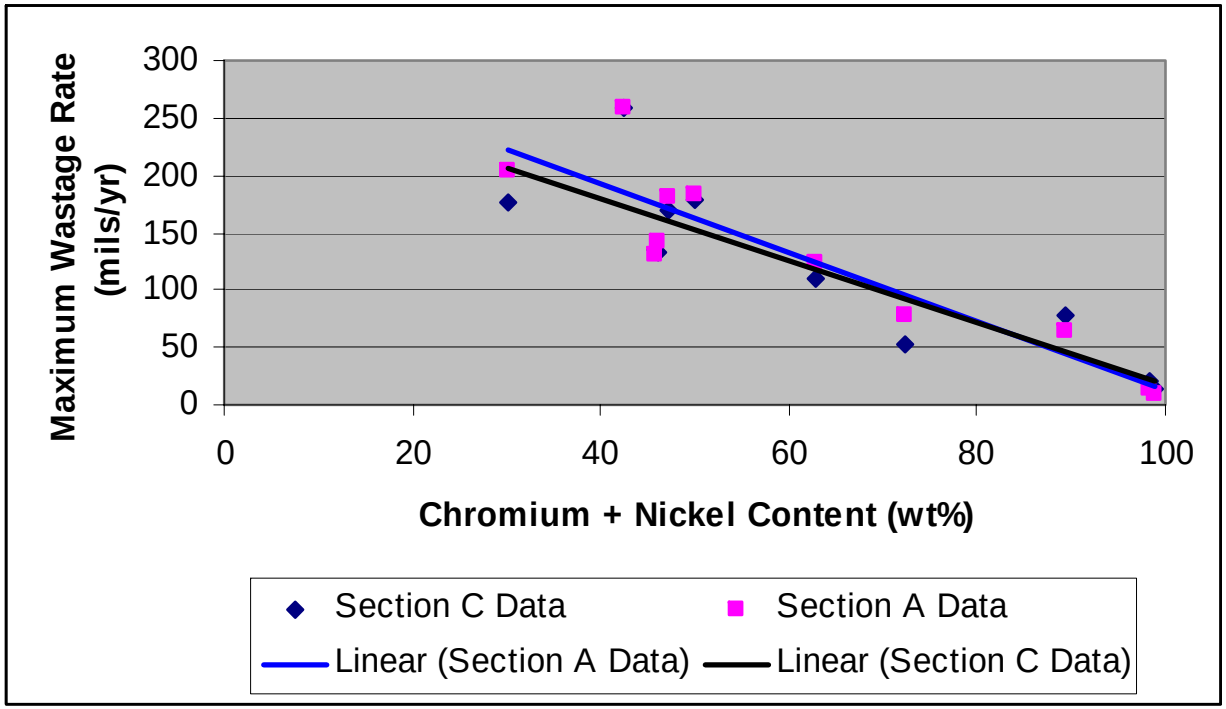

Chromium + Nickel Content vs. Wastage Rate

Corrosion rate is inversely related to nickel + chromium.

Corrosion rate is proportional to the iron content.

© 2004 The Babcock & Wilcox Company. All rights reserved.

Results - Section "C"

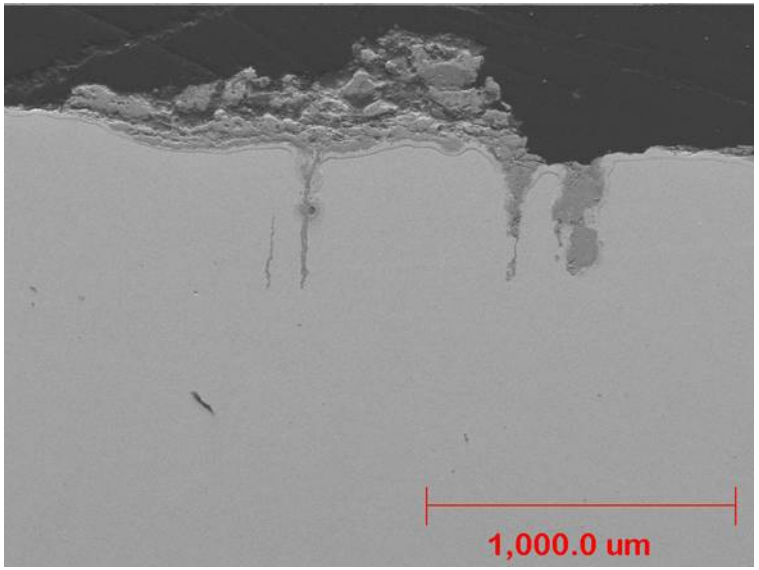

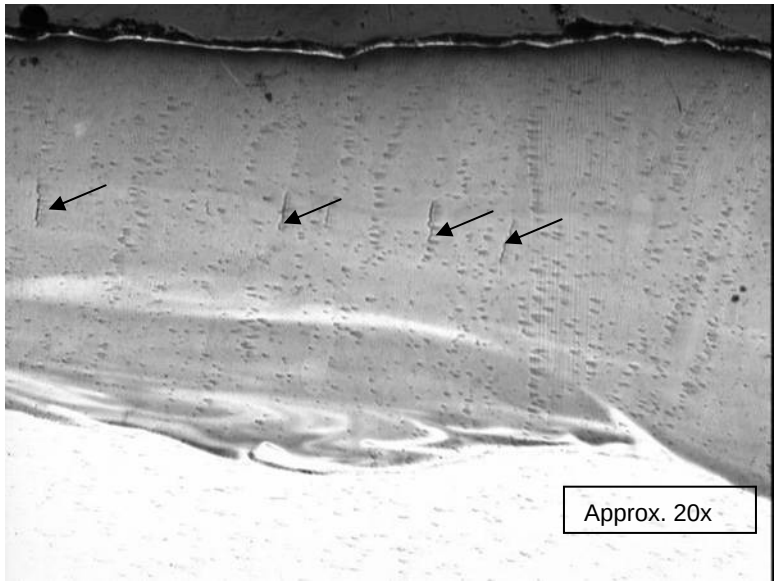

Weld Cracks Intersecting External Corrosion for INCO 72 Weld Overlay

Internal Cracking in INCO 72 Weld Overlay

© 2004 The Babcock & Wilcox Company. All rights reserved.

Results - Section "C"

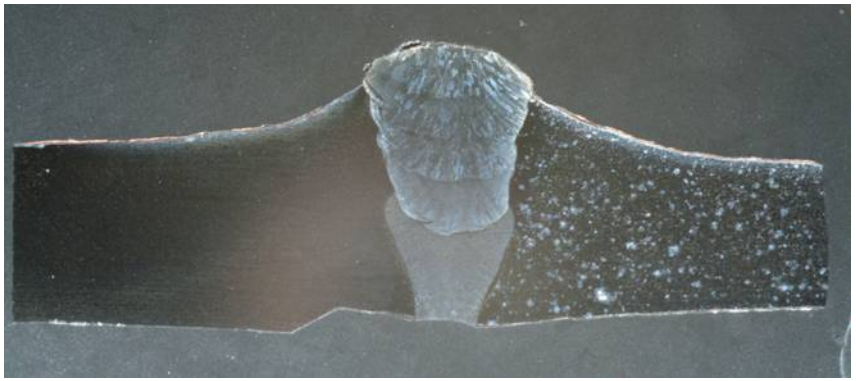

Typical Tube-to-Tube Weld Profile after Exposure

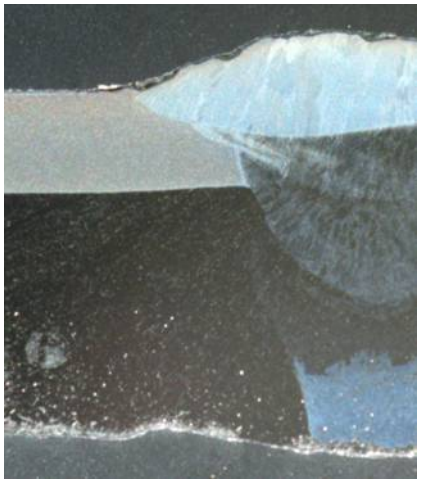

Weld at 1121º F
(showing no corrosion)

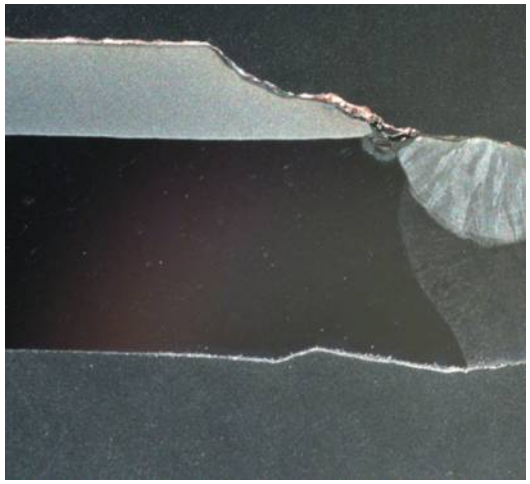

Weld at 1203º F
(showing weld corrosion affecting adjacent base metal

Incoclad 671 Weld Cross Sections

© 2004 The Babcock & Wilcox Company. All rights reserved.

Summary of Results - Sections "A" and "C"

- *Several of the materials tested are more resistant than the Type 304, 347, 321, and 316 stainless steels currently used in superheaters and reheaters.*

Alloy	Corrosion Rate Section A	Operating Temp. ºF	Corrosion Rate Section C	Operating Temp. ºF
Incoclad (48%Cr, 52%Ni)	13 mpy	1075	10 mpy	1086
Inconel 72 weld clad	21 mpy	1068	14 mpy	1079
Inconel 52	77 mpy	1062	63 mpy	1073
Thermie (now Inconel 740)	53 mpy	1160	77 mpy	1171
HR120	109 mpy	1077	79 mpy	1088

- *Corrosion rates for modified 310 stainless steel alloys (24- 26% chromium) were higher and the lower chromium alloys like NF709, modified 800, and Save 25 were higher yet.*

© 2004 The Babcock & Wilcox Company. All rights reserved.

Summary of Results - Section "C"

The evaluation of Section C, and consideration of Section A results, suggests the following:

1. ***Materials that corroded rapidly in Section A, also fared poorly in Section C.***

2. ***Materials that performed well in Section A also did so in Section C.***

3. ***Some materials that demonstrated a moderate wastage rate, showed a reduced wastage rate at intermediate temperature (both in Sections A and C) – probably due to practical positional and operational variations in conditions.***

© 2004 The Babcock & Wilcox Company. All rights reserved.

Summary of Results - Section "C"

4. ***The full cladding thickness of the iron-aluminide coated and IN 52 Weld Overlaid specimens was lost on Section "C" exposing the 800H base material which has a significantly higher wastage rate.***

5. ***Cracking was found in the IN 72 Weld Overlay specimens and was also discovered in the as-received material (independent of the corrosion mechanism). It increased quantity and length with time at temperature. Incoclad 671 is very similar in composition but did not exhibit cracking which suggests modification of the cladding process. If resolved, IN 72 Weld Overlay would be a cost-effective option.***

6. ***Weld cross-sections showed that the Inconel 625 filler metal serves well for most of the candidate materials. However, care must be taken to ensure that the weld filler metal has an equivalent wastage resistance to the materials being joined.***

© 2004 The Babcock & Wilcox Company. All rights reserved.

What's Ahead?

- ***Section B was removed April 26th and moved to B&W's Research Center where evaluation has begun. Results will be reported this fall.***

- ***Tests under the DOE/OCDO sponsored "Boiler Materials for Ultra-supercritical Power Plants" Project will determine the performance of several new materials at still higher temperatures. These sections were installed at Niles in December 2003. They are expected to be removed in the spring or fall of 2006.***

© 2004 The Babcock & Wilcox Company. All rights reserved.

a McDermott company

The Babcock & Wilcox Company

Generating Powerful Solutions℠

1-800-BABCOCK
www.babcock.com

© 2004 The Babcock & Wilcox Company. All rights reserved.

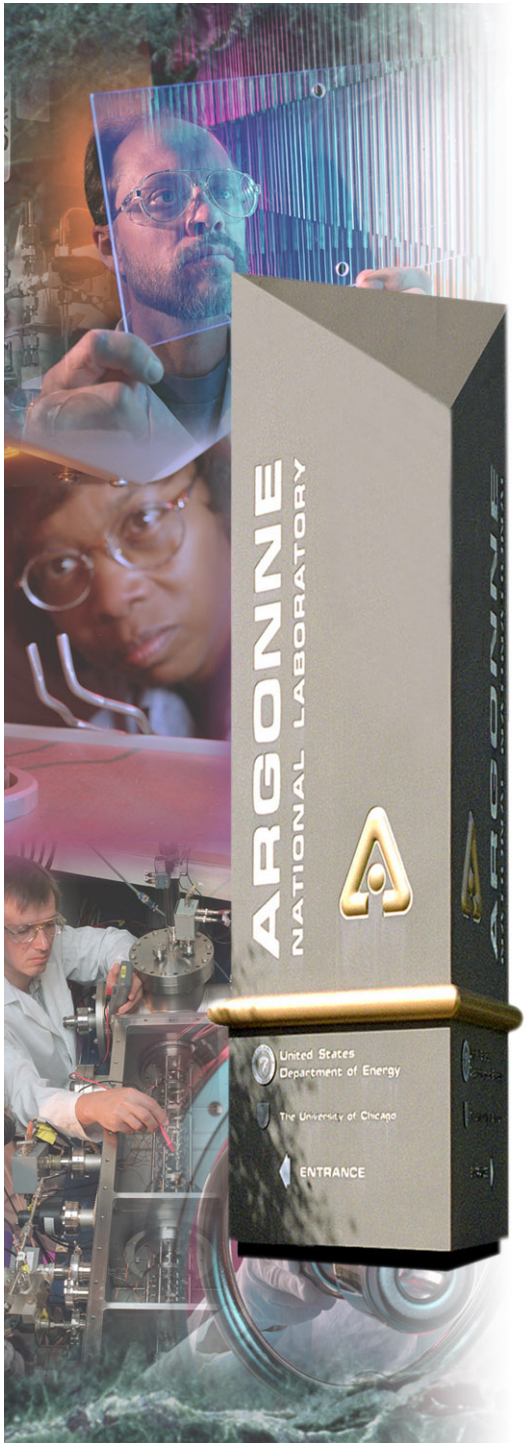

Fireside Corrosion of Alloys for USC Plants

K. Natesan, J. H. Park, and D. L. Rink

19th Annual Conference on Fossil Energy Materials, Knoxville, TN, May 9-11, 2005

Work supported by DOE/Office of Fossil Energy, Advanced Research Materials Program

Argonne National Laboratory

Office of Science
U.S. Department of Energy

A U.S. Department of Energy
Office of Science Laboratory
Operated by The University of Chicago

Outline of Presentation

- **Background**
- **Objectives**
- **Materials and experimental procedure**
- **Performance of Fe-base alloys**
- **Performance of Ni-base alloys**
- **Project summary**

Efficiency and Emissions for Coal-fired Boiler Technologies

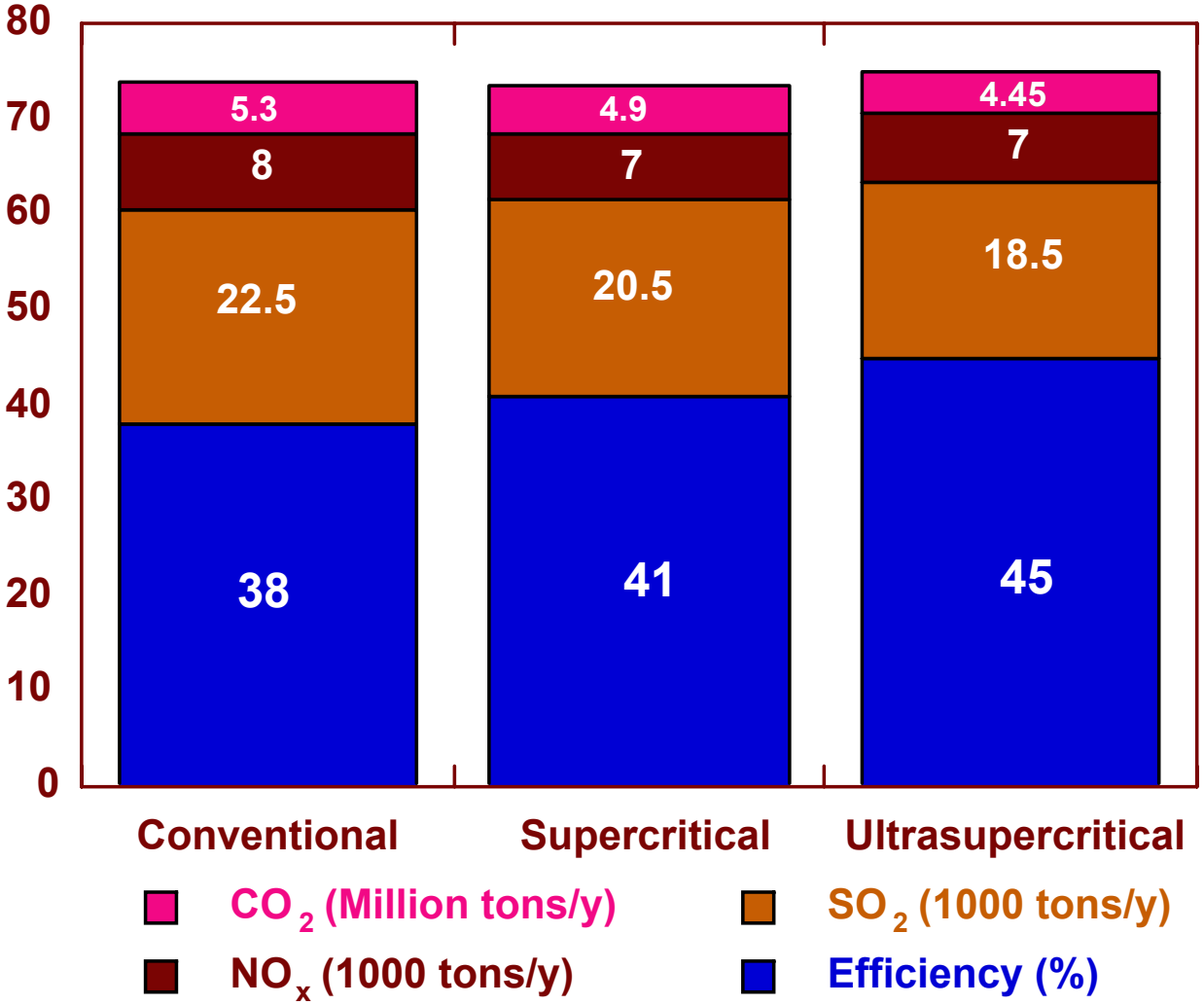

Pulverized Coal-Fired Boilers

Goal is to develop advanced steam cycles

Current: 16.5-24 MPa (2,400-3,500 psig), 540°C (1000°F) steam

Near-Term Goal: 34.5 MPa (5,000 psig), 650°C steam

Long-Term Goal: 34.5 MPa (5,000 psig), 760°C steam

Waterwall corrosion:	Formation of pyrosulfates, trisulfates
Superheater corrosion:	Formation of alkali-iron trisulfates Alkali sulfates/alkali chlorides induced corrosion Loss of mechanical properties

ANL Program Objectives

- Evaluate fireside corrosion performance of metallic materials in coal-ash environments typical of advanced steam cycle systems
- Evaluate the role of alkali sulfates and alkali chloride in the corrosion process
- Establish the relative corrosion performance of off-the shelf and experimental alloys
- Surface engineering of alloys to improve fireside and steamside corrosion resistance
- Perform comparative corrosion tests on candidate materials by exposures in coal-burning combustion test facility at NETL, Pittsburgh

Fe-base Alloys for use up to 650°C

Material	C	Cr	Ni	Mn	Mo	Fe	Other
Mod. 9Cr-1Mo	0.10	9	0.8	0.45	1.0	Bal	Nb 0.08, V 0.2, N 0.06
HCM12A	0.10	12	0.3	0.5	0.4	Bal	W 2.0, V 0.2, Nb 0.05, Cu 0.9, N 0.05
E911	0.12	9	0.25	0.51	0.94	Bal	W 0.9, V 0.2, Nb 0.06, N 0.06
NF616	0.10	9	0.06	0.46	0.47	Bal	W 1.84, V 0.2,

Fe-base Alloys for T up to 700°C

Material	C	Cr	Ni	Mn	Si	Mo	Fe	Other
Super 304H	0.10	18	9	1.0	0.3	-	Bal	Nb 0.45, Cu 3.0, N 0.09
347HFG	0.08	18	11	2.0	1.0	-	Bal	Nb + Ta = 10 x C min
HR3C	0.06	25	20	1.2	0.4	-	Bal	Nb 0.45, N 0.2
310TaN	0.05	25	20	1.0	0.2	-	Bal	Ta 1.5, N 0.2
NF709	0.07	20	25	1.0	0.6	1.5	Bal	Ti 0.6, Nb 0.2, N 0.18, B 0.004
SAVE 25	0.10	23	18	1.0	0.4	-	Bal	Nb 0.45,, W 1.5, Cu 3.0, N 0.2
Modified 800	0.10	20	30	1.5	0.2	1.5	Bal	Ti 0.25, Nb 0.25, V 0.05, N 0.03, B 0.004
HR120	0.05	25	37	0.7	0.6	2.5	Bal	Co 3, W 2.5, N 0.2, Cu 0.18, B 0.004, Al 0.1, Nb 0.7
671 clad/800H								
671	0.05	48	Bal	0.02	0.2	-	0.2	Ti 0.4
800	0.05	21	32	0.5	0.2	-	Bal	Ti 0.4, Al 0.4

Nickel-base Alloys for use at T up to 760°C

Alloy	Cr	Ni	Si	Mo	Fe	Other
601	21.9	Bal	0.2	0.1	14.5	Al 1.4, Ti 0.3, Nb 0.1
690	27.2	61.4	0.1	0.1	10.2	Ti 0.3, Al 0.2
617	21.6	53.6	0.1	9.5	0.9	Co 12.5, Al 1.2, Ti 0.3
IN 625	21.5	Bal	0.3	9.0	2.5	Nb 3.7, Al 0.2, Ti 0.2
602CA	25.1	62.6	0.1	-	9.3	Al 2.3, Ti 0.13, Zr 0.19, Y 0.09
230	21.7	60.4	0.4	1.4	1.2	W 14, Al 0.3, La 0.015
HR160	28.0	Bal	2.8	0.1	4.0	Co 30, Al 0.2
693	28.8	Bal	0.04	0.1	5.8	Al 3.3, Nb 0.67, Ti 0.4, Zr 0.03
740	23.5	49.0	0.5	0.4	2.1	Co 20, Ti 2, Nb+Ta 2, Al 0.7

Corrosion Test Facility

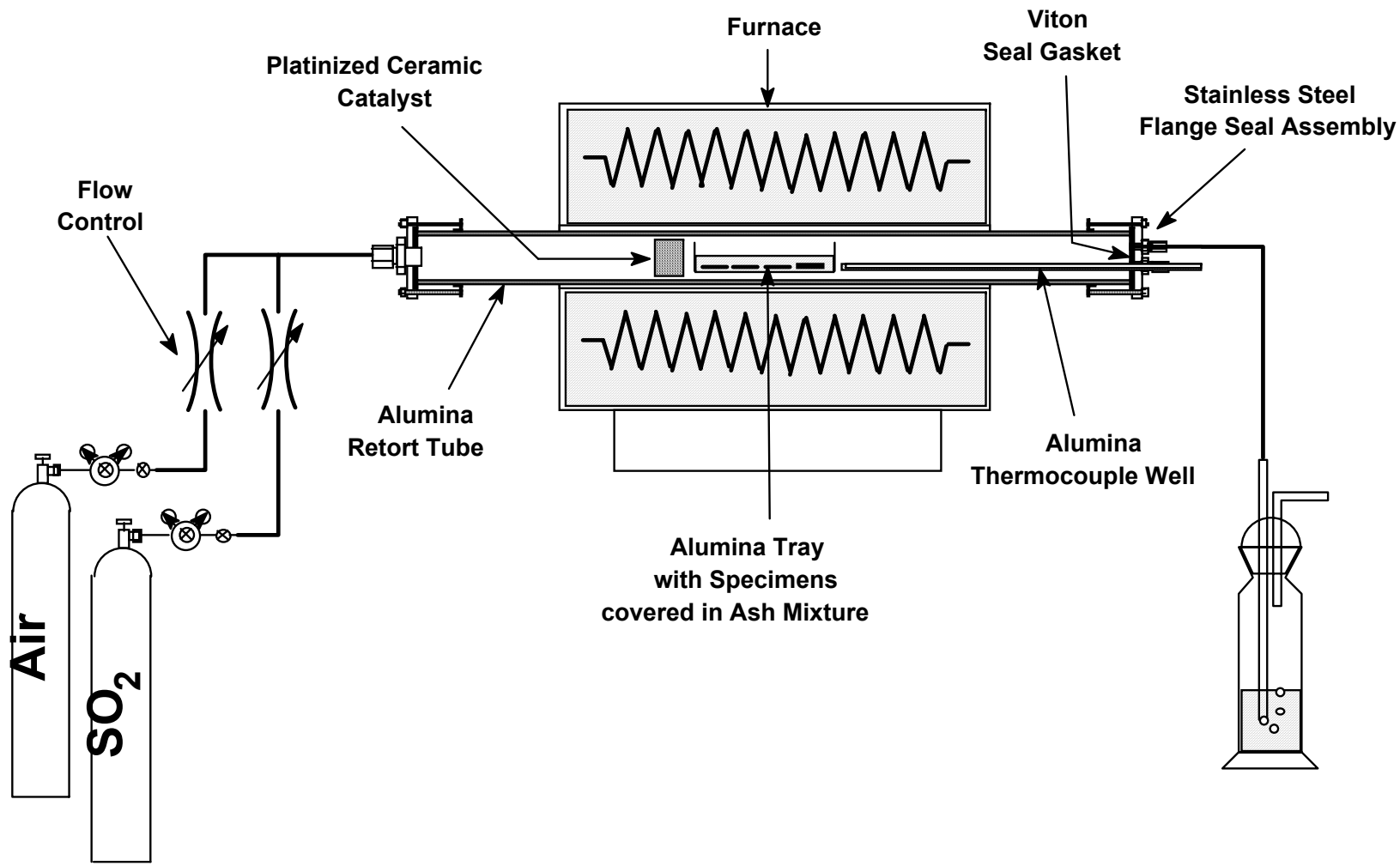

Deposit chemistry

(a) $SiO_2 : Al_2O_3 : Fe_2O_3 = 1:1:1$

(b) $Na_2SO_4 : K_2SO_4 = 1:1$

(c) NaCl

Ash 1: 90 wt.% (a) + 10 wt.% (b)

Ash 2: 85 wt.% (a) + 10 wt.% (b) + 5 wt.% (c)

Ash 3: 89 wt.% (a) + 10 wt.% (b) + 1 wt.% (c)

Laboratory Test Details

- **Key variables: temperature, time, alloy composition, deposit composition**
- **Materials: ferritics, austenitics, high-Ni alloys, claddings/coating**
- **Gas: 1 vol.% SO_2 in air (catalyzed)**
- **Test temperatures: 650, 725, and 800°C**
- **Test times: 300-2000h**
- **Specimen evaluation: weight change**
  scanning electron microscopy
  energy dispersive X-ray analysis
  X-ray diffraction

Corrosion Loss in Coal Ash + Alkali Sulfate

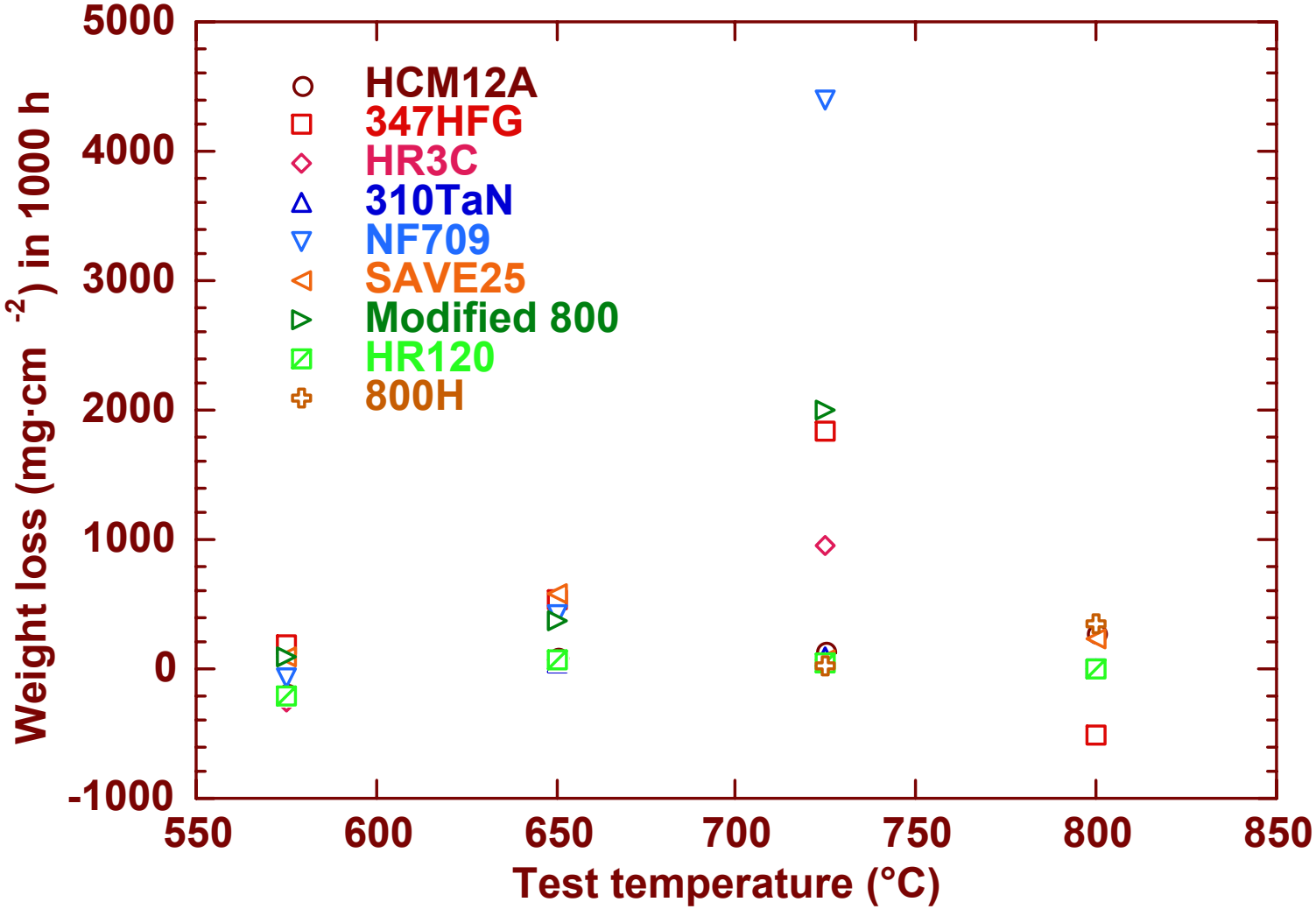

Corrosion Loss in Coal Ash + Alkali Sulfate + NaCl

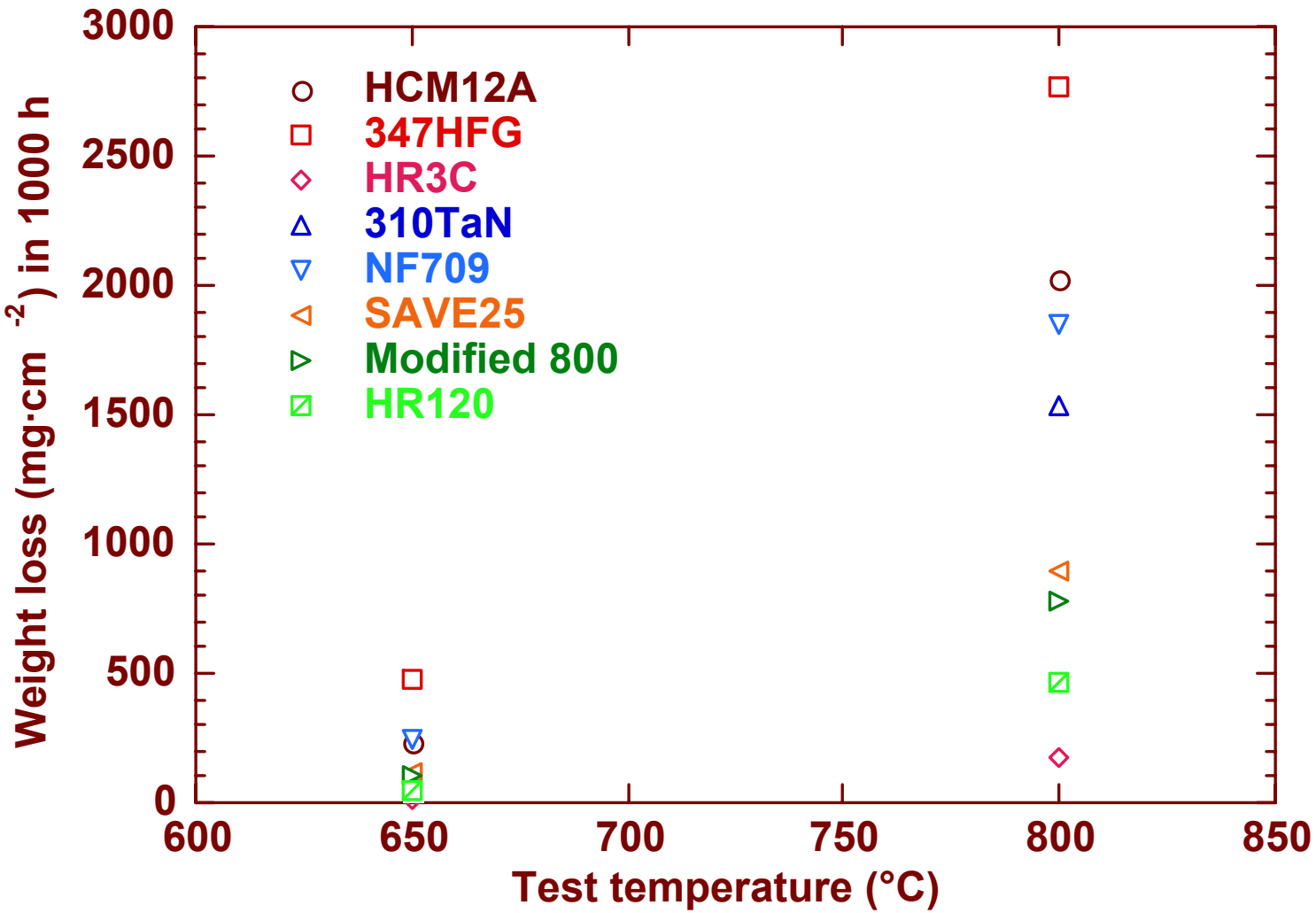

Effect of Deposit Chemistry on Corrosion of Fe-base Alloys

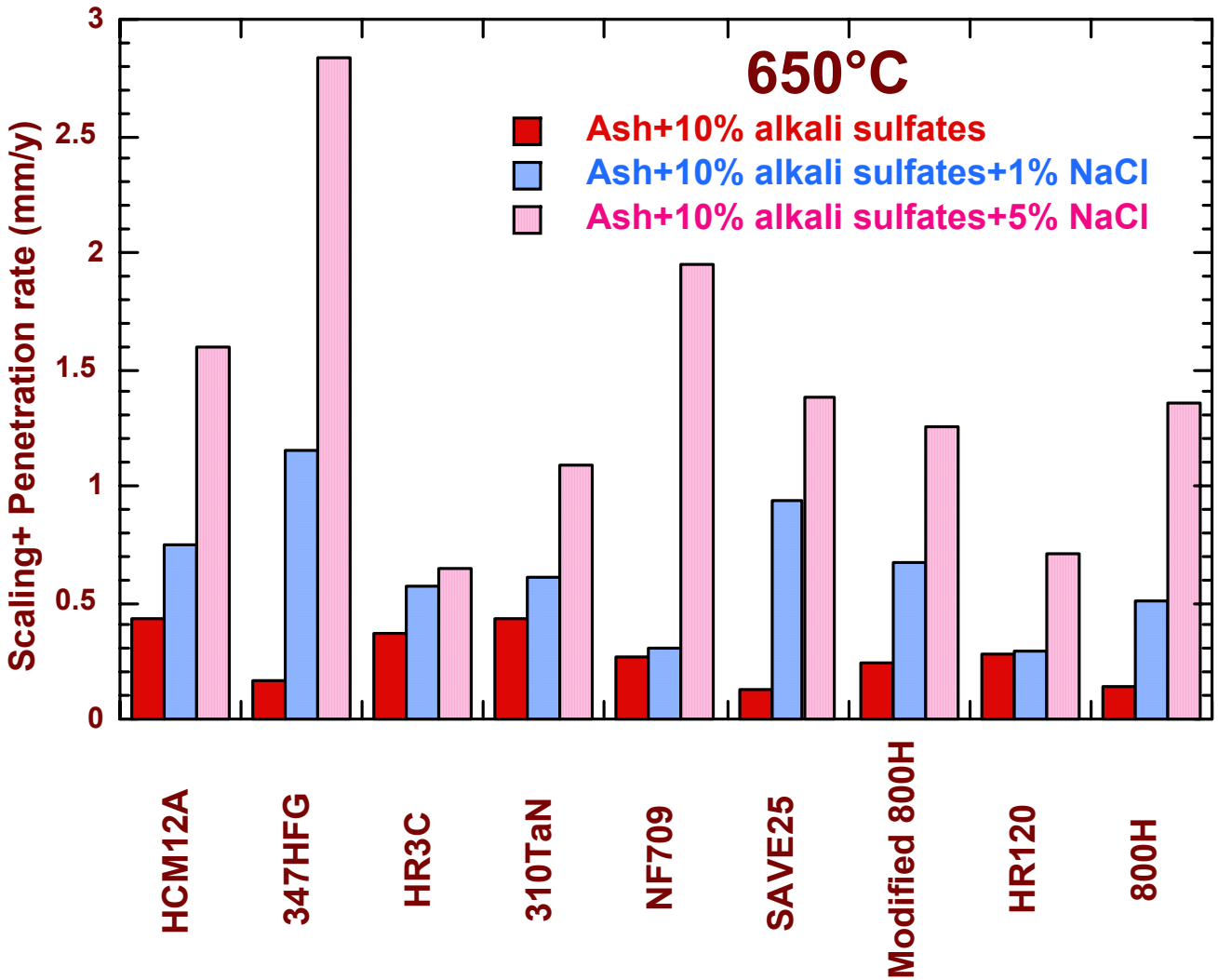

Effect of Deposit Chemistry on Corrosion of Ni-base Alloys

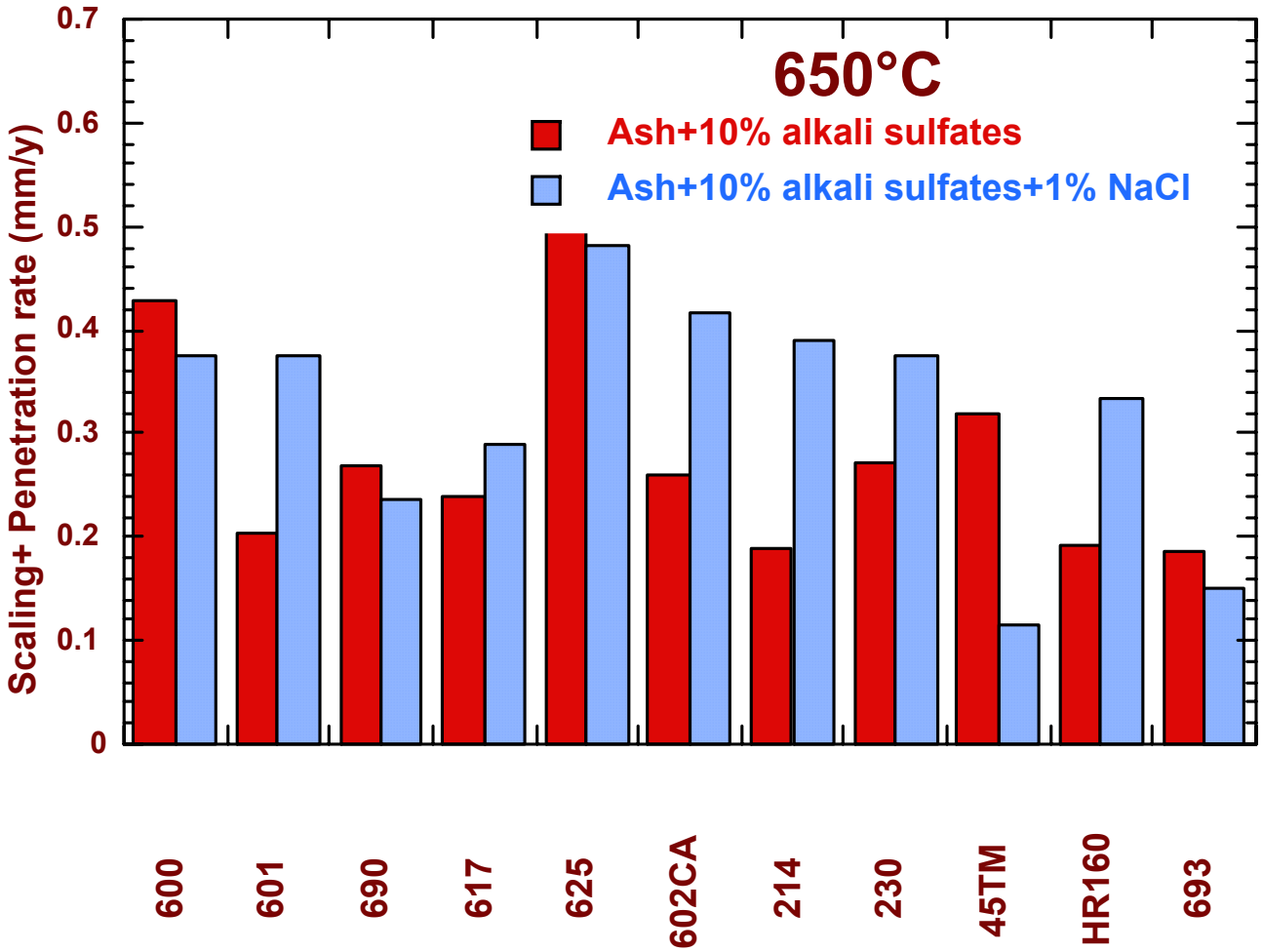

Comparison of Corrosion Rates for Fe- and Ni-base Alloys

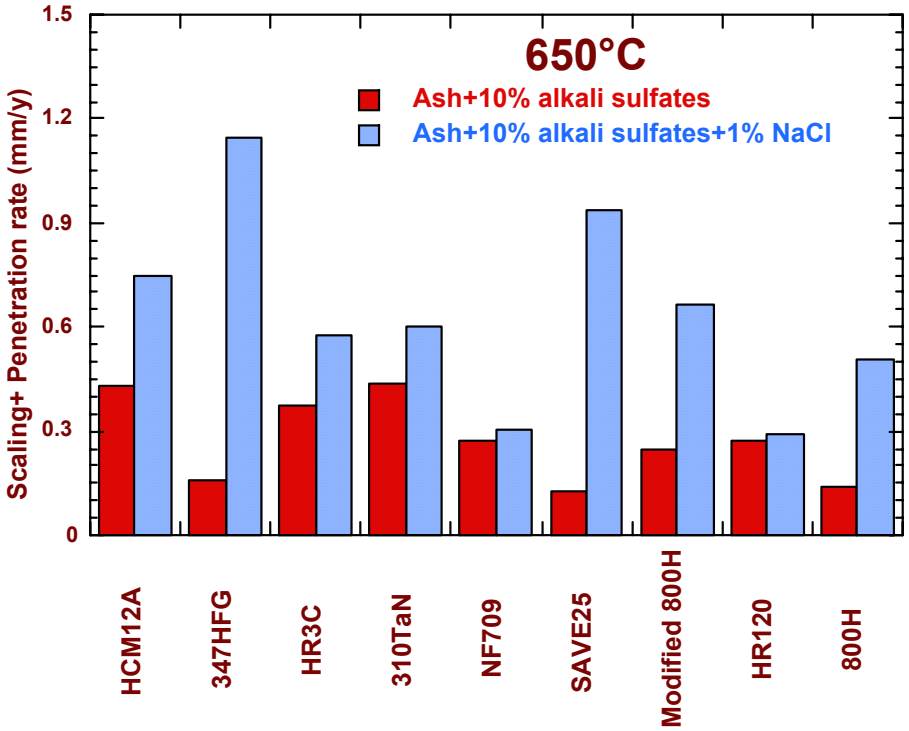

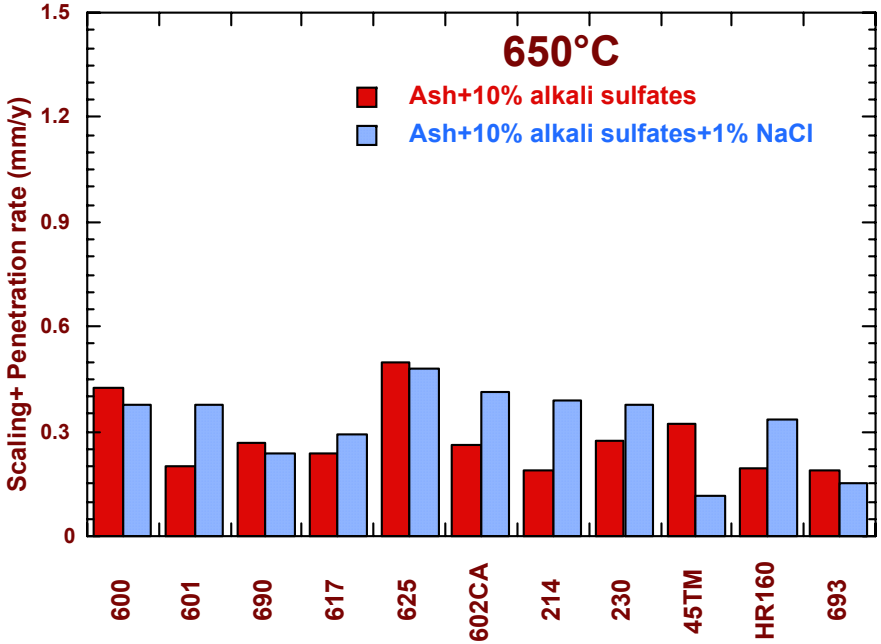

Cross section of a typical specimen before exposure

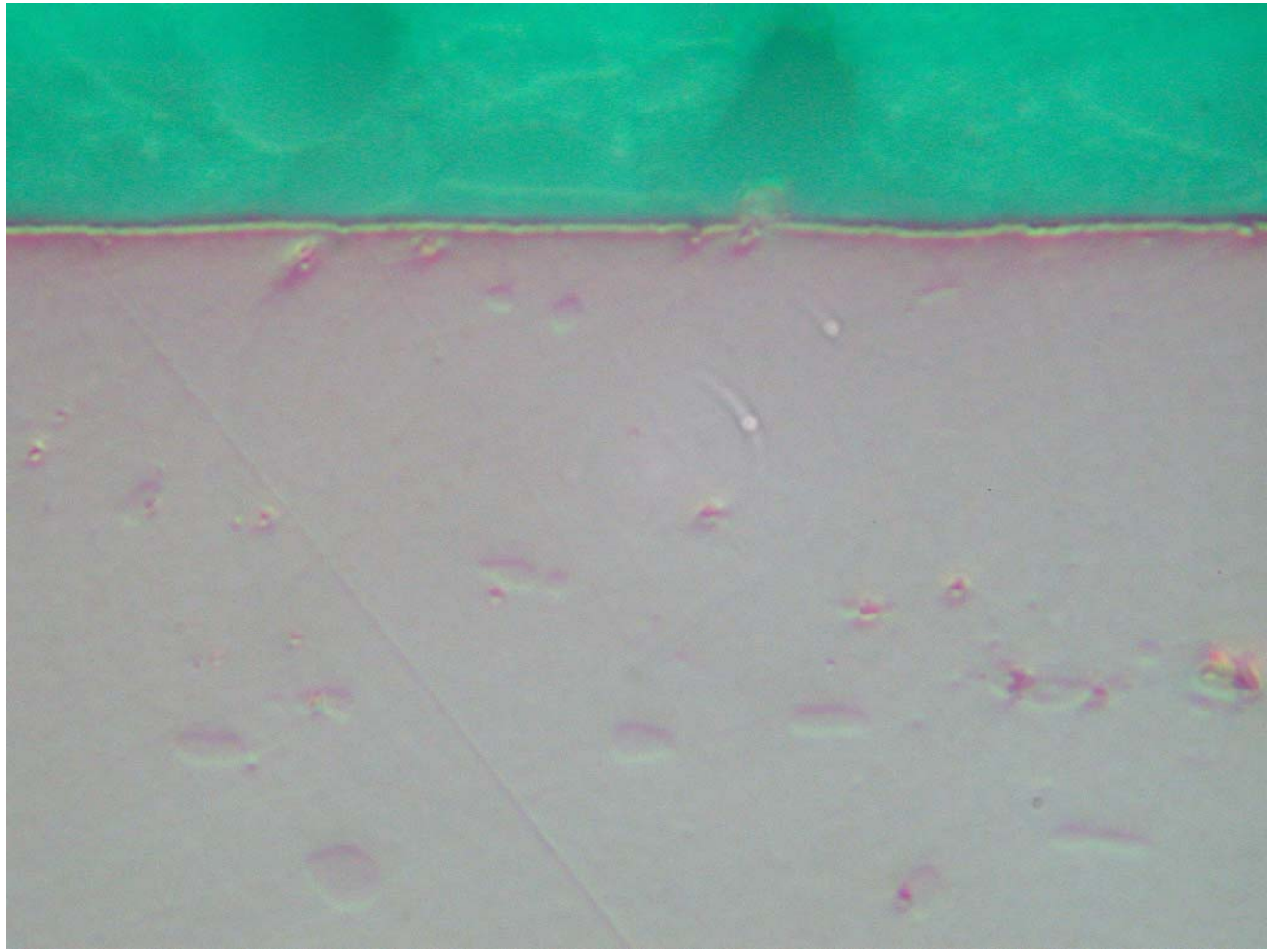

668 h exposure at 650°C in ash + sulfates

QuickTime™ and a
Photo - JPEG decompressor
are needed to see this picture.

671 **800**

900 h at 650°C in ash + sulfates+1%NaCl

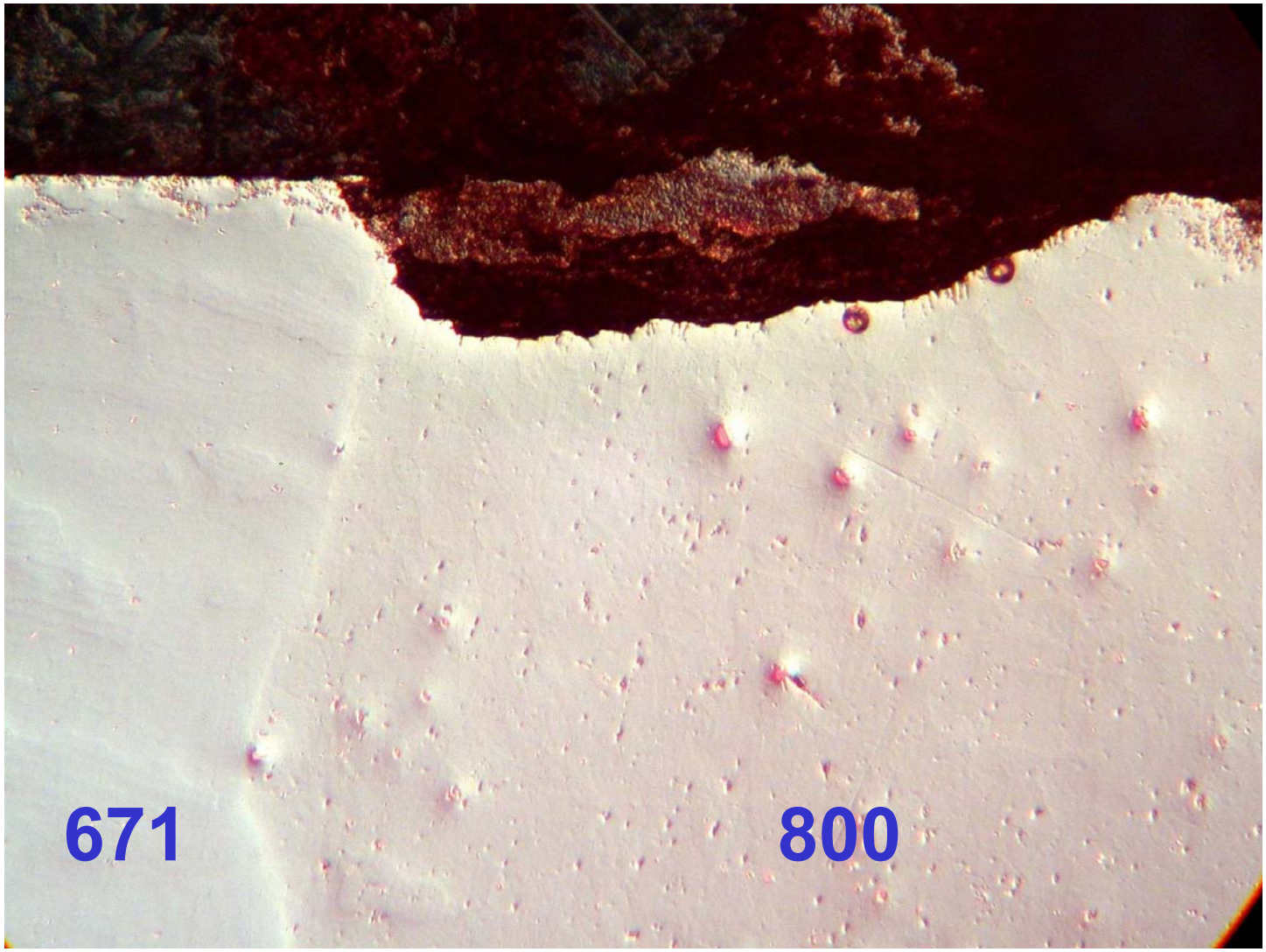

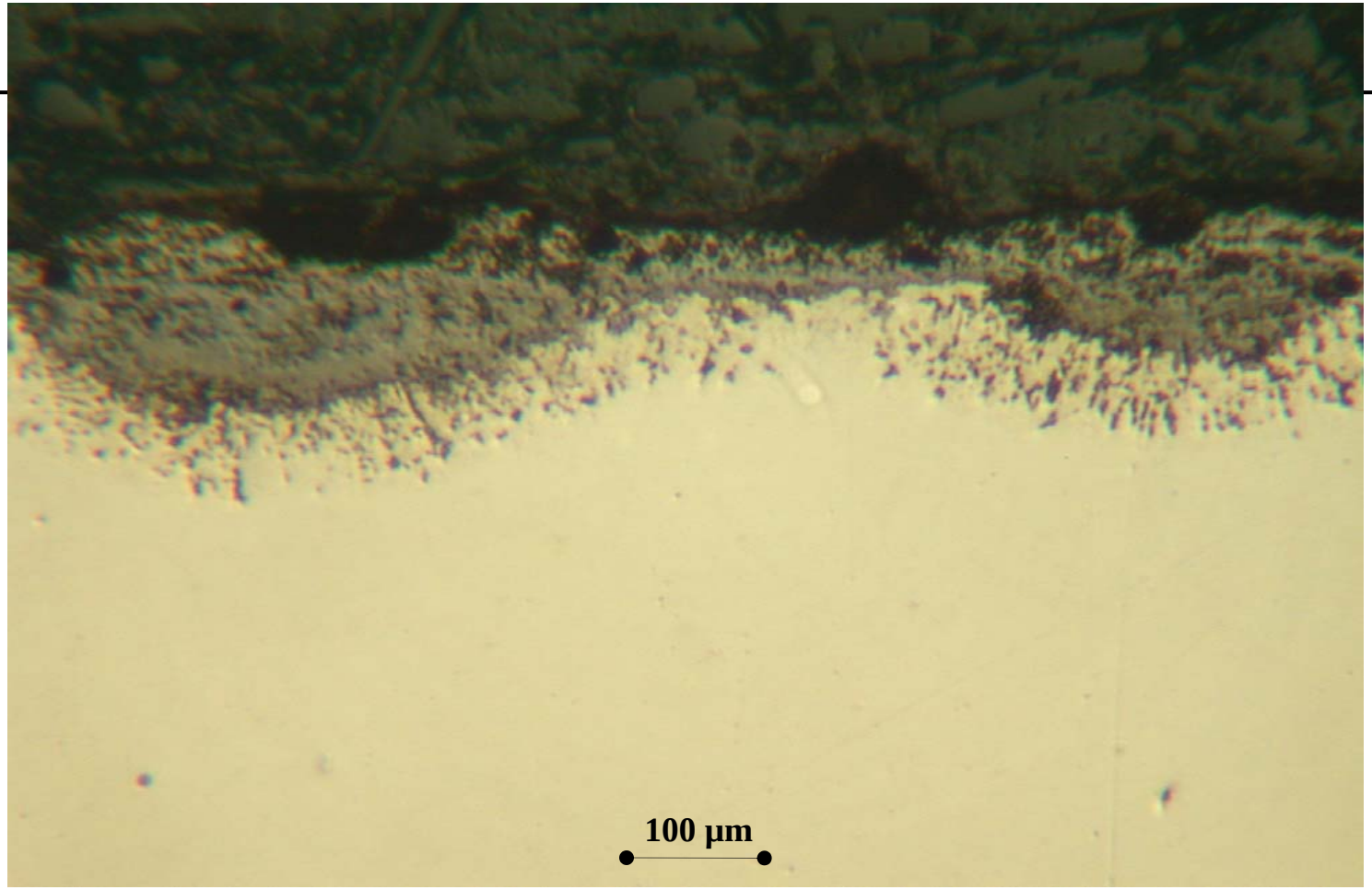

Alloy MA956, 900 h, 650°C
Ash + sulfates+ 1% NaCl

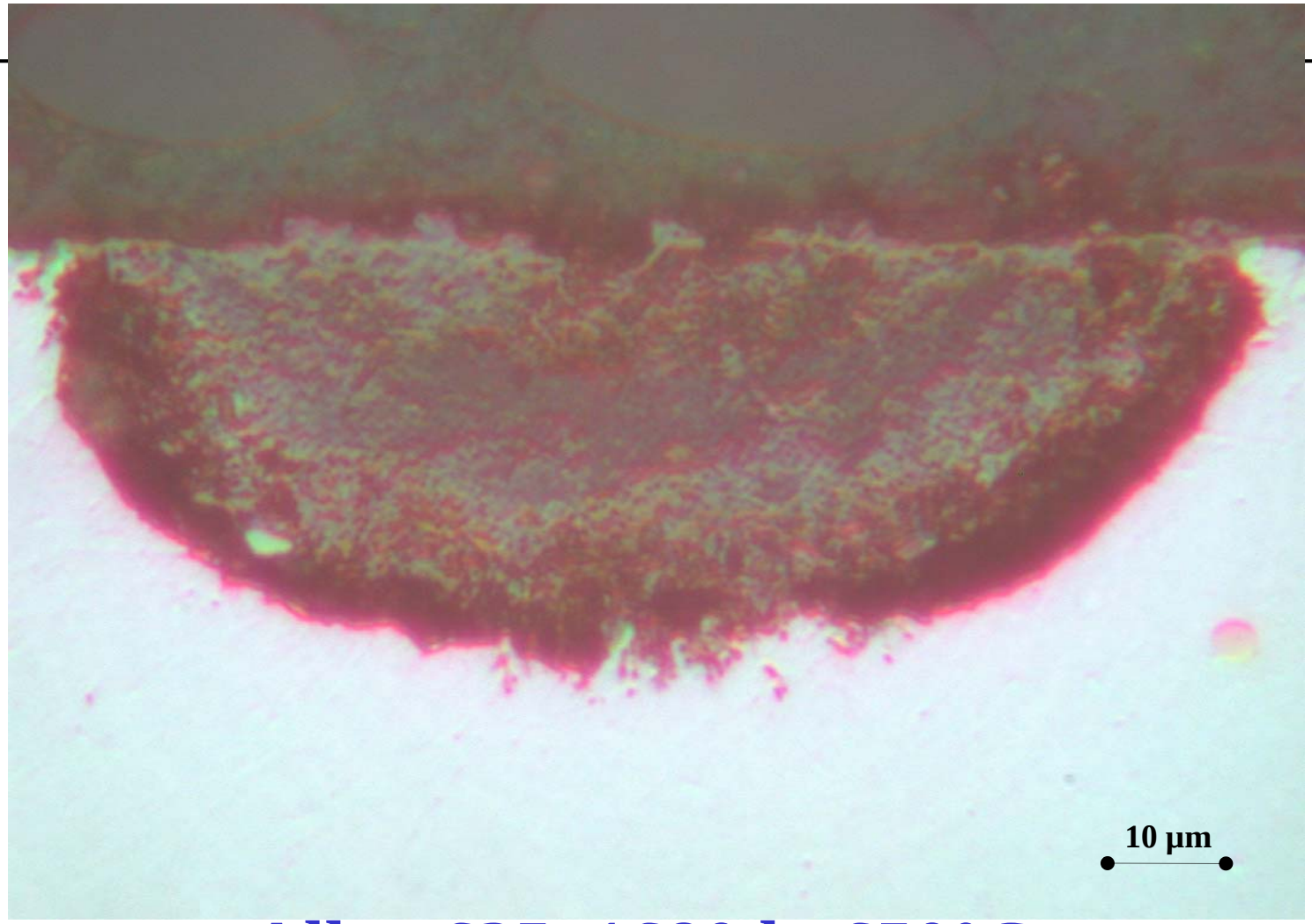

Alloy 625, 1680 h, 650°C
Ash + sulfates

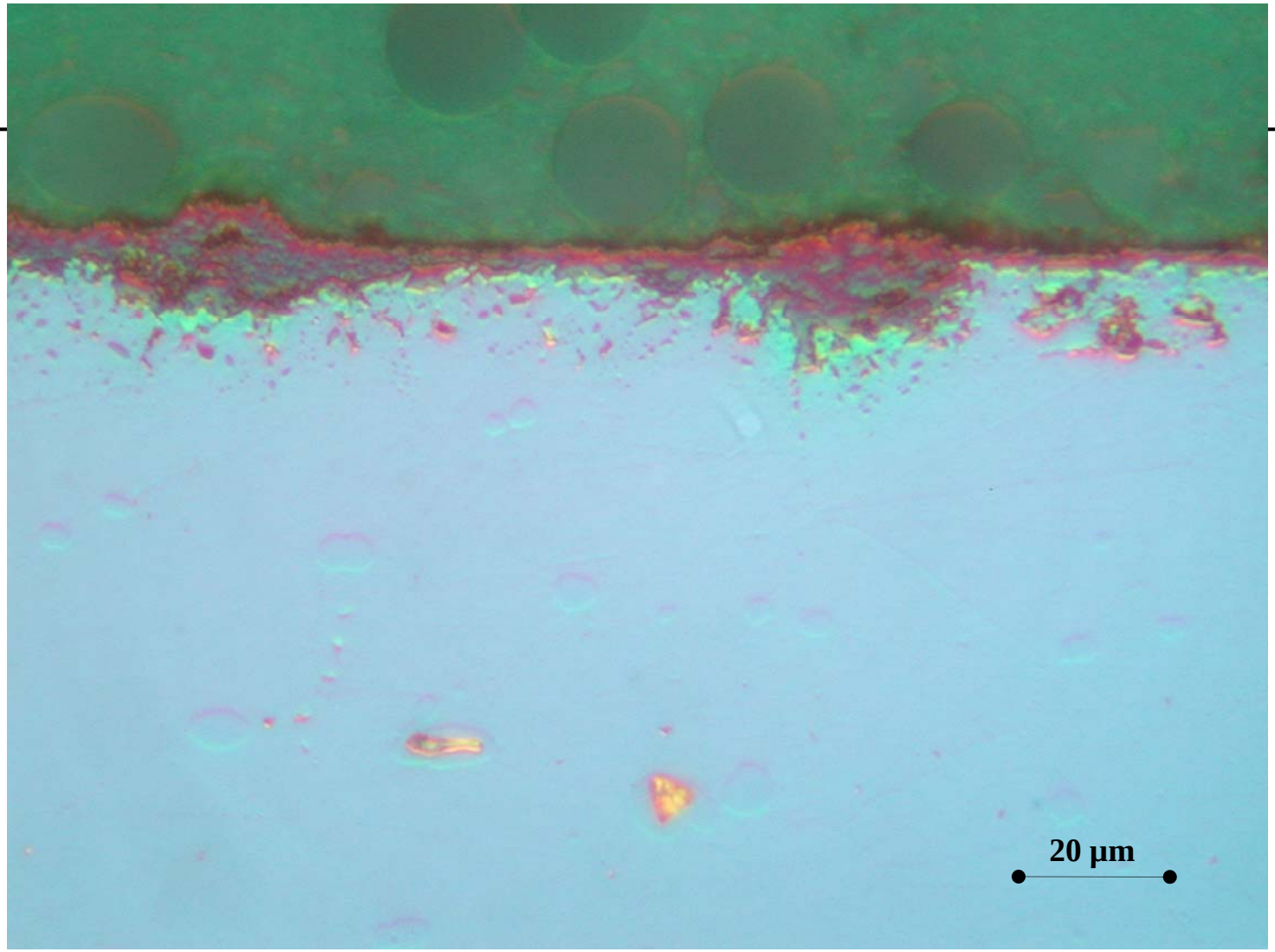

Alloy 602CA, 1680 h, 650°C
Ash + sulfates

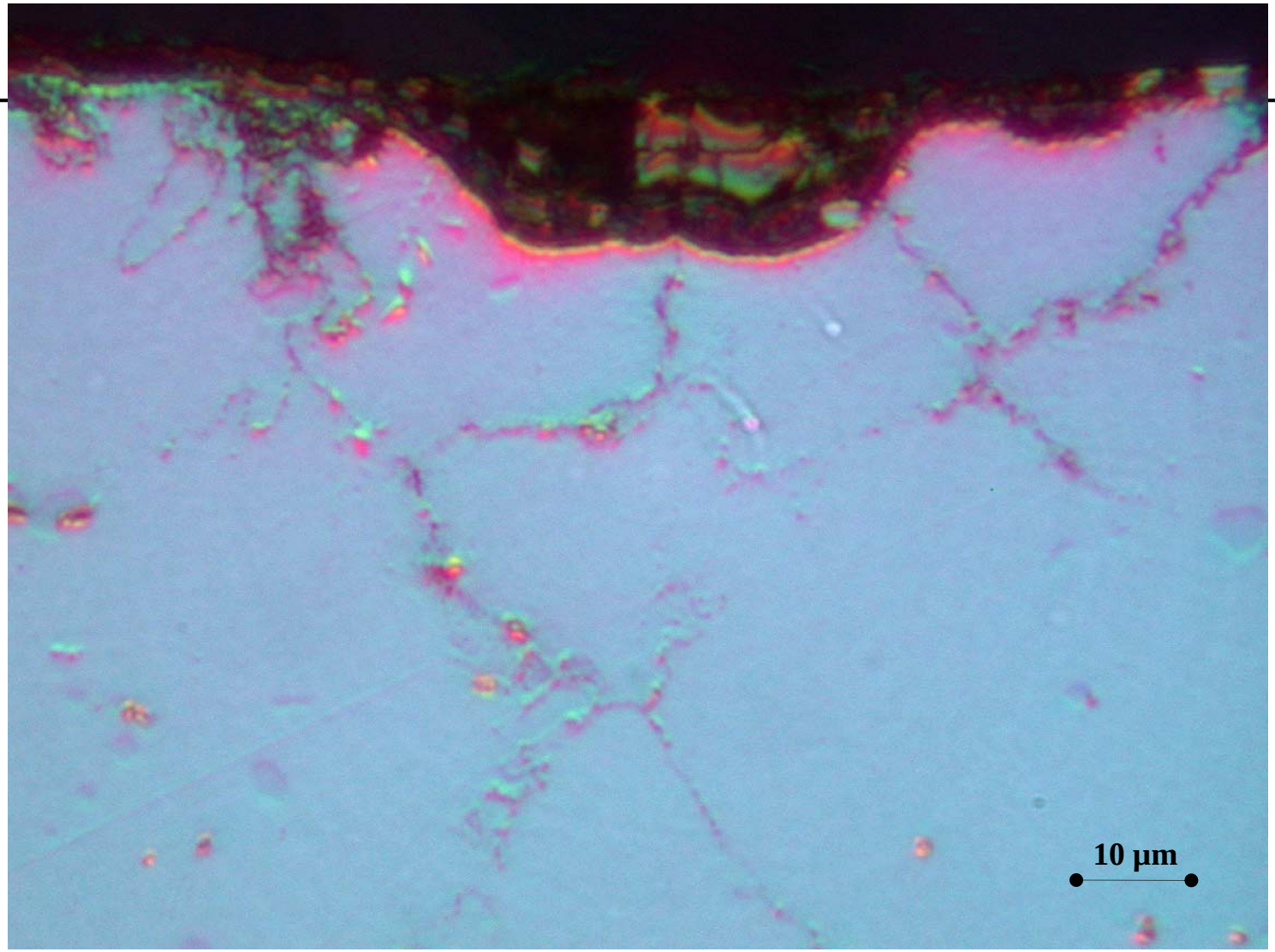

Alloy 230, 1680 h, 650°C

Ash + sulfates + 1% NaCl

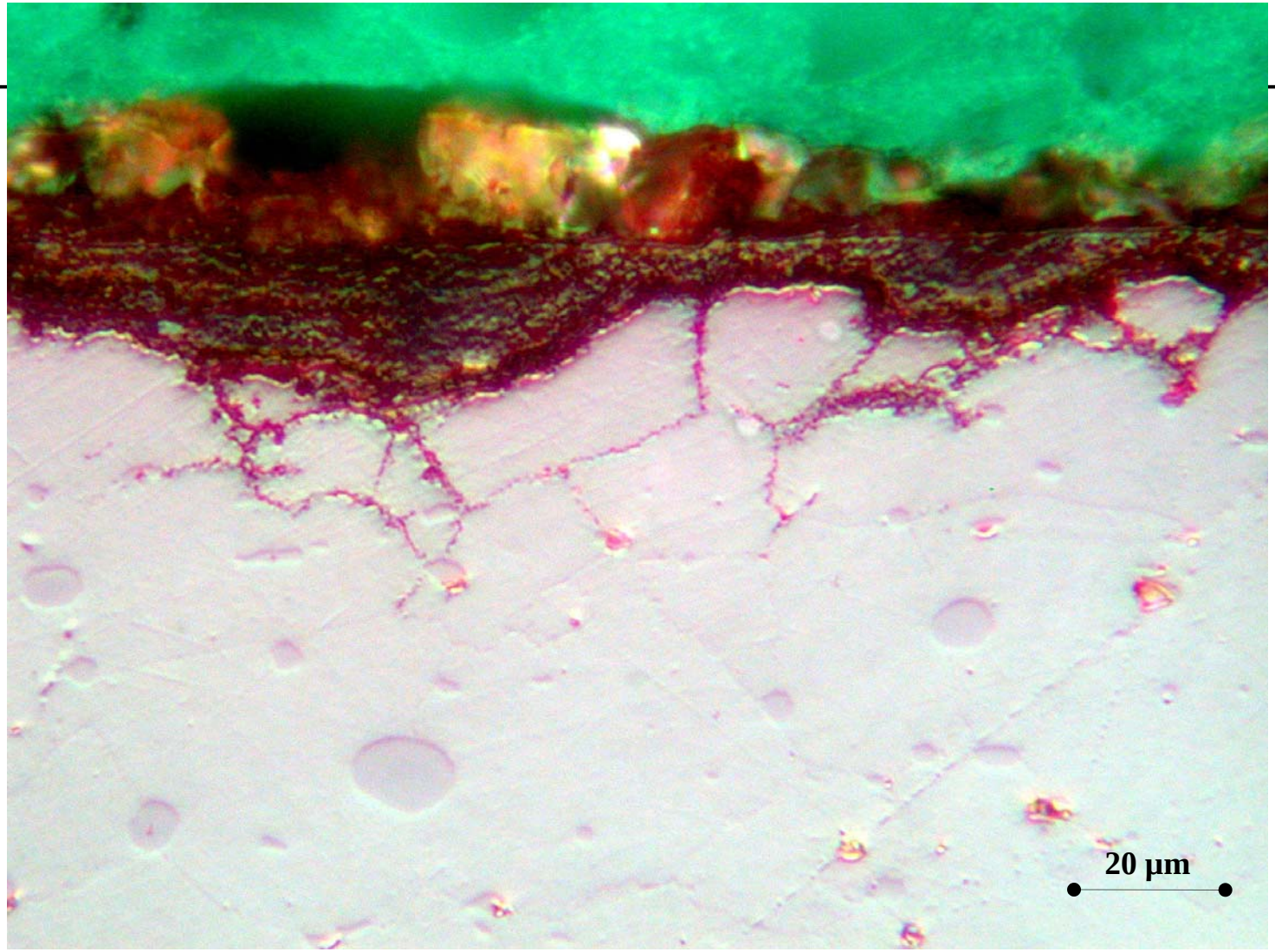

Alloy 230, 1680 h, 650°C

Ash + sulfates

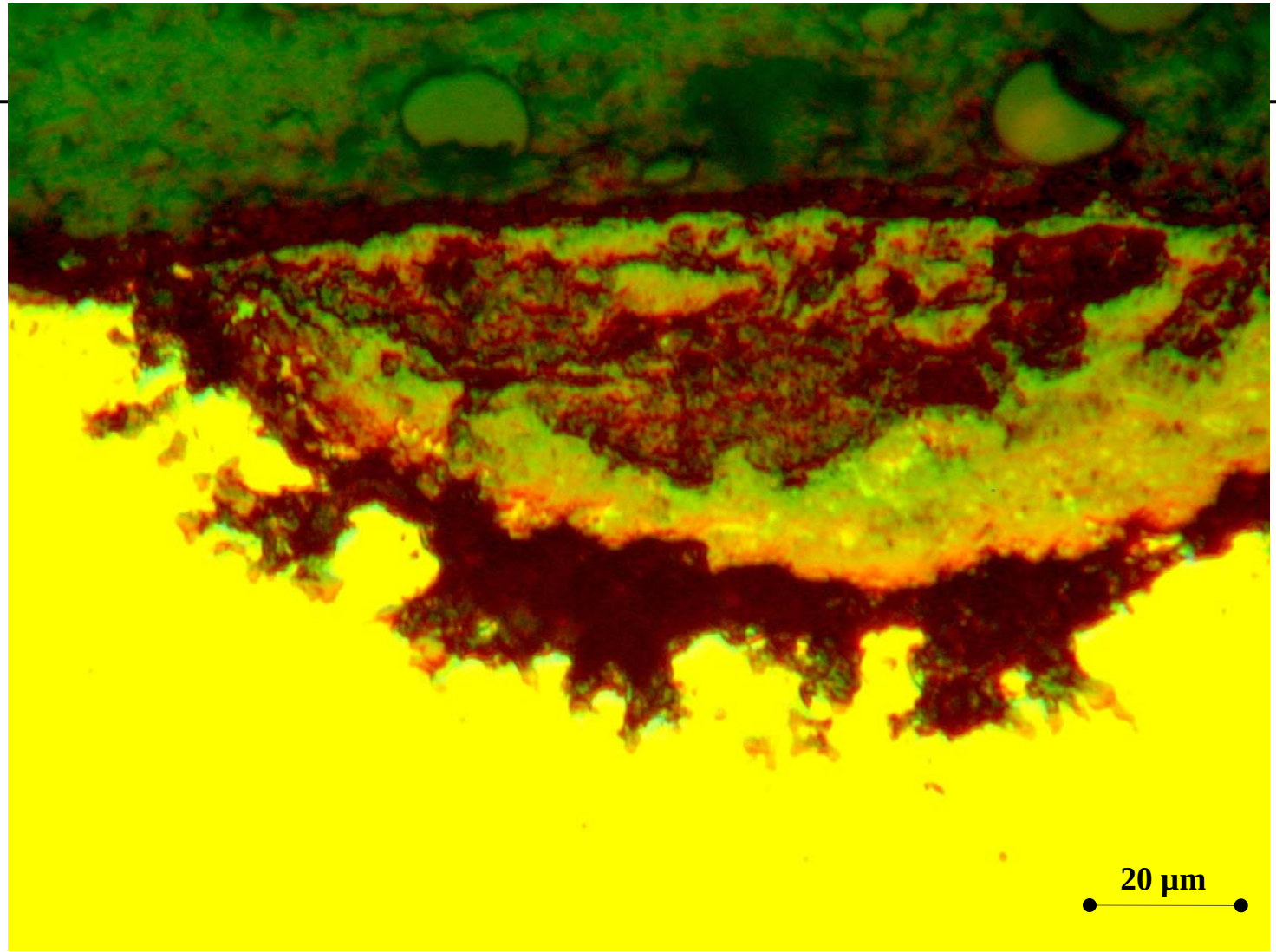

Alloy 45TM, 1680 h, 650°C

Ash + sulfates

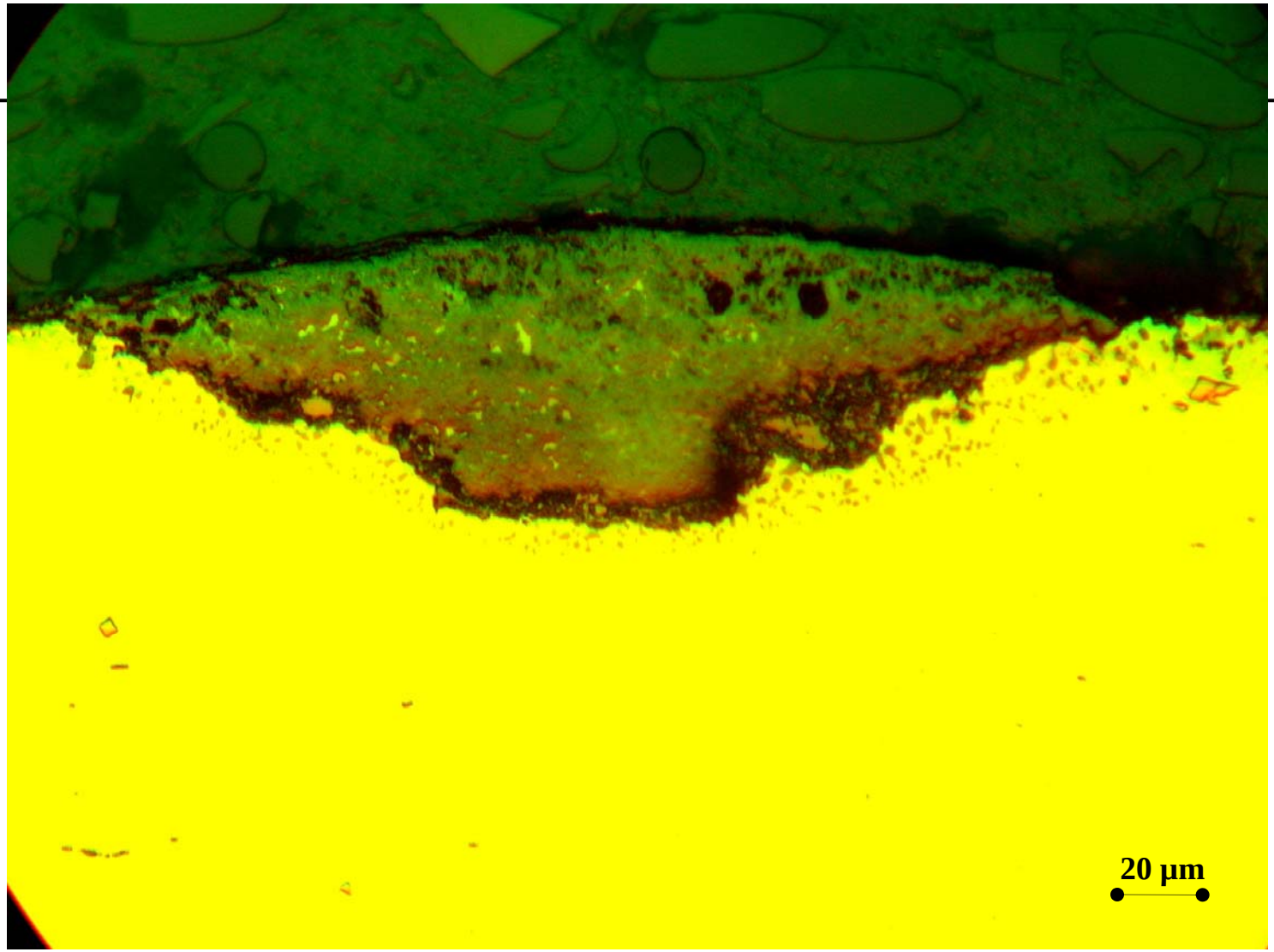

Alloy 45TM, 1680 h, 650°C

Ash + sulfates + 1% NaCl

Alloy 693, 1680 h, 650°C

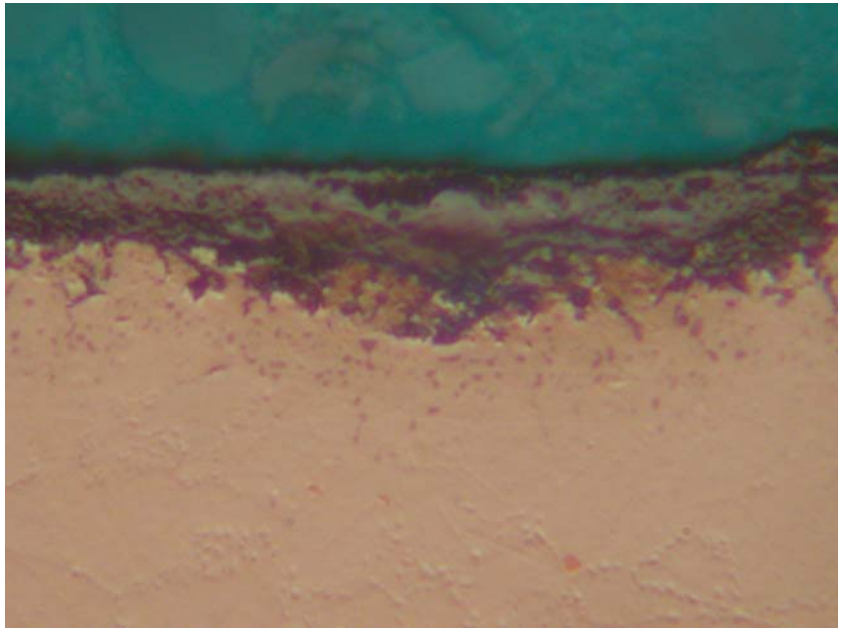

ash + sulfates

10 µm

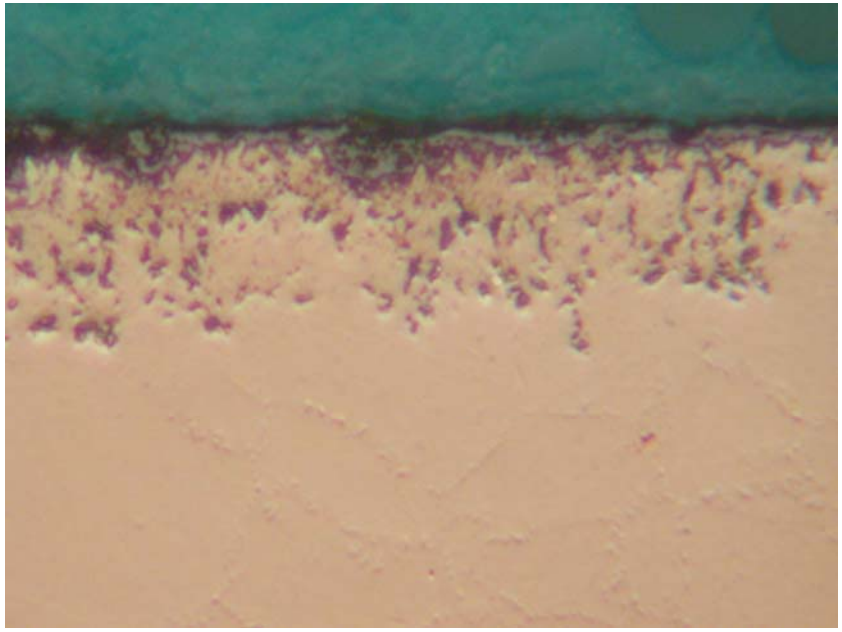

ash + sulfates + 1% NaCl

Alloy 601, 1680 h, 650°C, Ash + Sulfates

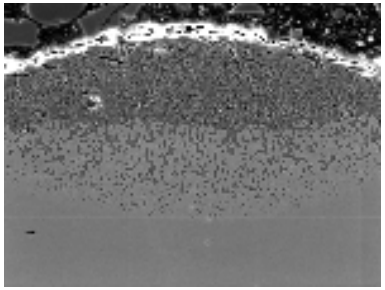

601, ash 1 650°C, 1680 h

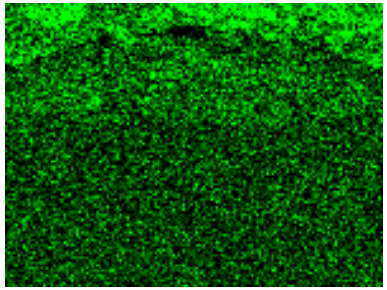

Al

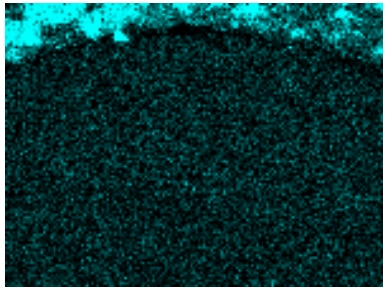

Si

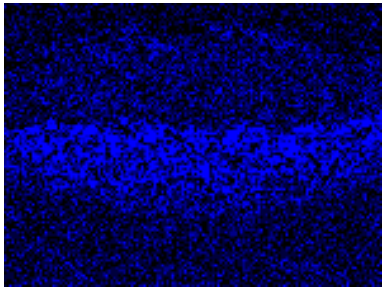

S

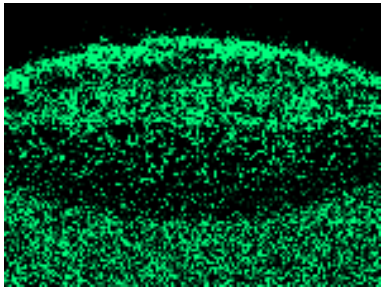

Cr

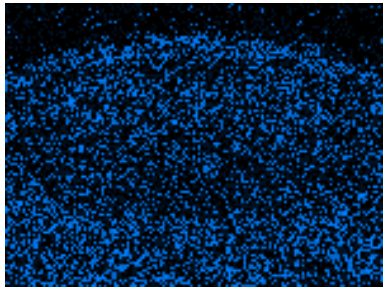

Mn

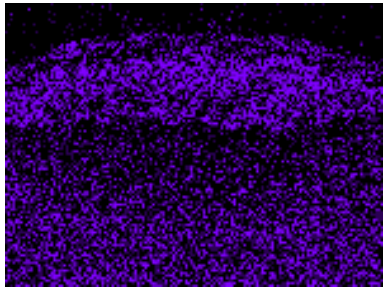

Fe

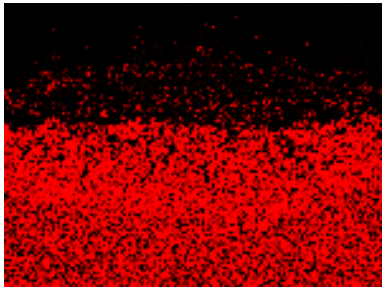

Ni

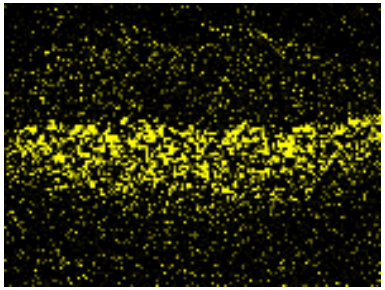

Nb

Alloy 601, 1680 h, 650°C, Ash + Sulfates + NaCl

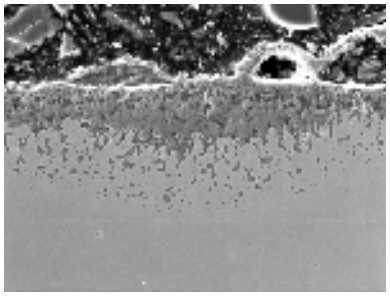

601, ash 3, 650°C, 1680 h

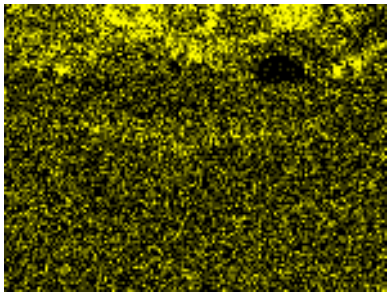

Al

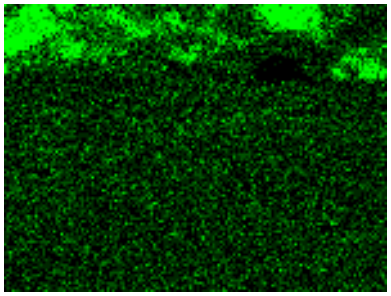

Si

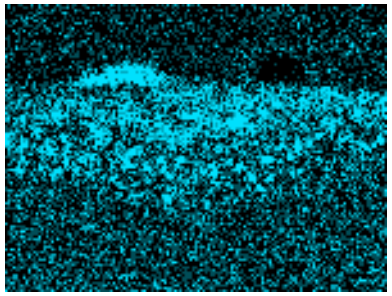

S

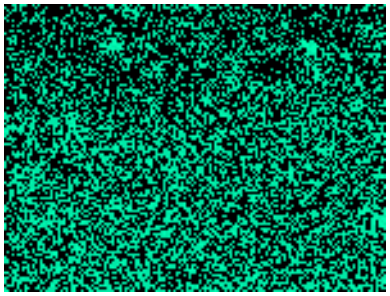

Ti

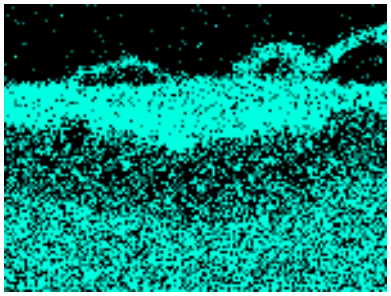

Cr

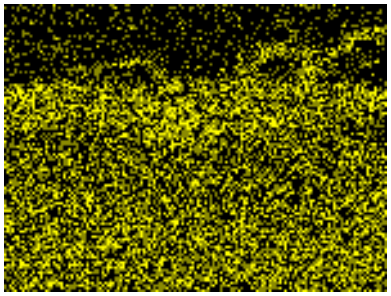

Mn

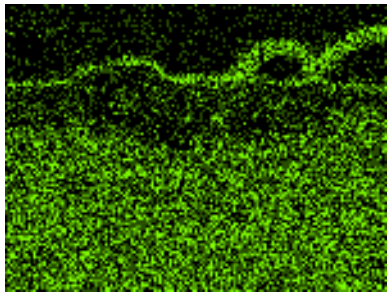

Fe

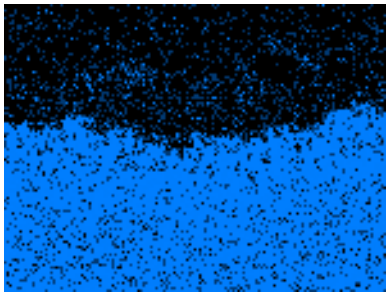

Ni

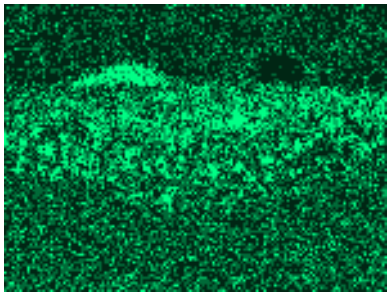

Nb

Hot Corrosion of Ni-Cr Alloys

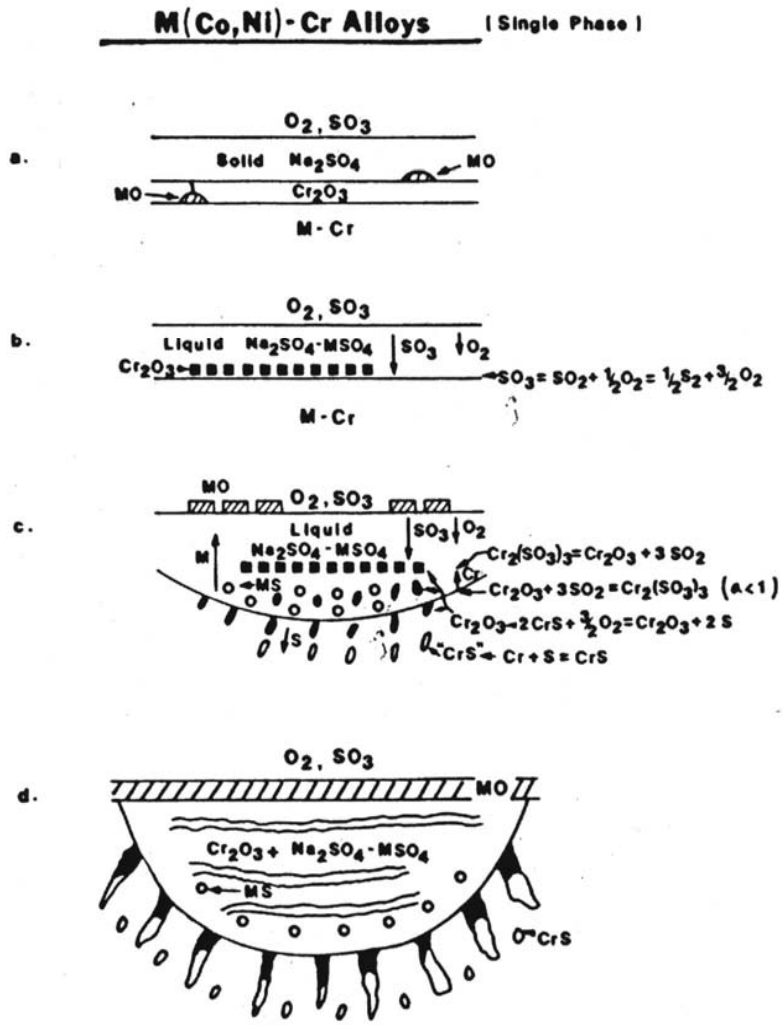

Facility for Corrosion Test in the Presence of NaCl Vapor

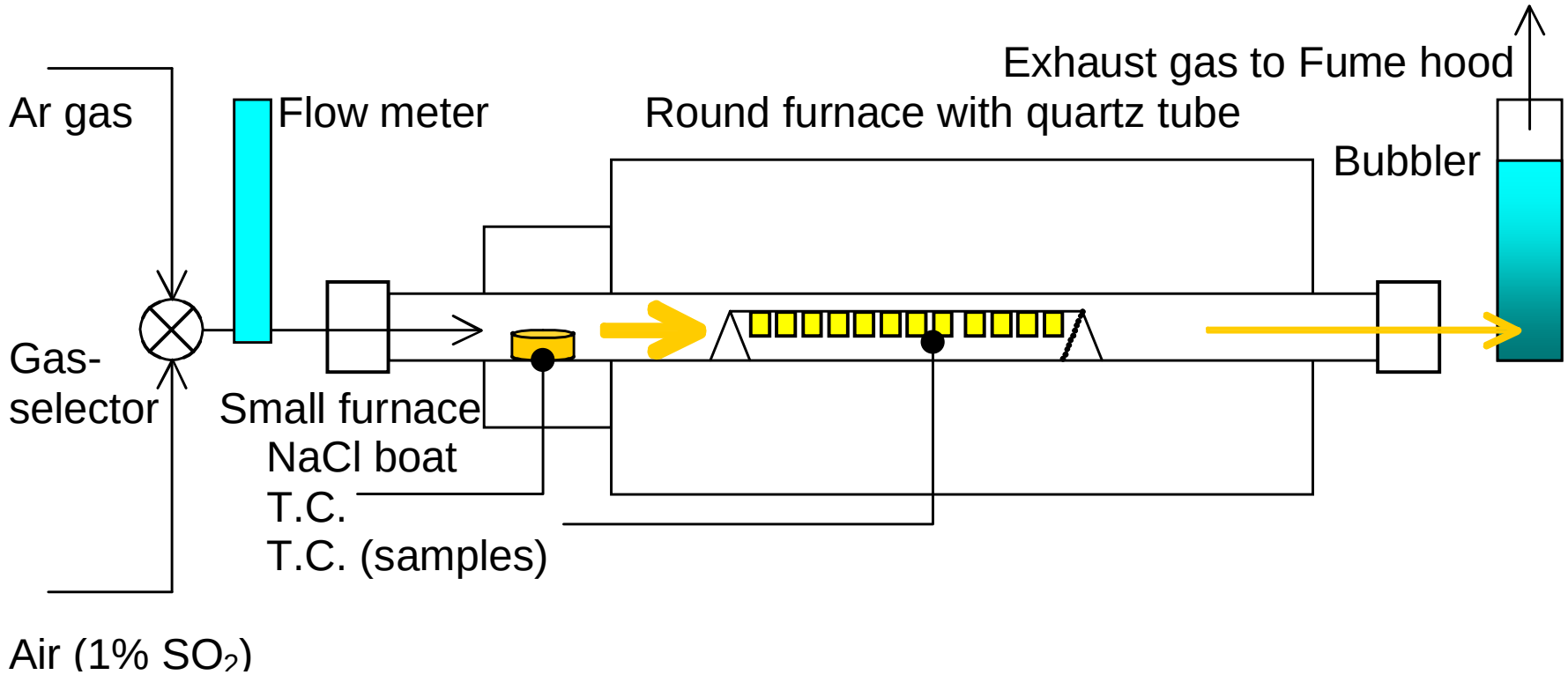

Specimens after 100-h Exposure in Air +1 % SO_2 + 300 vppm NaCl

Mod. 9Cr-1Mo | E911 | HCM12A | NF616 | Mod. 9Cr-1Mo | HCM12A | E911 | NF616

Cross section of E911 specimen after 100-h Exposure in Air +1 % SO_2 + 300 vppm NaCl

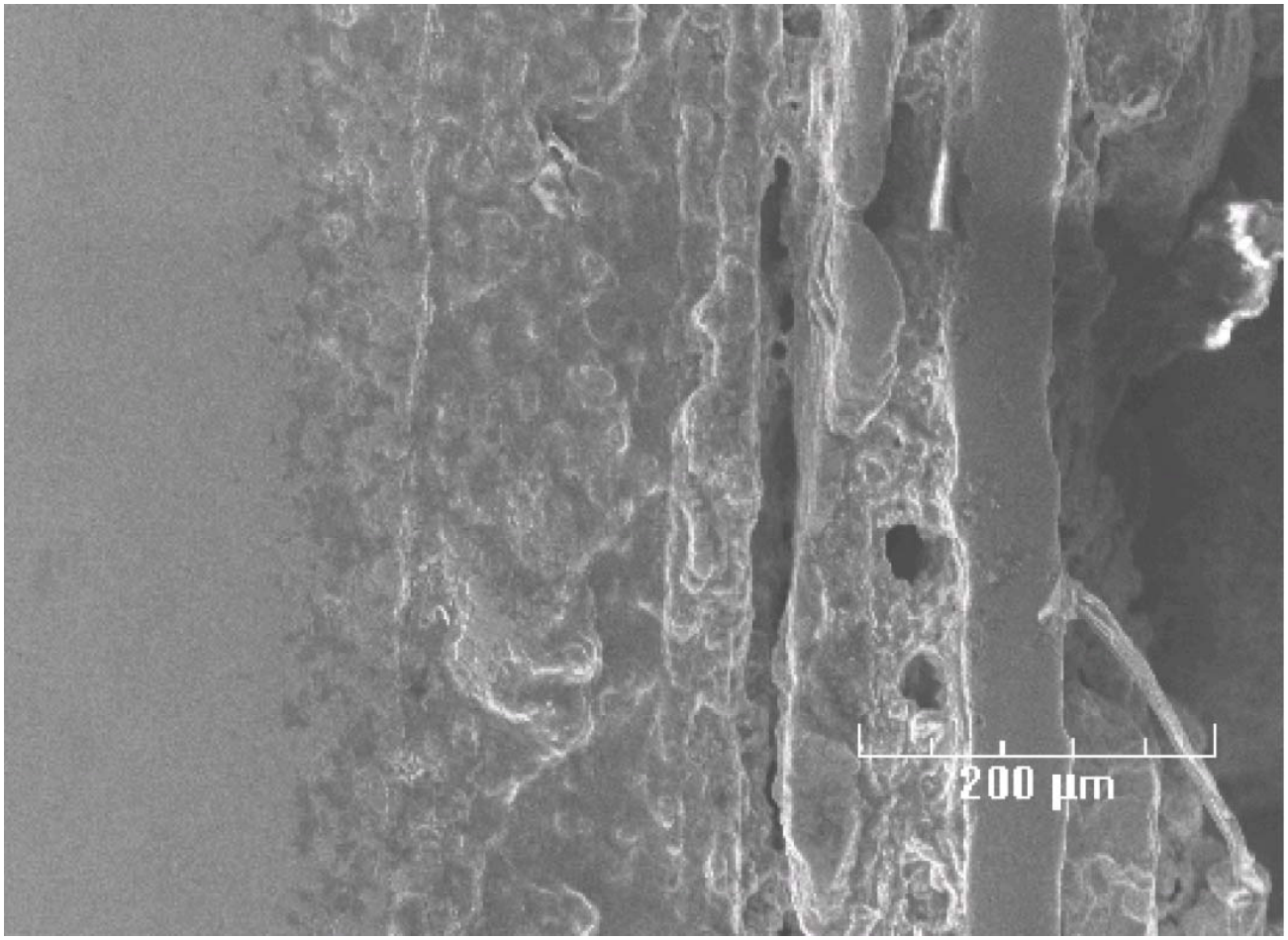

Schematic of morphology in ferritic alloys exposed in Air +1 % SO_2 + 300 vppm NaCl

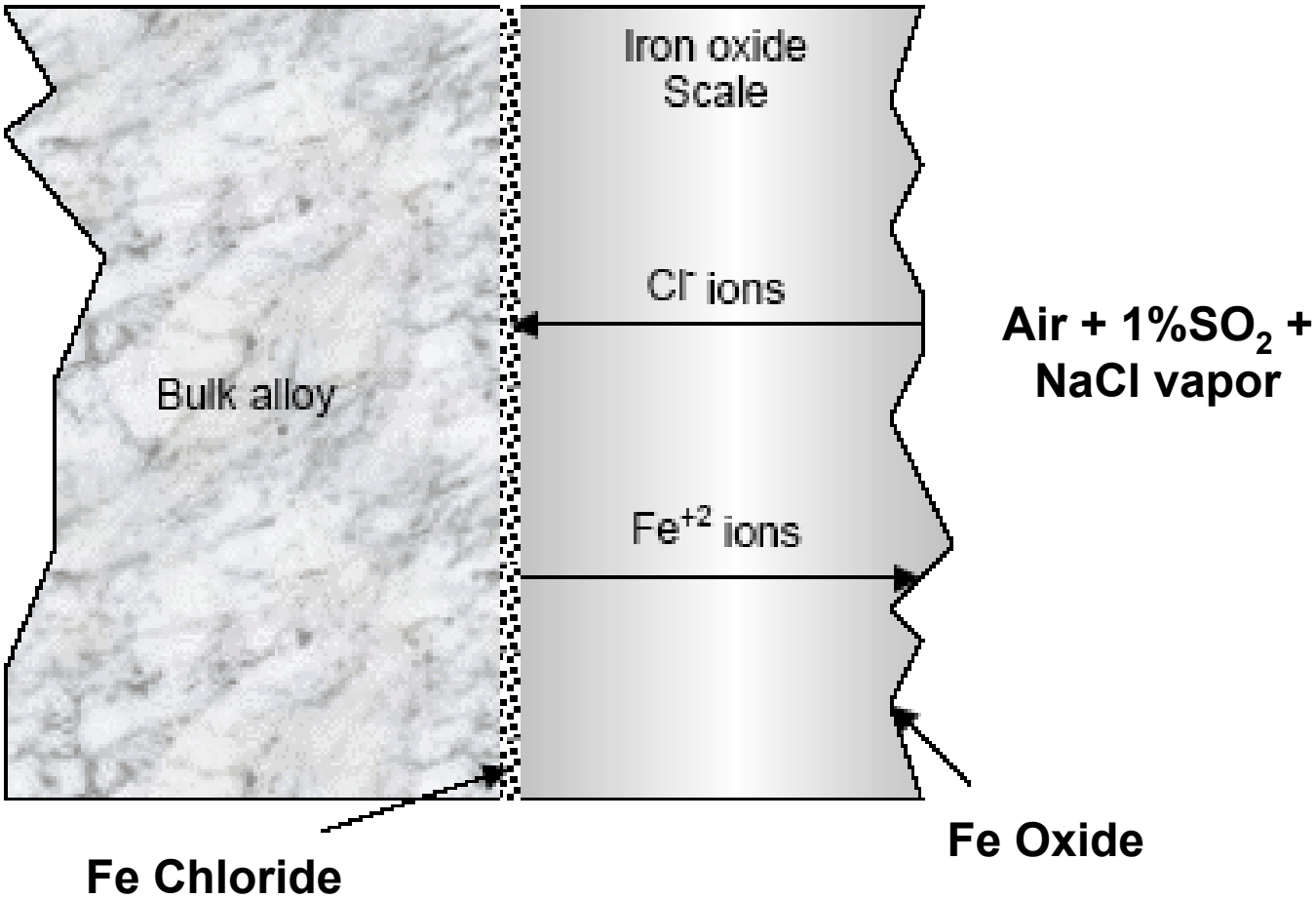

Coated Specimens after 200-h Exposure in Air +1 % SO_2 + 300 vppm NaCl

NF616 HCM12A E911 Mod. 9Cr-1Mo NF616 HCM12A E911 Mod. 9Cr-1Mo

Cross section of coated-E911 specimen after 200-h Exposure in Air +1 % SO_2 + 300 vppm NaCl

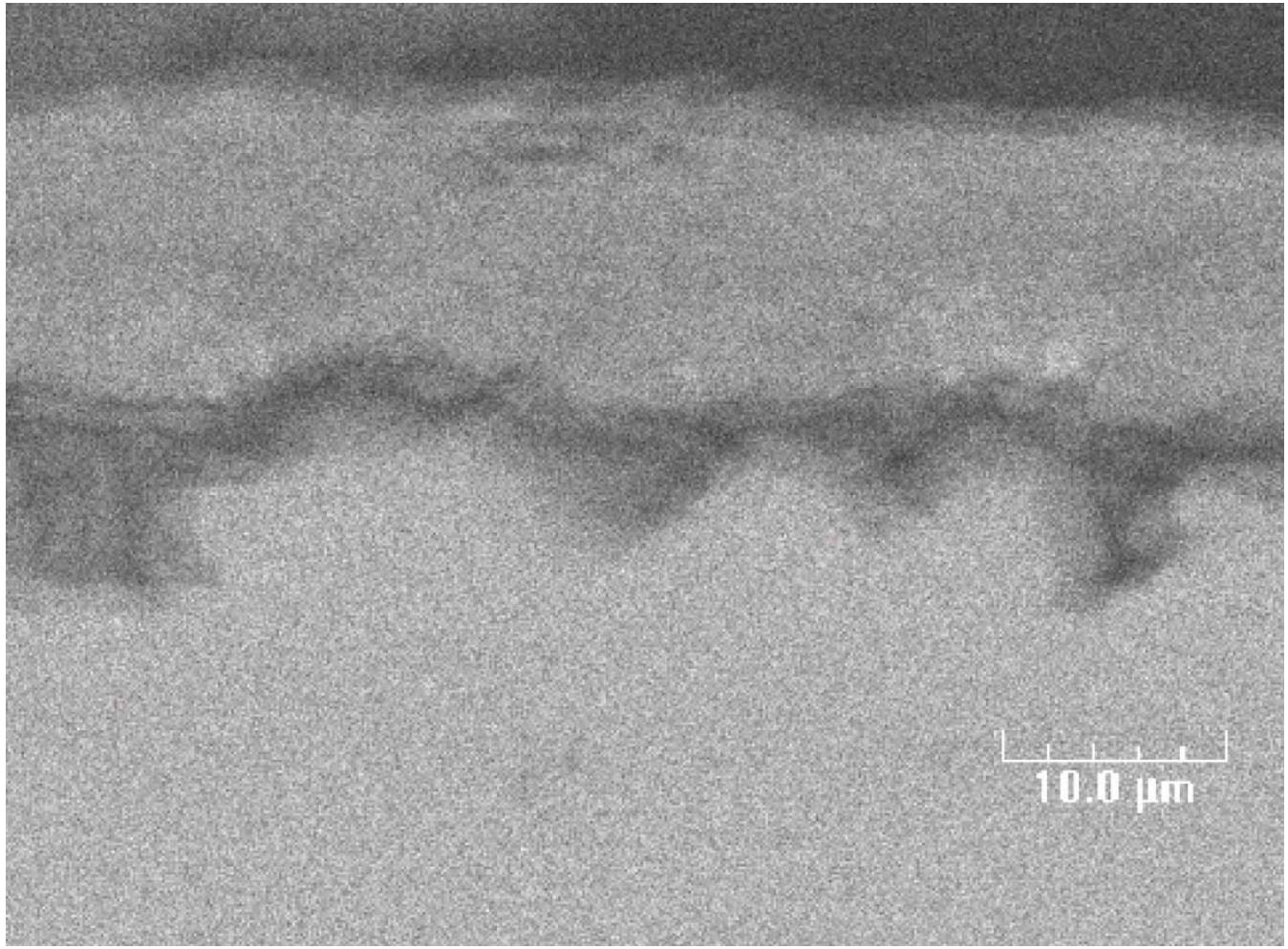

Exposure in NETL Facility: 1500-1600°F (≈ 815-870°C)

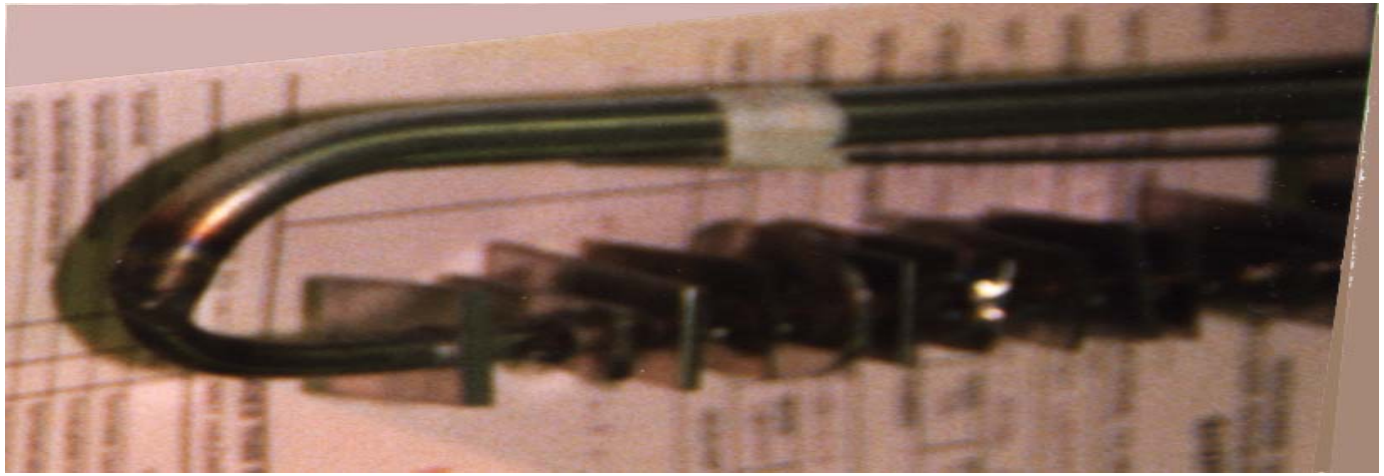

Before exposure

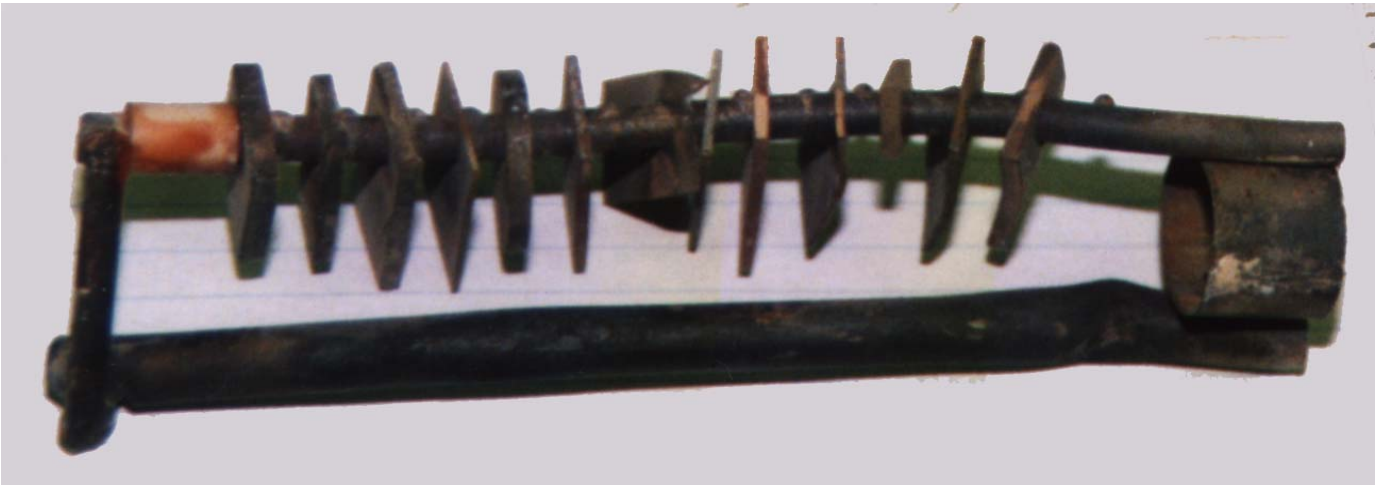

After exposure

Project Summary

- Fireside corrosion is a major issue in selection of materials for advanced steam cycles
- We have conducted studies at ANL to evaluate the corrosion performance of several Fe- and Ni-base alloys
- The laboratory tests simulated the combustion atmosphere and three deposit chemistries which included ash constituents, alkali sulfates, and two levels of NaCl
- Corrosion rates exhibited a bell shaped curve (for Fe base alloys) with peak rates around 725°C, and the rate itself is dependent on the alloy chemistr

Summary (continued)

- Several Fe-base alloys showed acceptable rates in the sulfate containing coal-ash environment; but, NaCl in the deposit led to catastrophic corrosion at 650 and 800°C

- Ni-base alloys, tested for 1680 h at 650°C, showed a local attack in the form of pits and associated sulfidation of the alloy. This form of attack is well established and is known as "low temperature hot corrosion" or Type II hot corrosion (in gas turbine terminology)

- Surface modification (including coatings) is a promising option to decrease the corrosion rate and wastage in ferritic alloys

- Need to establish the maximum levels for alkali sulfates and alkali chlorides in combustion environment (and their relationship to coal feedstock) for acceptable corrosion

Oxidation of Alloys for Advanced Steam Turbines

Albany Research Center

Gordon Holcomb, Bernie Covino,
Sophie Bullard, Malgorzata Ziomek-Moroz,
and David Alman

19th Annual Conference on Fossil Energy Materials
Knoxville, TN, May 9-11, 2005

Outline

- Introduction and Background
- Research Approach
- Results of Research in Progress
- Summary

Introduction

- Project funded out of the Advanced Research (AR) Program of Fossil Energy (FE) of DOE
- In support of DOE Advanced Power System goals of 60% efficiency from coal generation that require USC steam turbine conditions of:
  - 760°C (1400°F)
  - 37.9 MPa (5500 psi)

Efficiency Improvement over a Subcritical 16.5 MPa/538°C/ 538°C Plant

Steam Conditions	Recent Power Plant Examples	Net Percentage Point Increase in Efficiency	Net Plant Efficiency, %
		2.9	39.9
		4.0	41.0
		4.5	41.5
31.0 MPa/593/593°C	Lubeck – 1995 Alvedore 1 – 2000	4.9	41.9
31.0 MPa/593/621°C	Westfalen – 2004	5.2	42.2
31.0 MPa/593/593/593°C	Nordjylland - 1998	6.5	43.5

Each 1% increase in efficiency eliminates ~1,000,000 tons of CO_2 emissions over the lifetime of an 800-MW plant

Swanekamp, 2002

112 GW New Coal Capacity By 2025

(Accounts for 42% of New Capacity Additions)

New Electricity Capacity Additions

(EIA Reference Case)

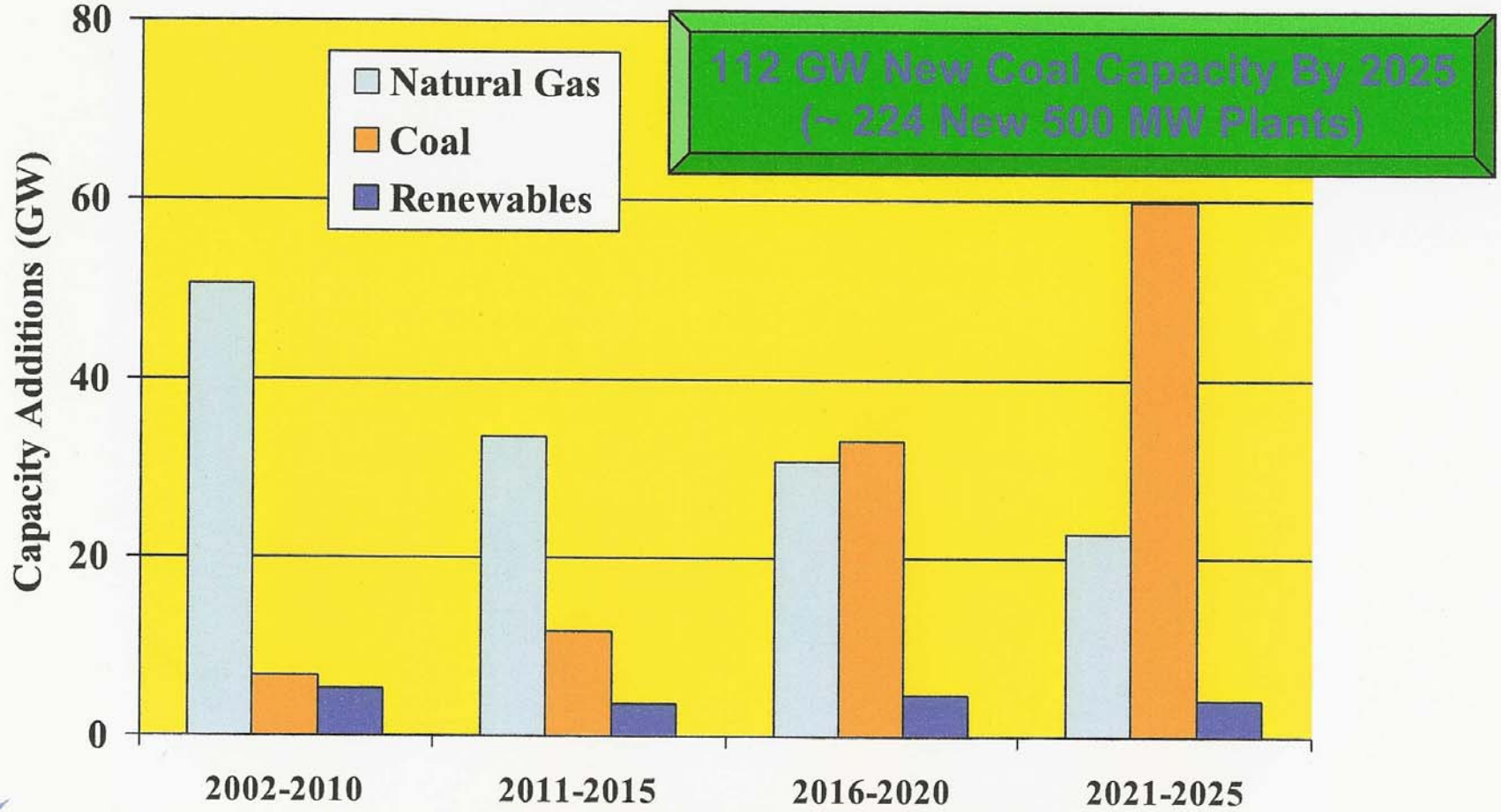

Source: Data Derived From EIA Annual Energy Outlook 2004

NETL Contacts: Scott Klara, klara@netl.doe.gov
Erik Shuster, erik.shuster@sa.netl.doe.gov

Coal's Resurgence in Electric Power Generation

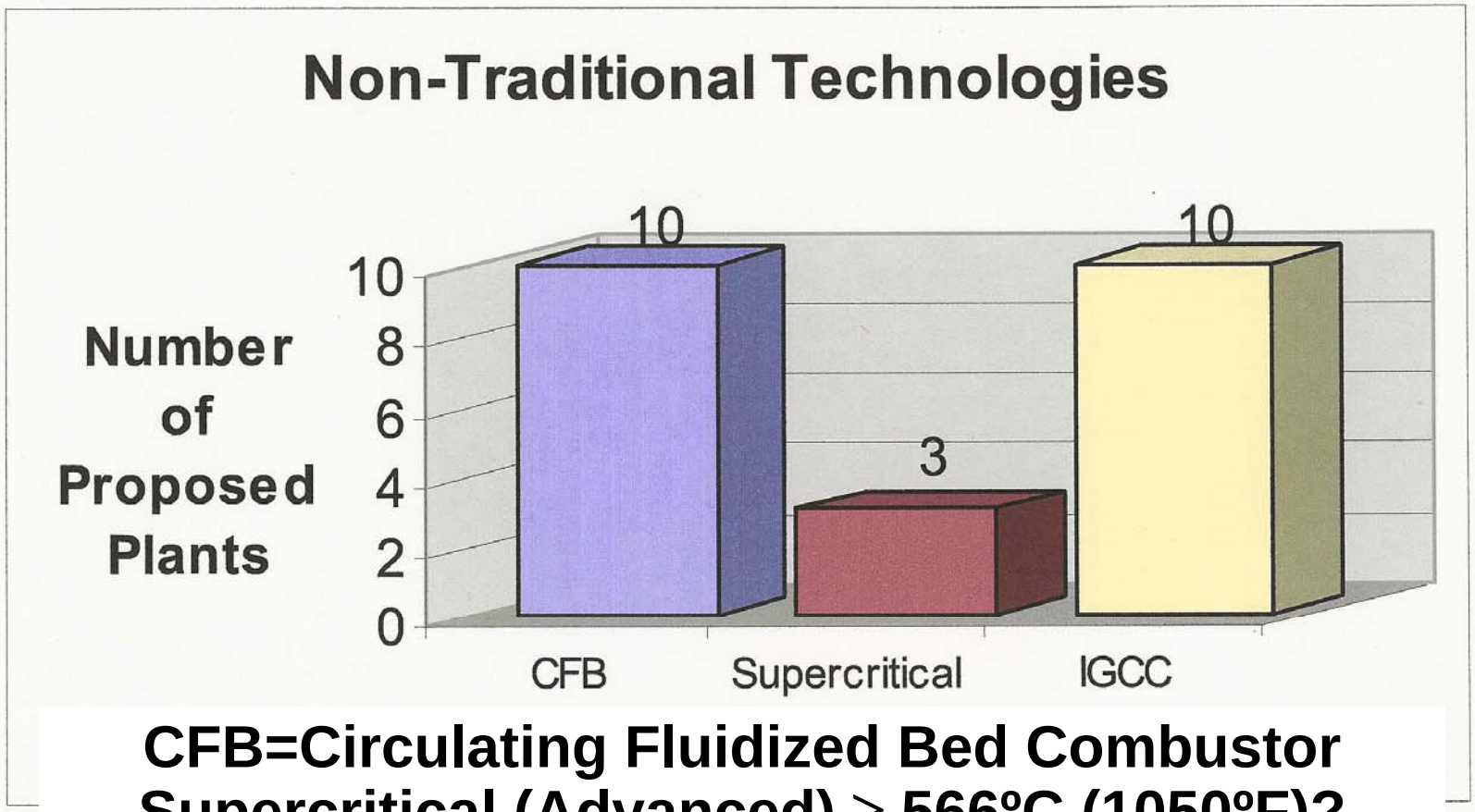

CFB=Circulating Fluidized Bed Combustor
Supercritical (Advanced) ≥ 566ºC (1050ºF)?
IGCC=Integrated Gasification Combined Cycle

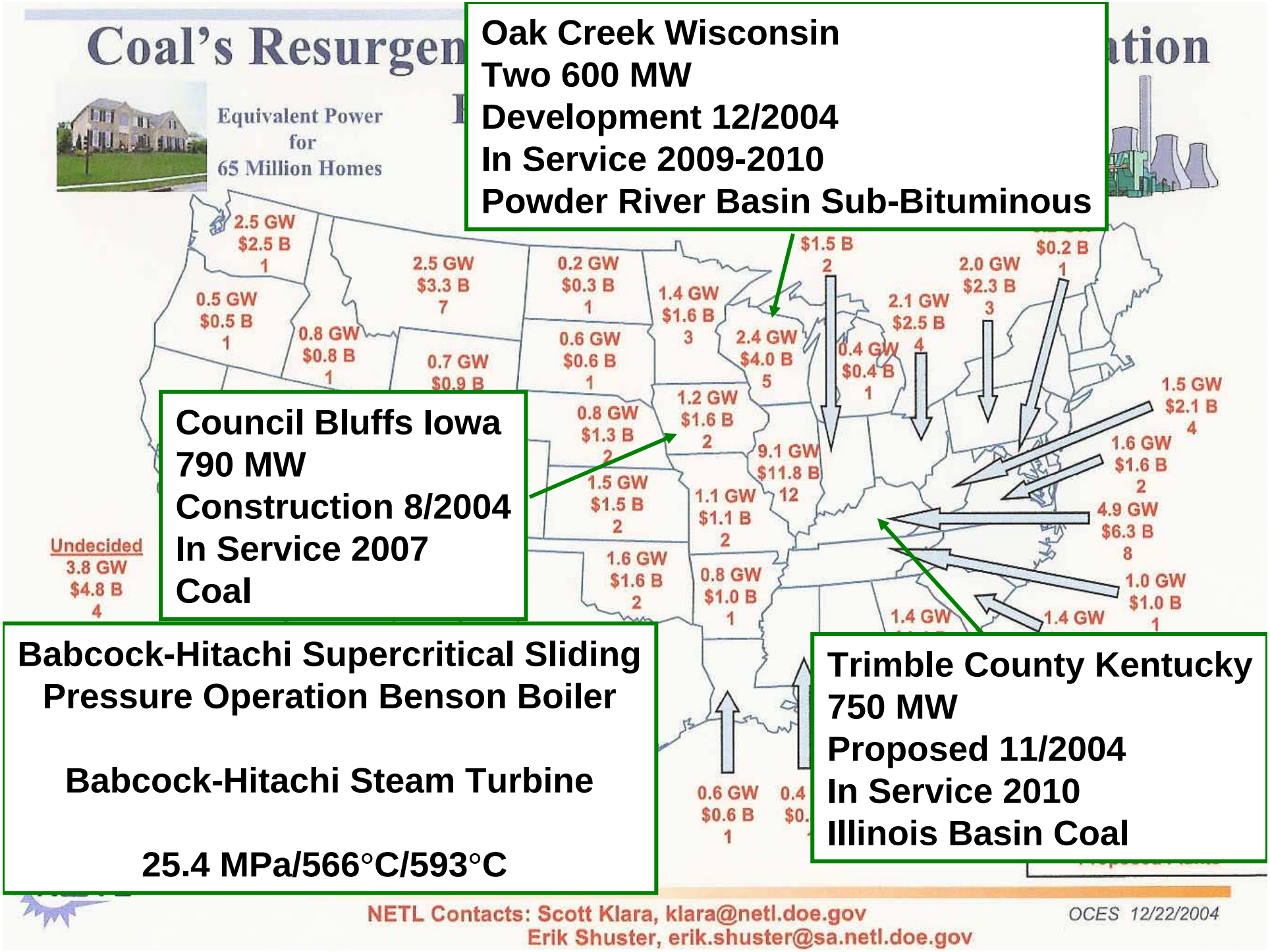
Coal's Resurgen
ation
Equivalent Power
for
65 Million Homes
Oak Creek Wisconsin
Two 600 MW
Development 12/2004
In Service 2009-2010
Powder River Basin Sub-Bituminous
Council Bluffs Iowa
790 MW
Construction 8/2004
In Service 2007
Coal
Babcock-Hitachi Supercritical Sliding
Pressure Operation Benson Boiler
Babcock-Hitachi Steam Turbine
25.4 MPa/566°C/593°C
Trimble County Kentucky
750 MW
Proposed 11/2004
In Service 2010
Illinois Basin Coal
2.5 GW $2.5 B 1
0.5 GW $0.5 B 1
0.8 GW $0.8 B 1
2.5 GW $3.3 B 7
0.7 GW $0.9 B
0.2 GW $0.3 B 1
0.6 GW $0.6 B 1
0.8 GW $1.3 B 2
1.5 GW $1.5 B 2
1.6 GW $1.6 B 2
1.4 GW $1.6 B 3
1.2 GW $1.6 B 2
1.1 GW $1.1 B 2
0.8 GW $1.0 B 1
2.4 GW $4.0 B 5
9.1 GW $11.8 B 12
$1.5 B 2
0.4 GW $0.4 B 1
2.1 GW $2.5 B 4
2.0 GW $2.3 B 3
$0.2 B 1
1.5 GW $2.1 B 4
1.6 GW $1.6 B 2
4.9 GW $6.3 B 8
1.0 GW $1.0 B 1
1.4 GW
1.4 GW
0.6 GW $0.6 B 1
Undecided
3.8 GW
$4.8 B
4
NETL Contacts: Scott Klara, klara@netl.doe.gov
Erik Shuster, erik.shuster@sa.netl.doe.gov
OCES 12/22/2004

Research Goals

- Determine the steamside oxidation behavior of target alloys for use in USC turbines
- Determine the role of pressure on oxidation mechanisms
- Examine curvature effects on spallation

Research Approach

- Ultra Supercritical Steam Exposures
  - Temperatures 593 to 760°C (1112-1400°F)
  - Pressures of 2400 to 5500 psi (16.5-37.9 MPa)
- Cyclical Oxidation in Moist Air
  - Hourly cycles to examine adhesion and spallation behavior of protective oxides
- TGA in Steam+Argon
  - Determine oxidation mechanisms, kinetics, activation energies
- Furnace Exposures in Moist Air
  - Economical long-term tests

Alloys

Highest Strength in Alloy Category

- **Original 6 alloys**
  - SAVE12 -- Alloy 230
  - Super304H -- Alloy 617
  - HR6W -- Alloy 740
- **Additional Ni-base superalloys** **Bolt Material**
  - Nimonic 90 -- Refractory 26
  - Alloy 718 -- M-252
- **Also**
  - Rene 41 -- J1 -- J5

Candidate Blade Materials (EPRI)

Low CTE Nickel Alloys

Alloy Strength

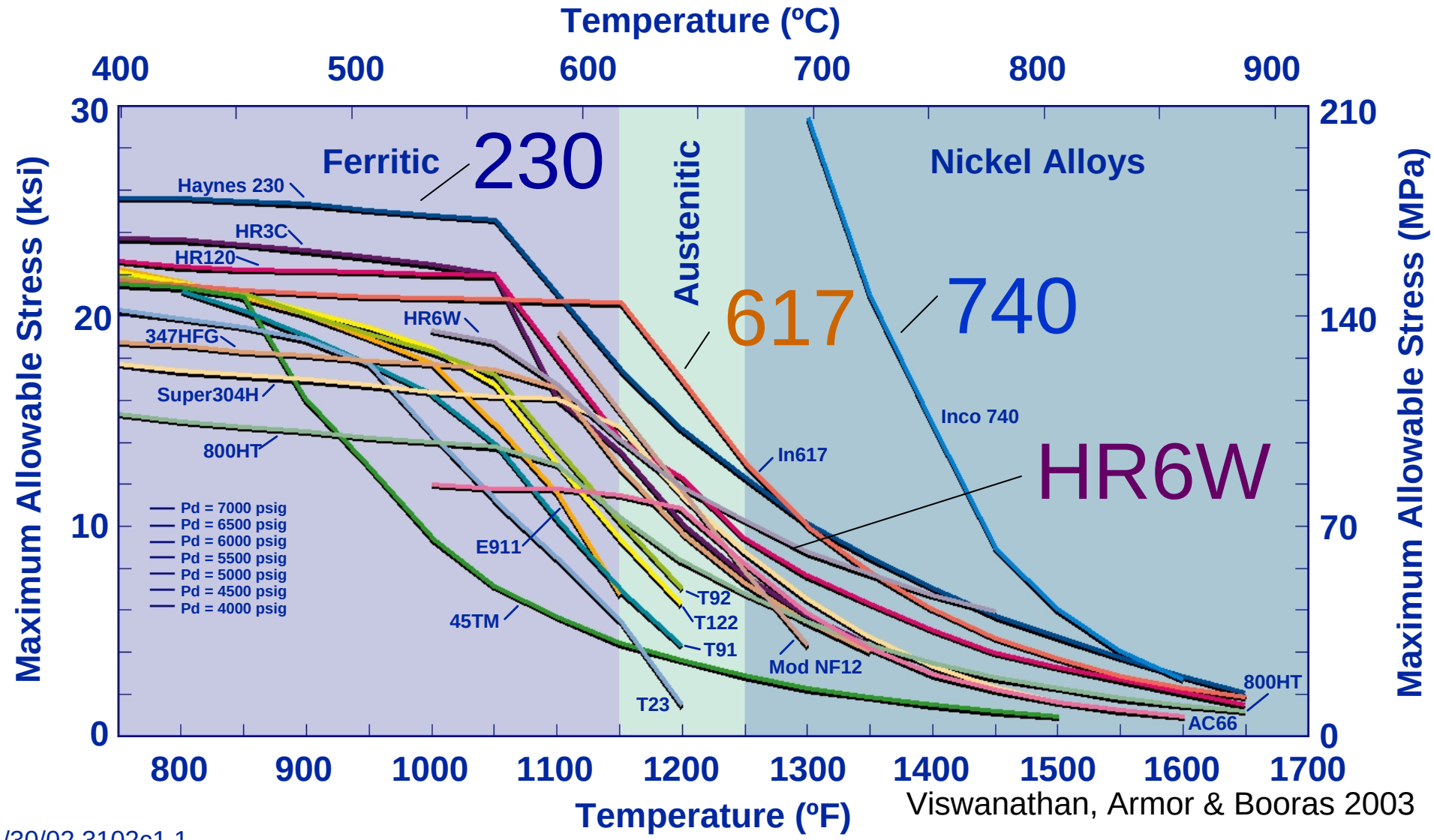

Viswanathan, Armor & Booras 2003

/30/02 3102c1.1

Section Comparison

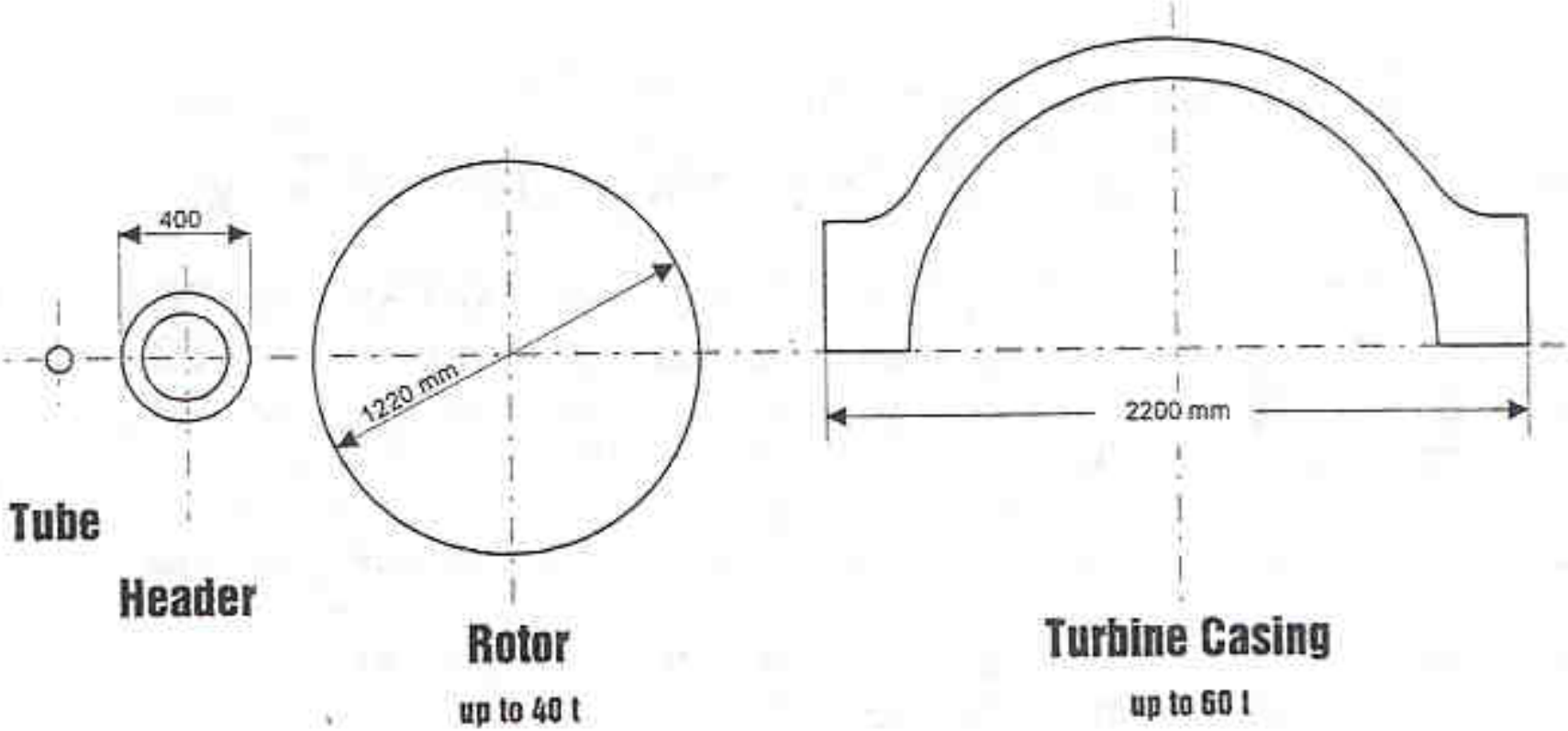

Thornton and Mayer, 1999

Thick section components are more susceptible to thermal fatigue issues.

SAVE12
10.5 Cr
2” O.D.
Concave
Convex

Stored Energy Model

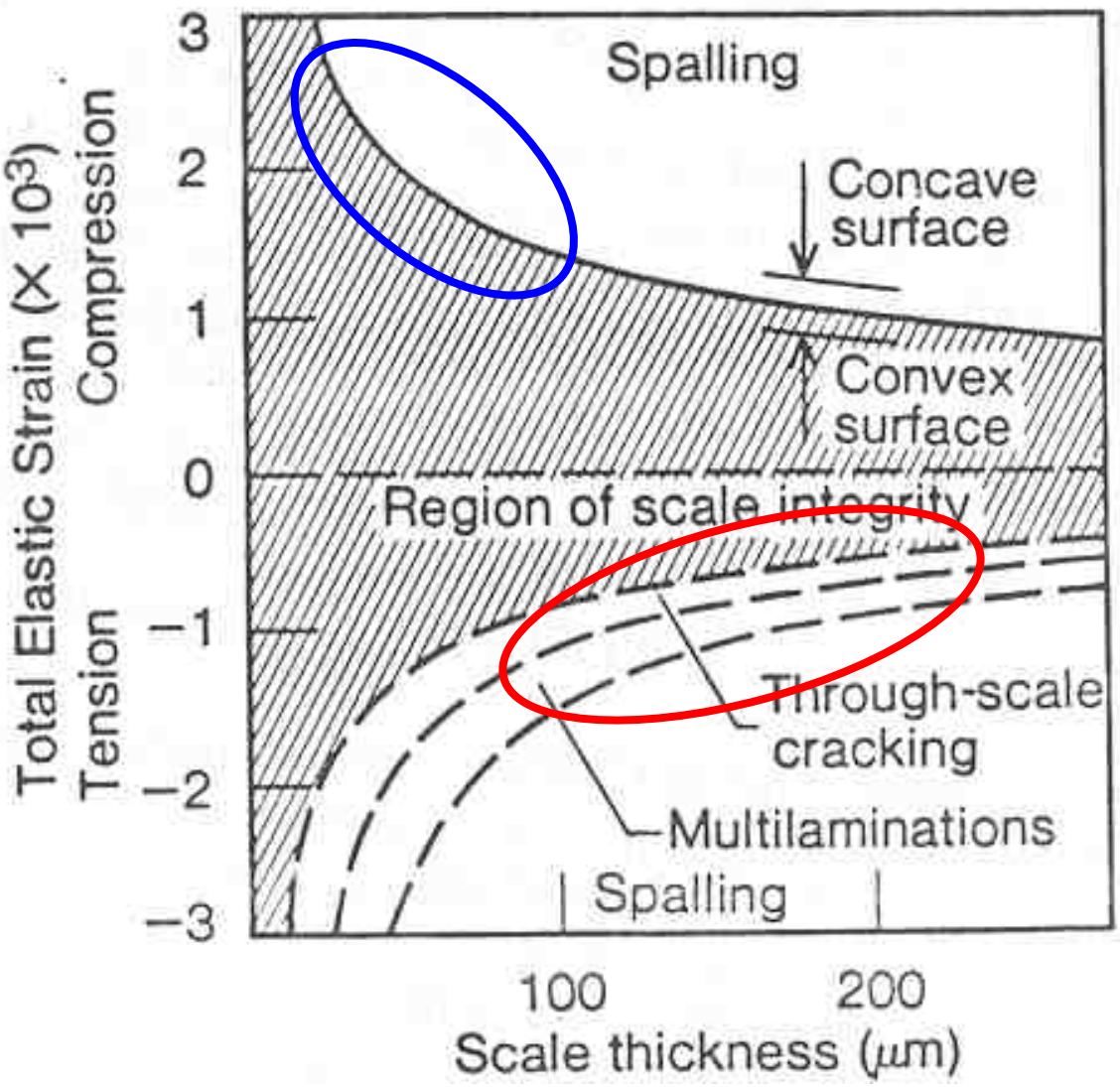

Austenitic Steels

Ferritic Steels

Armitt et al. 1978

USC Test Loop

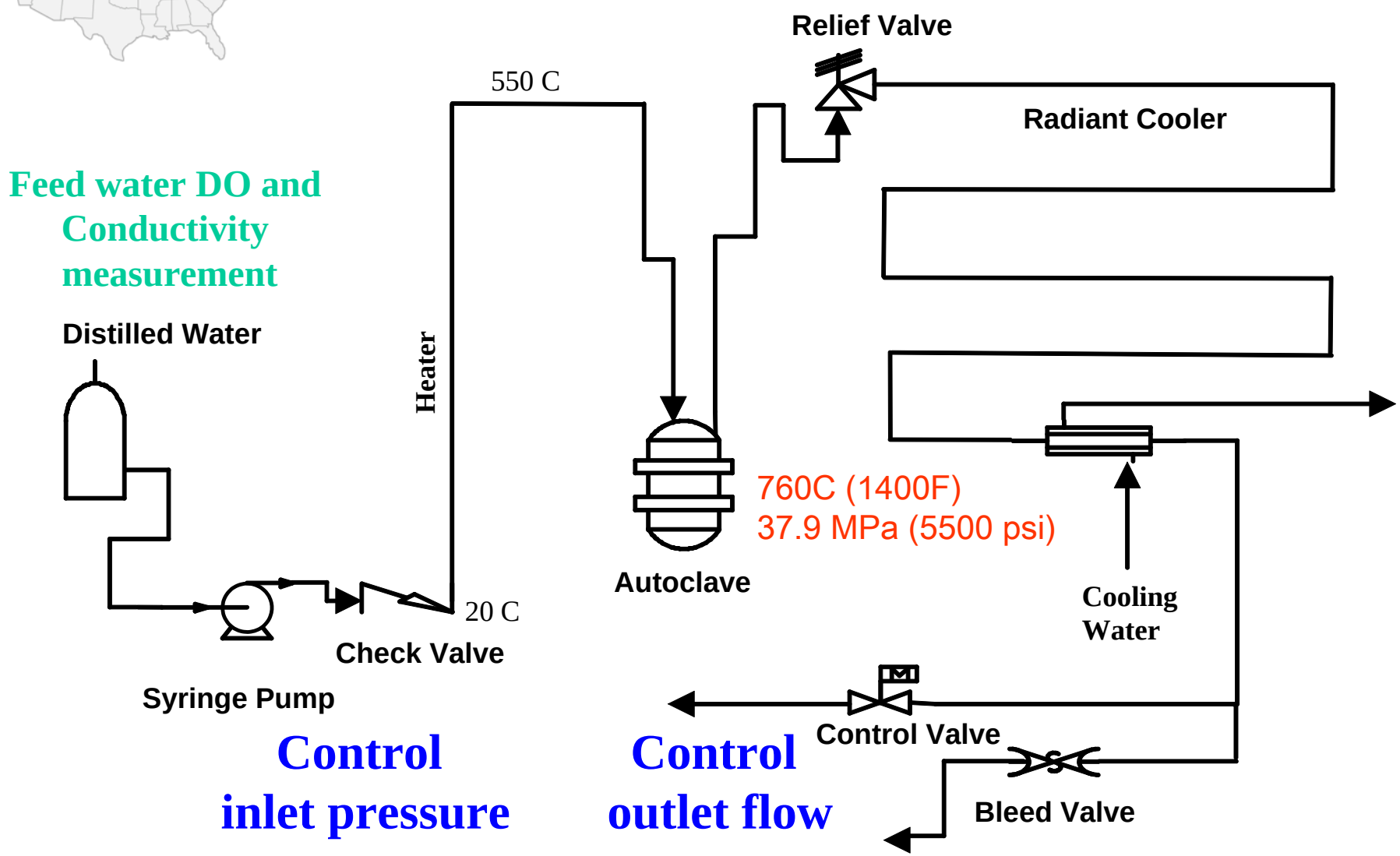

USC Feed Water System

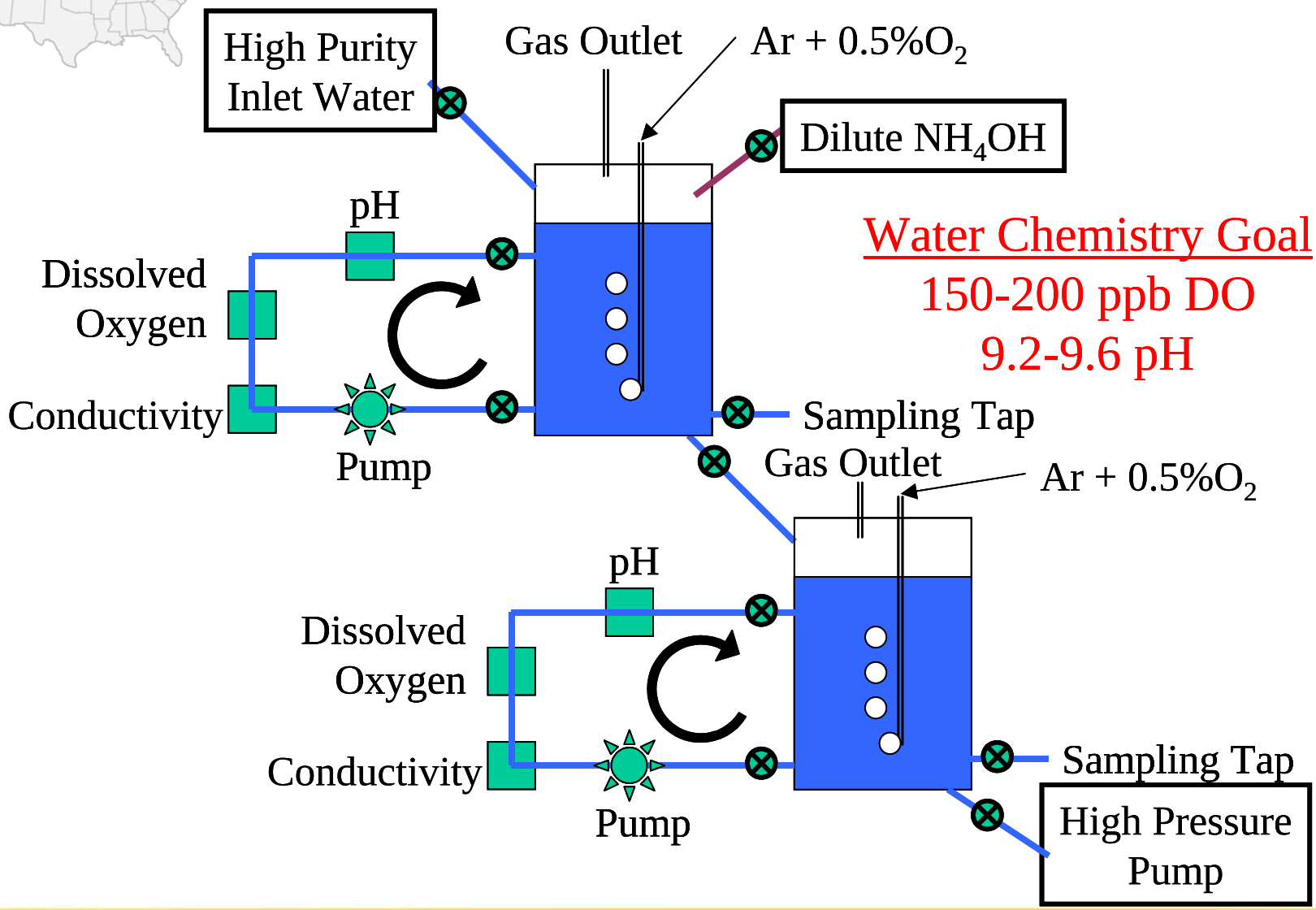

Water Chemistry Goal
150-200 ppb DO
9.2-9.6 pH

USC Exposure Facility

- Rene 41 autoclave had a delivery date of 12/31/04
- In February a letter stating that they could either
  - Make it out of 718
  - Add 1 year and $80,000 to make it out of Rene 41
- Unresponsive since we submitted questions about 718

Rene 41 vs 718

760°C
1400°F

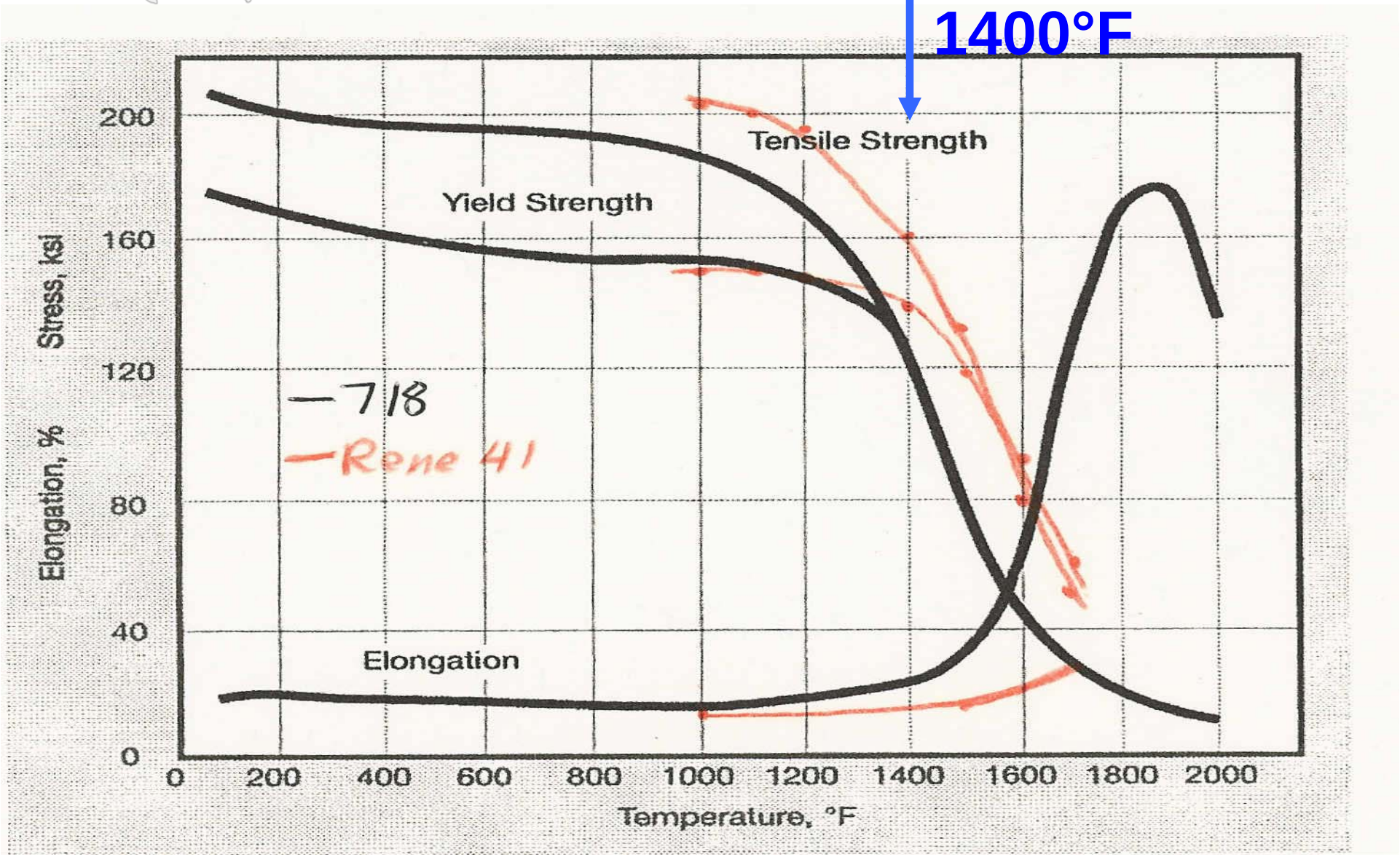

Cyclic Oxidation

Scale adhesion information during thermal cycles

Temperatures up to 800°C
Flowing steam/air mixture
Atmospheric pressure
Hourly cycles
7 samples at a time

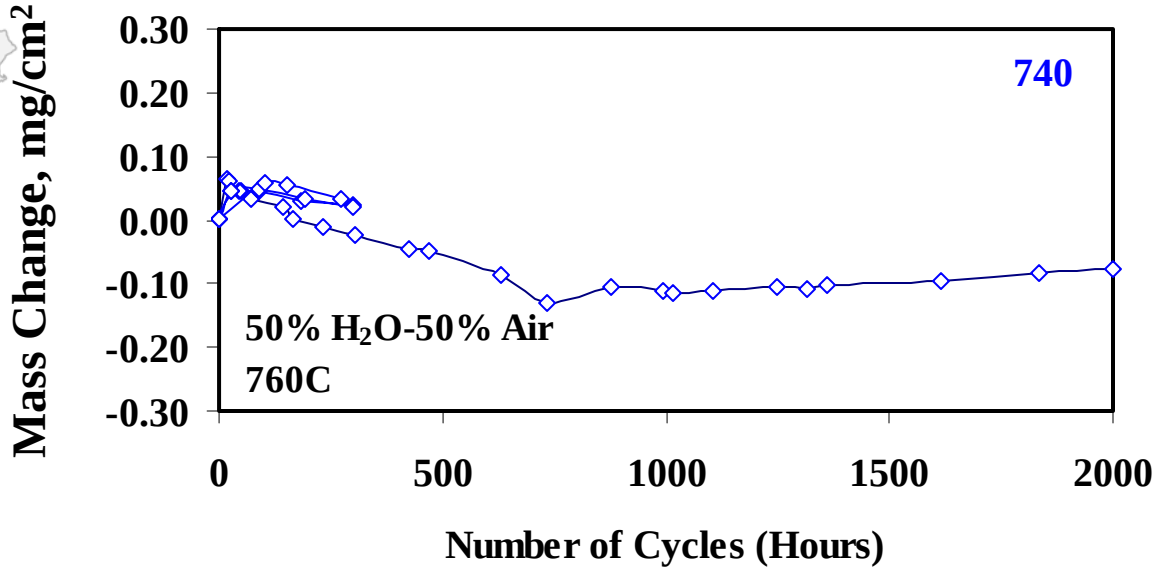

740

760°C
Air + 50% H_2O

4 mm

CY740-1(side-1)

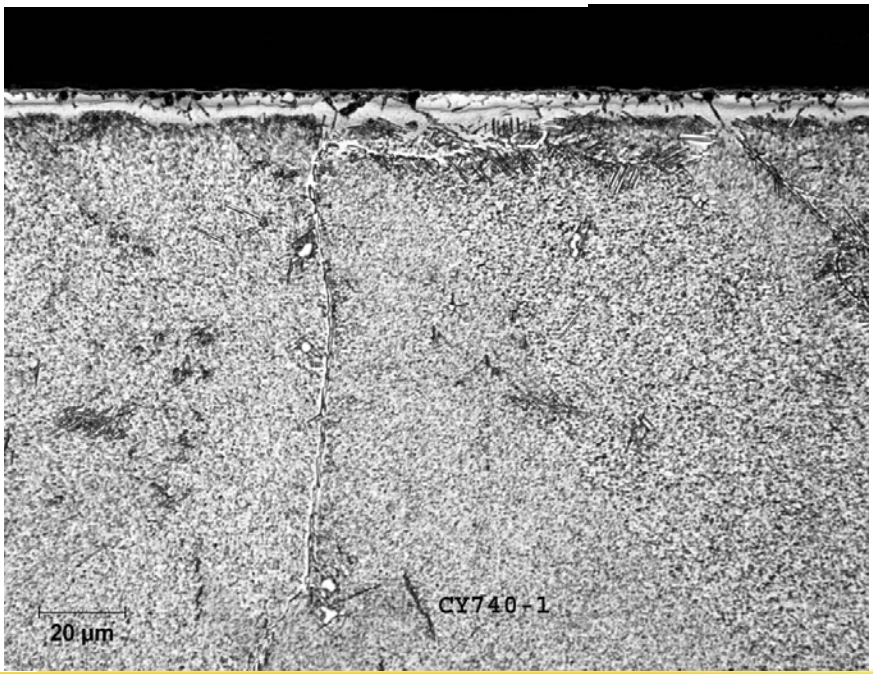

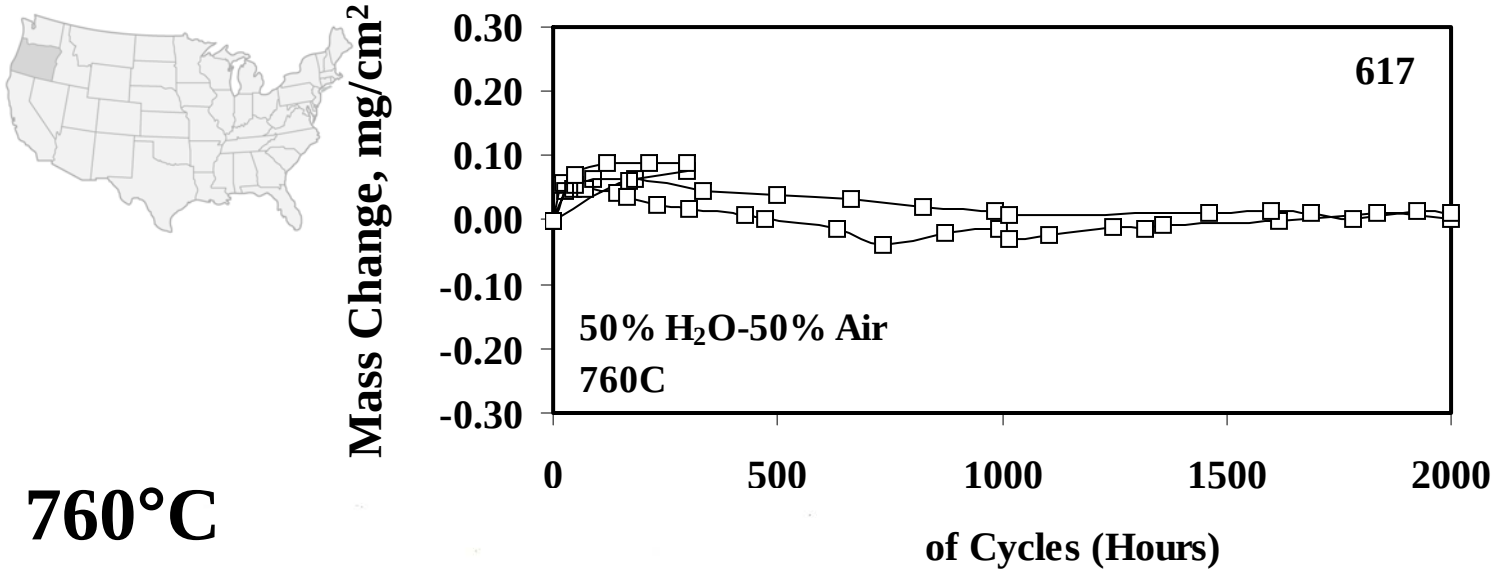

617

760°C
Air + 50% H_2O

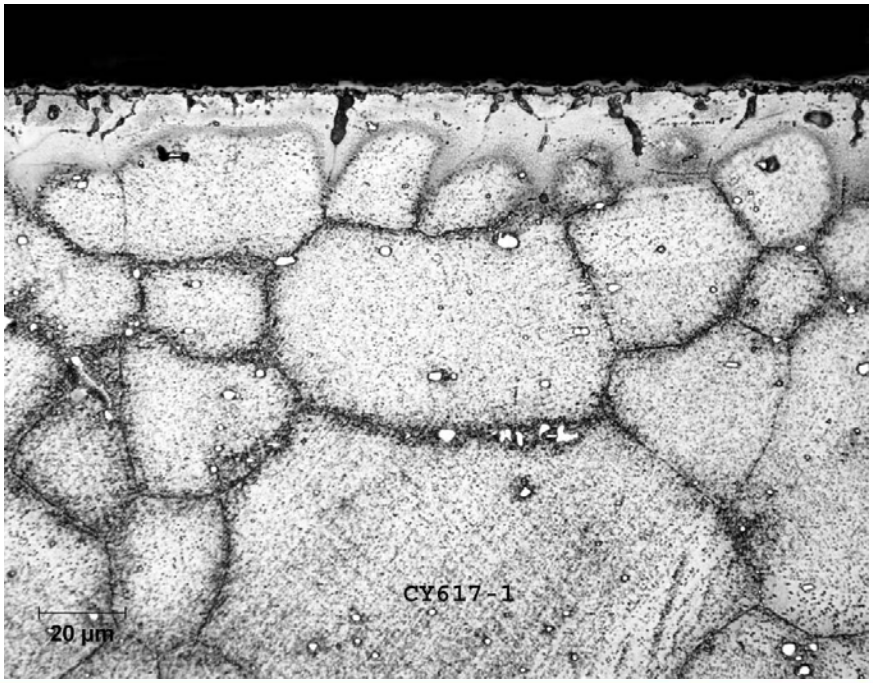

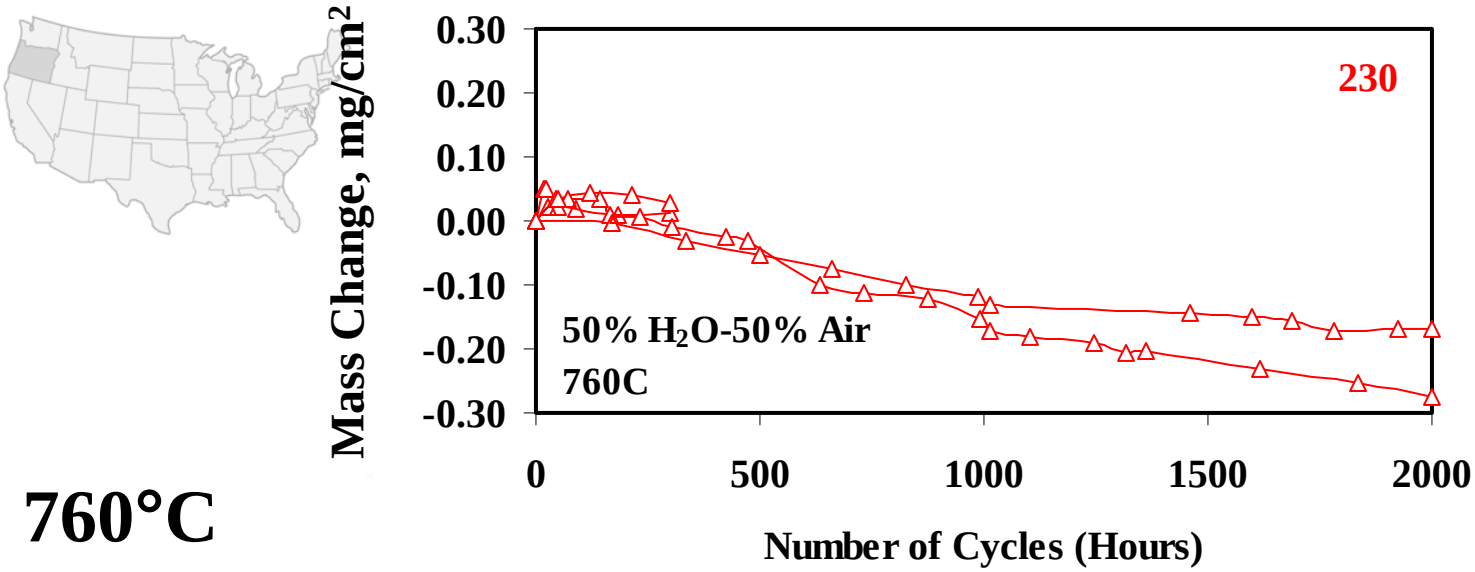

230

760°C
Air + 50% H_2O

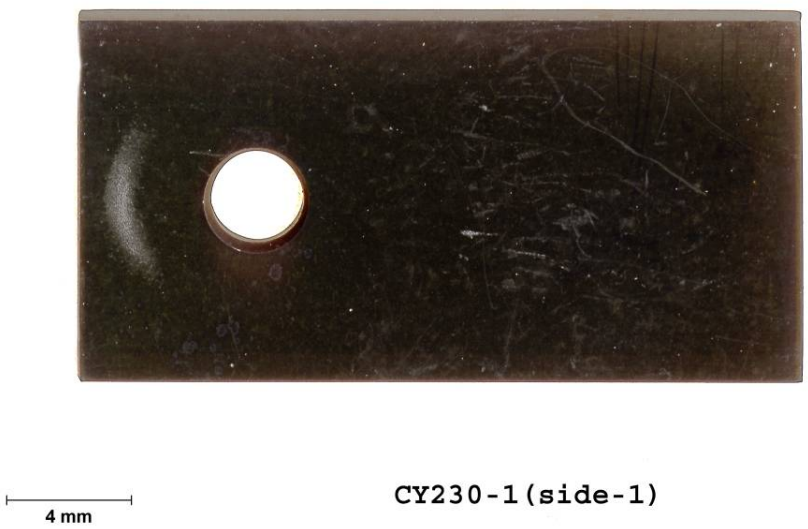

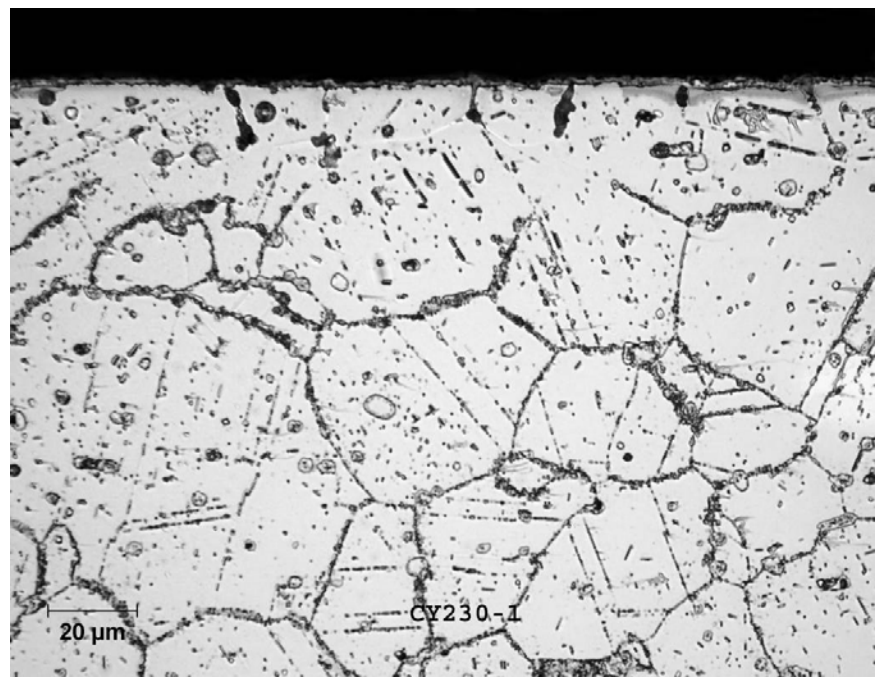

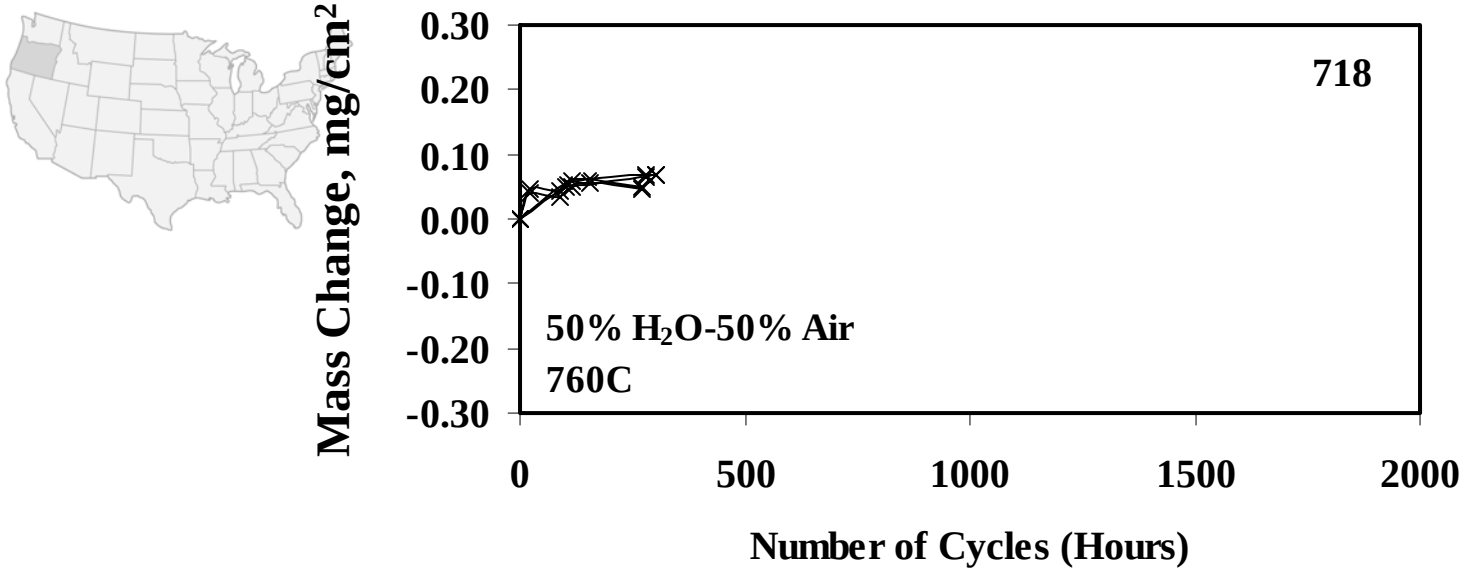

718

760°C

Air + 50% H_2O

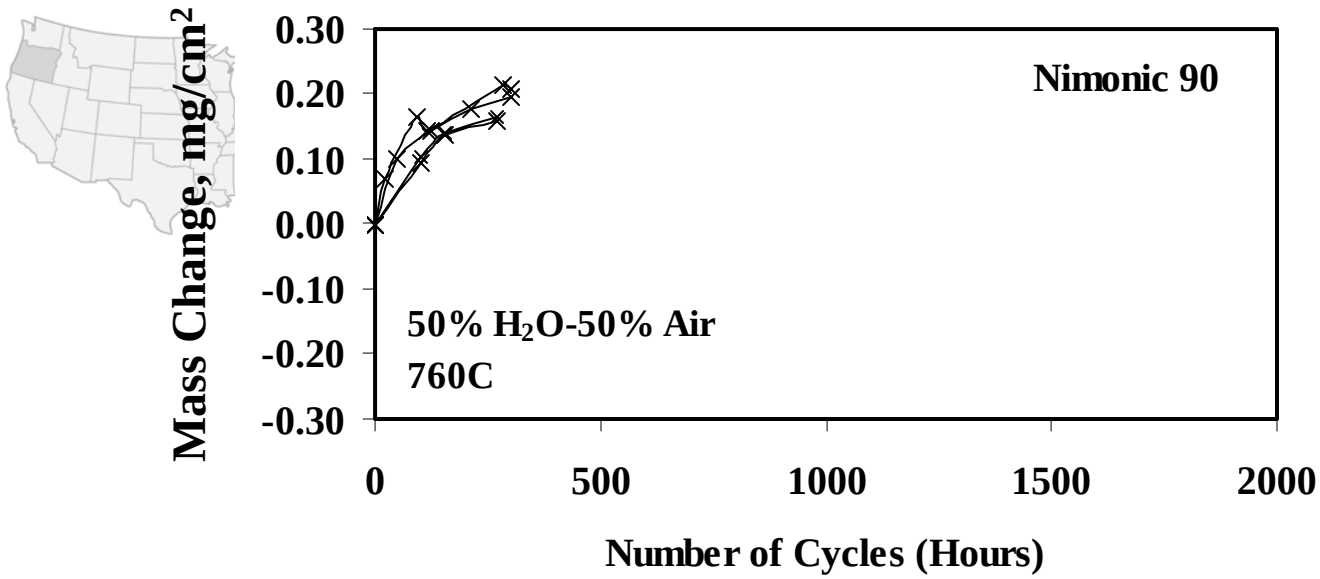

Nimonic 90

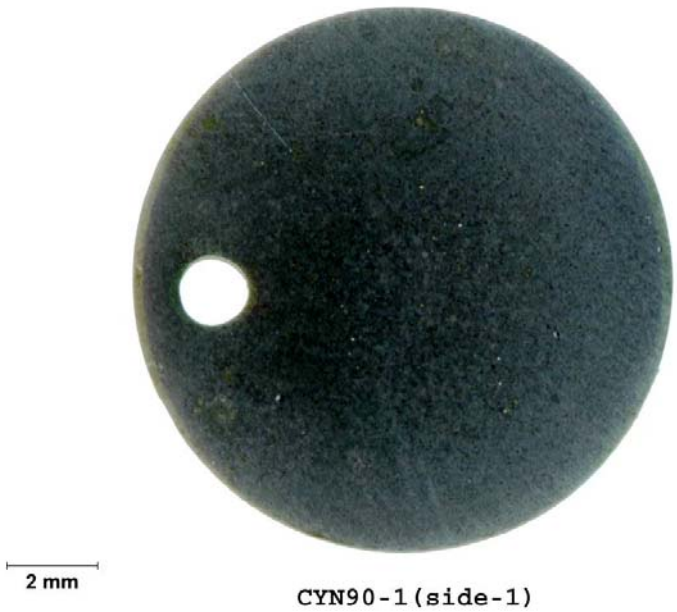

760°C

Air + 50% H_2O

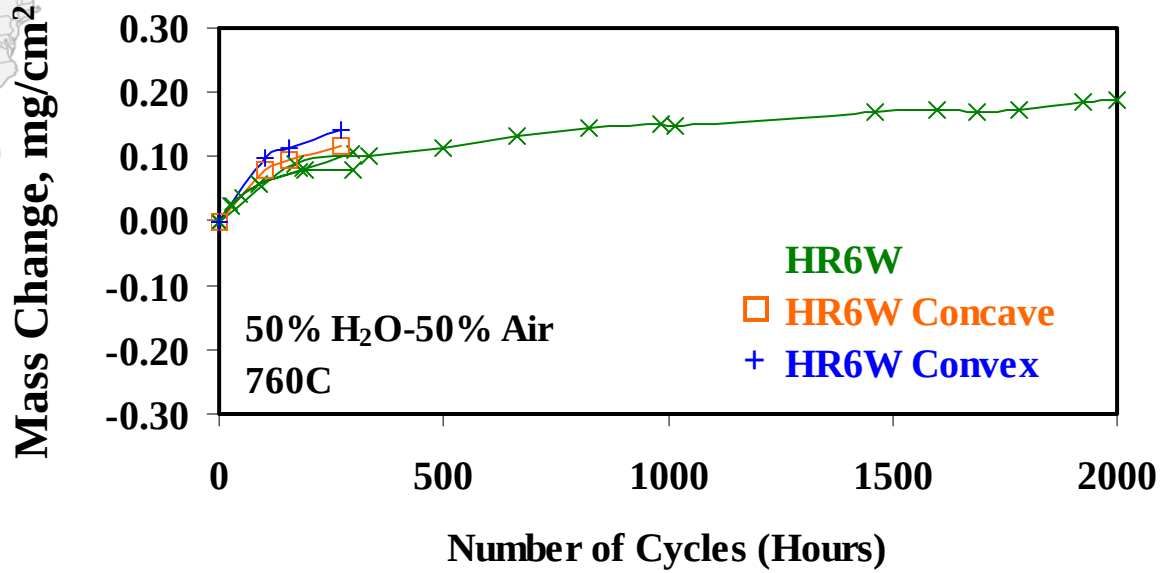

HR6W

4 mm

CYHR6W-1(side-2)

760°C

Air + 50% H_2O

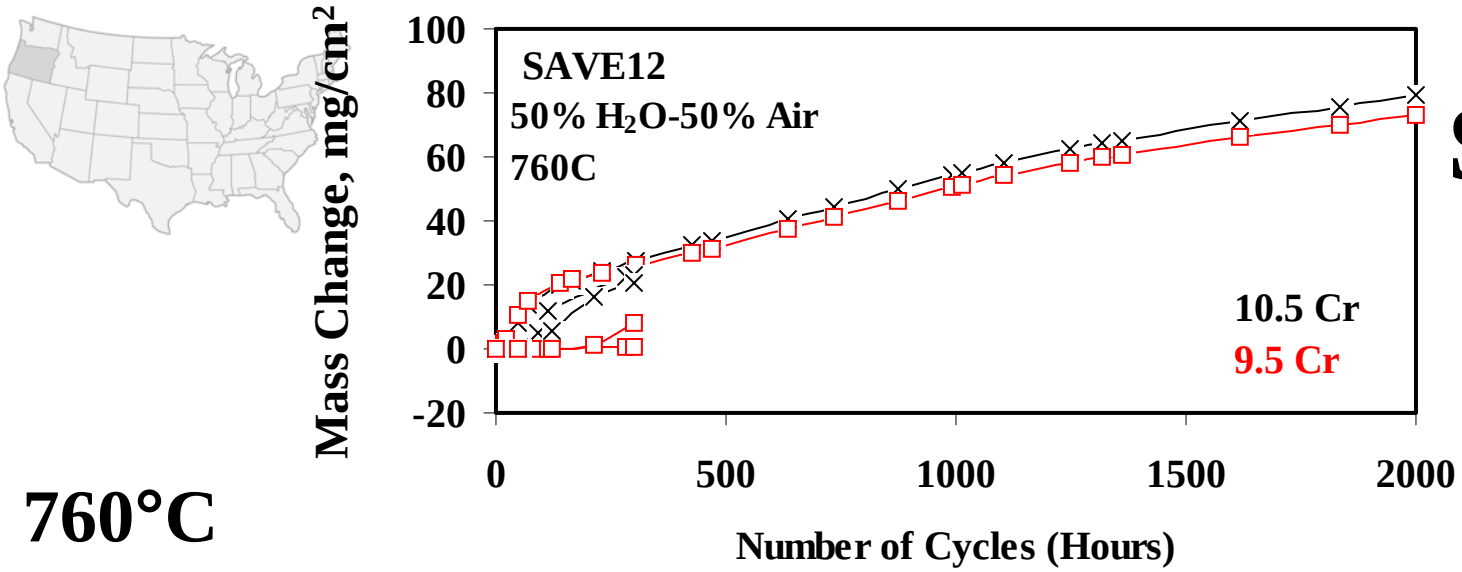

SAVE12

760°C
Air + 50% H_2O

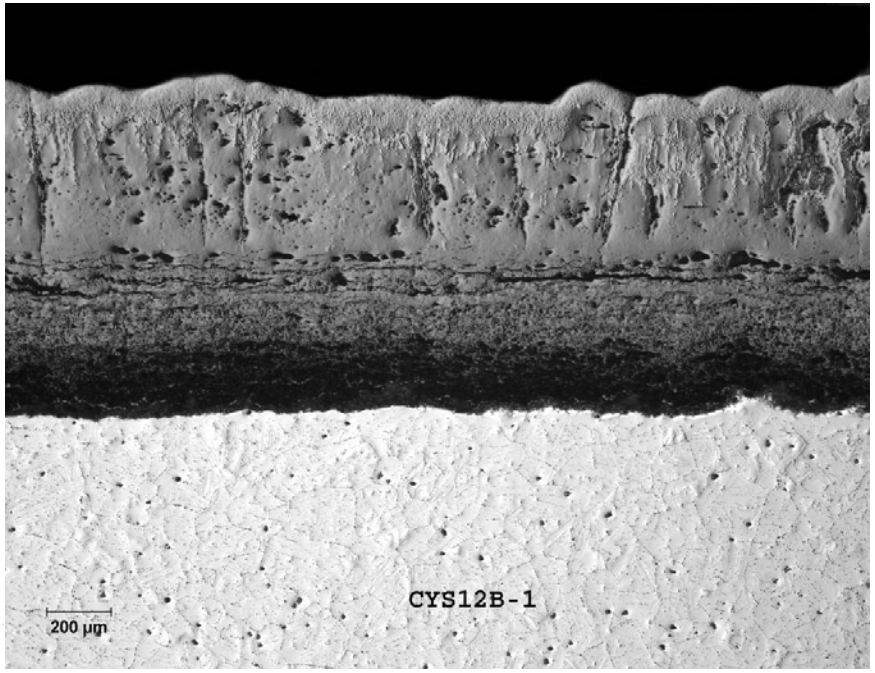

SAVE12 Curvature

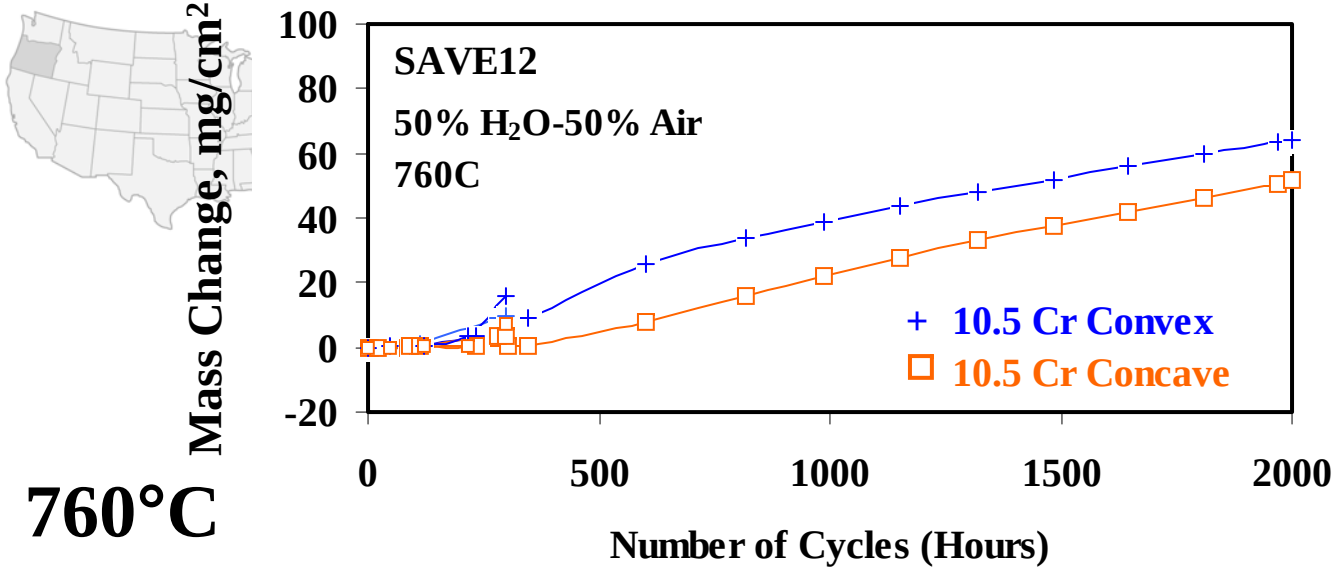

760°C

Air + 50% H_2O

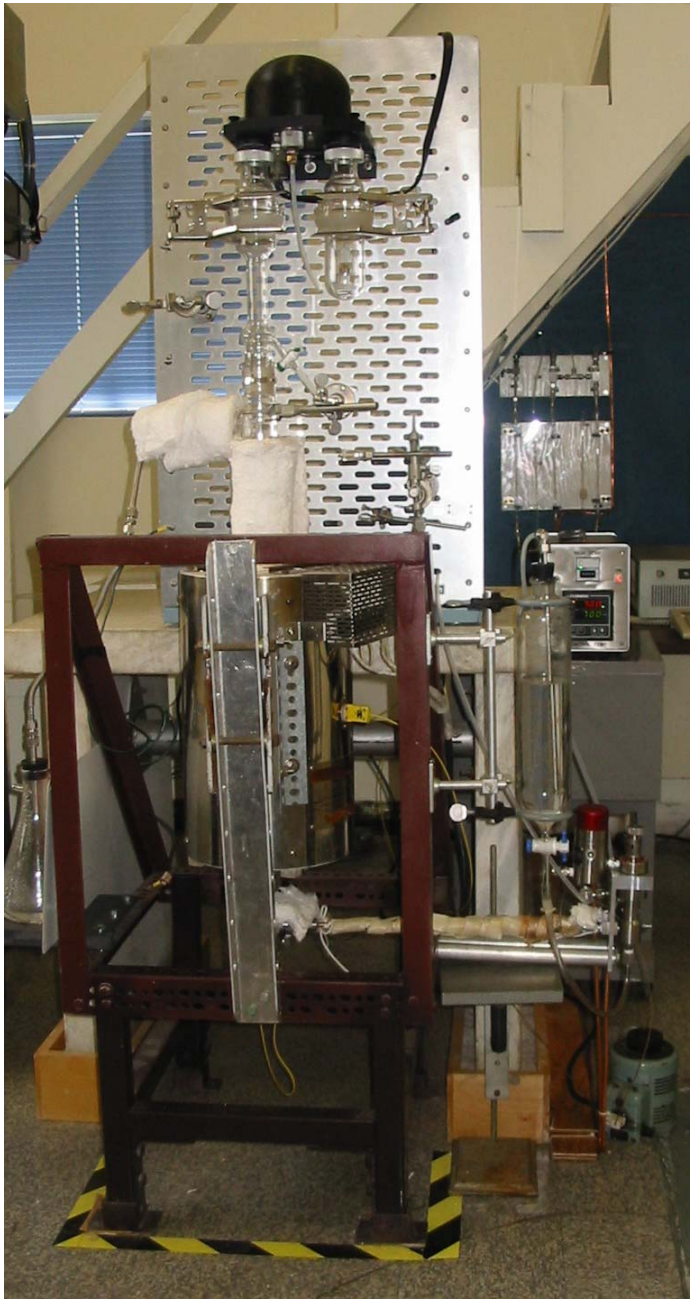

TGA Testing in Steam

Thermogravimetric analysis to give kinetics and corrosion mechanism information.

Temperatures up to 800°C
Flowing steam plus Ar
Atmospheric pressure

Feed water is oxygen saturated

TGA Results

THERMOGRAVIMETRIC ANALYSIS (TGA) FOR 300 HR TESTS IN O_2-SATURATED STEAM PLUS 60%Ar AT 800°C

Alloy	%Cr	Reaction Order, n	Parabolic R^2	Parabolic Rate Constant, k_p $mg^2cm^{-4}s^{-1}$
SAVE12 9.5Cr	9.5	1.78	1.000	1.4×10^{-3}
SAVE12 10.5Cr	10.5	1.70	1.000	1.9×10^{-3}
SAVE12 10.5Cr	10.5	1.76	0.995	2.0×10^{-3}
J1	12.1	1.73	0.990	3.8×10^{-7}
J5	12.5	1.91	0.990	1.7×10^{-7}
Alloy 617	22	1.62	0.960	1.4×10^{-7}
Alloy 617	22	2.63	0.585	3.9×10^{-8}
Alloy 230	22	1.78	0.878	6.9×10^{-8}
Alloy 230	22	1.79	0.645	3.7×10^{-8}
HR6W	23	1.87	0.524	3.8×10^{-8}
Alloy 740	24	2.20	0.527	2.0×10^{-7}

TGA Sensitivity

SAVE12 10.5Cr

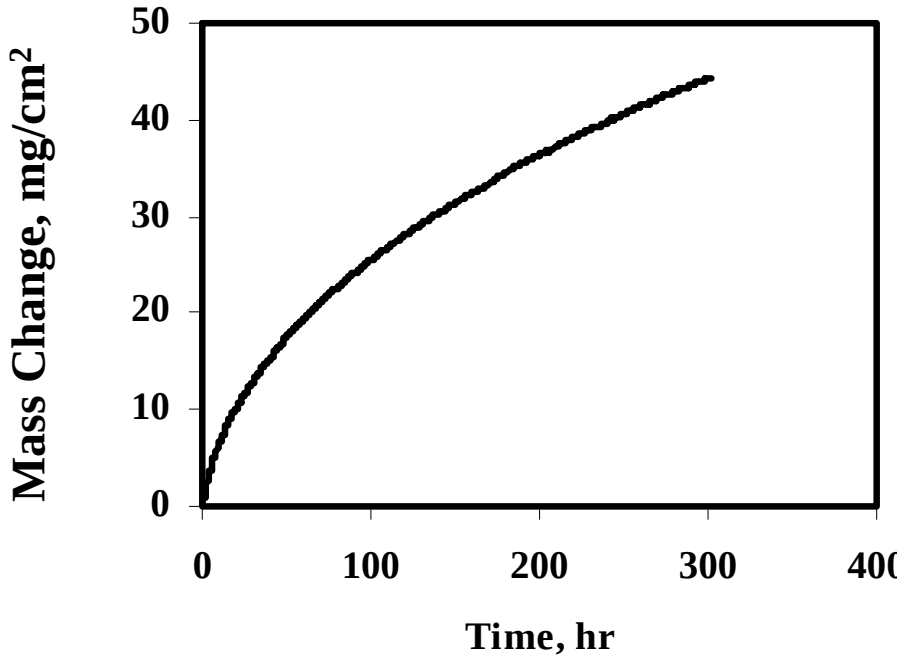

HR6W

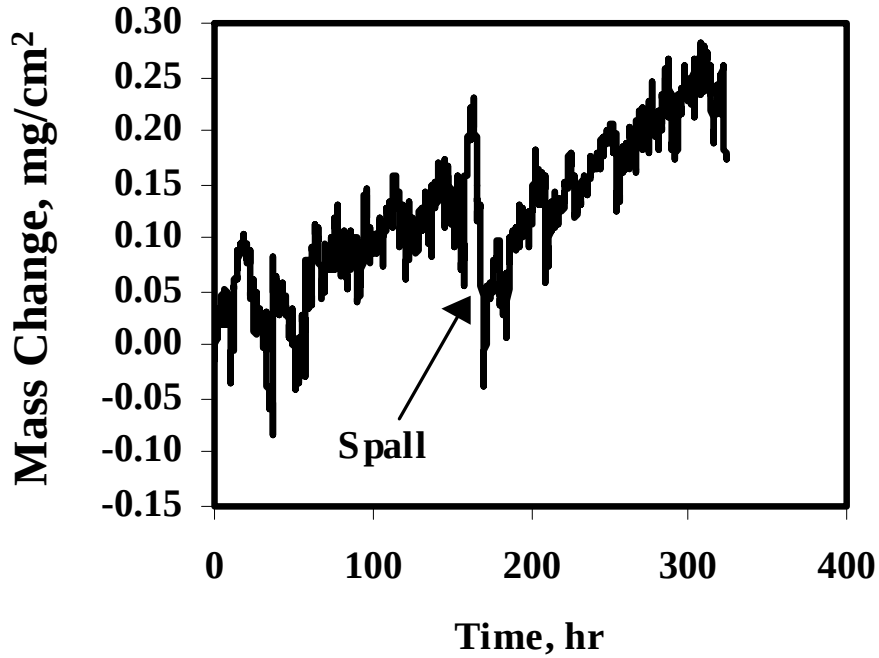

Furnace Exposures

- Air plus 3% water vapor
- Periodic removal for mass change measurements
- 700 and 800°C

Furnace Exposure
700°C in Moist Air

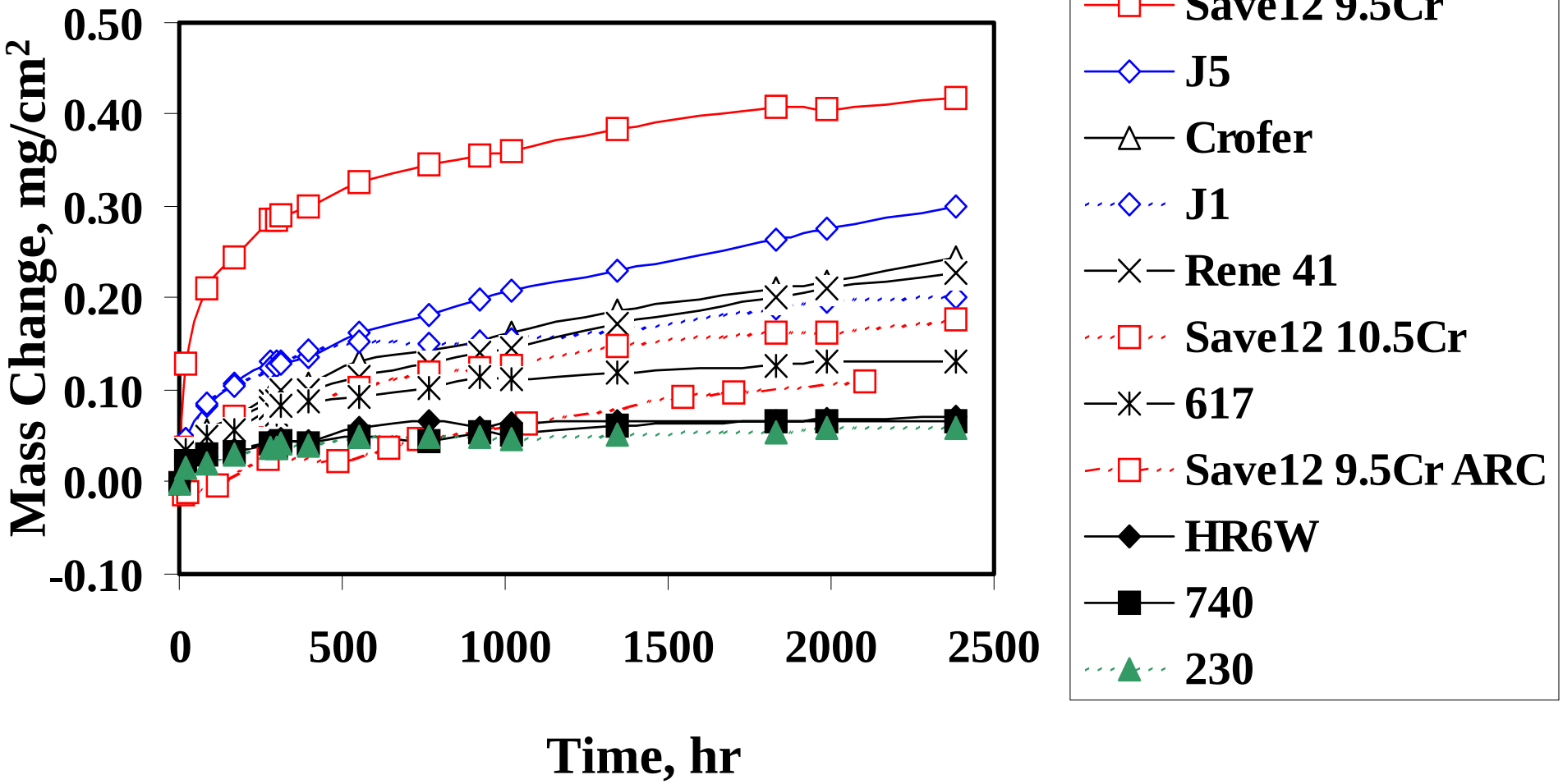

Furnace Exposure, 800°C in Moist Air

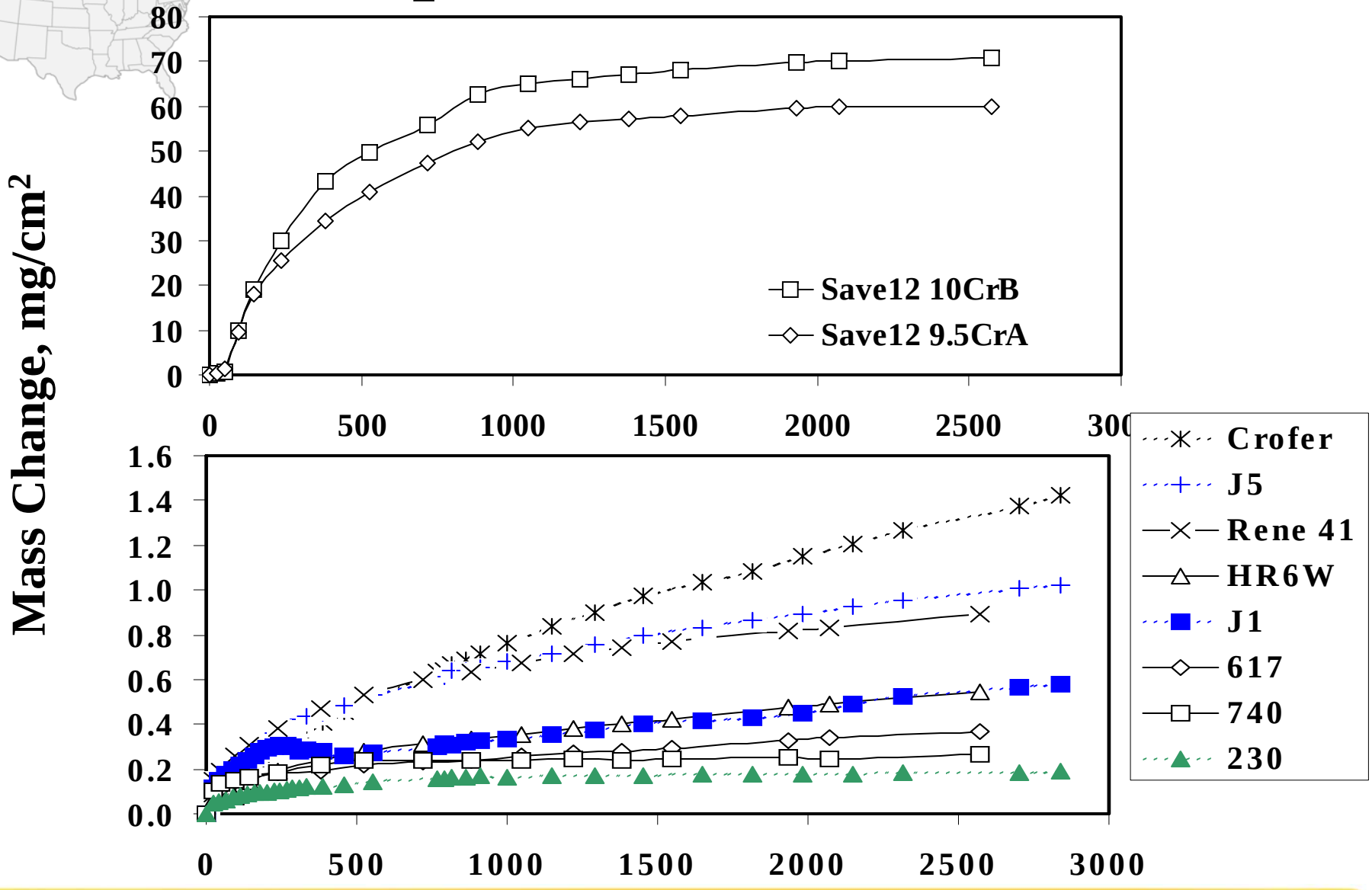

Summary

- DOE Advanced Power System goal of 60% efficiency from coal generation
  - Require USC steam turbine conditions of 760°C & 37.9 MPa
- Alloy Selection
  - Still looking for SUPER304H, M-252, Refractory 26
- Four types of exposure tests
  - USC steam at up to 760C and 37.9 MPa
    - In negotiations
  - Cyclic oxidation in air plus steam
  - TGA in Ar plus O_2 saturated steam
    - Sensitivity limitations
  - Furnace exposures in moist air

Optimization of ODS-Alloy Properties
for
High Temperature Oxidation Resistant Components

Bimal Kad

University of California – San Diego

Collaborators

I. G. Wright, Rod Judkins

Oak Ridge National Laboratory

Gaylord Smith

Special Metals Corporation

19th Annual Fossil Energy Meeting

May 9th – 11th 2005, Knoxville, TN

Goal: Oxidation Resistant Components

High Temperature Heat Exchangers–Vision 21, FutureGen
Combustor Liners – Energy Efficiency Programs

Target Product:
- 1-3” diameter 10’ft long tubes for heat exchangers
- oxidizing/sulphidizing service environments
- Operating pressure of 1000psi at 1000-1100°C

Material Options:
- Y_2O_3 strengthened Fe_3Al
- Y_2O_3 strengthened Fe-Cr-Al (MA956™)

Barriers:
- Grain shape dependent anisotropic properties
- In–service creep strength anisotropy
- Microstructure preserving non-fusion joining

Scientific approach:
- Hoop Creep enhancement via grain fibering,
- Enhancement via thermo-mechanical processing
- Component specific joining methodologies

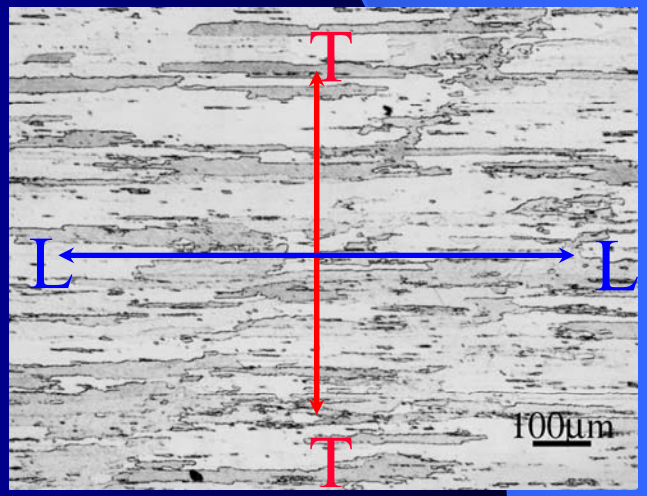

Today's presentation covers 2 themes

- Exploring non-fusion joining techniques

  - *Inertial welding: butt joint configurations*

  - *Magnetic pulse welding: lap joint configurations*

- Improving hoop creep response via processing

  - *Thermo-mechanical routes to altering the underlying grain shape*

  - *Motivation for cross-rolling/helical grain fibering*

Non-Fusion Joining Efforts

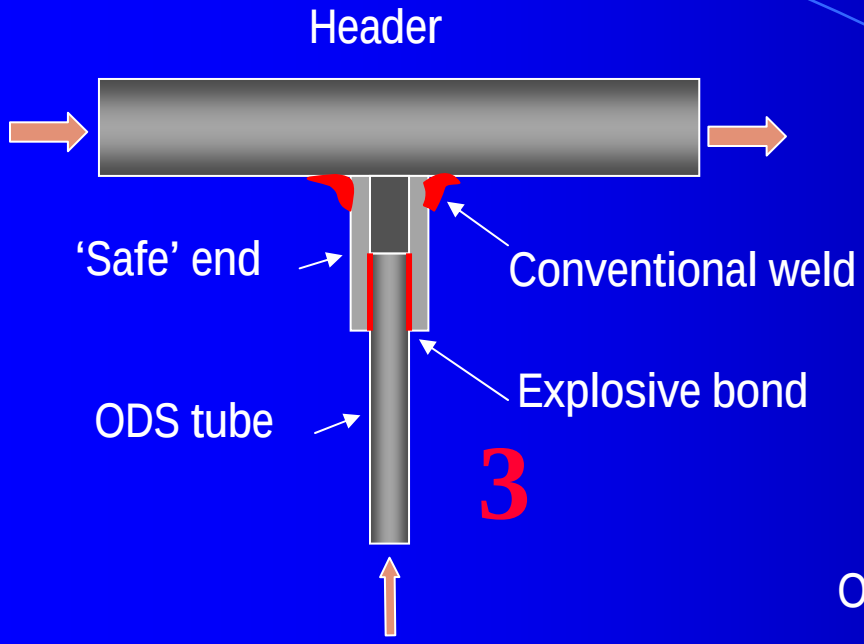

British Gas 'Harp' Joint

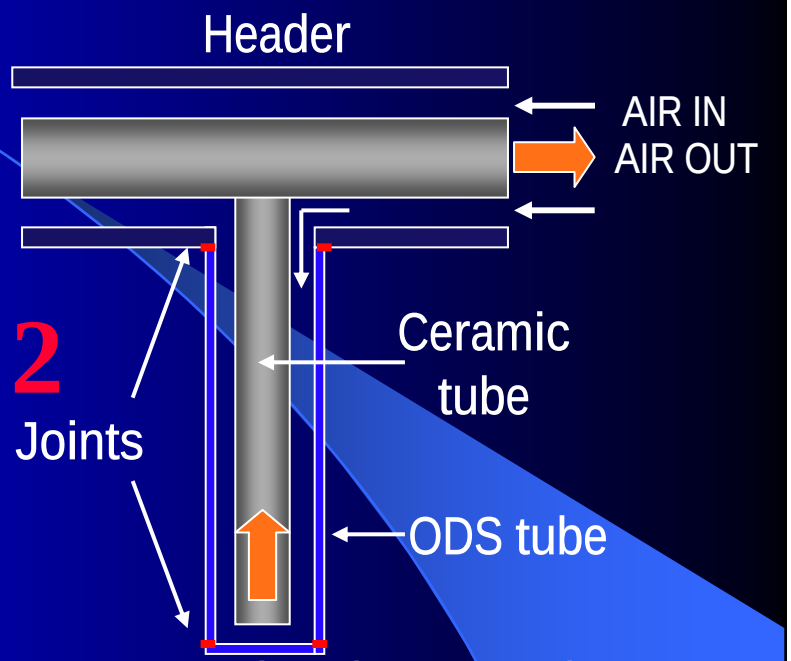

Bayonet tubes (COST-522)

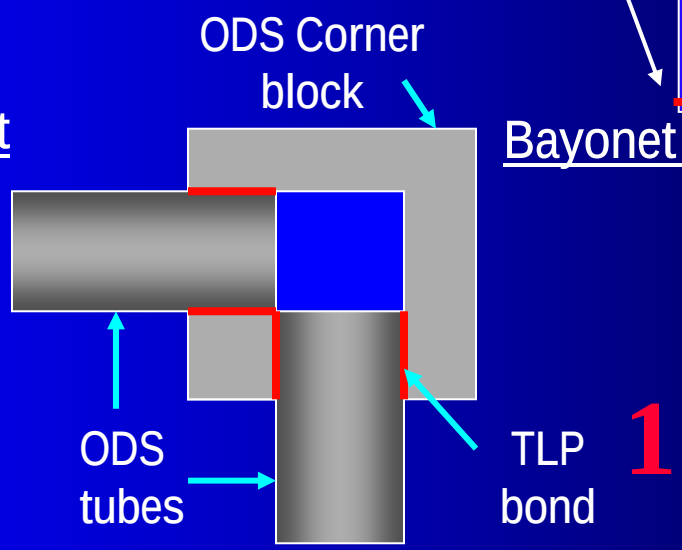

TLP joint: HiPPS program

Inertia welding of MA956 tube butt joint

For the Vision-21 heat exchanger program various configurations of 1) tube to tube, 2) tube to header block, and 3) tube to flange head can be explored for design development

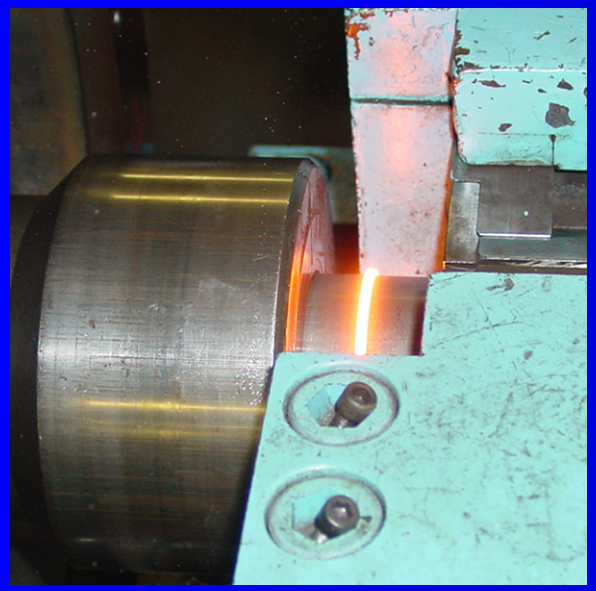

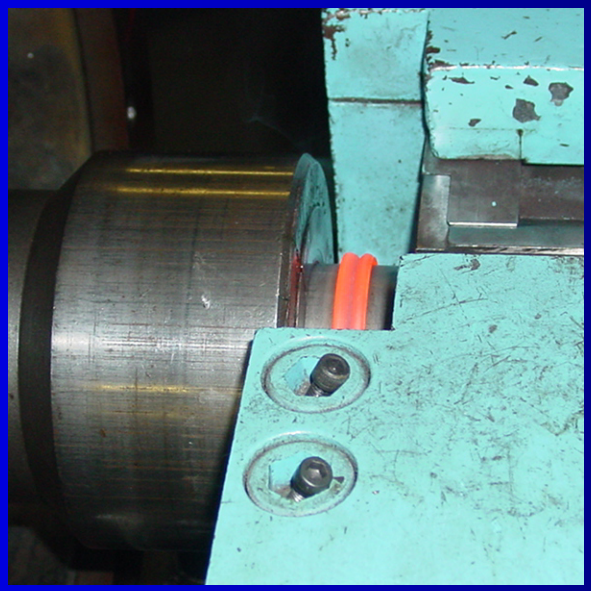

Material Condition: 2-1/2” OD, ¼” wall thickness unrecrystallized MA-956 Tube

Inertia Welded Joint Microstructures

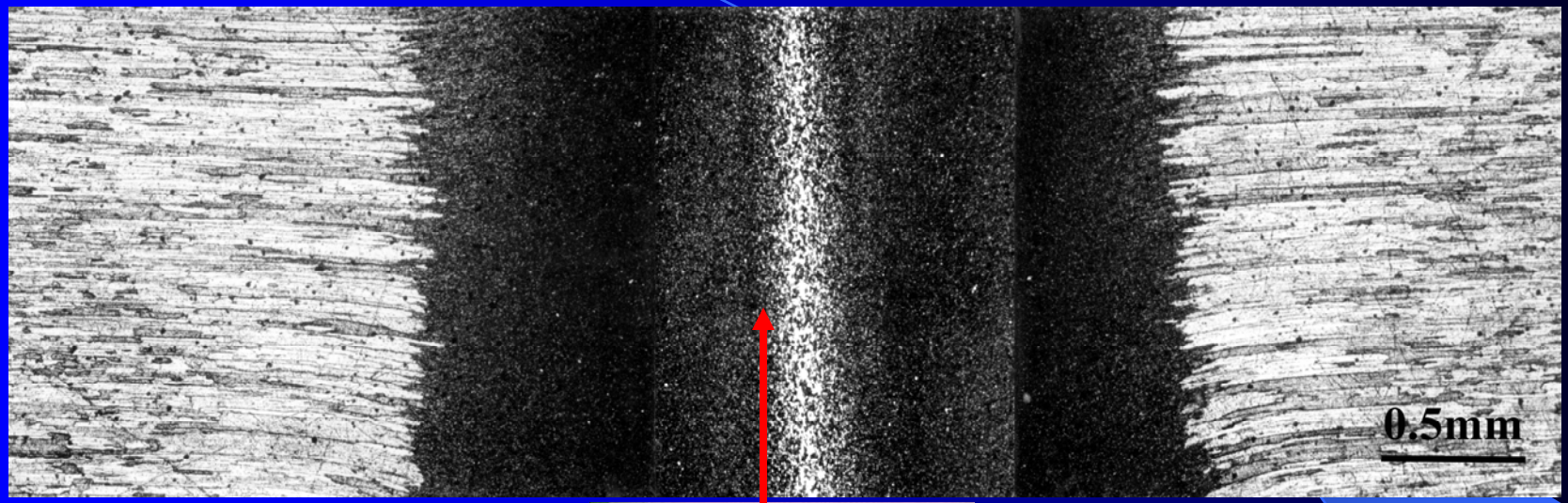

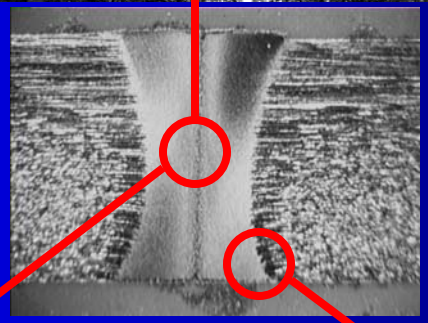

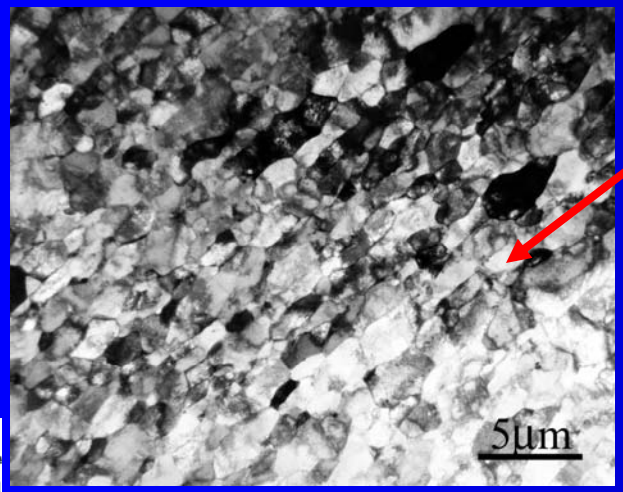

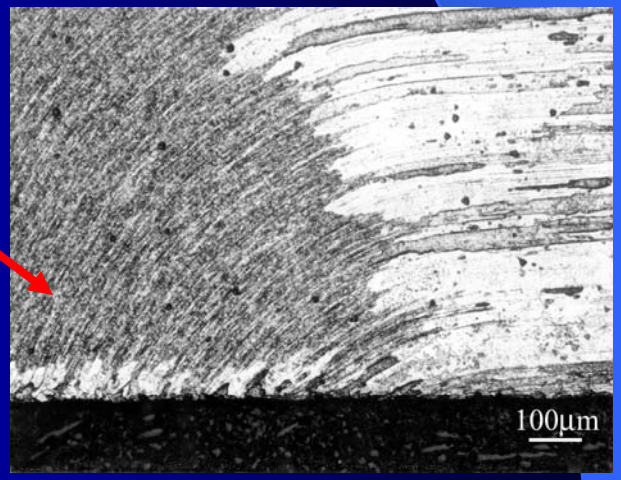

Inertial Welded Joint Integrity

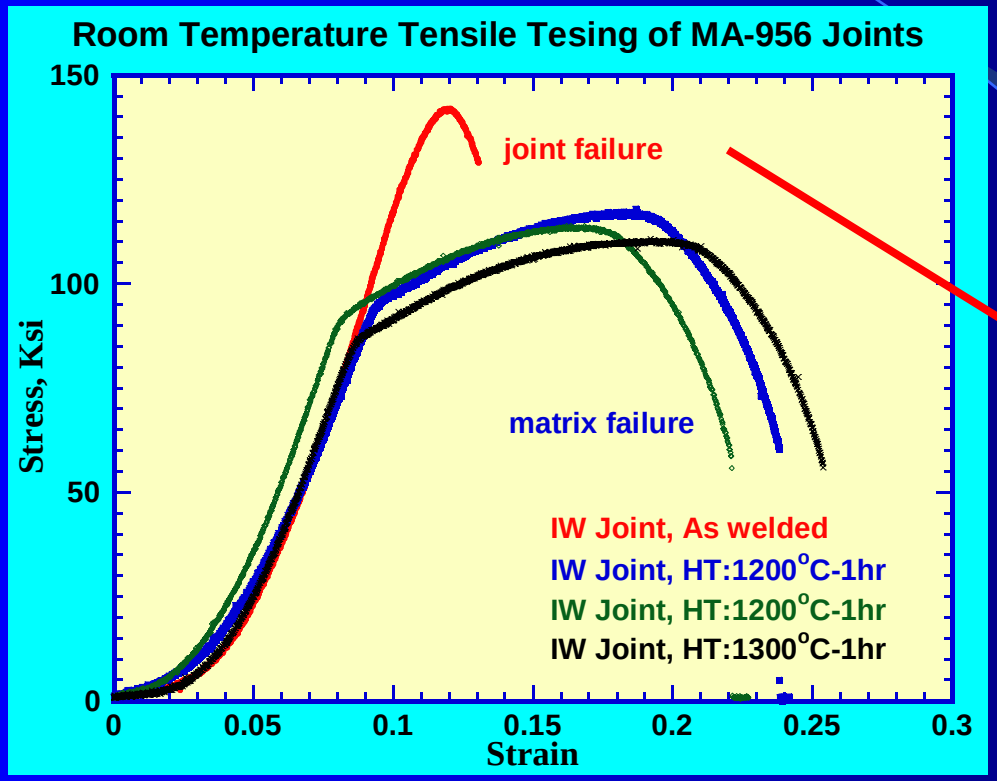

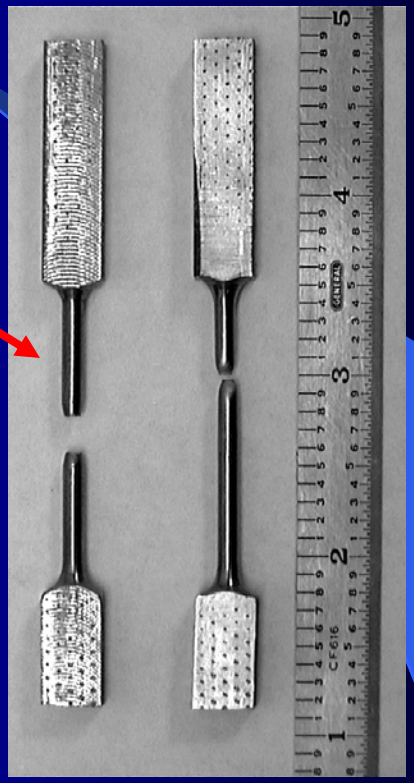

In as-welded condition: joint fails at about 90% of the unrecrystallized matrix strength

In the prescribed recrystallized end-use condition: joint is far superior than the matrix

Joint Deformation and Failure

As-welded, RT tensile test

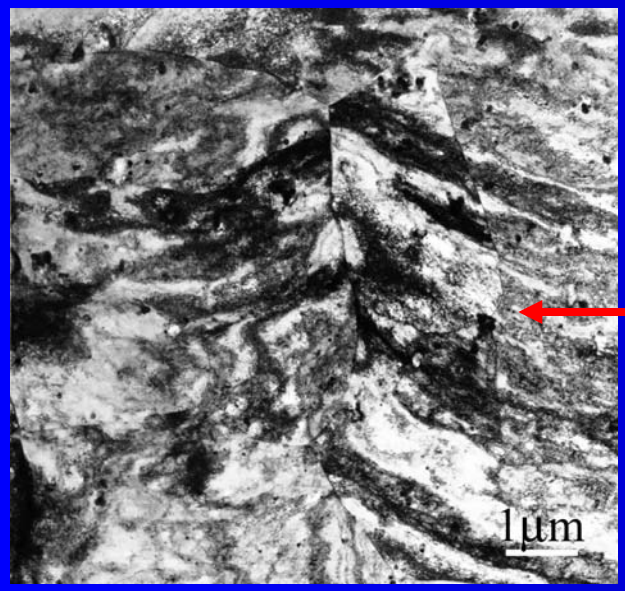

Cross-sectional view

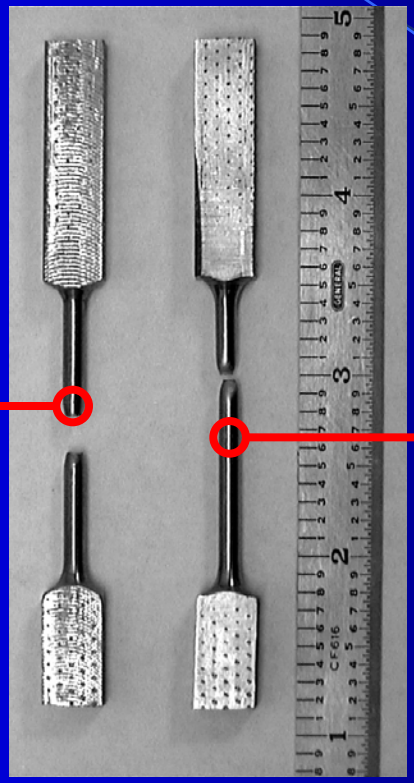

HT:1200°C-1hr, RT tensile test

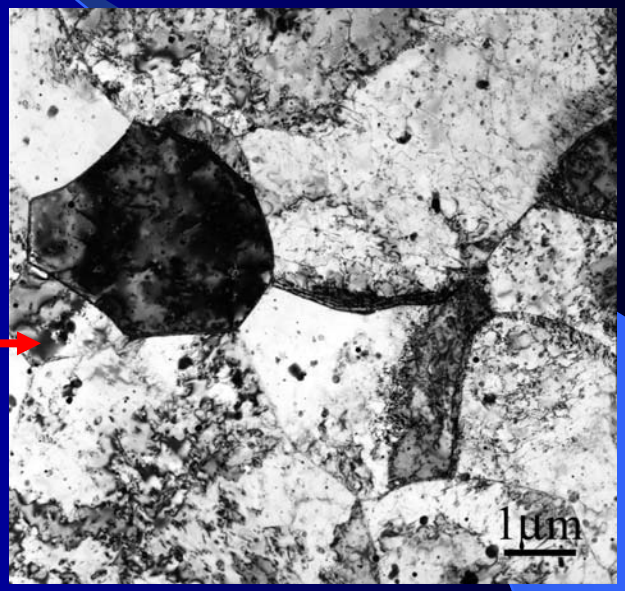

Cross-sectional view

As-welded condition: joint fails with severe deformation bands. Traces of grain flow suggests failure some distance away from interface.

Heat-treated condition: Joint region has the nominal deformation/dislocation activity.

High Temperature Longitudinal Response

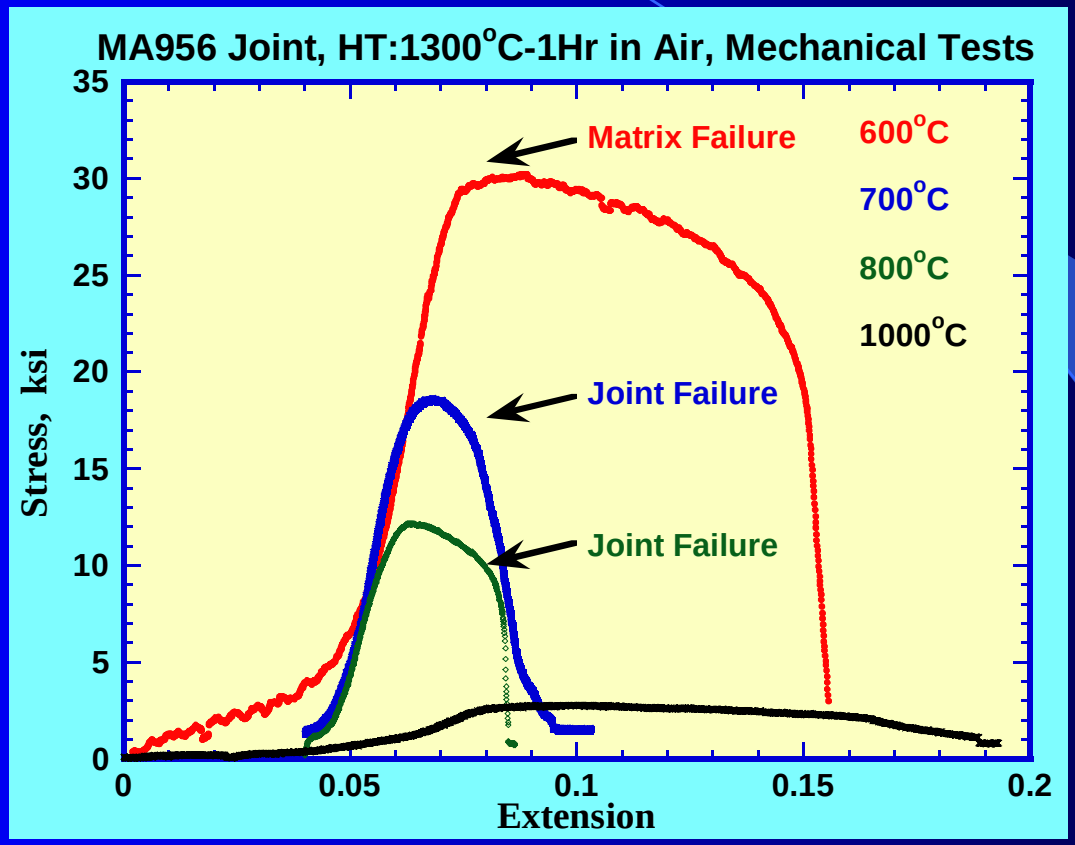

Joint sections heat-treated at 1300°C –1hr in air. Longitudinal joint sections are tested for high temperature integrity. At 600°C and below failure occurs in the recrystallized matrix. At 700°C and above failure occurs in the unrecrystallized joint regions.

Inertia Welded Joint
Creep Response: HAZ scale effects

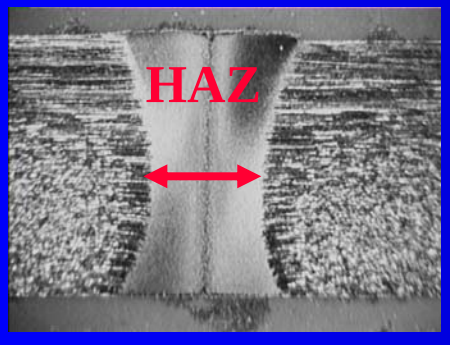

Sample	IW#7	IW#8
IW upset	0.195”	0.343”
HAZ	1-1.5mm	2.5-3mm
Stress	2ksi	2ksi
Creep rate	$4x10^{-4}$	$4.6x10^{-3}$
Creep strain	<1%	4%
L-M Para	47.54	42.72

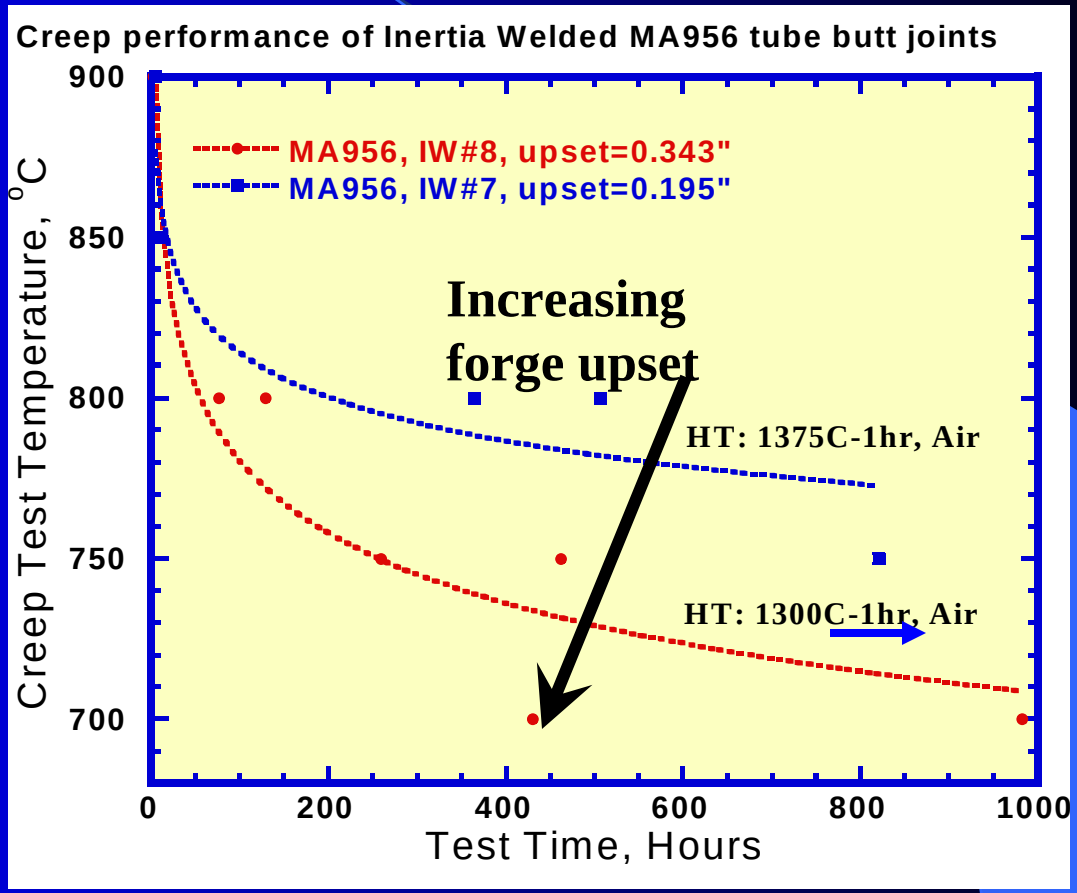

HAZ dimension control - promising

Inertial Welding: Challenges & Opportunities

1) best suitable for thick walled tubing

2) Joint about 100°C weaker than base microstructure creep response

3) benefit of contact aspect ratio (Δ/t), Δ=HAZ length, t=wall thickness

4) Δ/t reduced by manipulating energy input & forge upset parameters

5) Δ/t reduced by artificially increasing t by flaring and/or flange formation

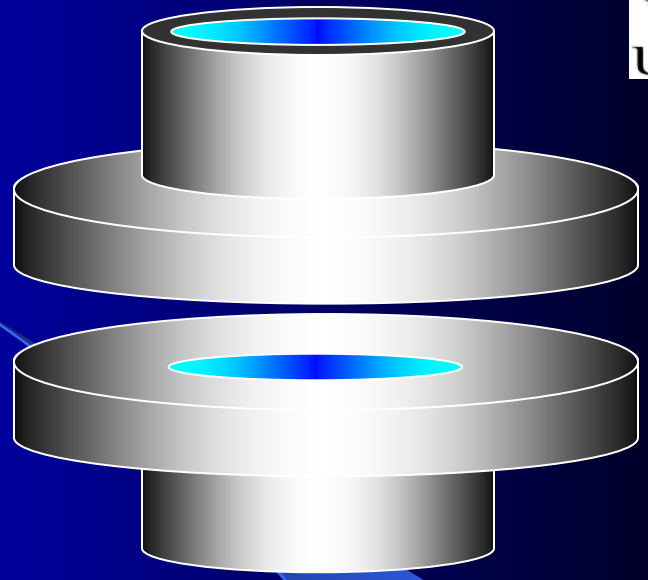

Inertia weld flange-to-flange joint

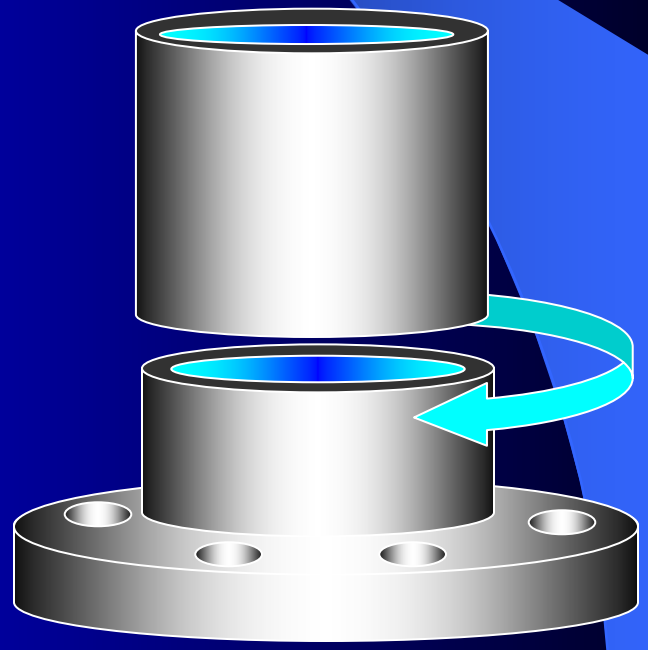

Inertia weld tube-to-flange joint

Magnetic Pulse Welding (MPW)

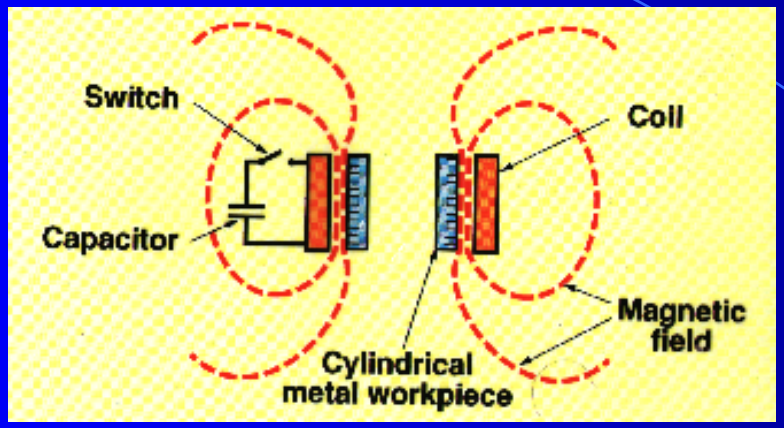

MA956 hollow tube onto 1018 steel rod

1018 steel core too soft, deforms but no weld!

MPW: MA956 tube on tube test protocol

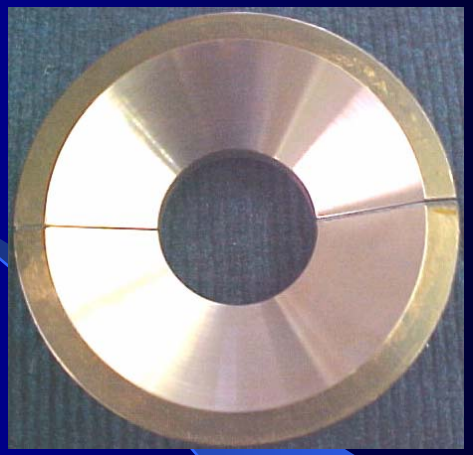

Inner Tube Assembly

Outer Tube Assembly

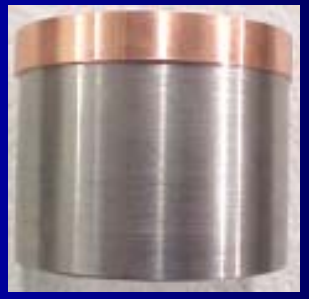

40kJ

52kJ

78kJ

78kJ

98kJ

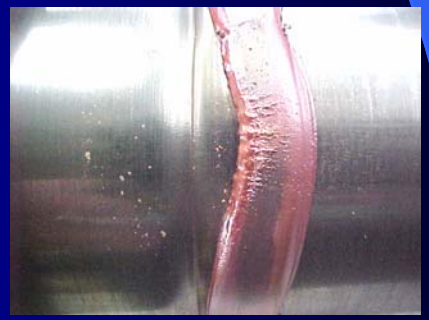

Magnetic Pulse Welding: Challenges & Opportunities

1) suitable for thin walled tubing; weld width scales with wall thickness

2) mandrel material choice is critical!

3) Substantial Air gap (Δ)=2t is required

4) Field fitted lap tubes/ rings promising for repair function.

5) End cap joining most promising for bayonet type heat exchanger design.

6) Combine IW & MPW process for optimum performance

Pulse welding of end caps

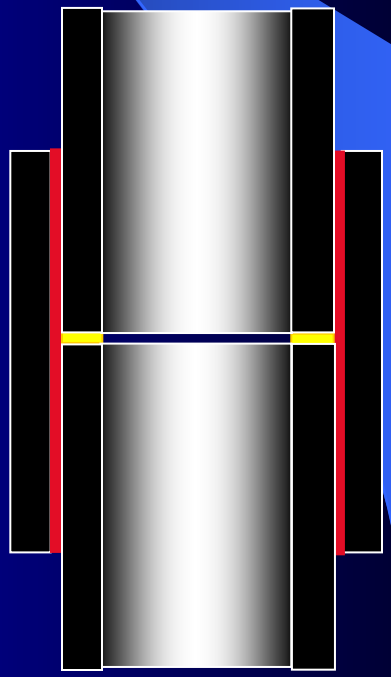

Combined IW + PMW joint

Creep Comparison for ODS-Materials

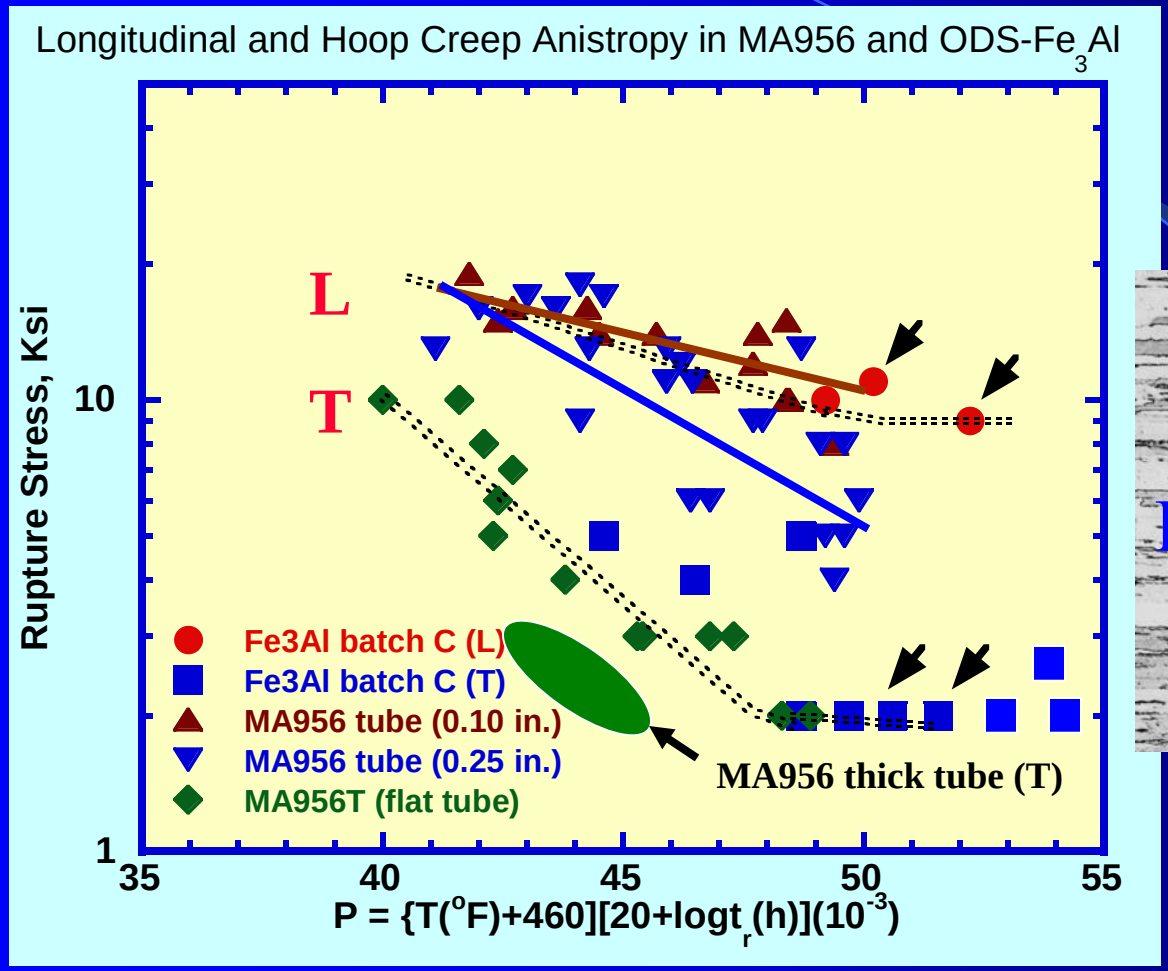

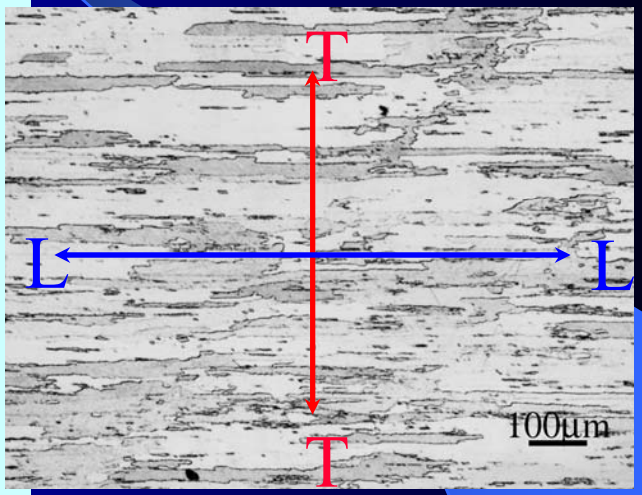

i) L superior than T

ii) ODS-Fe_3Al superior than MA956

iii) Thin walled MA956 better than thick walled MA956

Application Range for ODS Alloys

Objective: to improve the limited hoop creep performance of ODS-Alloys

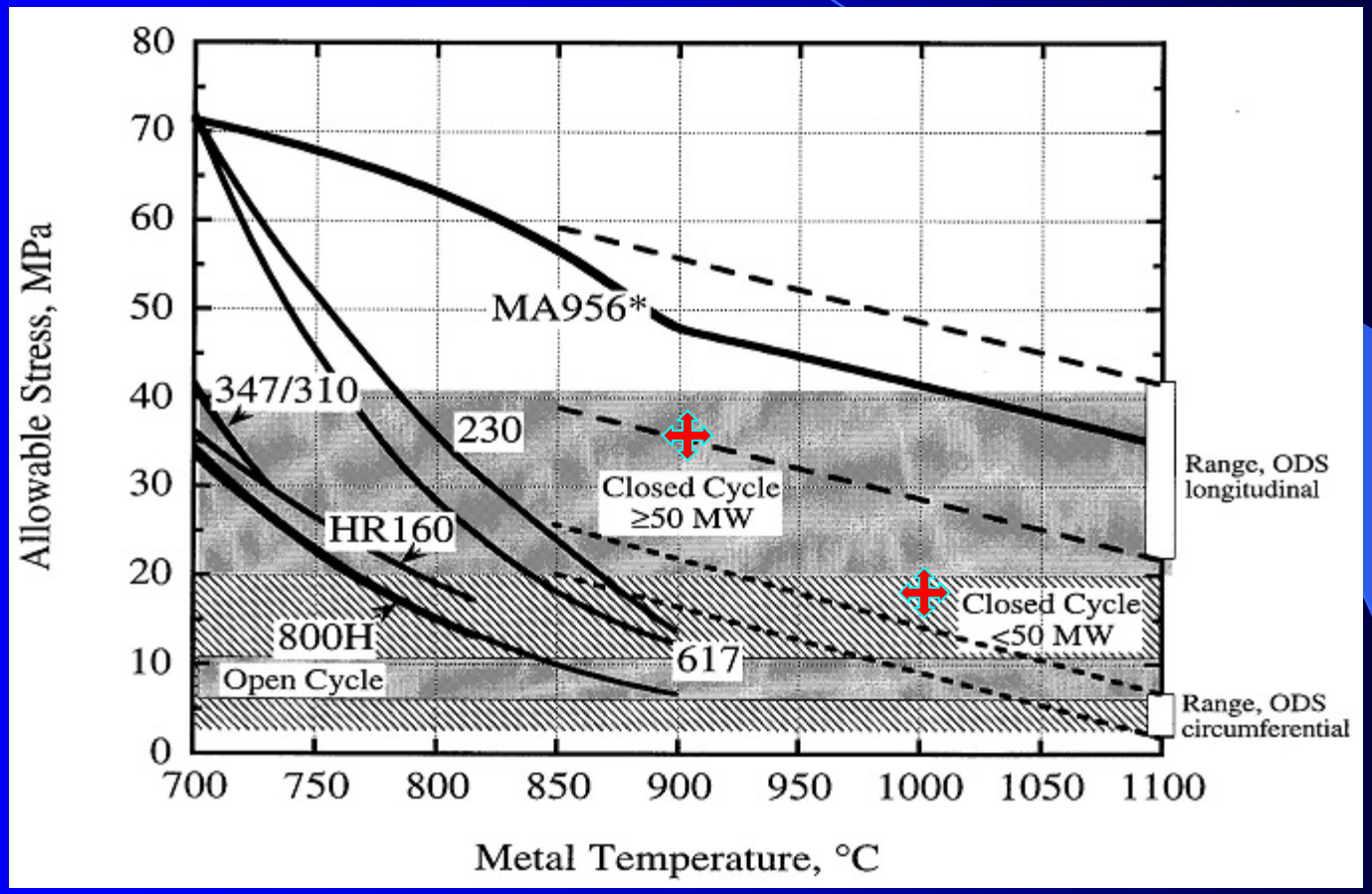

Current hoop performance metrics for ODS-Fe_3Al Alloys

Improvements in ODS-Fe_3Al Hoop Creep

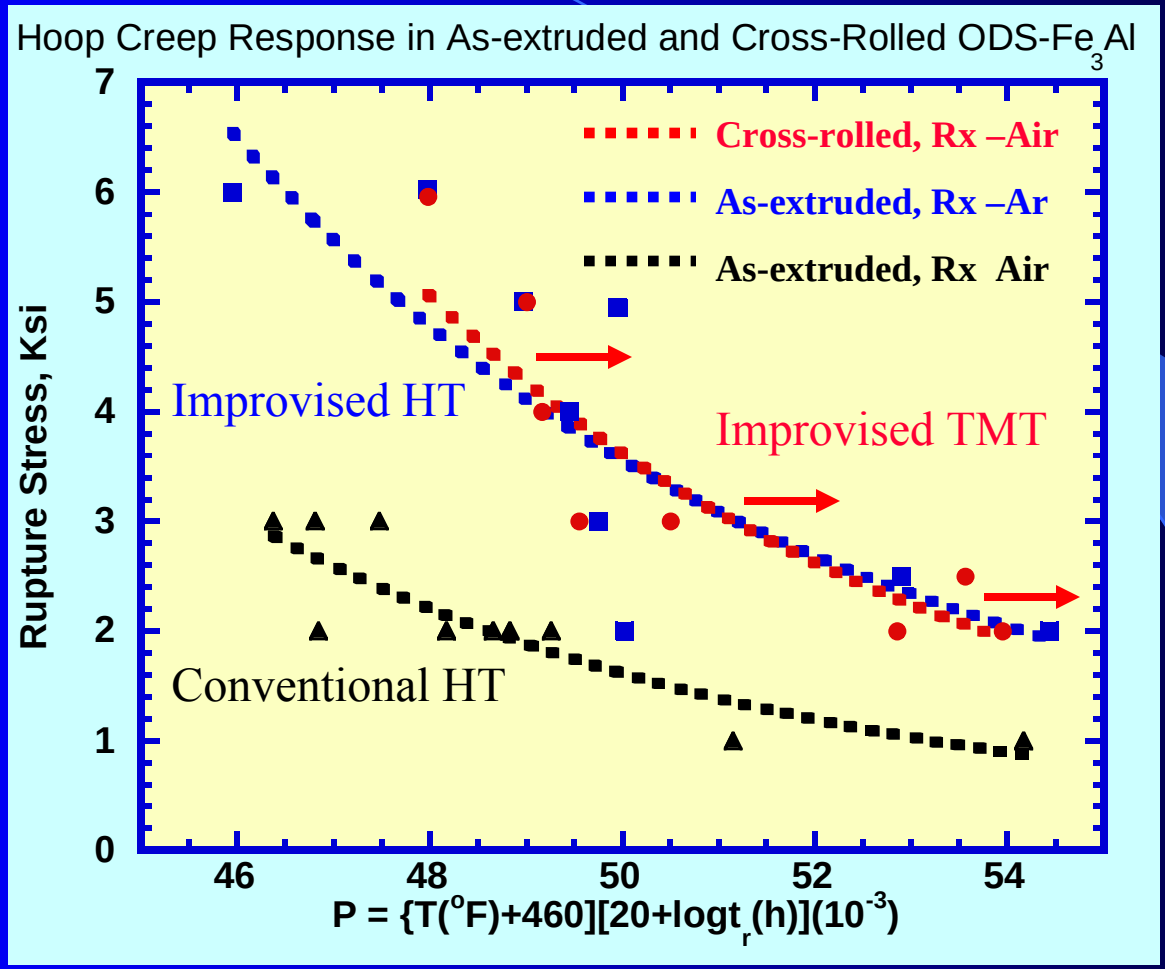

Hoop creep response is improved by control of recrystallization environment and temperature. Tests of cross rolled materials show significant improvements.

Grain realignment in the hoop direction

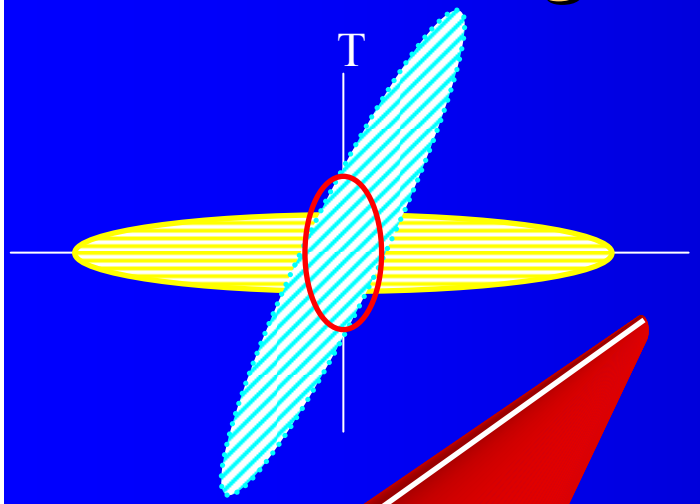

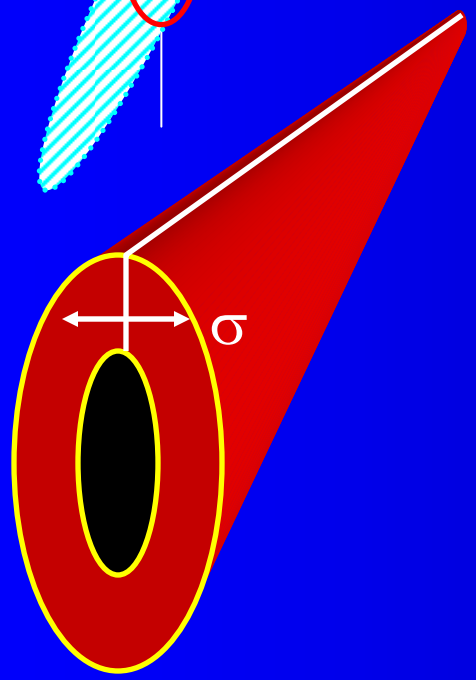

As processed grain boundaries normal to hoop loading axis

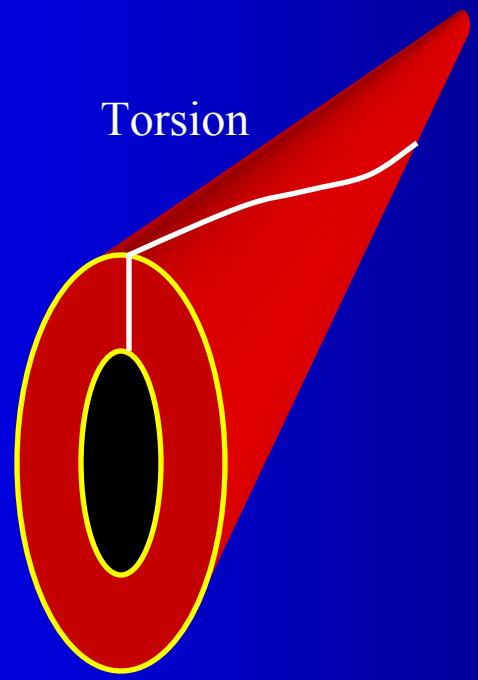

Grain realignment along length of tube

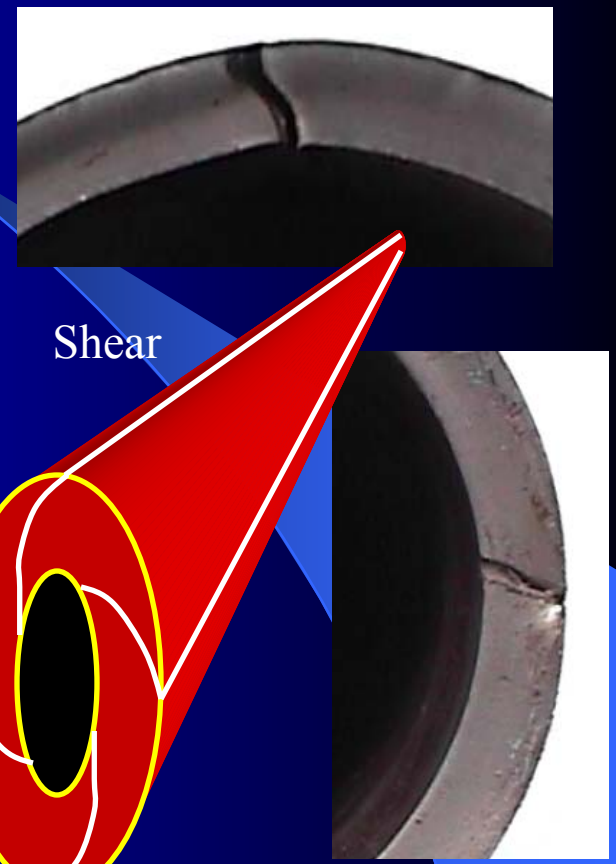

Grain realignment along radius of tube

Cross rolling technique

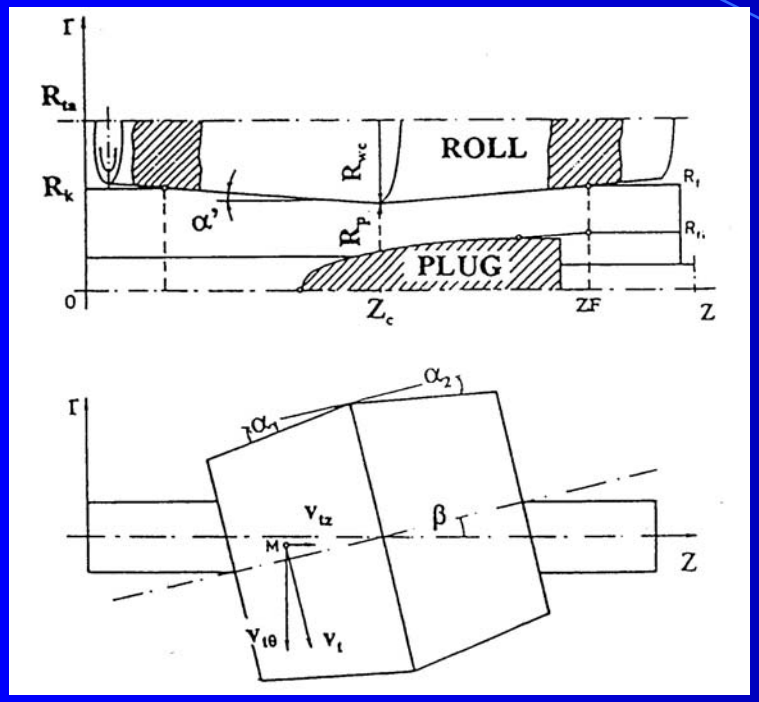

$$V_{tz} = V_t \sin\alpha = \omega R_{\omega z} \sin\beta$$

$$V_{t\theta} = V_t \cos\alpha = \omega R_{\omega z} \cos\beta$$

Grain shapes can be altered via torsion techniques.

Such helical grain modification is anticipated to improve hoop creep response.

<u>Improved Grain Aspect Ratio</u>

Grain Shape Changes via Cross Rolling

As-processed grain size

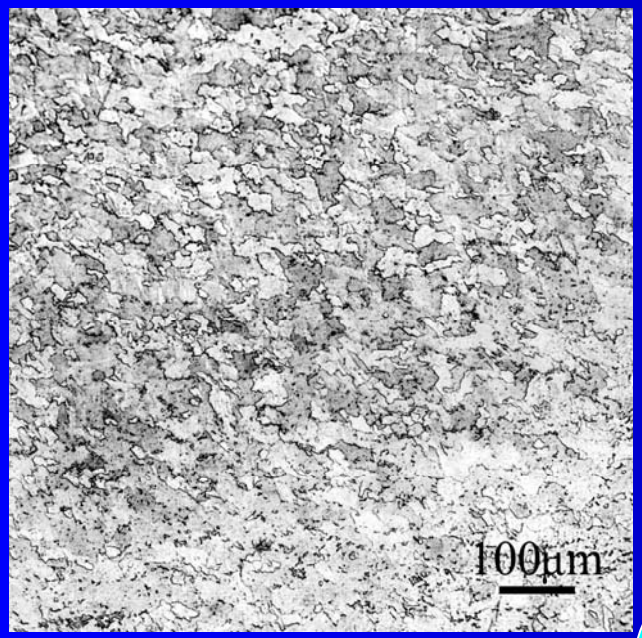

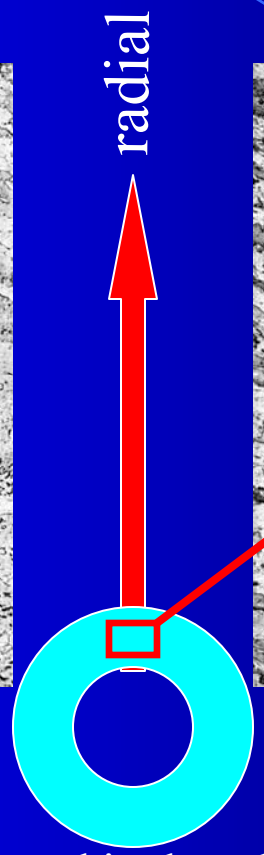

Cross rolled grain size

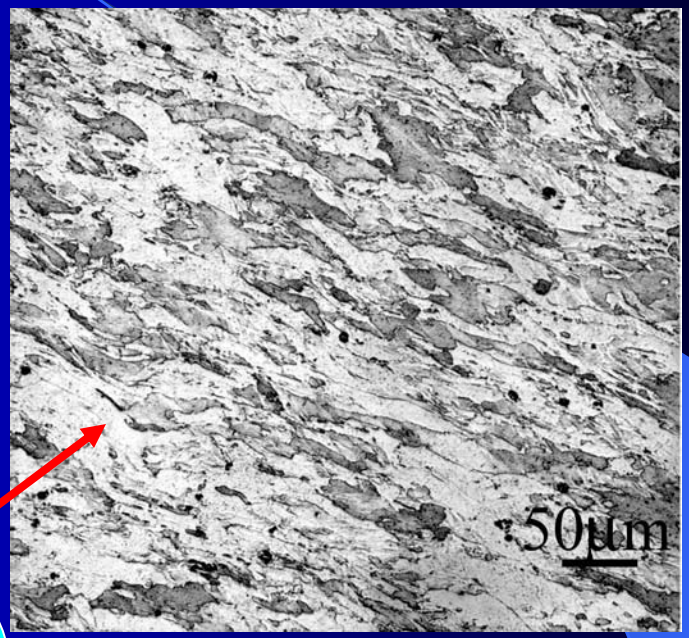

The as-extruded grain shape as viewed in the tube cross-section is roughly equi-axed. On cross-rolling the grain aspect–ratio is significantly enhanced in the hoop direction

Hoop Creep of Grain Modified MA956 Tubes

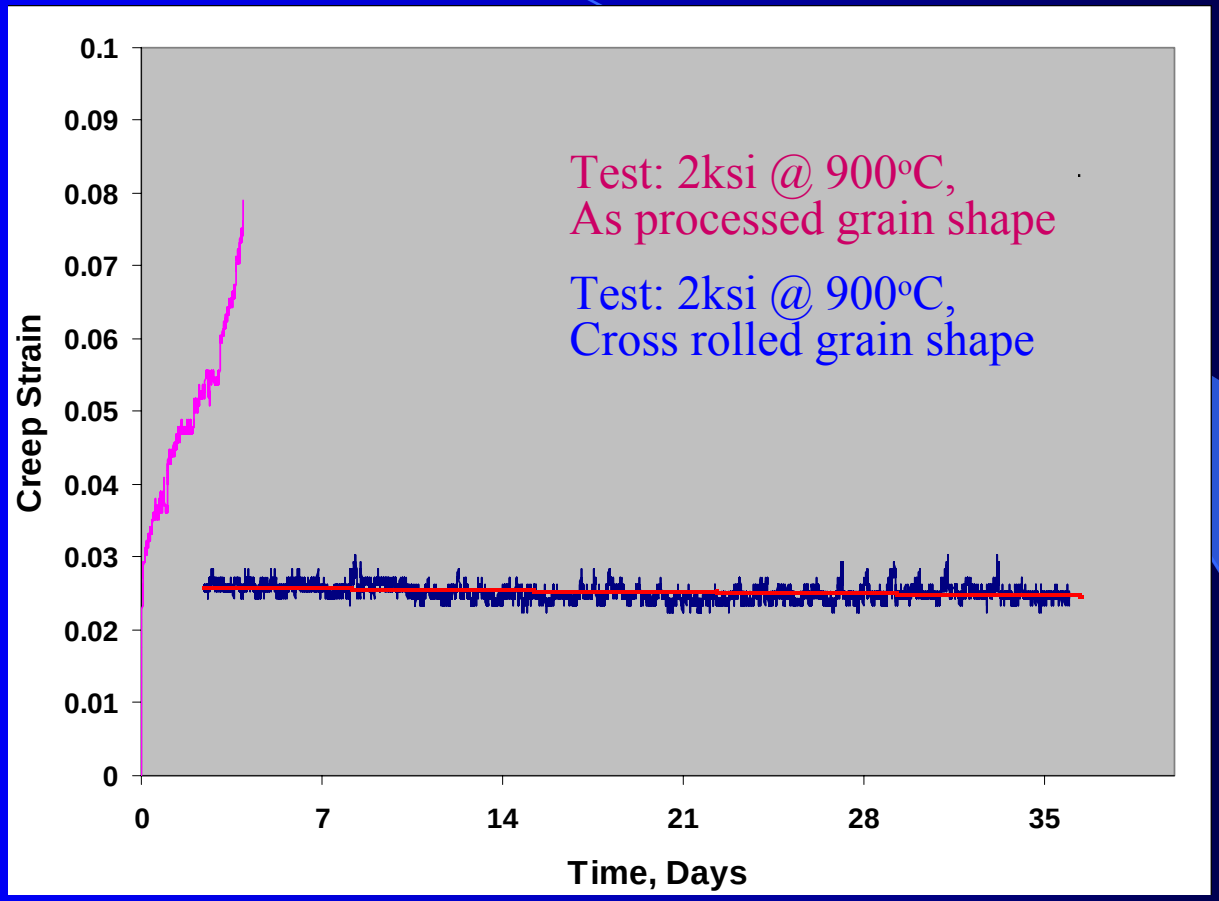

Hoop creep testing of cross-rolled MA956 tube shows a firm performance enhancement in comparison to the as-received tube. L-M Parameter improved from 45 to 49 (till date).

Summary of Results

- A firm threshold established for ODS-Fe_3Al transverse creep tested at 2Ksi at 1000°C. L-M parameter>54.4 at 2Ksi and >54.0 at 2.5Ksi
- Recrystallization environment play a dominant role in improving hoop creep response.
- Grain fibering offers significant hoop creep enhancement
- Non fusion joining methods still being developed – for specific joint configurations via IW and MPW techniques.

Recrystallization Microstructures

Transverse view

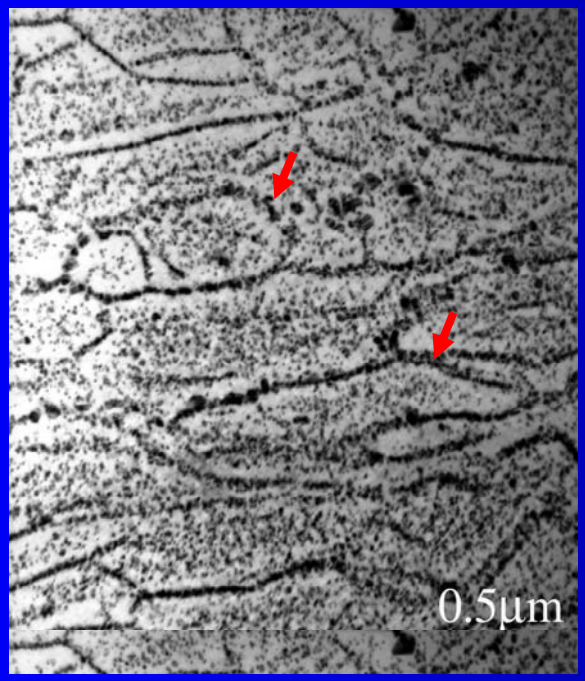

Longitudinal view

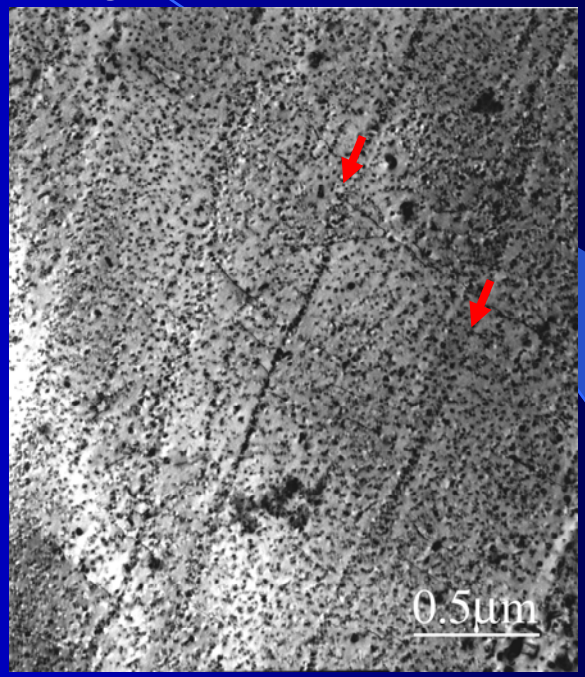

Specimens extracted from the high purity powder chemistry (PMWY-3) heat-treated tubes (HT: 1200°C-1hr in Air). Red Arrows indicate prior particle boundaries in transverse and longitudinal views

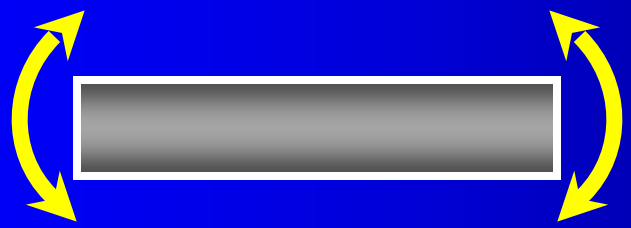

ODS tube

Header

British Gas ‘Harp’ Joint

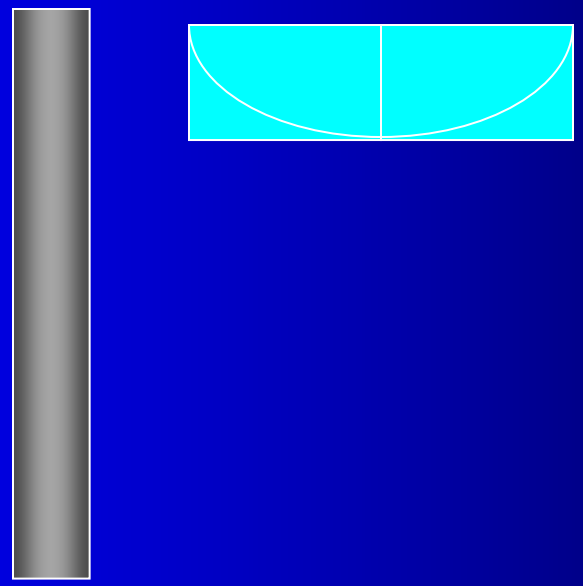

Reduction in Defect Content in ODS Alloys

THE UNIVERSITY of LIVERPOOL

J.Ritherdon and A.R.Jones

University of Liverpool

1. Recrystallisation behaviour in a PM2000 variant alloy

2. PM2000 tube torsion tests

- Trials at ORNL
- subsequent recrystallisation behaviour

3. Initial PM2000 tube torsion forming trial

- Forécreu, France

Recrystallisation in PM2000 variant alloy

THE UNIVERSITY of LIVERPOOL

1. Aim

Investigate recrystallisation behaviour in ODS alloys:

(i) with controlled Y_2O_3 - free regions introduced

ODS Fe_3Al

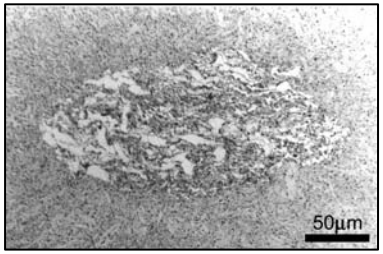

As-extruded / 1050^0C

(ii) with mild steel container (large Y_2O_3 - free region) retained during post-consolidation processing

2. **Alloy fabrication**

PM2000 alloy + 1wt.% ODS-free Fe powder
(25 µm< 100% <300µm; 127µm mean)

Recrystallisation in PM2000 variant alloy

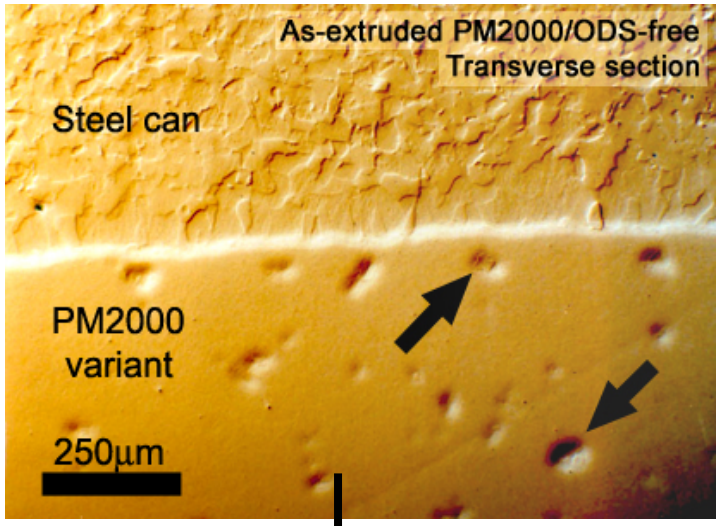

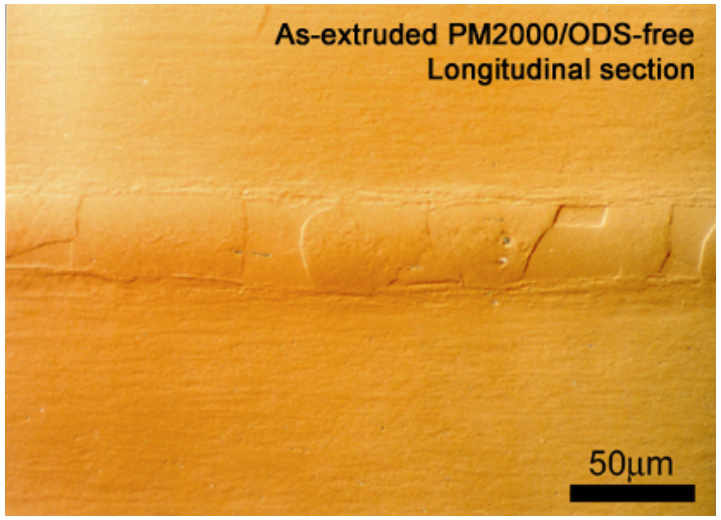

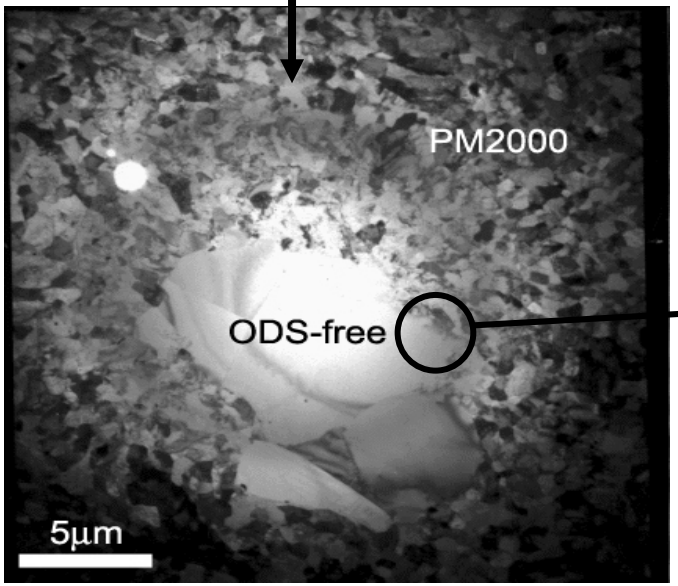

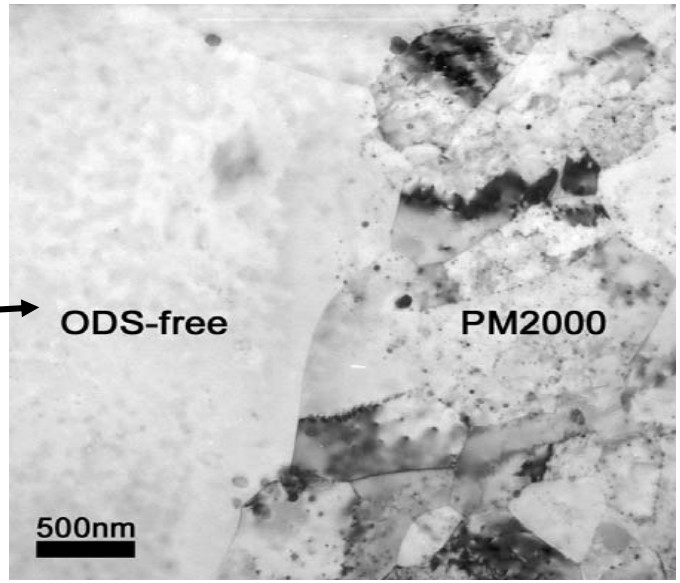

Recrystallisation in PM2000 variant alloy

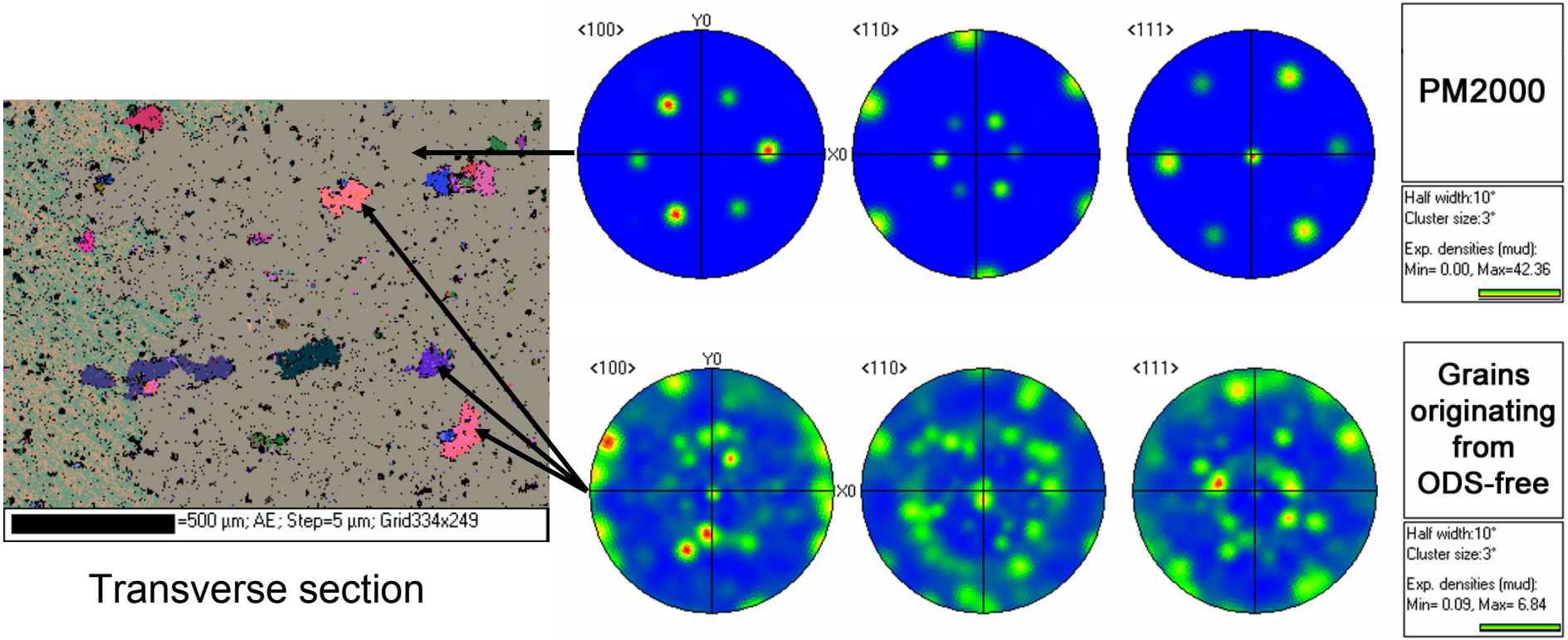

Transverse section

PM2000 + 1%Fe: consolidated (9:1 extrusion ratio / 1050^{0}C) + 1380^{0}C / 1h

Recrystallisation in PM2000 variant alloy

THE UNIVERSITY of LIVERPOOL

In the as-extruded alloy:

$\mathbf{T_{Rex}}$ ODS-free FeCrAl << $\mathbf{T_{Rex}}$ PM2000 ⇒ { Rex. as separate 'phases' / Hence limited Rex. interaction

To increase interaction during recrystallisation:

$\mathbf{T_{Rex}}$ ODS-free FeCrAl ↑ —ε_p ↓→ 'critical strain annealing'

$\mathbf{T_{Rex}}$ PM2000 ↓ —ε_p ↑→ increase cold work

Recrystallisation in PM2000 variant alloy

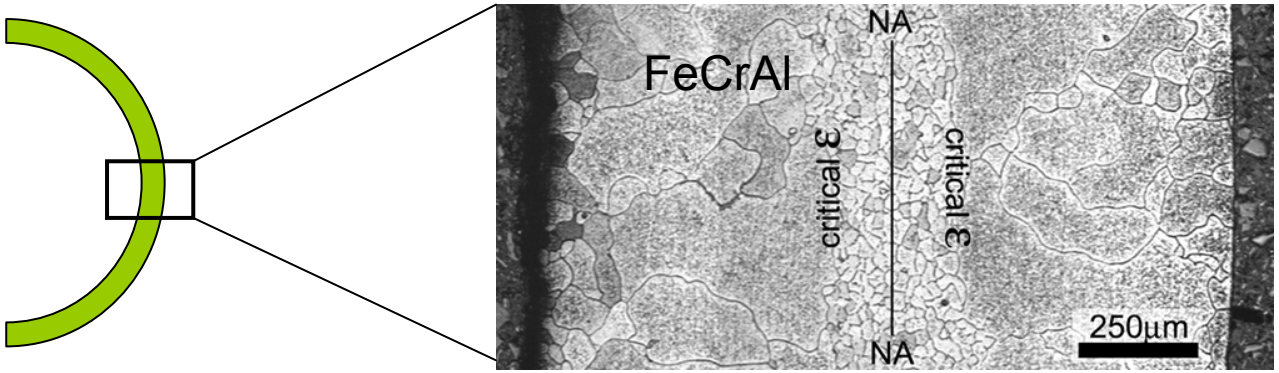

Deformation / annealing schedule

As extruded PM2000/ODS-free	+	cold roll ~ 26% (R_A))	+	1100^{0}C/1h	+	bending strain (~0.04)	+	Anneal > 1200^{0}C

PM2000 ⇒ recovery

1% FeCrAl ⇒ Rex.

Recrystallisation in PM2000 variant alloy

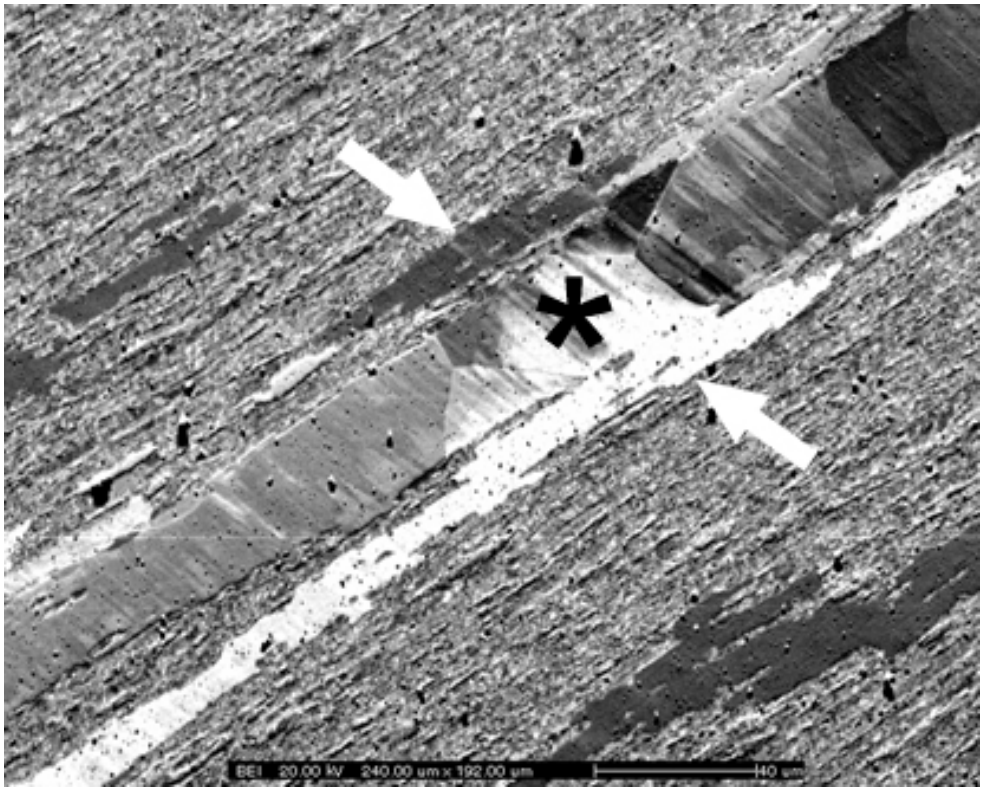

PM2000/ODS free - longitudinal section

As-extruded + cold rolled 26%

+ annealed 1100ºC/1hour

+ bent round former to ID20mm

+ annealed 1200ºC/15min

Recrystallised grains originating in ODS-free region (*) grow into surrounding unrecrystallised PM2000 (arrowed). Orientations confirmed by EBSD analysis. Grains grow preferentially parallel to the extrusion direction.

Recrystallisation in PM2000 variant alloy

THE UNIVERSITY of LIVERPOOL

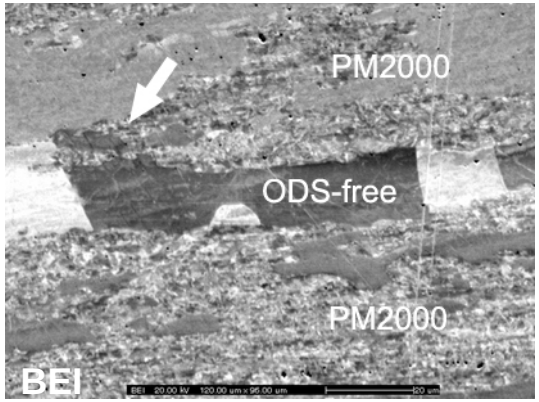

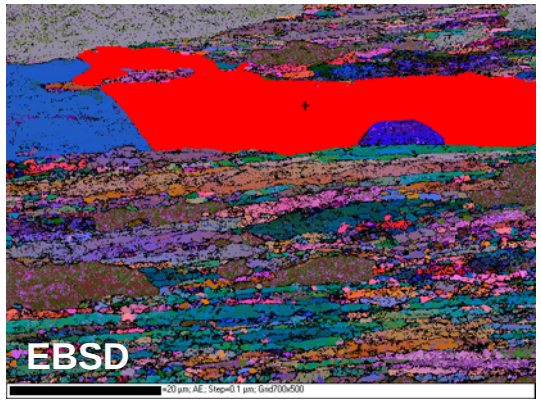

100µm

PM2000/ODS free - longitudinal section

As-extruded + cold rolled 26%

+ annealed 1100ºC/1hour

+ bent round former to ID20mm

+ annealed 1300ºC/5min

Grains originating in ODS-free stringer migrating into PM2000 during annealing

Recrystallisation in PM2000 variant alloy

THE UNIVERSITY of LIVERPOOL

PM2000/ODS free - longitudinal section

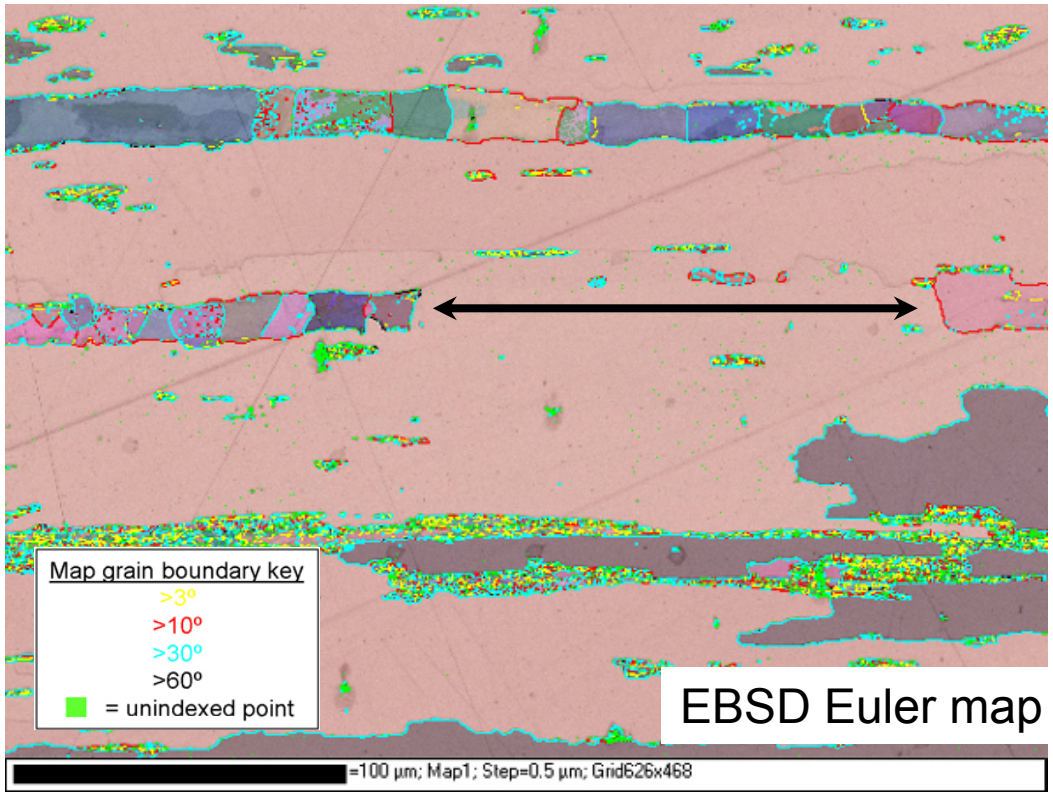

EBSD map of a large Rex. grain extending through an ODS-free region (arrowed) into PM2000 either side (longitudinal section).

As-extruded + cold rolled 26%

+ annealed 1100ºC/1hour

+ bent round former to ID20mm

+ annealed 1300ºC/15min

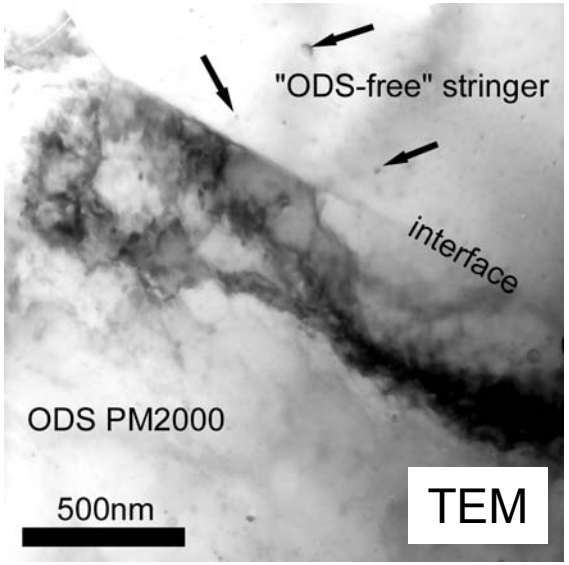

PM2000 / ODS-free interface migration into surrounding PM2000 at ~8µm.h^{-1}

Y_2O_3 particles (arrows) now located within recrystallised grain.

Recrystallisation in PM2000 variant alloy

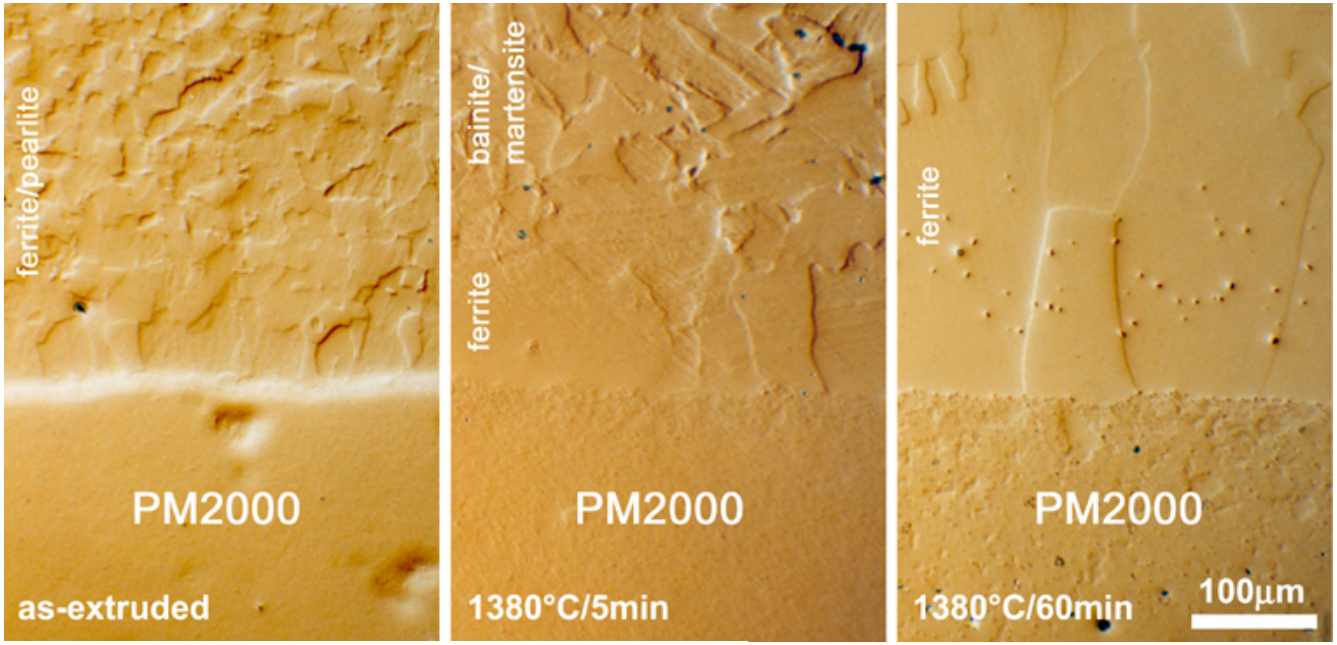

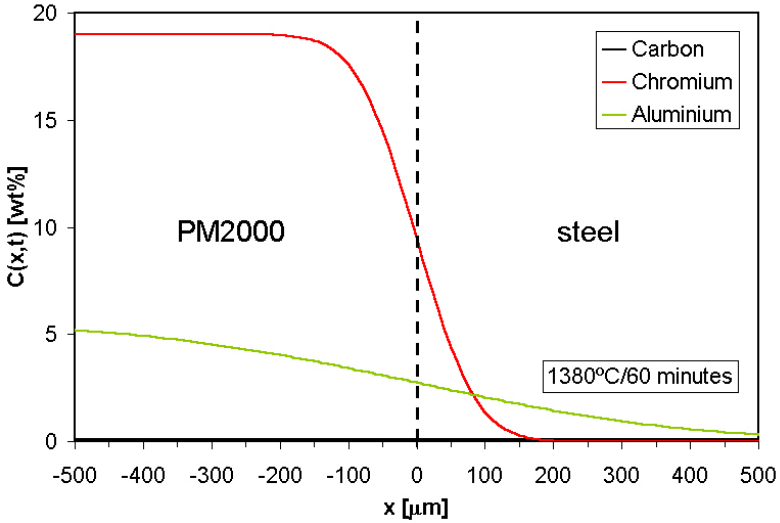

In the consolidated billet, further annealing causes Al, Cr to diffuse from PM2000 into the mild steel can.

The ambient microstructure in the extrusion can varies with distance from the PM2000/can interface.

The can microstructure adjacent to the PM2000 changes from transformable ferritic/pearlitic to stable ferritic.

Recrystallisation in PM2000 variant alloy

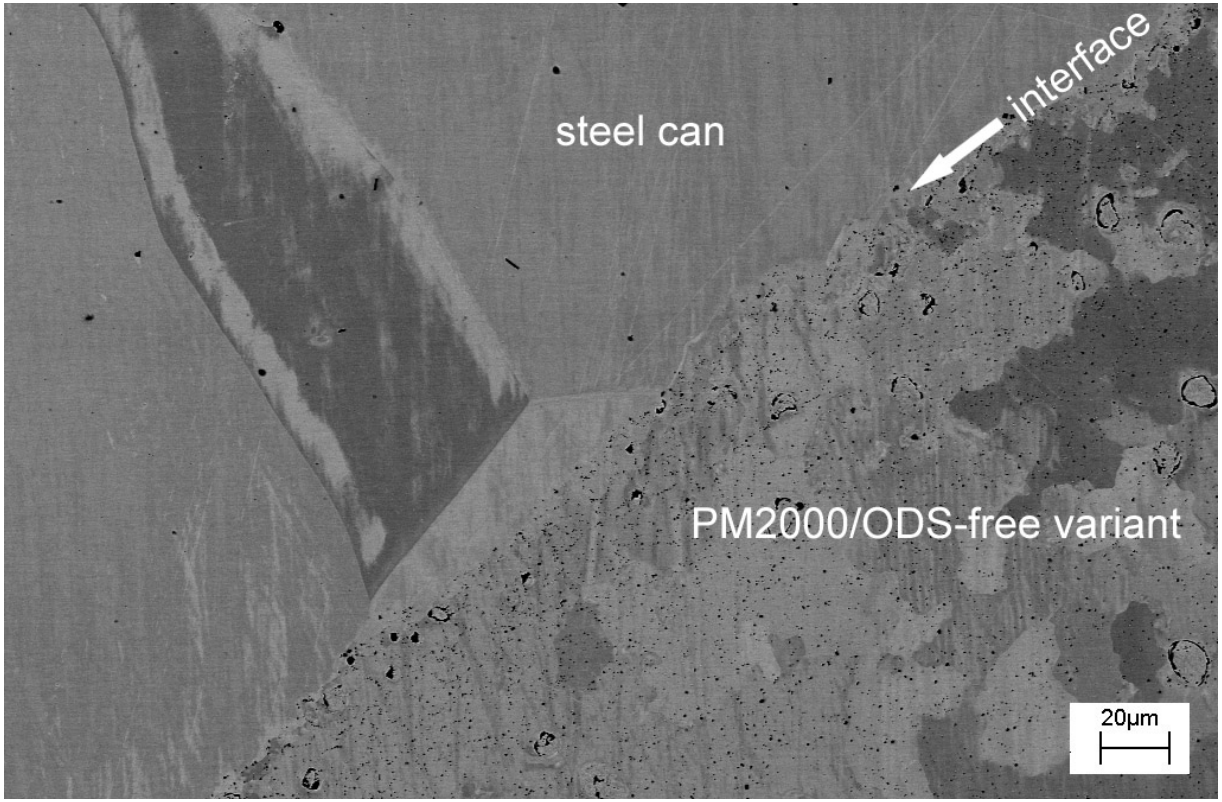

Cold rolled by 26% → Annealed 1100ºC/1hour →
Bent to ID20mm → Annealed 1200ºC/1 hour

No recrystallisation interaction found between the steel can and the PM2000.

PM2000 tube torsion tests

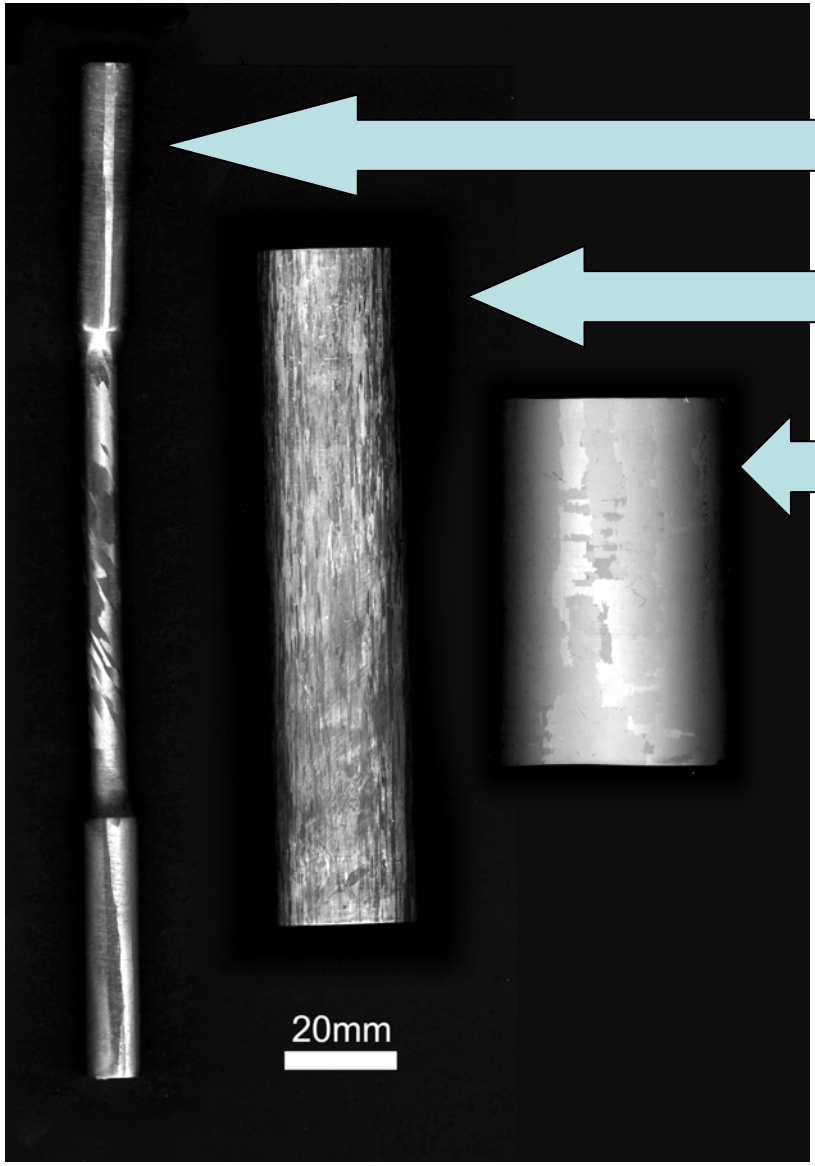

Hot torsion bar

Standard tube

Flow formed tube

Significant grain reorientation possibilities.
But tendency to through wall variation in:

- grain size
- grain orientation
- aspect ratio

PM2000 tube torsion tests

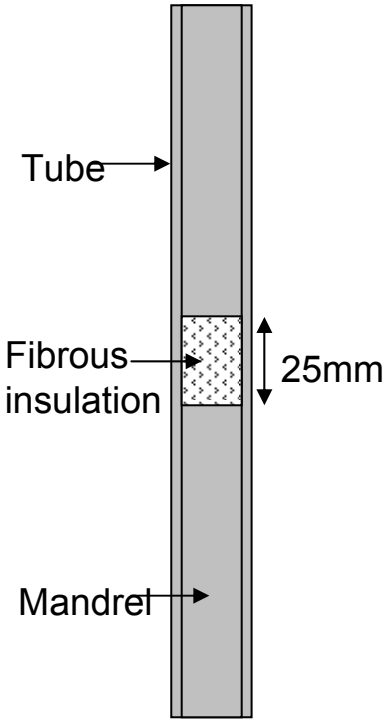

Schematic cross section

PM2000 tubes (9) subject to torsion trials at ORNL.
Test variables: $T^{o}C$; γ; γ_{Tot}; σ_{axial}; support mandrel

Tube: 200mm long x 25mm ∅ x 2.5mm wall

PM2000 tube torsion tests

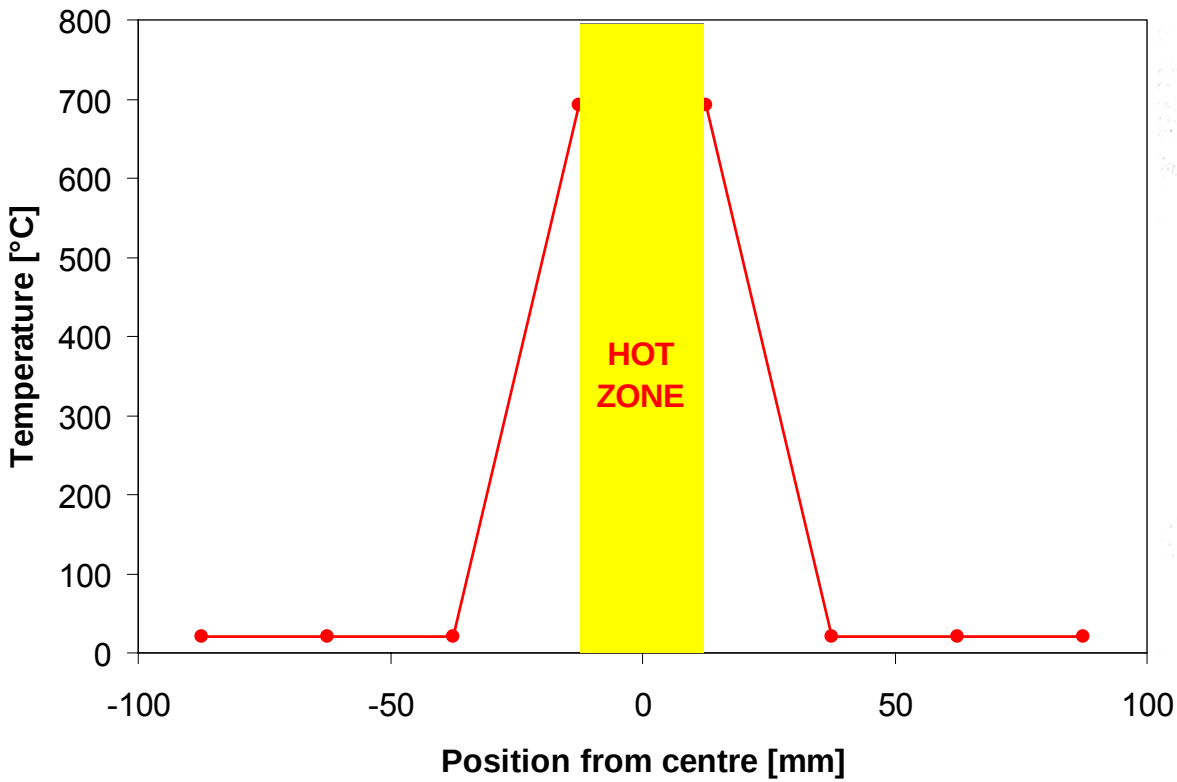

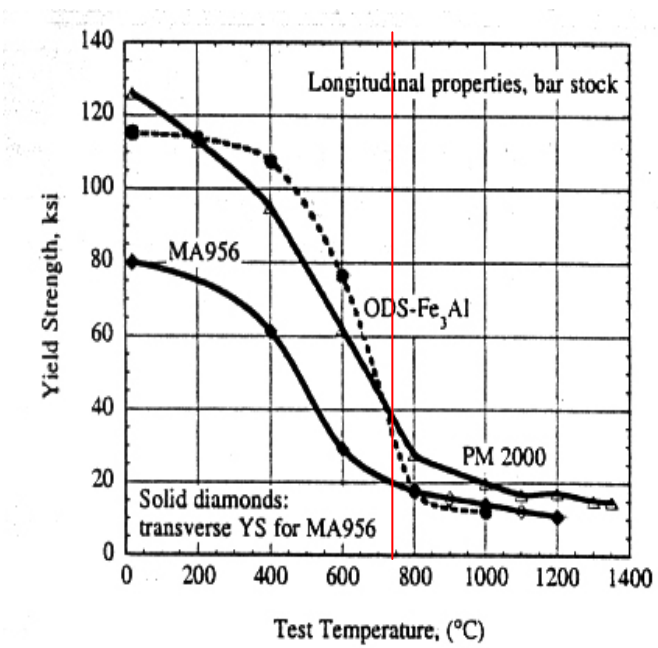

PM2000 tube torsion tests

Test Parameters			
	Torsion[3] / twisted length [º / mm]	**Inclination θ**	**Temp. [ºC]**
Tube 1	83 / 25	36º	750
Tube 2	123 / 25	47º	750
Tube 3[1]	119 / >25	~47º	750
Tube 4	160 / 50	35º	750
Tube 5[2]	80 / 25	35º	750
Tube 6	80 / 25	35º	750
Tube 7	80 / 25	35º	675
Tube 8	160 / 25	55º	750
Tube 9	95 / 25	40º	750

Notes:
1. 100mm support Mandrel
2. superimposed Axial strain (0.08)
3. torsion rate (0.12°.s^{-1})

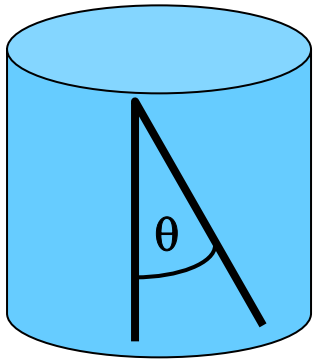

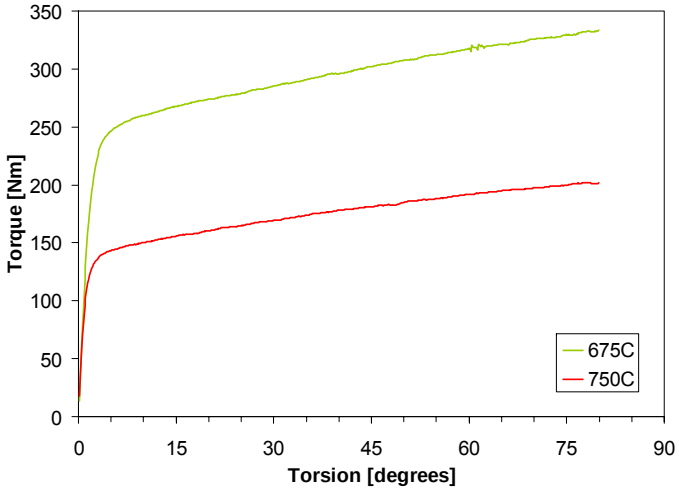

PM2000 tube torsion tests

THE UNIVERSITY of LIVERPOOL

160^0/ 50mm; $\theta = 35^0$

+

SR @ 1380^0C / 1h

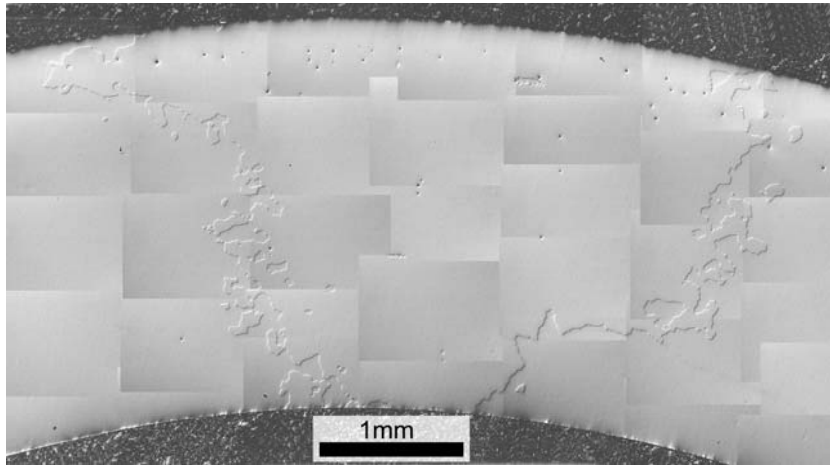

Transverse section

PM2000. Warm flow formed 72% (R_A)
Secondary recrystallisation 1380^0C / 1h

PM2000 tube torsion tests

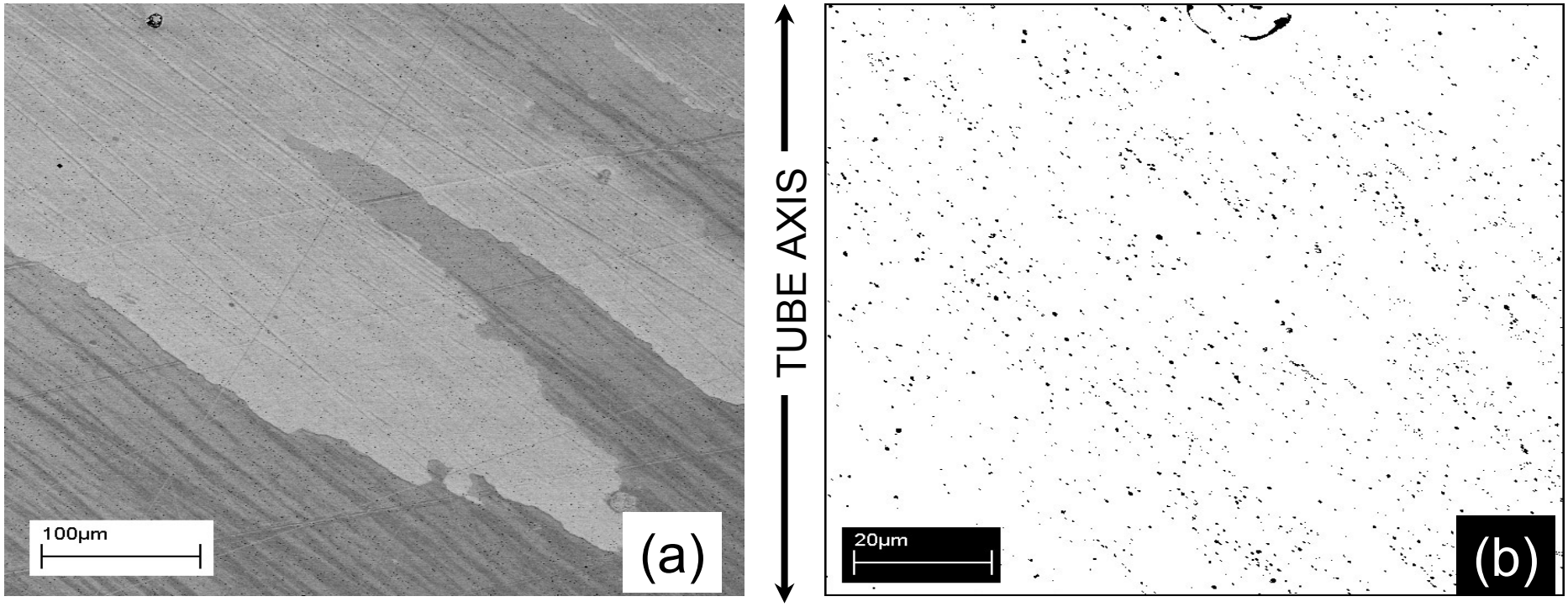

(a) SEM image of helically orientated grain growth in Tube 4.

(a) SEM image manipulated to reveal the helical distribution of oxide particles.

PM2000 tube torsion tests

Tube 5 : 1380'C/1h

80^0 / 25mm + σ_{Axial}

$\theta = 35^0$

75mm

Tube 8 : 1380'C/1h

160^0 / 25mm

$\theta = 55^0$

PM2000 tube torsion tests

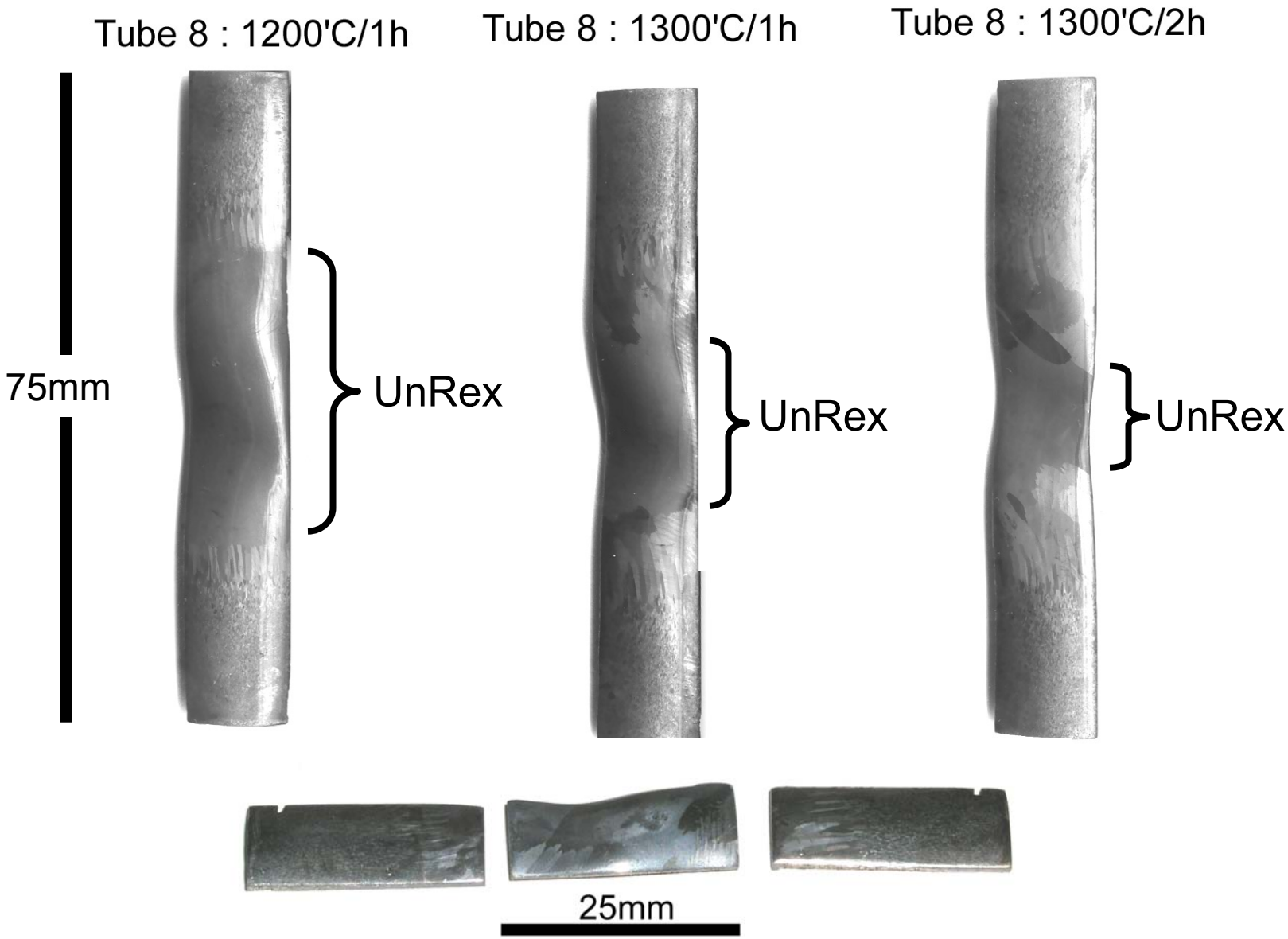

PM2000 tube torsion forming trial

Forécreu, Commentry, France

Manufacture special metallurgical profiles using: extrusion / drawing / twisting

Profiles up to 5m in length, 65mm ∅, with 1-3 (typically) straight / twisted axial coolant holes

High speed steels, tool steels etc

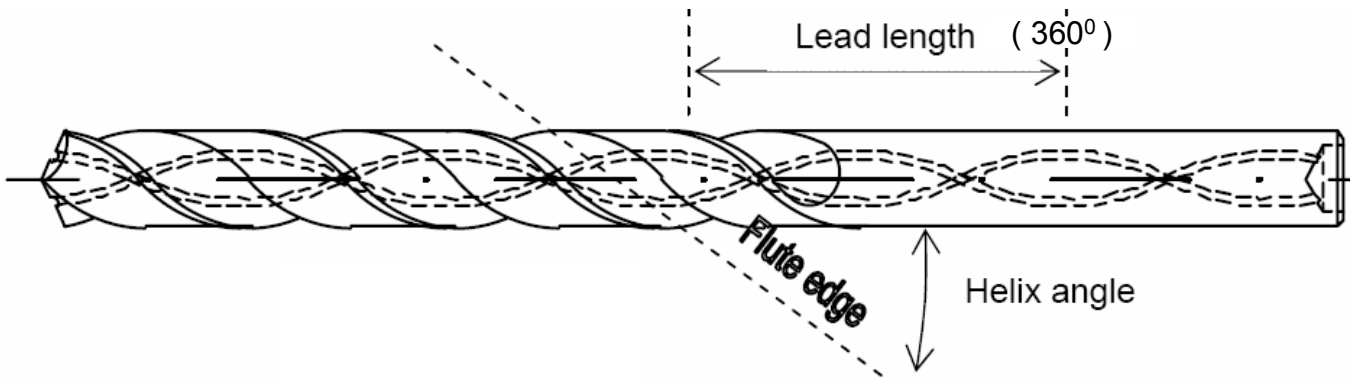

Schematic: drill made from Forécreu profile

PM2000 tube torsion forming trial

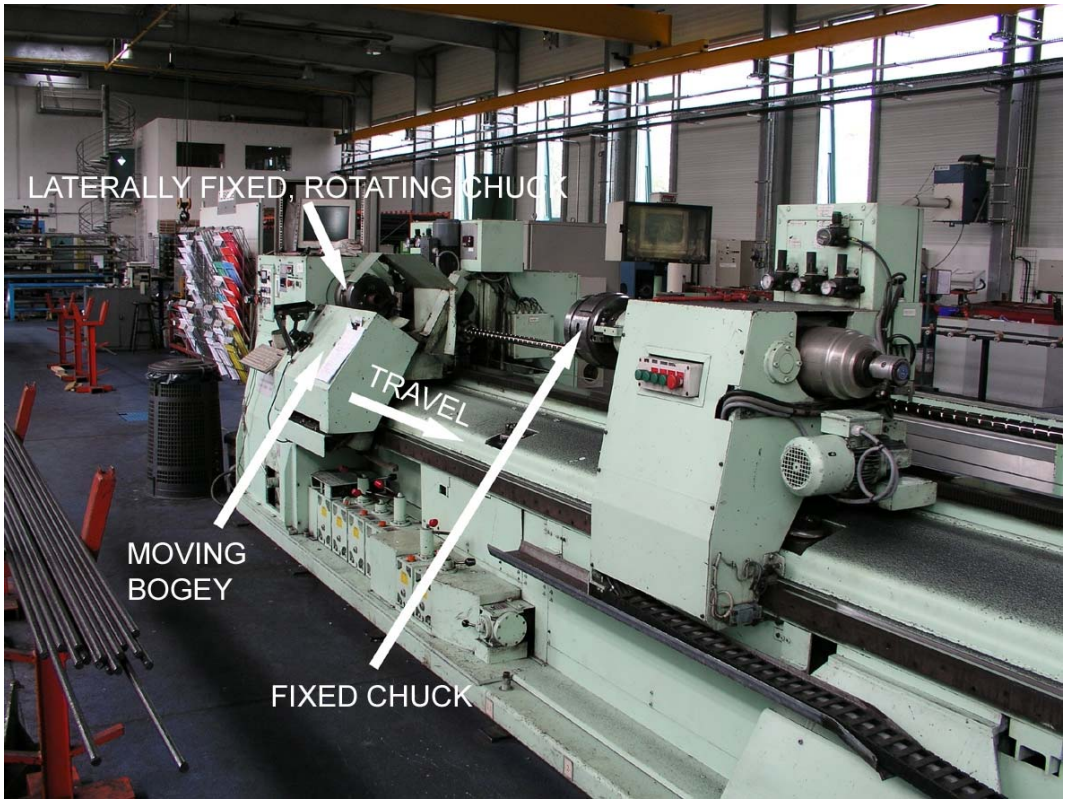

PM2000 tube torsion forming trial

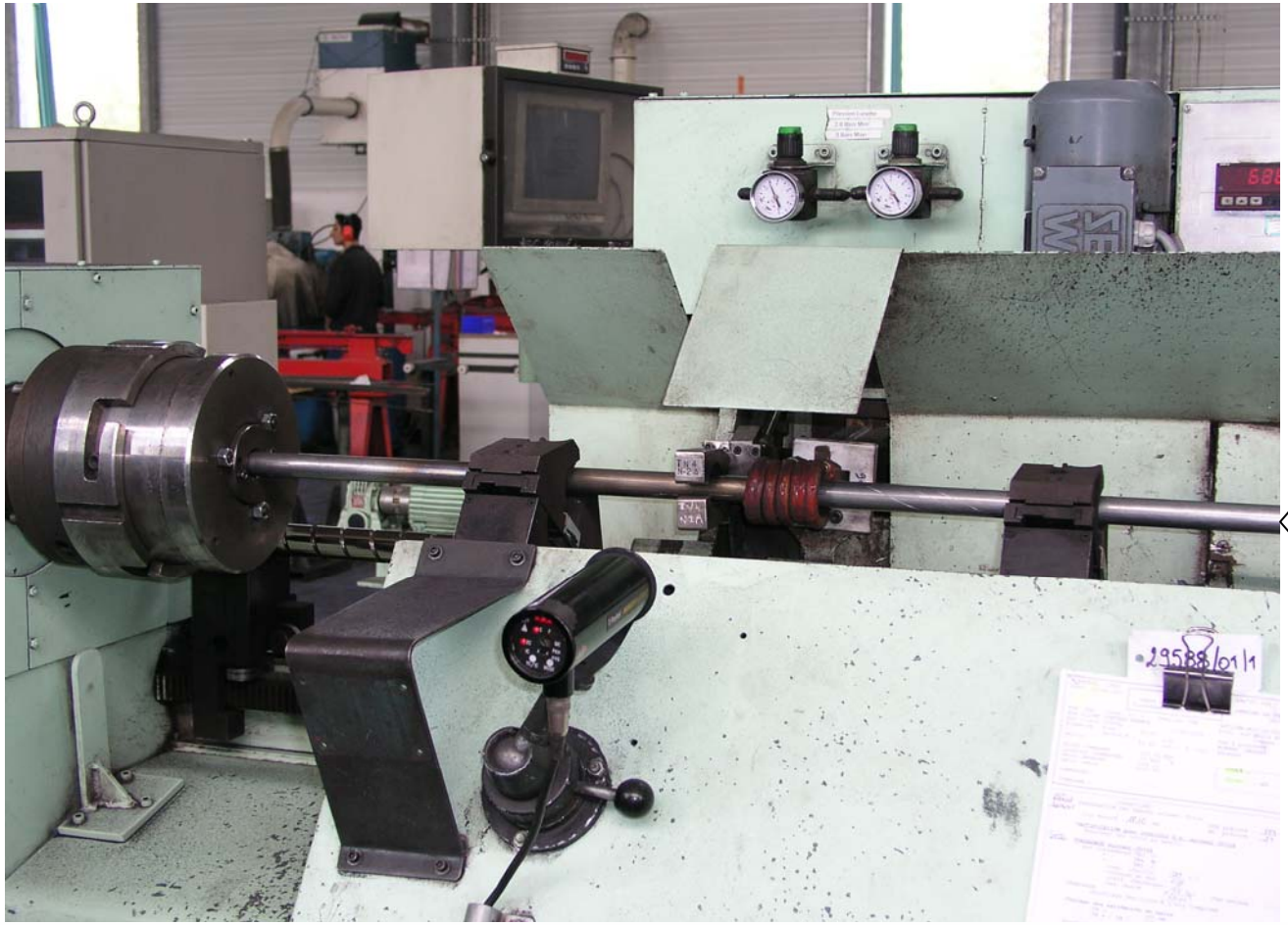

PM2000
fine grained
2m length
25mm ∅
2.5mm wall

FORÉCREU

PM2000 tube torsion forming trial

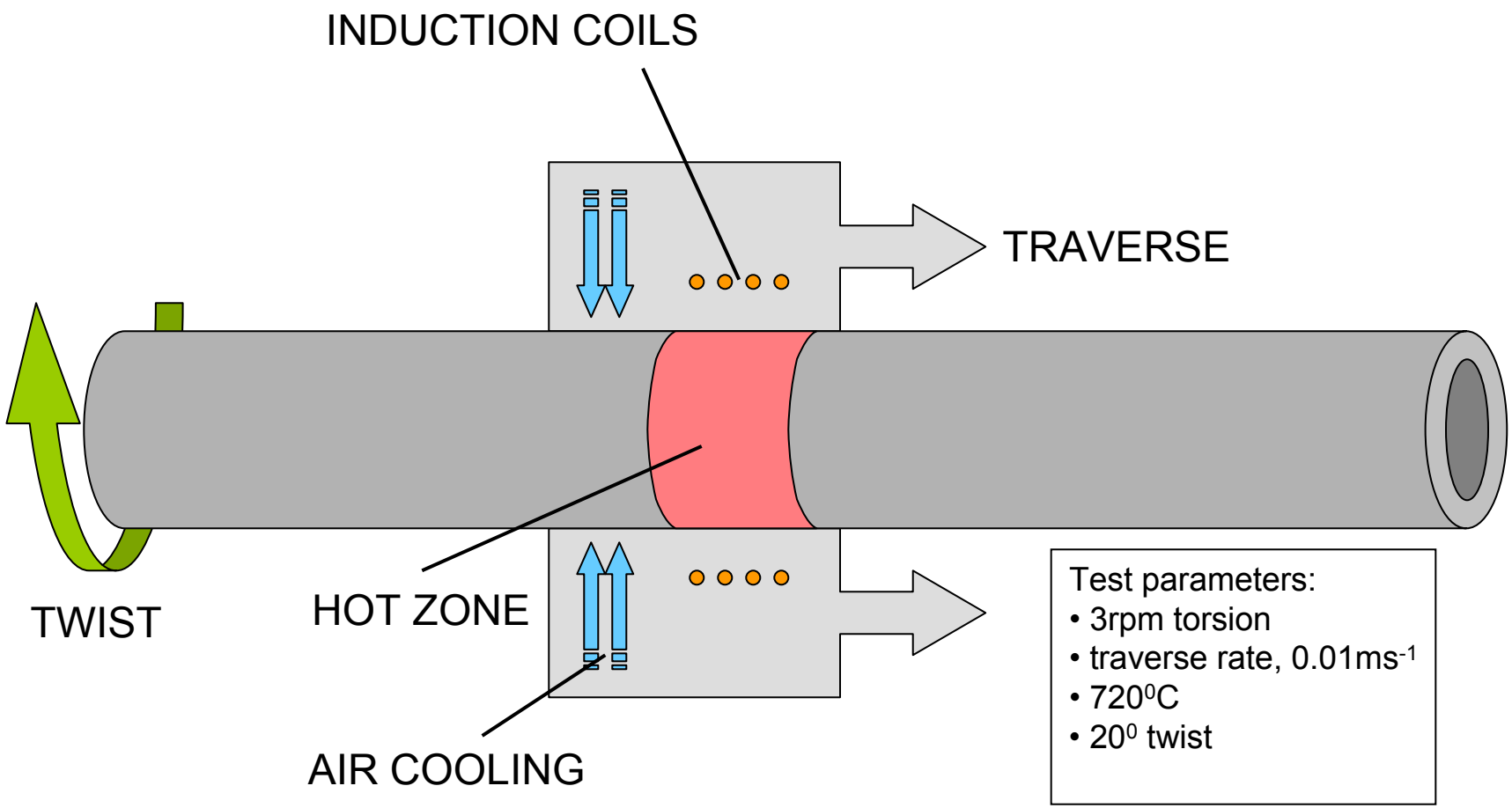

Test parameters:
- 3rpm torsion
- traverse rate, 0.01ms^{-1}
- 720^{0}C
- 20^0 twist

PM2000 tube torsion forming trial

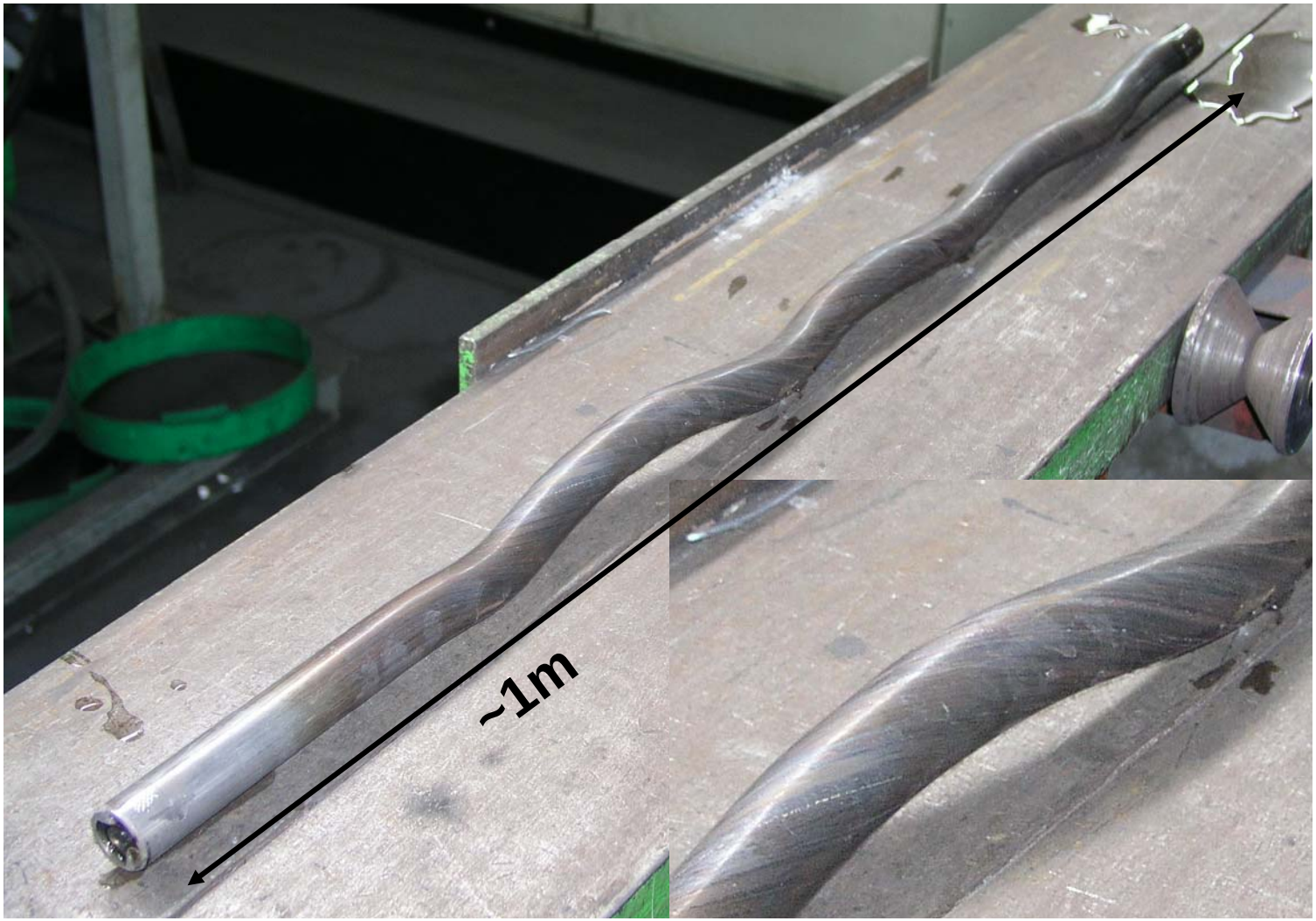

PM2000 tube torsion forming trial

Initial trial:
- Tube spiralling
- No ‘shell’ buckling

Subsequent trials:
- axial tube restraint?
- thicker wall tube?

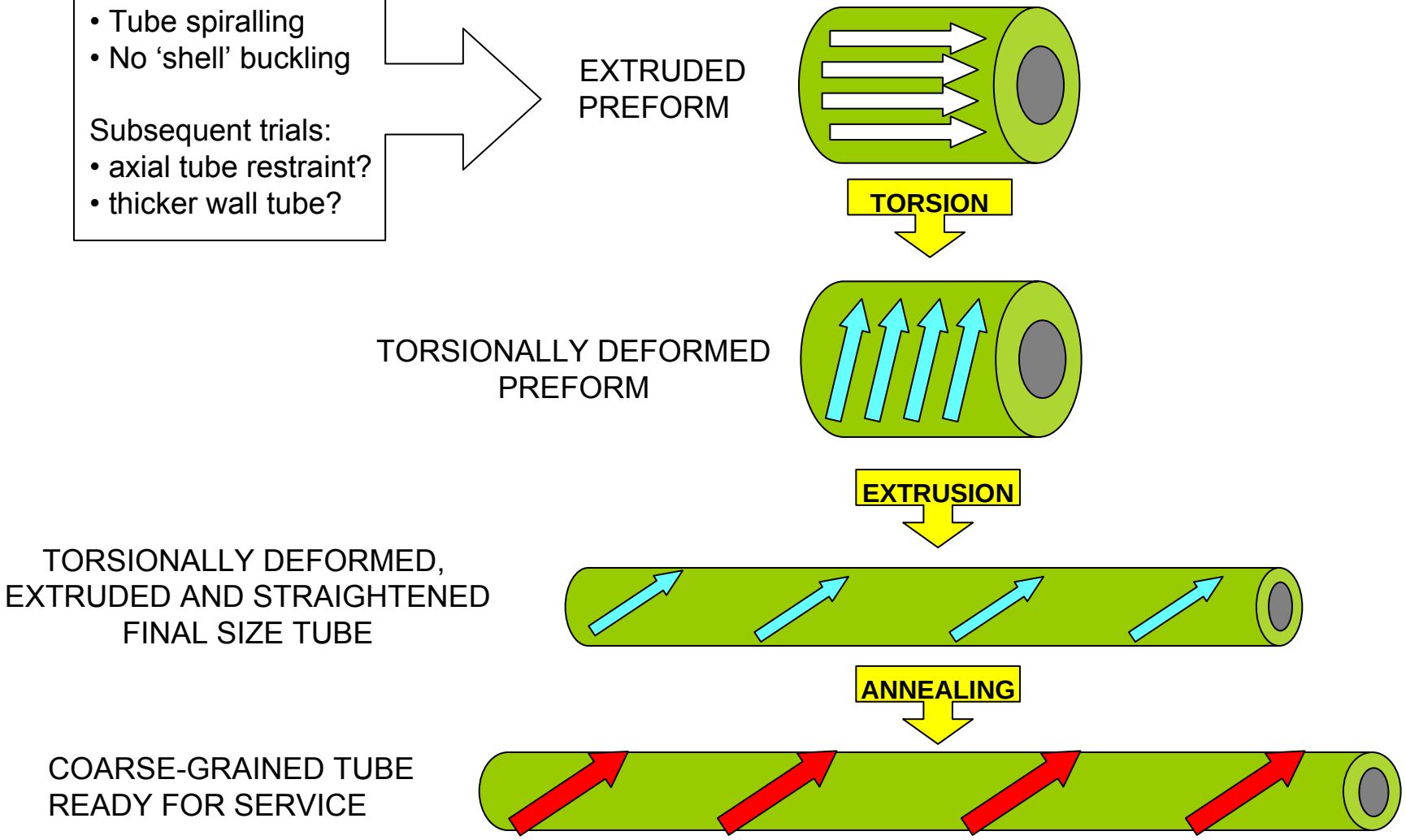

PM2000 tube torsion tests

Mathematical Modelling of Thin Walled Tubes under Thermal Loading

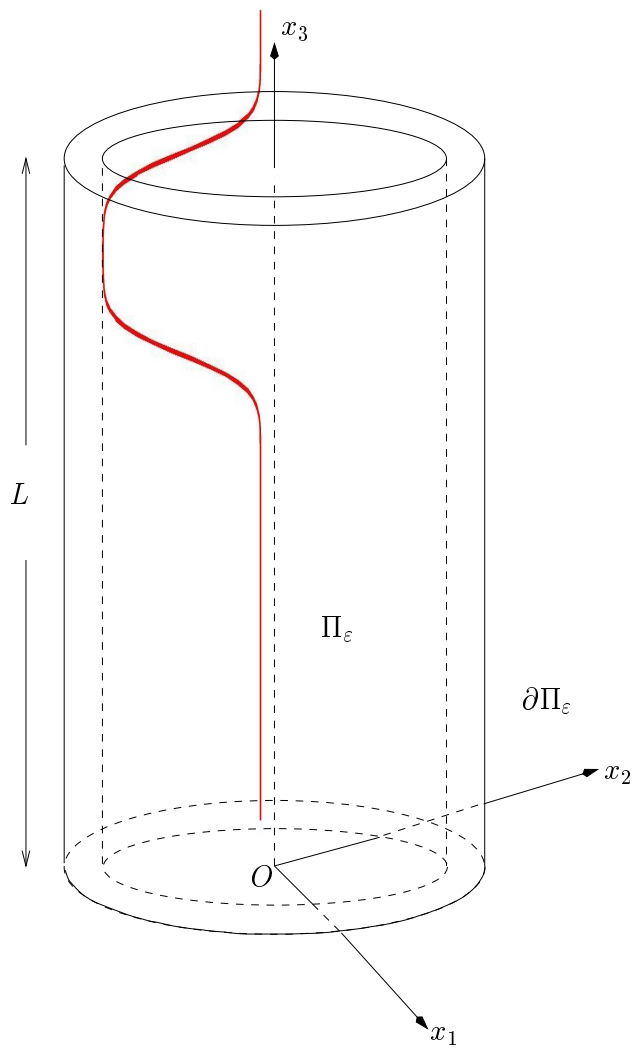

The effect of a heated region modelled as *inhomogeneity* in modulus along the *axis of the tube*

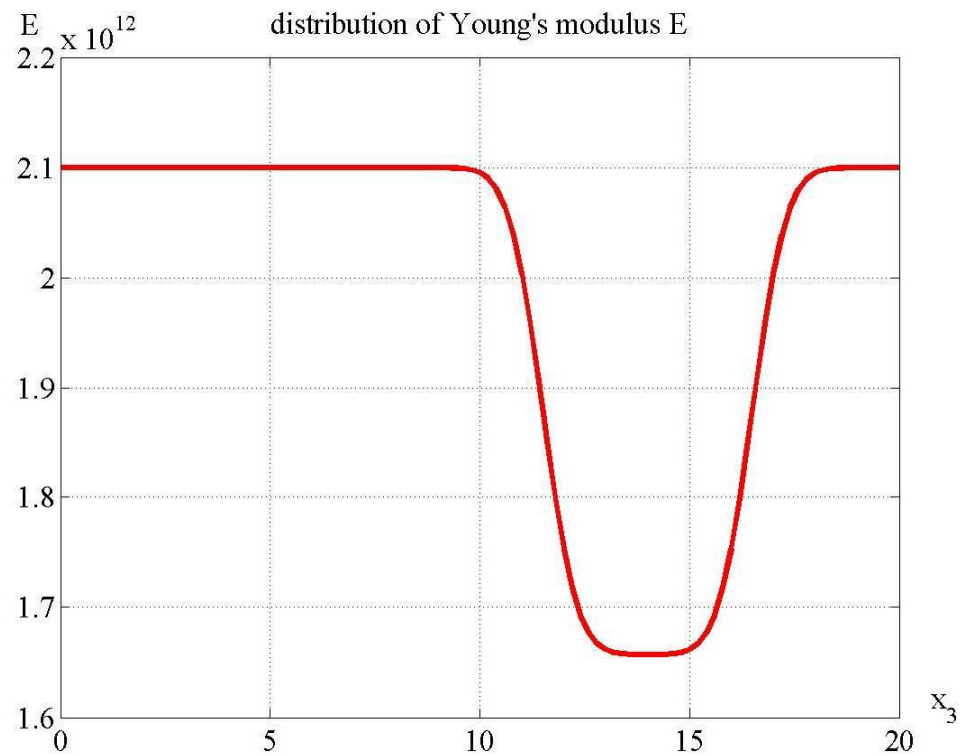

Heated region moves along the axis of the tube.

PM2000 tube torsion tests

THE UNIVERSITY of LIVERPOOL

Mathematical Modelling of Thin Walled Tubes under Thermal Loading

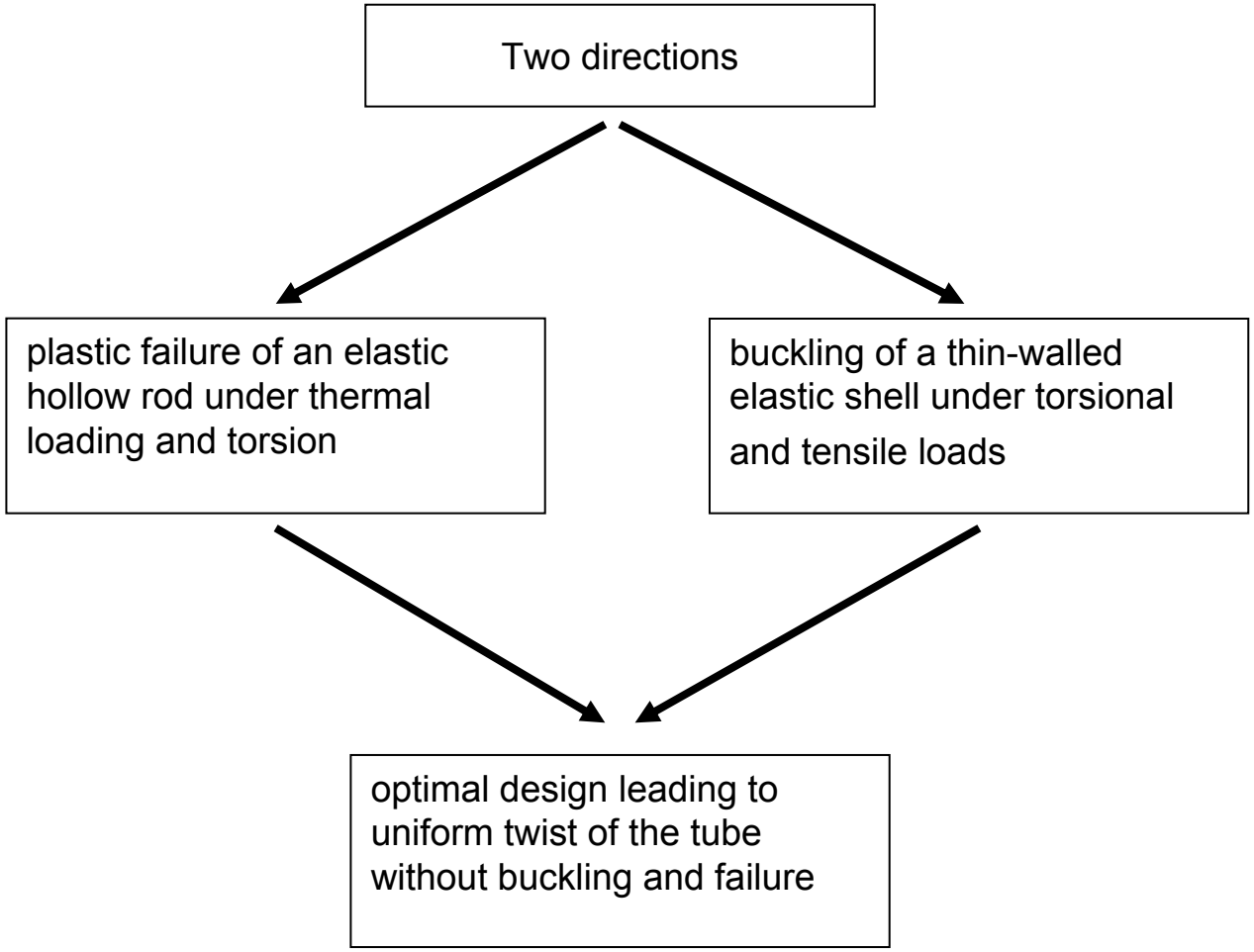

Conclusions

Recrystallisation in PM2000 variant alloy

- Conventional thermo-mechanical processing (TMP) leads to, essentially, independent recrystallisation of the PM2000 and ODS-free regions (PM2000: <111> fibre texture; ODS-free: random texture)
- TMP that increases stored energy levels in PM2000 and *simultaneously* facilitates 'critical strain annealing' in ODS-free regions, brings $T_{Rex\ PM2000}$ and $T_{Rex\ ODS\text{-}free}$ into sufficient proximity to encourage interaction during recrystallisation
- Post extrusion annealing and interdiffusion can create a stable ferritic layer in the 'mild steel' can at the alloy / can interface; but this ODS-free region does not interact with adjoining PM2000 during recrystallisation.

PM2000 tube torsion tests

- High temperature (675^0C,750^0C) tube torsion tests have been performed on PM2000 tube (25mm ∅,2.5m wall)
- Secondary recrystallisation produced through-wall coarse grained microstructures with up to 55^0 microstructural twist (tube 8) aligned with the twisted oxide stringers
- In torsion, tubes exhibited a tendency towards buckling collapse rather than plastic failure

PM2000 torsion forming trial

- A hot (720^0C) torsion trial has been performed on PM2000 tube (2m x 20mm x 2.5mm wall) using a custom profiling m/c at Forécreu, France
- 20^0 twist was achieved; but the trial was terminated because the tube spiralled: this first result suggests the technique has promise.

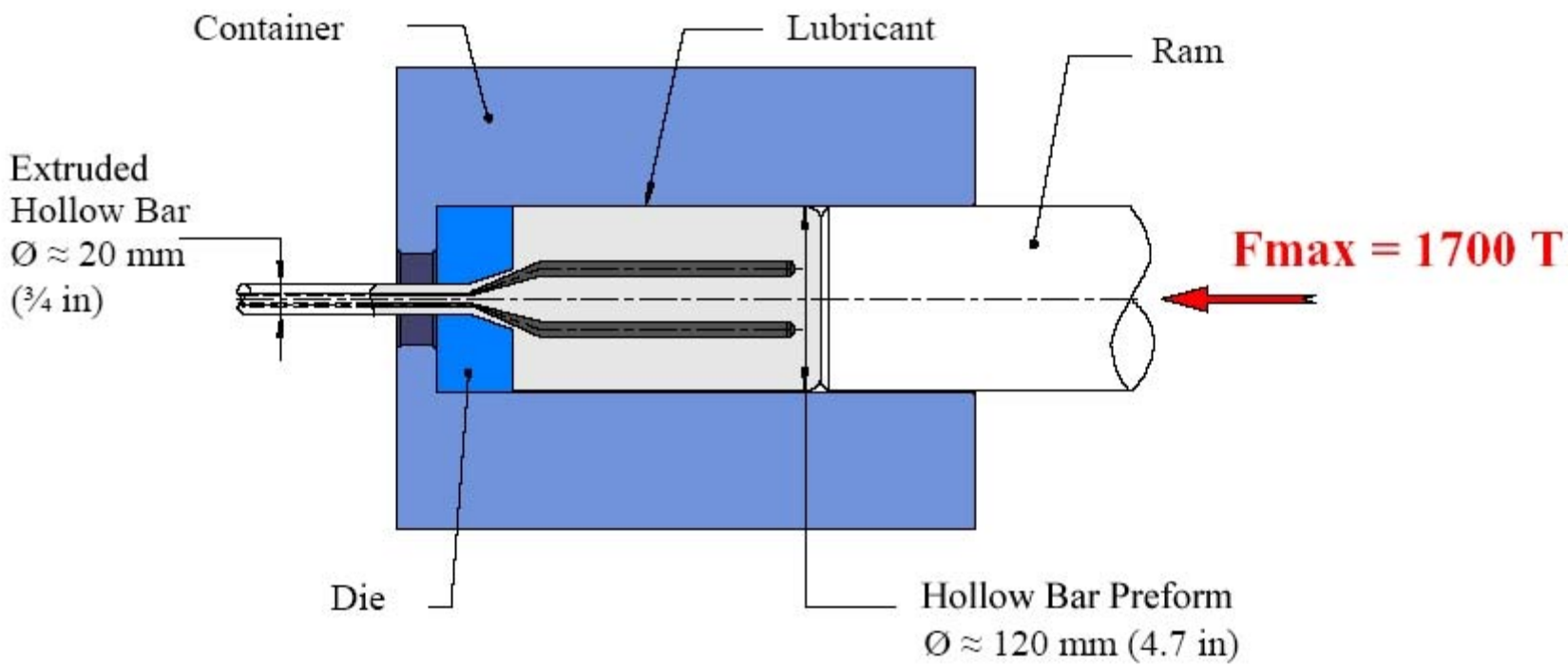
Container
Lubricant
Ram
Extruded
Hollow Bar
Ø ≈ 20 mm
(¾ in)
Fmax = 1700 T
Die
Hollow Bar Preform
Ø ≈ 120 mm (4.7 in)

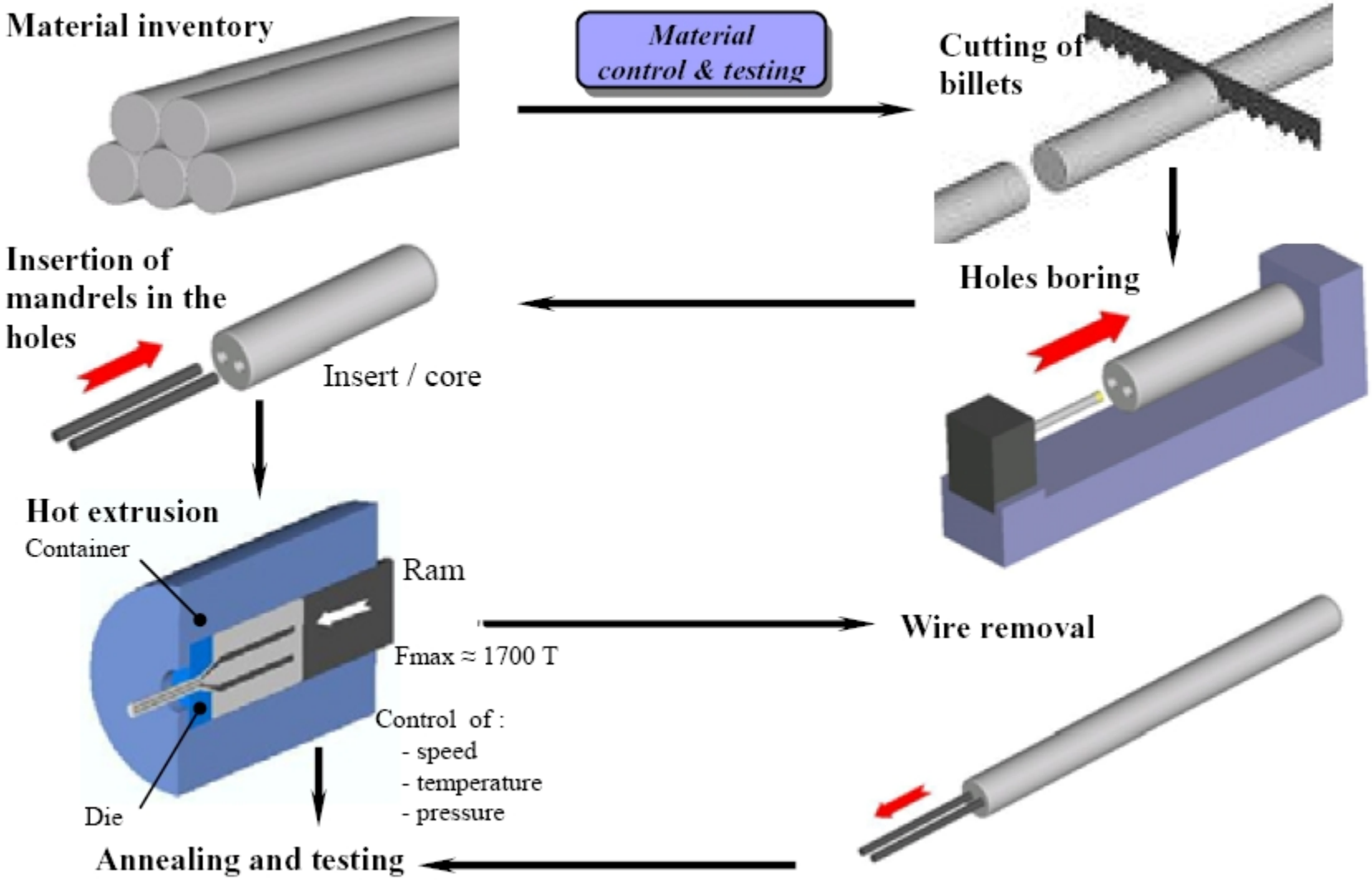
Material inventory
Material control & testing
Cutting of billets
Holes boring
Insertion of mandrels in the holes
Insert / core
Hot extrusion
Container
Ram
Fmax ≈ 1700 T
Control of :
- speed
- temperature
- pressure
Die
Wire removal
Annealing and testing

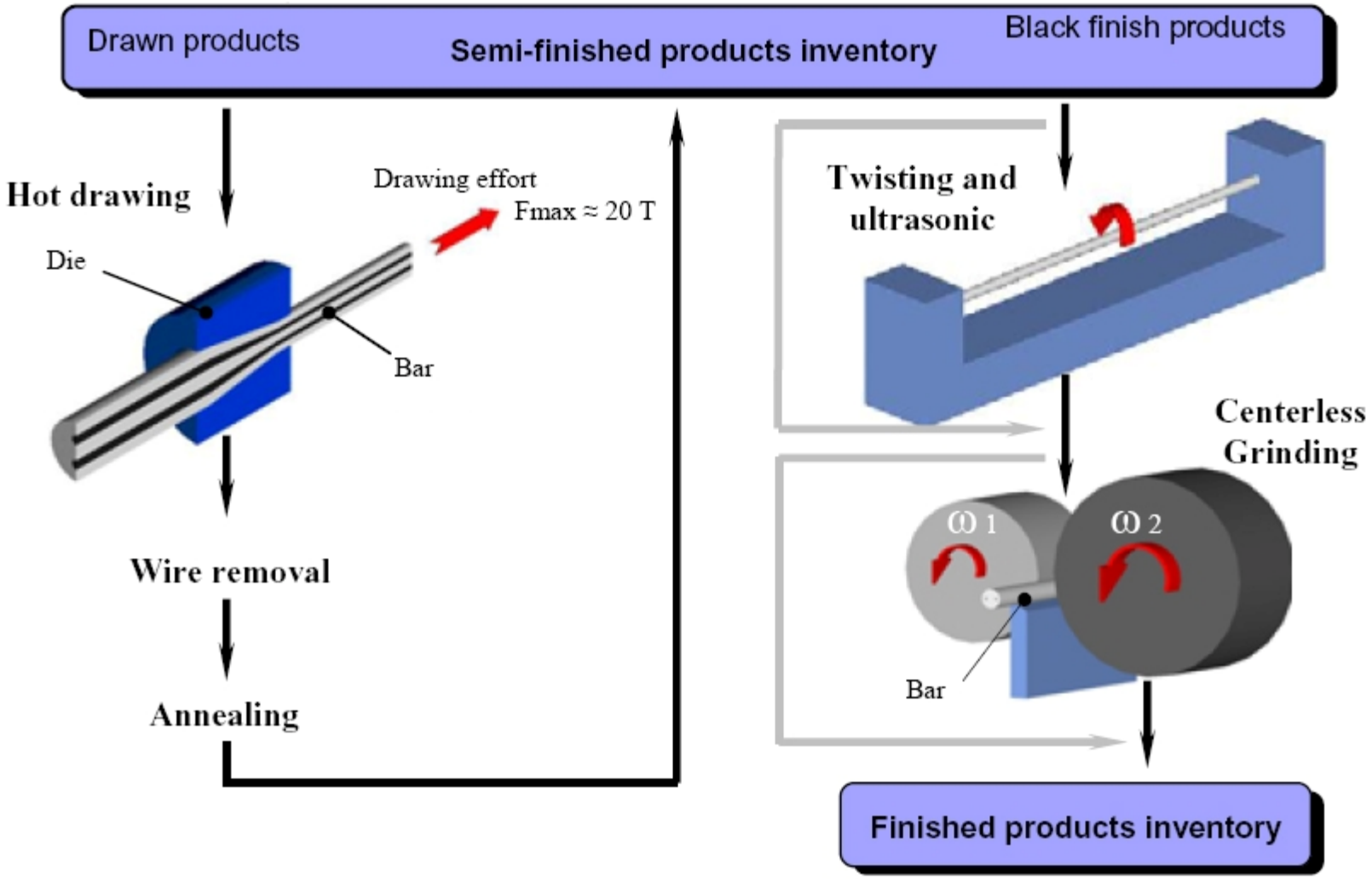
Drawn products
Semi-finished products inventory
Black finish products
Hot drawing
Drawing effort
Fmax ≈ 20 T
Die
Bar
Wire removal
Annealing
Twisting and
ultrasonic
Centerless
Grinding
ω 1
ω 2
Bar
Finished products inventory

Development of Mo-Si-B Silicide Intermetallics

J. H. Schneibel[1], M. P. Brady[1], H. M. Meyer III[1], J. A. Horton[1], J. J. Kruzic[2] R. O. Ritchie[3]

[1]Oak Ridge National Laboratory, Oak Ridge, Tennessee

[2]Oregon State University, Corvallis, Oregon

[3]Lawrence Berkeley National Laboratory and University of California, Berkeley, California

Support: Department of Energy - Office of Fossil Energy

Outline

- **Key Mechanical Property Issues for Mo-Si-B**
  - **Multi-phase alloys**
- **Strategy: Optimize the Ductility and Toughness of the Mo Solid Solution Phase**
  - **Zr Alloying**
  - **Spinel Additions**
  - **Focus on Mechanistic Insight**

Driver

Higher-Strength Materials for Aggressive Environments

Multi-Phase Alloys: Mo-Mo_3Si-Mo_5SiB_2 Phase Triangle $T_m \approx 2000^oC$

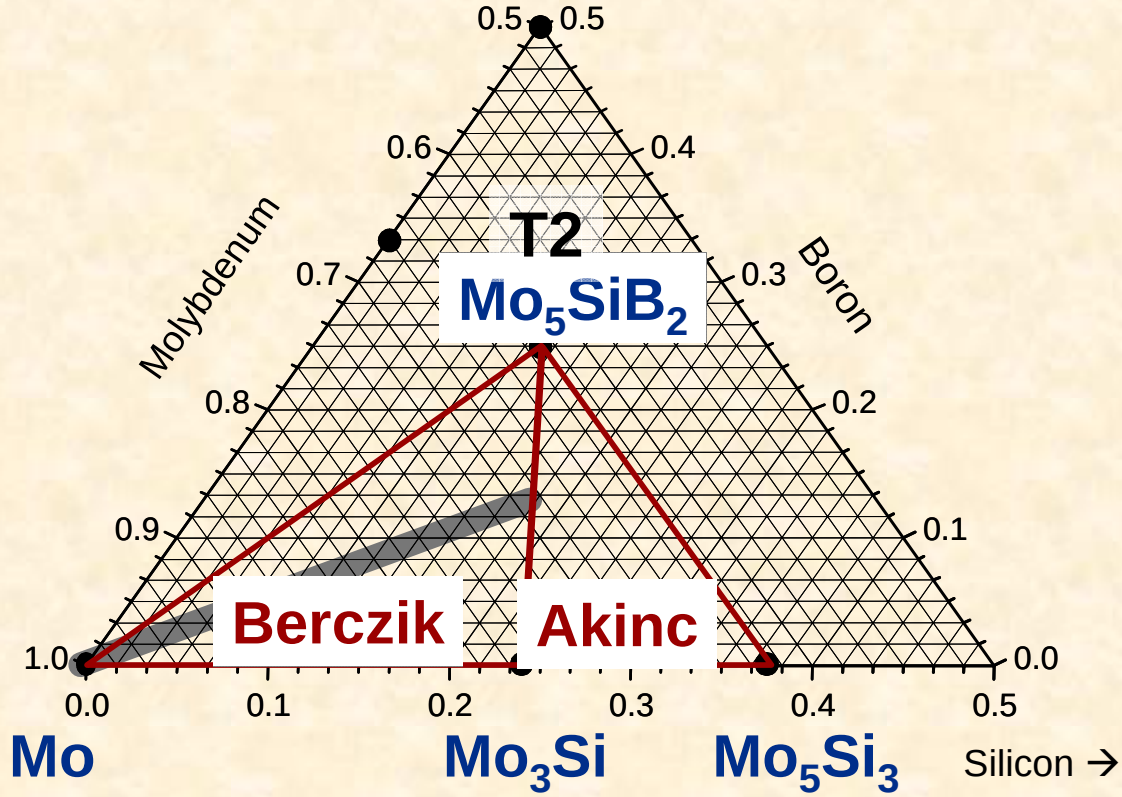

- Akinc: oxidation-resistant but brittle
- Berczik: better toughness but oxidation issues

Room Temperature Fracture Toughness Increases with α-Mo Volume Fraction

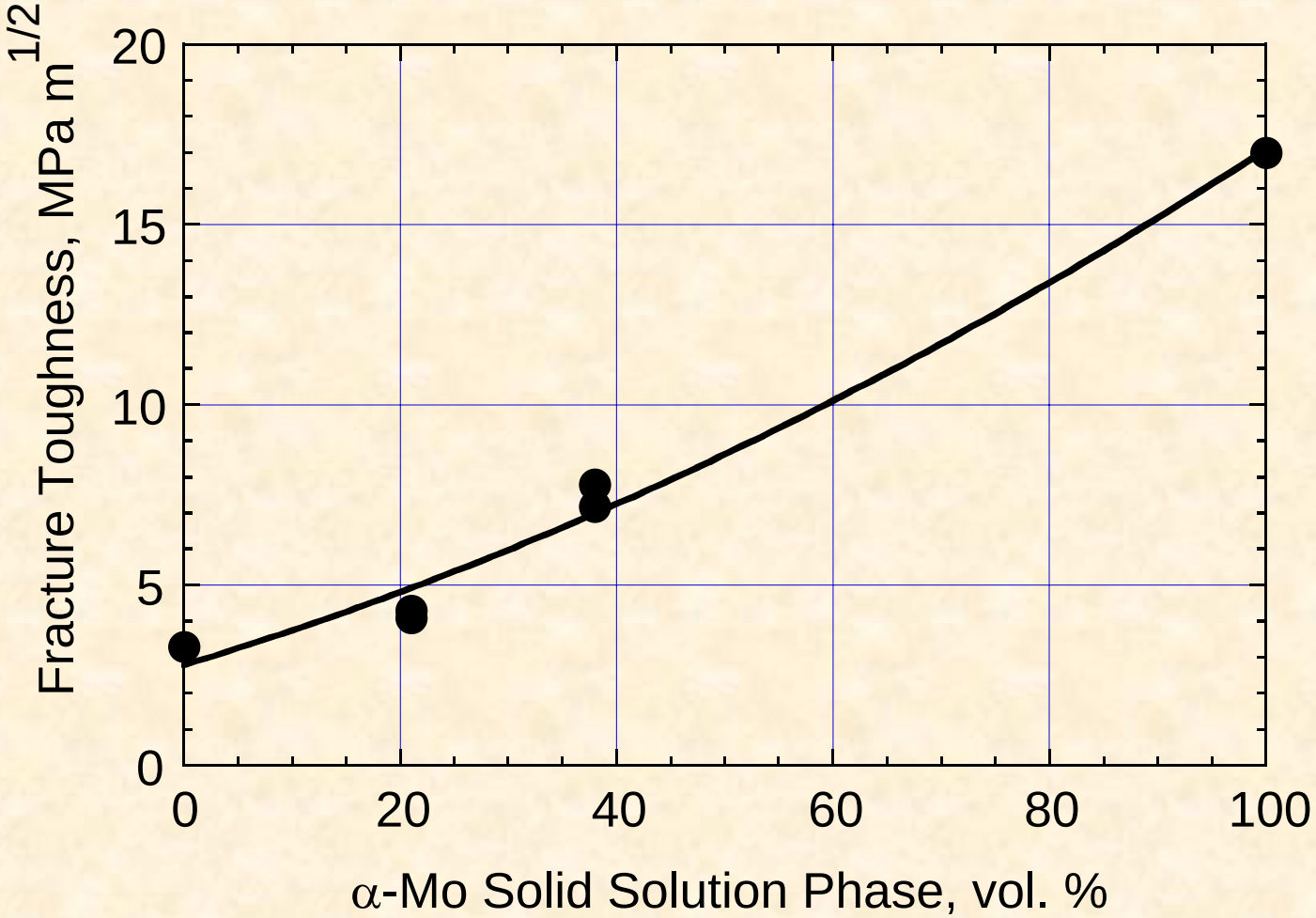

But, Oxidation Resistance and Creep Strength Decrease w/α-Mo

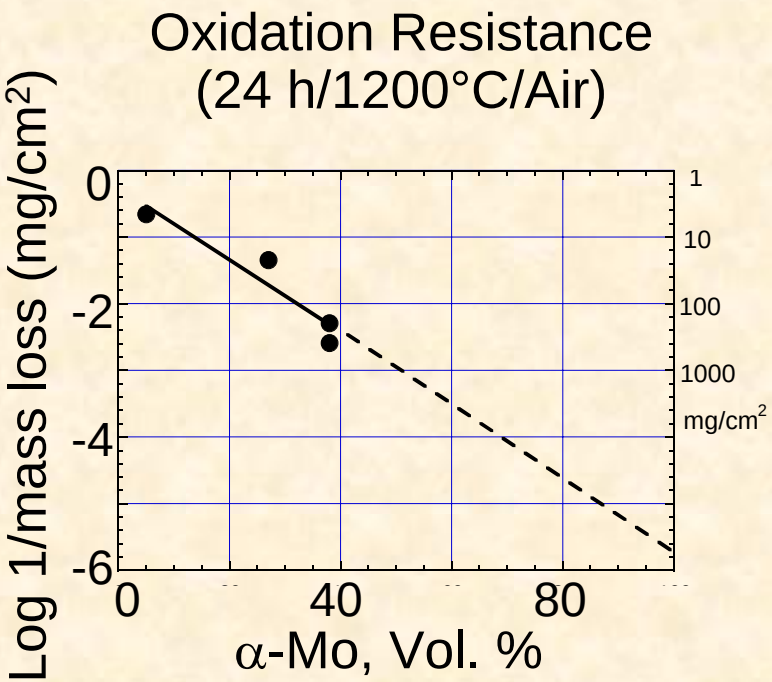

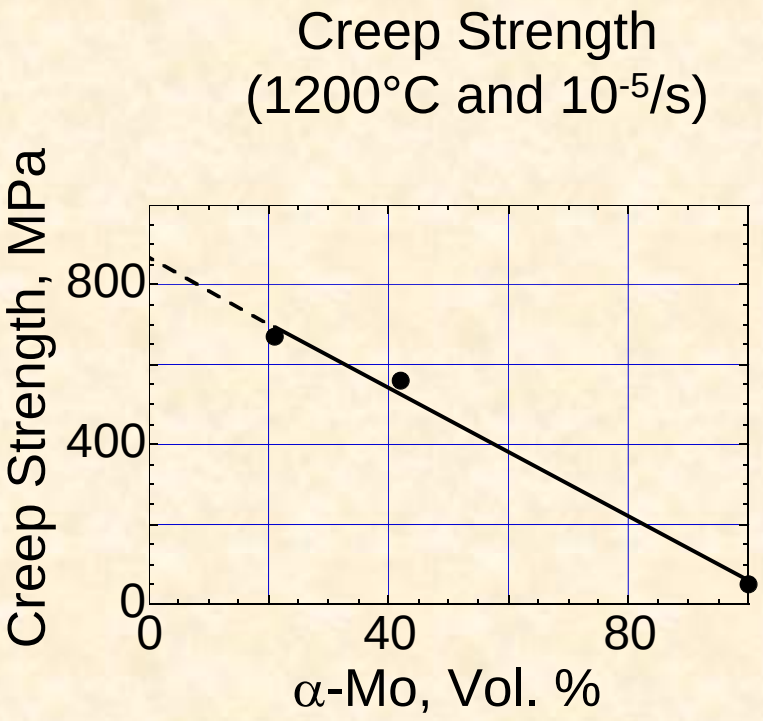

Balance of Properties via α-Mo Optimization

- **The Problem: In Mo-Si-B we can achieve:**
  - Good fracture toughness
  - Good oxidation resistance
  - Good creep resistance
  - **But not all at the same time!**

- **Design Strategy:**
  - Improve ductility and fracture toughness of the Mo phase to make more efficient use of it, i.e., to get by with smaller volume fraction of Mo phase
  - Need discontinuous Mo for oxidation/creep strength

What Can We Do to Improve the Toughening Effectiveness of α-Mo?

- Microalloying with Zr
- Addition of $MgAl_2O_4$ spinel particles
- Additions of rhenium
  - -Re reduced DBTT of Mo (Rhenium Effect)
  - -Cost issues: explore other approaches first

Toughening of Mo-Si-B by Zr Additions

- **Zr Used in TZM Mo alloys**
- **Zr to getter O, strengthen grain boundaries**

1-3 at.% Zr Improved Toughness of Mo-Si-B

Room-Temp. Fracture Toughness of Cast/Annealed Mo-12Si-8.5B-xZr (at.%), Chevron-Notched/3-Point Bend

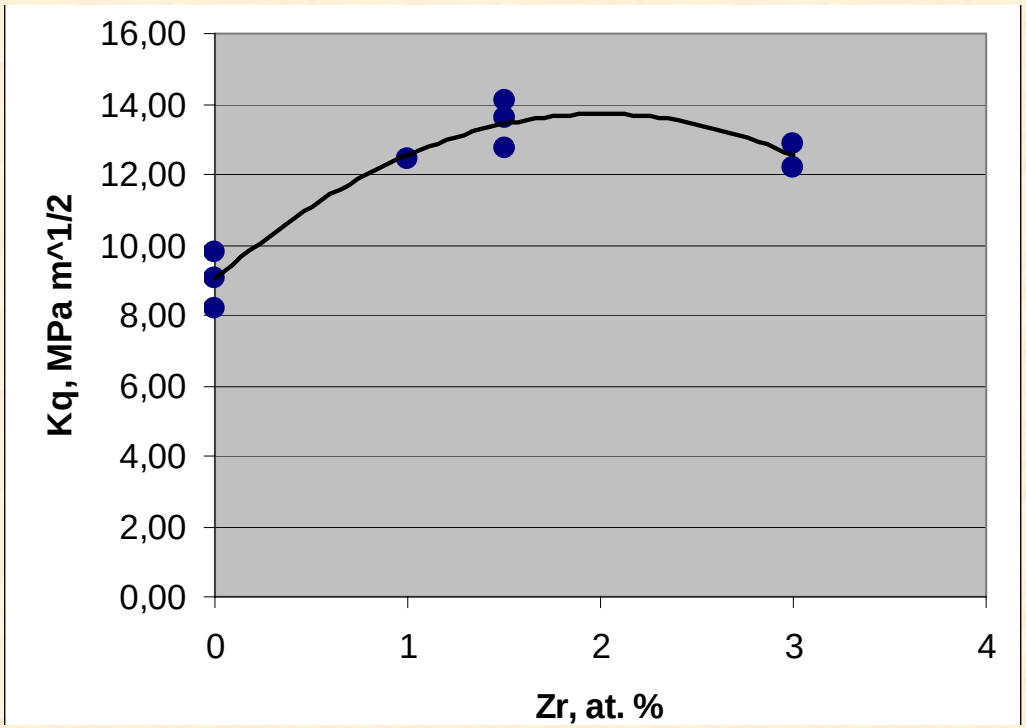

- Semi-quantitative measurement method- useful to show trends
- Mo-12Si-8.5B discontinuous α-Mo alloy (need for oxidation/creep)

Zr Additions to Model α-Mo(Si) Alloys to Explore Mechanism of Effect

Room-Temp. Fracture Toughness
Chevron-Notched/3-Point Bend

Mo-2.5Si-0.1Zr: **23.3, 22.8 MPa $m^{1/2}$**

Mo-2.5Si-0.5Zr: **24.0, 23.3, 22.6 MPa $m^{1/2}$**

- Single-Phase α-Mo(Si) alloys (lower Zr levels to keep single phase)
- Little difference in fracture toughness between 0.1-0.5Zr at 2.5 Si

Simultaneous Changes in Grain Size and Fracture Mode with Zr to α-Mo(Si)

Mo-2.5Si-0.1Zr, at.%

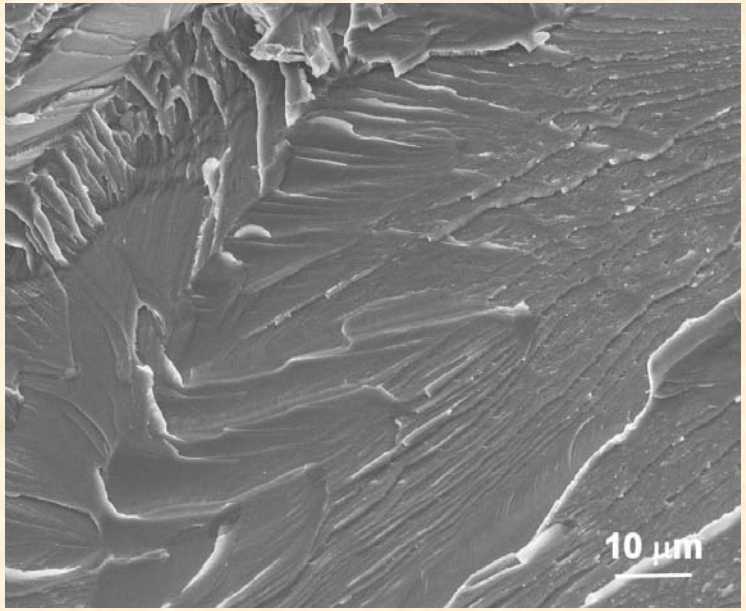

Mo-2.5Si-0.5Zr, at.%

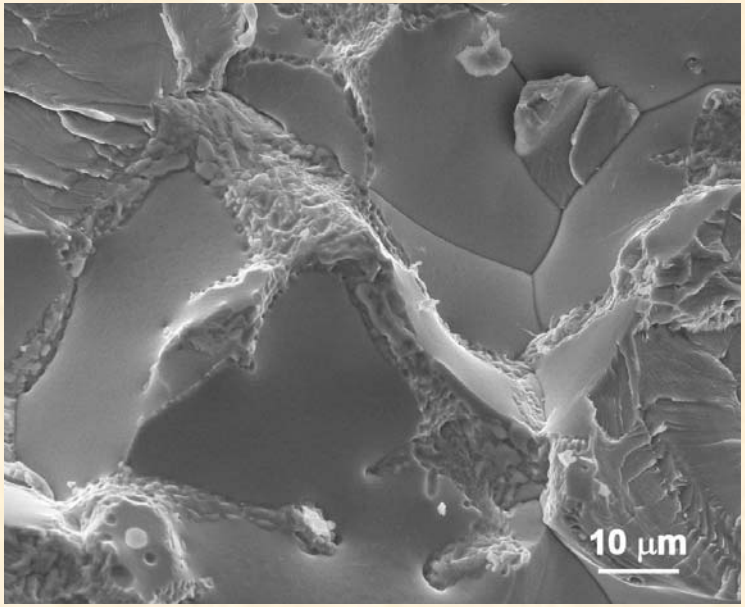

- Transgranular fracture with 0.1 Zr (pure Mo intergranular)
- 0.5 Zr finer grain size/but shift to partial intergranular fracture
- No clear mechanistic insight for effect of Zr on Mo-Si-B alloys

Microstructure Analysis: Zr Reduces the Level of Si in α-Mo for Mo-Si-B Alloys

EDS Measurements of α-Mo(Si) Phase in Annealed (24h/1600°C/Vac) Alloys

Mo-12Si-8.5B, at%	**4.0 ± 0.6 at% Si**
Mo-12Si-8.5B-1.5Zr, at%:	**3.1 ± 0.1 at% Si**

Toughening of Mo-12Si-8.5B by Zr Additions – Working Hypothesis

- Si Strengthens Mo but also Embrittles It
- Zr Reduces the Amount of Si that Dissolves in the Mo Solid Solution, and Thus Reduces the Level of Hardening and Increases Fracture Toughness
- Moderate Gains in Toughness via Zr

Ductilization of Mo by Spinel Particles ($MgAl_2O_4$)

Bendix Corp./Scruggs et al. (Mid 1960's) Ductilized Cr via Additions of MgO/Spinel

- Additions of MgO to commercial-purity Cr powder partially convert to $MgCr_2O_4$ spinel during consolidation

- $MgCr_2O_4$ spinel postulated to getter nitrogen and other impurities that embrittle Cr: 10-20% tensile elongation at room temperature
  - (93-97)Cr-(3-6)MgO-0.5Ti wt.% typical alloy

- Revisited under Fossil ARM Program
  - impurity gettering mechanism refined
  - industrial scale-up in progress with Plansee (joint paper 2005 Plansee seminar/spin-off applications under investigation)

Scruggs Also Reported Ductilization of Mo by Spinel Additions

- **Mo-$MgAl_2O_4$ and Mo-$NiAl_2O_4$ exhibited higher room temperature ductility than "pure" Mo**

- **Proposed mechanism based on impurity gettering**
  -oxygen can embrittle Mo grain boundaries

- **Revisit this effect in Mo as basis for strategy to improve α-Mo phase toughening in Mo-Si-B alloys**

First Attempt at Spinel Ductilization of Mo Successful

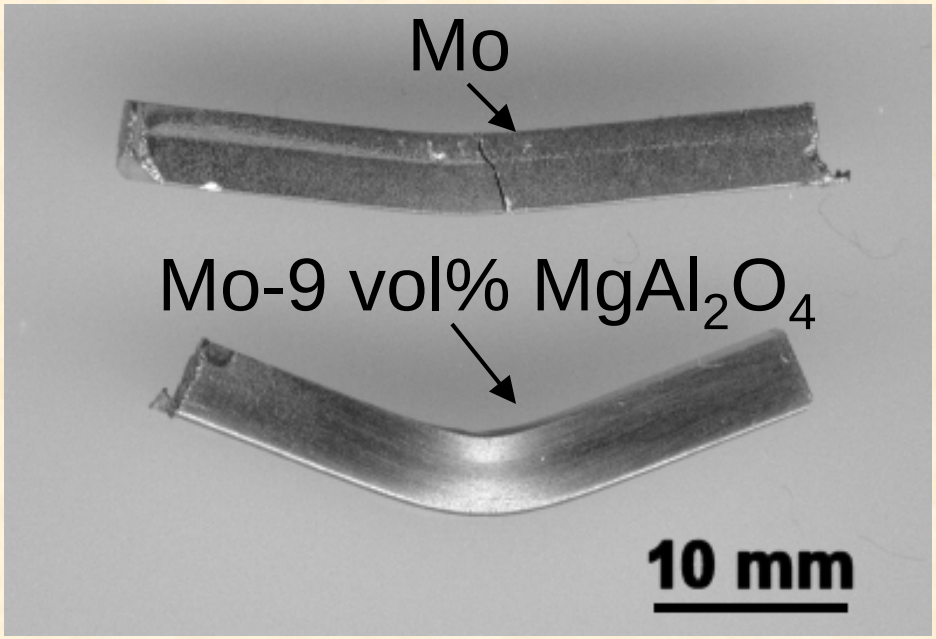

- Some initial difficulties in repeating

Explore Mechanical Properties of Mo as a Function of $MgAl_2O_4$ Addition

- **0.1, 2.5, 5 vol% $MgAl_2O_4$ to explore effects**
  - **"pure" Mo mechanical property scatter makes control alloy difficult, use 0.1 $MgAl_2O_4$**
- Hot-pressing 1 h/1800°C/21 MPa/vacuum
- Mo powder, 3-7 μm/ Additions of Zr and B (as Mo_2Zr and MoB)
- $MgAl_2O_4$ powder, < 20 μm

Microstructure of Mo-2.5 vol% $MgAl_2O_4$

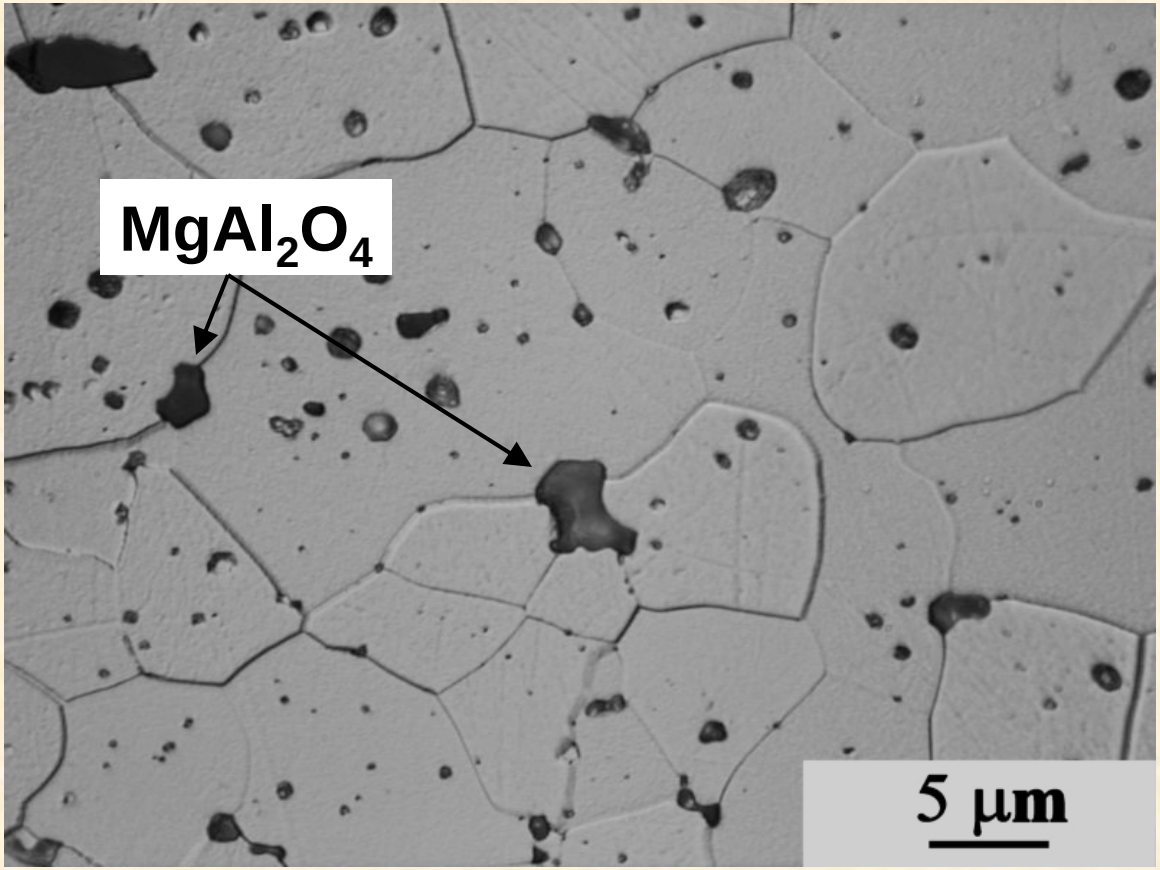

- $MgAl_2O_4$ predominately at Mo grain boundaries

Mo-Spinel Showed Good Tensile Elongation at Room Temperature

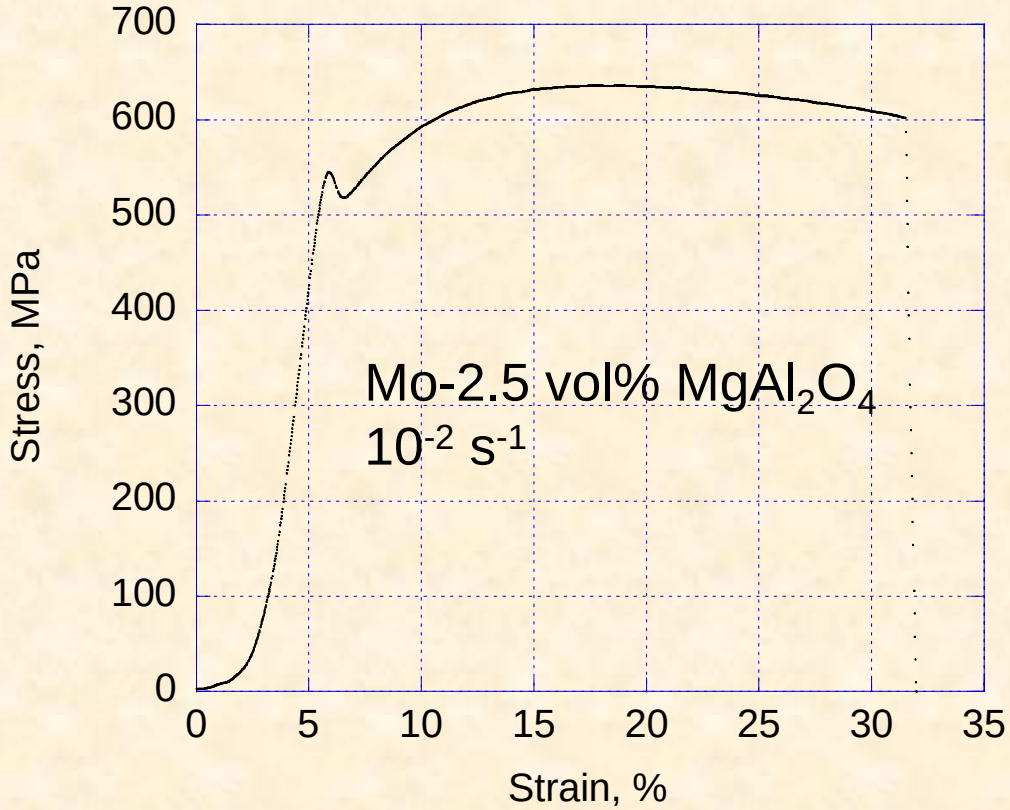

- **Fracture by crack propagation – no necking**

How is $MgAl_2O_4$ Spinel Improving Ductility?

Check Scruggs Impurity Gettering Mechanism First

Impurities (C, N, S) Segregated at Oxide Dispersion/Cr Matrix Interfaces in Cr-MgO Alloys

Auger Maps of In-Situ Fractured Cr-MgO Alloys

SEM of Fracture Surface

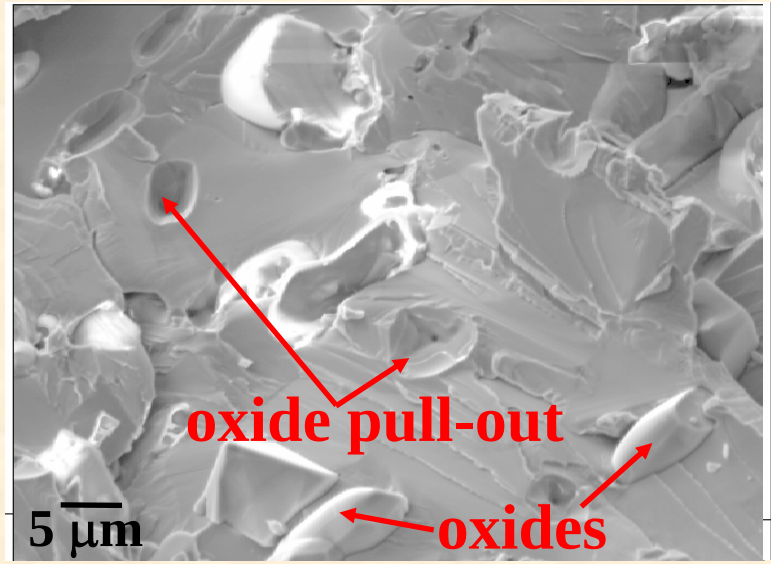

Nitrogen Map

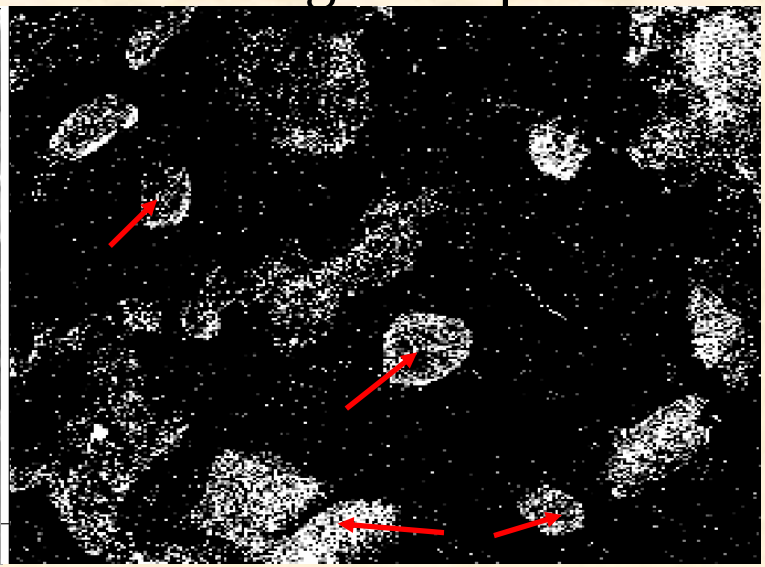

•Impurities managed by segregation at $MgO/MgCr_2O_4$ spinel

In-Situ Fracture in Auger to Explore Impurity Distribution in Mo-2.5 $MgAl_2O_4$

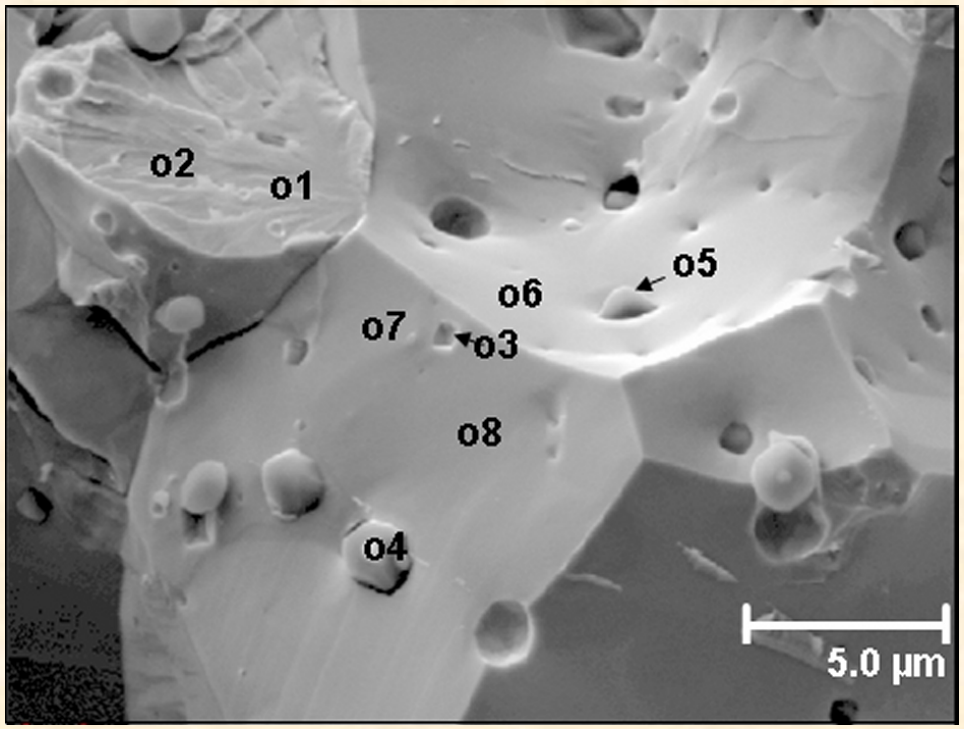

- Spinel particle surfaces, spinel pull-out regions, intergranular and transgranular fracture areas examined for impurities

No Clear Impurity Trends Emerged

- Key embrittlement species in Mo is O at grain boundaries
  - -intergranular failure/low ductility
- $MgAl_2O_4$ spinel oxide particles make tracking of oxygen complex
- Fracture primarily intergranular but little O was detected in Auger
- Little C also detected
  - -C decreases O at grain boundaries/strengthens them and results in trangranular fracture/greater ductility (Wadsworth, Nieh, Stephens; Kumar and Eyres)
  - -Schneibel comment: you can't go wrong citing the lab director!

How is $MgAl_2O_4$ Spinel Improving Ductility?

Look at Tensile Behavior Trends and Microstructure

Ductility maximum for 2.5 vol% $MgAl_2O_4$

Strain rate 10^{-2} s^{-1}

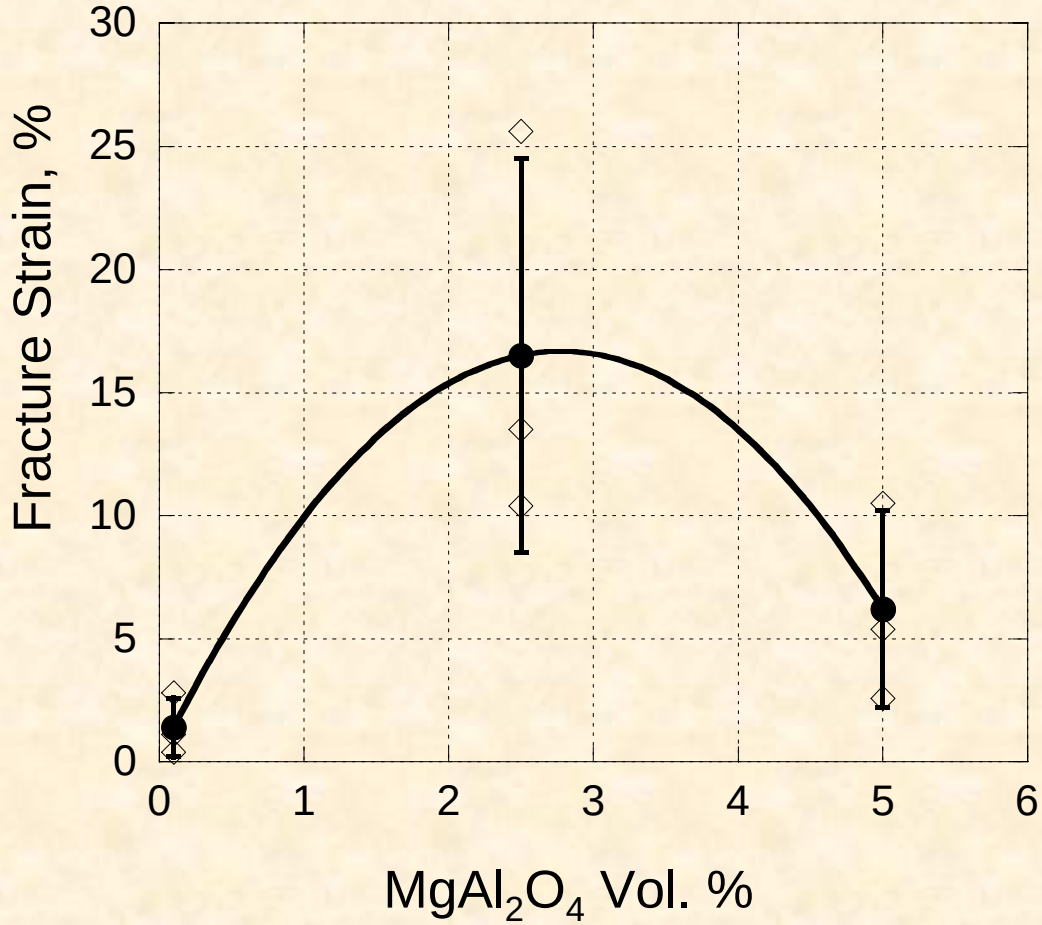

- **Large scatter in fracture strain/ductility**

Yield Stress Increased with Increased $MgAl_2O_4$ Volume Fraction and Strain Rate

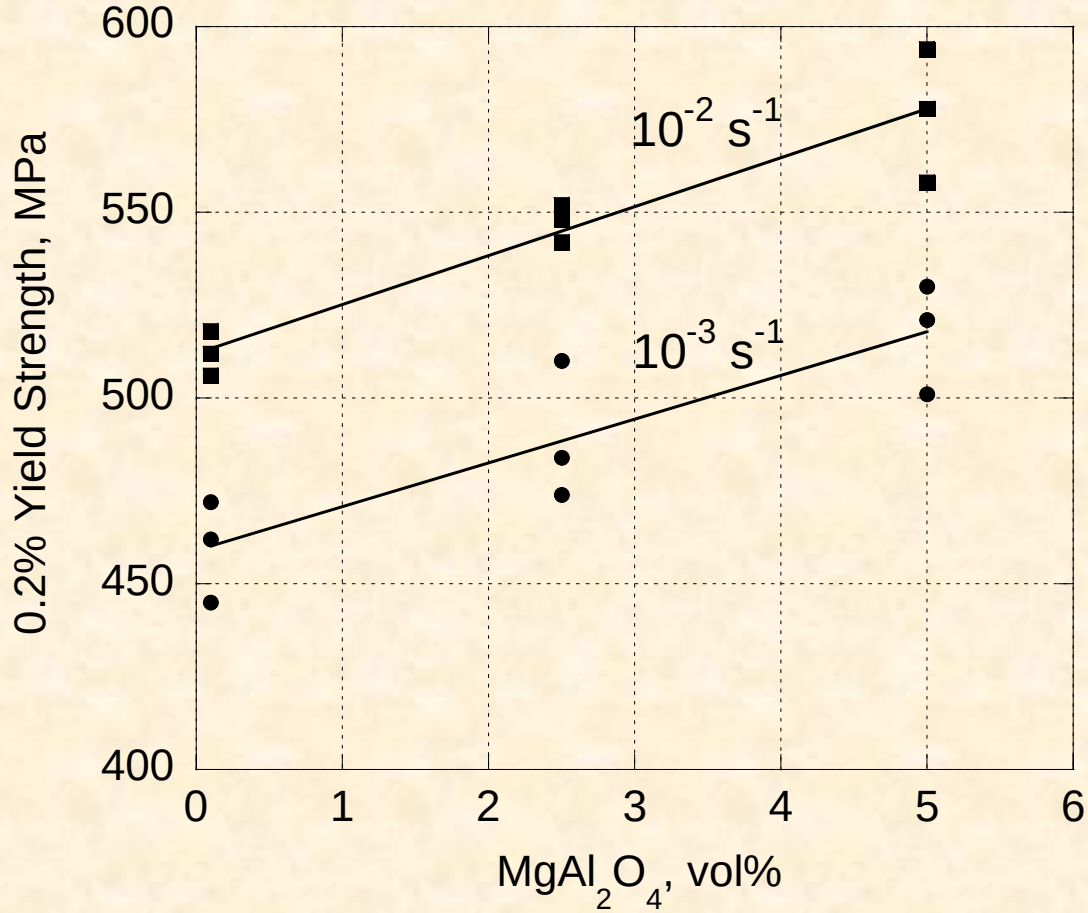

- Mo (BCC) known to be strain rate sensitive

Ultimate Tensile Stress Increased/Leveled Off with Increased $MgAl_2O_4$ Vol.%

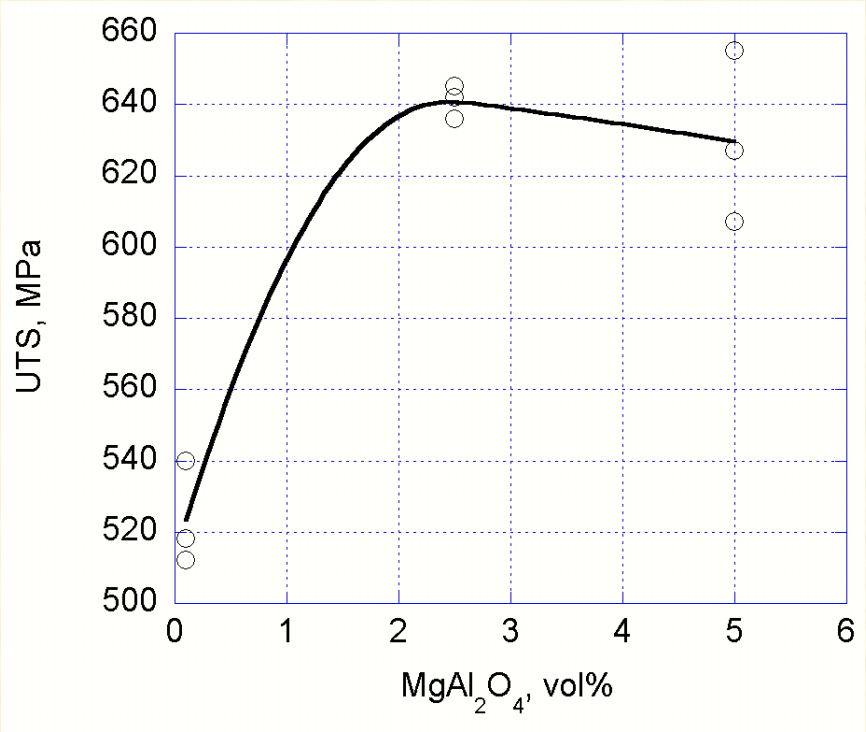

- UTS leveled off between 2.5 and 5 vol.% spinel
- Consistent with ductility decrease at 5% spinel

Decreased Mo Grain Size with Increased $MgAl_2O_4$ Spinel Additions

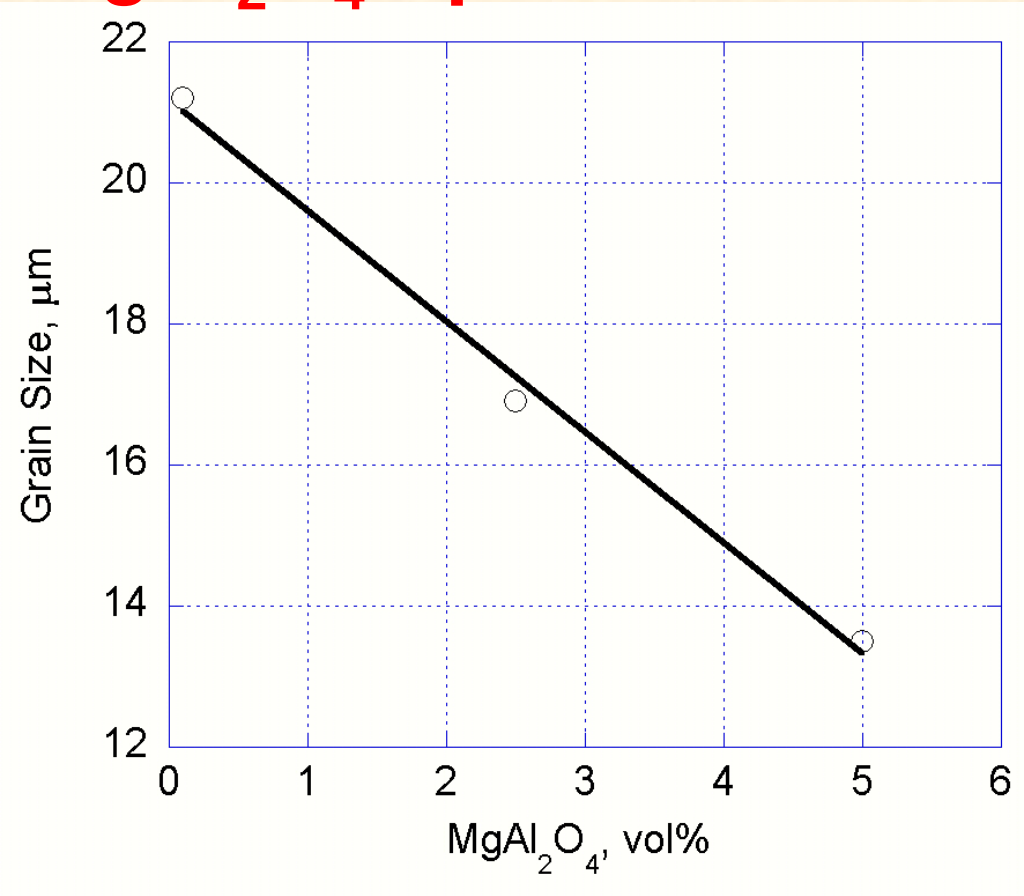

•Spinel additions yielded fine Mo grain size

Hall-Petch Relationship

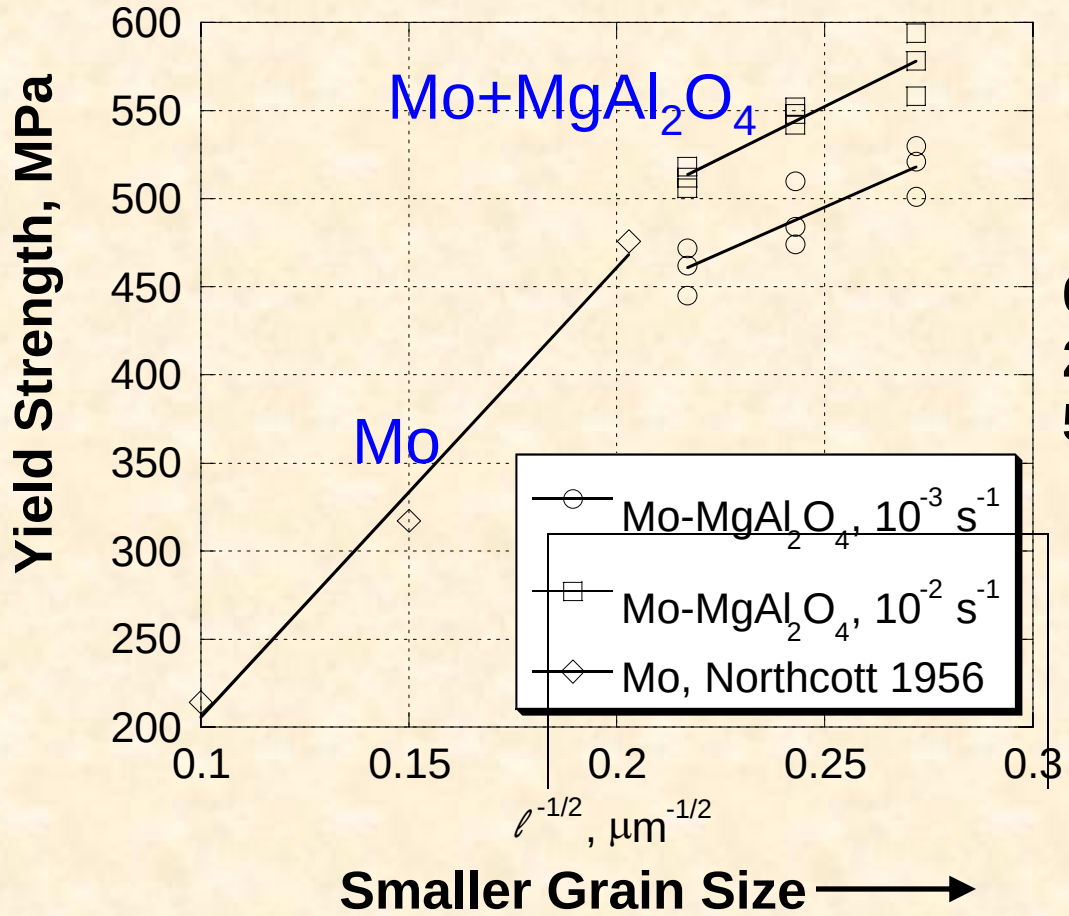

0.1 vol% 21.9 μm
2.5 vol% 16.9 μm
5.0 vol% 13.5 μm

•Slope differences likely artifact of limited grain size range in spinel alloys

Grain Boundary Cracking at Spinel Partcles

Surface of Polished Specimen after Tensile Test

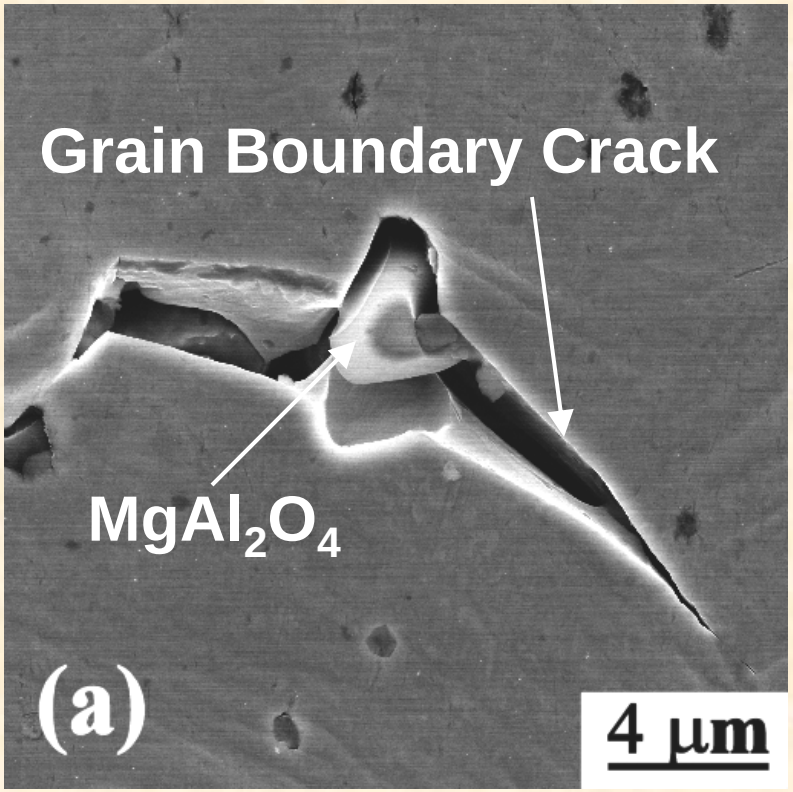

- Brittle spinel particles can act as crack initiators

Decohesion of Mo/$MgAl_2O_4$ Spinel Interfaces

Surface of Polished Specimen after Tensile Test

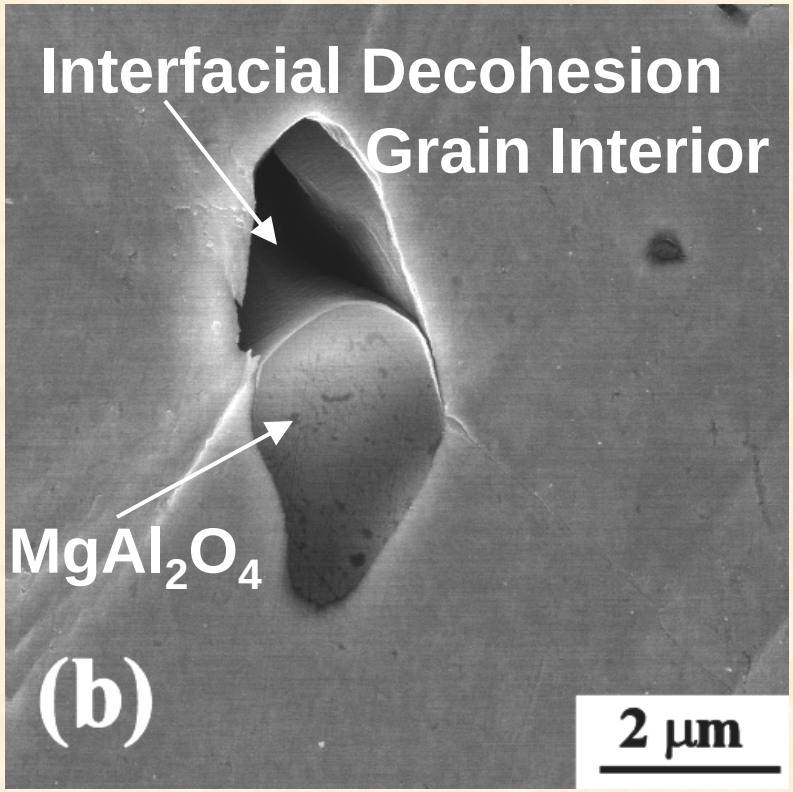

- Suggests Mo/spinel interfaces were weak
- High local strains in Mo

Cross-Section Through Gage Length After Tensile Test Revealed Surface Microcracks

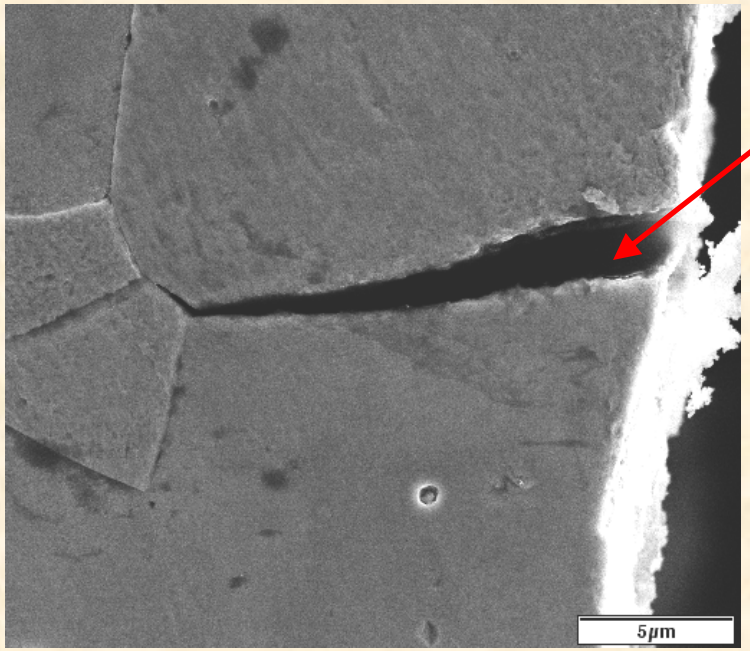

Surface Microcrack

- Surface microcracks source of failure fracture (no necking of tensile specimens observed)
- Microcracks spaced 0.1-0.2 mm along the gage length

ℓ

Assume Microcrack Length Scales with Grain Size

Hypothesis: fracture occurs when the largest surface microcrack reaches a critical local stress intensity factor K_q and propagates

$$K_q = 1.12\,[\sigma_{UTS}/(1-c)]\,(\pi\, 2\ell)^{1/2}$$

c = $MgAl_2O_4$ volume fraction

2ℓ = microcrack length, where ℓ = grain size

- UTS modification for weak Mo/spinel interface, spinel does not carry load

Hypothesis Supported: Kq was Same for All Conditions Studied

$MgAl_2O_4$, vol%	Strain Rate, s^{-1}	K_q, MPa $m^{1/2}$
0.1	0.001	7.3
2.5	0.001	7.1
5.0	0.001	6.6
0.1	0.01	6.9
2.5	0.01	7.6
5.0	0.01	6.8

- Smaller the grain size/smaller the surface microcrack, the larger stress (more strain) to drive the crack to reach fracture

Suggests Ductility with Increased $MgAl_2O_4$ Can be Explained by Grain Size Reduction

- Consistent with Reported Behavior of Mo
  - -Mo grain size decrease from 100 μm to 45 μm increases tensile reduction in area from 6 to 67% (Northcutt, 1956)

- Too high a $MgAl_2O_4$ volume fraction and fracture initiated at brittle $MgAl_2O_4$ particles (decreases ductility)

The Scruggs Mechanism for Mo: More Questions than Answers

- The ductility improvement by $MgAl_2O_4$ particles may be interpreted as a grain size effect
- More Auger data needed to determine whether the oxygen concentration at the grain boundaries depends on the $MgAl_2O_4$ volume fraction - do we have a gettering effect as well?
- Would a ductility maximum be observed if the grain boundaries would be strengthened, e.g. by Zr, and fracture would be transgranular?
- How is the Scruggs effect influenced by Si in solid solution?

Summary and Conclusions

- Moderate Toughening of Mo-12Si-8.5B by Zr
  - -linked to decrease of Si in α-Mo phase

- Scruggs Spinel Ductilization of Mo Replicated
  - -effect can be explained by grain size refinement of spinel particles-located on grain boundaries
  - -extent of spinel impurity gettering not clear
  - -possible applicability to Mo-Si-B

Dispersions of MgO in Cr Impart Ductility at Room Temperature

(D.M. Scruggs, 1963)

Powder Processed 93.5Cr-6MgO-0.5Ti wt.%

Tensile Behavior

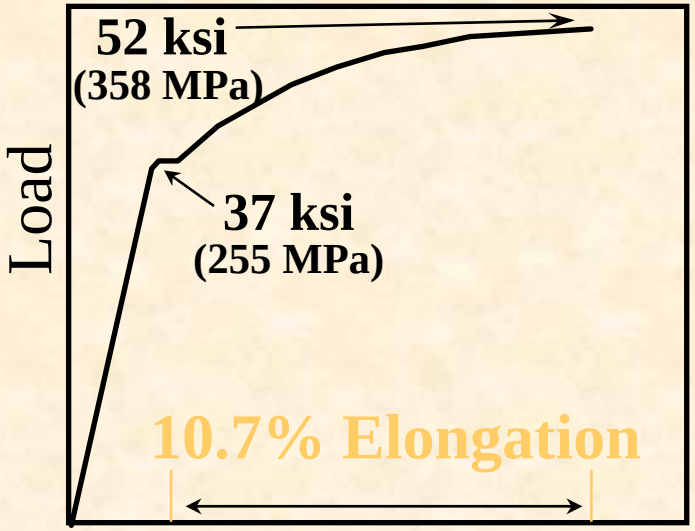

Microstructure (SEM)

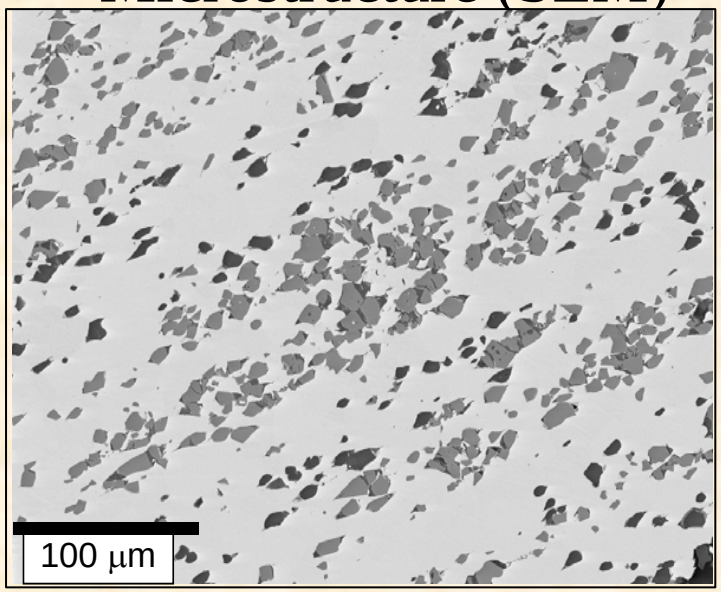

Cr Matrix (light), $MgCr_2O_4$ (gray)
MgO (dark)

Grain Boundary Strengtheners Zr and B Oxidized During Processing/Ineffective

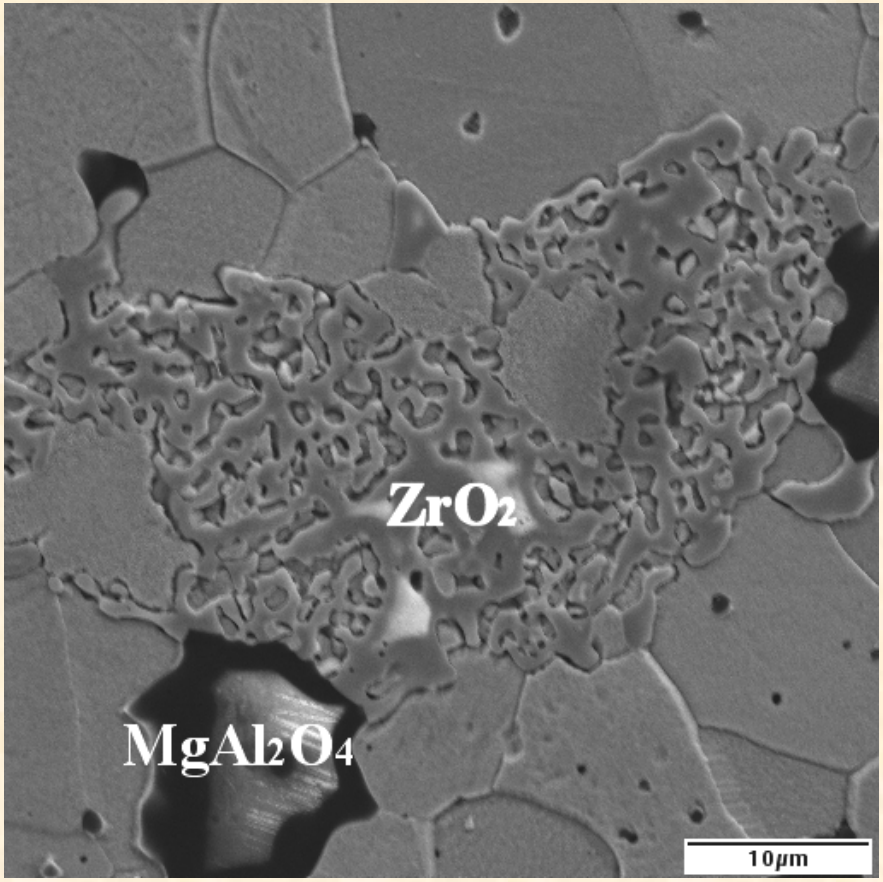

Two Subsequent Attempts to Produce Ductile Mo-$MgAl_2O_4$ Failed

- $MgAl_2O_4$ particle size too large
- Oxygen-contaminated Mo powder (formation of brittle MoO_2)
- Property gradients in hot-pressed disks

Explore Mechanical Properties as a Function of $MgAl_2O_4$ Addition

- Mo powder, 3-7 μm/ Additions of Zr and B (as Mo_2Zr and MoB)
- $MgAl_2O_4$ powder, < 20 μm
- **0.1, 2.5, 5 vol% $MgAl_2O_4$ to explore effects**
- Hot-pressing 1 h/1800°C/21 MPa/vacuum
- Final carbon concentration 0.024 at% (30 wppm)
- Cannot easily determine bulk C/O concentration (spinel addition)

  (Generally, an atomic C/O > 2 eliminates intergranular failure in Mo alloys)

Cr Brittle at Room Temperature

- Impurities a major contributor to room-temperature brittleness in Cr: raises brittle to ductile transition temperature, BDTT (> ≈10-50 wppm level degrades ductility)

- Nitrogen particularly deleterious
  - high elevated temperature solubility, near zero at room temp
  - precipitates as fine, acicular grain boundary phase
  - as little as 5-10 wppm Nitrogen can be embrittling

Toughness Improvements via Control of α-Mo Continuity and Volume Fraction

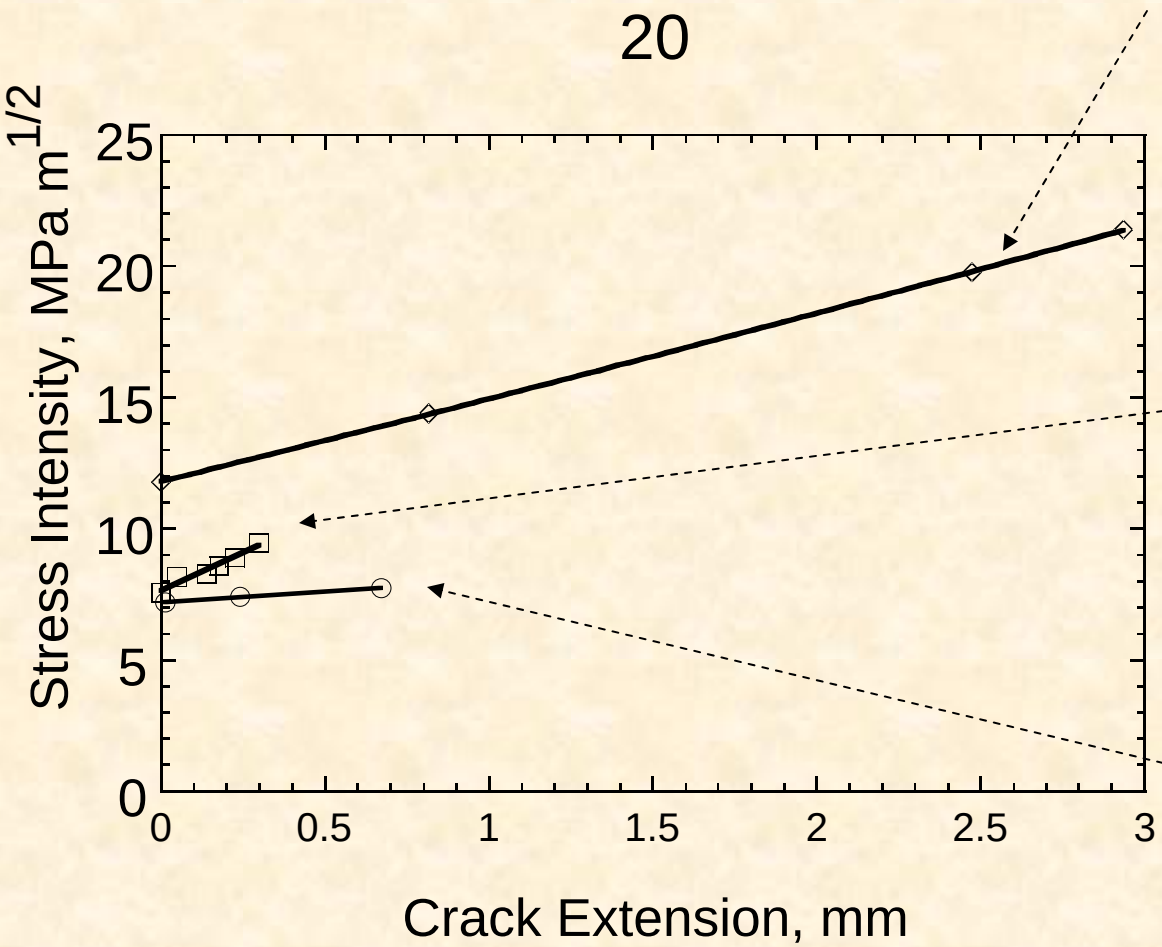

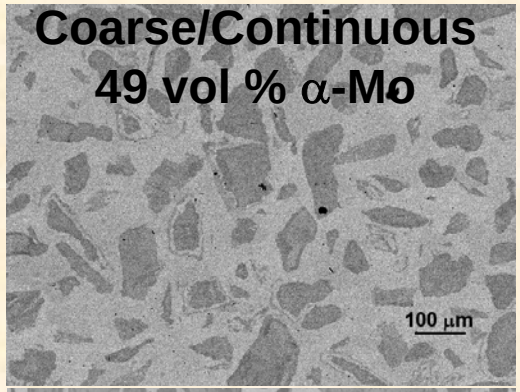

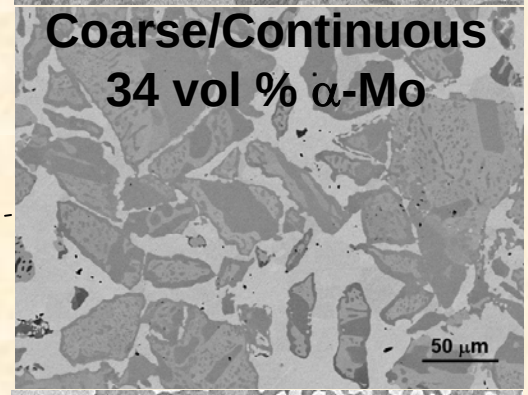

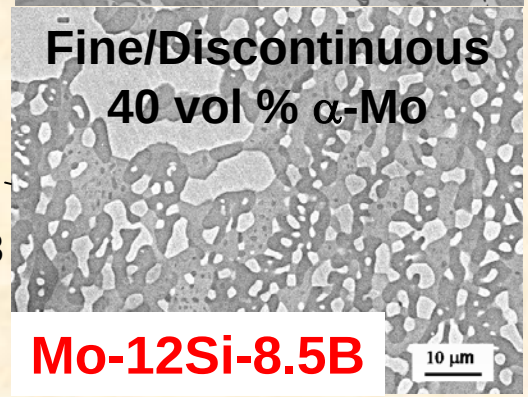

Mo-12Si-8.5B

Multi-Phase High Temperature Alloys: Exploration of Laves-Phase Strengthening of Steels

C. T. Liu, Y. Yamamoto, Z.P. Lu, H.M. Meyer, and M. P. Brady

Oak Ridge National Laboratory

19th Annual Conference on Fossil Energy Materials

Knoxville, TN May 9-11, 2005

Outline

- New Effort: Builds on Laves-Cr Alloy Effort

- Austenitic and Ferritic Alloys
  - -potential for Laves strengthening
  - -suitability for Al-modification for improved oxidation resistance

- Early Results of Microstructure Control Attempts
  - -oxidation
  - -tensile/creep strength

Extensive Discussions and Technical Input from Phil Maziasz, Bruce Pint, John Shingledecker, and Ian Wright Gratefully Acknowledged

Improved Creep Strength and Oxidation-Corrosion Resistance Needed for DOE/ARM Program Targets

- **Ferritic steels (Fe-base): > 600°C (1110°F)**
- **Austenitic steels [(Fe,Ni) base): > 700°C (1290°F)**
- **ODS/Intermetallics: > 800°C (1470°F)**
- **Need oxidation resistance to accompany strength increases (water vapor, sulfidation, hot corrosion, etc.)**

Strengthening Approaches for Austenitic and Ferritic Stainless Steels

- **Solid solution hardening**
- **Particle strengthening**
  - **Carbide/Nitride particles:** complex MX containing Nb, Ti, V, etc. (much recent success/gains have outstripped oxidation resistance)
  - **Intermetallic particles**

    A_2B (Laves) and A_3B phases (some exploration but mixed success)
- **Slow diffusion processes: slow precipitation and coarsening kinetics**

Apply Insights Gained in Laves-Cr Effort to Ferritic/Austenitic Alloys

Microstructure Manipulation in Cr_2Ta-Cr(X) Alloys

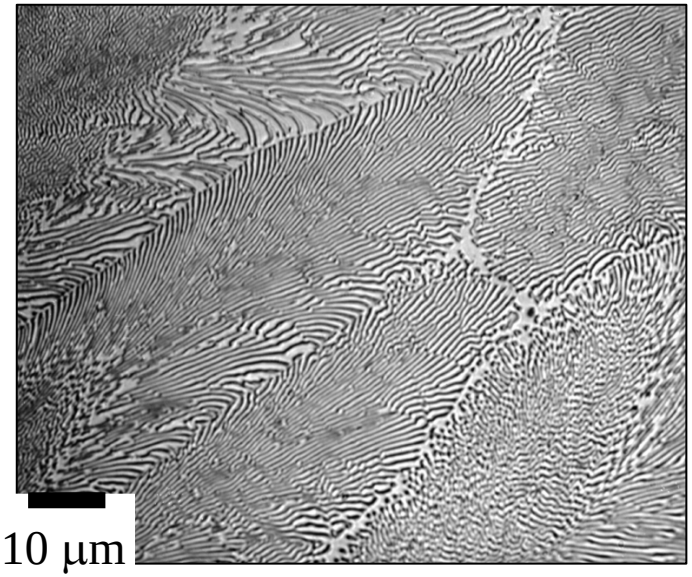

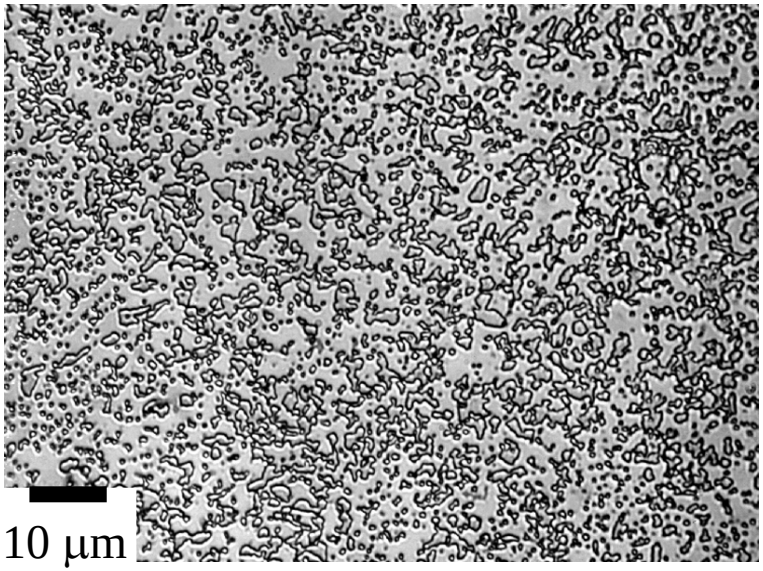

Cr_2X → Cr_2Nb-Cr → Cr_2Ta-Cr → Cr_2Ta-Cr(Fe)

- Very high strength but limited ambient toughness
- Attempt extension to Fe(Cr), <u>Fe(Ni,Cr)</u>

Intermetallic Phases in Equilibrium with γ in Ni-Nb-Fe-20Cr System

(Takeyama et al. 2001)

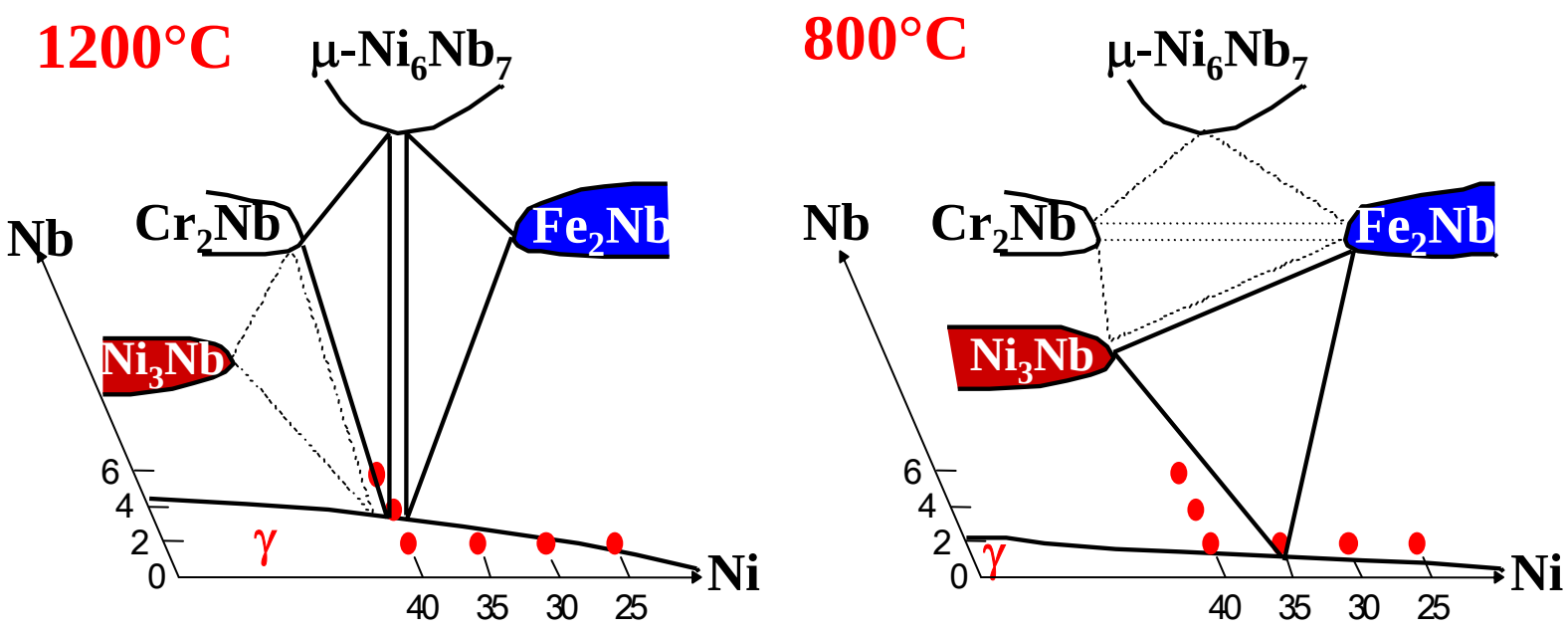

- Phase equilibria provides opportunities for **Ni_3Nb** and **Fe_2Nb** intermetallic precipitates in γ–Fe(Ni,Cr)
- The Ni content strongly affects the amount and morphology of intermetallic-precipitates

Multi-Pronged Alloy Strengthening Strategy

Solid solution + Carbides + Intermetallic

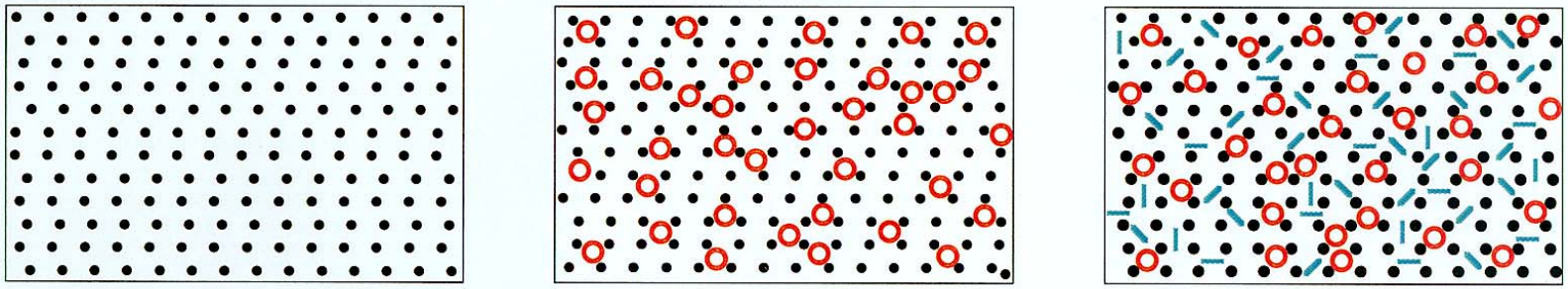

Solid Solution Hardening | Solid Solution + Carbide Hardening | Solid solution + carbides + intermetallic-phase Hardening

- Fe-(10-20)Cr-(15-25)Ni-(>1) Nb base (austenitic focus)
- Minor alloy additions are added for controlling second phase composition and morphology (B, C, Mo, Ti, V, W)
- Exploratory arc-castings: forging and/or ageing

Key Goal is to Explore Strengthening in Al-Modified Austenitic Alloys

- Al a significant benefit for oxidation at levels sufficient to form Al_2O_3 or possibly M_2O_3 where M = (Al, Cr, Fe, …)
(variation on McGurty et al. alloys from the 1970-80's)

- Al additions major complication for strengthening
  - -BCC stabilizer/delta ferrite formation
  - -may interfere with N additions
  - -stacking fault energy/cross-slip effects

- Want to use as little Al as possible to gain oxidation benefit
  - -risk internal oxidation issues

- Initial evaluation in water vapor environments
  - -present in all combustion environments
  - -volatilization of Cr-base oxide scales key problem

2.4 wt.% Al Imparts Improved Oxidation Resistance in Water Vapor at 800°C

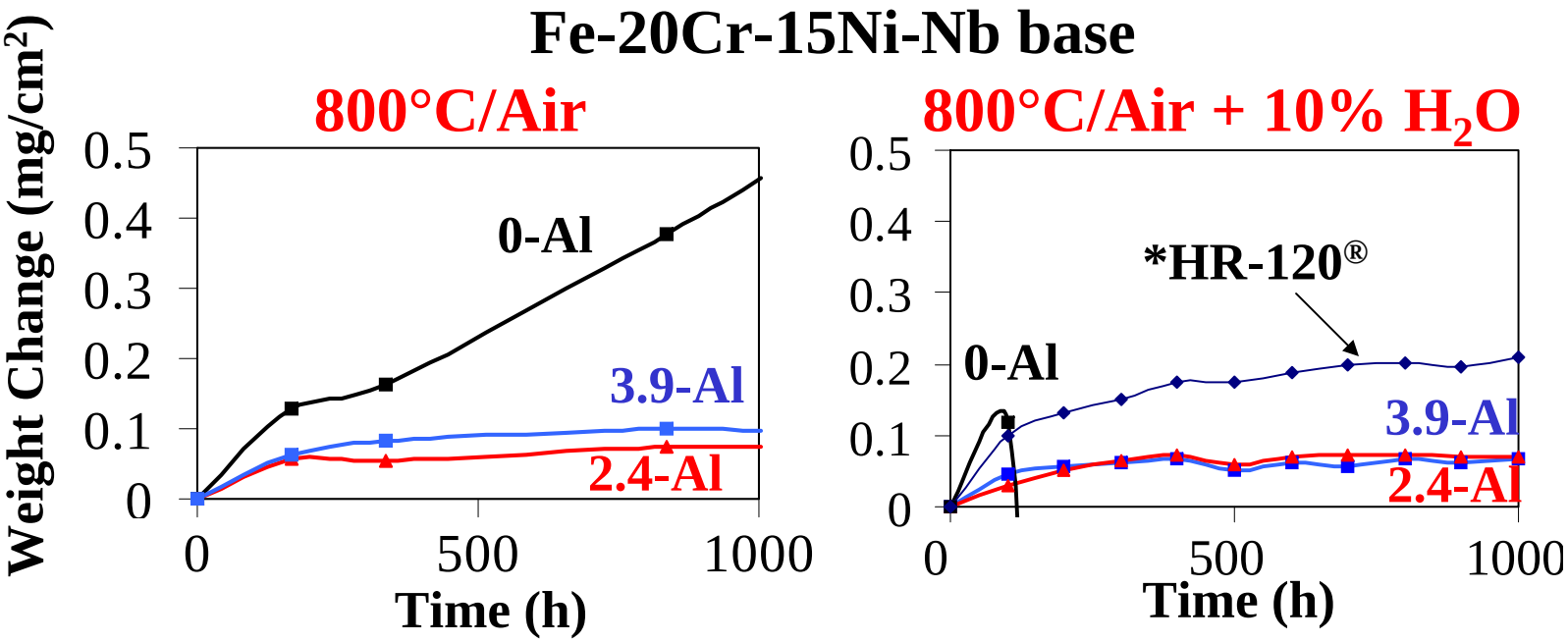

- Poor behavior of Fe-20Cr-15Ni-Nb base despite 20% Cr
- 2.4 and 3.9 wt.% Al additions significantly improve oxidation resistance in water vapor
  - -lower weight change kinetics than HR®-120

*data courtesy B.A. Pint (HR®-120 data from foil)

The 2.4 Wt.% Al Addition Also Effective at 700°C in Air + 10% H_2O

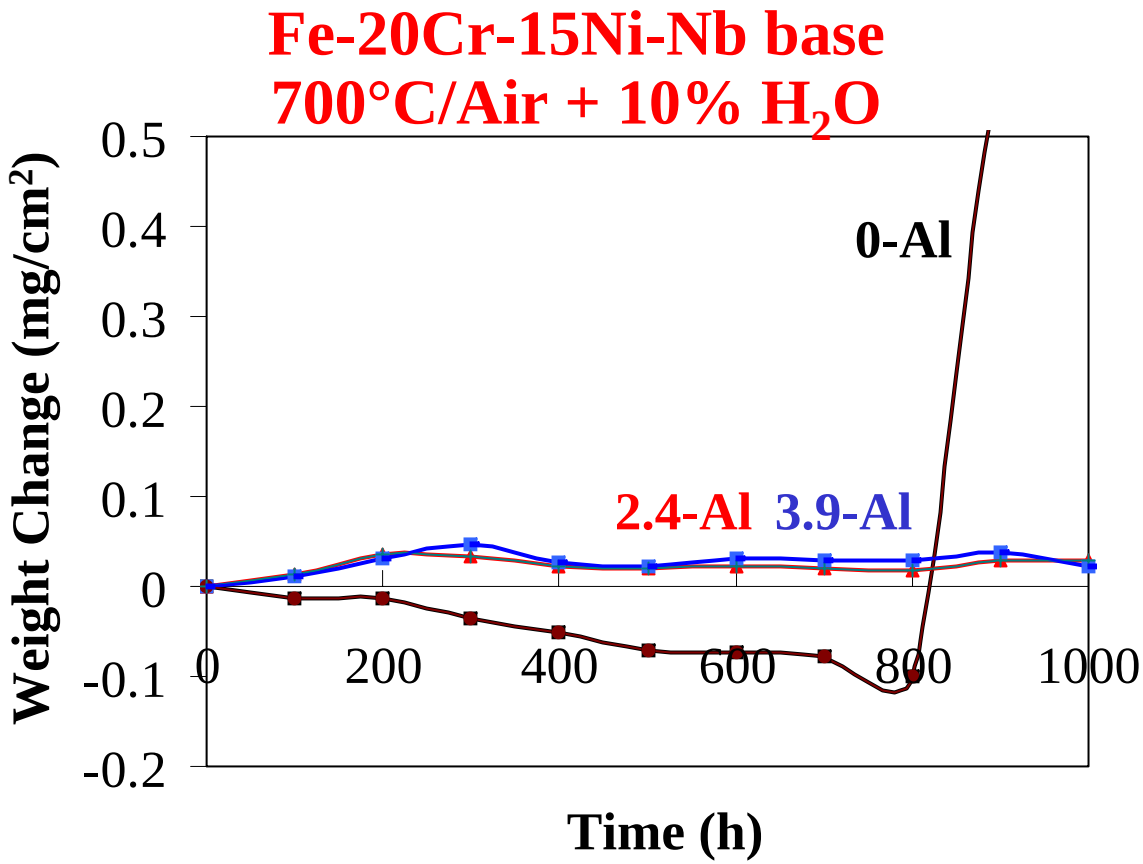

- Lower temperature water vapor environments can be more aggressive than higher temperatures (Pint-650°C was more aggressive than 700°C w/Cr_2O_3 formers)

Nodular Fe-rich Oxide Growth in Water Vapor without Al Additions

Fe-20Cr-15Ni-Nb base

800°C/1000 h/Air

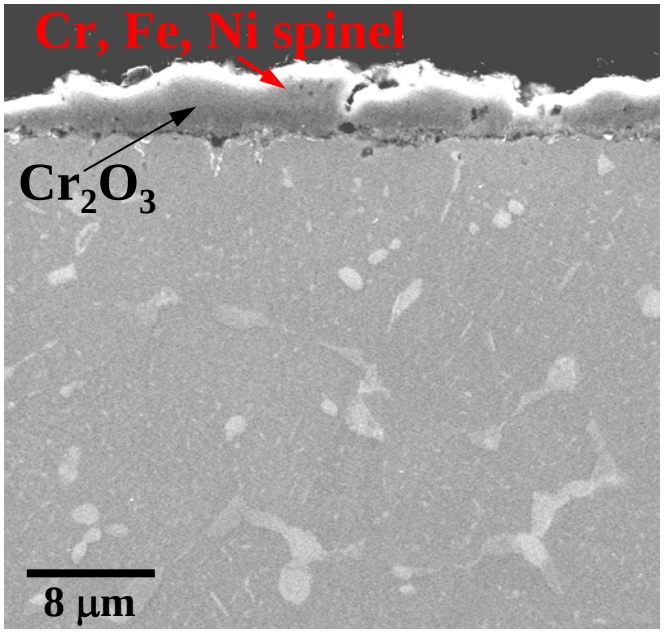

800°C/500 h/Air + 10% H_2O

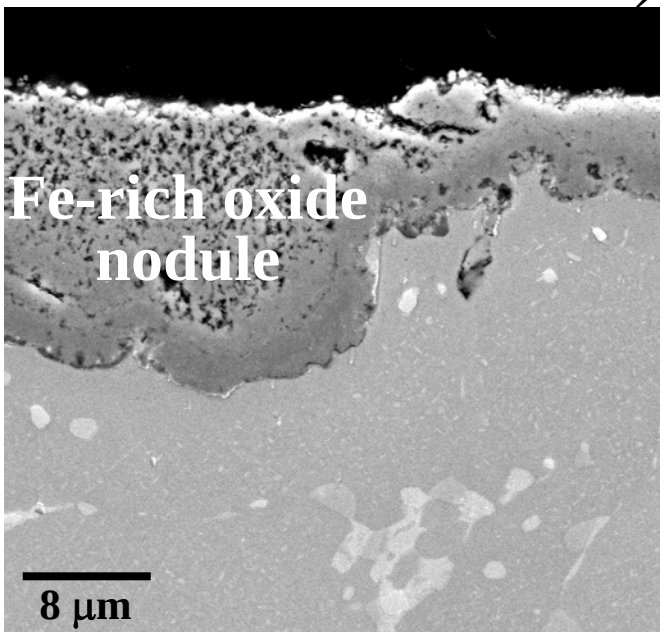

- Borderline 800°C oxidation behavior accelerated by H_2O
- Nodules classic start of breakdown of Cr_2O_3 in H_2O
- Microstructure: NbC/Fe_2Nb fine intragranular/coarse at grain boundaries- more later

Water Vapor Had Little Effect on Oxidized Surface of the 2.4 wt.% Al alloy at 800°C

XPS Survey scans on Fe-20Cr-15Ni-Nb base + 2.4 Al

Oxidized at 800°C

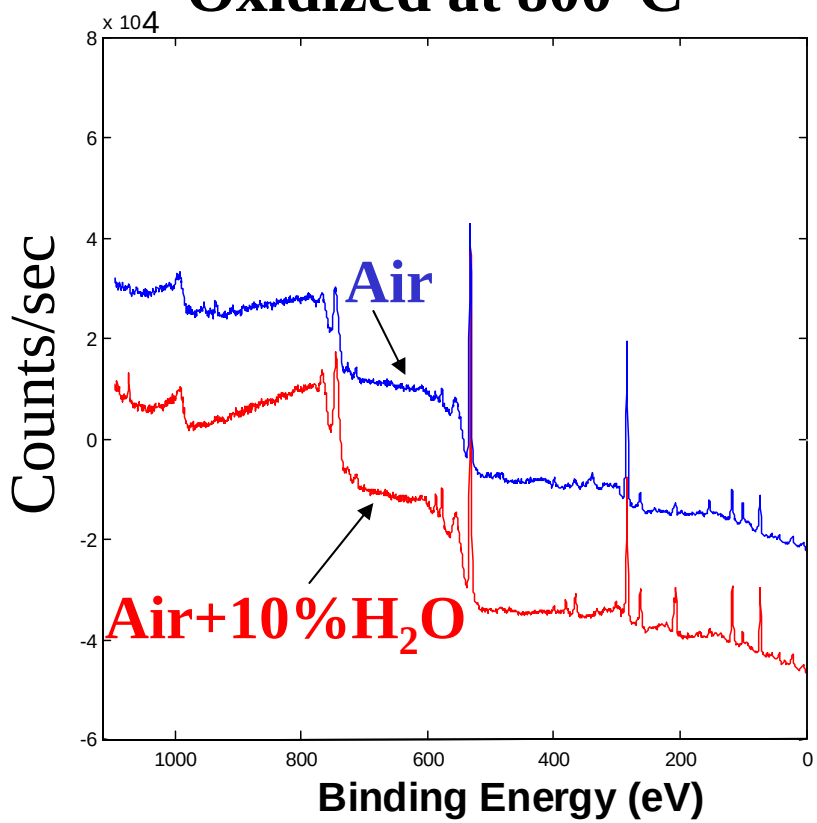

•Similar surfaces after 800°C oxidation in air and air+10%H_2O

Auger Data Indicates the Scale was Primarily Al-Oxide

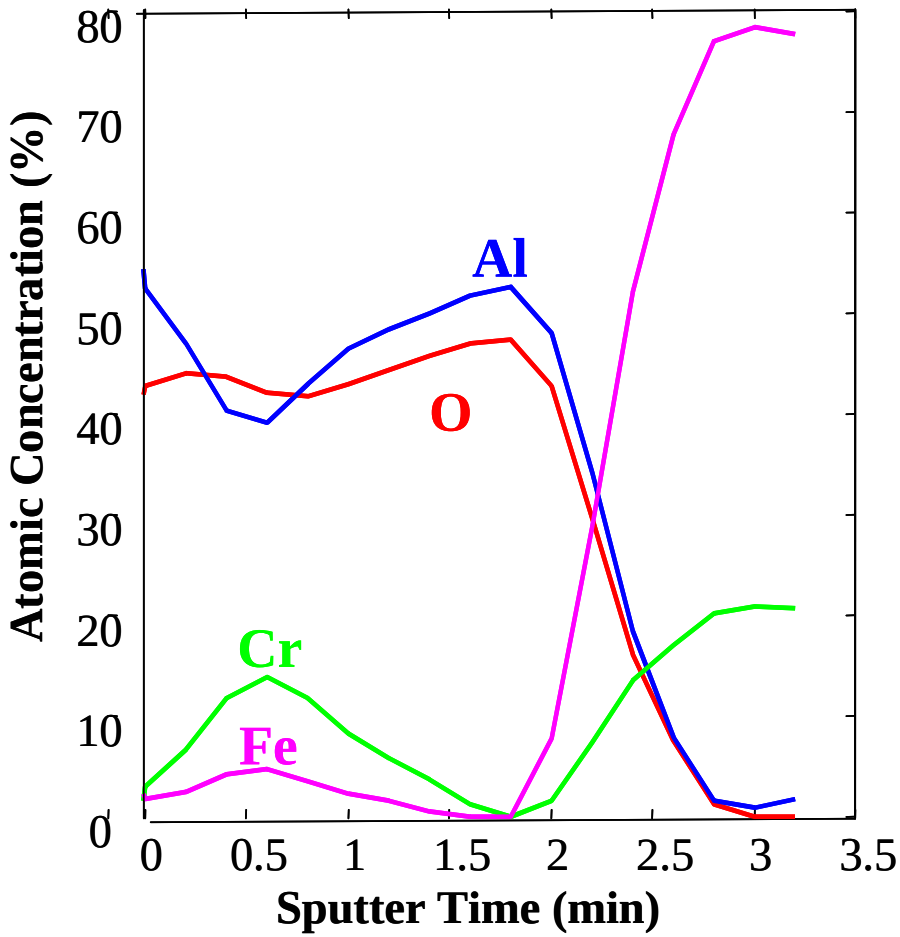

- Surface closer to Al-rich $(Al,Cr,Fe)_2O_3$ than exclusive Al_2O_3
- XRD inconclusive: likely based on transition Al_2O_3's (not α)

Submicron Scale and No Internal Attack in 2.4 Al Alloy at 800°C in 10% H_2O

SEM Cross-Section of Fe-20Cr-15Ni-Nb base + 2.4 Al 800°C/1000 h/Air + 10% H_2O

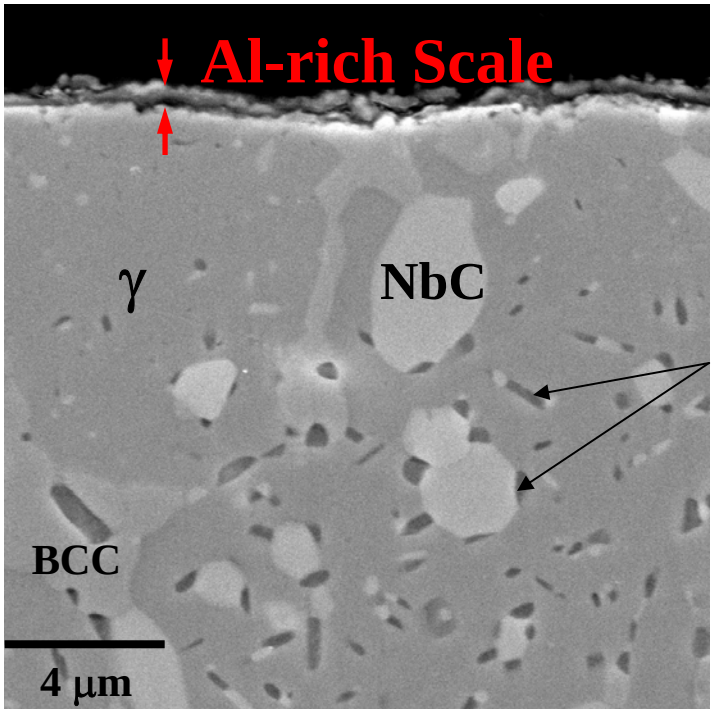

NiAl (dark rods)

- B2 NiAl base precipitates dissolve to support Al-rich oxide
- Duplex/coarse structure not ideal for strengthening-more later

Al as Nanoscale B2 NiAl-Base Precipitates

Solution Treated and Water Quenched 3.9 wt.% Al

B2 NiAl-Base Spherical Precipitates (30 nm)

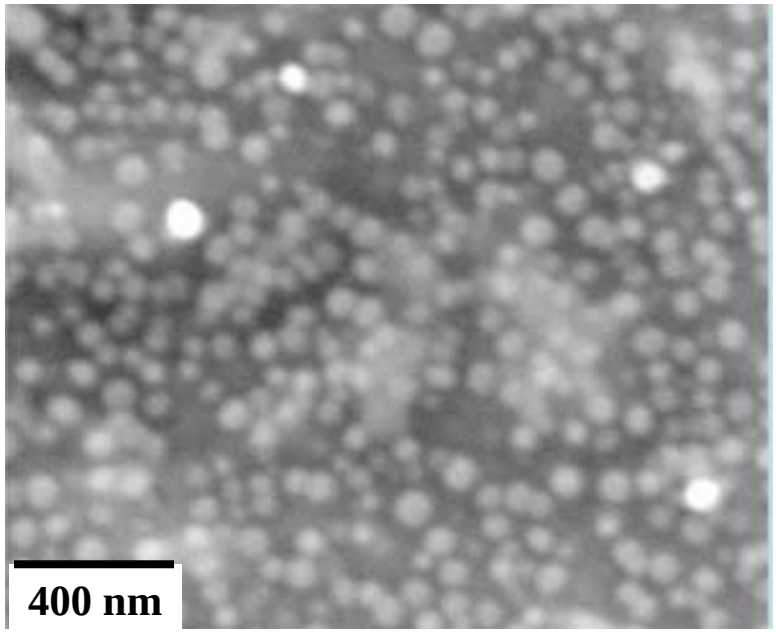

C14 Laves Fe_2Nb Base Needle Precipitates (0.5μm)

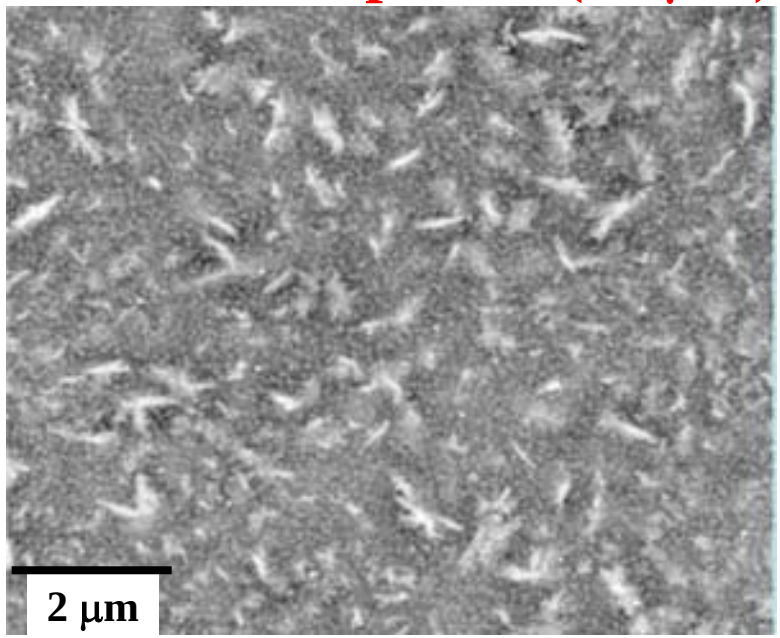

- Similar trends with 2.4 Al wt.% addition

B2 NiAl Precipitates Coarsen Significantly

TEM Bright Field Image of 800°C Annealed 3.9 wt.% Al

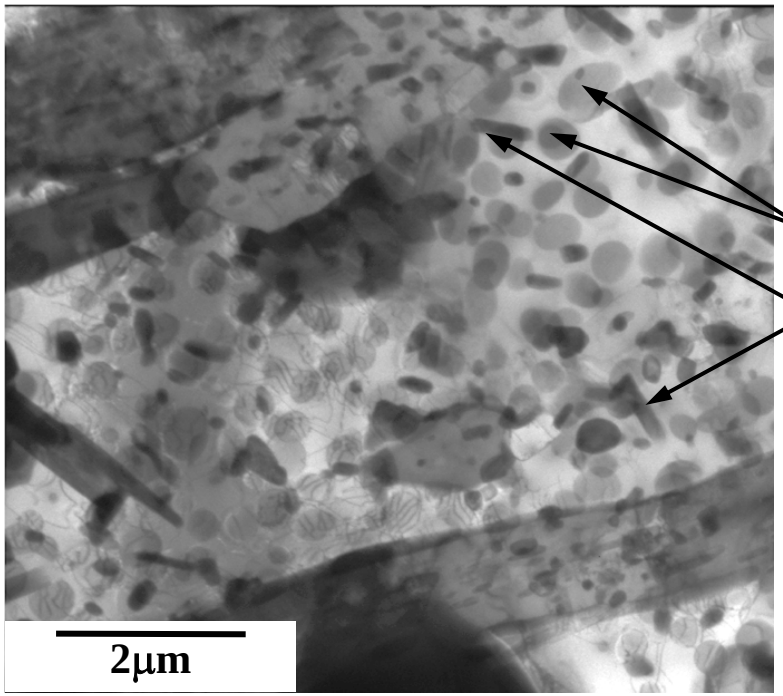

NiAl: spherical, 0.3 μm
Fe_2Nb: rod, 0.5 μm

- Coarsening of NiAl well known-still useful for oxidation
- Laves Fe_2Nb was stable

Initial Series of Alloys Show Balance of RT Ductility and High Temp Strength

Tensile Properties for Al-Modified Fe-Ni-Cr-Nb Base Alloys (FNC)

Alloy No.	Yield (ksi, MPa)	Ultimate tensile (ksi)	Elongation (%)
		room temperature	
FNC-5	122 (840)	141	5.1
-6	113 (780)	132	4.7
-8	102 (700)	121	6.6
		700°C	
FNC-5	52.0 (360)	44.5	68.1
-6	62.6 (430)	84.2	26.5
-8	60.0 (414)	82.4	40.5
		750°C	
FNC-5	41.2 (284)	51.9	81.8
-6	51.0 (352)	65.5	58.8
-8	54.3 (375)	76.1	48.3

- Decent levels of ductility despite Fe_2Nb precipitates

Two Key Microstructural Problems in First Series of Alloys

Backscatter SEM of 2.4 wt.% Al Modified Alloy

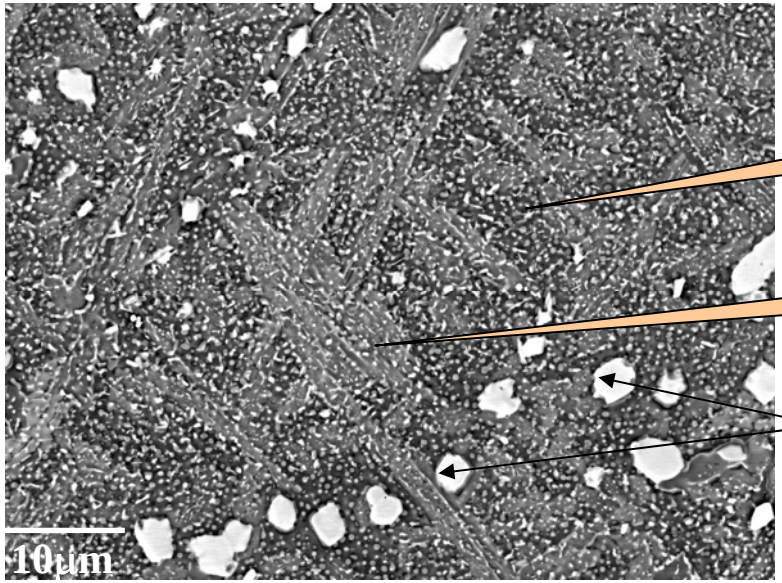

Dark area: BCC

Gray band: FCC

Coarse primary NbC/Fe_2Nb (light)

- Microstructure is duplex, not austenitic
- Regions of coarse primary NbC/Fe_2Nb
  - also have fine, intragranular NbC/Fe_2Nb (desired)

First Series of Alloys Did Not Exhibit Any Appreciable Creep Resistance

750°C/15 ksi (100 MPa) Creep Rupture Behavior

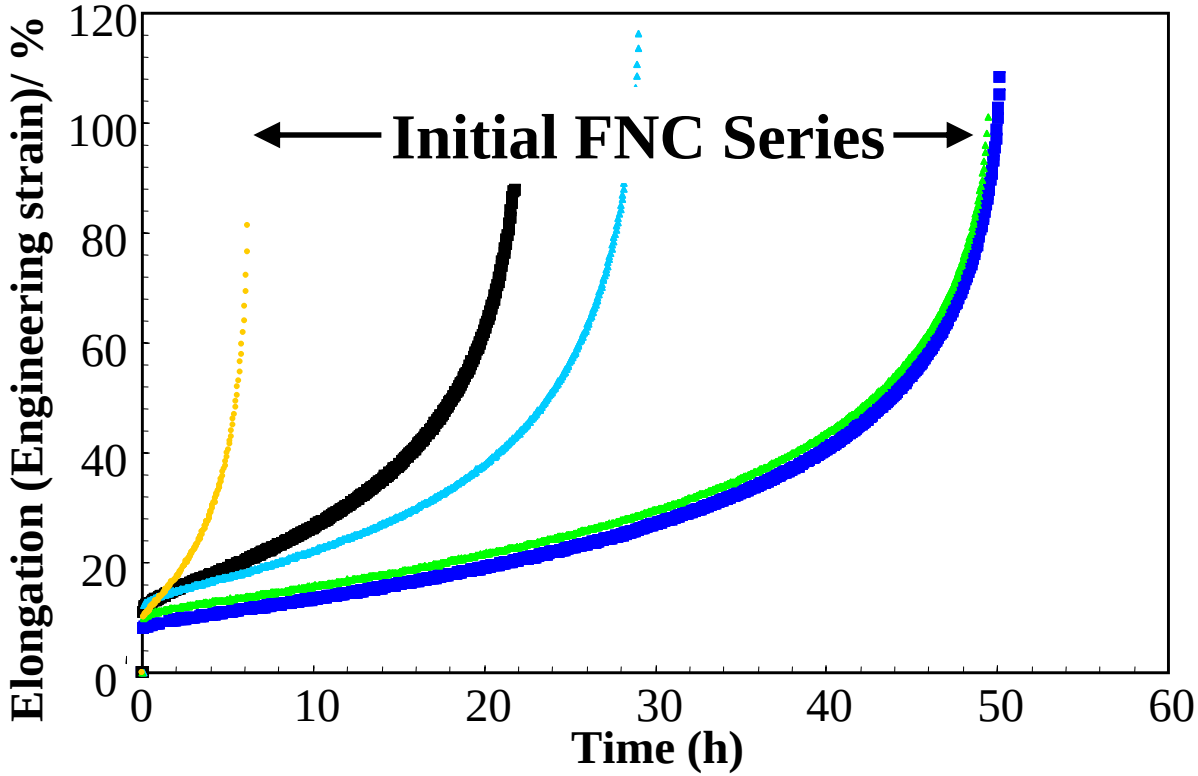

- In range of un-optimized conventional austenitics
- Optimized alloys 1000's h under these conditions

BCC Regions Converted to Sigma During Creep Exposure (BAD!)

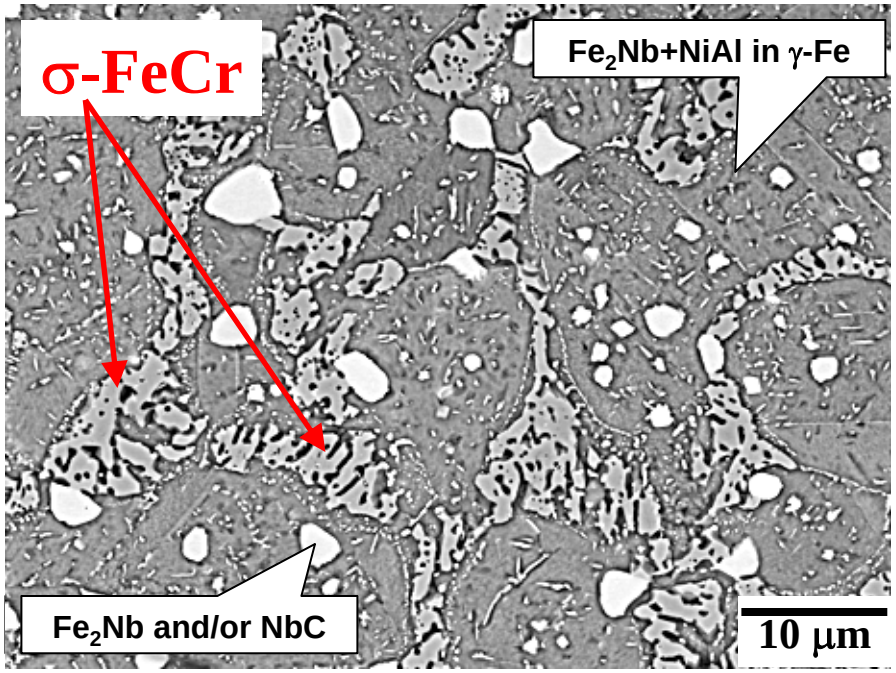

- Modify alloy composition to yield single-phase austenitic structure

Some Promising Aspects to Initial Alloy Series Microstructure

TEM Bright Field Image of γ Matrix in 800°C Aged Duplex Alloy (2.4 wt.% Al)

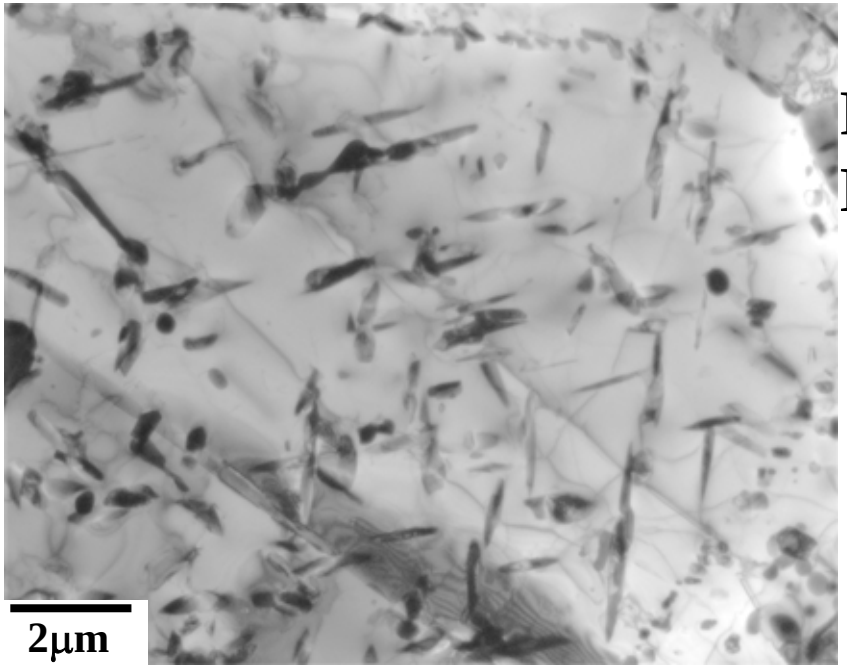

Fe_2Nb (black)
NiAl (light gray)

- High density of Fe_2Nb and NiAl precipitates
  - starting point to build on

Modified Composition to Yield Fully Austenitic Matrix

750°C/15 ksi (100 MPa) Creep Rupture Behavior

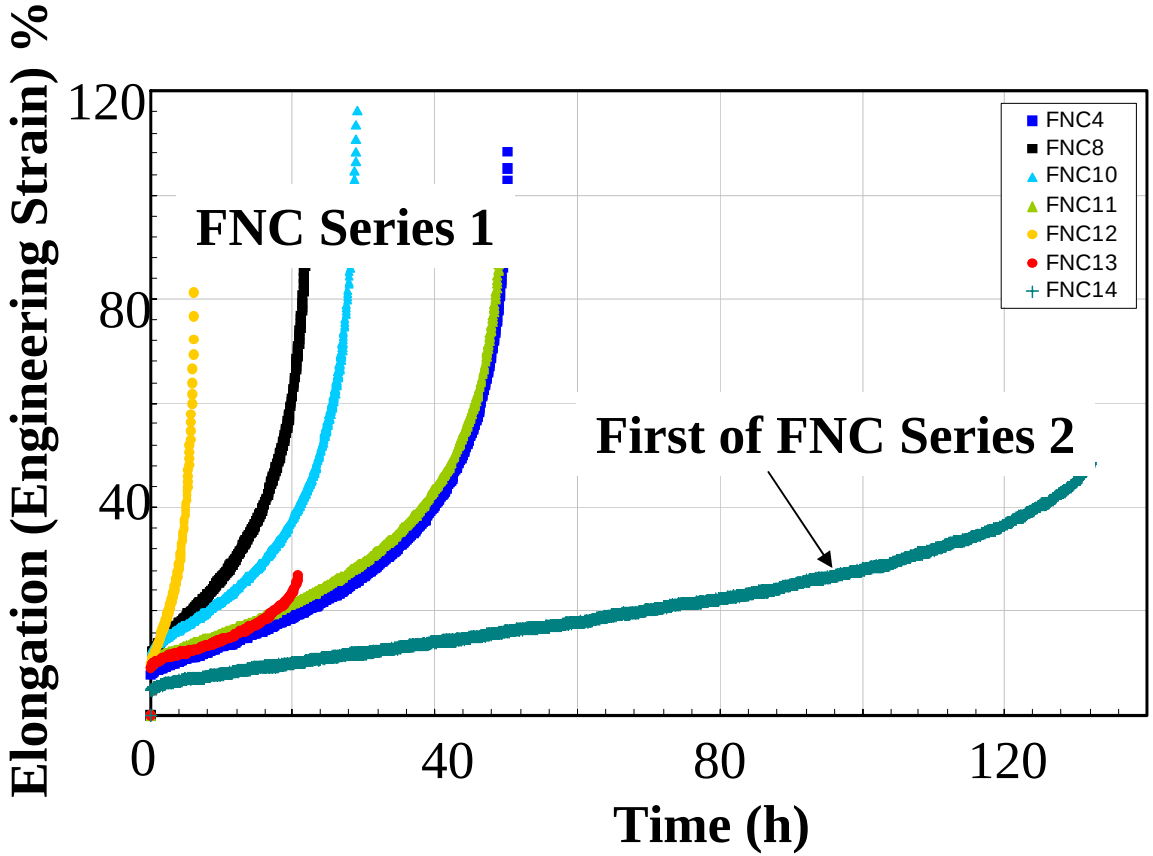

- 1st alloy of new series- significant improvement still needed

Coarse Fe_2Nb/NbC Not Helpful for Creep Resistance

SEM Images of Initial Series 2 FNC Alloys

As cast

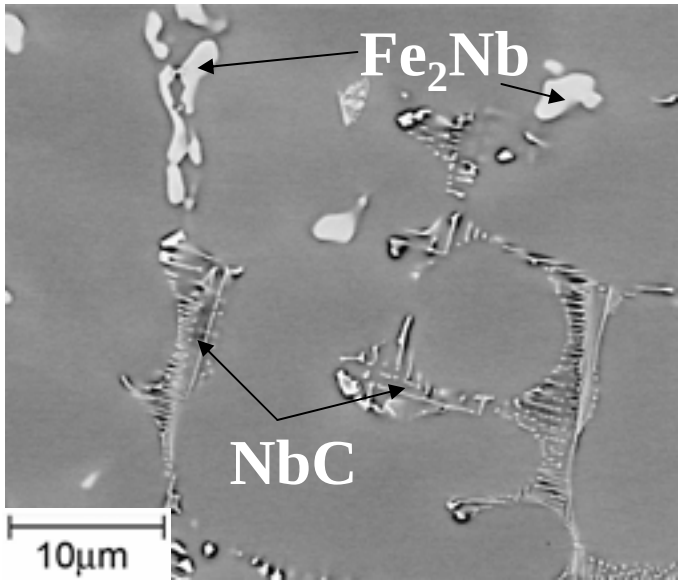

As aged

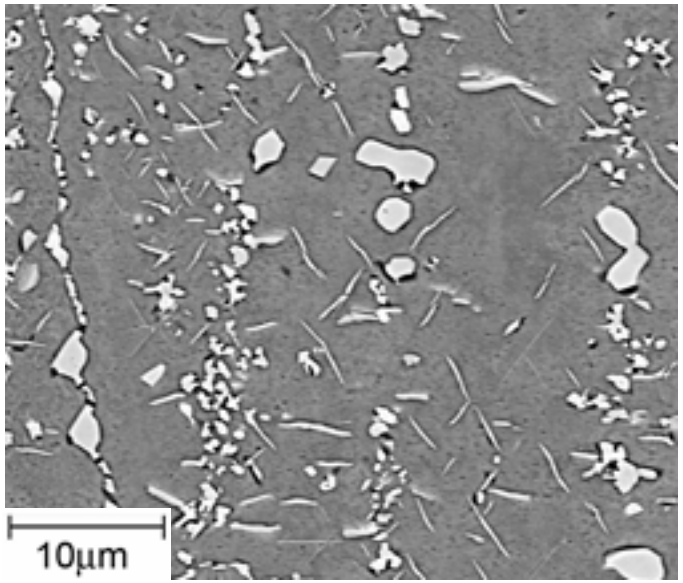

- Decreasing Nb level/modified processing should eliminate coarse primary NbC and Fe_2Nb: new alloys in progress

Initial Alloy Design Efforts Very Aggressive

- **Started with complex alloys with multiple minor additions**

- **Rapidly moving up learning curve for controlling microstructure and 2nd phase morphology**

- **Also taking step back to focus solely on Laves phase/Al effects**

Revisiting Takeyama et al. 2001 Alloys

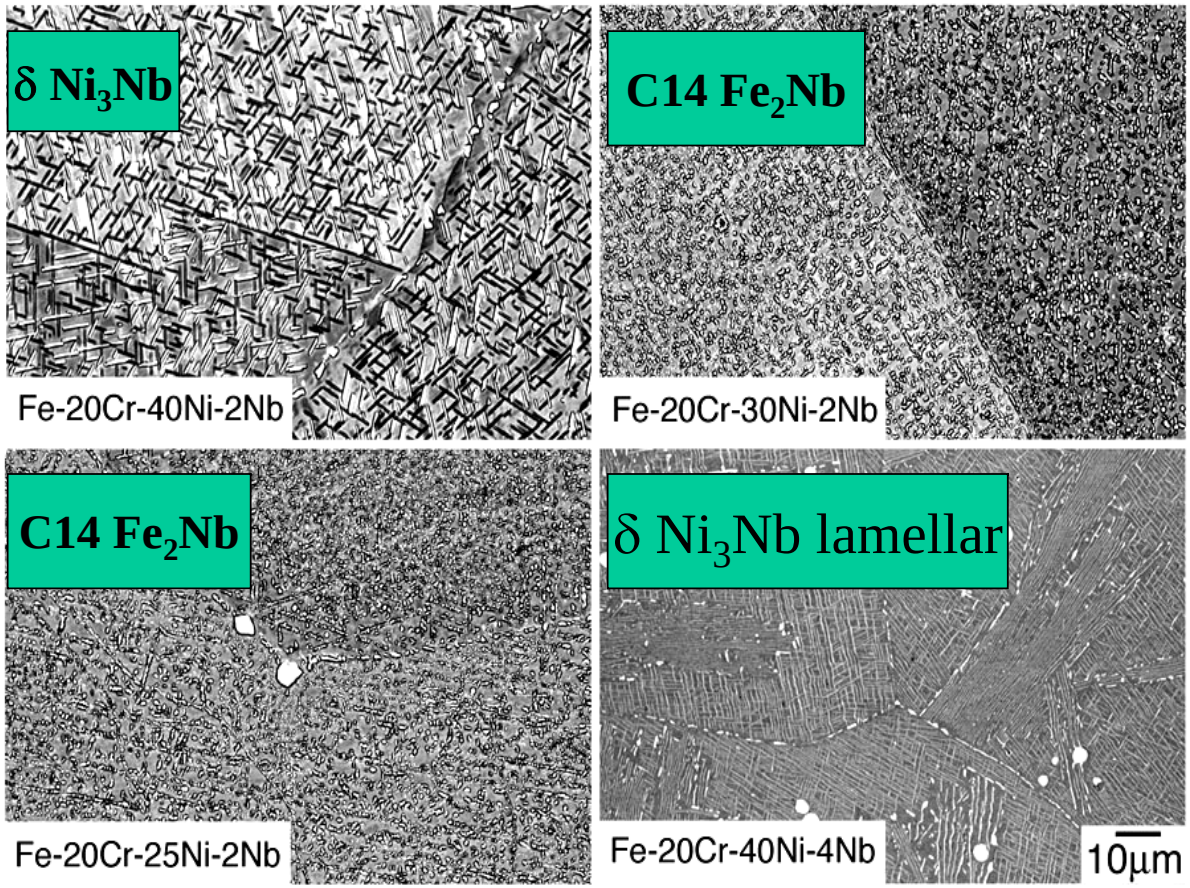

- Establish baseline tensile and creep strengths of 40 Ni (Ni_3Nb) and 30 Ni (Fe_2Nb) alloys (at.%)
- Establish effects of Al additions in phase equilbria/properties

Summary

- Relatively small Al addition (2.4 wt.%) effective in imparting Al-base oxide scale, improving resistance to water vapor environments
  - -Al in fine B2 NiAl base precipitates
  - -oxidation tests in duplex alloys/? similar in fully austenitic (will investigate)
- Progress made in understanding/manipulating Laves phase and MC carbides in Al-modified alloys
  - -no gains in creep resistance yet
  - -close to achieving desired microstructures
- Key in the next year will be to answer (go/no go decisions)
  - 1) Can Fe_2Nb strengthening of γ be effective?
  - 2) Can it be accomplished in Al-modified alloys?

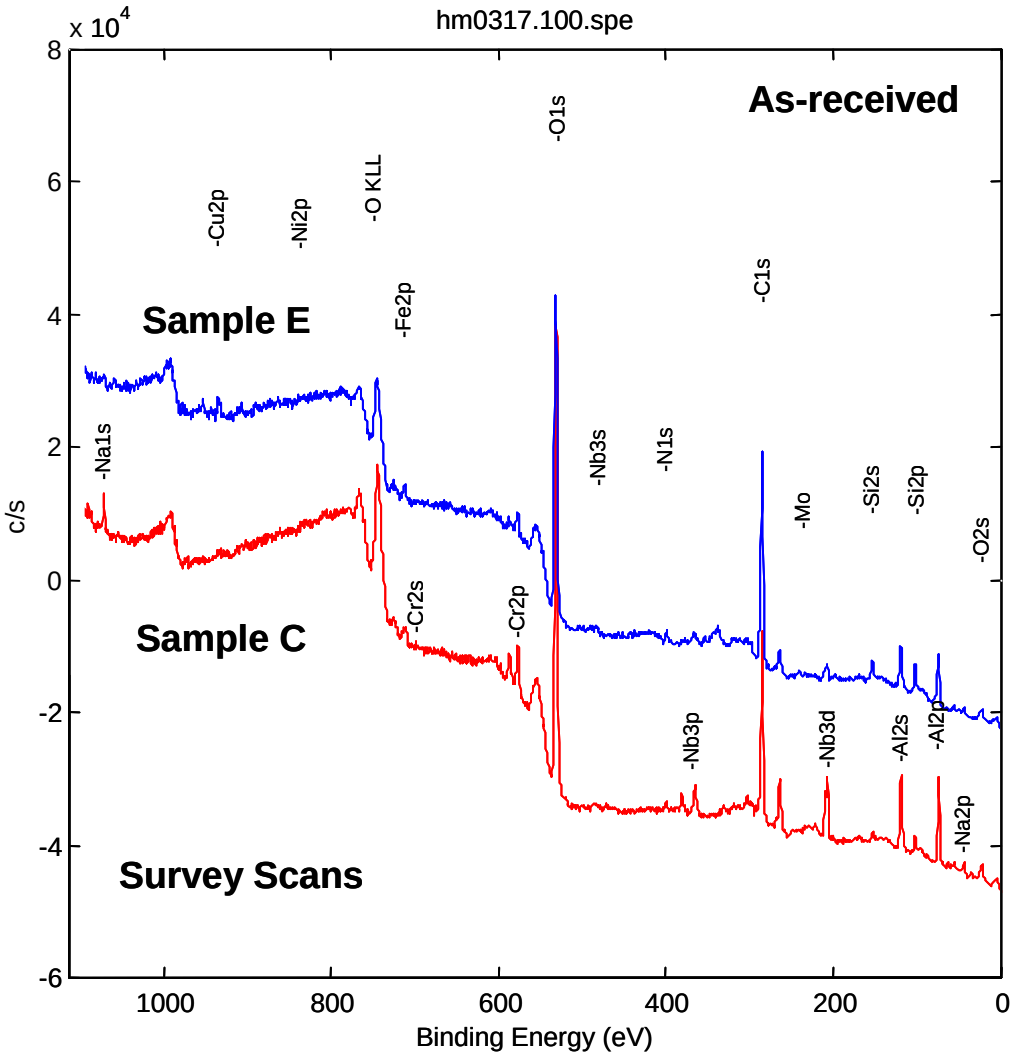
hm0317.100.spe
x 10^4
As-received
Sample E
Sample C
Survey Scans
-Cu2p
-Ni2p
-O KLL
-Fe2p
-O1s
-C1s
-Na1s
-Nb3s
-N1s
-Mo
-Si2s
-Si2p
-O2s
-Cr2s
-Cr2p
-Nb3p
-Nb3d
-Al2s
-Al2p
-Na2p
c/s
Binding Energy (eV)
8
6
4
2
0
-2
-4
-6
1000
800
600
400
200
0

IOWA STATE UNIVERSITY
OF SCIENCE AND TECHNOLOGY

AMES LABORATORY

Coating Strategies to Improve the Oxidation Resistance of bcc-Mo-Based Mo-Si-B Alloys

M. J. Kramer, A. J. Thom, Z. Tang, and M. Akinc
Ames Laboratory and Iowa State University

19th Annual Conference on Fossil Energy Materials
May 9-11, 2005
Knoxville, TN

Ames Laboratory is operated for the U.S. Dept. of Energy (DOE) by Iowa State University under contract No. W-7405-ENG-82. This work was supported in part by the Office of Energy Research, Office of Computational and Technology Research, and Advanced Energy Projects Division. This work was also supported by the U.S. Dept. of Energy (DOE) National Energy Technology Laboratory under Contract No. AL-00-360-011.

Presentation Outline

AMES LABORATORY

- Project goals
- Overview of Mo-Si-B alloys
  - Si-rich ($Mo_5Si_3B_x$-based) and Mo-rich (bcc Mo-based) alloys
  - Suitability for 3000°F applications
- Coatings by plasma spraying
  - Resulting phase equilibria
  - Coating phase stability upon annealing
- Coatings by pack cementation
  - HAPC process to siliconize surface of Alloy 3
  - Overview of properties
- Conclusions
- Thermodynamic Modeling and Alloy Design

Vision 21, FutureGen Goals

AMES LABORATORY

- Vision 21 Power Generation Goals
  - 60% efficient for coal-based, 75% efficient for gas-based by 2015
  - Near zero emissions
  - Heat exchanger and turbine component target: 1000 hours at 3000°F (~1650°C) in combustion environment

- Near Term
  - Mo-Si-B
  - T1-based alloys now meet temperature criteria for heat exchangers
  - ⇒ Issues to be addressed:
    - – Corrosion
    - – Improvements with minor alloy additions
    - – Low fracture toughness

- Future
  - Derivative Mo-Si-B alloys
  - T1-based alloys now meet creep resistance criteria for turbine applications
  - ⇒ Issues to be addressed:
    - – Near-net shape processing
    - – Low temp oxidation resistance
    - – Cyclic oxidation resistance

Mo-Si-B Intermetallic System

AMES LABORATORY

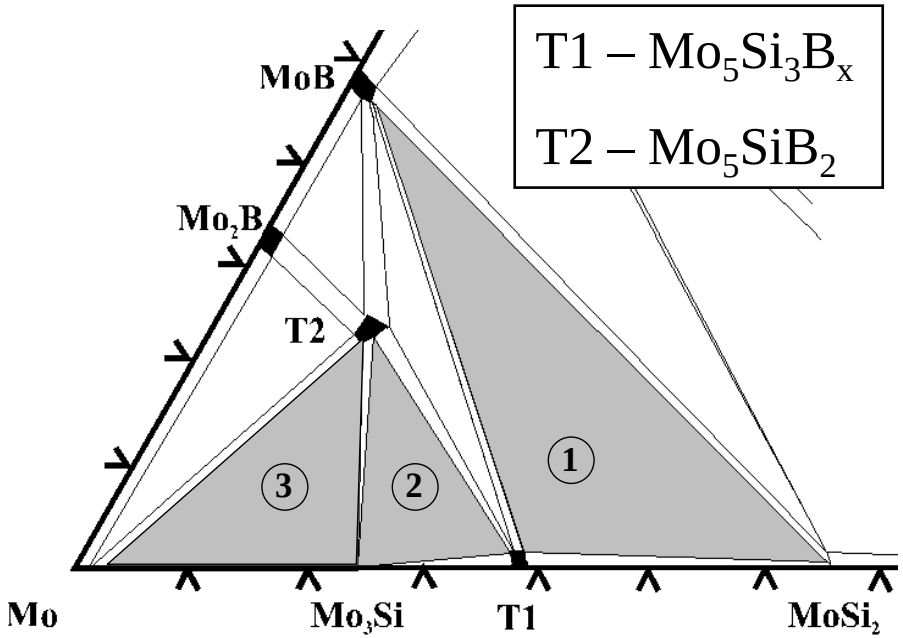

- T1-containing assemblages (1&2)
  - Excellent oxidation resistance and creep strength to near 1600°C
- Mo-containing assemblage (3)
  - Improved fracture toughness

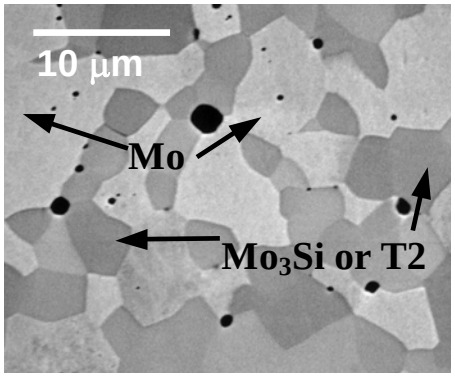

3: Mo-4.3Si-1.1B (wt%)

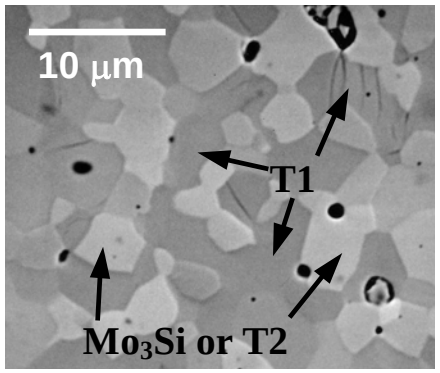

2: Mo-10Si-1.5B

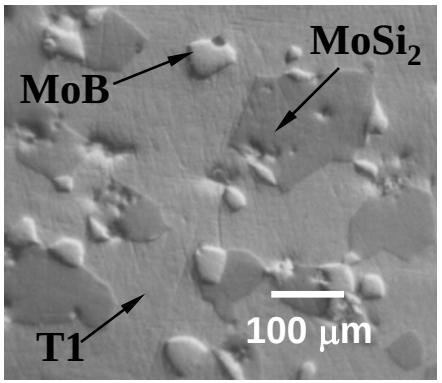

1: Mo-13Si-2.4B

Mo-Si-B Oxidation at 1600°C in Dry Air

AMES LABORATORY

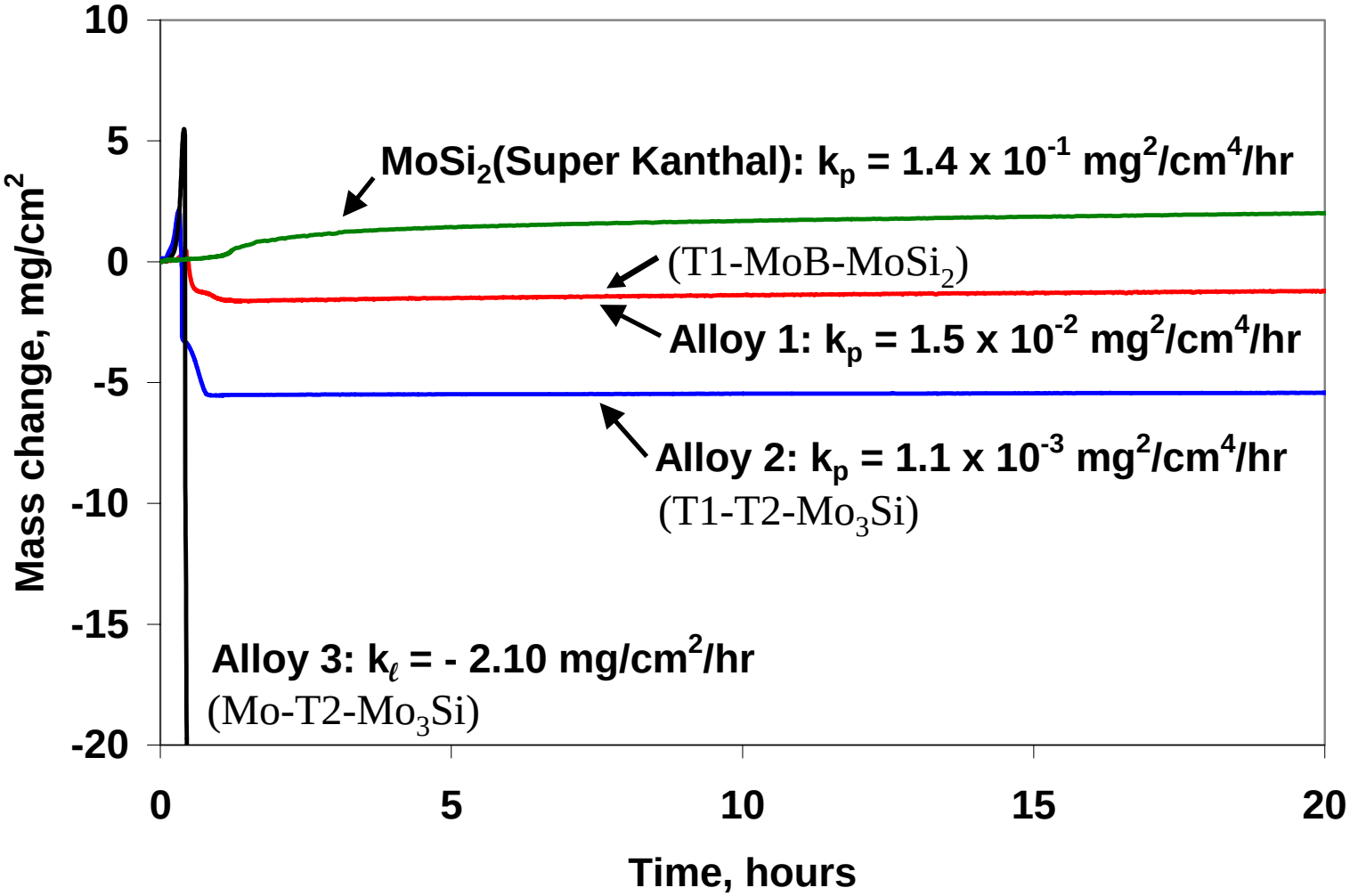

⇨ *T1-based alloys presently meet Vision 21 oxidation metric*

Alloy 3 Mechanical Behavior

AMES LABORATORY

- Room temperature crack growth resistance

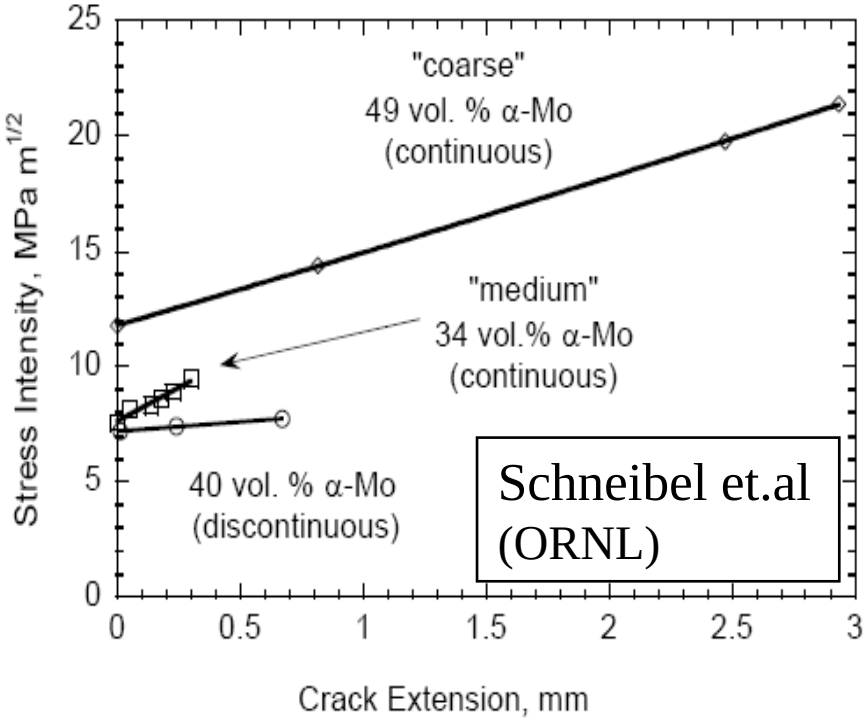

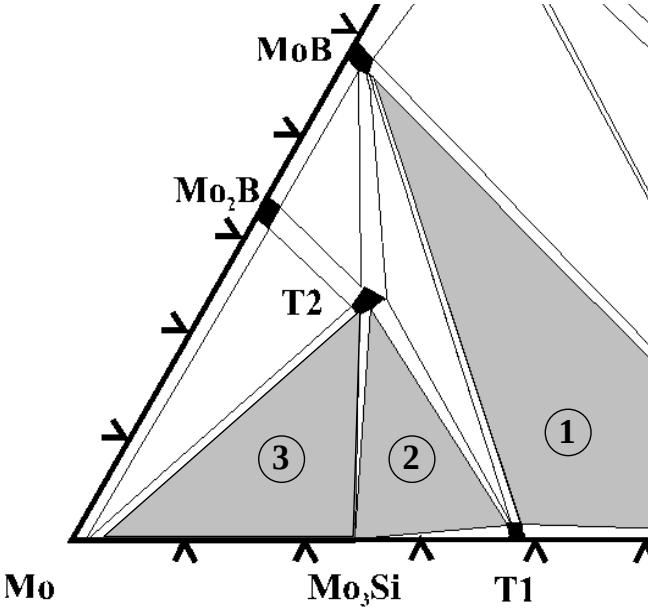

⇨ *Tradeoff of poor oxidation resistance with improved fracture resistance for Alloy 3*

⇨ *Use Alloy 1-based coatings to protect mechanically tough, but oxidatively unstable Alloy 3-based substrates (ie- FGM's)*

Experimental

AMES LABORATORY

- Air plasma spraying (APS) of Mo-Si-B alloys (with INL)
  - Substrate: grit-blasted Mo foil, 2 x 2 inch tiles
  - 100 mm standoff, air cooled back plate
  - Side 1: ~500 μm Alloy 1; Side 2 ~ 500 μm Alloy 3
  - Ar annealing at 1600°-1800°C
- Characterization of APS coatings
  - As-sprayed: XRD, chemical analysis, cross-sectional SEM
  - Annealed: XRD, cross-sectional SEM
  - Oxidation testing at 1600°C in air
- Siliconizing surface of Mo+T2 alloys
  - Halide Activated Pack Cenmentation (HAPC) process using Si, NaF (activator), Al_2O_3 (inert filler)
  - Co-deposition of B and Si to effect borosilicate glass formation
  - Coating characterization and oxidation

Alloy 1 APS Coating

- As-sprayed Alloy 1 coating

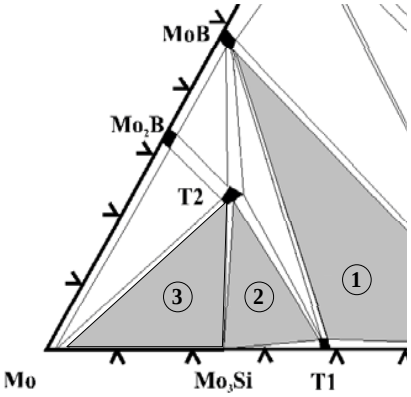

AMES LABORATORY

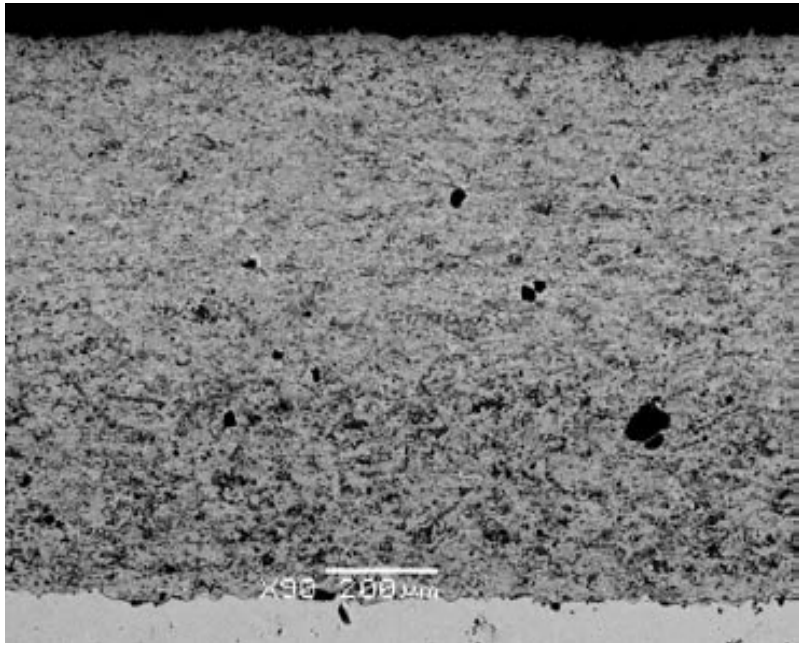

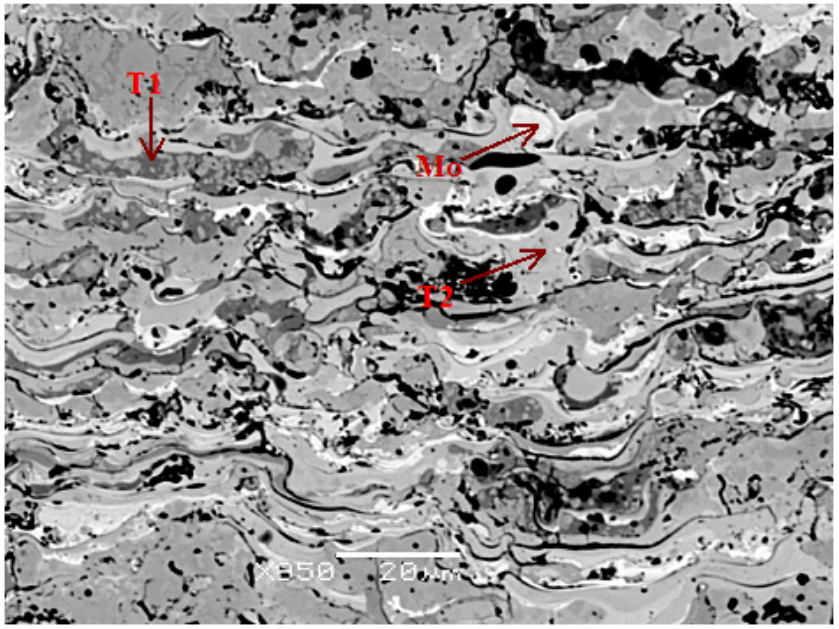

- Higher pore density near Mo substrate
- Non-equilibrium phase constitution: Mo, MoB, $MoSi_2$, T1, T2

Alloy 1 APS Coating

AMES LABORATORY

- Annealed coating: 1800°C/2 hrs/Ar

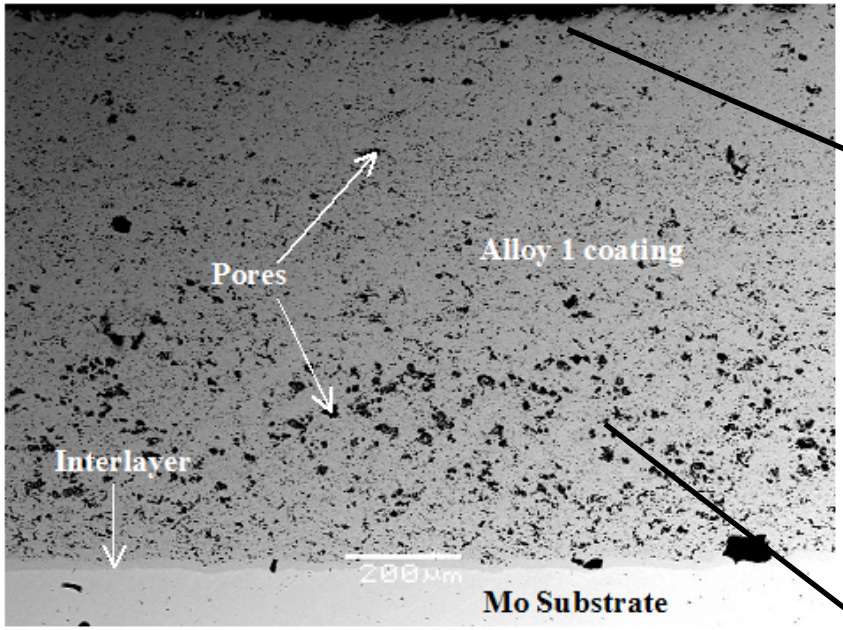

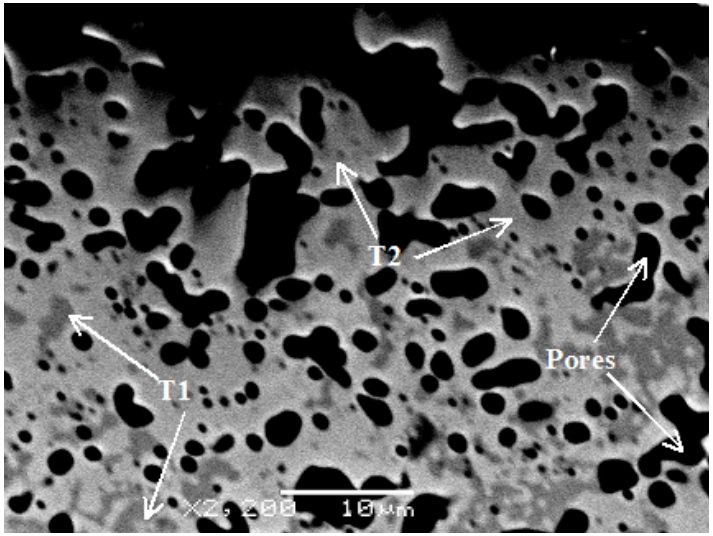

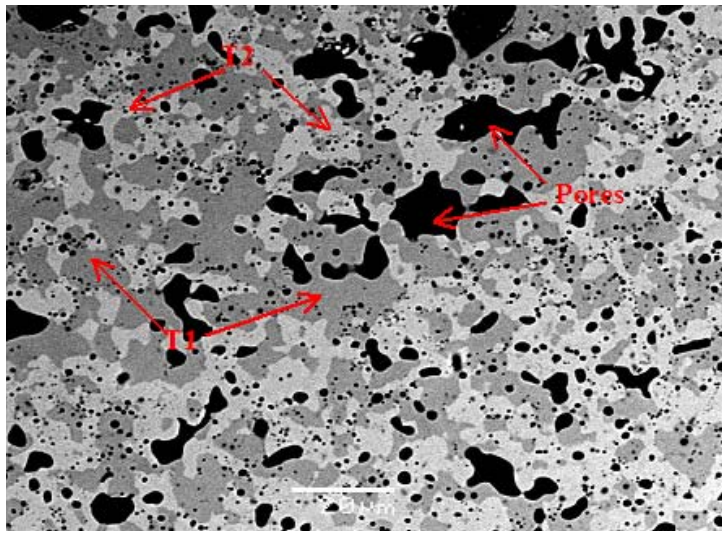

- Mo-enrichment of coating
  - Exclusive T2 formation at surface
  - T1 + T2 at interior

Alloy 1 APS Coating

AMES LABORATORY

- Reaction layer between Mo and Alloy 1 coating at 1800°C/2 hrs

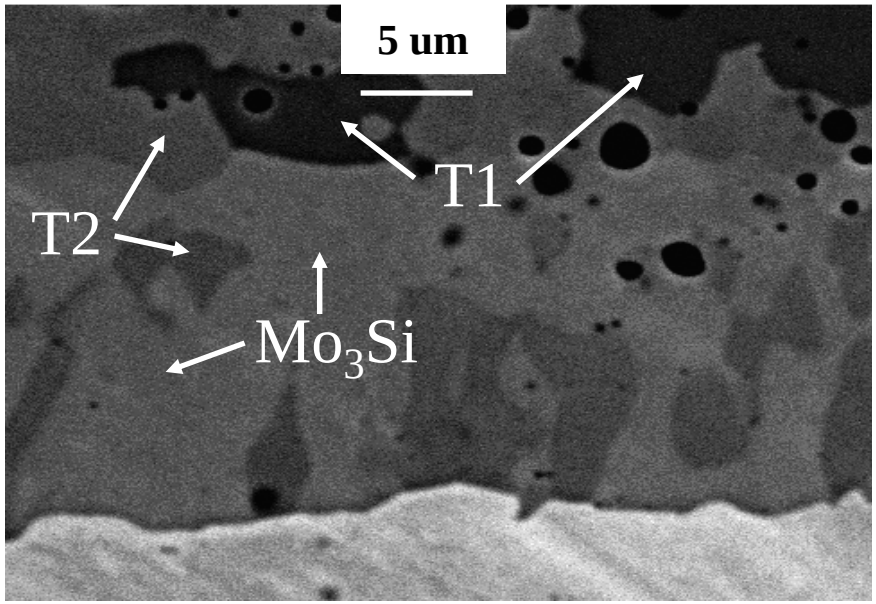

Alloy 1 coating

Reaction zone

Mo substrate

Alloy 1 APS Coating

AMES LABORATORY

- Formation of reaction layer between Mo and Alloy 1 coating

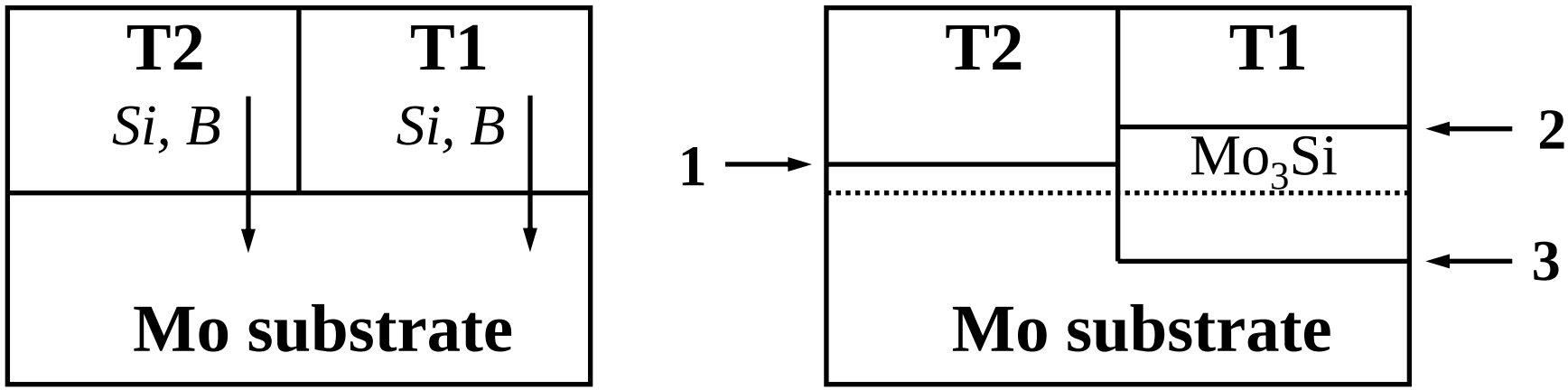

- Interface 1: $Mo_5SiB_2 \rightarrow Mo(Si,B)$ ⇨ minor growth into T2
- Interface 2: $Mo_5Si_3B \rightarrow Mo_3Si + Si$ ⇨ major growth into T1
- Interface 3: $Si + Mo \rightarrow Mo_3Si$ ⇨ major growth into substrate
- Uneven interface growth
- D_{Si} strongly dependent upon temperature

Coating Evolution with Annealing Time

AMES LABORATORY

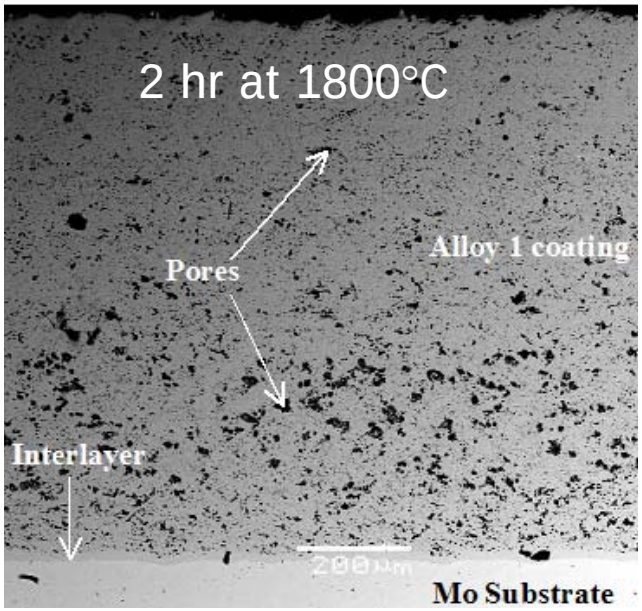

50 hr at 1800°C

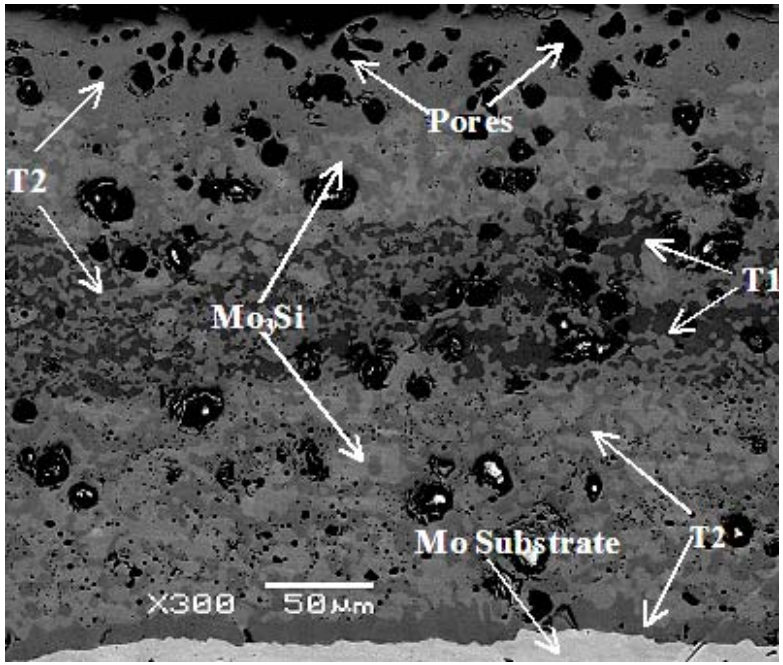

100 hr at 1800°C

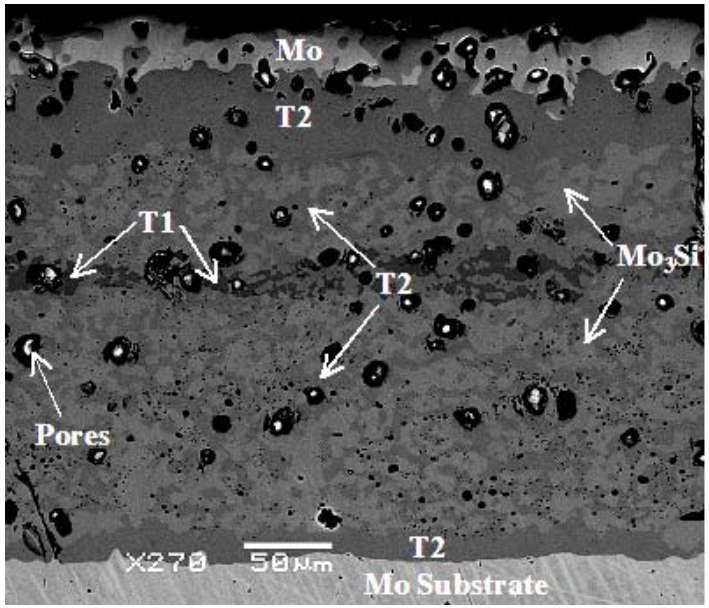

Evolution of Annealed Alloy 1 Coating

AMES LABORATORY

1. Inward progression of decomposition of T1 into Mo_3Si
2. Formation of continuous T2 layer adjacent to Mo substrate

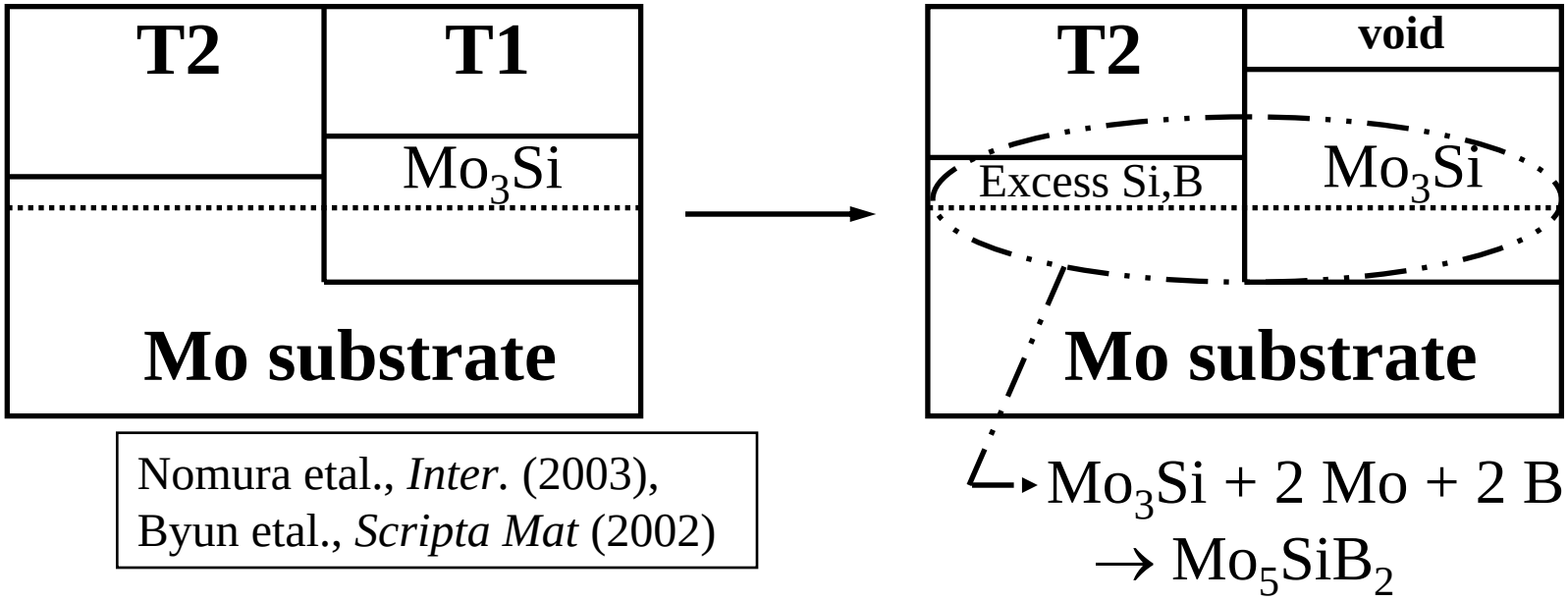

Nomura etal., *Inter.* (2003),
Byun etal., *Scripta Mat* (2002)

3. Volatility of Si, B from surface during extended low PO_2 anneal leads to formation of metal-enriched surface

Coating Composition with Annealing

AMES LABORATORY

Composition	Wt.%		Mol.%		Mo/Si
	Mo	Si	Mo	Si	
Powder					1.83
As-sprayed (M3)					2.07
2hrs@1600ºC annealing (M5)					2.35
2hrs@1800ºC annealing (M3)					2.26
50hrs@1800ºC annealing (M3)					3.24

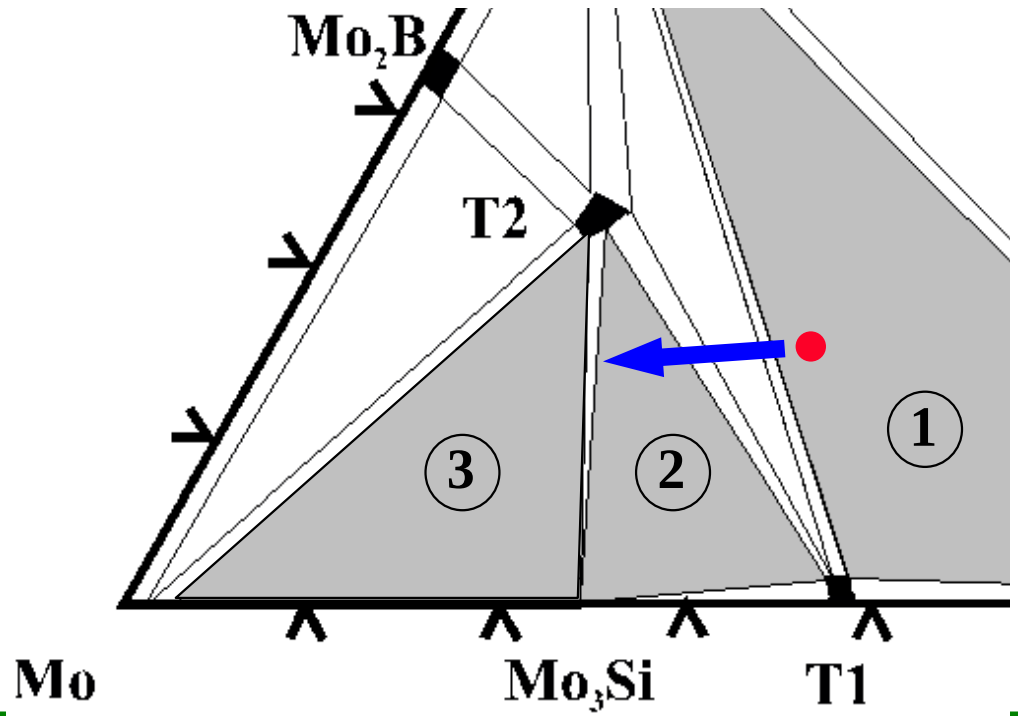

Coating Oxidation at 1600°C in Air

AMES LABORATORY

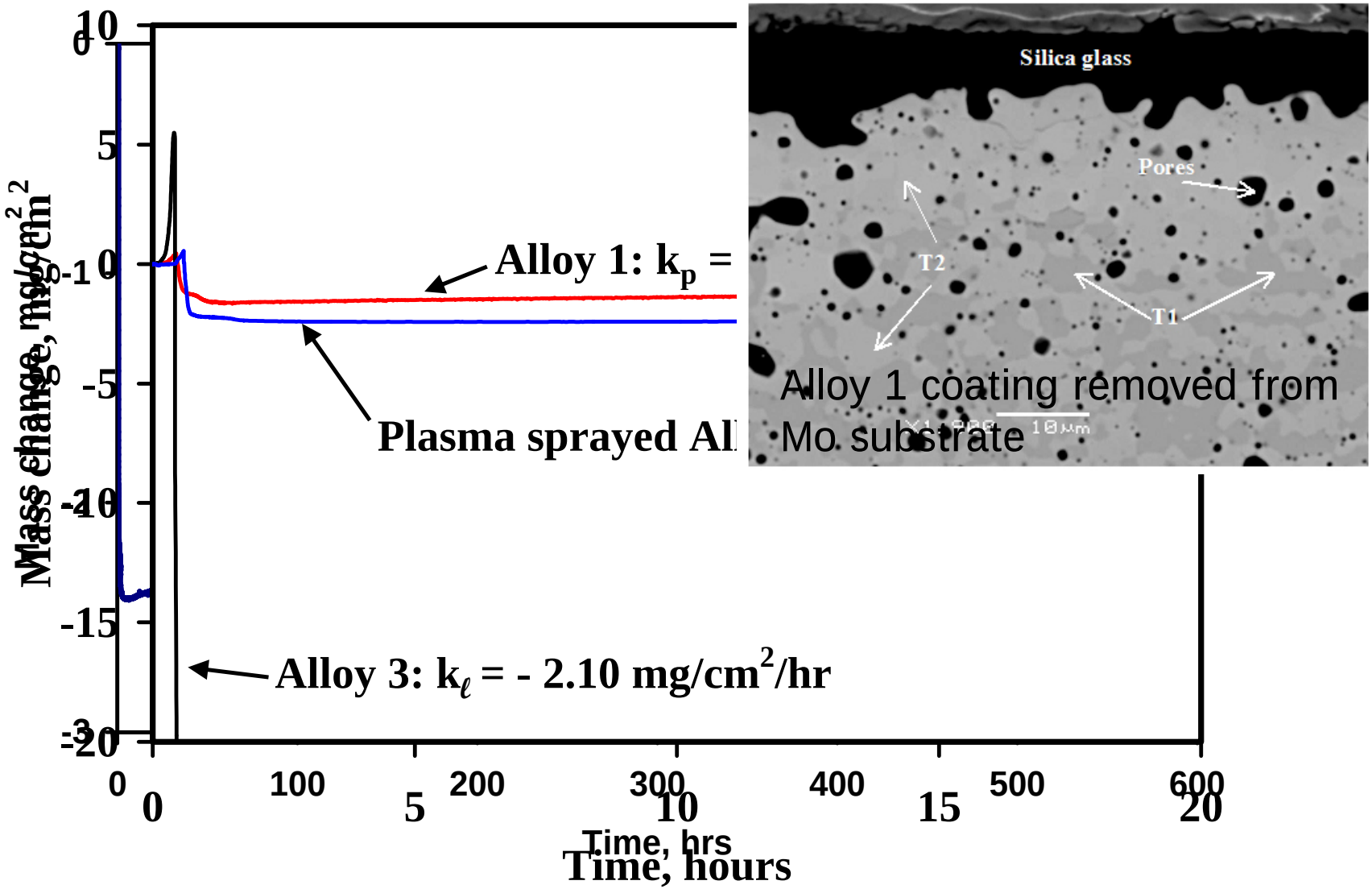

Alloy 3 APS Coating

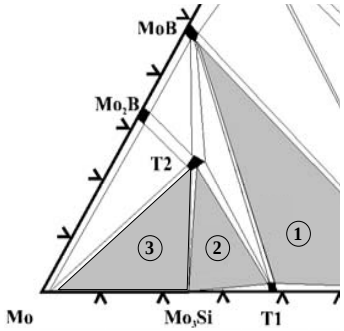

AMES LABORATORY

- Annealed coating: 1800°C/2 hrs/Ar

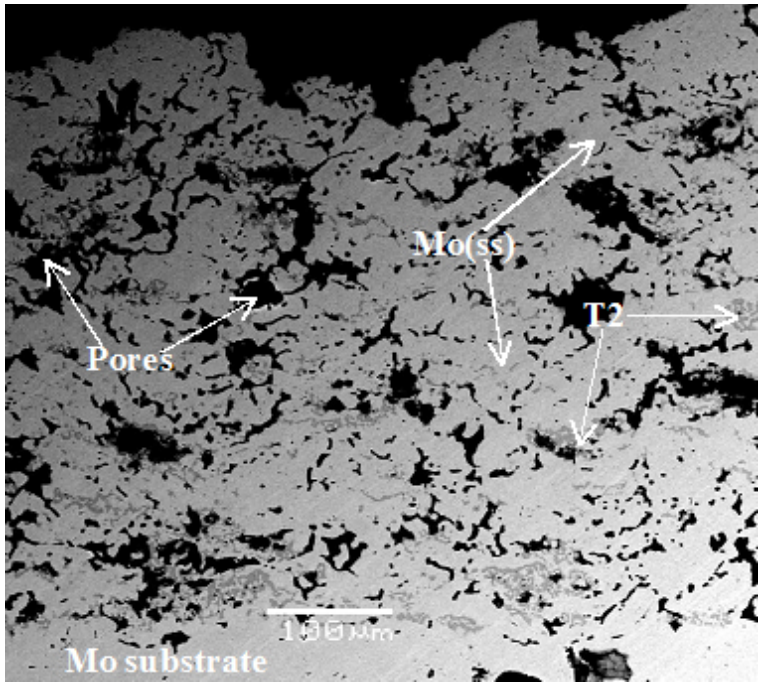

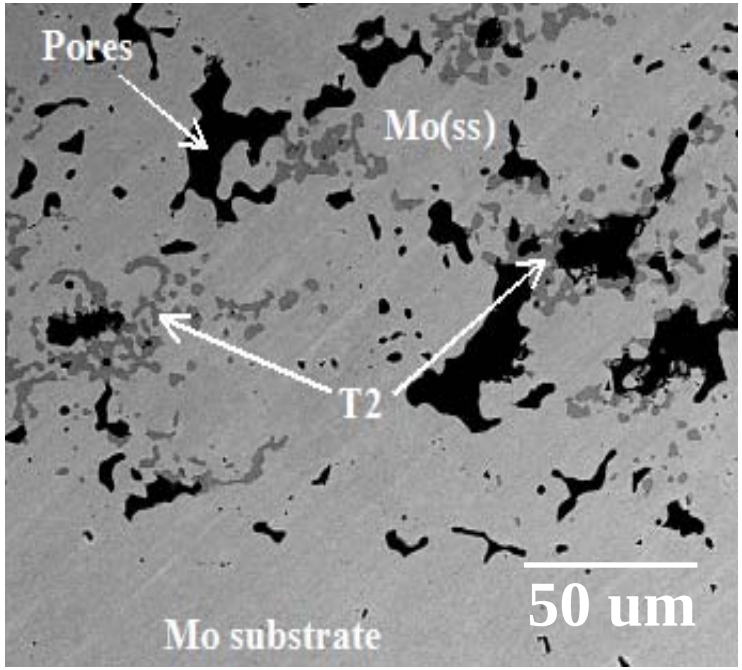

- Significant pore density within coating
- Extensive loss of Si for APS
- Minor amount of T2 within Mo matrix
- Complete oxidation of coating after 1 hour in air at 1100°C

Siliconizing Alloy 3 Coupons

AMES LABORATORY

- Halide activated pack cementation (HAPC) process
- Pack mixture (wt%)
  - $NaF:Si:Al_2O_3$ = 2:10:88
  - $B:NaF:Si:Al_2O_3$ = 1:2:9:88
- Pack conditions
  - 900°C for 16 hrs in argon
  - Alumina cement sealed alumina crucible

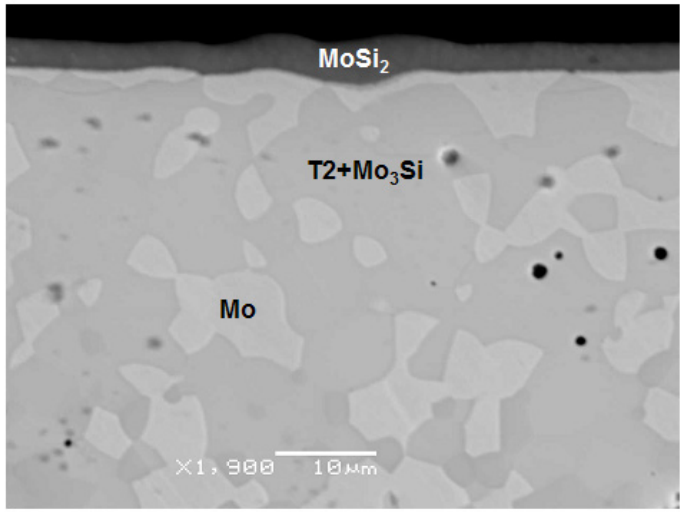
MoSi2
T2+Mo3Si
Mo
X1,900 10μm

y HAPC

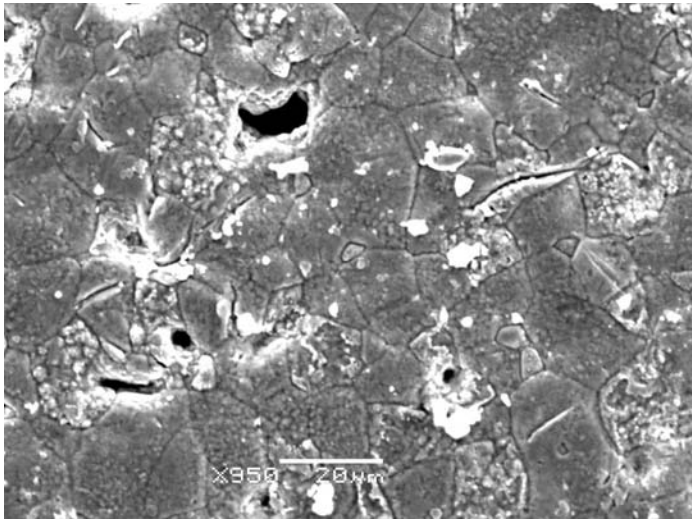
X950 20μm

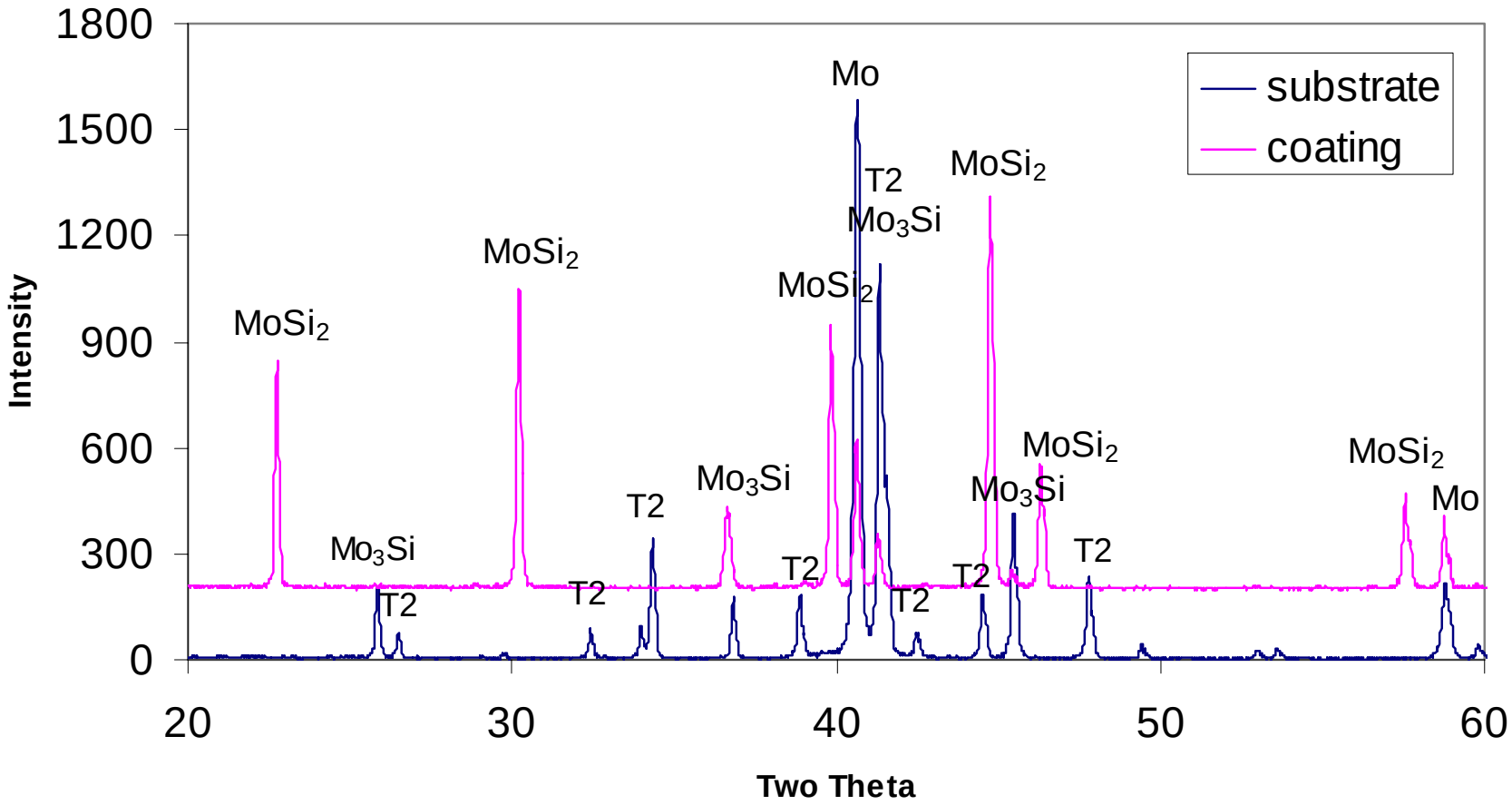
substrate
coating
Intensity
Two Theta
1800
1500
1200
900
600
300
0
20
30
40
50
60
MoSi2
Mo3Si
T2
Mo
MoSi2
Mo3Si
T2
MoSi2
Mo3Si
T2
MoSi2
Mo

Coating Defects

AMES LABORATORY

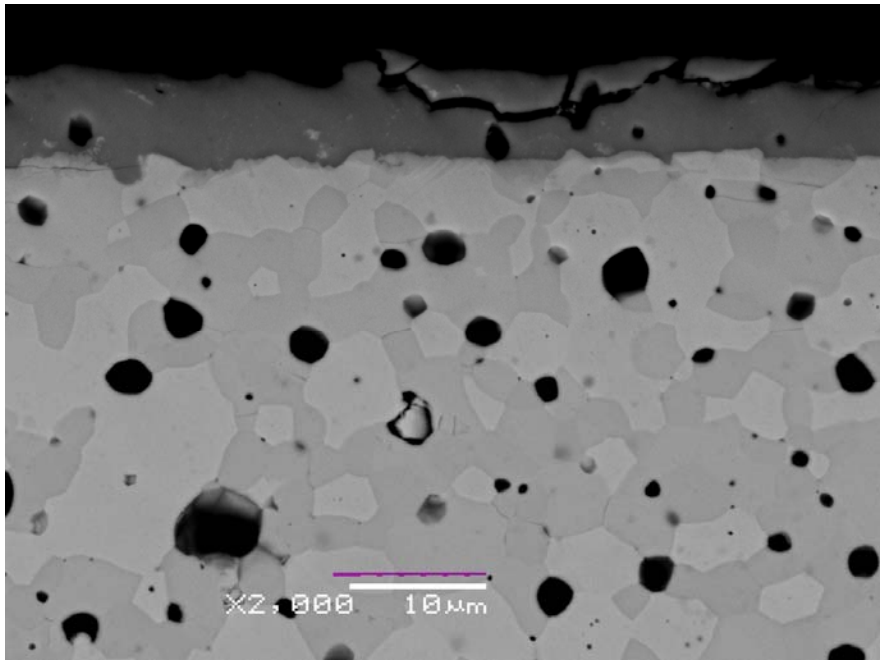

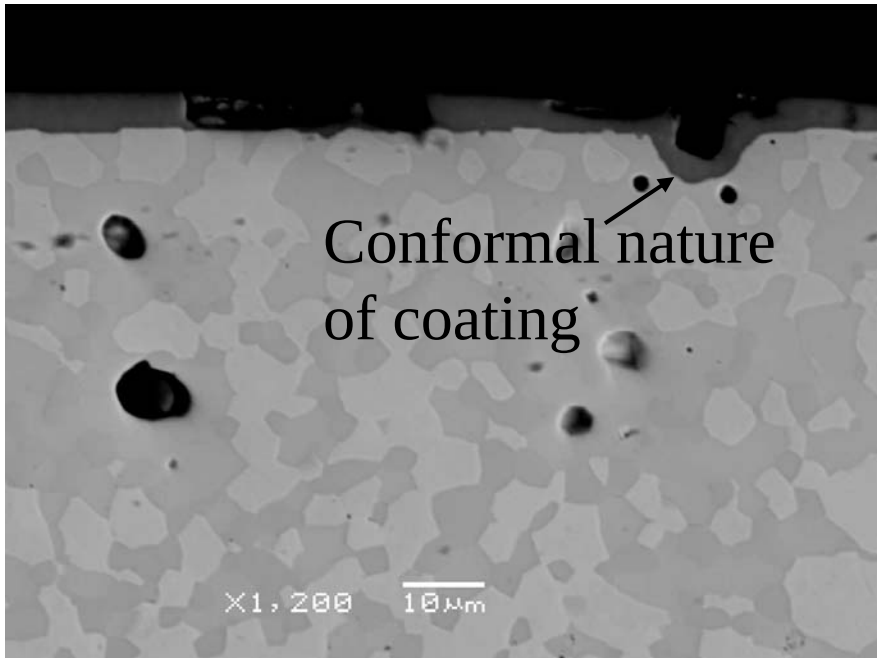

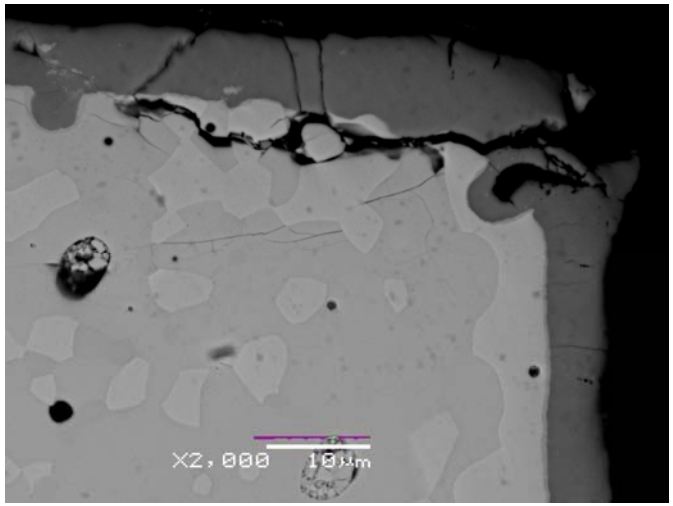

- Incomplete coverage at surface and corners
- Increase thickness without spalling due to growth stresses?

⇒ Add B to coating and form borosilicate glass to improve coverage of scale

Co-deposition of B and Si by HAPC

AMES LABORATORY

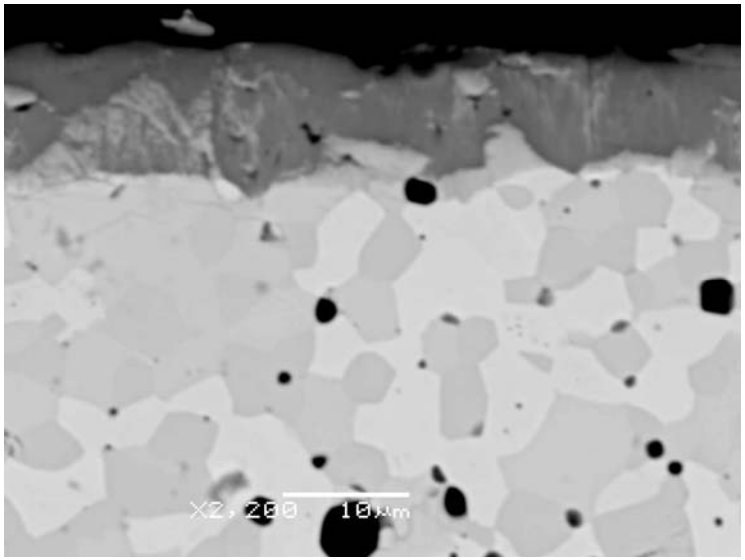

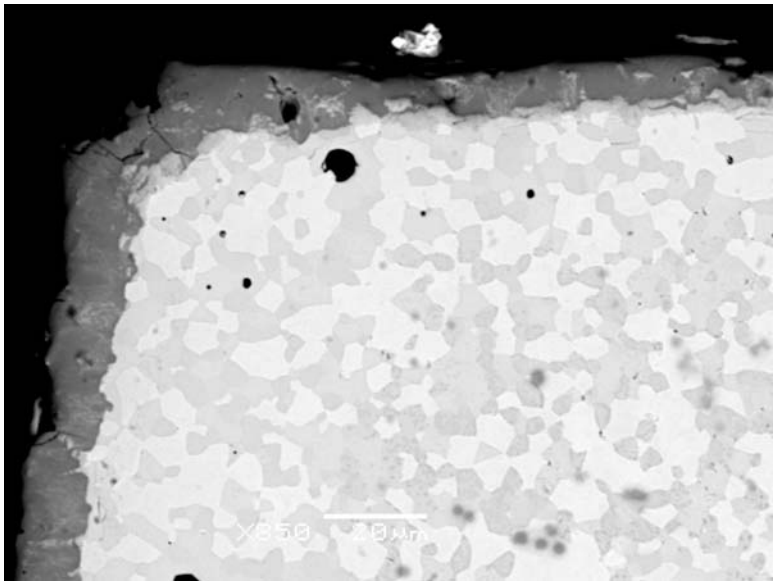

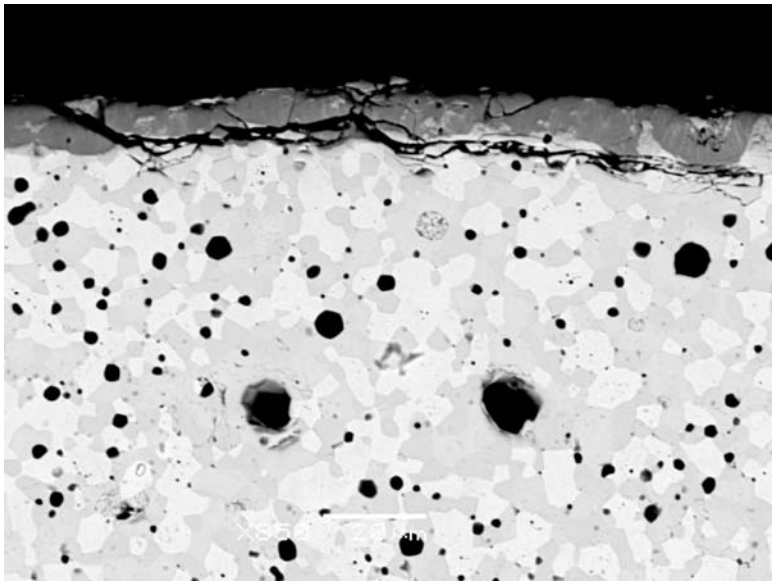

- $MoSi_2$-based coating with (MoB?)
- Continued problems with complete coverage at surface and corners

Conclusions

AMES LABORATORY

- Significant loss of Si and B during APS, but not detrimental to Alloy 1 coatings
- Significant interdiffusion between Alloy 1 APS coating and Mo substrate at 1800°C
- Alloy 1 APS coating oxidatively stable at 1600°C
- Conformal $MoSi_2$ coatings deposited onto Alloy 3 by HAPC process
- Incomplete coverage leads to rapid oxidation of Alloy 3 substrate (nearly consumed after 50 hrs at 1600°C in air)

Future Work

AMES LABORATORY

- Deposit continuous Alloy 1 coating onto Alloy 3 substrates by LPPS and verify oxidation protection
  - Reduced B and Si loss for LPPS
  - Obtain complete coverage for thicker coatings (> 200 μm)
- Optimize HAPC process to co-deposit complete layer containing both B and Si
  - Thicker layer to ensure complete coverage without spalling
  - Form borosilicate glass to improve coverage of underlying defects
- Use thermodynamic modeling to optimize alloy design of multicomponent alloys (ie- Nb-Mo-Si-B)

Thermodynamic Modeling /Alloy Design

AMES LABORATORY

- **Objective**

  - **Develop a thermodynamic model to predict microstructure and performance of the Mo-Si-B system**

  - **Investigate the effects of major element additions (such as Nb) and minor alloying additions (such as Al) to establish guidelines for intelligent alloy design**

General Structure of Thermo-Calc Package

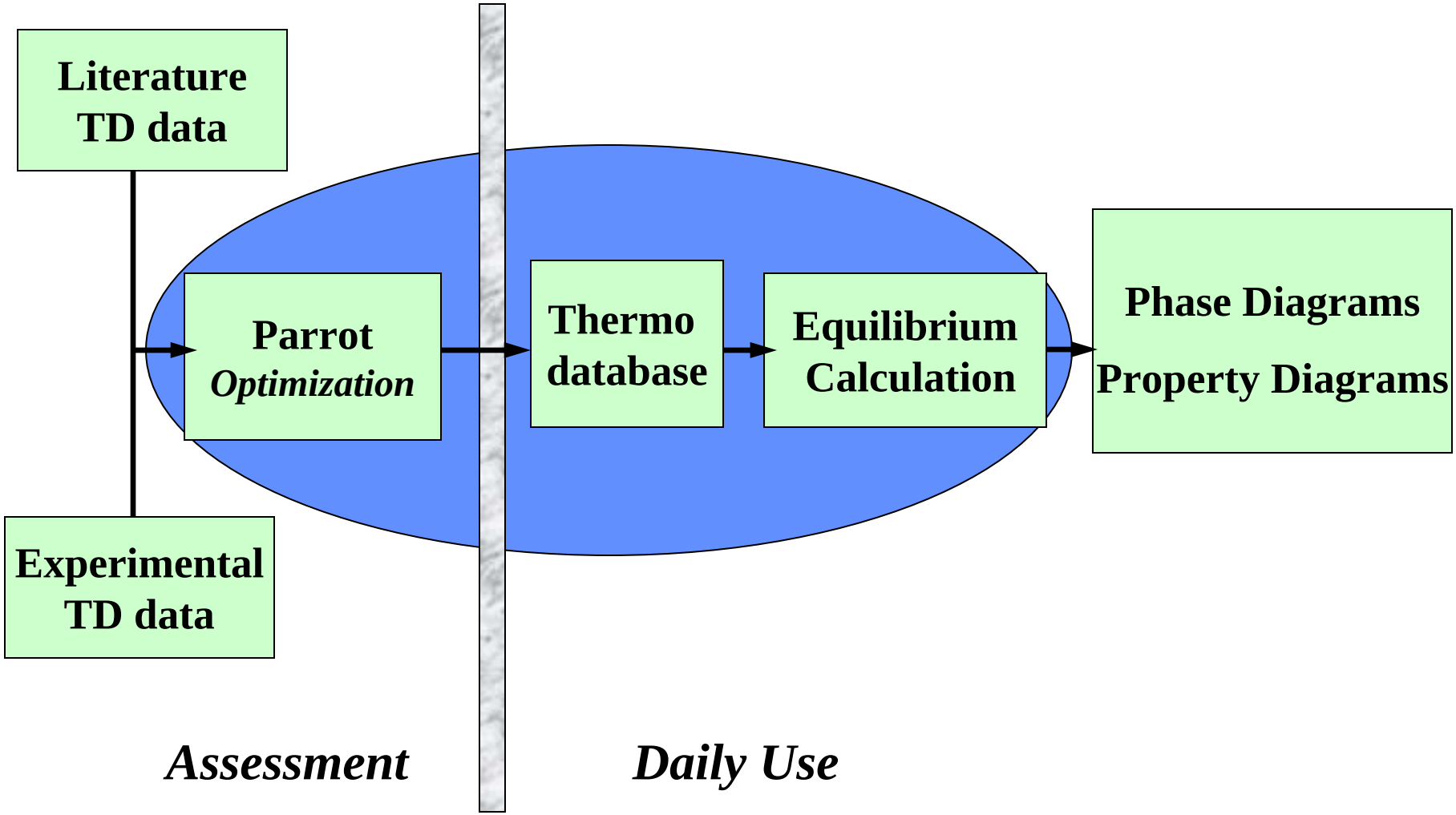

Modeling of Ternary Systems

AMES LABORATORY

- Construct a thermodynamic database for Mo-Si-B system with data provided by Yang et al. at University of Wisconsin-Madison
- Predict equilibrium phase fields using Thermo-Calc and compare these predictions with literature data and predictions from Pandat
- Expand investigation to consider Nb-Si-B, Nb-Mo-Si, and Nb-Mo-B systems

AMES LABORATORY

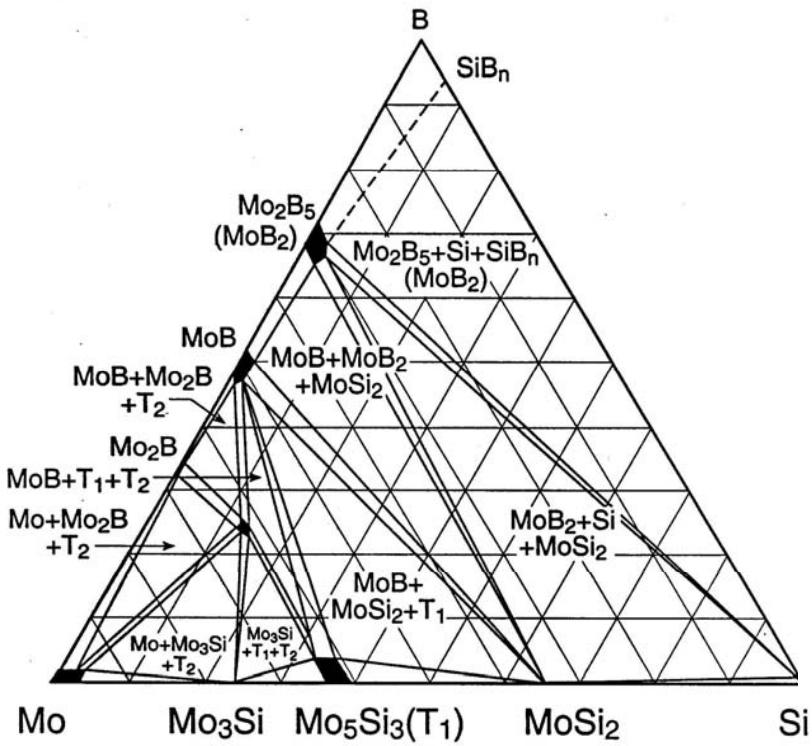

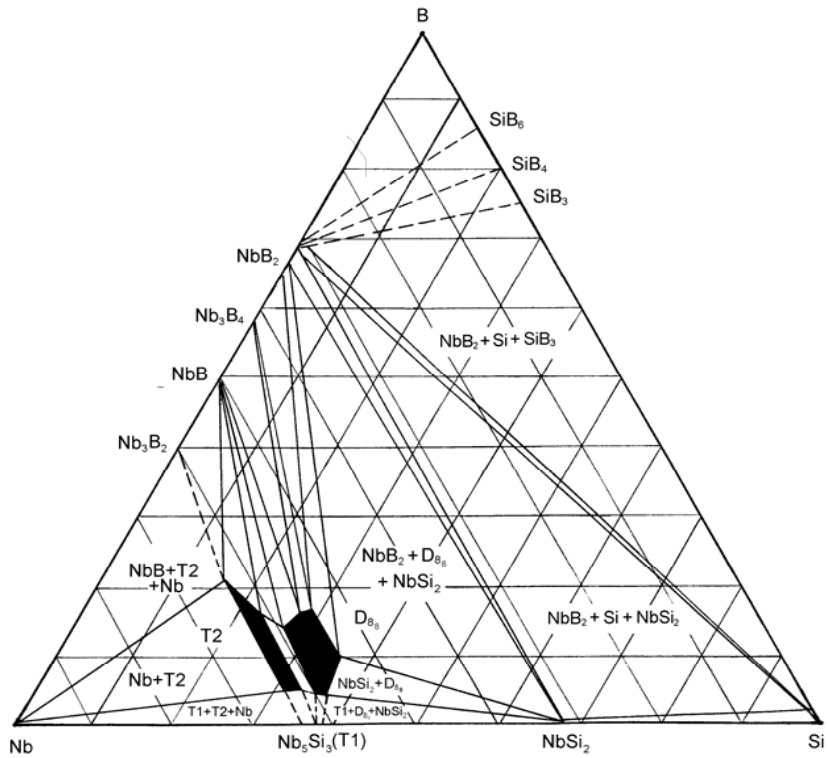

Modeling of Nb-Mo-Si-B system

AMES LABORATORY

- Construct a thermodynamic database for Nb-Mo-Si-B system by extrapolating thermodynamic descriptions of four constituent ternary systems and optimizing thermodynamic model parameters with experimental data
- Design optimal multiphase microstructures with appropriate alloy compositions

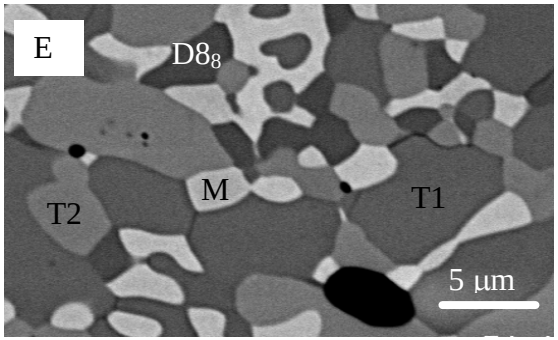

Vol%: 23(Nb,Mo)-
41 T_1 $(Nb,Mo)_5Si_3B_x$ -
26 T_2 $(Nb,Mo)_5(Si,B)_3$ -
9 $D8_8$ $(Nb,Mo)_5Si_3B_x$

*Optimization module (PARROT)**

AMES LABORATORY

Experimental Information

Empirical Rules

Fundamental Theories

Models for thermodynamic properties of each phase $G(T,P,X_1, \ldots)$

Databases for modeling parameters

Predictive calculations:

- Thermodynamic properties
- Equilibrium states, metastable states
- Phase diagrams, property diagrams

*** from Thermo-Calc Users' Guide**

Alloy 1 Coatings by LPPS

AMES LABORATORY

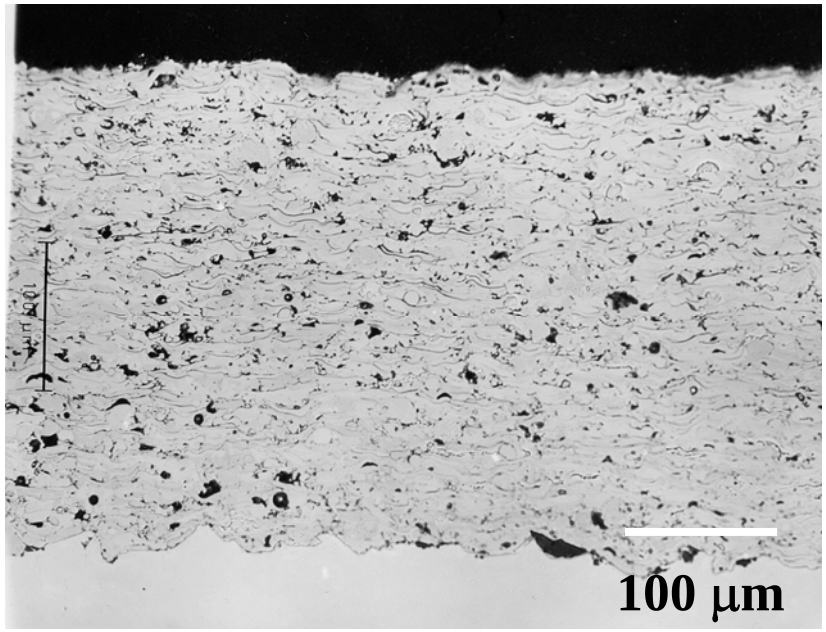

- 15-45 µm size powders
- Uniform coating with reasonable density
- Complete recrystallization after 2 hour anneal at 1800°C

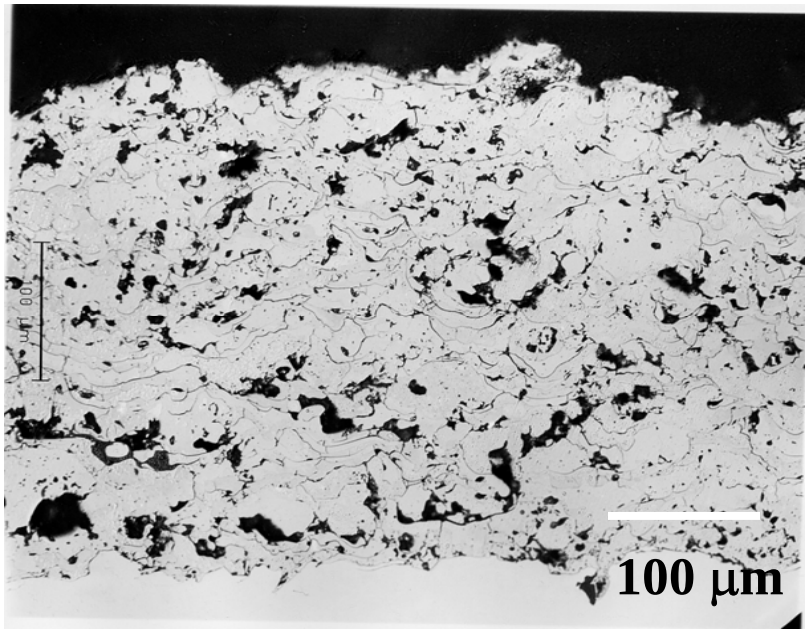

- 45-75 µm size powders
- Higher observed porosity

DOE-Fossil Energy (ORNL/NETL)

AMES LABORATORY

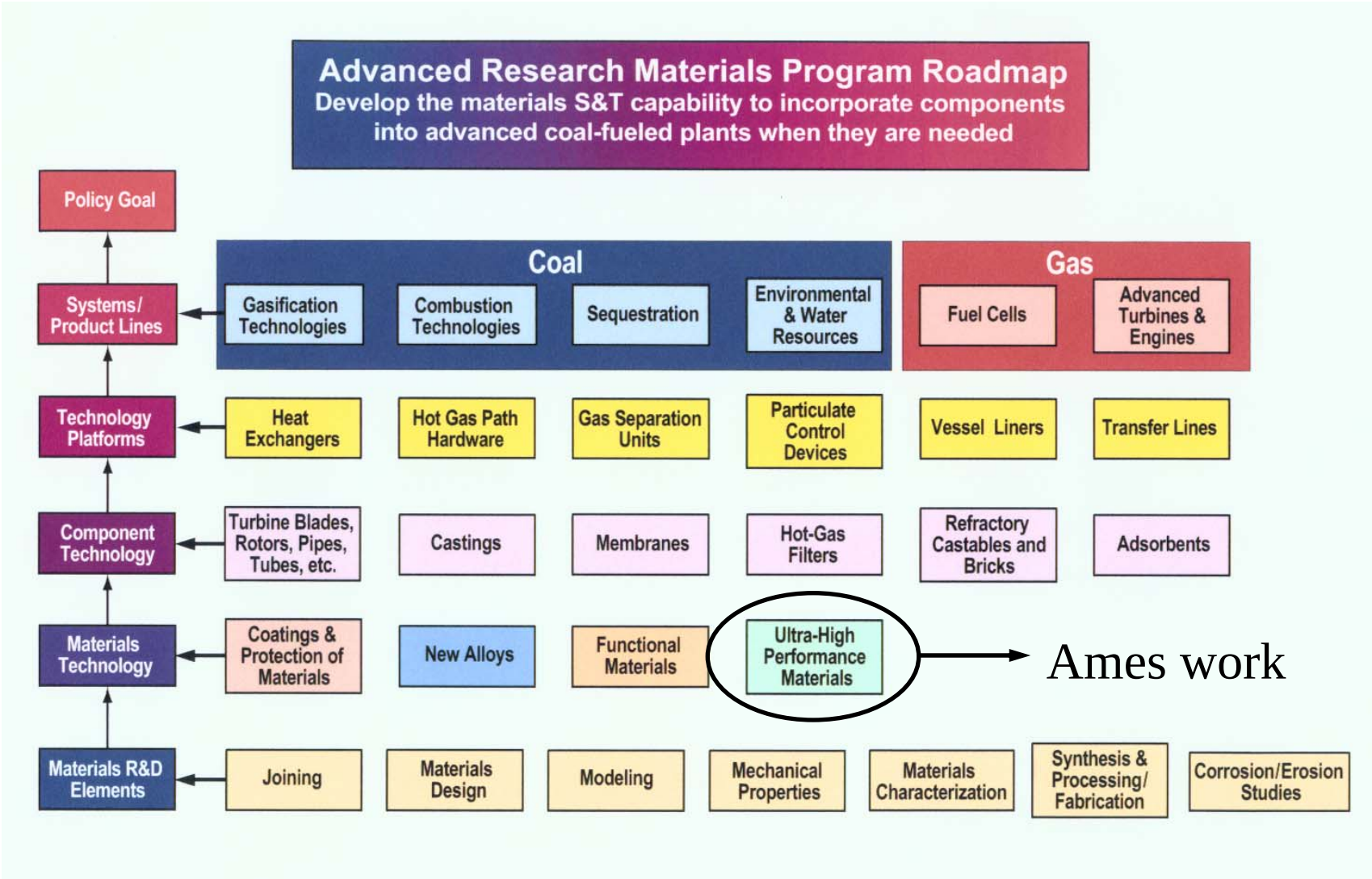

EERC Technology… Putting Research into Practice

TESTING OF A VERY HIGH-TEMPERATURE HEAT EXCHANGER FOR IFCC POWER SYSTEMS

19th Annual Conference on Fossil Energy Materials, Knoxville, May 9-11, 2005

John P. Hurley and Nathan J. Kadrmas
Energy & Environmental Research Center

Fred Robson
kraftWork Systems, Inc.

Acknowledgments

Funding for this work was provided by the U.S. Department of Energy (DOE)–United Technologies Research Center high-performance power system program, DOE–EERC biomass and fossil energy cooperative agreements, DOE Advanced Research Materials program, North Dakota Industrial Commission, and Xcel Energy.

EERC
Energy & Environmental Research Center®

IFCC Schematic

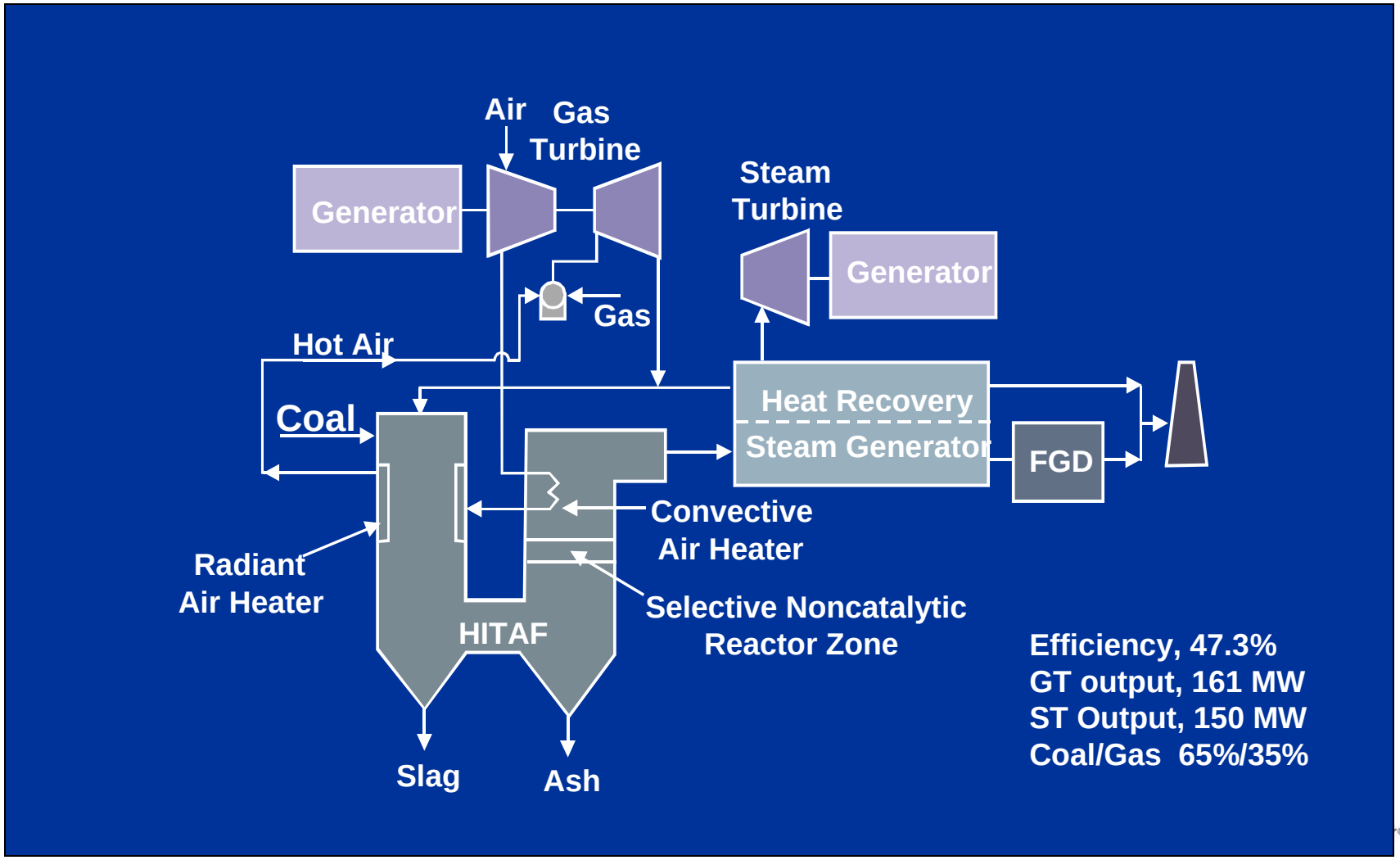

Advantages of Indirectly Fired Combined Cycles (IFCC)

- Operations very similar to PC-fired boilers
- Nearer term technology
- Higher efficiencies – 45% when firing coal, over 50% with NG supplement
- Half the water usage of a typical steam-based plant because of the Brayton cycle
- Slagging heat exchangers are self-cleaning
- Best technology for oxy-fuel combustion

EERC
Energy & Environmental Research Center®

Oxy-fired IFCC vs NGCC

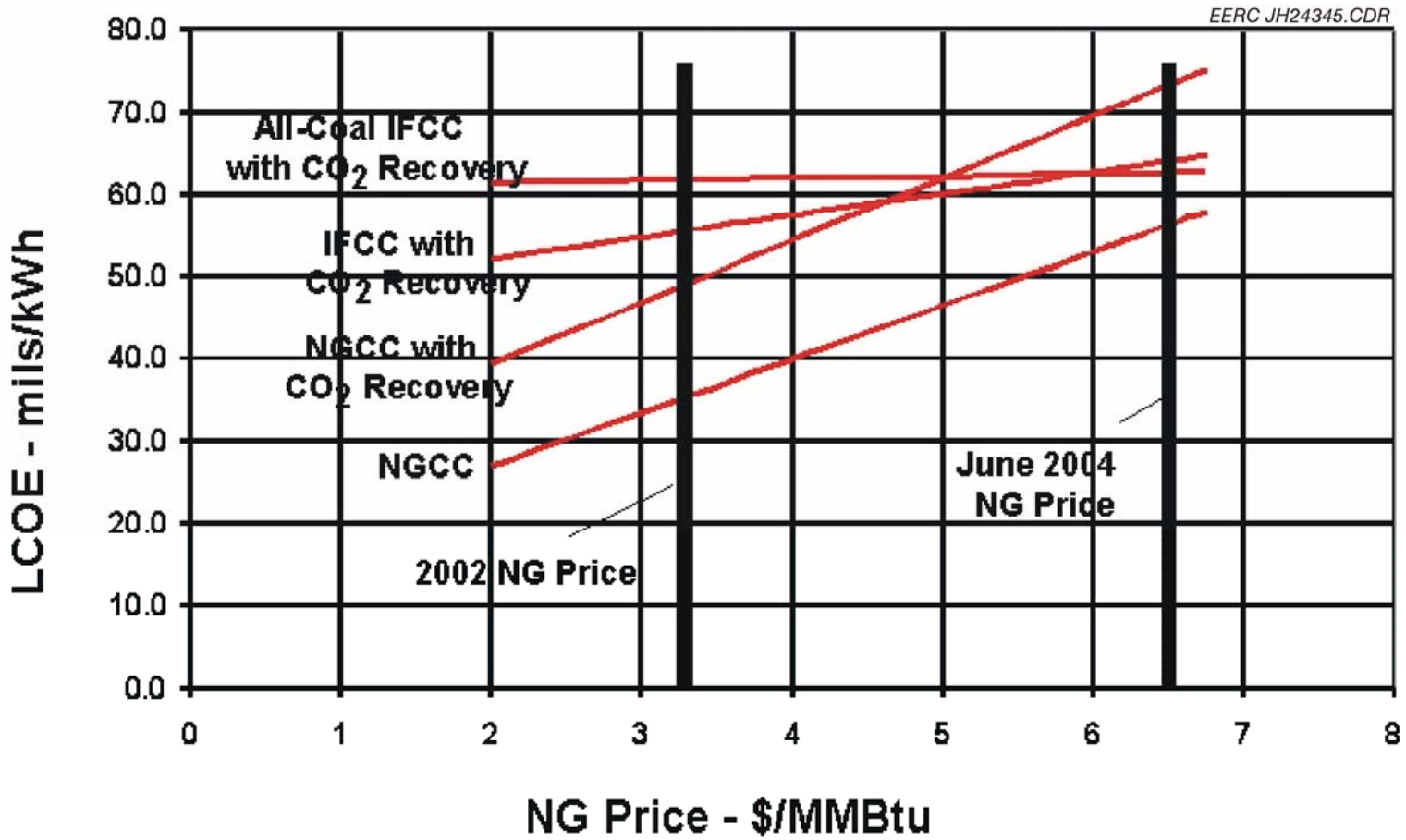

EERC
Energy & Environmental Research Center®

CO2 Recovery - PC versus Oxy-Fired IFCC vs IGCC

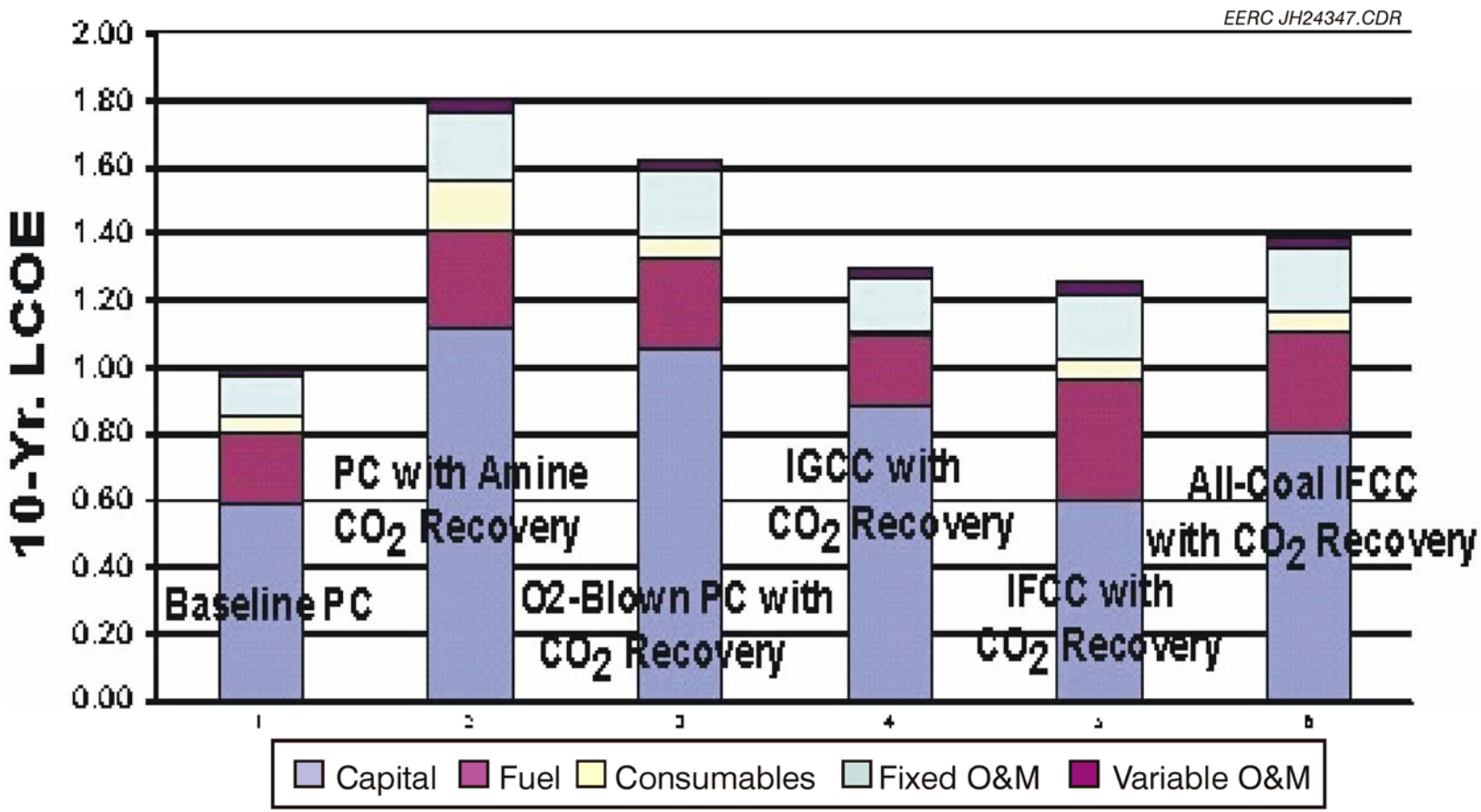

EERC
Energy & Environmental Research Center®

Comparison of LCOEs - Effects of Carbon Tax

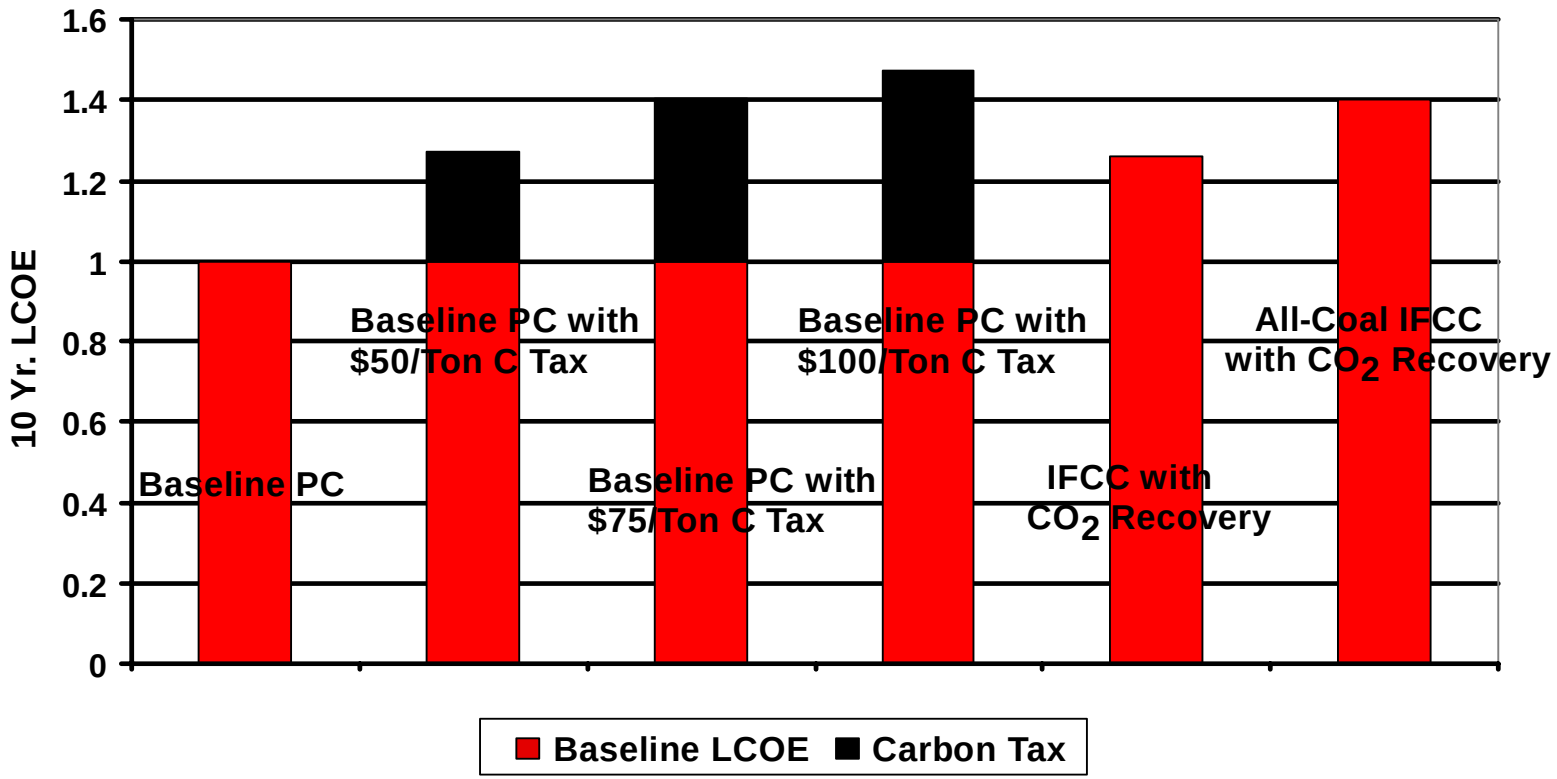

EERC
Energy & Environmental Research Center®

Air-Blown SFS Configuration Modified for Biomass Cofiring

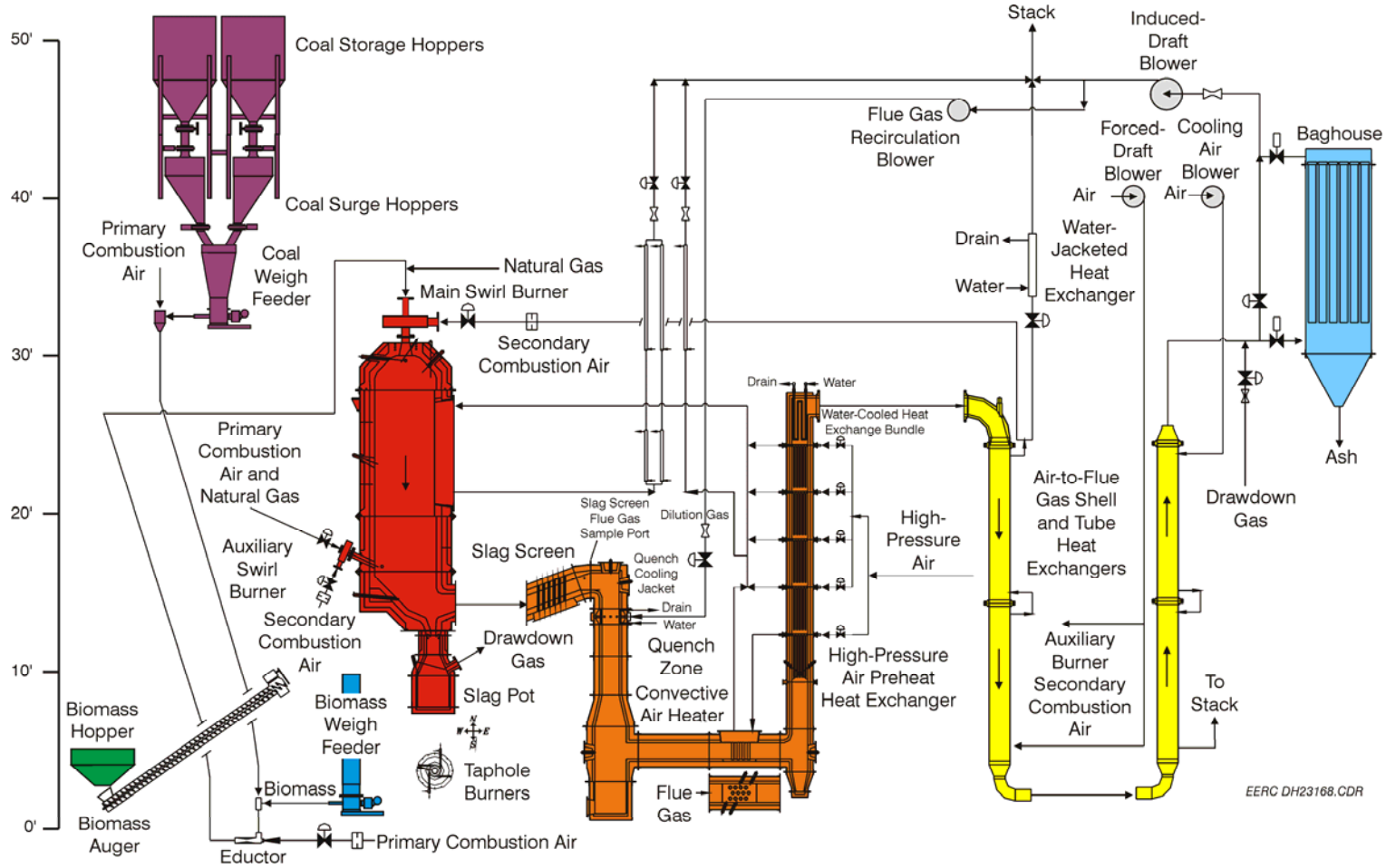

MA 956 Tube Installed in the HTHX

EERC JK21927.CDR

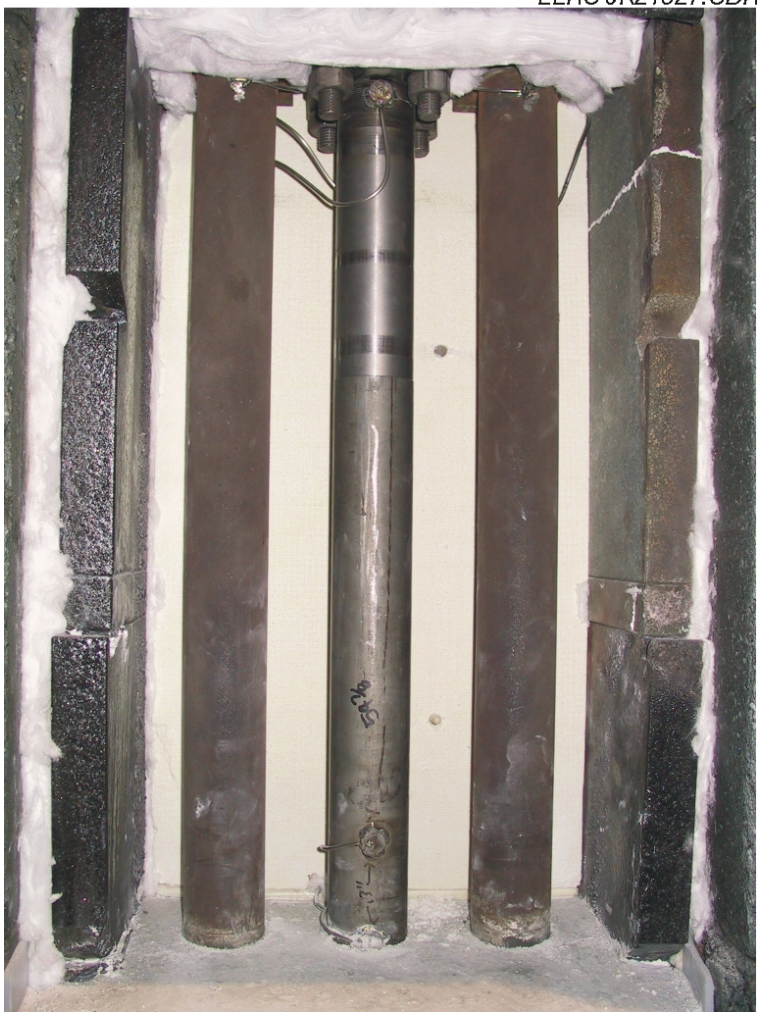

EERC
Energy & Environmental Research Center®

Summary of Previous Experience

- Over 2300 hours of operation on coal and NG
- Routinely produce process air at 1750F and 150psi
- Air as hot as 2000F and 100 psi produced for short time
- Slag layers only 1mm thick on bare tubes greatly reduce loss in heat transfer due to slagging
- Corrosion tests show that alloy lifetimes could be commercially acceptable at alloy temps up to 2150F but less than the slag solidus temperature
- One test with oxygen-enriched combustion which is a pathway to a zero emission coal fired plant

EERC
Energy & Environmental Research Center®

Impacts of Cofiring on the Operation of a Next-Generation Power System

- Funding is ½ Xcel Energy and ½ DOE
- 3 pilot-scale tests of operation of slagging IFCC and heat exchanger while firing coal/biomass blends
  - 20% biomass substitution reduces environmental impacts (mining and emissions) of coal-based power production
  - Fuels are North Antelope WY coal, hog fuel (wood processing residue), corn stover (ag residue), and switchgrass (energy crop)

EERC
Energy & Environmental Research Center®

Fuel Ash Analyses for the Coal–Biomass Cofiring Tests

Wt. % as Oxides	Coal	Hog Fuel	Corn Stover	Switchgrass
SiO_2	25.9–27.2	33.3	57.3	70.3
Al_2O_3	17.0–18.3	2.5	3.2	0.0
Fe_2O_3	7.2–7.6	3.2	1.4	0.25
TiO_2	1.5	0.3	0.3	0.03
P_2O_5	1.2	1.8	3.8	4.8
CaO	26.3–26.9	43.2	9.5	9.4
MgO	6.9–7.2	3.9	12.6	4.9
Na_2O	0.8–1.2	3.9	0.4	0.03
K_2O	0.2–0.3	7.9	10.0	7
SO_3	8.9–12.4	0.0	1.5	3.3
Ash Fusion, °C				
Initial	1209–1224	1349	1232	1348
Softening	1212–1229	1375	1245	1353
Hemisphere	1218–1233	1417	1251	1448
Fluid	1227–1258	1467	1288	1459

[1] Fuel and slag oxide concentrations normalized to an SO_3-free basis.
[2] Fuel and slag SO_3 concentrations normalized with other oxides.

EERC
Energy & Environmental Research Center®

Slagging Furnace System Operation Coal/Biomass Cofiring

- Furnace temperatures lower than for pure coal firing
  - inadequate HTHX air supply
  - Lower allowable surface temperature (1050C)
- Heat recovery same as for pure coal firing at same furnace temperature
- IFCC can be cofired without impact on furnace operation
- Baghouse cleaning more difficult because of fine particulates

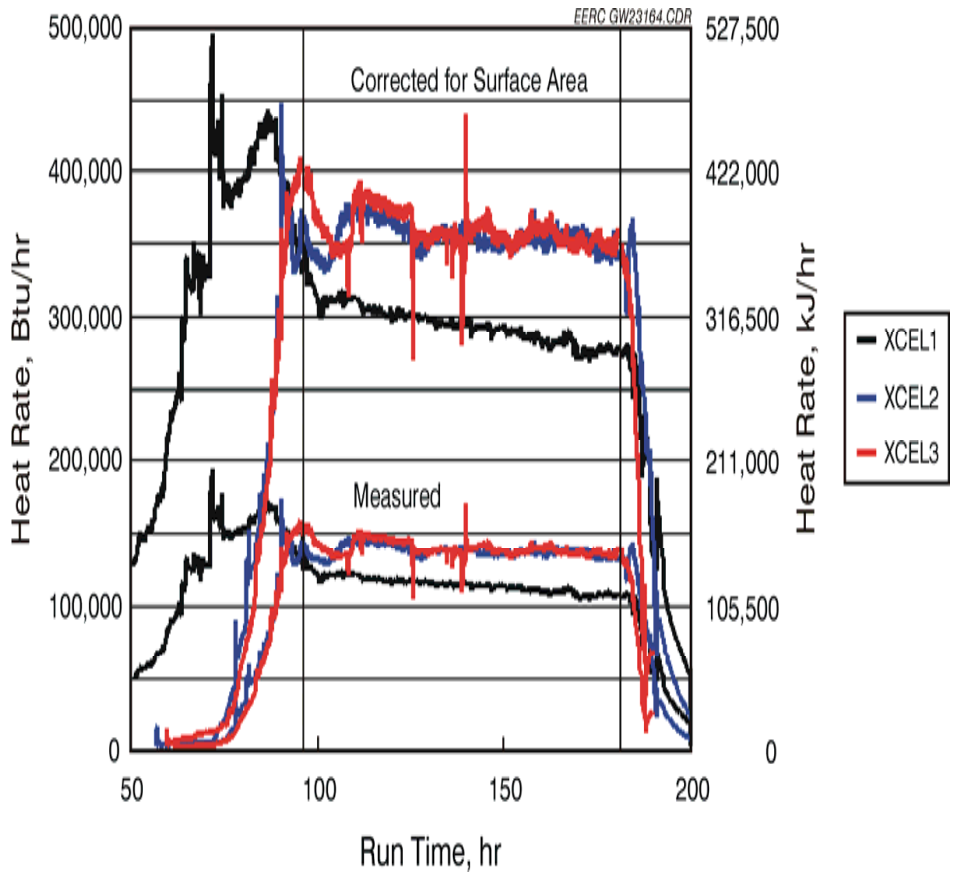

EERC
Energy & Environmental Research Center®

HTHX Ash and Slag Samples from the Coal–Hog Fuel Test

Oxides,[1] wt%	North Antelope Coal	Hog Fuel	Slag	Outer Sintered Layer	Inner Powdered Layer
SiO_2	25.9–27.2	33.3	37.7	51.5	35.6
Al_2O_3	17.0–18.3	2.5	20.1	10.3	17.0
Fe_2O_3	7.2–7.6	3.2	5.4	4.3	7.3
TiO_2	1.5	0.3	1.1	0.8	1.3
P_2O_5	1.2	1.8	0.9	1.0	1.4
CaO	26.3–26.9	43.2	28.0	23.2	20.1
MgO	6.9–7.2	3.9	4.4	2.6	6.6
Na_2O	0.8–1.2	3.9	1.2	3.5	7.1
K_2O	0.2–0.3	7.9	1.1	2.9	3.7
SO_3[2]	8.9–12.4	0.0	0.0	0.0	16.2

[1] Oxide concentrations normalized to an SO_3-free basis.
[2] SO_3 concentrations normalized with other oxides.

EERC
Energy & Environmental Research Center®

HTHX Tubes After August 2001 Test

- Slag layer self cleaning
- 3 mm thick maximum
- Reduces heat flow by 15% as compared to 50% for sintered ash
- Over construction 20% rather than 100%
- No sulfur in the deposits

EERC
Energy & Environmental Research Center®

HTHX After Coal/Corn Stover Cofiring

EERC GW23091.CDR

EERC
Energy & Environmental Research Center®

Typical High-Temperature Upstream Deposit

- Larger, flattened particles
- Inertial impaction mechanism
- Primarily complex silicates, no sulfur

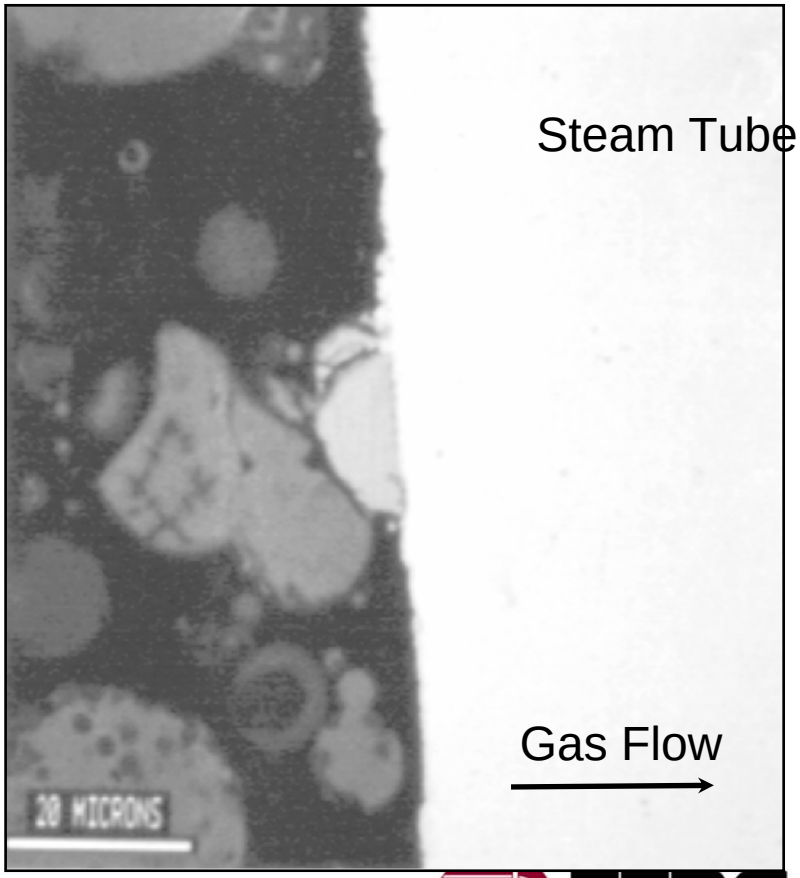

EERC
Energy & Environmental Research Center

Typical Low-Temperature Upstream Deposit

- Small particles
- Thermophoretic deposition
- Primarily alkali metal and alkaline earth sulfates

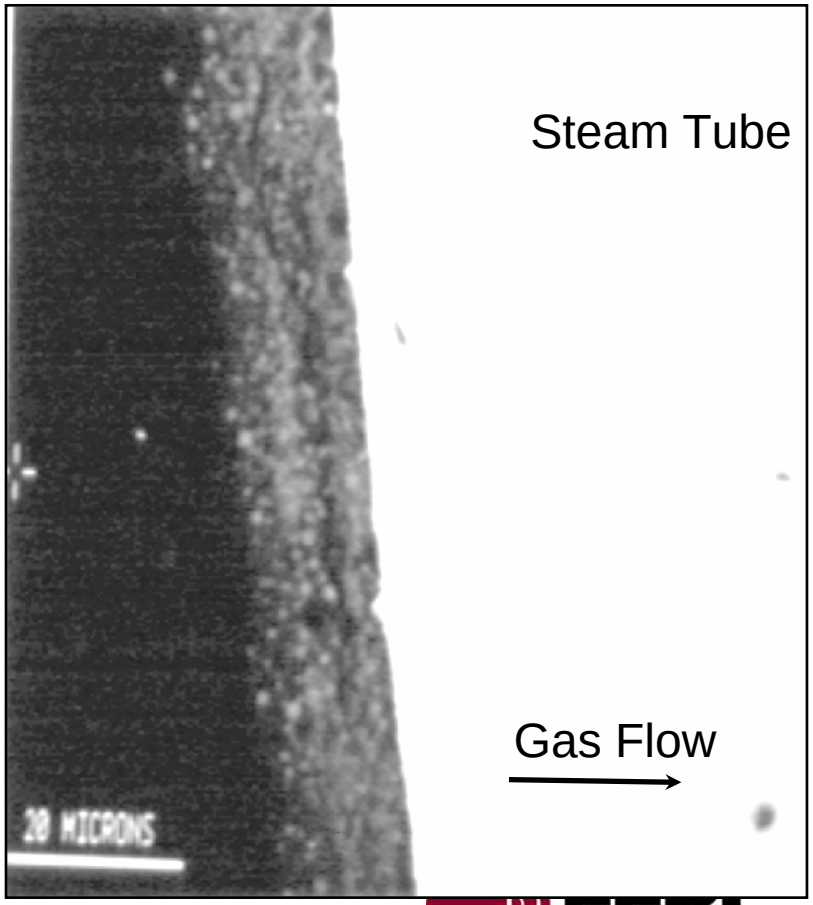

EERC
Energy & Environmental Research Center®

Distribution of Bonding Phases A Function of Deposit Temperature

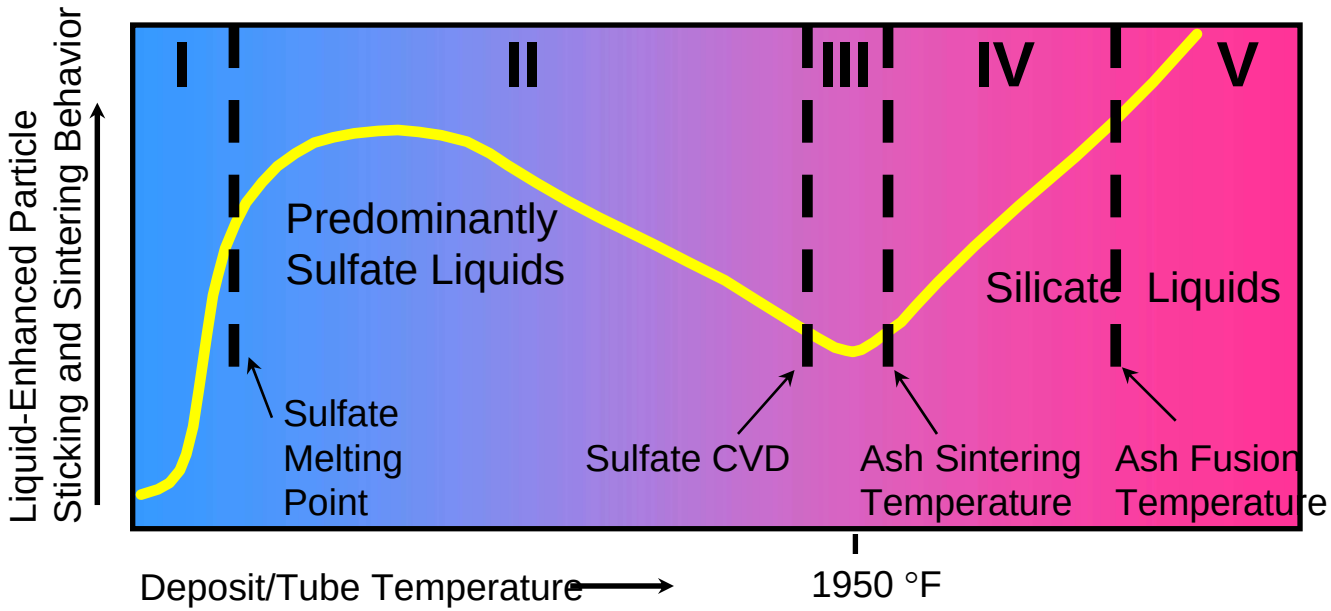

Deposition Regimes:

I. Dry-sticking regime: no glue
II. Vapor or thermophoretically deposited liquid glue
III. Glue produced by heterogeneous chemical reactions at vapor–ash interface
IV. Ash particle softening on impact
V. Wet limit (sticking coefficient nearly unity) Liquid

EERC
Energy & Environmental Research Center®

EERC Computational Fluid Dynamics Modeling
Deposit Temperature (ºF)

Baseline case

Reconfiguration

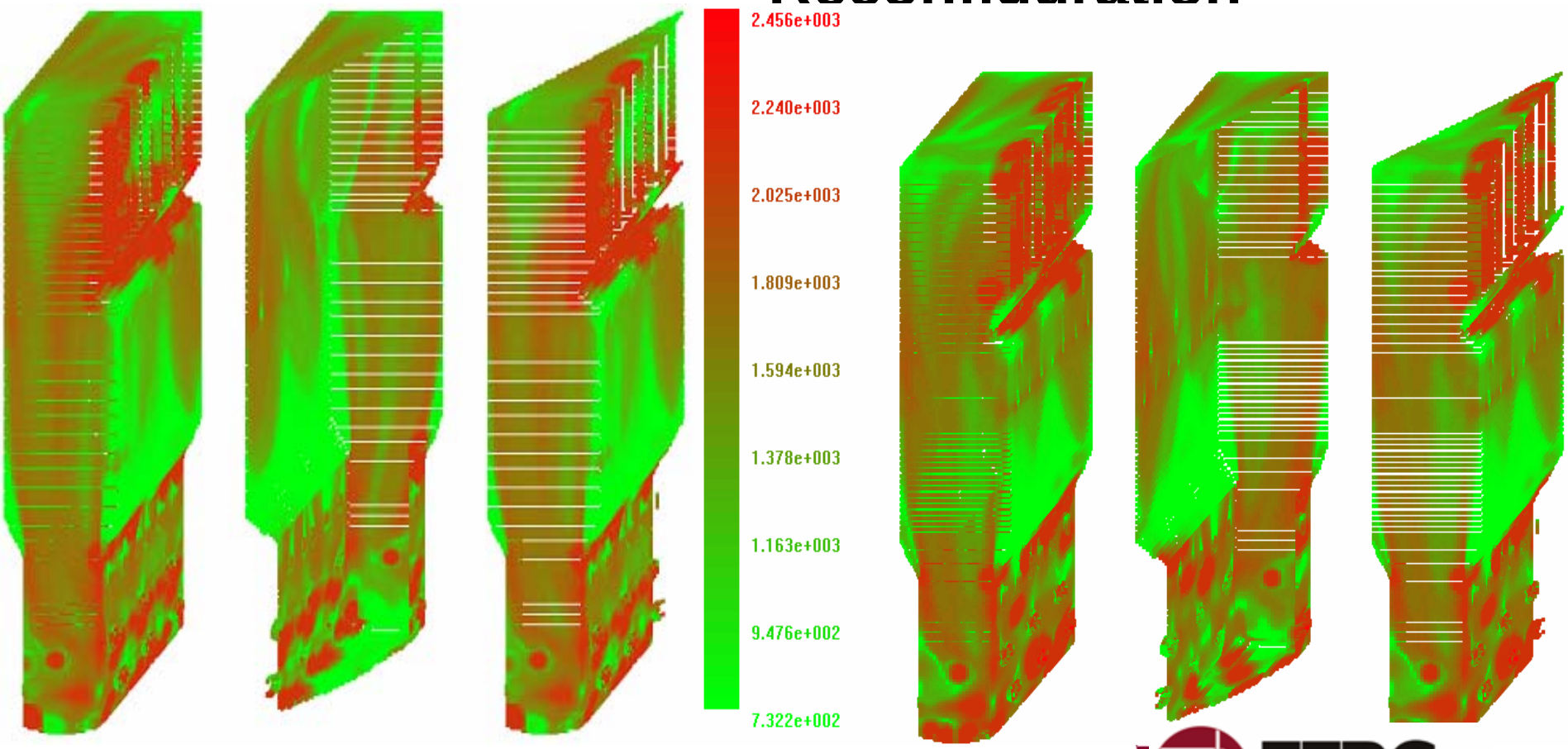

EERC
Energy & Environmental Research Center

DSAF Modified For Alloy Testing

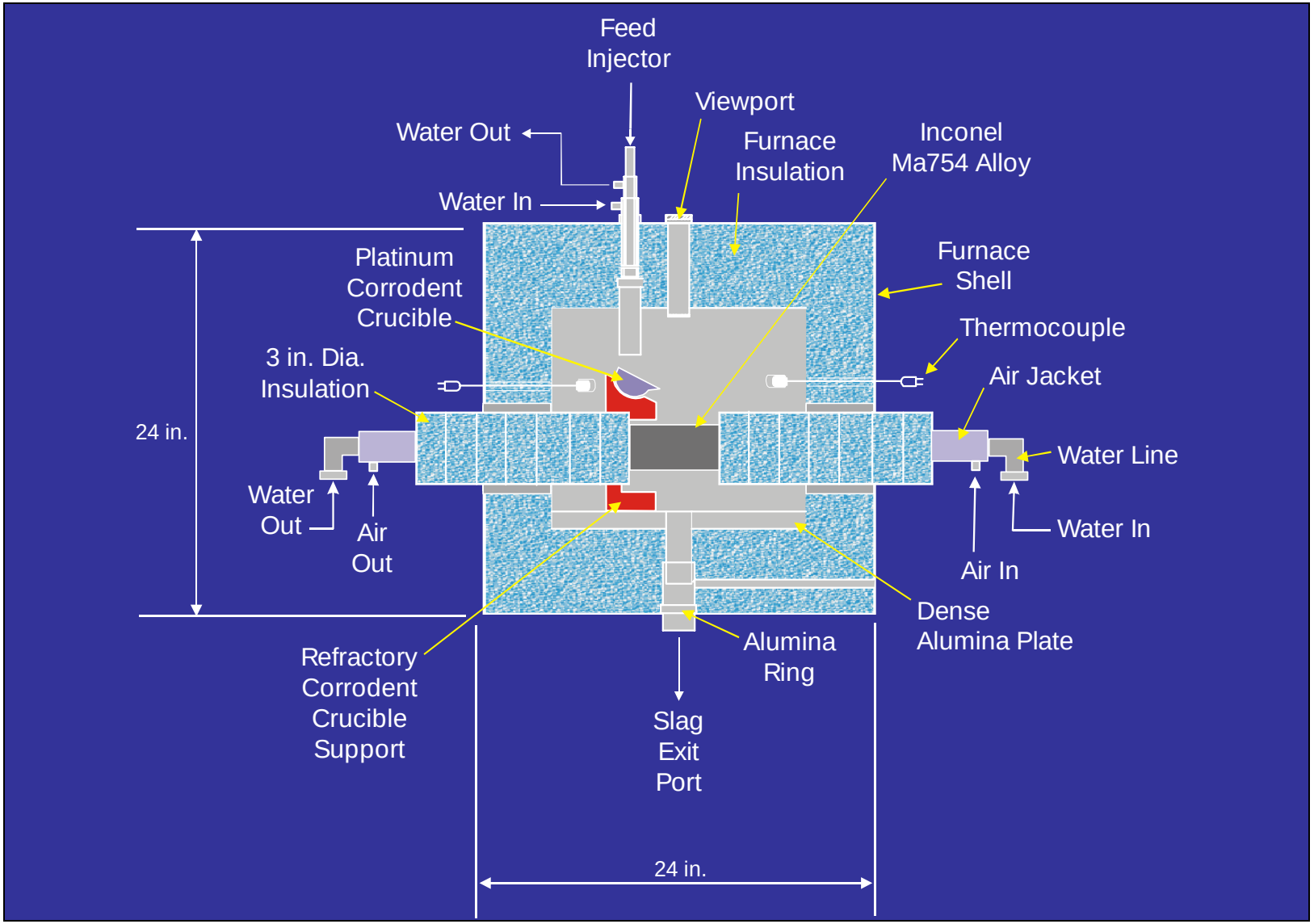

MA956 After Flowing Slag Corrosion (100 hours at 1050C)

EERC
Energy & Environmental Research Center®

Biomass/Coal Slag Corrosion of MA956 at 1050 and 1150C

- Slag remains attached to surface upon cooling except for switchgrass at 1150C
- Attached slag is enriched in potassium and phosphorus
- Phosphorus is in the oxide layer but not the alloy

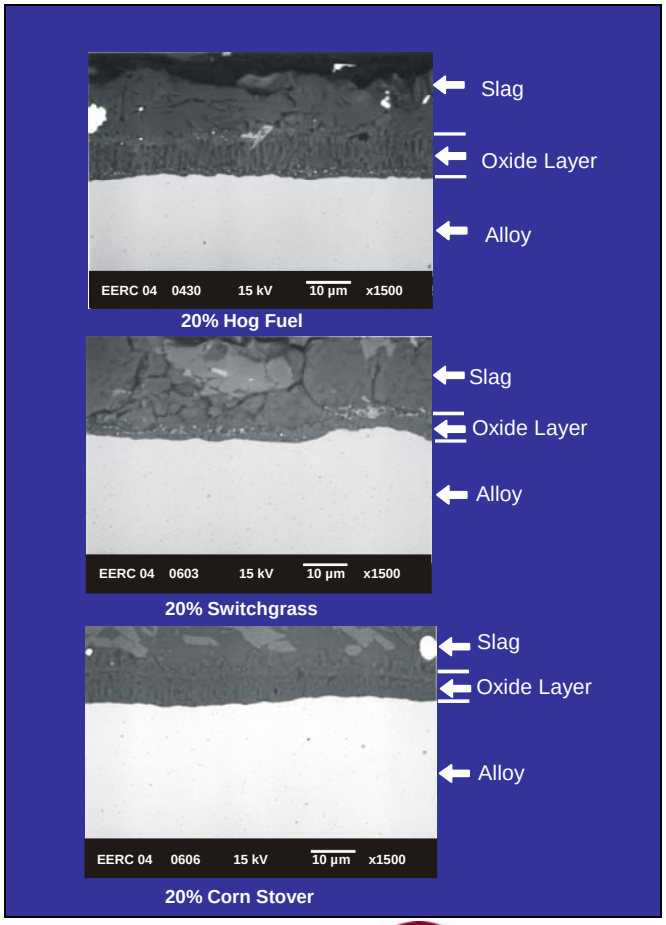

EERC
Energy & Environmental Research Center®

TLP Joint in MA956

EERC JH23173.CDR

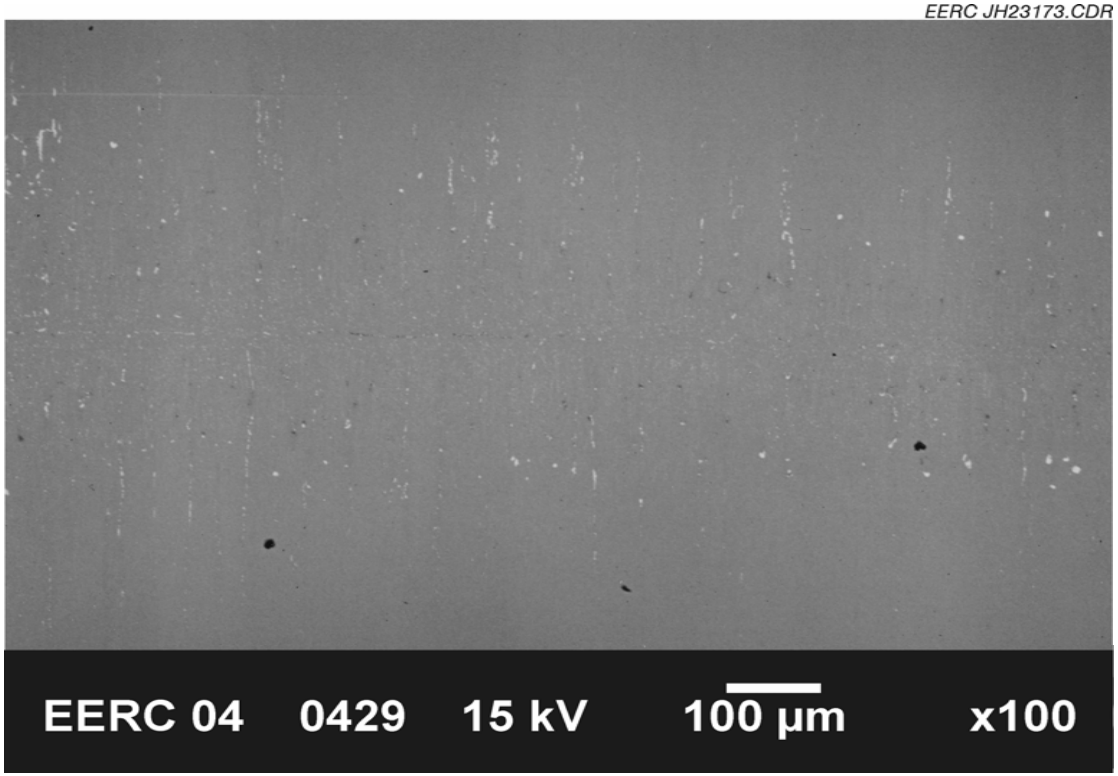

EERC
Energy & Environmental Research Center®

Conclusions on IFCC Operation With Coal/Biomass Cofiring

- Furnace temperatures lower than for pure coal firing
  - Lower allowable surface temperature (1050C)
  - Inadequate HTHX air supply
- Heat recovery same as for coal firing at same furnace and HTHX temperature
- Inner ash layer on HTHX enriched in sulfate at 1050C – must determine corrosion rates
- Inner ash layer would not be enriched in sulfate at 1150C which is allowable for hog fuel and corn stover cofiring
- TLP joining method promising, but contamination is an issue

EERC
Energy & Environmental Research Center®

Concepts for Smart, High-Temperature Corrosion-Resistant Coatings

P.F. Tortorelli. M.P. Brady, and I.G. Wright

Oak Ridge National Laboratory

19th Fossil Energy Materials Conference

May 10, 2005

Advanced Research Materials Program
Office of Fossil Energy

Motivation

- Adequate resistance to environmental degradation is a critical material barrier to the operation of advanced fossil energy systems
  - Reactive species (O_2, H_2S, H_2O, H_2, CO, HCl, etc.)
  - Slags, salts
  - High temperatures
  - Varying conditions
    - operation
    - fuels of opportunity

- Need breakthrough advances in materials and materials protection that require new research, development, synthesis and/or performance approaches

- Coatings offer possibilities for corrosion protection under aggressive (and changing) environmental conditions while the substrate provides strength or other desired properties

Research Objective

Explore

Feasibility of “different” high-temperature protective coatings for advanced fossil systems

Using

State-of-the-art alloying and microstructural approaches to high-temperature corrosion resistance

Approach

- Focus on concepts, not synthesis or detailed corrosion studies
- Pursue compositions and structures that can react with the environment in various ways determined by the nature of the reactive species and temperature such that effective protective barrier layers can form in various environments
- Specifically examine the response of multiphase alloys and composite structures to various reactive gases and salts
  - Mo-Si-B
  - Ti-Al-Cr+

Multiphase Phenomena As A Basis For Design Of Alloys For High-Temperature Corrosion Resistance

Two Limiting Cases

Gesmundo & Gleeson 1992

Cooperative Mode

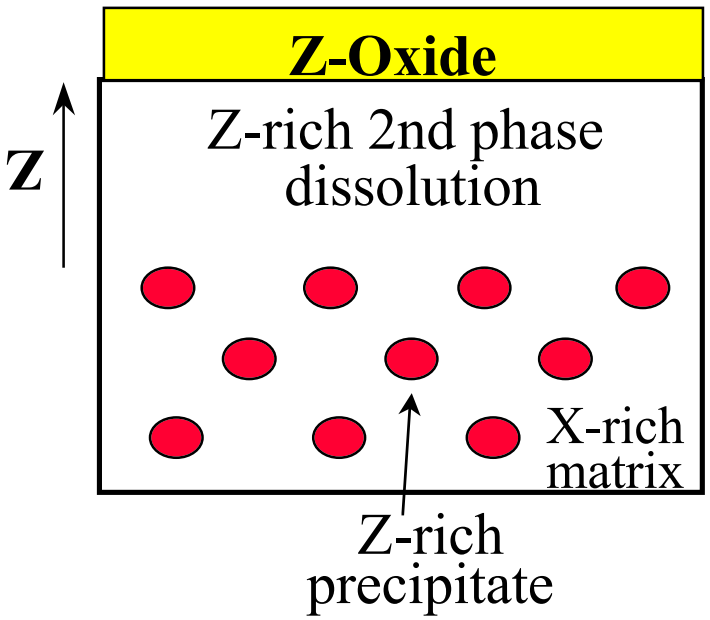

Independent (In-Place)

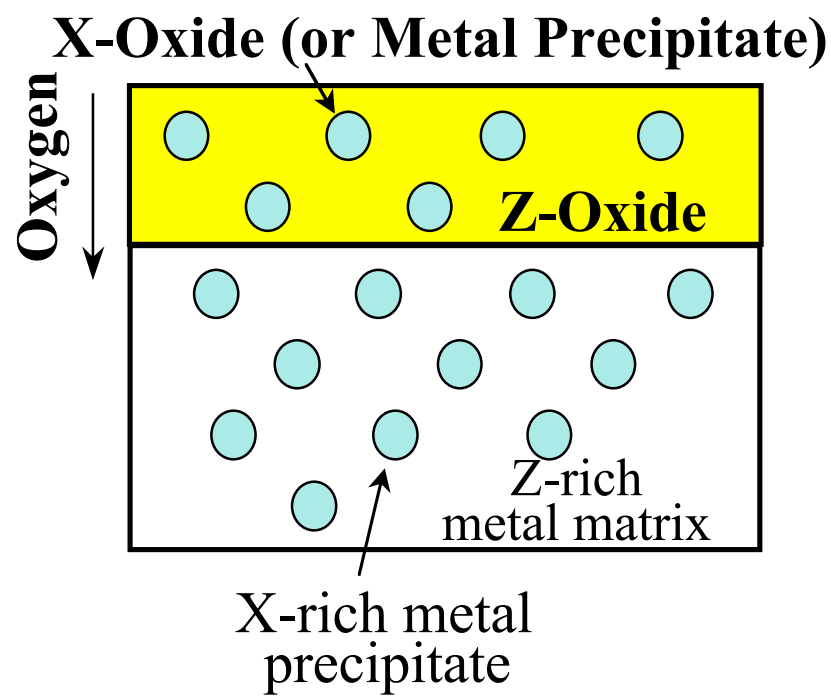

- Cooperative: single-phase reaction product
- Independent (In-Place): composite surface which mimics underlying alloy structure

Smart Protective Coatings For High-Temperature Corrosion Protection

- Smart = sense and respond appropriately
- In present context, materials that sense particular environmental conditions and form protective barrier layers to provide high-temperature corrosion protection
- To date, focus has been on concepts for compositions that yield good resistance in air (oxygen) as well in severe sulfidizing/oxidizing environments
  - p_{S_2} = ~10^{-6} atm, p_{O_2} = ~10^{-22} atm (coal gasification conditions)
  - H_2S-H_2-H_2O, 800°C

We Seek Compositions That Form The Appropriate Product(s) In A Given Environment

Previously, have examined the multiphase Mo-Si-B system

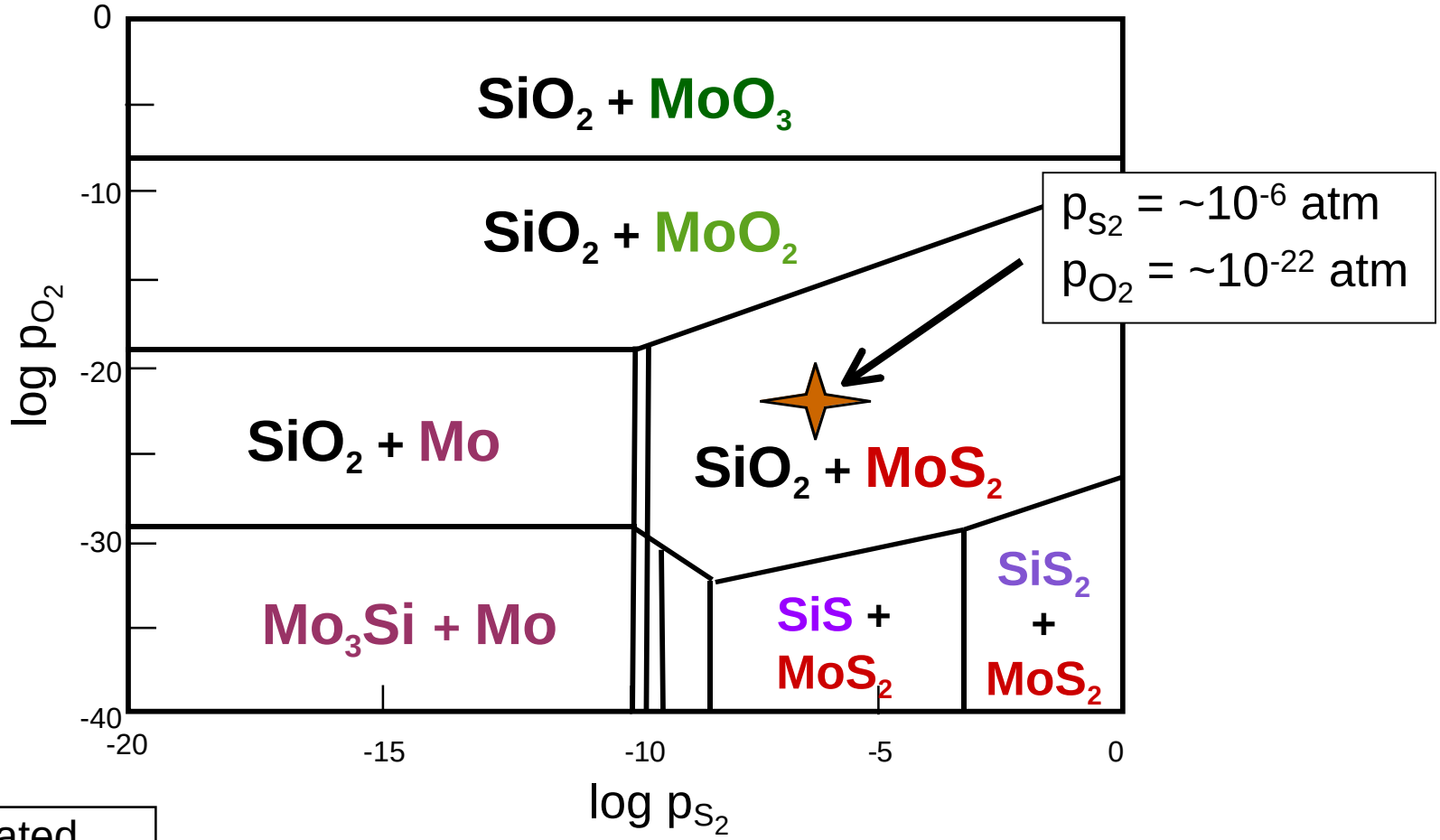

Calculated Phase Stabilities

Mo-Si-B Systems Looked Promising

- Si can provide means to establish protective silica or borosilicate layers (Meyer et al., Thom et al., Mendiratta et al., Natesan, Tortorelli et al., Schneibel et al., Supatarawanich et al., Pettit & Meier, etc.)
- Mo sulfidizes slowly (cf. Mrowec, Douglass et al.)
- MoS_2 more stable than Si sulfides

Can we manipulate the phase assemblage of Mo-Si-B so that effective barrier layers can form in different environments?

Mo-Mo_3Si-Mo_5SiB_2 Showed Very Good Sulfidation Resistance

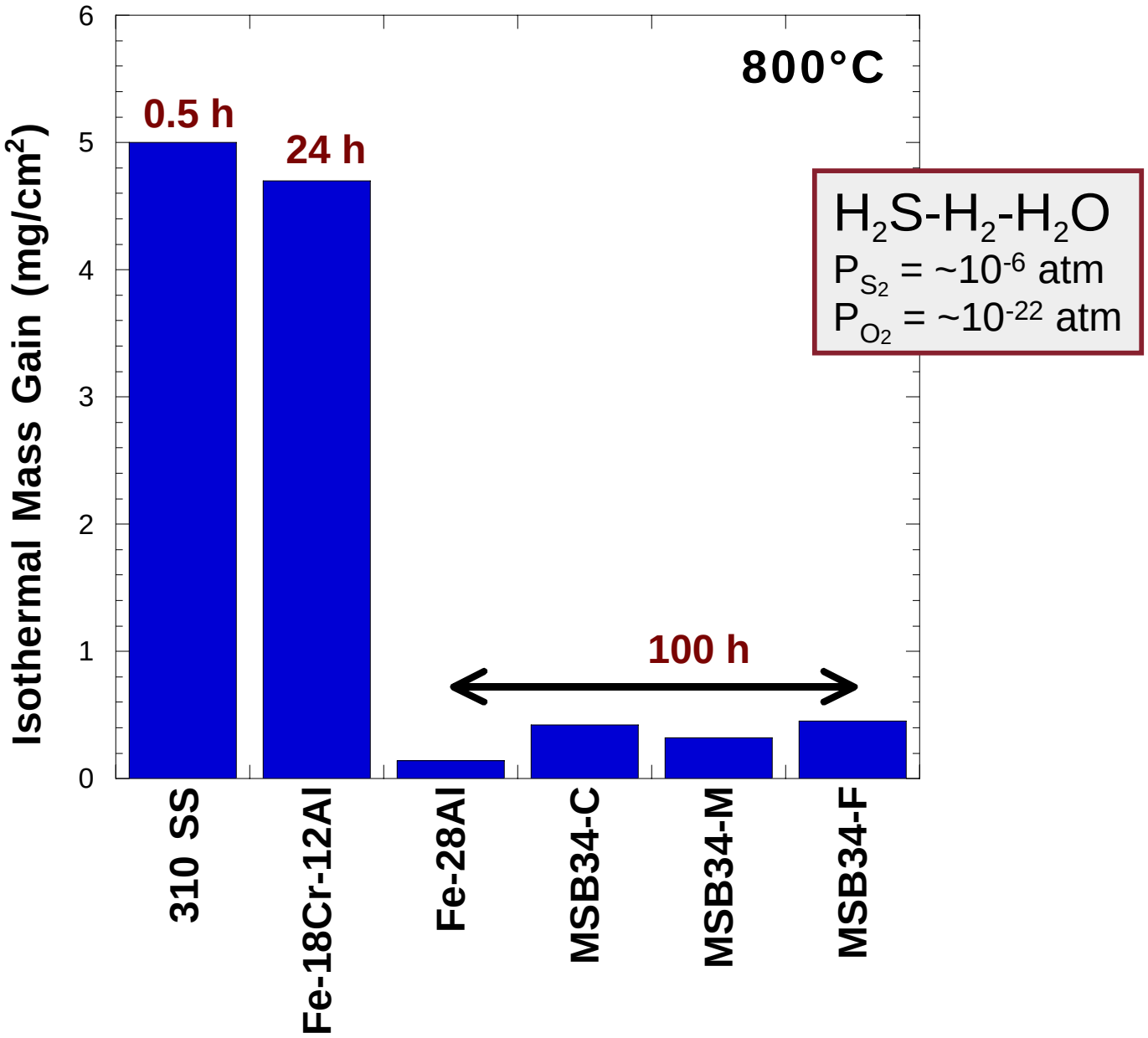

Thin Corrosion Products Were Observed

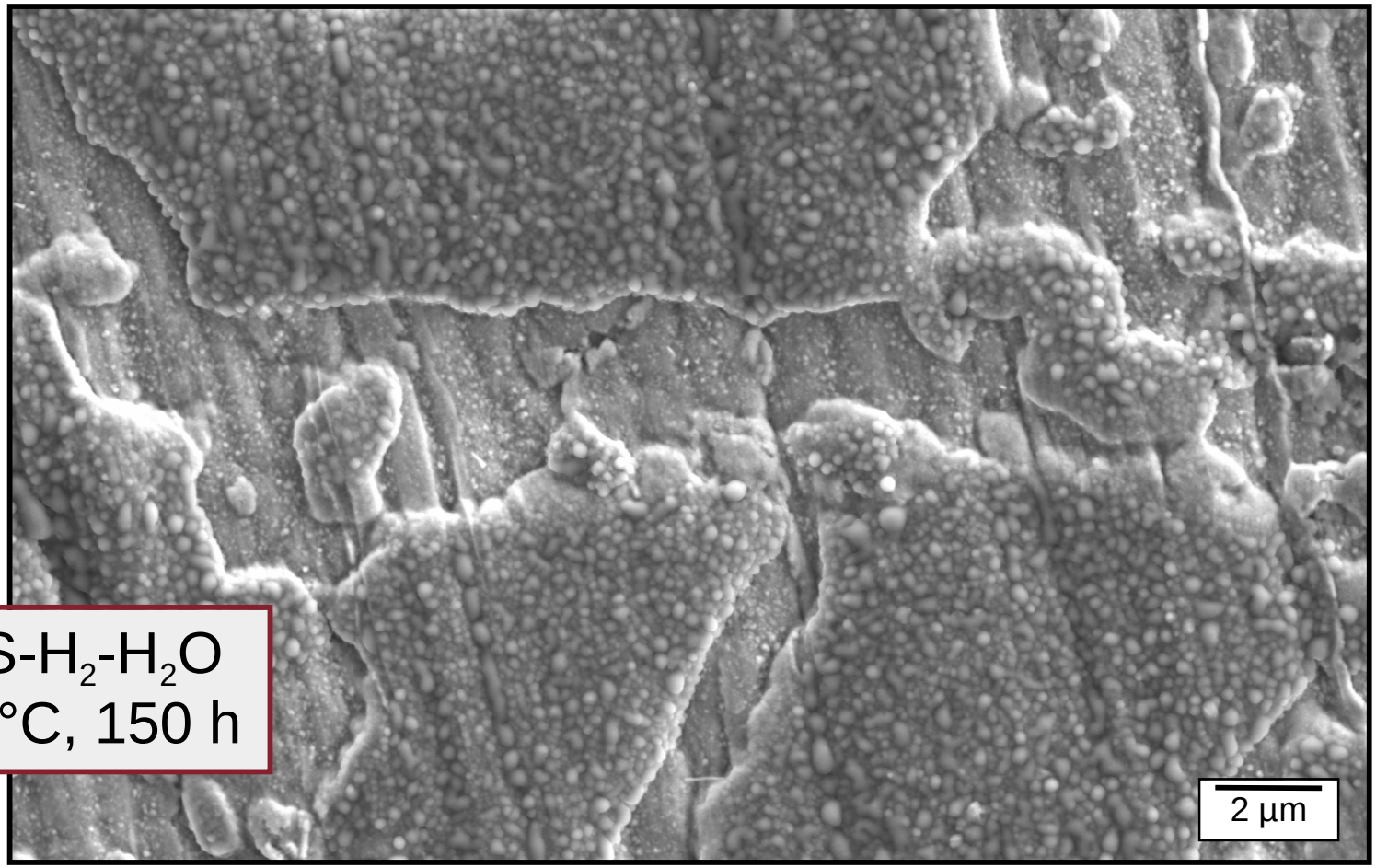

H_2S-H_2-H_2O
800°C, 150 h

- XRD: small but distinct peaks for MoS_2, SiO_2
- Phases appeared to react independently of each other

Can Be Considered As A Variant Of Gesmundo & Gleeson Classification For Multiphase Oxidation

Independent (In-Place)

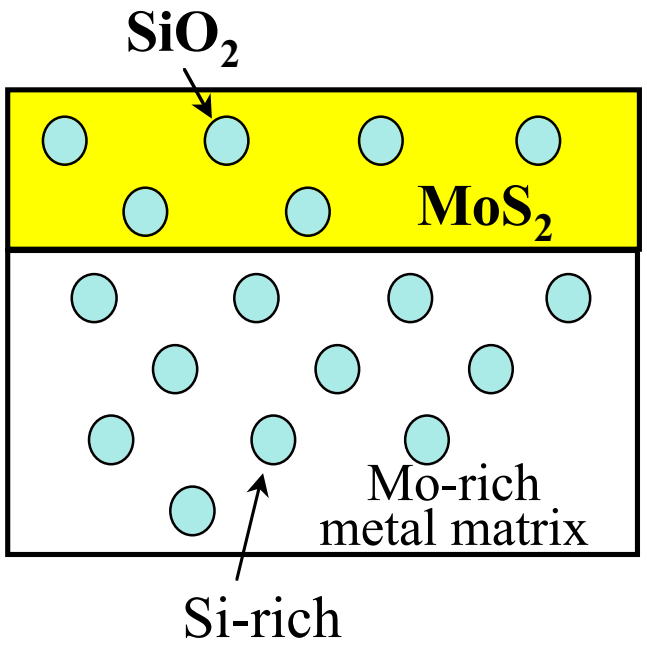

Usually, High-Temperature Corrosion Resistance Relies on Formation Of A Continuous Product Layer

$$aM + bR_2 = M_aR_{2b}$$

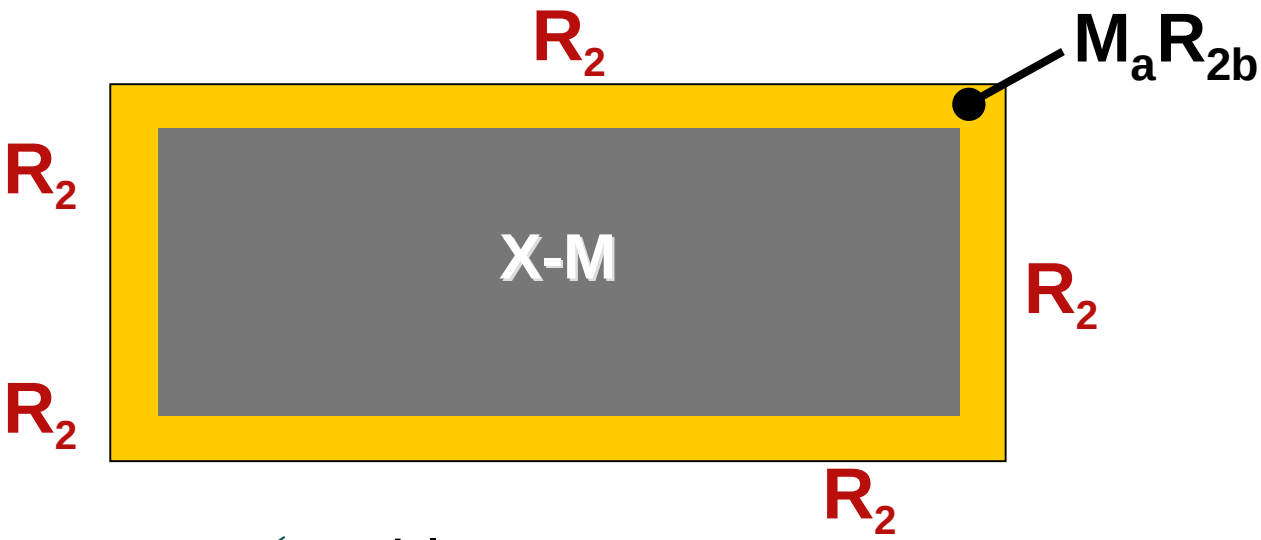

- ✓ stable
- ✓ continuous
- ✓ slowly growing
- ✓ mechanically sound
- ✓ adherent

Many Factors Control The Ability To Form And Maintain Such Layers

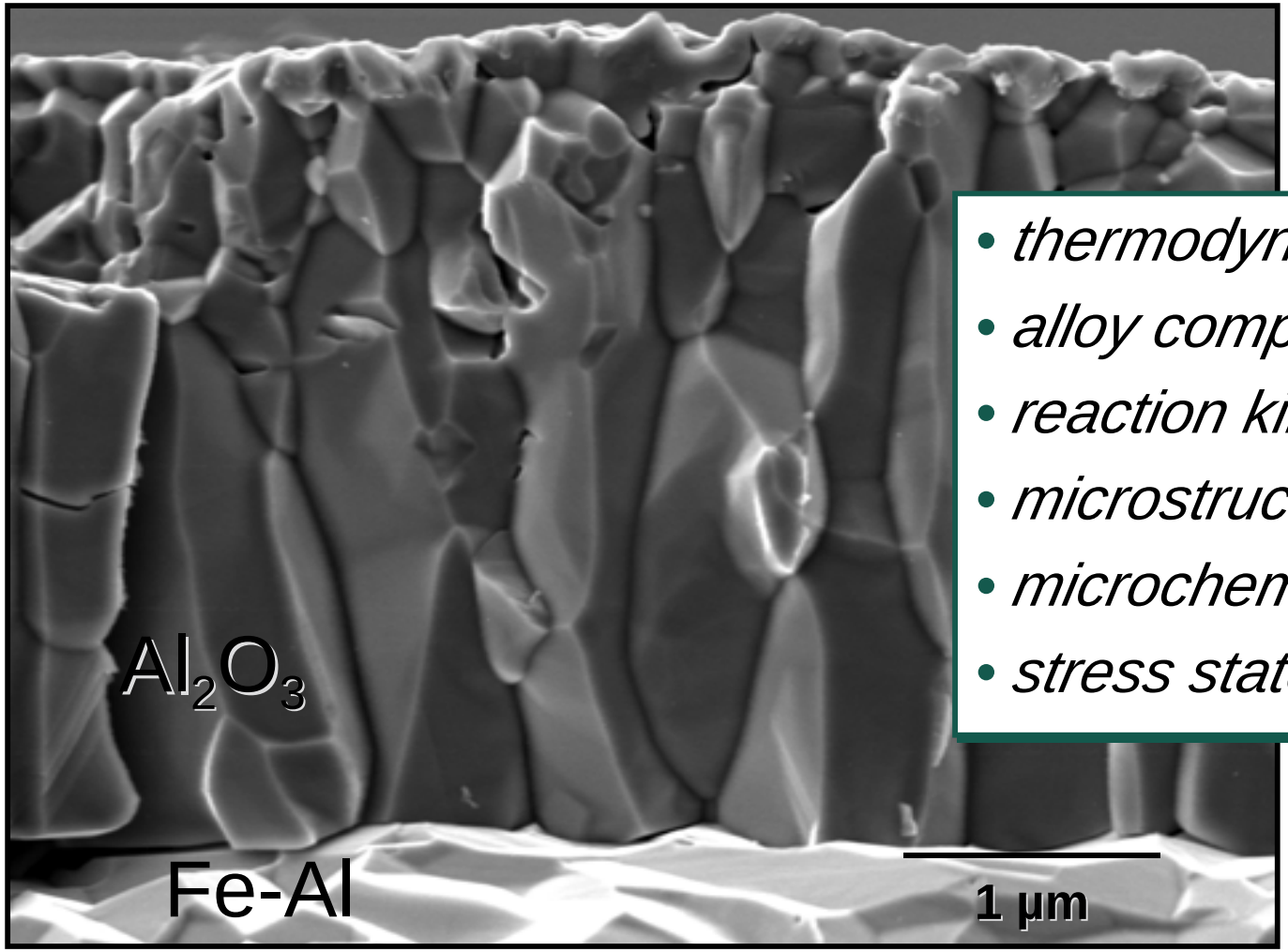

- *thermodynamics*
- *alloy comp'n.*
- *reaction kinetics*
- *microstructure*
- *microchemistry*
- *stress states*

With Some Exceptions, Sulfides Typically Show Rapid Growth Kinetics Compared To Oxides

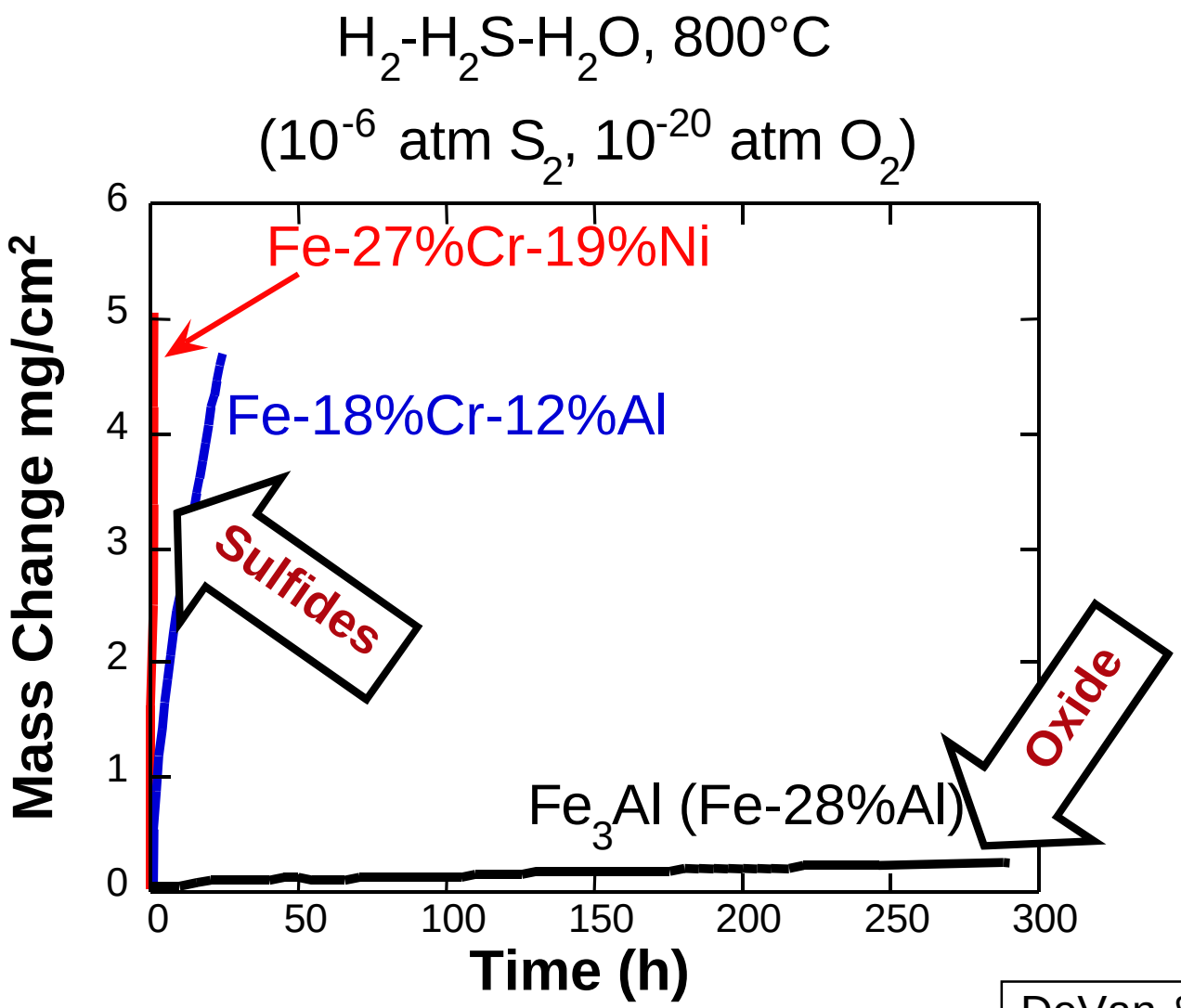

DeVan & Tortorelli 1993

So, We Look To Using Surface Oxides As A Permeation Barrier To Sulfur

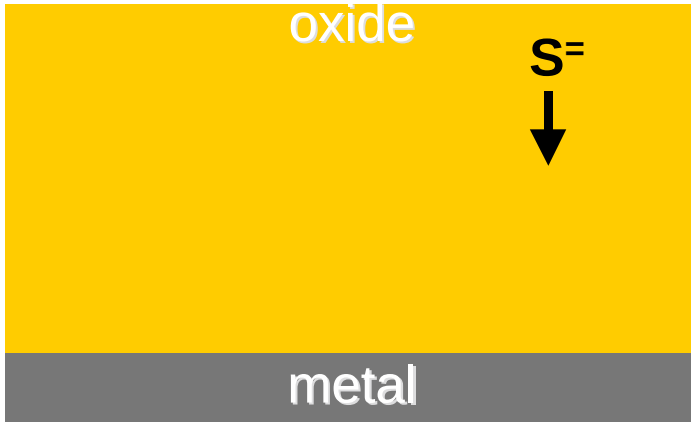

High-Temperature Protective Oxides

- Cr_2O_3
- Al_2O_3
- SiO_2
- BeO

Intermediate-Temperature Protective Oxides

- ~~Iron oxides~~
- ~~Nickel~~
- ~~mixed oxides~~

Alumina Layers Can Be Particularly Effective Permeation Barriers

- Sulfur-bearing gases
- Water vapor (avoids volatility problems associated with Cr_2O_3 and SiO_2)
- Carburizing environments

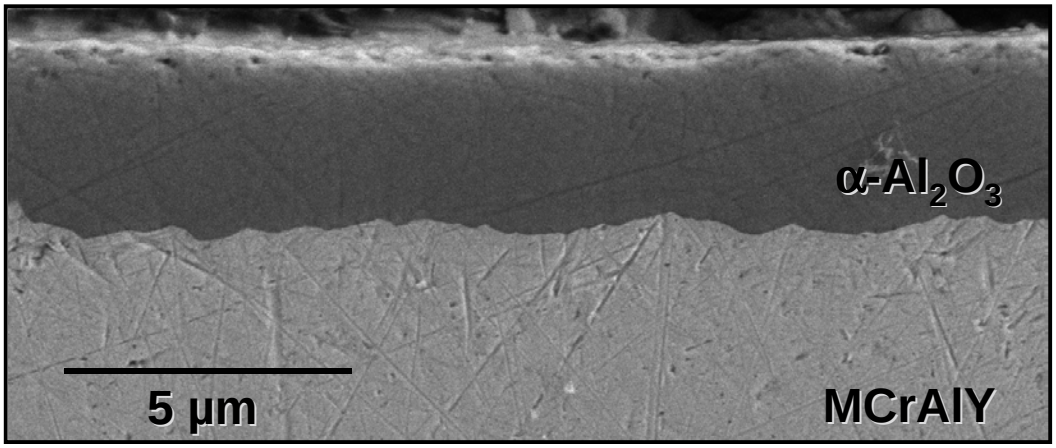

We Are Now Exploring Ti-Al-Cr Systems

- TiAl has been shown to have some sulfidation resistance (Schütze)
- When optimized, can form alumina even at low oxygen partial pressures
- Mulitphase nature allows manipulation to better achieve continuous alumina formation and good oxidation resistance at 800°C (Brady et al.)
- Coatings have been developed (Brady, Smialek, and Brenly)

Cr Additions to Ti-Al Reduce O Solubility And Thus Promote External Alumina Formation

Ti-43Al exposed for 48 h at 1000°C in Pure Oxygen

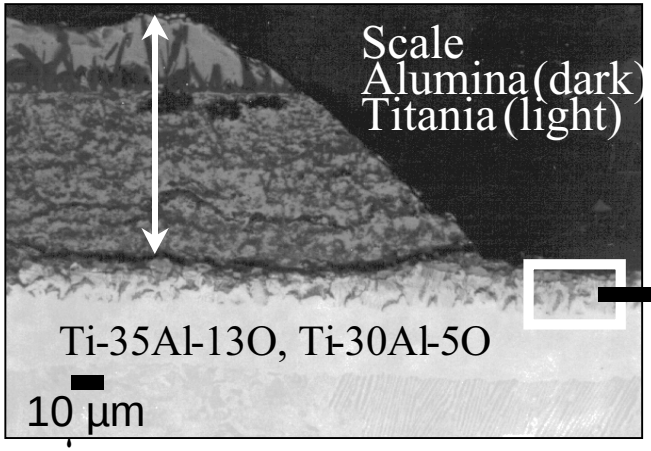

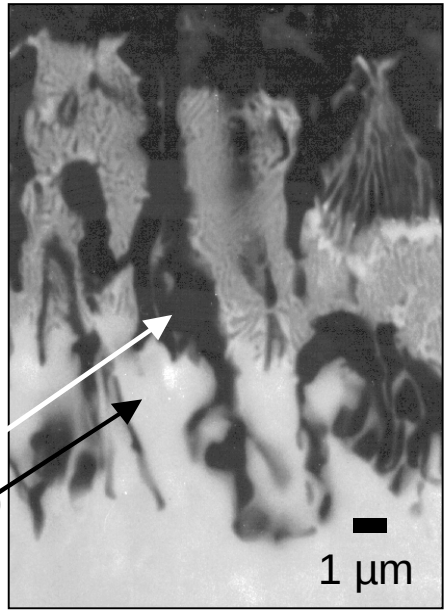

Ti-42Al-27Cr FORMS CONTINUOUS ALUMINA

Exposed for 100 h at 1000°C in Pure Oxygen

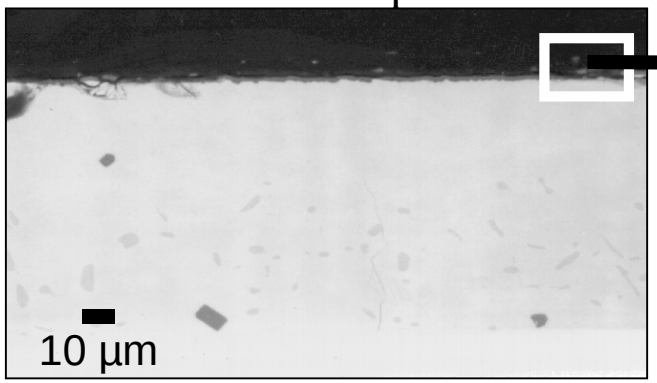

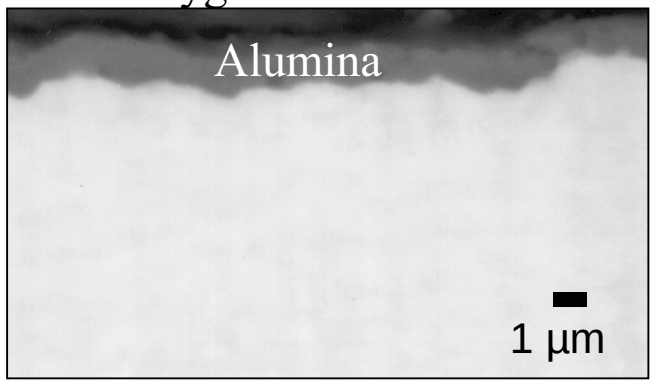

Brady et al.

We Have Recently Examined Several Variants Of Ti-Al-Cr

- Ti-51Al-12Cr (at.%)
- Ti-45Al-15Cr-15Nb
- Ti-45Al-15Cr-15Ta
- Ti-48Al-13Cr-10Nb-5Ta

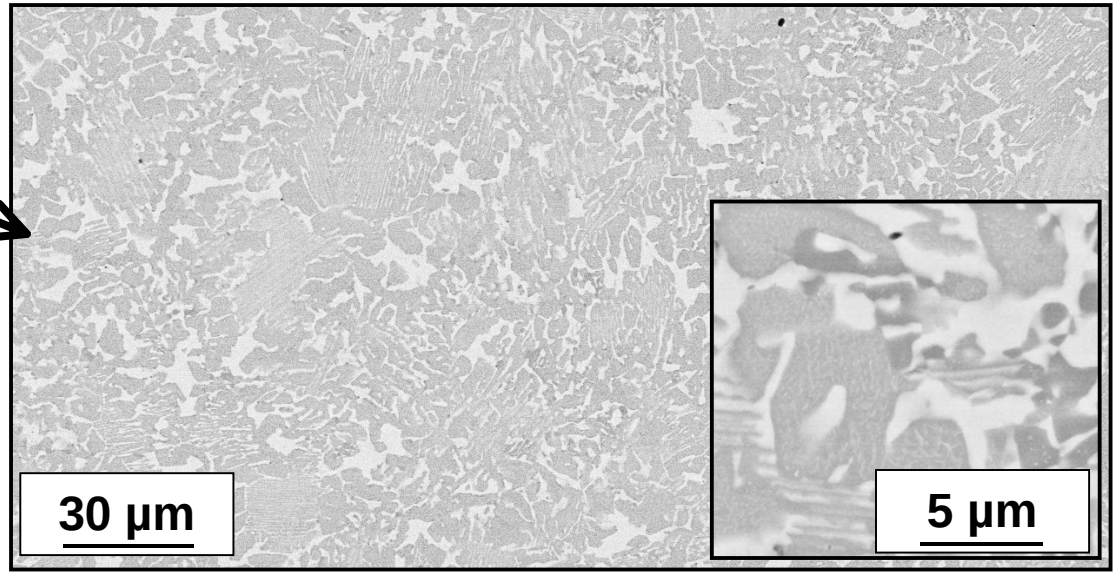

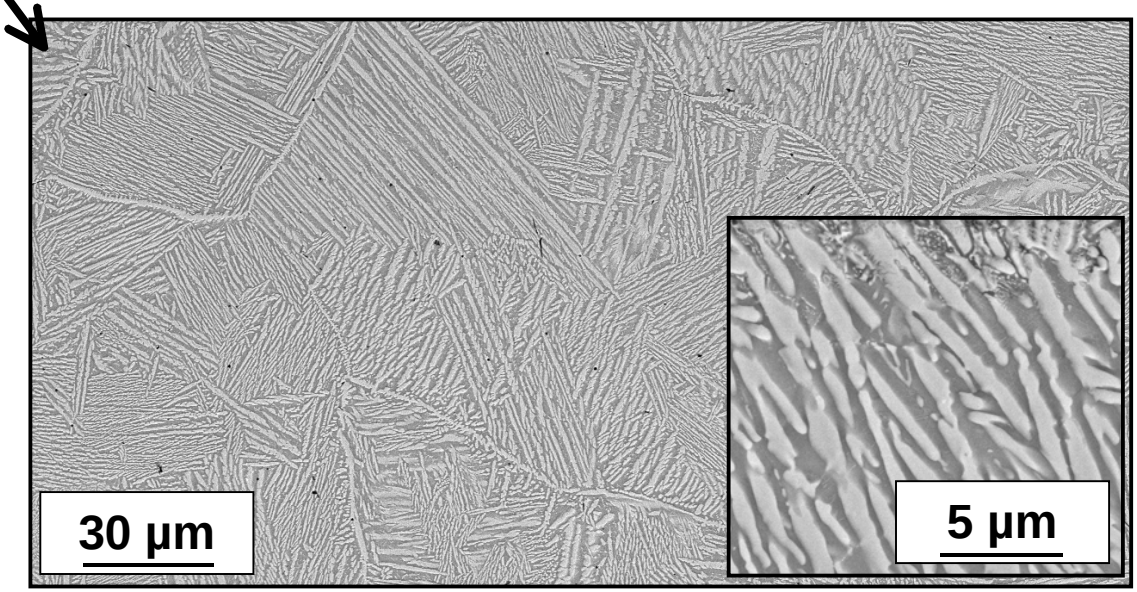

- 100 h, dry air, 800°C
- 50 h, H_2S-H_2-H_2O, 800°C
- Preliminary results

Alumina Should Be Stable On TiAlCr In Our H_2S-Containing Environment

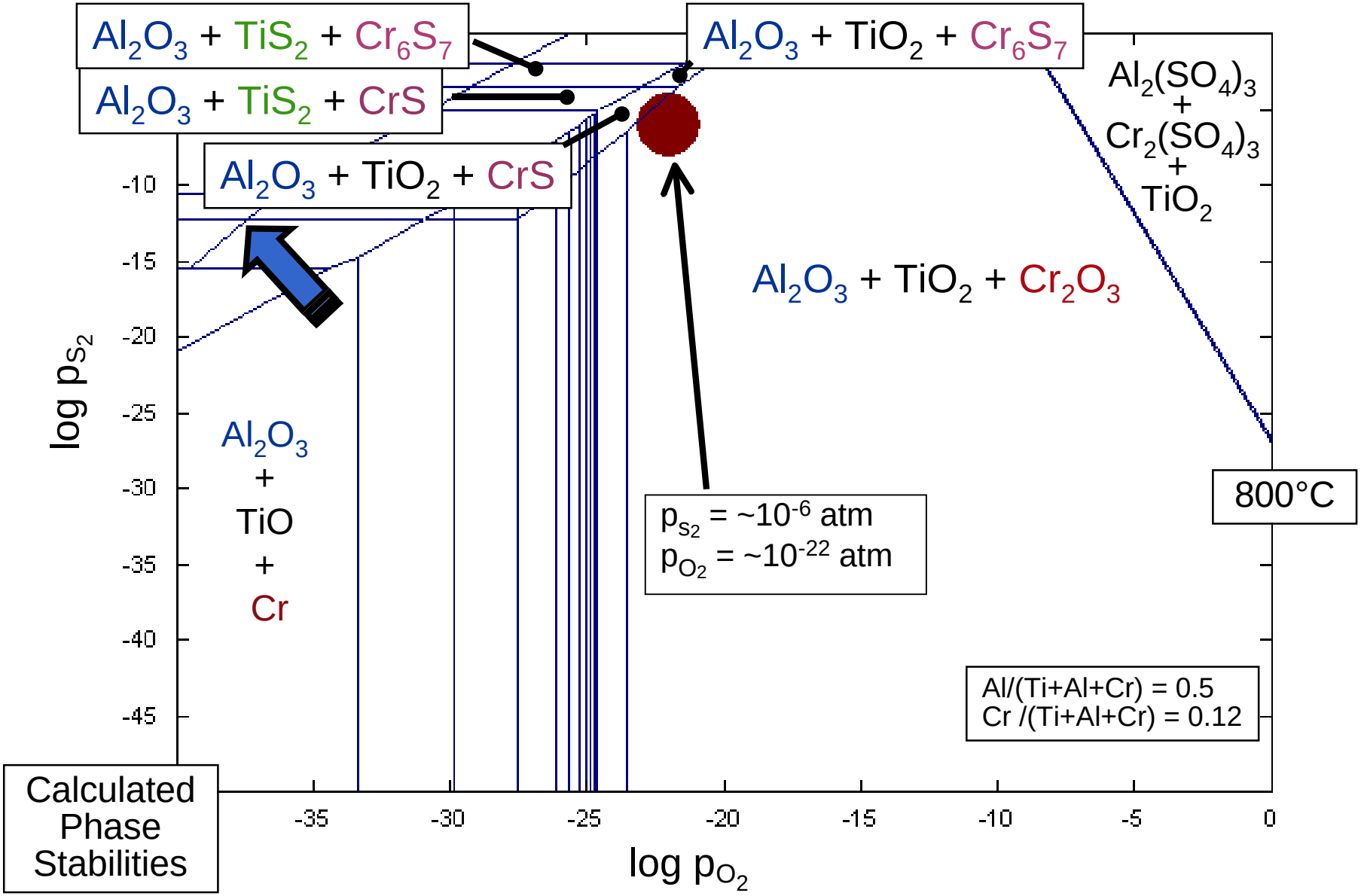

Niobium Sulfide Can Be Stable, But Should Grow Slowly

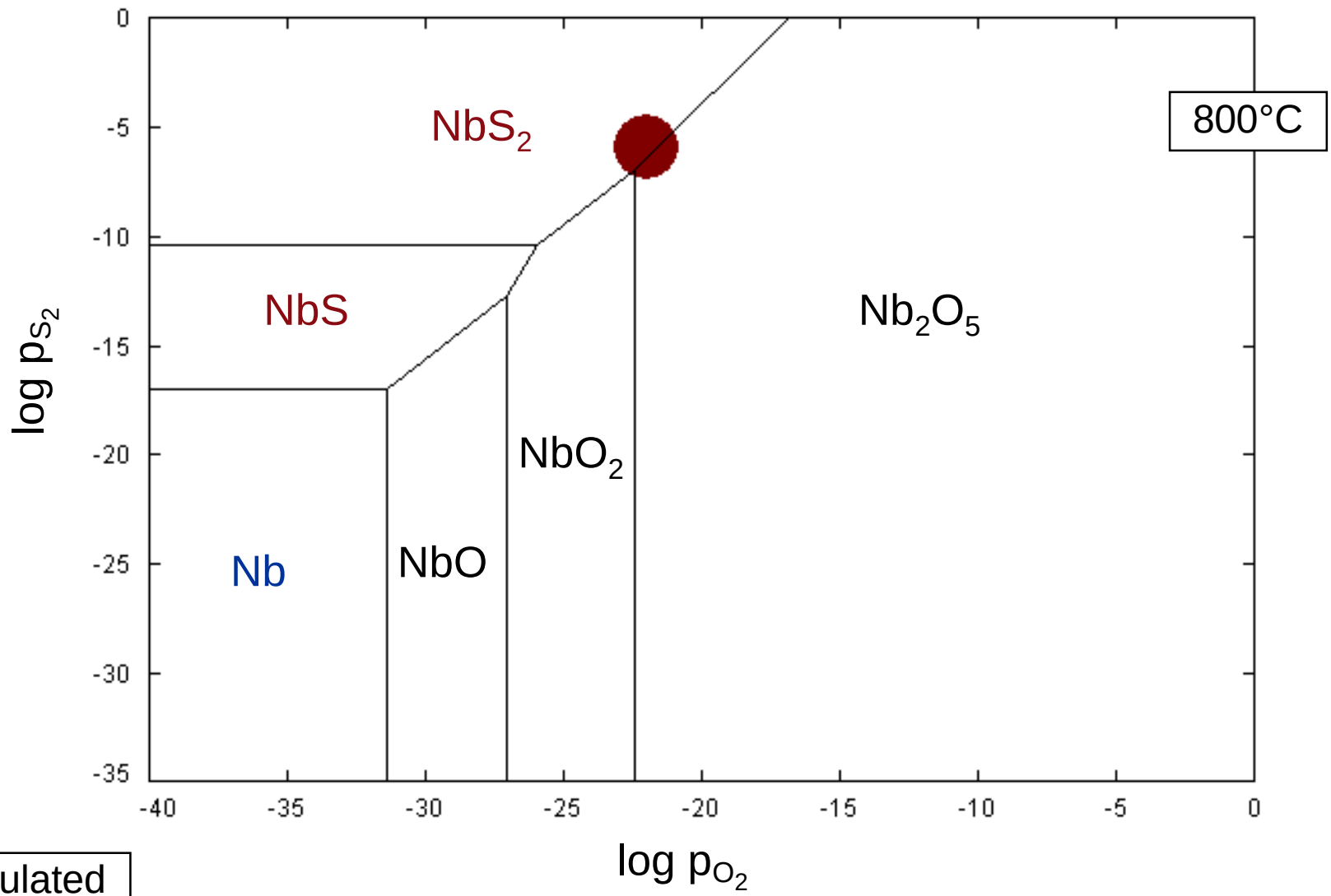

Calculated Phase Stabilities

Oxidation Exposures Yielded Small Mass Gains And Continuous Alumina Layer On TiAlCr

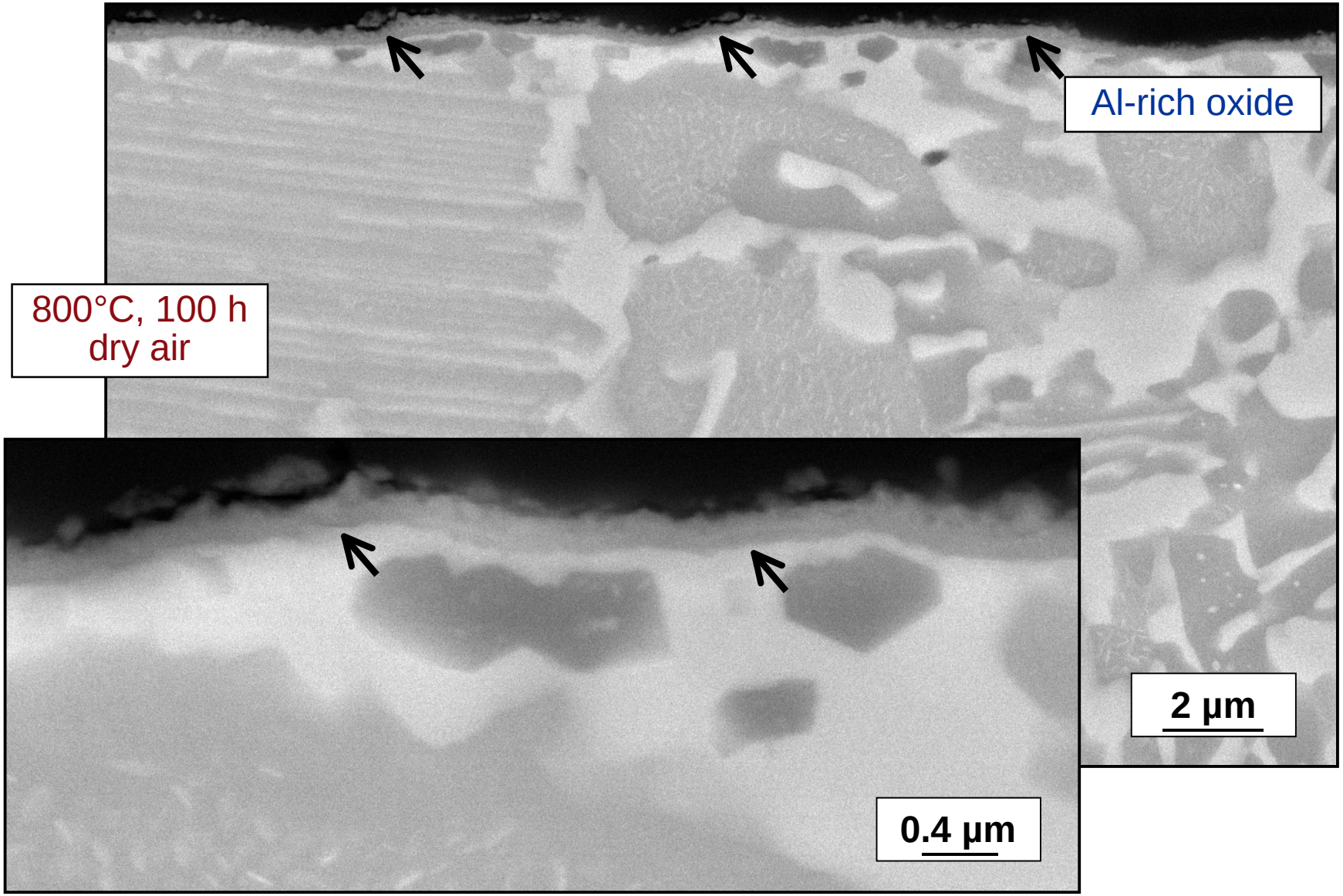

On Some TiCrAl's, A Continuous Alumina-Rich Layer Also Formed In H_2S-Containing Environment

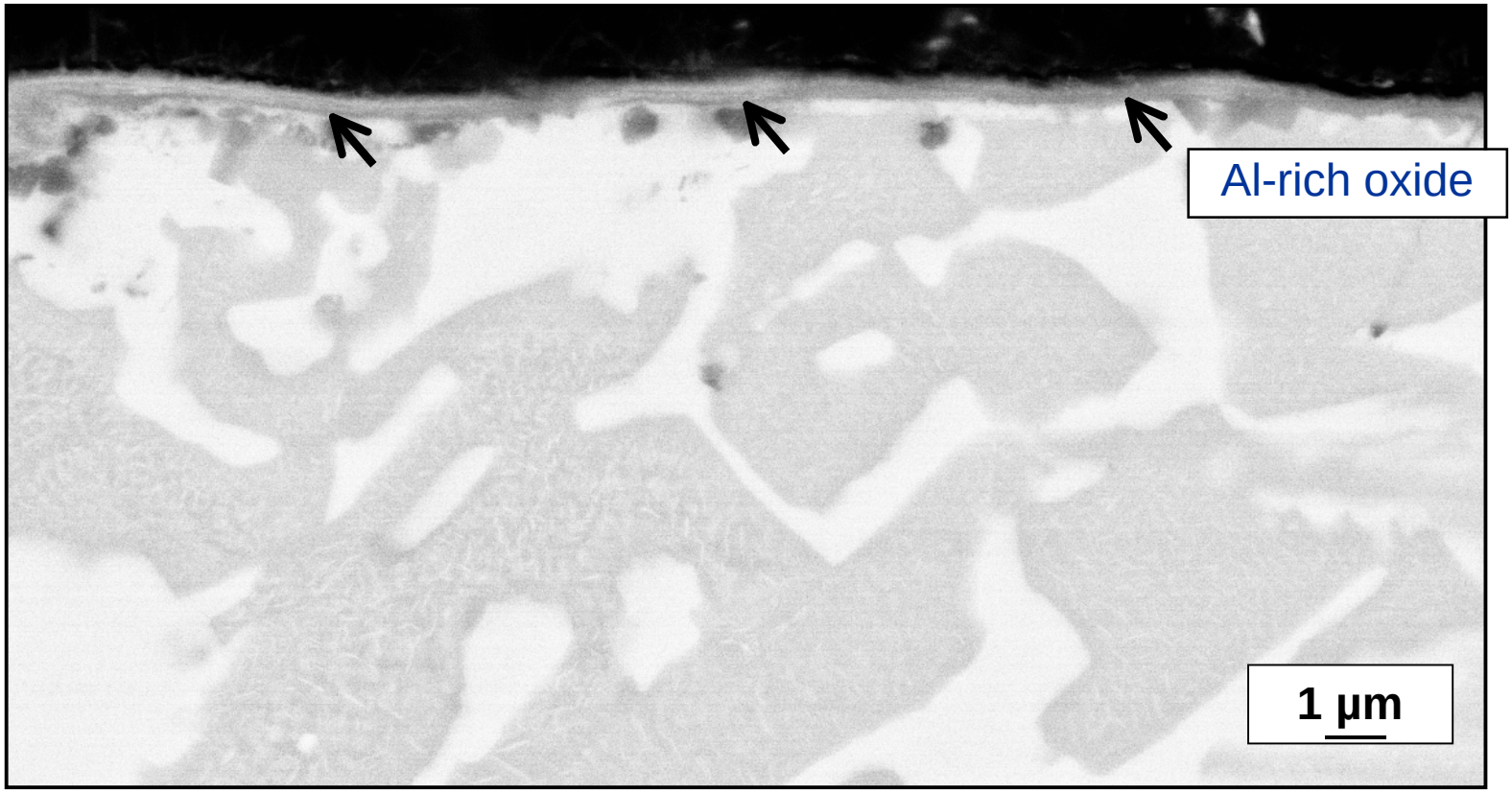

TiAlCr, 800°C, 50 h, H_2S-H_2-H_2O

On Some TiCrAl's, A Continuous Alumina-Rich Layer Also Formed In H_2S-Containing Environment

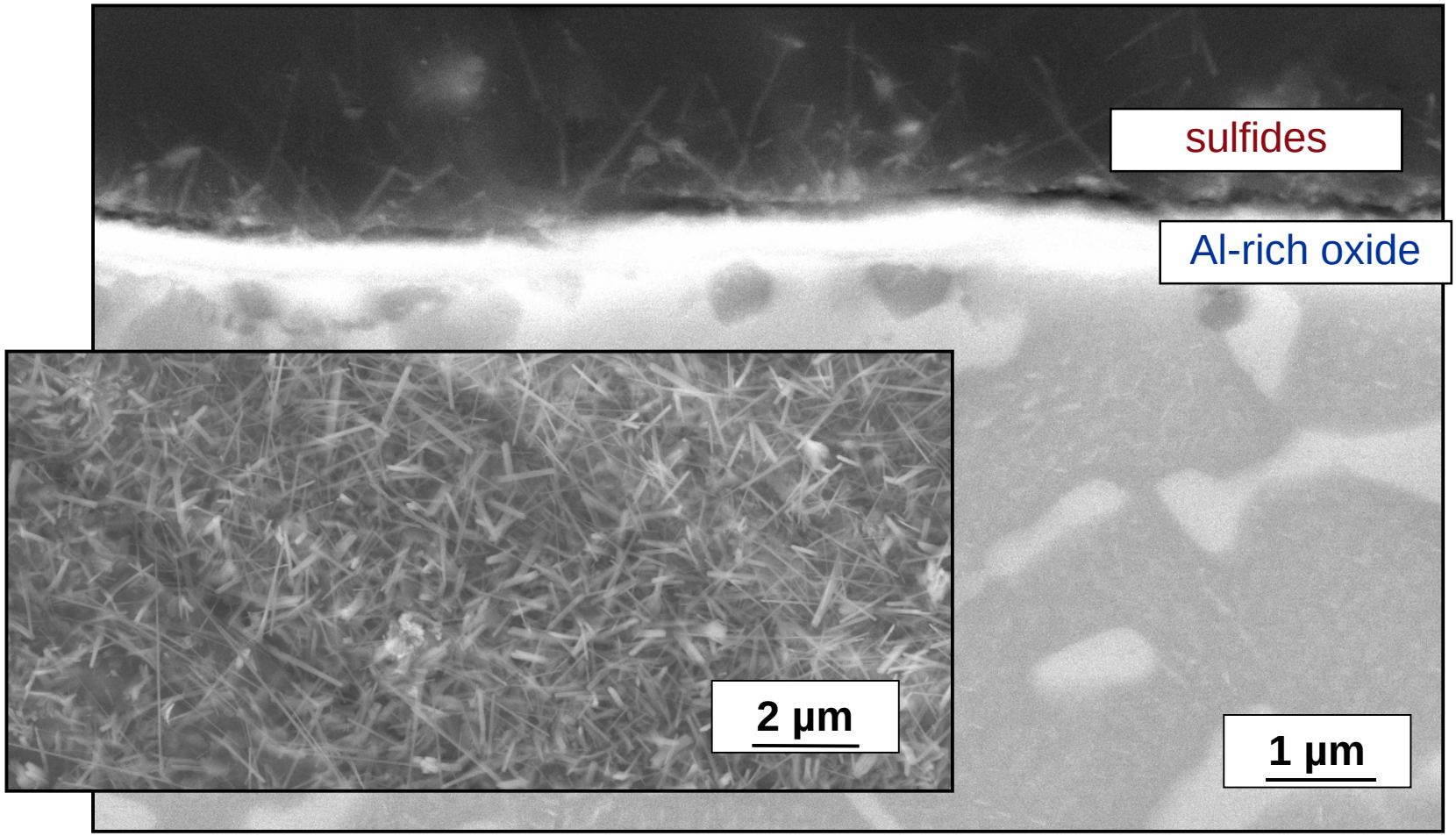

TiAlCr, 800°C, 50 h, H_2S-H_2-H_2O

Presence Of This Al-Oxide Layer Prevented Substantial Sulfidation

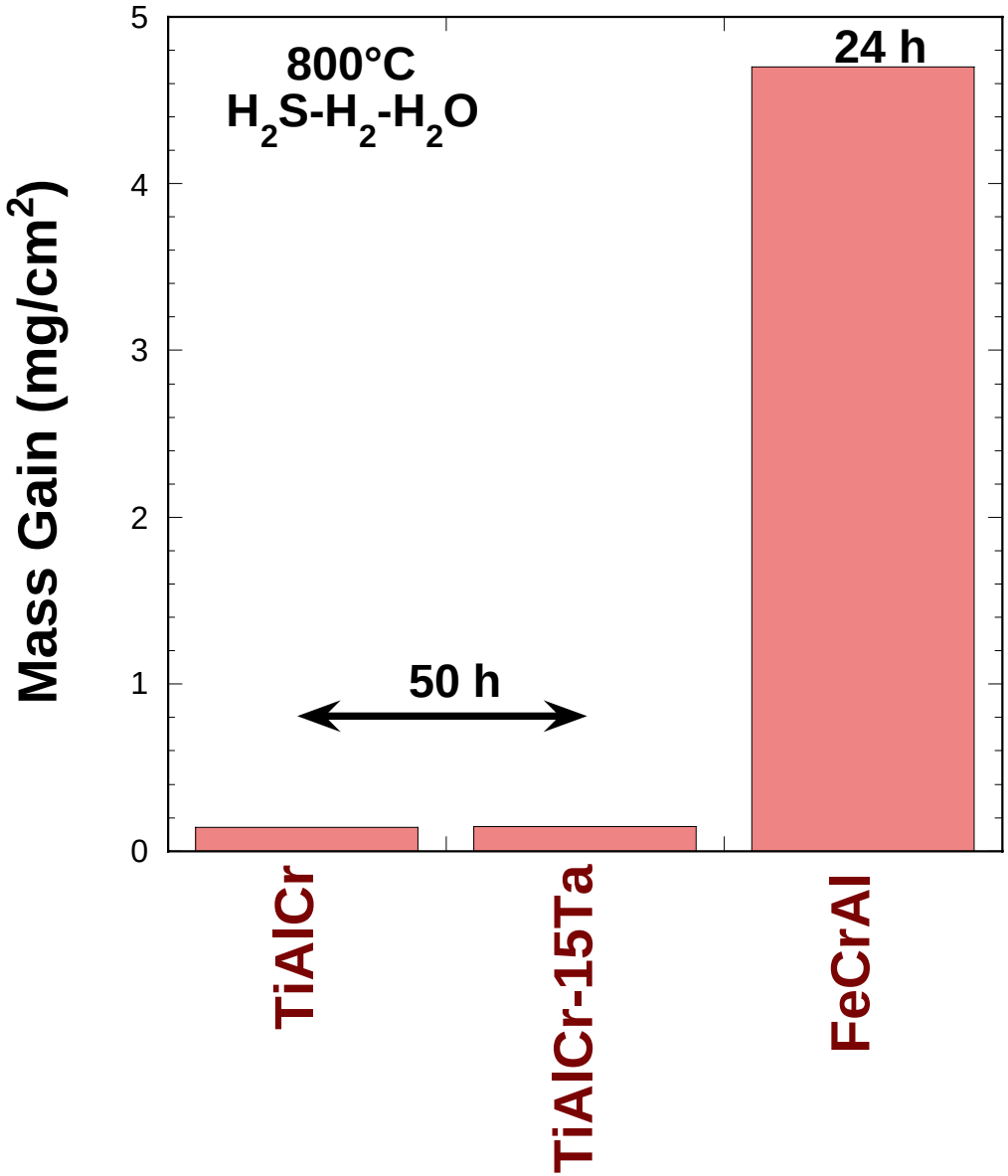

But, Mass Gains Of TiAlCr-15Nb For Exposures With Sulfidizing Potential Were Significantly Higher

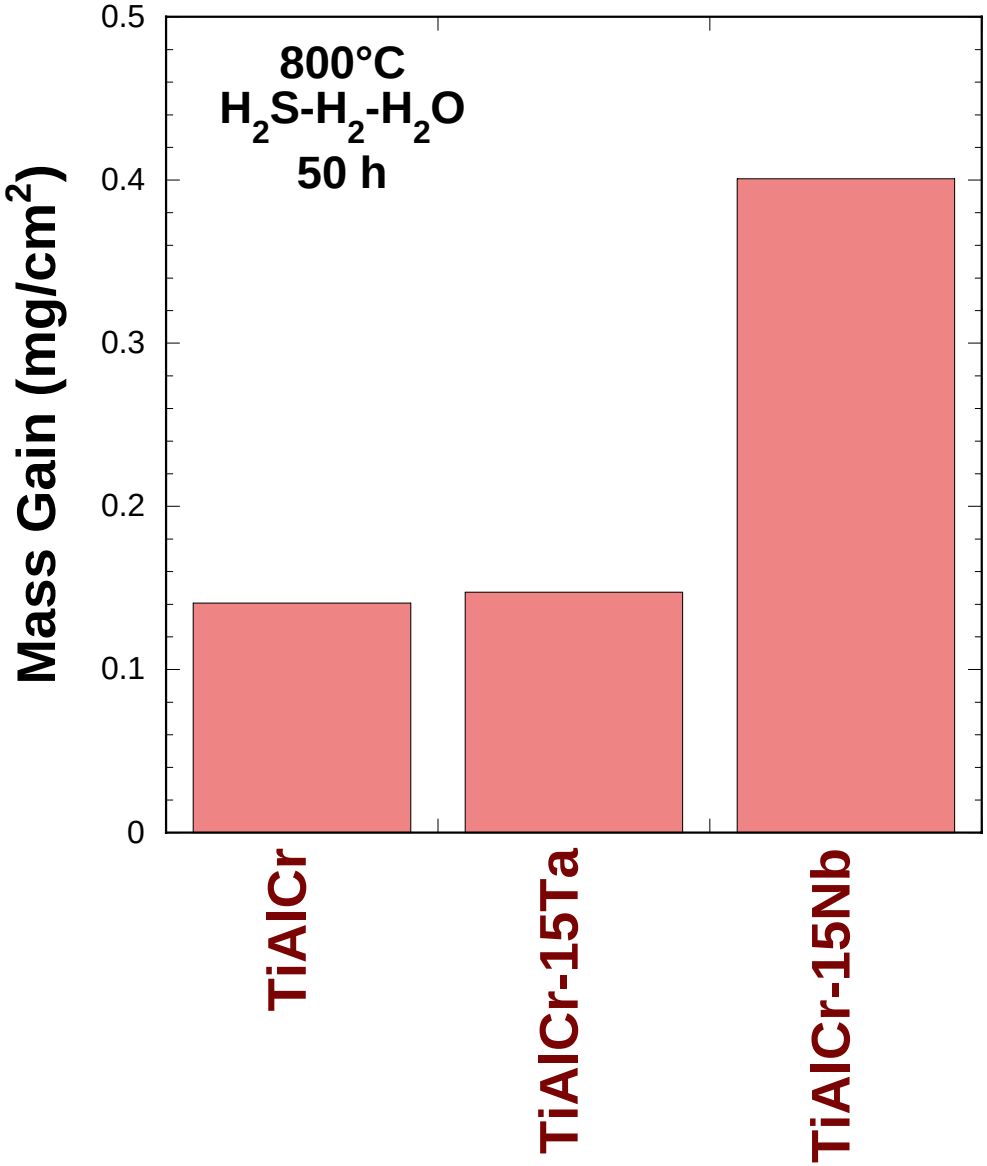

A Mixed Al-Ti Oxide Layer Formed On The TiCrAl-Nb Alloy Upon Oxidation

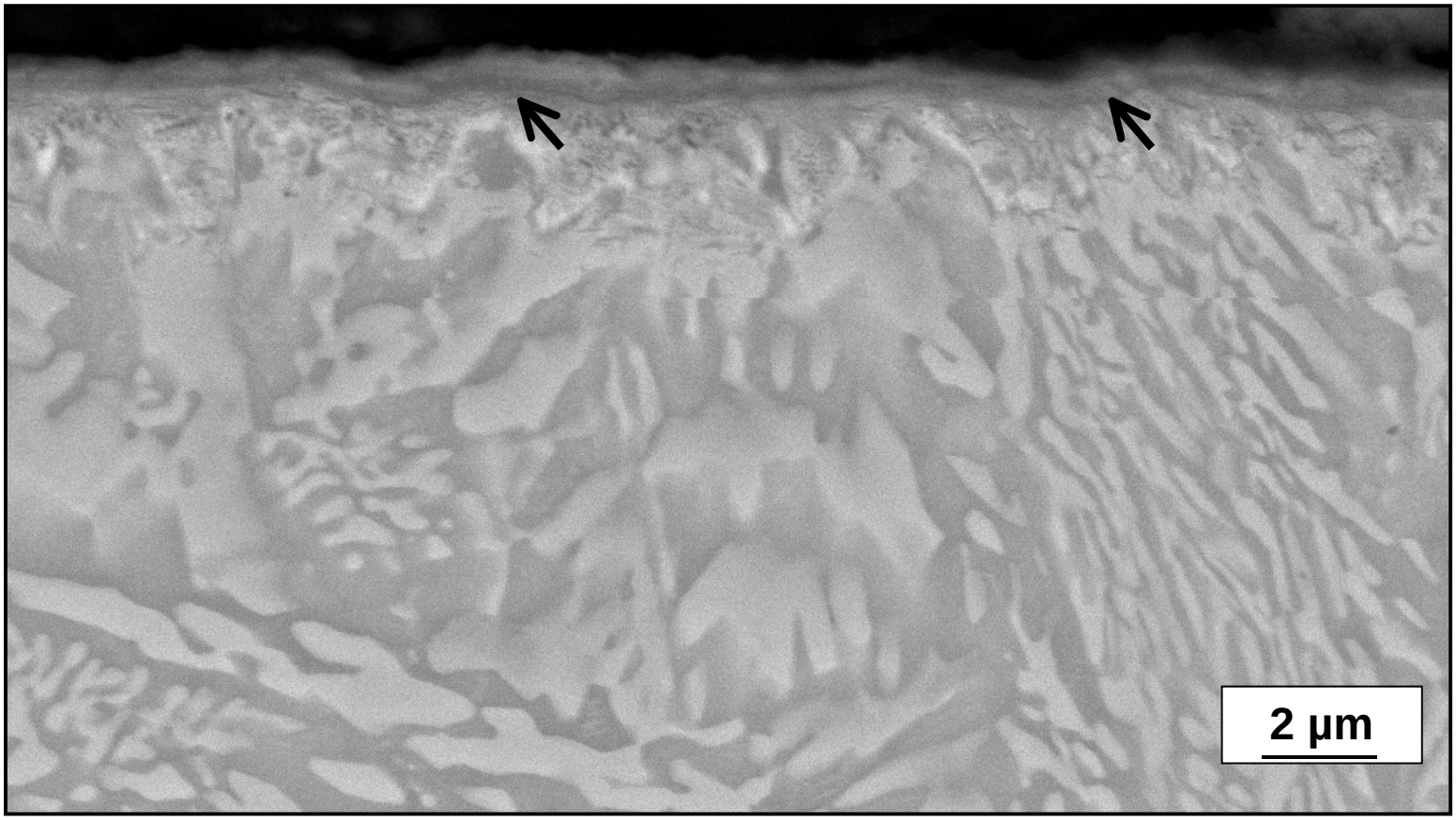

800°C, 100 h, dry air

The Inability To Form Protective Alumina On This Alloy Was Manifested As Greater Sulfidation

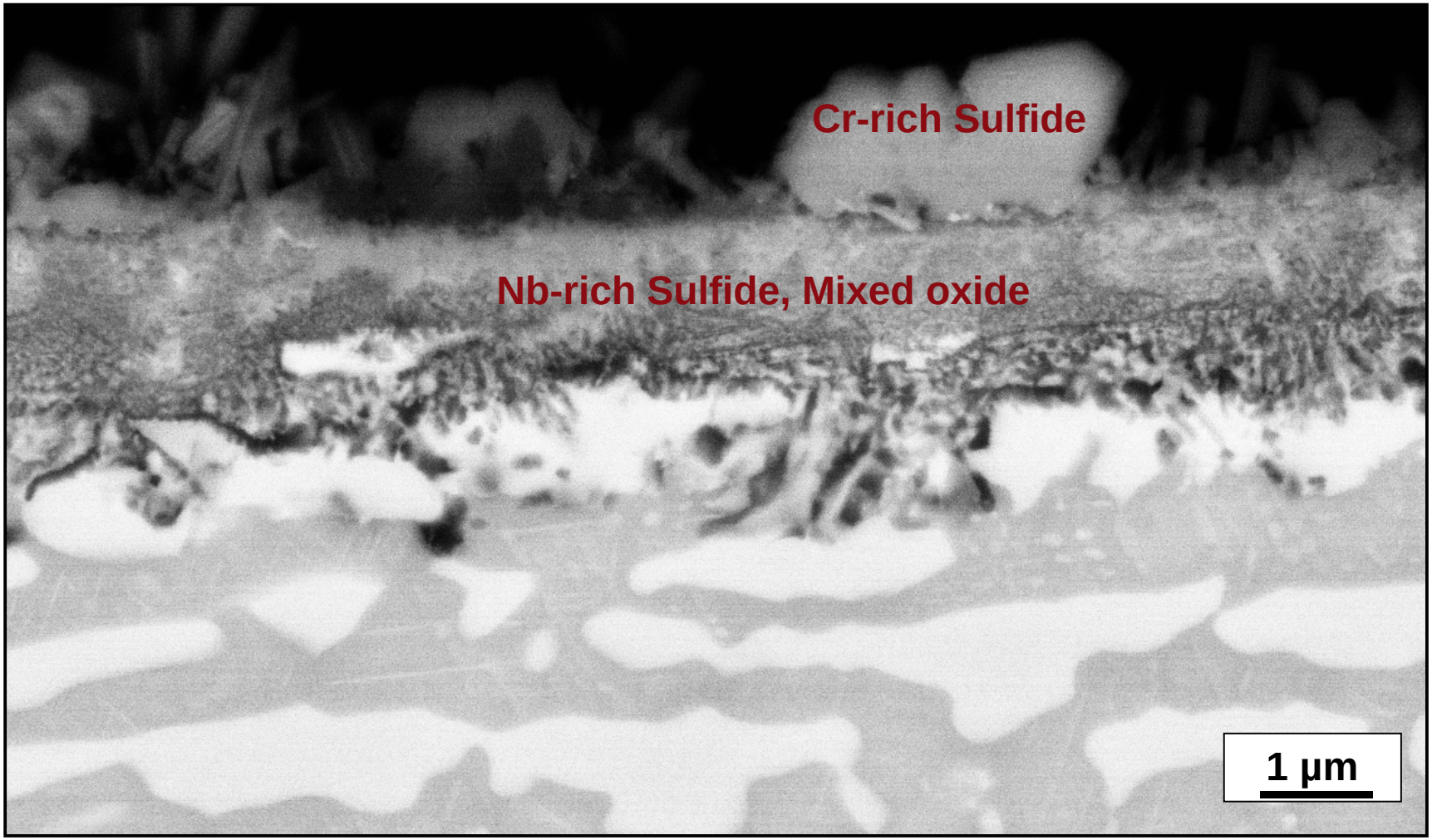

TiAlCr-15Nb, 800°C, 50 h, H_2S-H_2-H_2O

The Inability To Form Protective Alumina On This Alloy Was Manifested As Greater Sulfidation

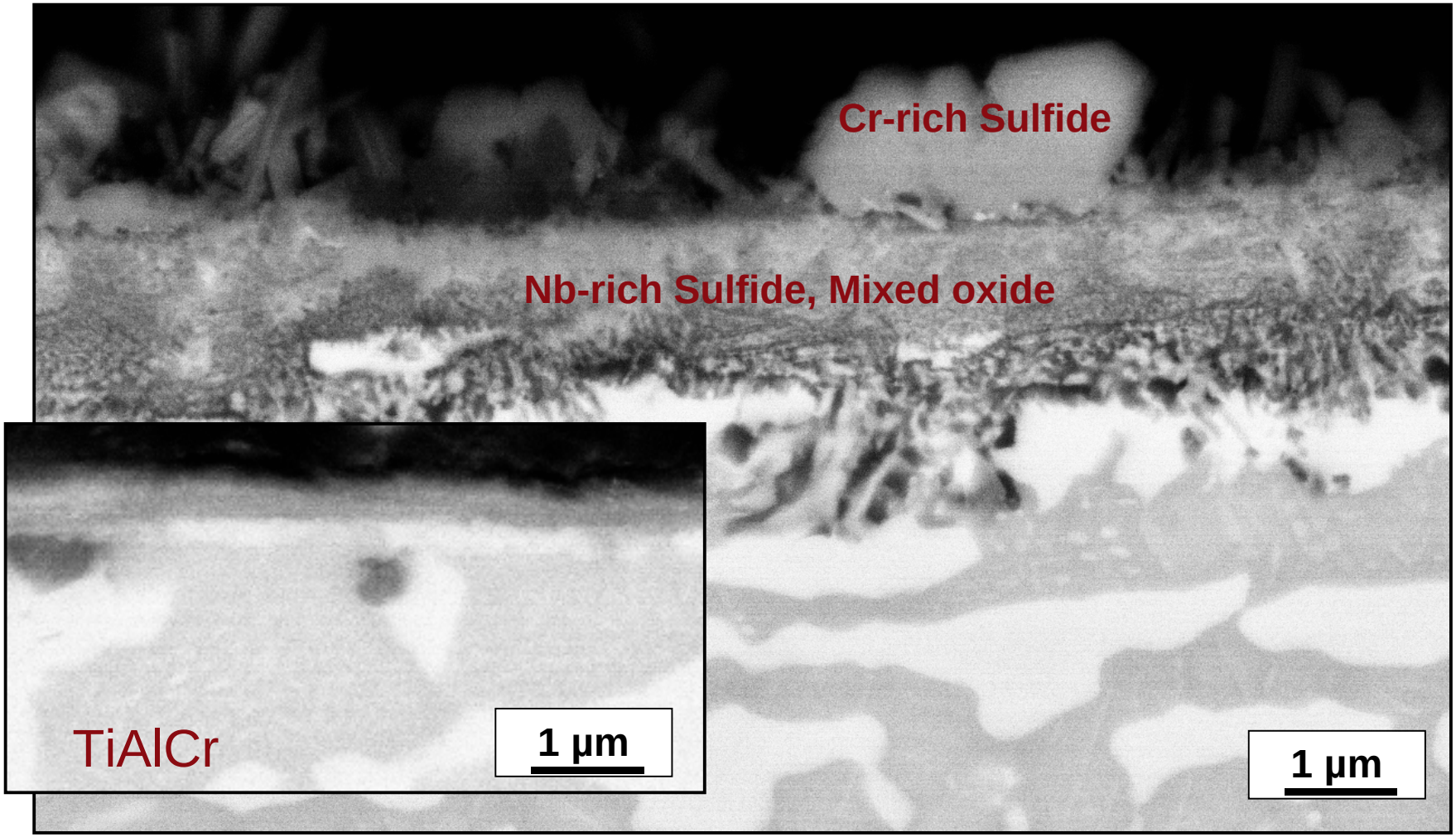

TiAlCr-15Nb, 800°C, 50 h, H_2S-H_2-H_2O

Various Sulfides Had Different Morphologies

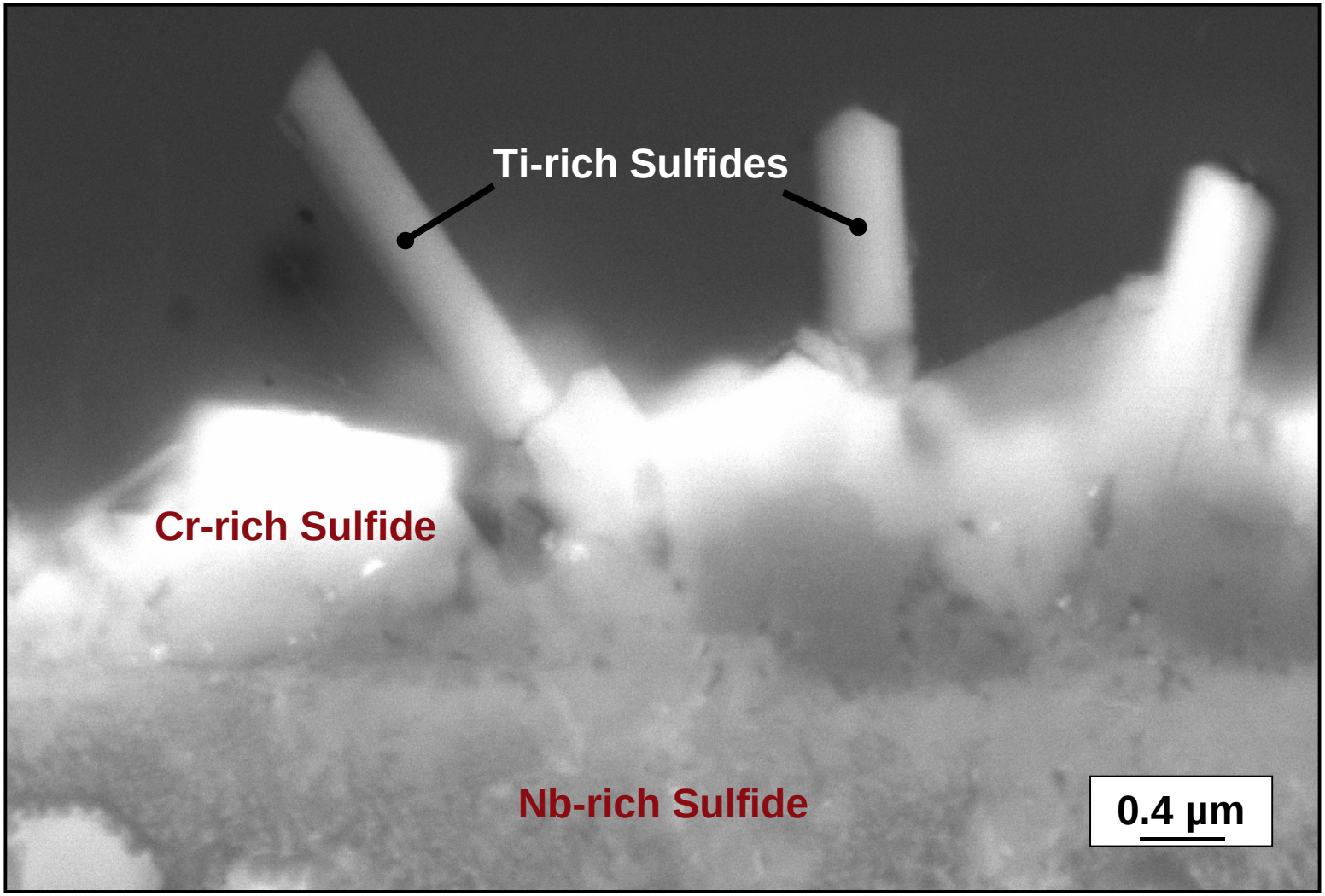

TiAlCr-15Nb, 800°C, 50 h, H_2S-H_2-H_2O

Various Sulfides Had Different Morphologies

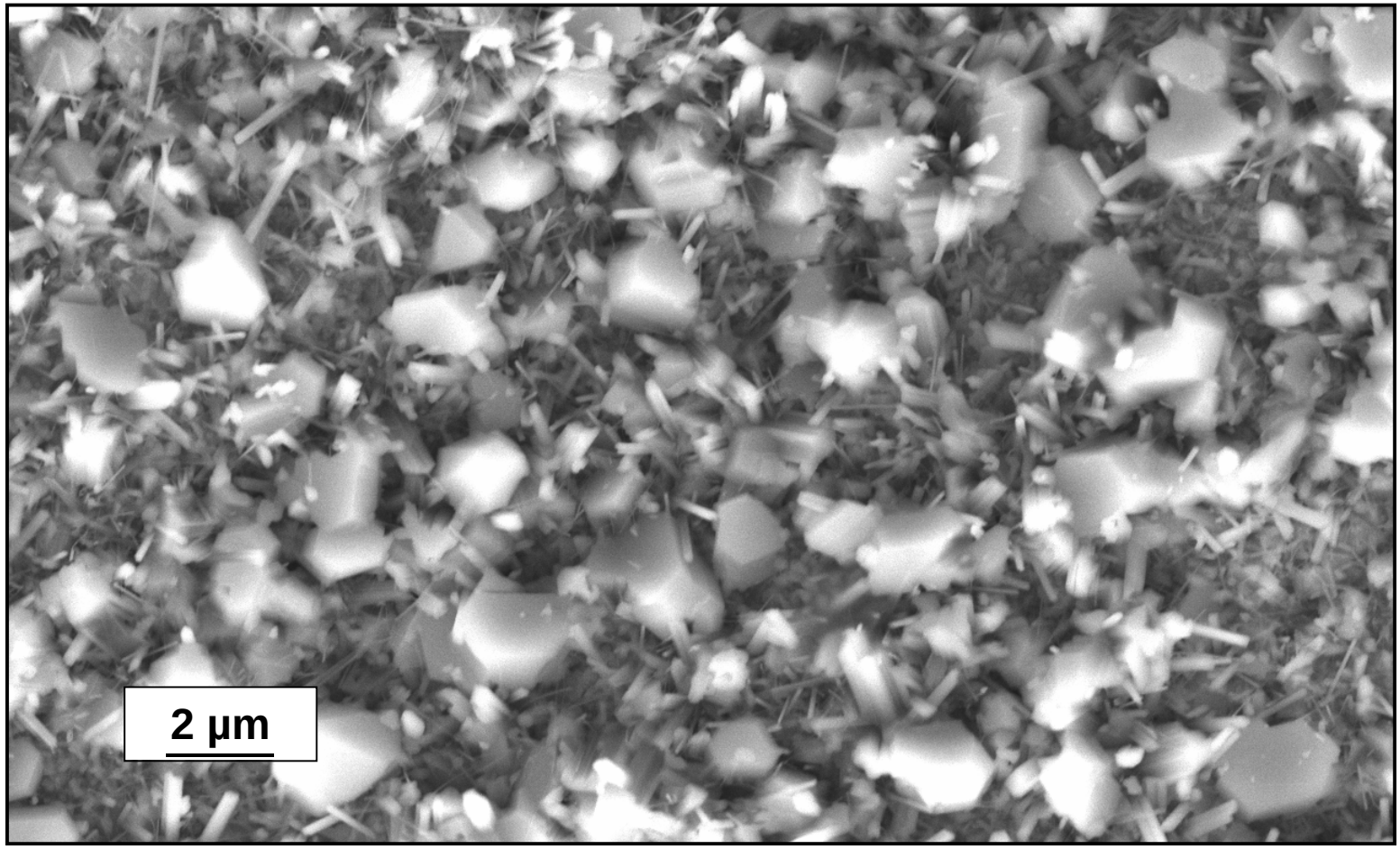

TiAlCr-15Nb, 800°C, 50 h, H_2S-H_2-H_2O

Similar To What Has Been Observed For Fe-Al-Cr Systems Exposed Under Same Conditions

The TiCrAl System Appears To Have Some Promise For Sulfidation Resistance

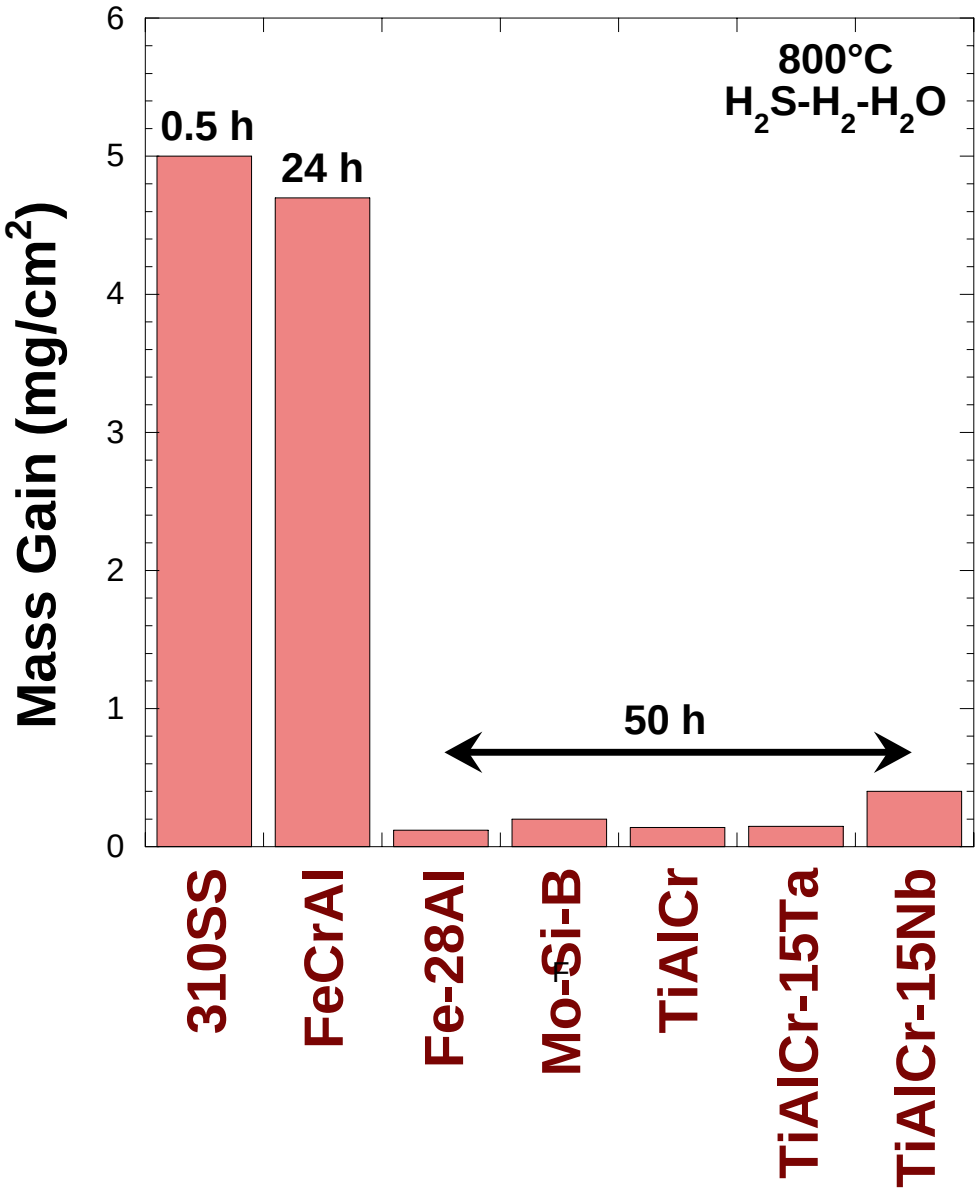

More Work Needed To Confirm And Fully Characterize

Ongoing And Future Work

- Complete
  - detailed analysis of sulfidized specimens
  - extended exposures
- Optimize compositions and microstructures of Ti-based systems
- Examine resistance under changing p_{O_2}-p_{S_2} conditions for Mo- and Ti-based systems

Summary

- The high-temperature response of multiphase alloys and composite structures to gas mixtures containing oxygen and sulfur was studied for TiAlCr systems

- TiAlCr alloys can offer good sulfidation resistance when compositions and microstructures yield protective alumina at low oxygen partial pressures associated with gasification processes

Back-Up

Smart Protective Coatings For High-Temperature Corrosion Protection

- Smart = sense and respond appropriately
- In present context, materials that sense particular environmental conditions and form protective barrier layers to provide high-temperature corrosion protection

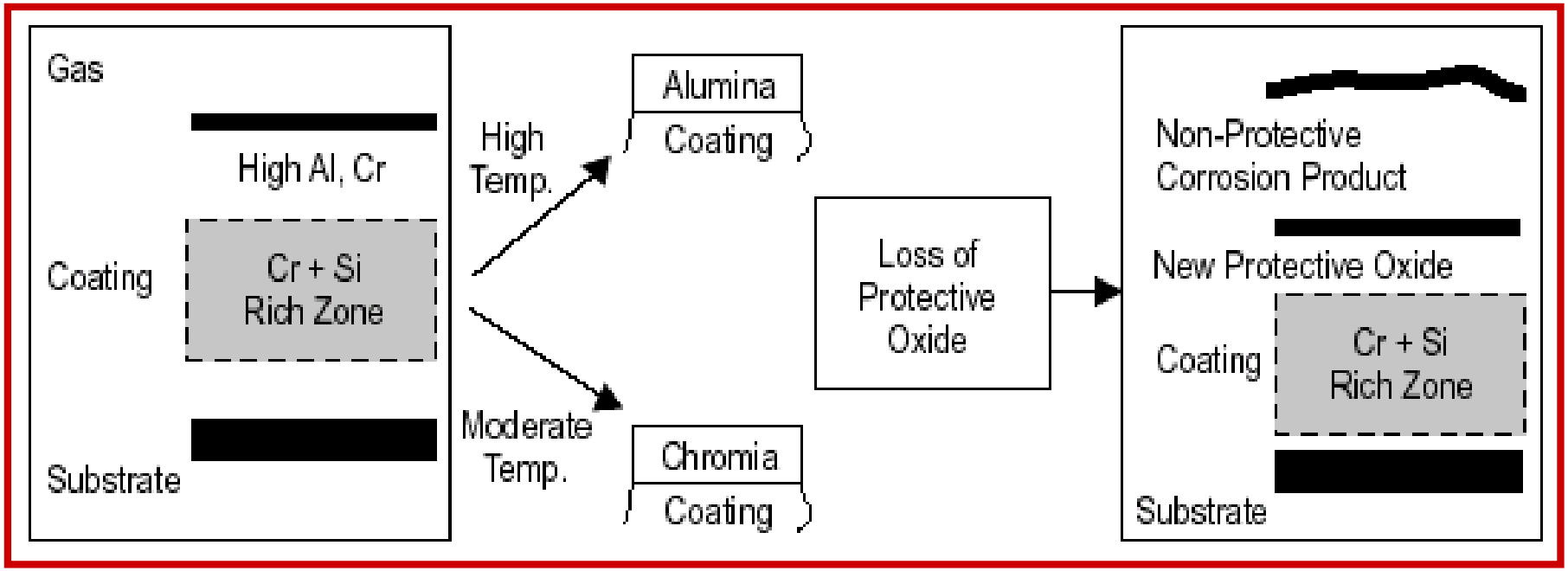

J.R. Nicholls, "Smart Coatings—A Bright Future", *Materials World*, vol. 4, 1996

Cr ENRICHMENT LIMITS a_{Al}/a_{Ti} DECREASE DUE TO Al DEPLETION TO FORM ALUMINA

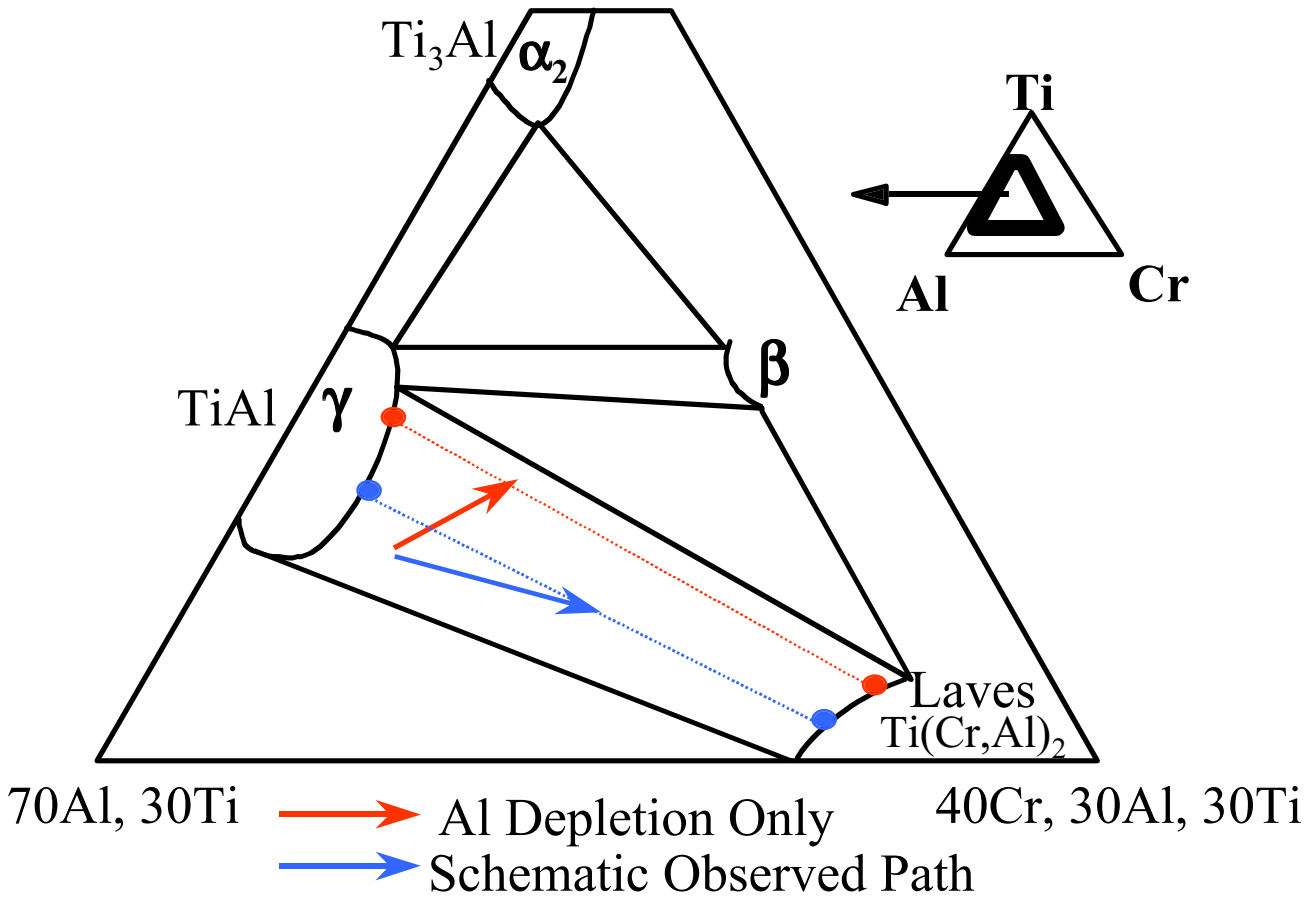

- Composition at Alloy/Scale Interface Stays Well Within γ + Laves Two-Phase Field: Little Decrease in a_{Al}/a_{Ti} with Al Depletion

A Minimum M Is Needed To Achieve External Product Formation

(Shown for oxide, same for other products)

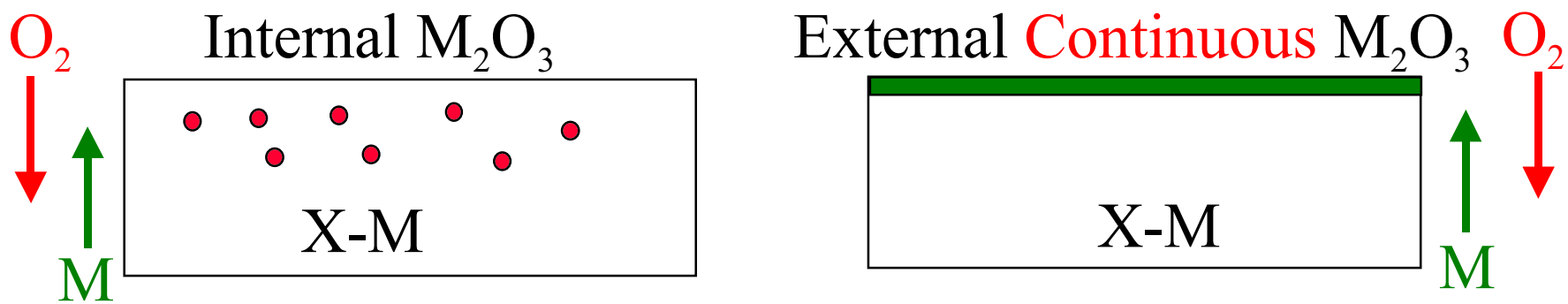

Minimum M for Continuous M_2O_3 $\propto \sqrt{(O\ sol.) \bullet \frac{D_O^{metal}}{D_M^{metal}}}$

Wagner, 1952

- AT WT
  Ti 37.00000 46.9818
  Al 51.00000 36.4778
  Cr 12.00000 16.5403

  Not as low in Cr as I had thought once converted to weight.

  Certainly much higher in Al than any FeCrAl, NiCrAl.

Iron, Chromium, and Aluminum Sulfides Preferentially Formed On Cycled Surfaces

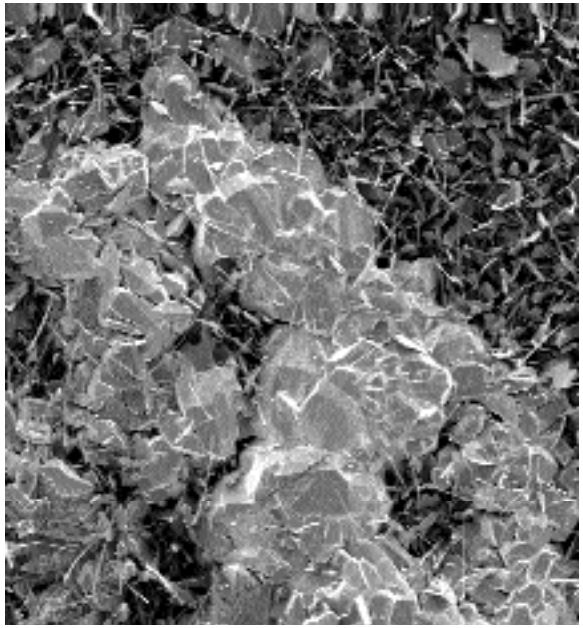

100 µm

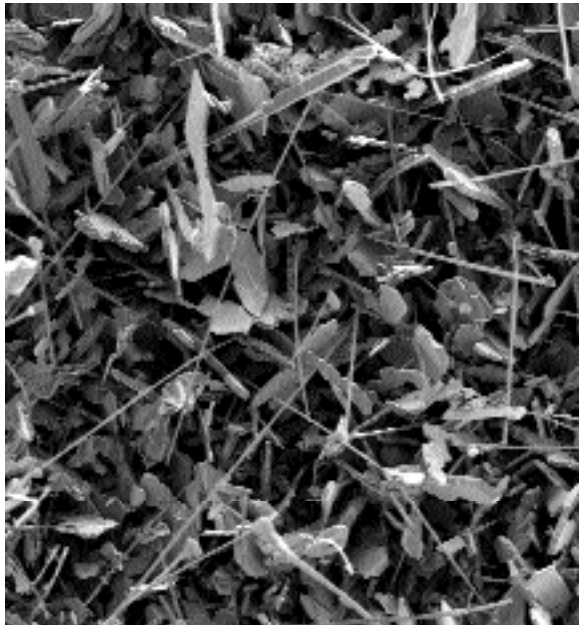

40 µm

GMA - 21Al-6Cr, 3 Thermal Cycles

B. A. Pint, SEM
C. S. MacDougall, XRD
S. J. Bobrowski, EDX

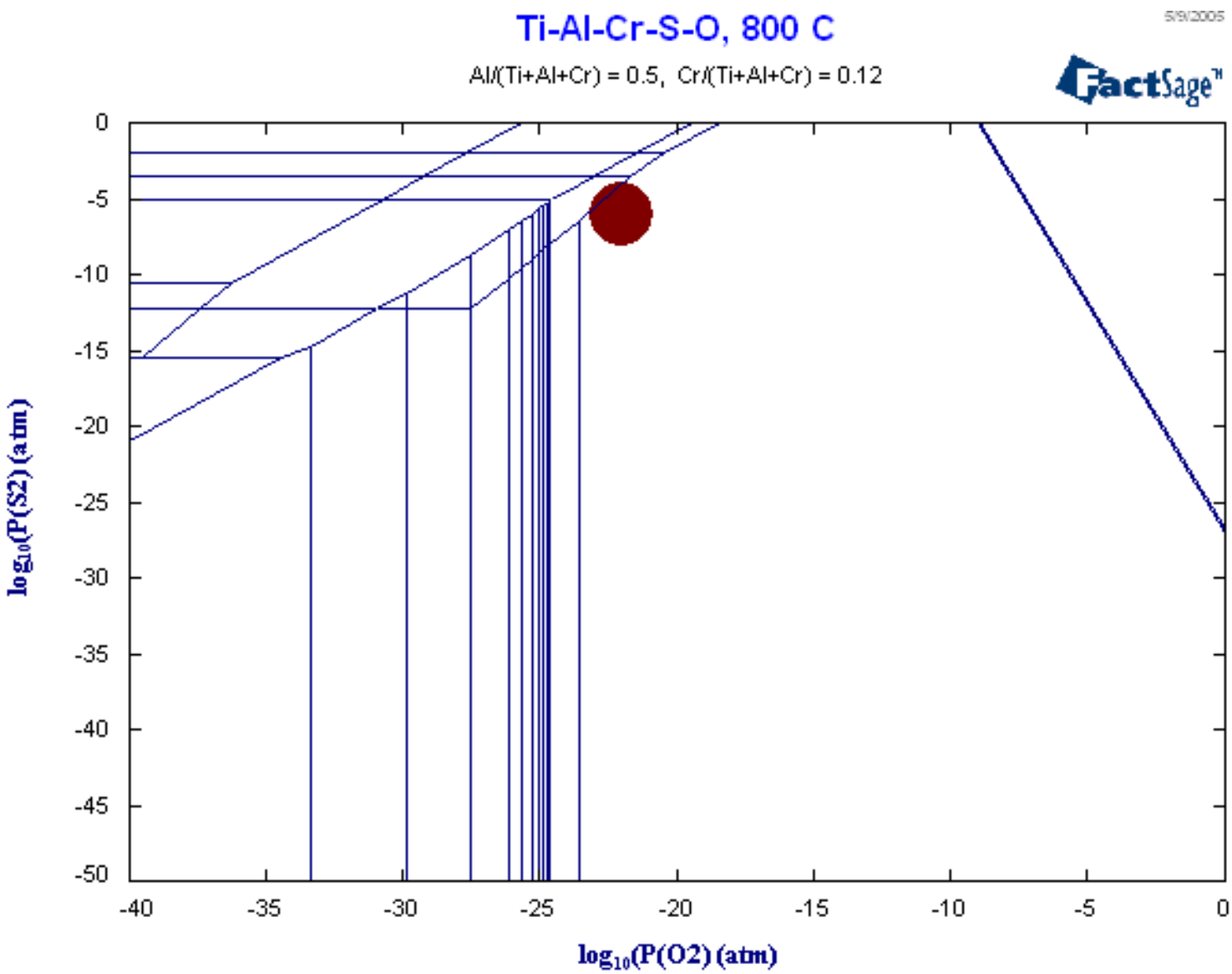
Ti-Al-Cr-S-O, 800 C
5/9/2005
Al/(Ti+Al+Cr) = 0.5, Cr/(Ti+Al+Cr) = 0.12
FactSage™
0
-5
-10
-15
-20
-25
-30
-35
-40
-45
-50
-40
-35
-30
-25
-20
-15
-10
-5
0
log10(P(S2) (atm)
log10(P(O2) (atm)

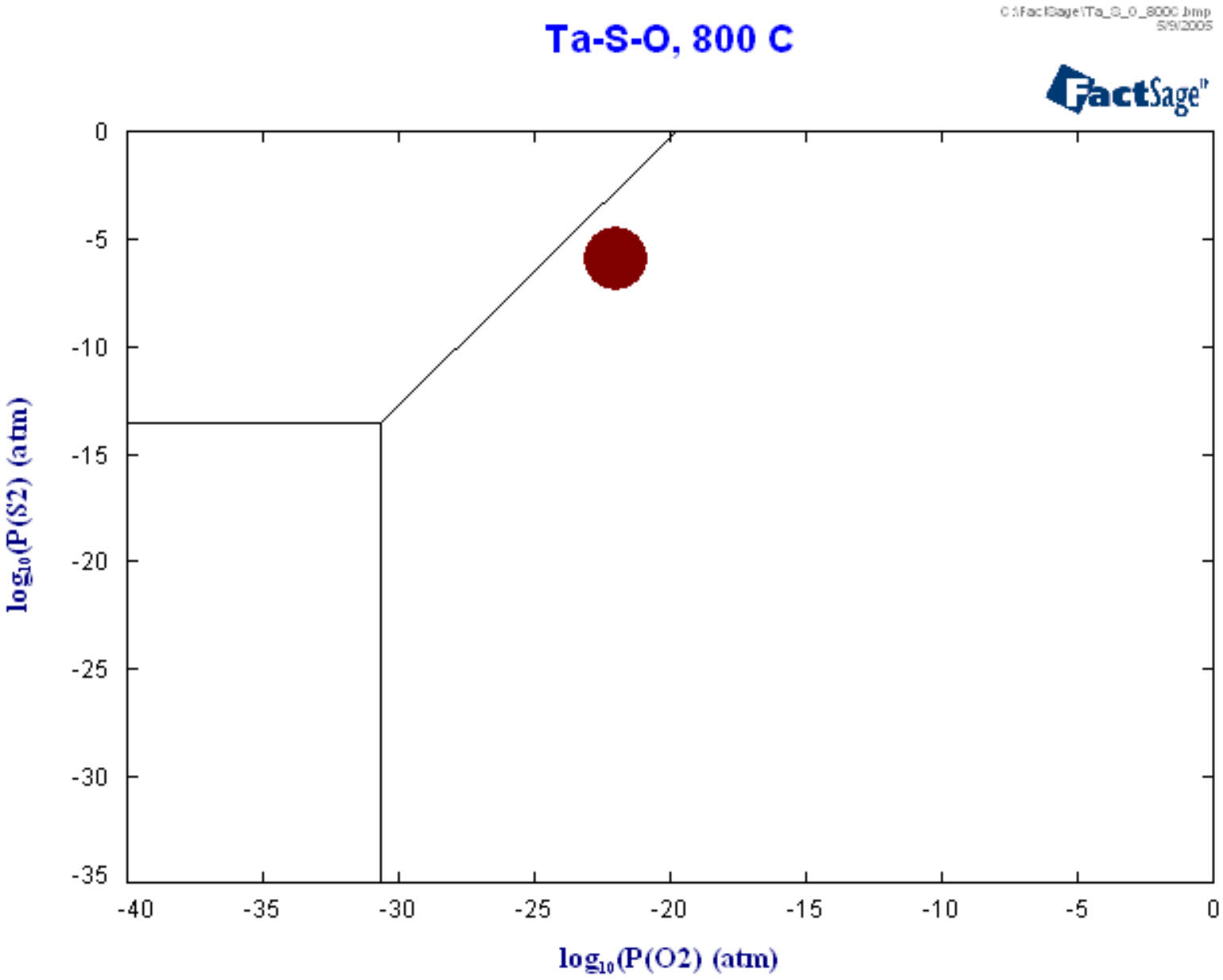
C:\FactSage\Ta_S_O_8000.Jmp
5/9/2005
Ta-S-O, 800 C
FactSage
0
-5
-10
-15
-20
-25
-30
-35
-40
-35
-30
-25
-20
-15
-10
-5
0
log10(P(S2) (atm)
log10(P(O2) (atm)

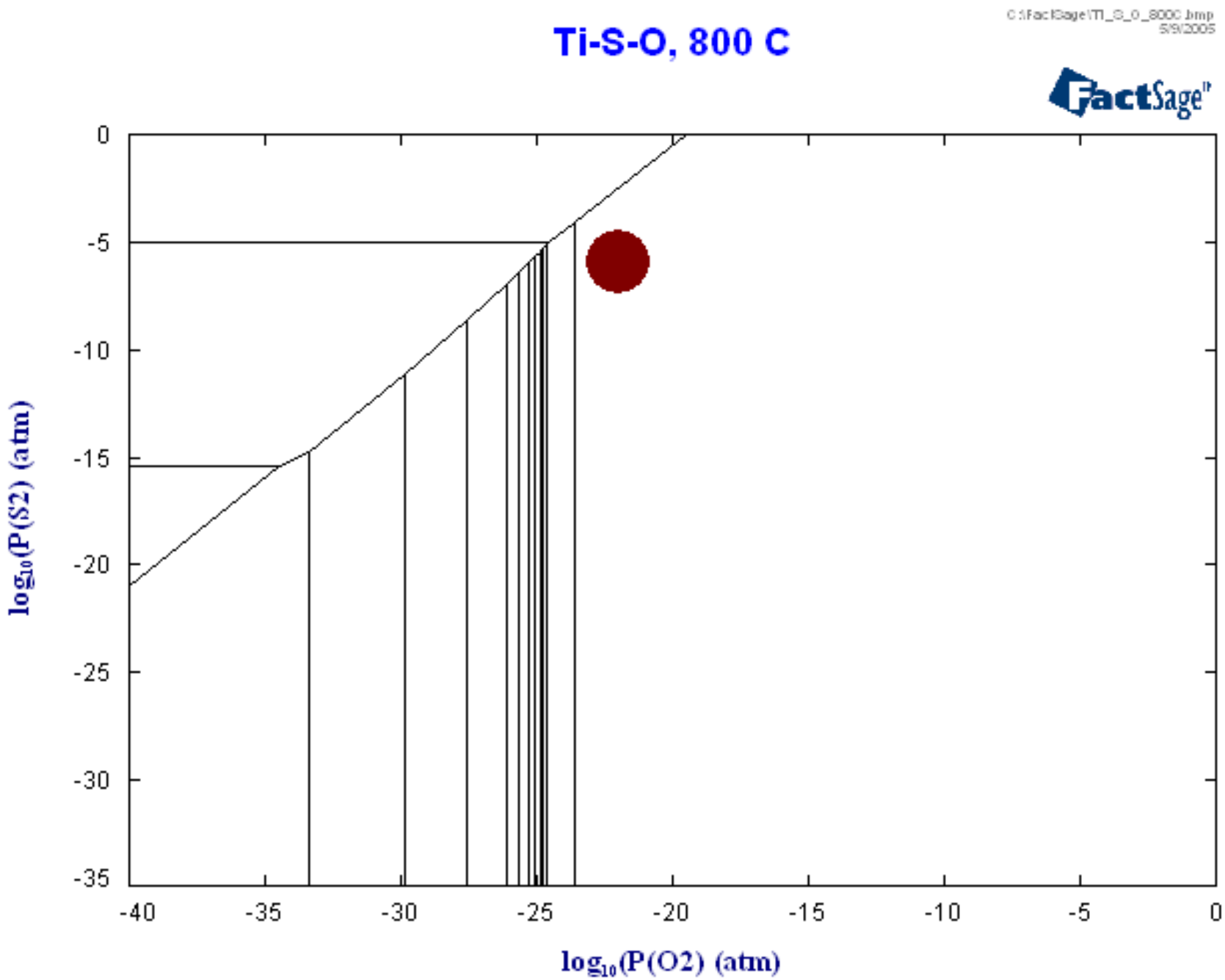
C:\FactSage\Ti_S_O_8000.Jmp
5/9/2005
Ti-S-O, 800 C
FactSage
0
-5
-10
-15
-20
-25
-30
-35
-40
-35
-30
-25
-20
-15
-10
-5
0
log10(P(S2) (atm)
log10(P(O2) (atm)

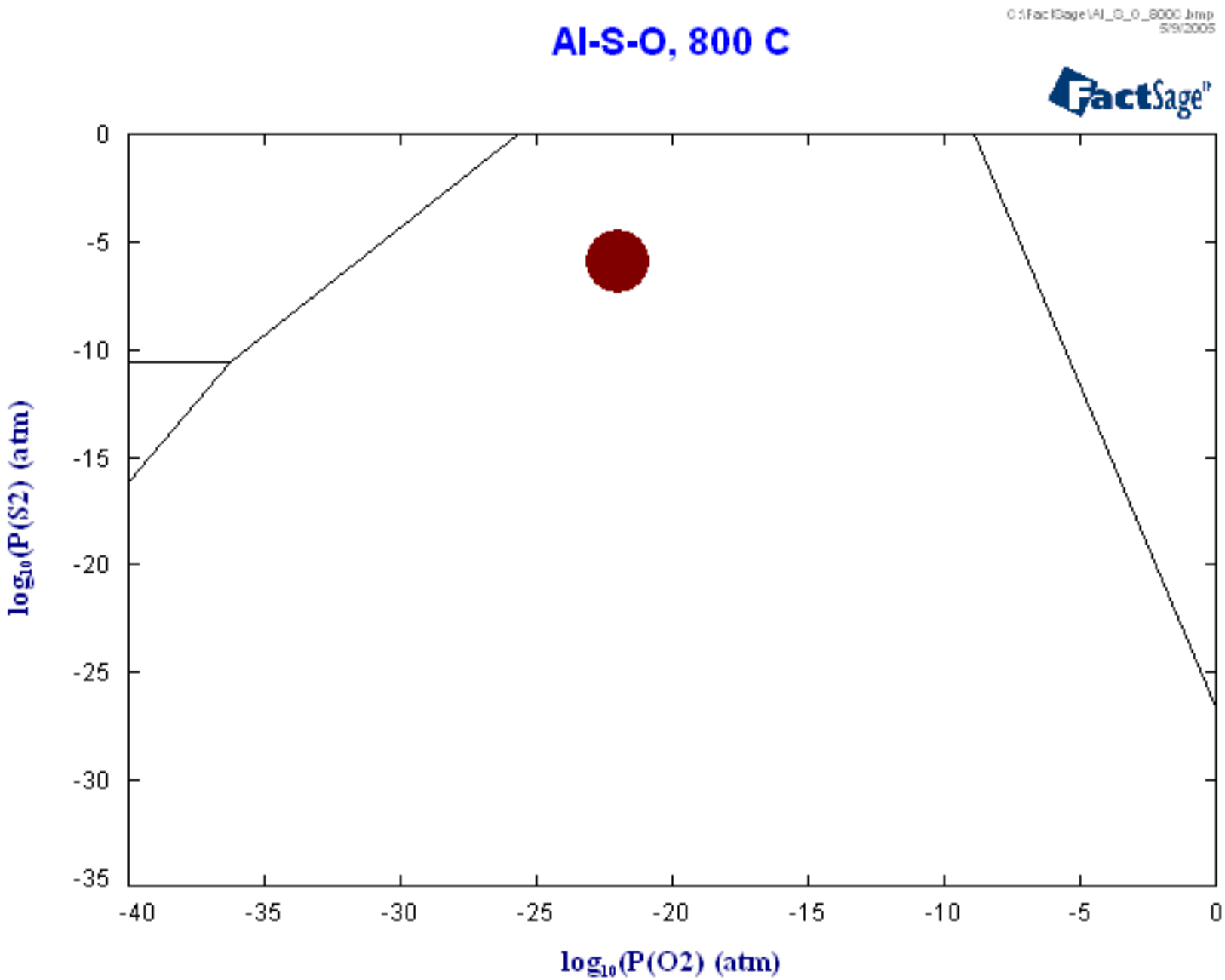
C:\FactSage\Al_S_O_800C.bmp
5/9/2005
Al-S-O, 800 C
FactSage
0
-5
-10
-15
-20
-25
-30
-35
-40
-35
-30
-25
-20
-15
-10
-5
0
log10(P(S2) (atm)
log10(P(O2) (atm)

Albany Research Center

Solutions that make the Nation's energy systems safe, efficient and secure

Improved Refractories for Slagging Gasifiers in IGCC Power Systems

19th Annual Fossil Energy Materials Conference – Knoxville, TN

Associate Research Director –
Cindy Powell

Researchers –
James Bennett, Rick Krabbe, Jasper Kwong, Hugh Thomas

U.S. DOE – Albany Research Center
Office of Materials Performance
1450 Queen Ave. SW
Albany, OR, USA 97321

Phone: 541-967-5983
Fax: 541-967-5845
E-Mail: jbennett@alrc.doe.gov

Program Review Outline

- Background/Issues
- Program Objectives/Goals
- Chrome Oxide Refractory Development
- No/Low-chrome Oxide Refractory Development
- Summary
- Acknowledgements

Integrated Gasification Combined Cycle (IGCC) System

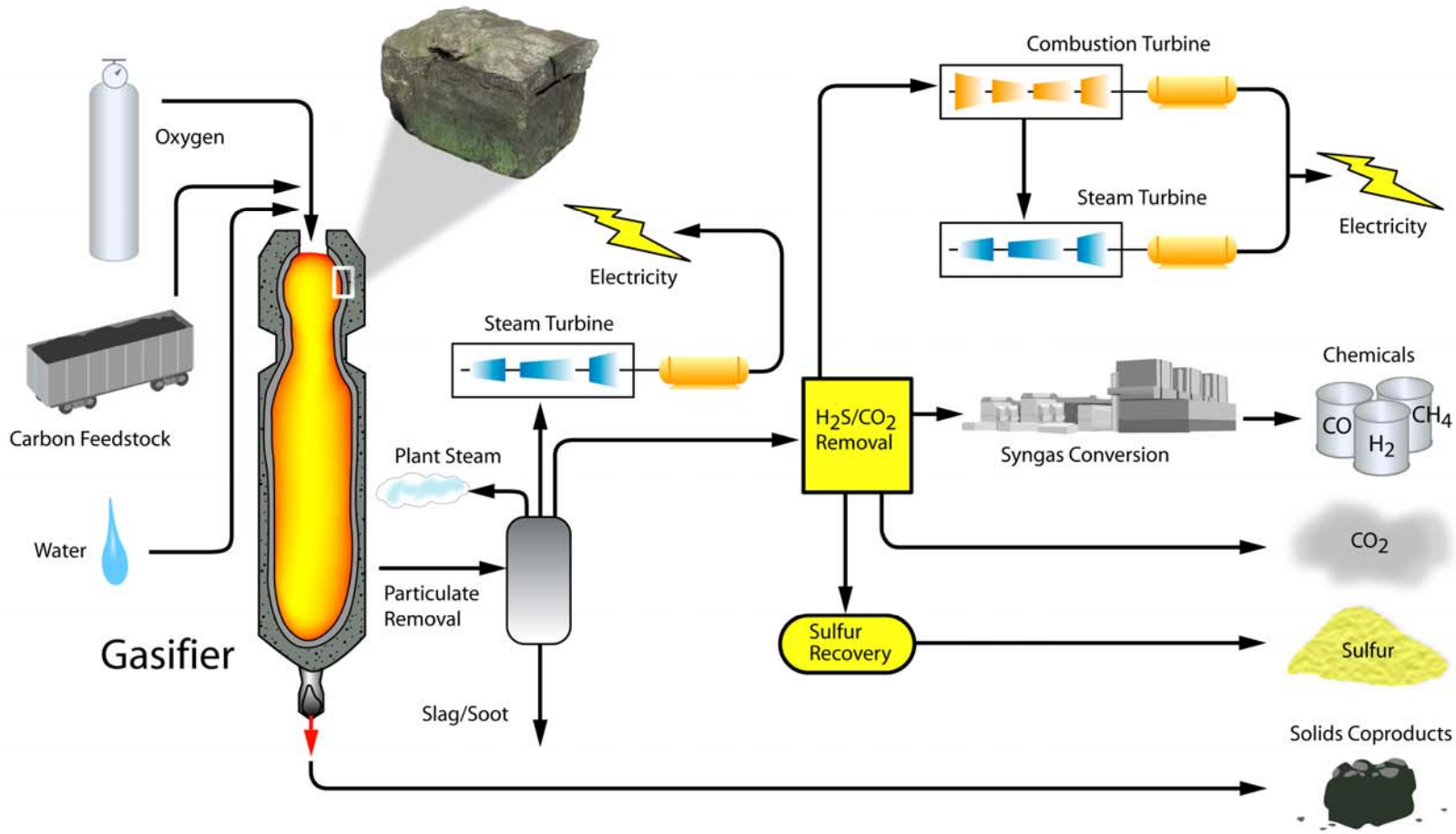

Material Challenges Inherent to Slagging Gasifier Technology

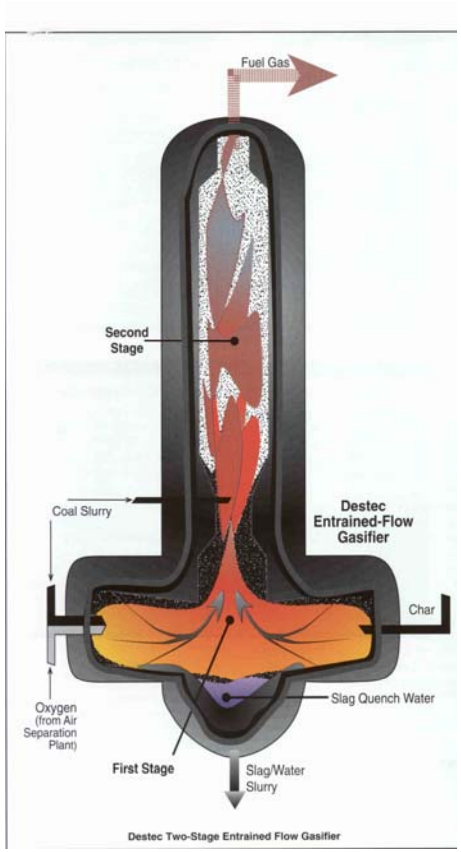

- Operating Temperatures of 1325° to 1575°C
- Thermal Cycling
- Alternating Reducing and Oxidizing Environment
- Corrosive Slags of Variable Chemistry
- Corrosive Gases
- Pressures ≥ 400 psi

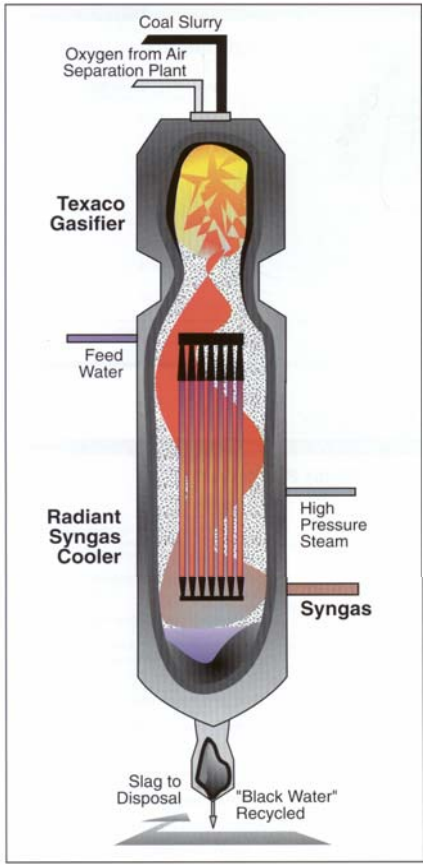

Gasifier Containment Strategy

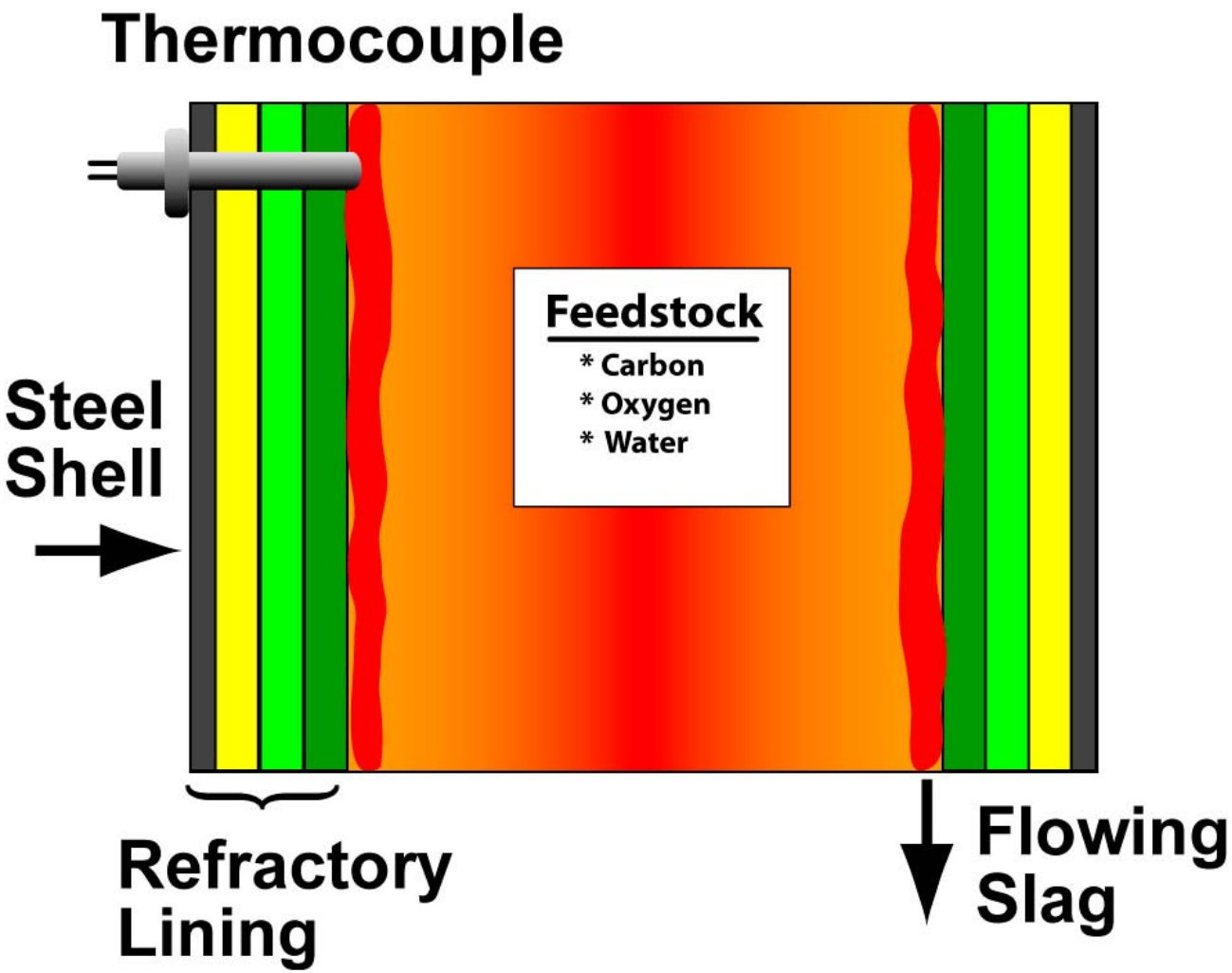

Refractory Material Issues

- Slagging Gasifiers -

Gasifier users identified refractory service life as ***the*** most important limitation to on-line availability

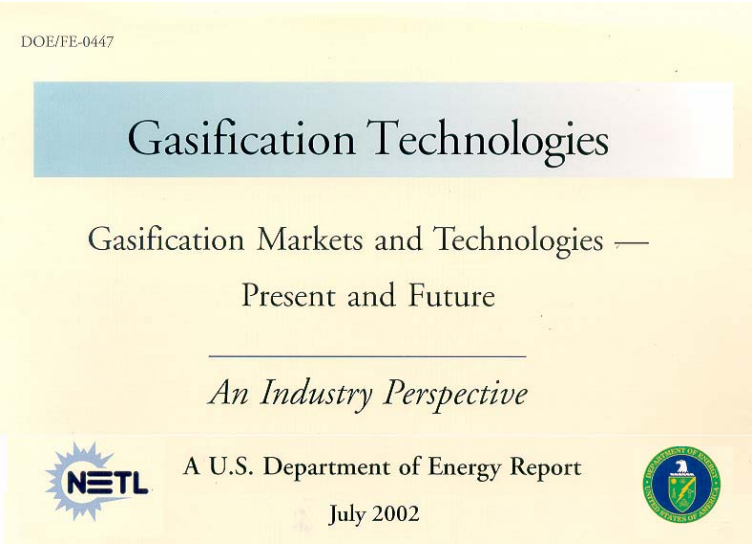
DOE/FE-0447

Gasification Technologies

Gasification Markets and Technologies —
Present and Future

An Industry Perspective

A U.S. Department of Energy Report

July 2002

Gasifier Refractory Liner

Current “best” refractories last 3 to 24 months, with a replacement cost of up to $1,000,000 and 2-3 weeks downtime.

Material Issues - Consequences

1. Low system reliability, on-line availability
   - *gasifier down as frequently as once/month*
2. Lost opportunity costs
3. Lack of temperature control
4. Frequent maintenance/high costs
5. High material repair costs
   – *up to $1 million for refractory lining*
6. Excessive safety margins

Material Needs – Program Objectives

Develop new/improved performance materials with:

1. **Enhanced resistance to slag penetration**
2. **Corrosion resistance to molten slag**
3. **Resistance to thermal cycling**
4. Creep (load bearing) stability
5. Corrosion resistance to hot gasses
6. Hot abrasion resistance
7. Stability in oxidizing/reducing environments

Project Goal

Enhance gasifier reliability and economics through the development of improved refractory materials with a longer service life – *target is 50 pct improvement.*

Researching two refractory systems:

1. *High-chrome oxide refractory materials*
2. *No/low chrome oxide refractory materials*

1. Improving the Service Life/Developing New High-Chrome Oxide Refractories

Research To Date

- *Post-mortem* evaluation of spent materials identified failure mechanisms.
- Engineered new material capable of resisting slag penetration failure, tested in laboratory (*developed and patented phosphate containing high chrome oxide refractory)*
- Worked with industrial cooperator for commercial scale-up of phosphate containing refractory
- Phosphate containing refractory undergoing pilot plant testing in a commercial gasifier

Phosphate Containing High Cr_2O_3 Refractory Commercially Manufactured for Plant Trials

Causes of Refractory Wear

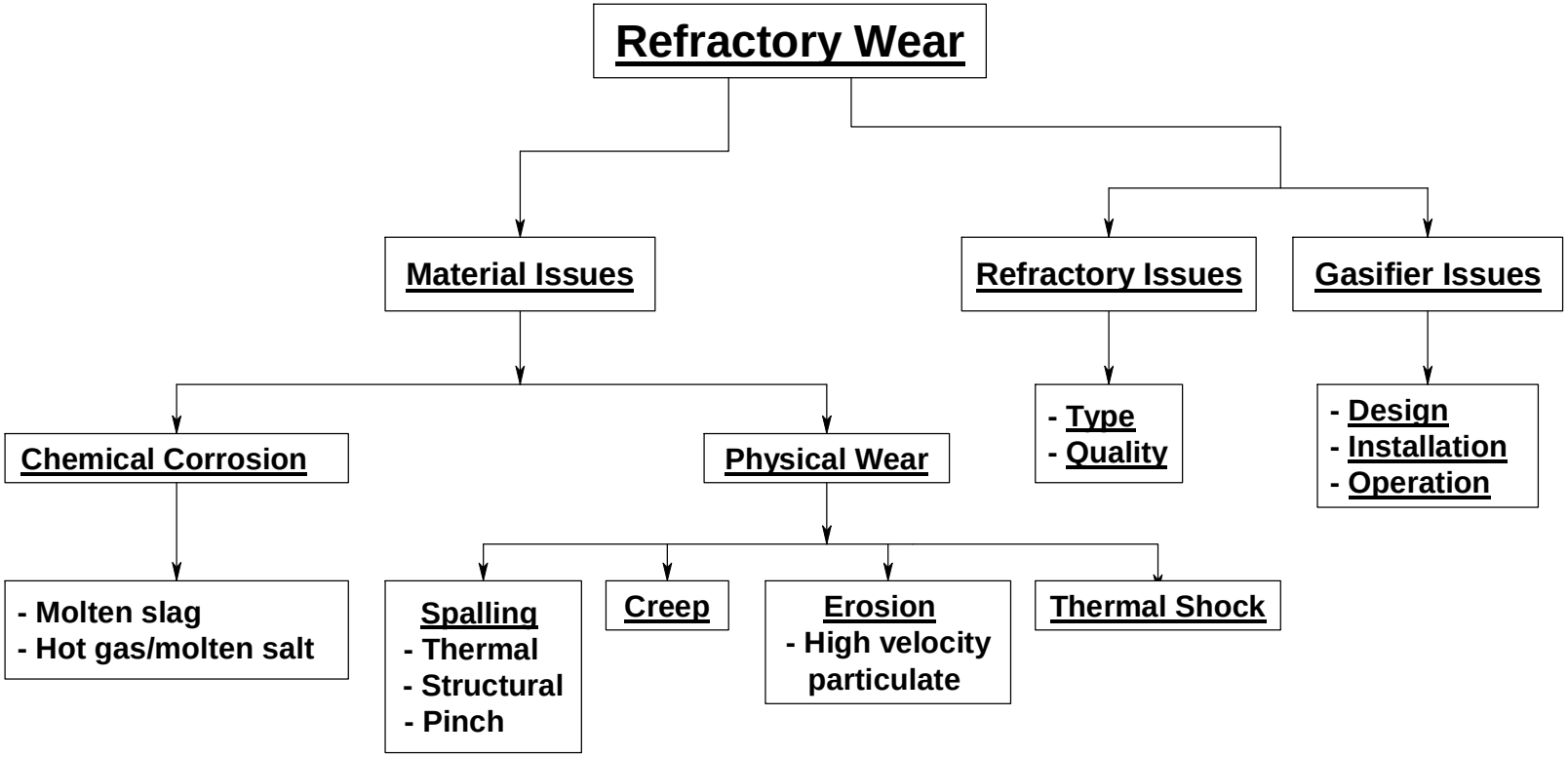

Phosphate Containing Test Panels in Gasifier Service *(coal feedstock)*

Lower Cone – 17 Days

Sidewall – 100 + Days

Coal/Petcoke/Coal-petcoke Refractory Testing

- Gasifier operators have not seen any refractory service life differences caused by petcoke or coal slags
- Laboratory testing has not shown any difference between petcoke and coal slags
- Decision jointly made between Harbison and ARC to evaluate the current phosphate containing high chrome oxide refractory in petcoke/coal-petcoke gasifier slags

Current/Scheduled Test Panels

Coal

- Eastman – Lower cone (17 days)
  - Sidewall panel (100 days +)
  - 2nd lower cone fabricated, waiting installation

Coal/Petroleum Coke

- TAMPA Power and Electric (TECO) – Throat area planned

Petroleum Coke

- Wabash – Sidewall panel installed, waiting gasifier start
- Coffeyville – Discussions underway, lower cone

2. Developing No/Low-chrome Oxide Refractory Materials

Slagging Gasifier Refractory Materials

- Early material evaluation
  - mid 70's to late 80's
  - DOE, EPRI, industry driven
  - evaluated high Al_2O_3, SiC, Si_3N_4,Cr_2O_3, ……. fused cast and sintered shapes
  - high Cr_2O_3 refractory materials identified as best
- Current refractory liners *(60 to 90 pct Cr_2O_3)*
  - High chrome/alumina
  - High chrome/alumina/zirconia
  - Chrome/magnesia (historical)

- Material Issue -

Chrome Oxide is the Main Component of Refractory Liners (60 to 90 pct)

<u>However - High Cr_2O_3 refractories:</u>

- have not met the service life requirements
- have a high cost
- are difficult to produce
- have a high density (impact material weight, size, number joints)
- have possible long-term supply issues
- have perceived/real safety concerns
- limit gasifier repair, turnaround speed
- each material has a unique failure mechanism – greater zoning may be needed

Project Research Goal

- Enhance gasifier reliability and economics through the development of improved refractory materials with longer service life that eliminate or minimize the use of chrome oxide

Intelligent Materials Design

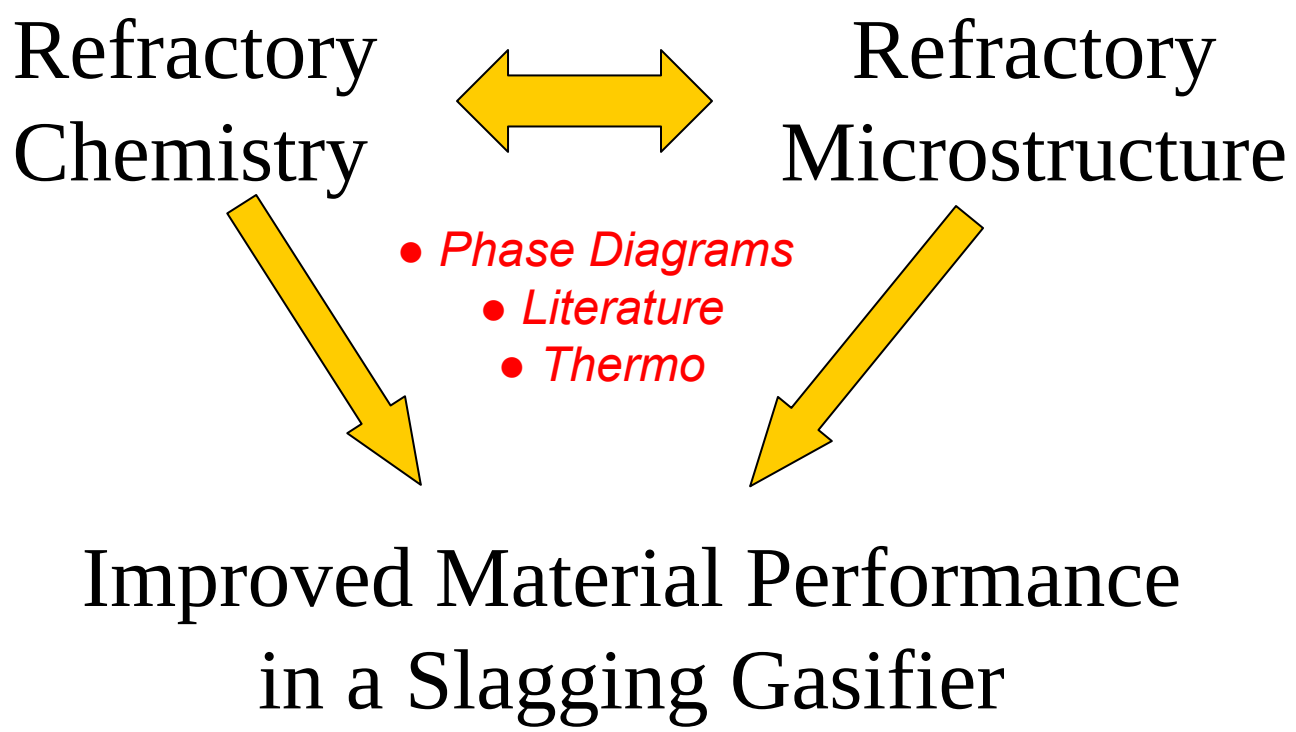

Technical Difficulties - New Refractory Material Development

- only so many materials exist suitable for use in severe service environments
- difficult to get new materials commercially
- difficult to make new refractories
- unique testing often required

No-chrome/Low-chrome Oxide Refractory Development

- Identifying potential no-chrome/low-chrome materials for lab testing
- Lab tests (*small and large cup, rotary slag*) to evaluate critical properties developed
- Test samples of first generation refractory materials being evaluated
- Limited laboratory testing underway

Small Scale Cup Test Evaluation of Alternative Materials

<u>Type Materials Evaluated</u>

- ZrO_2, Al_2O_3, TiO_2, MgO, SiO_2, CaO, SrO, phosphates
- Mixtures to form new systems for refractory testing
- Low Cr_2O_3 materials

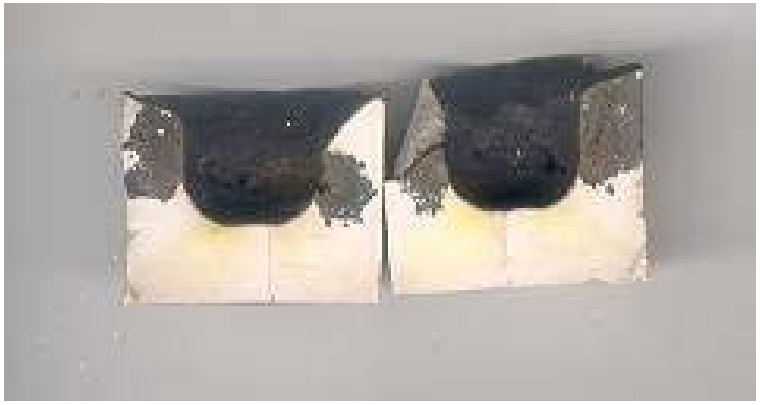

Engineered Refractory Systems: Chemistry + Microstructure Selection/Control

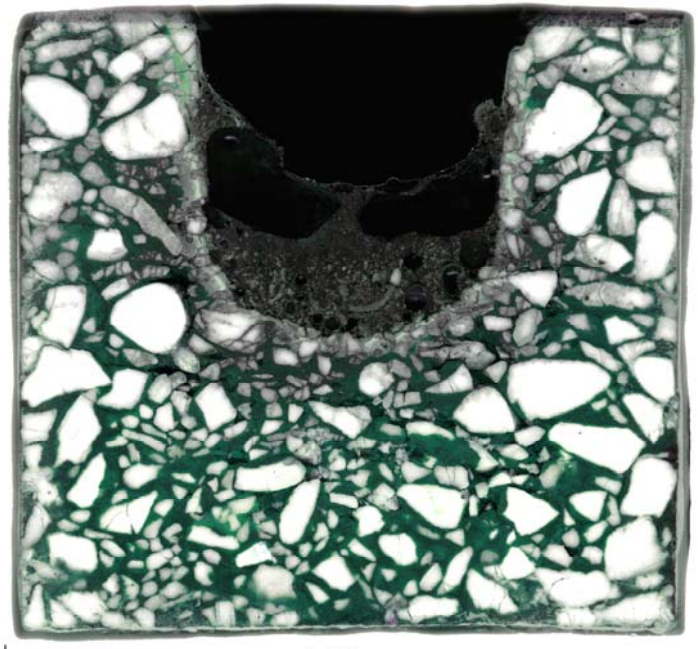

10 mm

(C)

In static cup tests, some compositions look promising, but more rigorous, dynamic rotary slag testing is needed.

Dynamic Laboratory Testing Necessary

Static test result suggests excellent slag resistance…

But dynamic tests indicate performance issues

Dynamic Laboratory Tests

90% Chromia//10% Alumina - no measurable wear

Spinel: > 20% wear

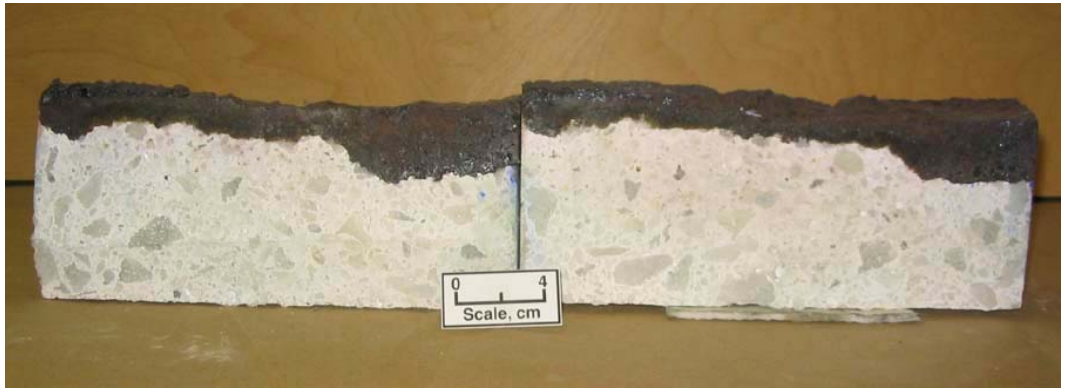

Summary

- Current goals/milestones are met
- Major wear mechanisms identified through post-mortem analysis – used to engineer new/improved refractory liner materials for gasifier applications
- ARC has developed and patented a phosphate-modified chromium oxide refractory, currently undergoing field trials

Summary

- Alternatives to chromium oxide are needed
- New chrome-free and low-chrome engineered refractories are currently undergoing laboratory tests. Static tests look promising; dynamic tests ???

Acknowledgements

- Fossil Energy - USDOE
  - Advanced Research – Materials
  - Advanced Gasification Technologies
- Albany Research Center - USDOE
  - Advanced Metallurgical Processes
- Cooperators
  - Eastman Chemical Co.
  - Conoco-Phillips
  - Tampa Electric Co.
- Three refractory companies

  (one chrome, two non-chrome)

CORROSION RESISTANT CERAMIC COATINGS

Beth L. Armstrong, Glen H. Kirby, Kevin M. Cooley, and H.T. Lin
Oak Ridge National Laboratory

in collaboration with

Jasper (Kyei) Kwong and Cynthia Powell
Albany Research Center

19TH Annual Conference on Fossil Energy Materials
Knoxville, Tennessee
Tuesday May 10, 2005

Outline

- Background: Advanced ceramics for fossil energy applications
- Problem: Limitations of ceramics in aggressive environments
- Objective: Develop & fabricate low-cost protective coatings
- Slurry processing of protective coating materials
  - Review
  - Progress
- Research Highlights
- Future Research
- Acknowledgements

Advanced Ceramics for Fossil Energy Applications

- **Temperatures up to 1550 ^{o}C**

- **Aggressive species include:**
  - **Sulfur**
  - **Nitrogen**
  - **Trace heavy metals**
  - **Alkali salts**
  - **Steam**
  - **Molten slag**

- **Ceramics have many attractive features for use in such environments, e.g., high temperature strength**

- **The efforts in this project are aimed at developing a cost effective process for applying potentially corrosion resistant coatings**

Are Protective Coatings Necessary?

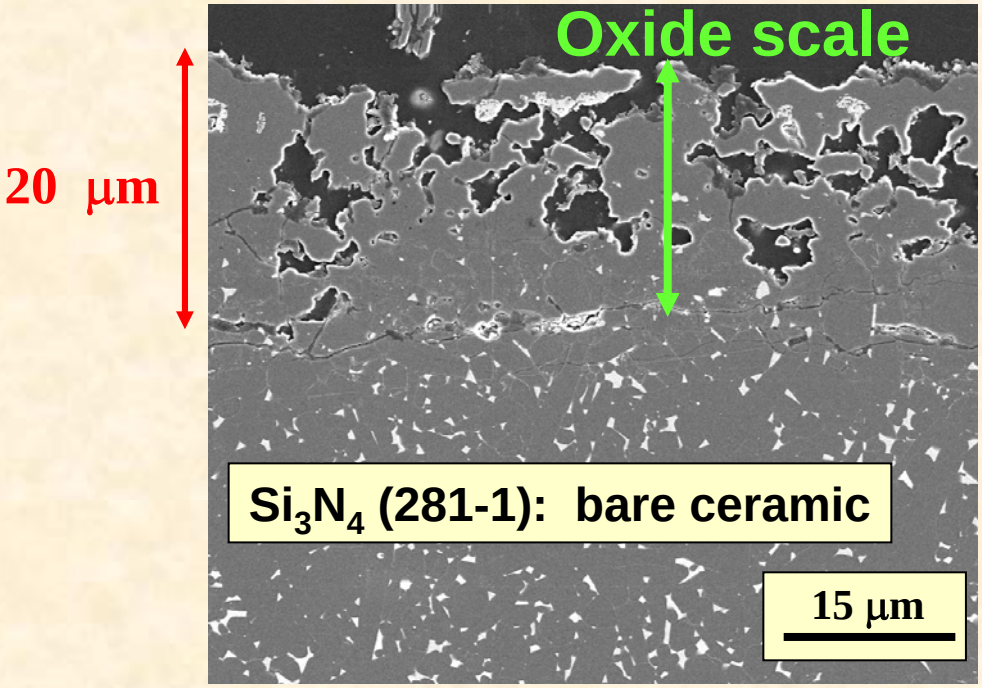

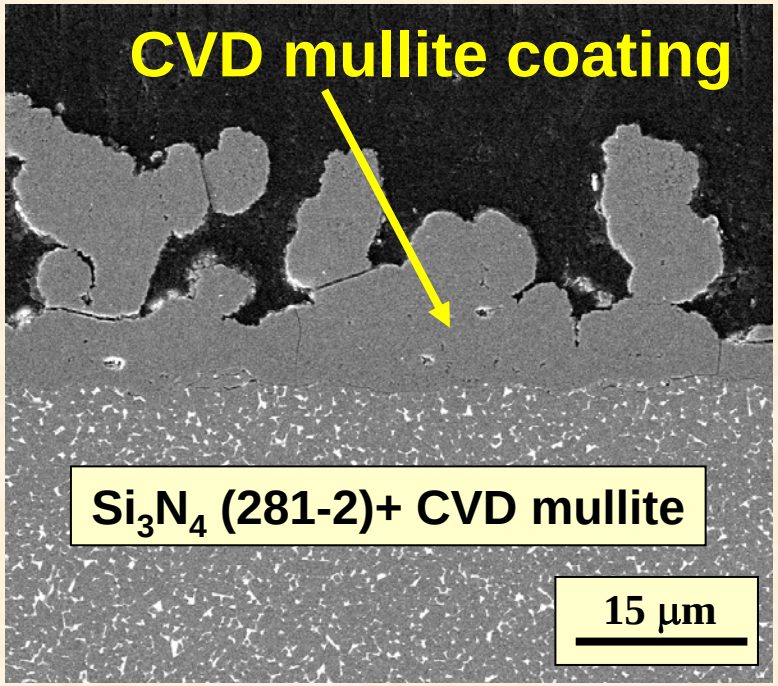

500-h, 1200°C, 10 atm, 15% H_2O

- **Protective coatings will be necessary to provide adequate ceramic component lifetimes.**
- **Coatings must be adherent, stable and protective in high temperature water vapor, thermal expansion matched with SiC or Si_3N_4, easy to manufacture, and cost effective.**

* Micrographs courtesy of J.A. Haynes/Oak Ridge National Laboratory

Yet More Evidence…

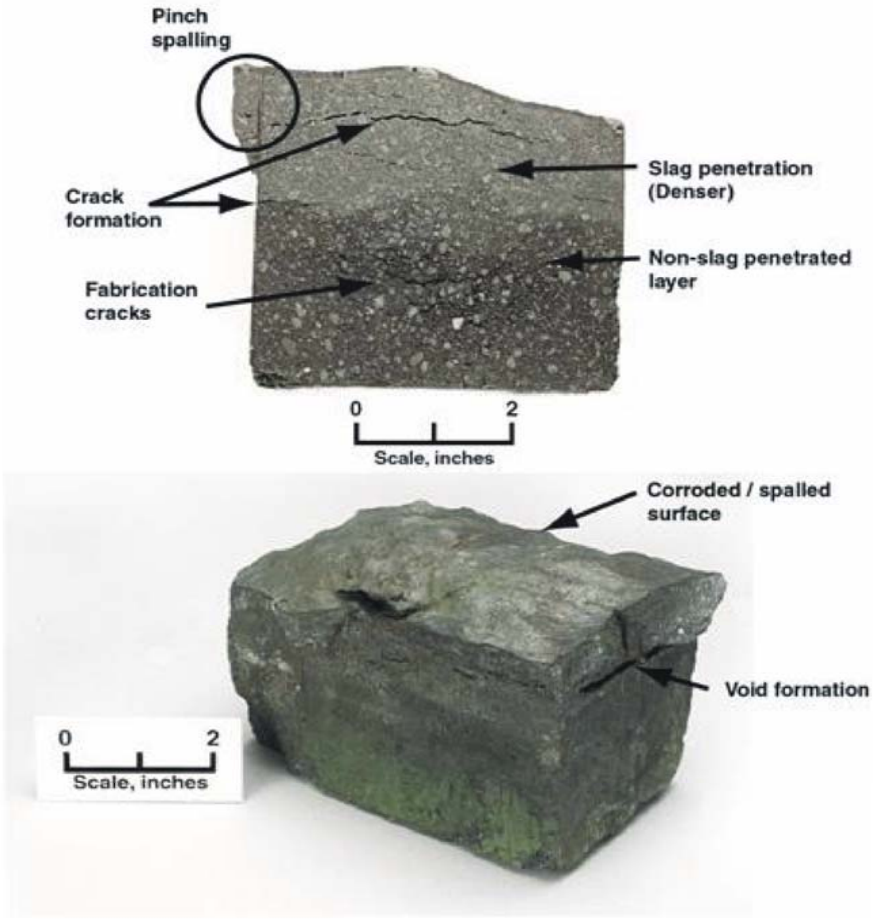

* Photo courtesy of K. Kwong/Albany Research Center

Objectives

- **Develop low cost coatings for protection of corrosion and/or environmentally sensitive ceramic substrates.**
  - **Dip coating (aqueous, slurry based) selected as process**
  - **Work focused on two systems: silica formers and non-silica formers (refractory brick)**
    - **SiC (Hexaloy) as substrate and mullite (Baikowski MuLCR) as coating system for demonstration**
    - **Commercial and Albany Research Center (ARC) refractory systems as substrate and coatings**

Key Issues

- **Demonstration of basic principles developed last year**
- **Collaboration with ARC to ensure scaleability and commercial issues addressed**

FY 2004 Accomplishments

- Demonstrated feasibility and flexibility of process
- Established "generic" process parameters
- Reduced sintering temperatures to minimize damage to substrate

Rare earth silicate coating on a complex-shaped component (NT154 Si_3N_4 Blade)

- The process is flexible, i.e., it can be modified to incorporate a wide range of ceramic particles (e.g., mullite, BSAS, zirconia, rare-earth silicates and disilicates, aluminates, and aluminosilicates) and solvents (e.g., aqueous and organic)
  - Complex-shaped components to be coated are dipped into a slurry (ceramic particles suspended in a solvent medium).
  - As-dipped coatings are dried and heat treated at elevated temperatures to promote densification
  - Can be used as a patch for damaged coatings
  - Resultant coating quality depends upon slurry rheology and wetting behavior

Silica Formers

Putting Scientific Principles to Practice

- **Applied colloidal principles to develop slurry formulation**
  - **Surface Charge (dispersant selection)**
  - **Rheology (flow behavior as a function of dispersant concentration)**
- **Expose mullite coated SASiC substrates to simulated environment**

Tailoring Interactions Between Colloidal Building Blocks

Colloidal particles --> basic "building blocks"

- **must control interparticle forces to tailor structure, rheological properties, and drying**

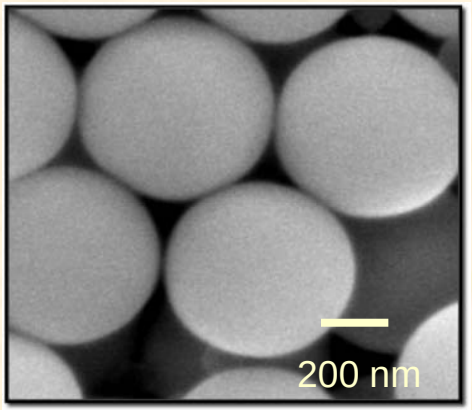

Hard sphere

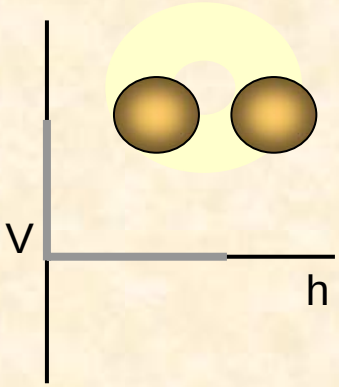

indexed matched
highly screened

Attractive

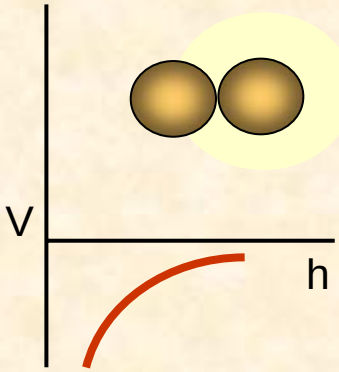

VdW forces
depletion forces

Soft Sphere

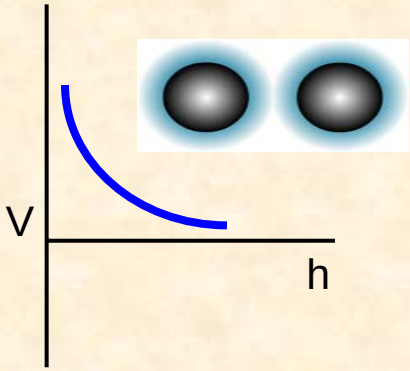

steric-stabilized
charge-stabilized

Flow Behavior of Mullite-PEI Suspensions

(Mullite Suspensions: 45 vol%, pH 7)

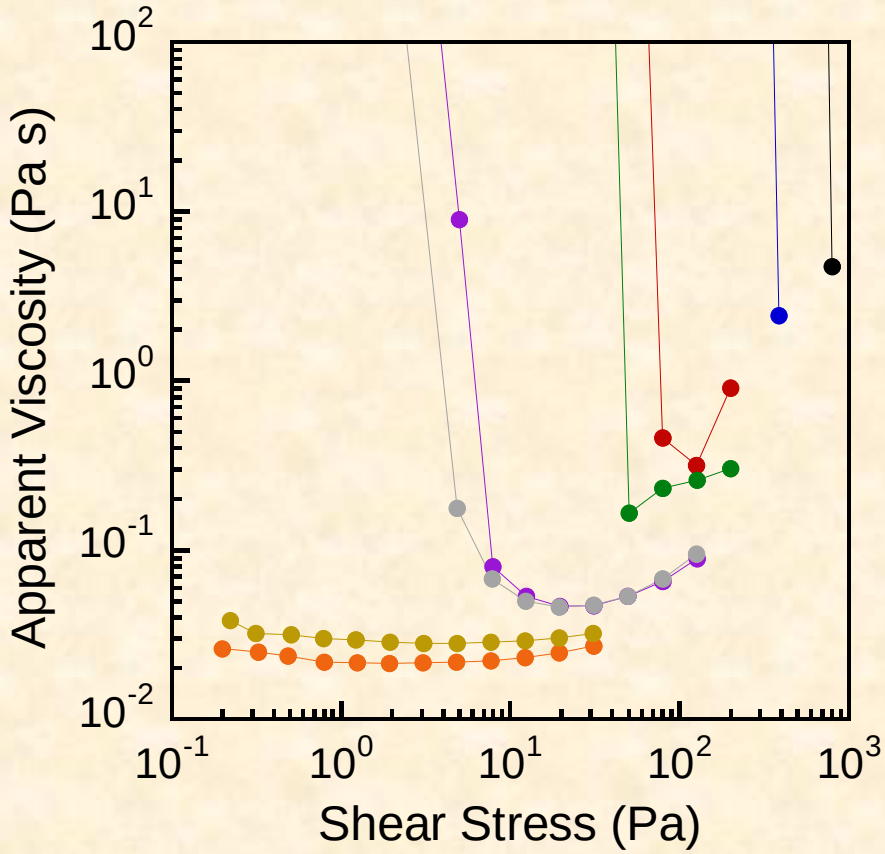

Legend

Varying PEI Addition
(mg PEI/m^2 MulCR)

- 0.125
- 0.135
- 0.15
- 0.1625
- 0.175
- 0.1875
- 0.2
- 0.25

Excellent Coating Precursors!

Resulting Coating Quality Depends Upon Slurry Rheology and Wetting Behavior

Coatings formed by dipping substrates into mullite slurries (45 vol%) of varying PEI Concentration, $[PEI]/[PEI]_{crit}$

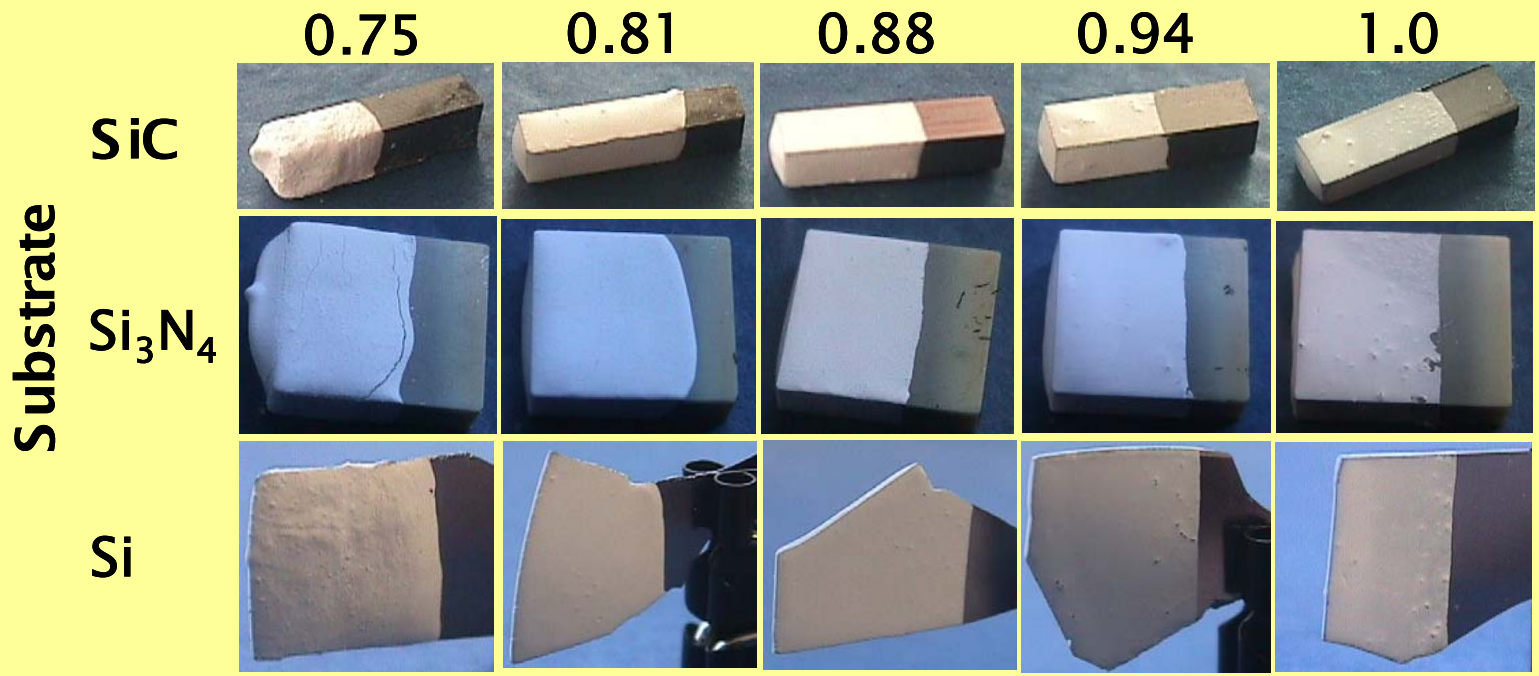

Dense, Uniform Coatings Achieved

Green coating, from
25 vol% mullite suspension

Sintered in air, 1400°C

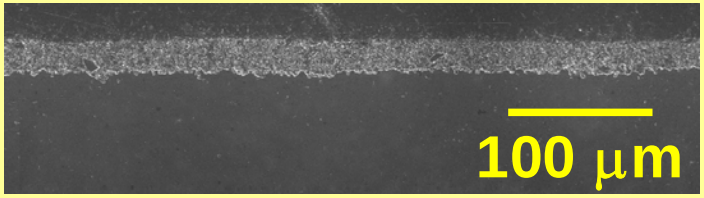

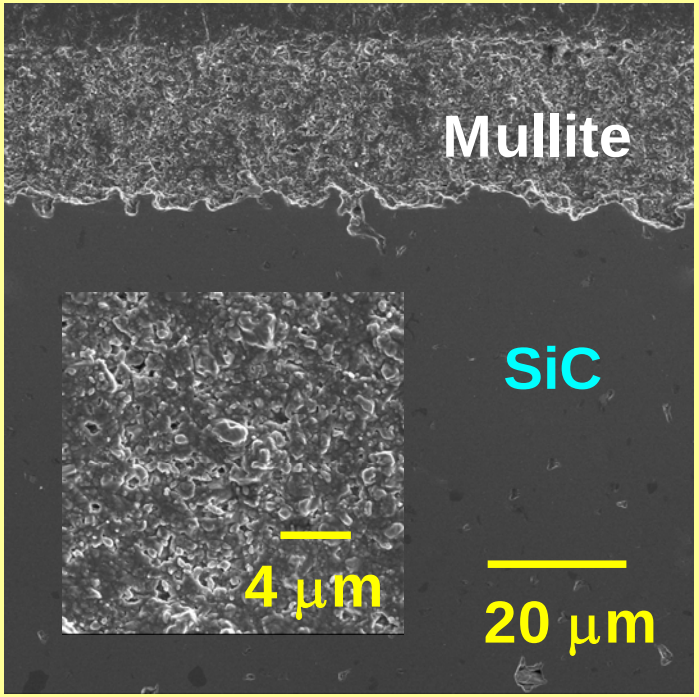

Mullite coating on a silicon carbide substrate

Strength Can Be Influenced by Coating Properties

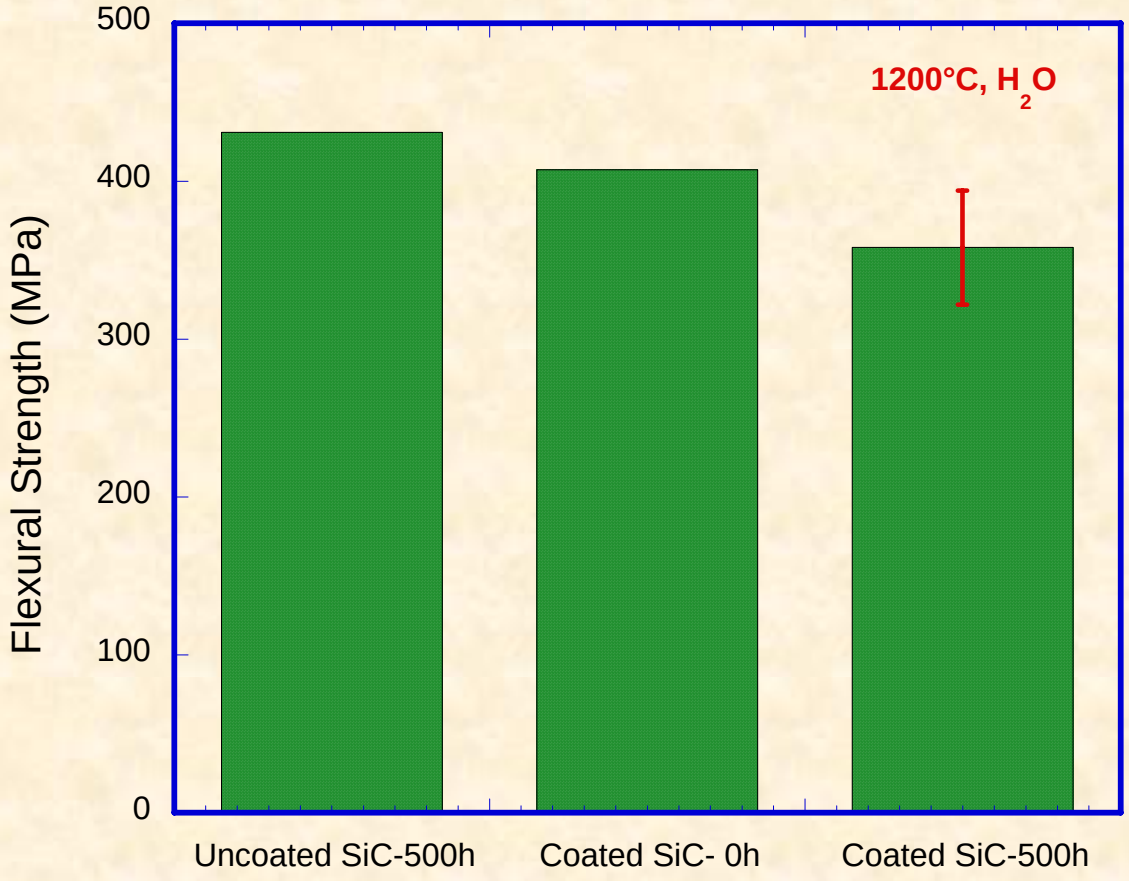

Minor Strength (~10%) Degradation Observed After 500h Steam Exposure at 1200°C

*Not exposed, uncoated SASiC room temperature 4 point bend = 380 MPa

As-Coated Strength Governed by Intrinsic Processing Flaws in SA SiC Substrate

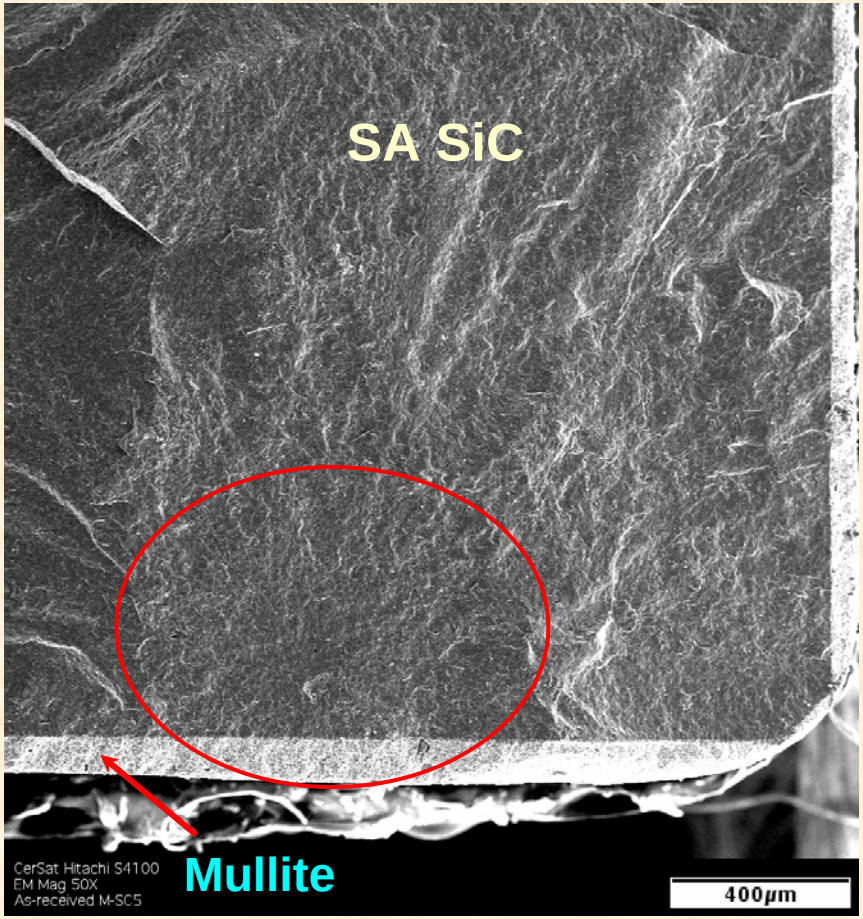

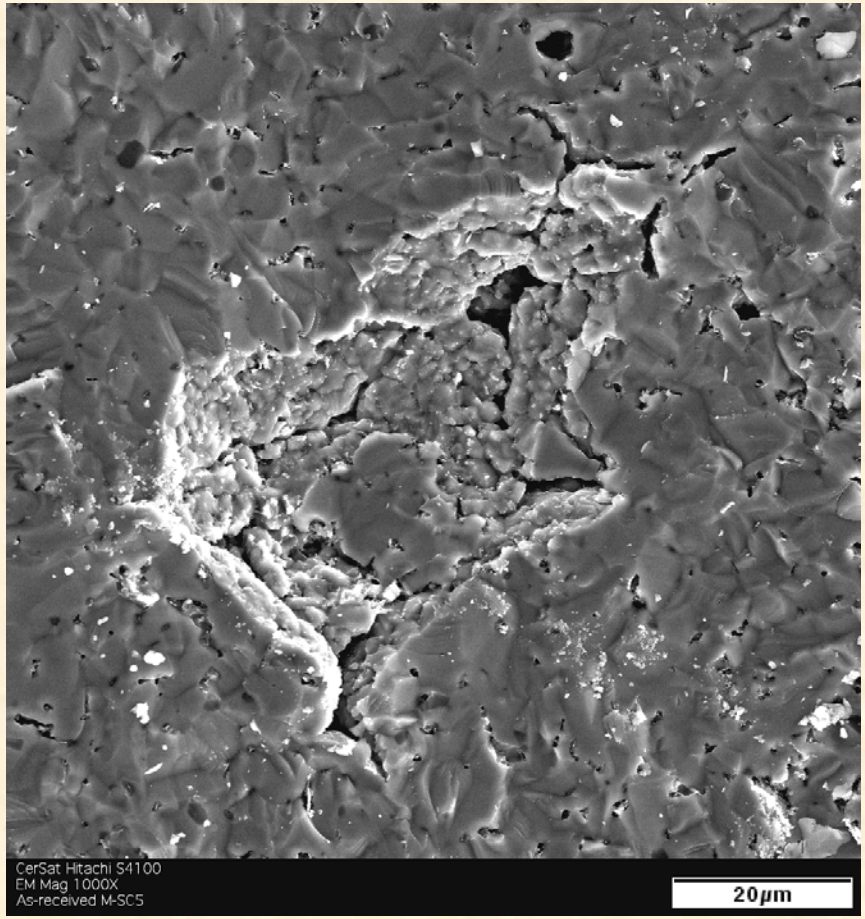

Minor Reaction Occurred Between Mullite and SASiC Substrate During the Sintering

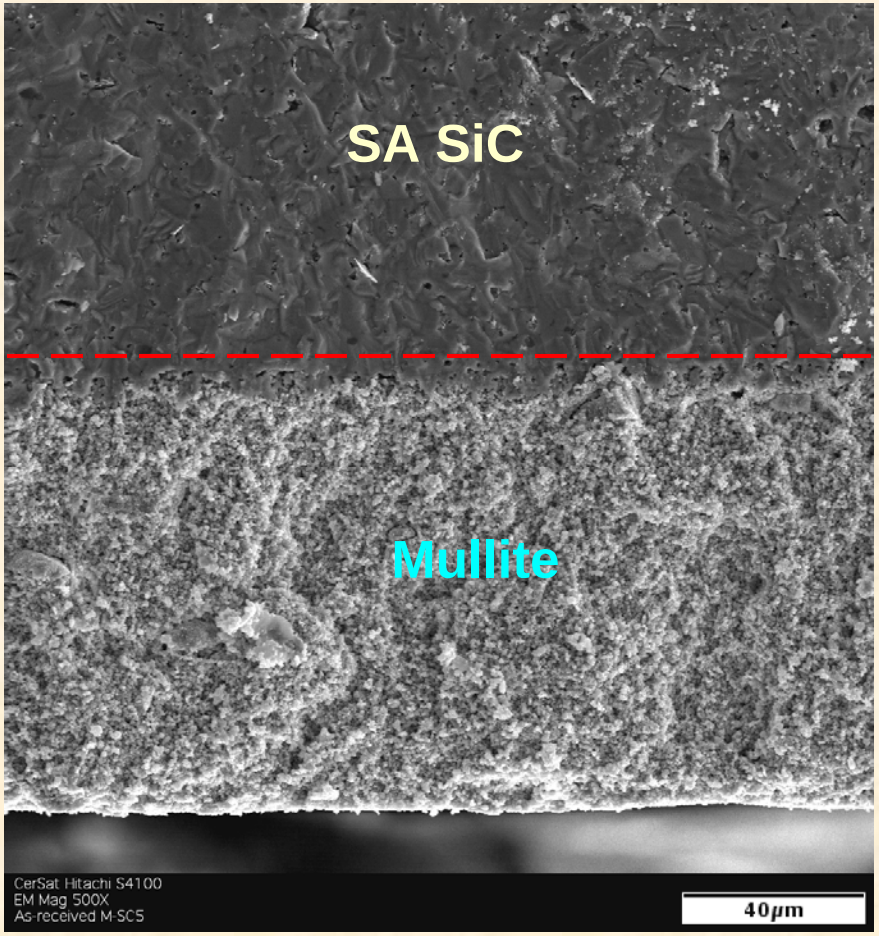

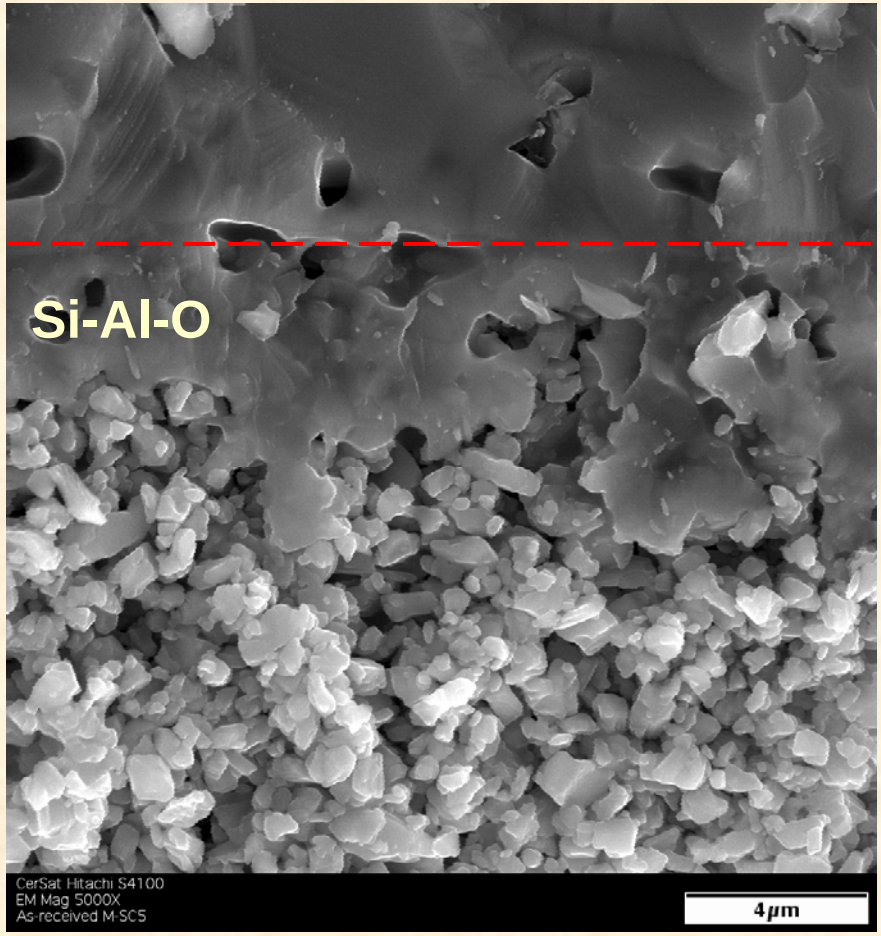

Interaction at the interface promotes adhesion

Strength Degradation Caused by Formation of Porous SiO_2 due to Oxidation of SiC Substrate

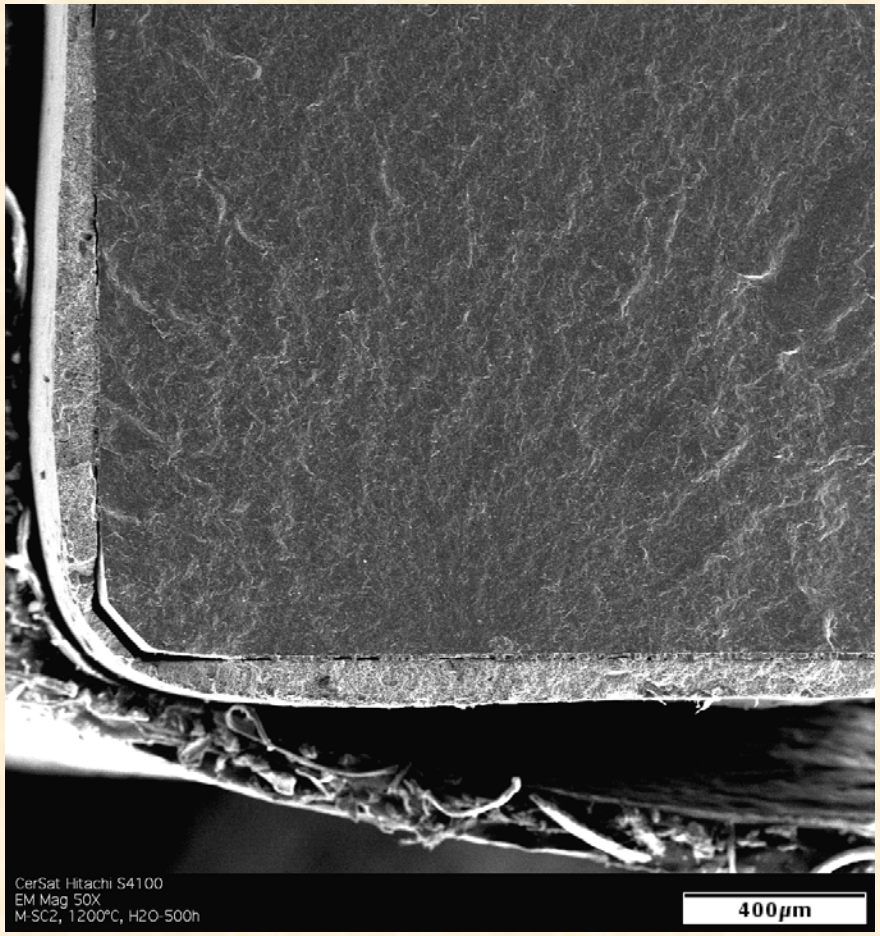

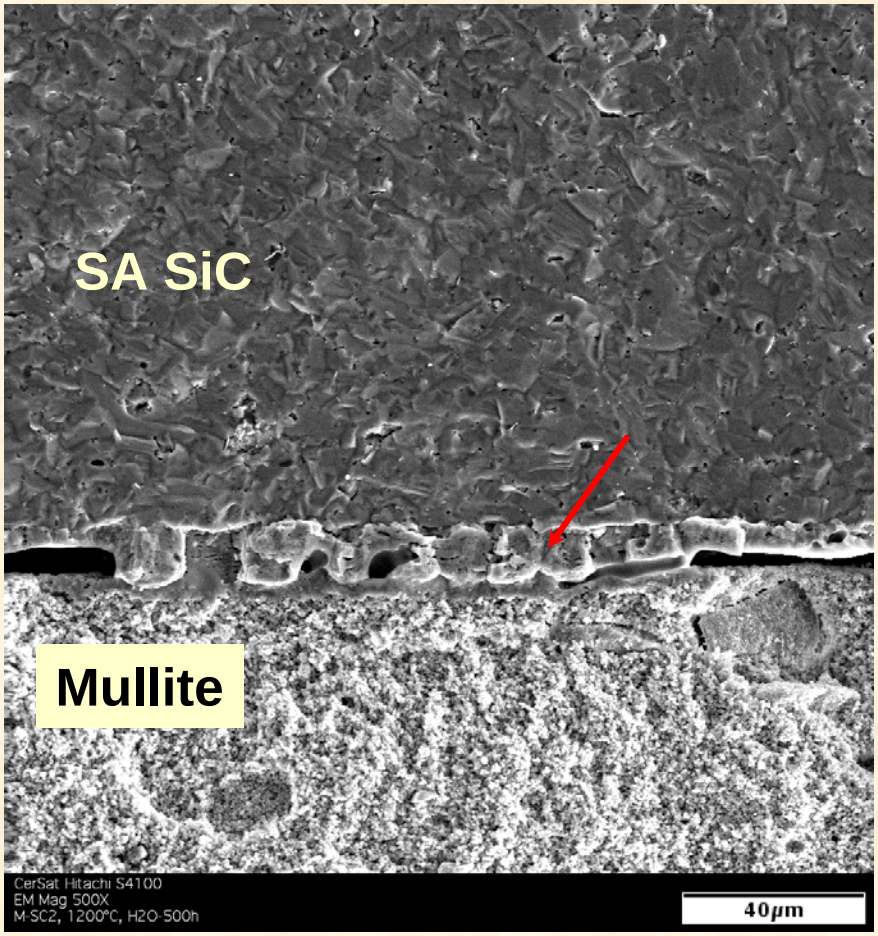

After 500h Steam Exposure Silica Formation Occurs: Conduction of O_2 through Porous Mullite Layer

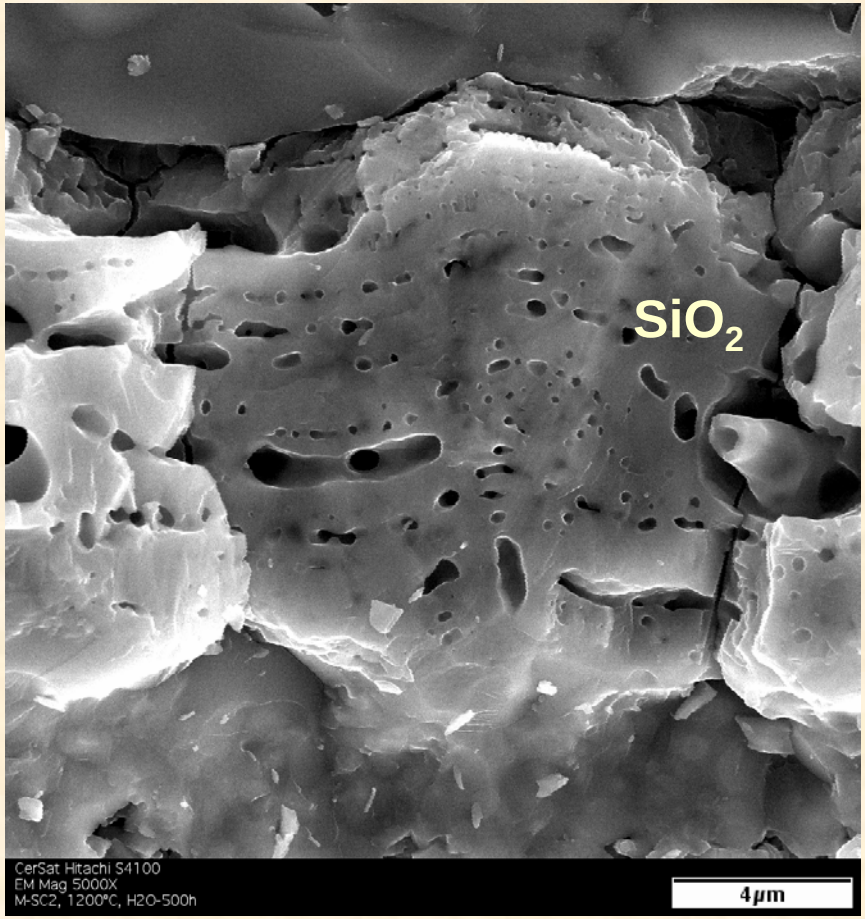

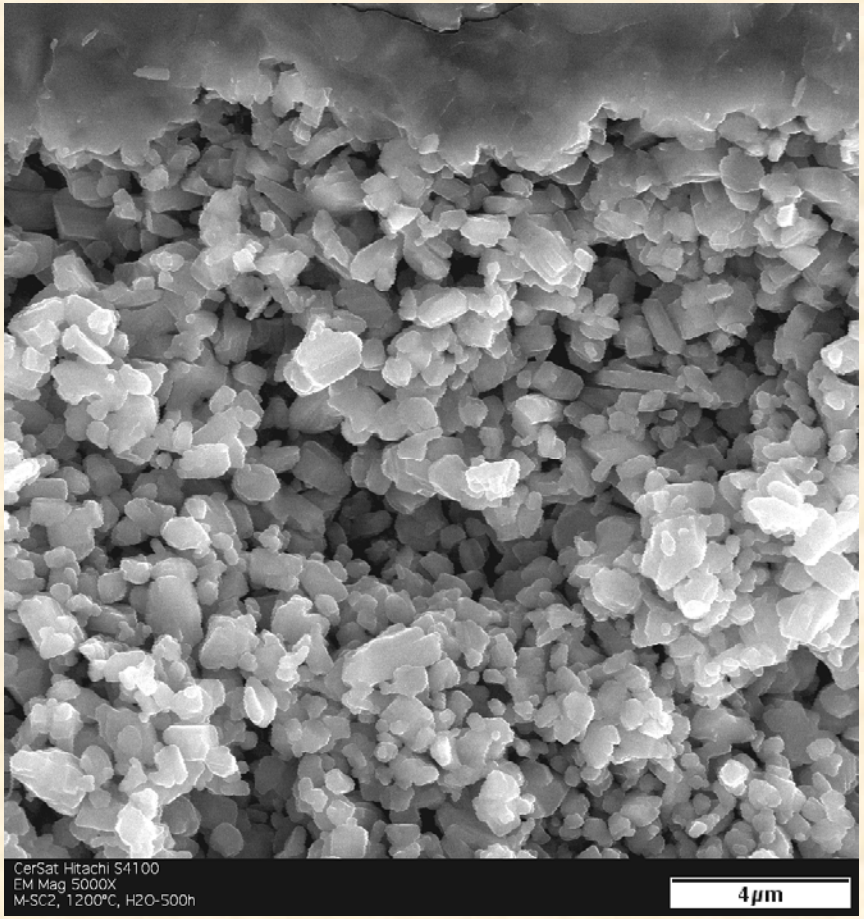

Collaboration with ARC: Refractory Systems

Collaboration Goals

- **Determine if the dip coating process can be applied to refractory brick, i.e., can a dense coating on a porous brick extend the service lifetime of the refractory**
- **Apply colloidal principles to develop slurry formulation for 3 selected commercial and the ARC developed refractory brick systems**
  - **Surface Charge (dispersant selection)**
  - **Rheology (flow behavior as a function of dispersant concentration and solids loading)**
  - **Optimize processing conditions to maximize coating density (sintering)**
  - **Coat test cups for molten slag testing at ARC**

Optimization of Dispersant Concentration and Solids Loading

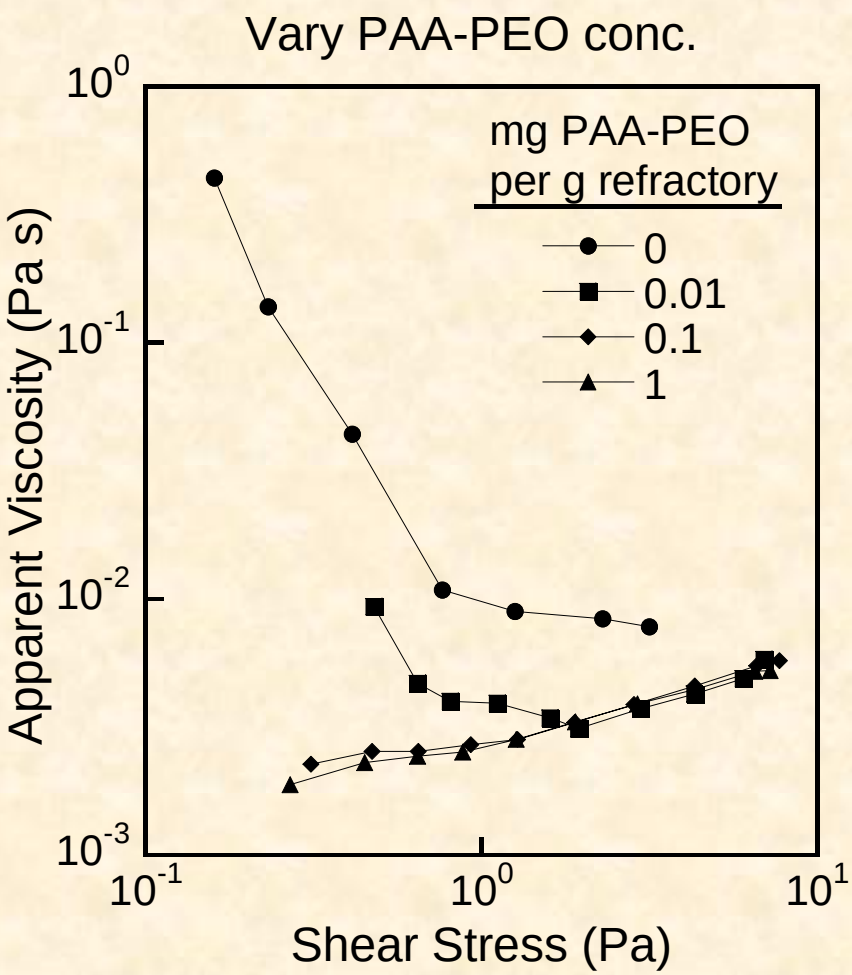

Constant: 20 vol% solids, pH 9

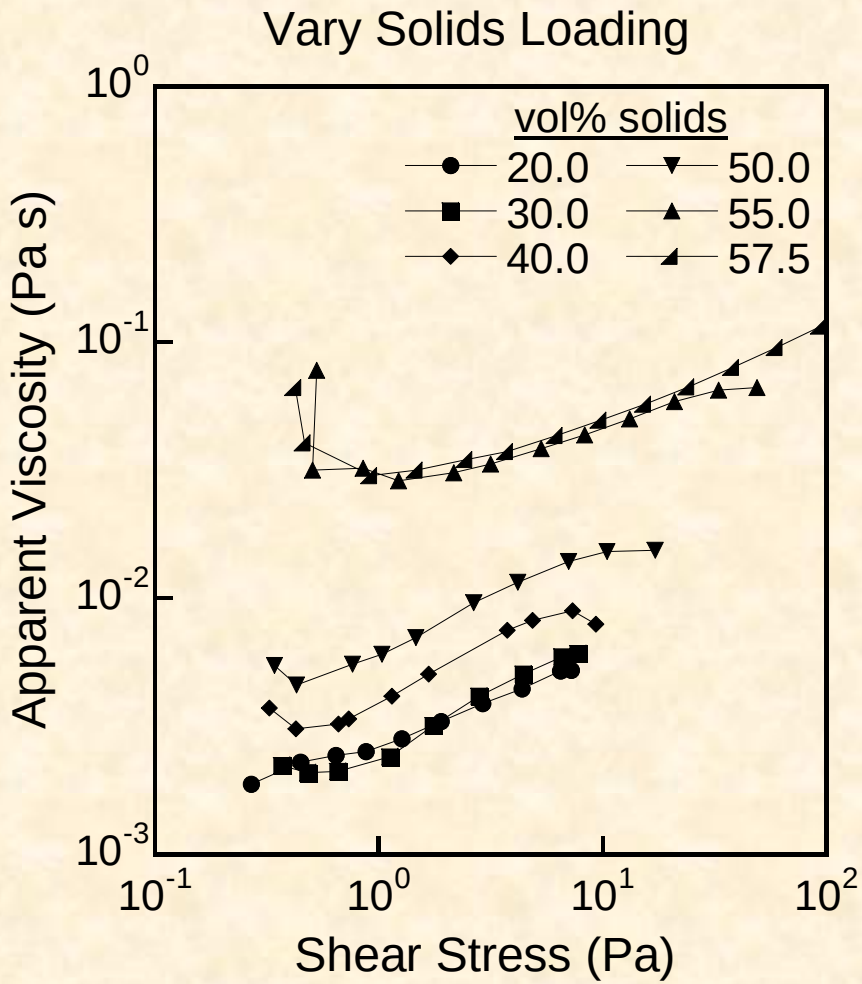

1 mg PAA-PEO per g refractory, pH 9

Rheology Similar for Selected Systems at Optimum Solids Loadings

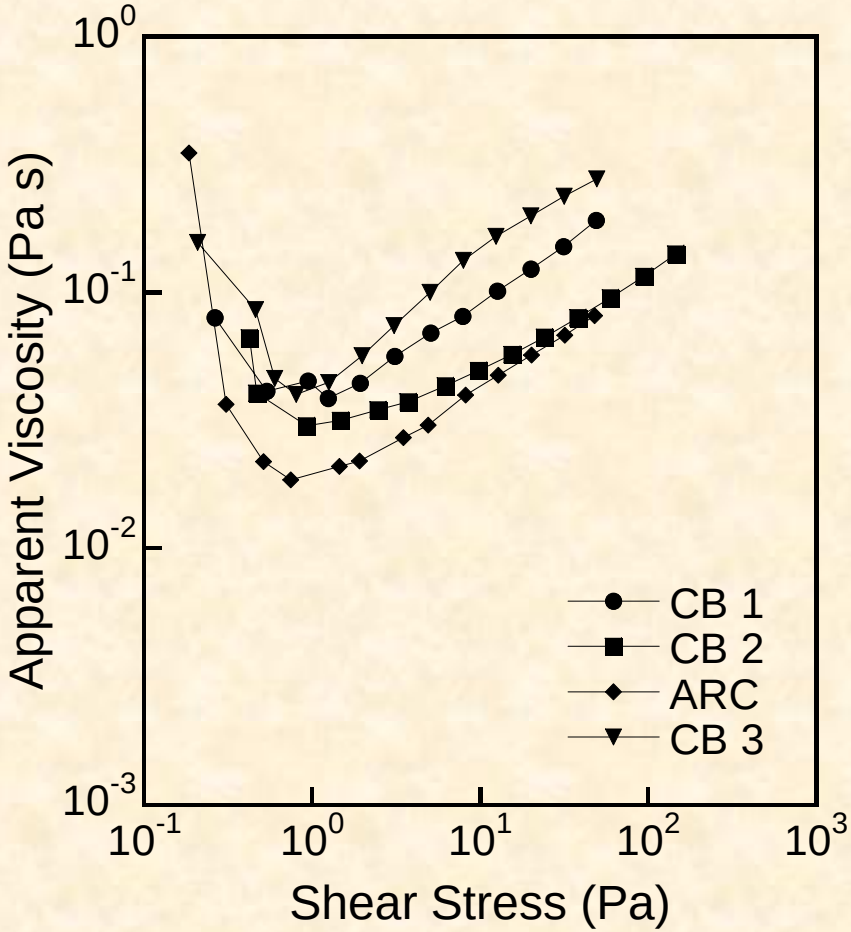

Commerical Brick = CB
ARC Developed Brick = ARC

Constant: 57.5 vol% solids, 1 mg PAA-PEO per g refractory, pH 9

Refractory Coatings on Refractory Brick

After Heat Treatment

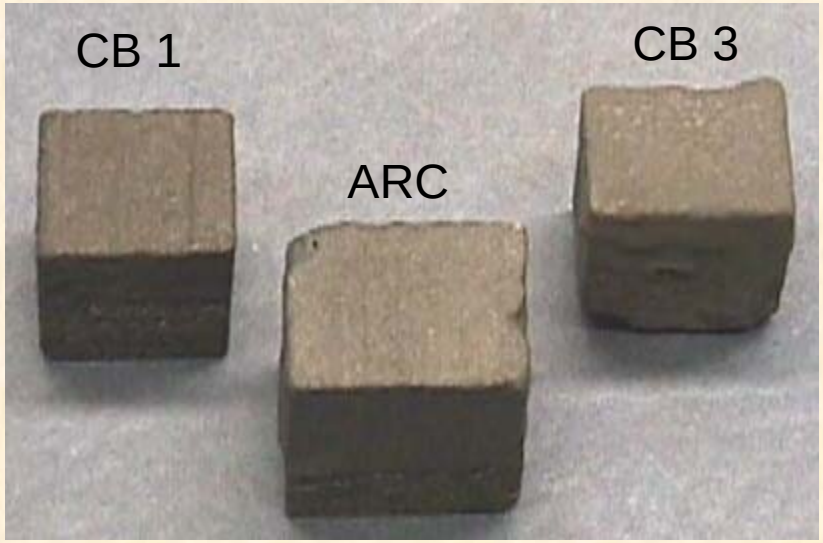

Heat Treatment:

120°C to 600°C, 2 h soak
300°C to 1600°C, 2 h soak

As-received brick

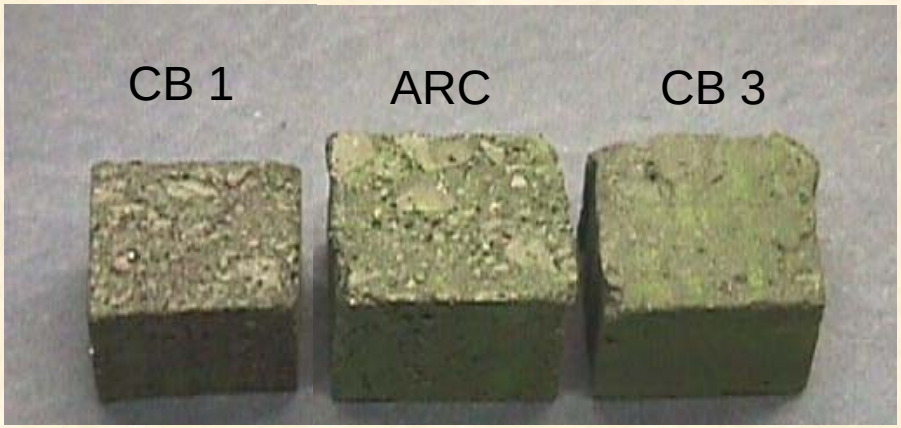

*** Similar results were obtained for the CB 2 system**

Coating Density Optimized with Sintering Conditions

57.5 vol% suspension
1600°C, 2h in air (1 atm)

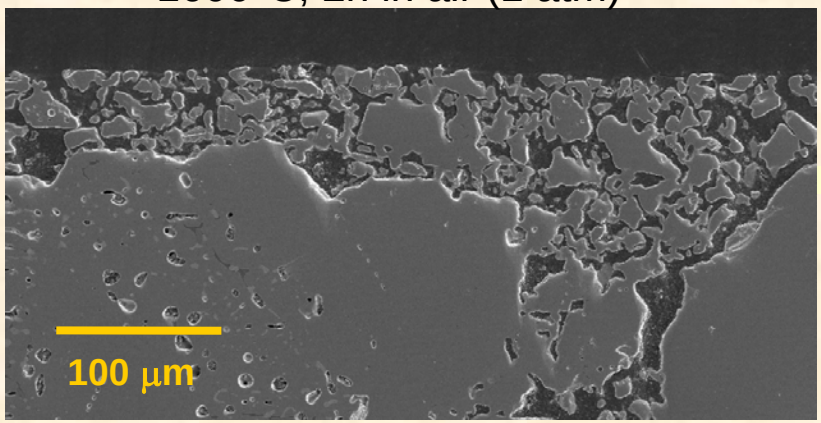

57.5 vol% suspension
1600°C, 12h in air (1 atm)

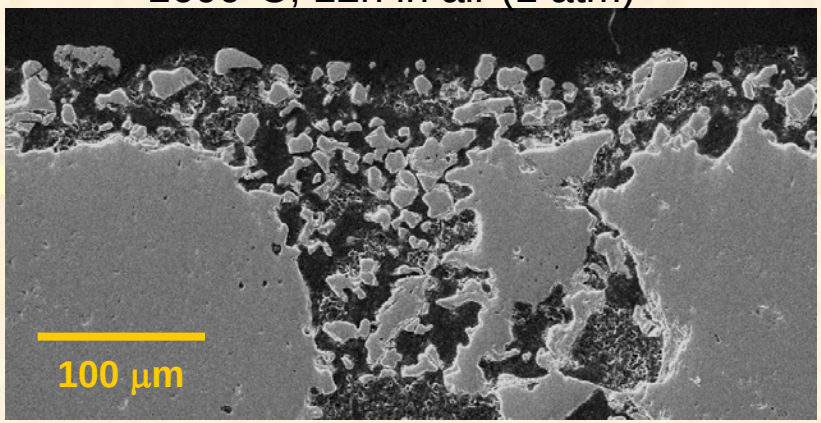

57.5 vol% suspension, 0.5*M* sintering aid
1600°C, 2h in air (1 atm)

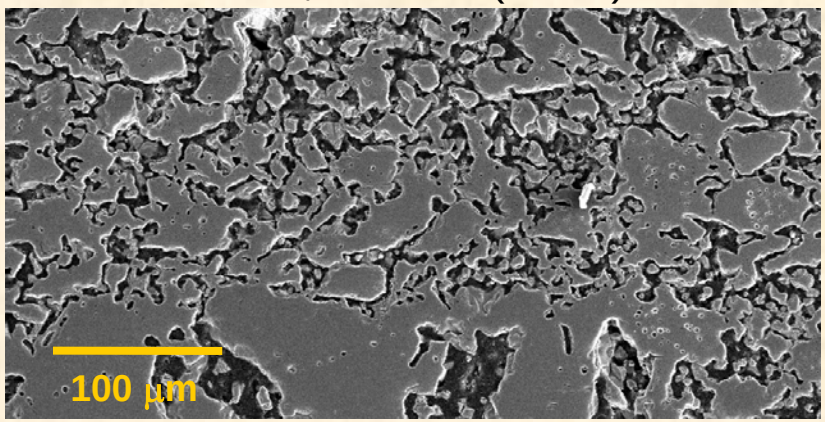

57.5 vol% suspension
1600°C, 2h in argon (1 atm)

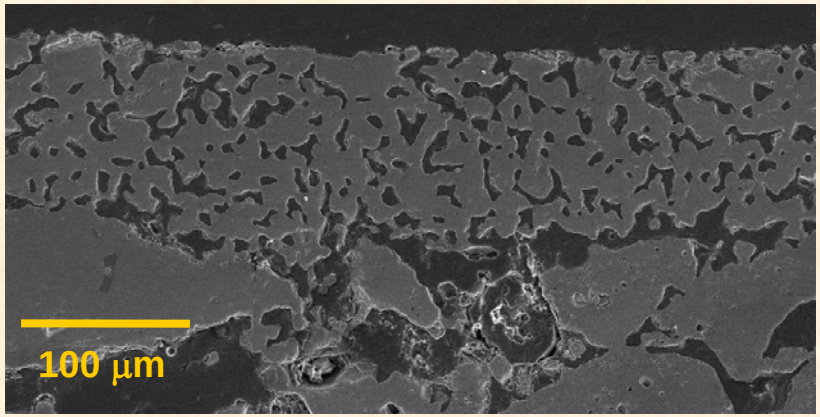

Conclusions

- A variety of materials and shapes can be coated by controlling slurry rheological behavior and processing parameters
- Dip coating is a viable process for protection in fossil environments
- Interaction at the interface between mullite and silicon carbide can promote adhesion yet the strength can be reduced due to silica scale formation if the coating is not dense
- Refractory coating density optimized with use of sintering aid and sintering environment

Future Work

- **Continue evaluation of mullite coating and process efficacy**
  - **Improve coating densities**
  - **Test in simulated fossil environments**
- **ARC testing in fossil environments to obtain confirmation of performance and feedback**
- **Continue evaluation of alternative material systems (baseline material studies)**

Acknowledgements

A special thanks to Matt Ferber/ORNL for mechanical properties testing

This research was co-sponsored by U. S. Department of Energy, Office of Fossil Energy Advanced Research Materials Program under Work Breakdown Structure Element ORNL-1B and U.S. Department of Energy, AE Mining Research under Work Breakdown Structure, FEAA075.

ORNL is operated by UT-Battelle for U. S. Department of Energy under contract DE-AC05-00OR22725.

Questions?

A Commercial Process For Production Of Silicon Carbide Fibrils

19th Annual Conference On Fossil Energy Materials

Knoxville, TN
May 10, 2005

Richard D. Nixdorf

ReMaxCo Technologies, Inc.
1010 Commerce Park Drive
Oak Ridge, TN 37830

Work funded by U.S.DOE Fossil Energy Department
Advanced Research Materials Program
through Oak Ridge National Laboratory under Roddie R. Judkins

What Are Silicon Carbide Fibrils?

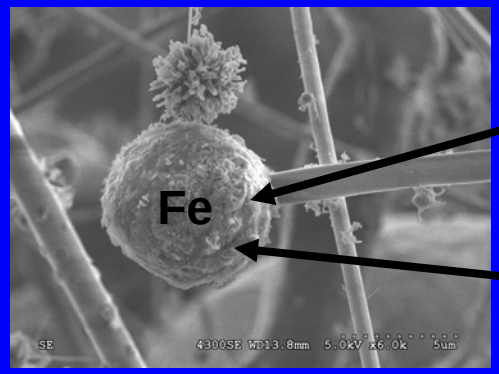

SiO

\+ = SiC

CO

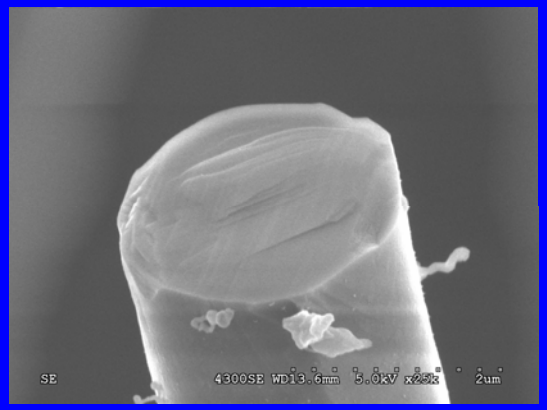

- 5 to 10 um diameter single crystal needles x 0.2 to 10 mm in length
- Respiratory health hazards eliminated with large diameter
- Use temperature to 1,600^{o}C
- Tensile Strength to 2,300,000 PSI (16,000 MPa)
- Elastic Modulus to 84,000,000 PSI (580,000 MPa)
- Stronger and more durable than any existing SiC fiber materials

Value of Silicon Carbide Fibrils as a Fossil Energy Material

- Demonstrated oxidation resistance to 1600º in air
- Composite-wall tubes for high temperature heat exchangers in the combustion chamber
- Combustion chamber refractory tile fatigue durability improvement (perhaps other refractory materials?)
- 2.5 PM compliant filter media for hot gas filters

Overview and Program Objective

- The U.S. DOE Fossil Energy Advanced Research Materials Program requires higher temperature materials for corosive environments.
- A process is required to produce the silicon carbide fibrils in volume quantities to allow consideration for commercial use.
- The commercial process must provide a reasonable product price of ~ $300 per pound (previous best by researchers = $2,000/lb)

History of Fibrils Development

1965 - VLS silicon carbide fibrils were discovered by Phillips Electronics in Sweden

1980 - Los Alamos National Laboratory spent several years on developing the technology for the US Government

1985 - Los Alamos turned the development over to MER and ACMC funded by DOD

1990 - DOE Fossil Energy Program funded Carborundum to resume the research. Carborundum abandoned the program when purchase by St Gobain

1998 - DOE requested ReMaxCo to continue the development effort after Carborundum

1999 - ReMaxCo studied that past work and determined that a new approach was necessary to attain commercial viability. Microwave synthesis was selected as this new approach

2000 - ReMaxCo conducted the first microwave synthesis bench-top proof-of-concept with significant success

FY 2000 Proof-of-Concept Experiments

- Increased Fibril Growth Rate from Carborundum's 0.17 mm/hour to 0.75 mm/hour - 4.4 X Improvement
- Melted Catalyst Particles and Sustained Fibril Growth with Microwave Energy rather than heating entire furnace chamber
- Grew Fibrils with no Deposit of SiC on Reaction Chamber Components - All MTS Gas Feeding Fibril Growth Balls to significantly reduce reactant gas cost
- Proved Potential for Microwave Growth Concept to reduce SiC fibril cost from $2,000/lb to a potential $300/lb

FY 2002 Scale-Up Experiments

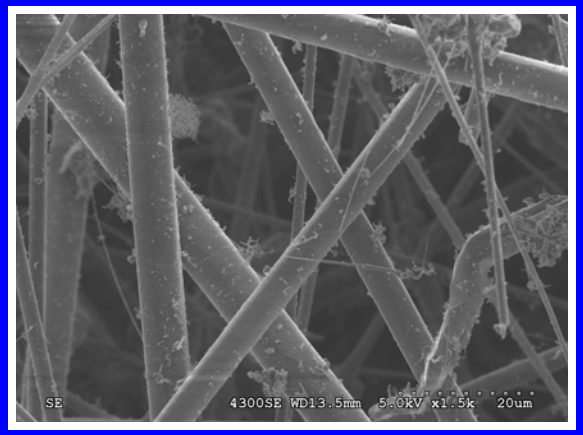

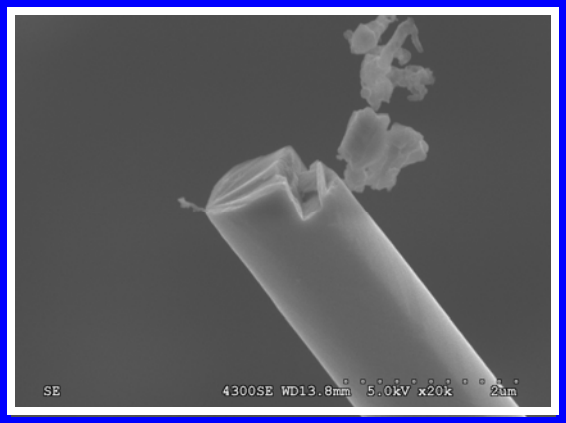

Microwave Reactor Operation Using Only Microwave Energy to Heat Fibril Growth Balls

Al_2O_3 furnace tube

Al_2O_3 boat

Microwave-heated catalyst and fibril growth

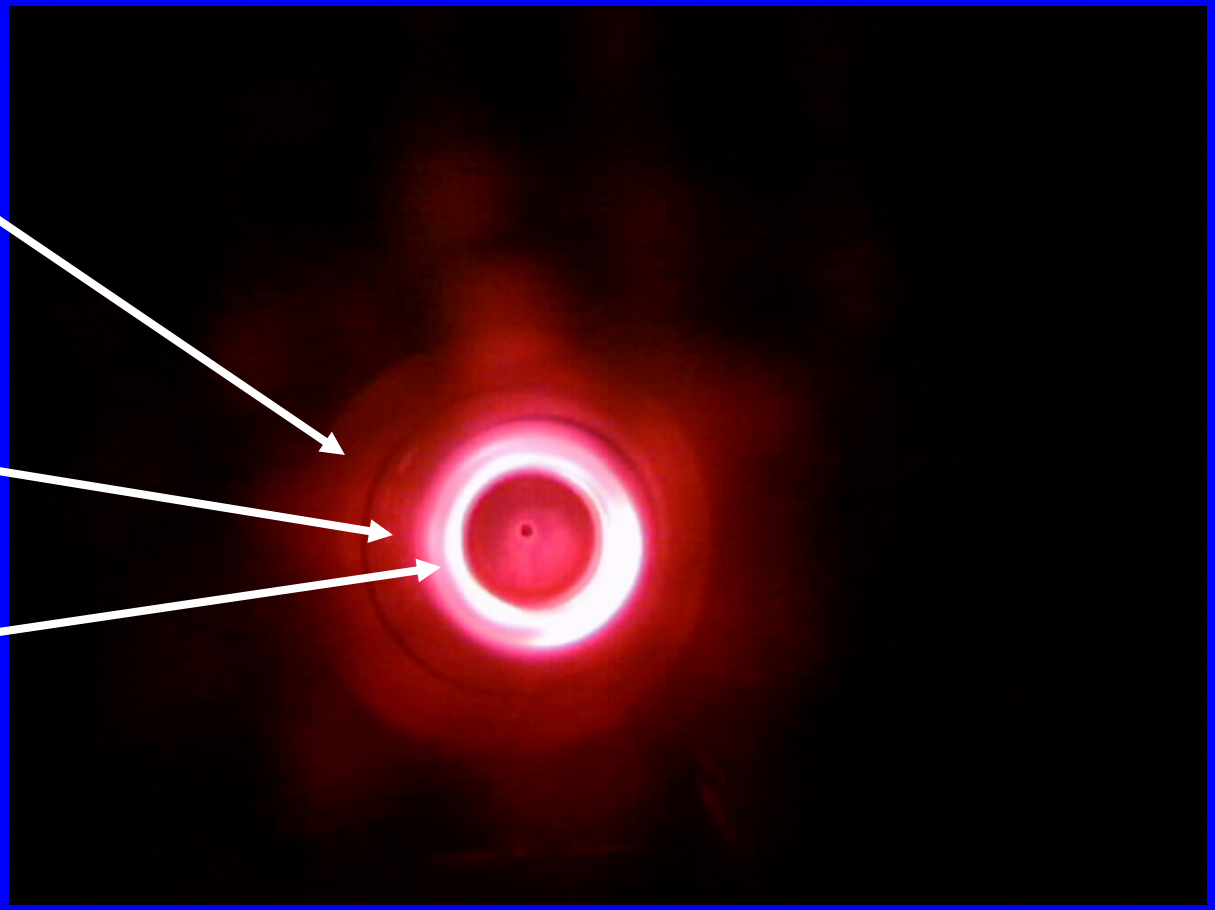

FY 2004 Fibrils Reactor Design
World-Class Engineering Expertise

First Two Reactors resulted in problems with <u>reactant gas distribution and control</u> and <u>microwave field uniformity</u>

<u>FY 2005 Reactor Designed by Known Experts in each System Component</u>

- **MS&E Engineering – 25 years experience in gas distribution systems for CVD reactors**
- **RF Technologies – 28 years experience in industrial microwave systems**
- **McCormick Engineering – 25 years experience in vacuum furnace design**
- **Starfire Systems – SiC precursor increases yield from reactant gas by a factor of three, without producing hazardous and expensive HCl acid offgas – compared to the previous standard MTS reactant gas**

FY 2005 Volume SiC Fibril Reactor

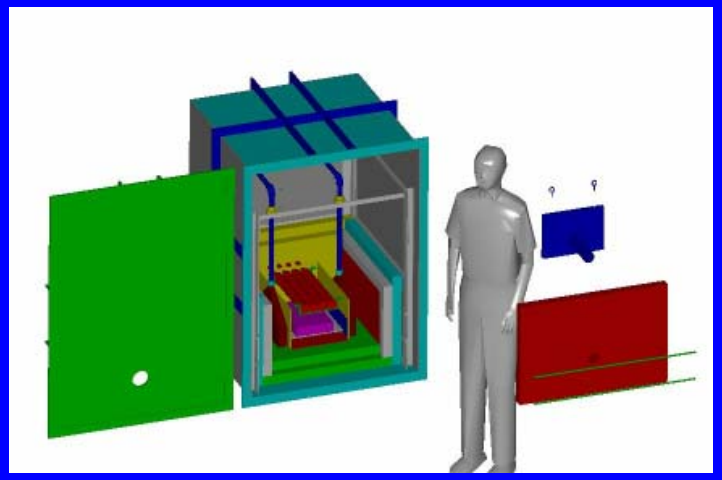

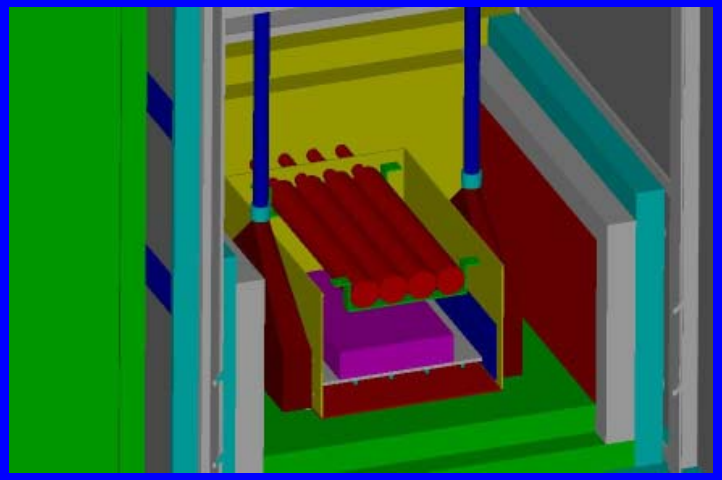

Furnace is estimated to make 200 to 400 grams/day of Fibrils

Furnace will be operable by July 2005

Sample of Fibrils should be available to DOE research scientists by 3rd Qtr. 2005 for materials testing

FY 2005 Volume SiC Fibril Reactor

Unit Assembled for Firing

FY 2005 Volume SiC Fibril Reactor

Microwave Feed System

FY 2005 Volume SiC Fibril Reactor

Fibrils Growth Chamber

Commercial Applications of Silicon Carbide Fibrils for Coal-Fired Power Plants

Heat Exchanger Tubes

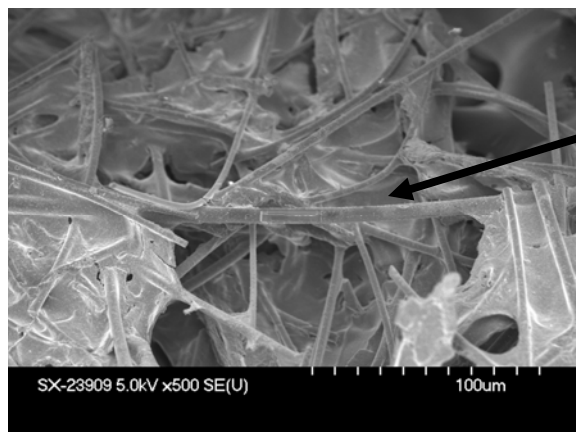

Silicon Carbide Fibrils can be formed into a paper

The paper can be rolled into tubes and joints prior to rigidifying

The tubes can be infiltrated with CVD ceramic materials to rigidify the tube after shaping tube arrays

The result is a heat exchanger tube capable of operating at 1,200 to 1,400^{o}C

Commercial Applications of Silicon Carbide Fibrils for Coal-Fired Power Plants

Fibrils Increase of Fatigue Strength and Life of Combustion Chamber Refractory Tiles

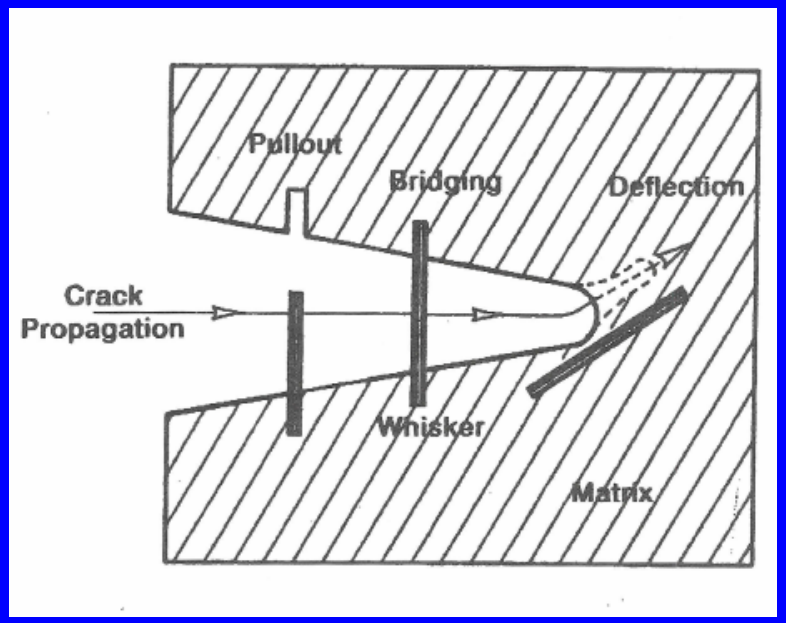

SiC Fibrils perform as rebar in concrete to add strength and stop cracks that cause fatigue failure

Refractory ceramic tiles exhibit significant fatigue failure above 1,200°C, Fibril reinforcement can move that limit to above 1,400°C

No current reinforcement material can perform at temperatures above 1,200°C

Commercial Applications of Silicon Carbide Fibrils for Coal-Fired Power Plants

Hot Gas Filters

Fibrils can be formed into an inexpensive pleated filter media capable of withstanding 1,400^{o}C gas temperatures

Filter efficiency of 95% on 0.01 um particle size is achievable

Filter size is unlimited; moving belts could handle the total exhaust of a coal-fired steam plant

Summary of Microwave Process Benefits for Silicon Carbide Fibril Production

- Lower energy consumption
- Higher Fibril growth rates
- Consistent reactant gas feed
- 40X increase in reactant gas efficiency
- Lower cost raw materials and capital equipment reduces Fibril Price

SiC Fibrils Contribution to Fossil Energy Program's Materials Requirements

High Temperature Heat Exchanger Tubes

Improve Creep Strength of Combustion Chamber Refractory Materials

High Temperature Filter Media for Fine Particulate removal from Combustion Gases (2.5 PM regulations)

Reinforcement to Improve Toughness of Refractory Metals (TiN and TiC Fibrils are possible)

Other Major Commercial Applications for Silicon Carbide Fibrils

- Silicon Carbide Computer Circuit Boards – reinforce CVI silicon carbide for heat dissipation (increases number of circuit capacity on a computer chip)
- Metal Cutting Tools – replace hazardous SiC whiskers with a non-respirable product; also, move into machining ferrous alloys
- High Temperature Filter Media – diesel exhaust, chemical processing, and fossil energy plant emissions
- Metal and Ceramic Reinforced Matrix Composites – high performance structural components in military and commercial applications (Air Force Tactical Fighter Jet)

Future Work on Silicon Carbide Fibrils

- ReMaxCo will be capable of supplying fibril samples and fibril composite parts to fossil energy researchers and others by 2005
- A corporate partner is needed in the energy or materials business to move the technology into commercial production
- ReMaxCo and Starfire Systems are seeking funding from NYSERDA for a small production facility near Albany, NY
- It is estimated that approximately $3 million dollars and two years of scale up will be required to move silicon carbide fibril production into the first phase of commercial volumes

Monitoring Power Plant Corrosion Using Corrosion Probes

Bernie Covino

Sophie Bullard, Malgorzata Ziomek-Moroz, Gordon Holcomb

Outline of Talk

- **Introduction**
  - **Why, What, and Where of corrosion probes**
  - **Past Research Results**
- **Isothermal Probe Research**
  - **Corrosion – Incinerator Ash**
  - **Corrosion – Coal Ash**
- **Air-cooled probe construction**

Corrosion in the Fireside

- Paradigm Change - corrosion can be treated proactively rather than reactively.
- New Capabilities - corrosion probes will allow power plant owners to monitor the condition of their biggest asset, the Power Plant.
- Bottom Line Improvements - NACE is working with the U.S. Congress to change corrosion expenditures to a capital expense.

Corrosion Probes?

- Electrochemical Corrosion Rate probes are:
  - A probe for inserting into aggressive environments with the ability to measure corrosion rate or corrosivity using electrochemistry
  - Consists of 2 or 3 sensing elements or electrodes (Sensors)
  - Needs the presence of an electrolyte
    - Allows for electron transfer between electrodes
    - Could be the deposited ash, the corrosion product, the potting compound, etc.
  - Includes an electrochemical technology capable of accurately measuring corrosion rates

Major Goal of Research

- To show that electrochemical corrosion probe technology is viable for coal and refuse burning power plants and that this technology adds value to the energy conversion process.

How Will Probes be Used?

- Near-instantaneous feedback on corrosion of key components
  - A process variable that can be monitored and controlled based on, for example, changes in coal type, coal composition, temperature, coal moisture content, combustion oxygen content (oxy-fuel), biomass, etc.
- Cumulative corrosion attack of key components
  - scheduling of maintenance when corrosion allowance is exceeded

Research Approach

Isothermal Probes

Quantitative

Responsive to process changes

Air-Cooled Probes

Isothermal Probe Properties

Field Probe Prototype

Thermal Gradients

Field Probes

Isothermal Probe Properties

Validated Measurements

Rugged and Long-lasting

Ash-Covered Isothermal Corrosion Probe

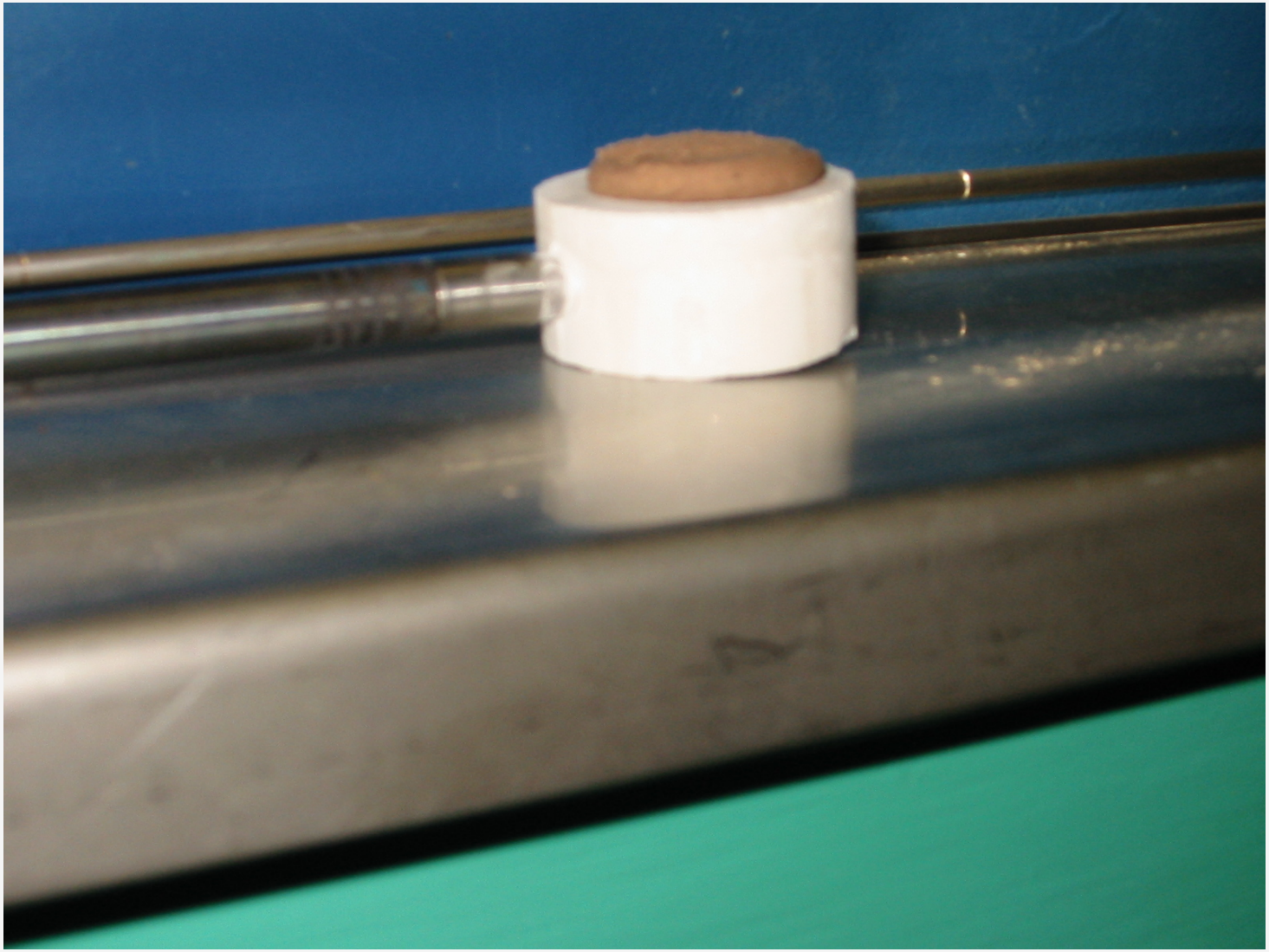

Past Isothermal Corrosion Probe Research

- What have we demonstrated to date?
  - Zero baseline of < 0.001 mm/y (0.04 mil/yr)
  - Close to Quantitative
  - The need to measure accurate Stern-Geary constants
  - LPR data gives best fit

SmartCET® Corrosion Monitoring System

- Linear polarization resistance (LPR)
  - Corrosion rate
- Electrochemical Noise (EN)
  - Corrosion rate
  - Localized corrosion index
- Harmonic distortion analysis (HDA)
  - Corrosion rate
  - Stern-Geary constant (B)

Software Output

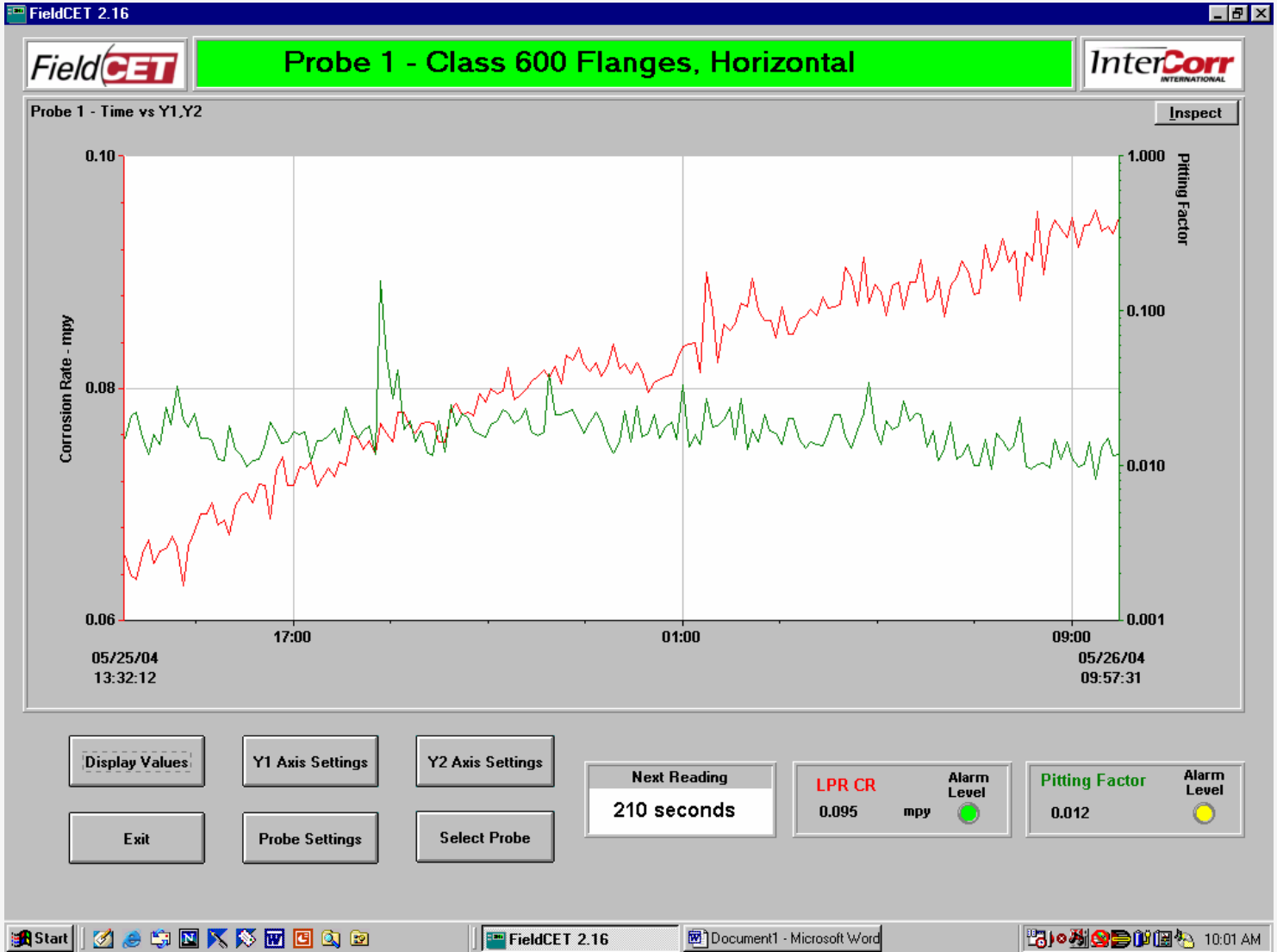

Corrosion Rate Reported Every 7 Minutes

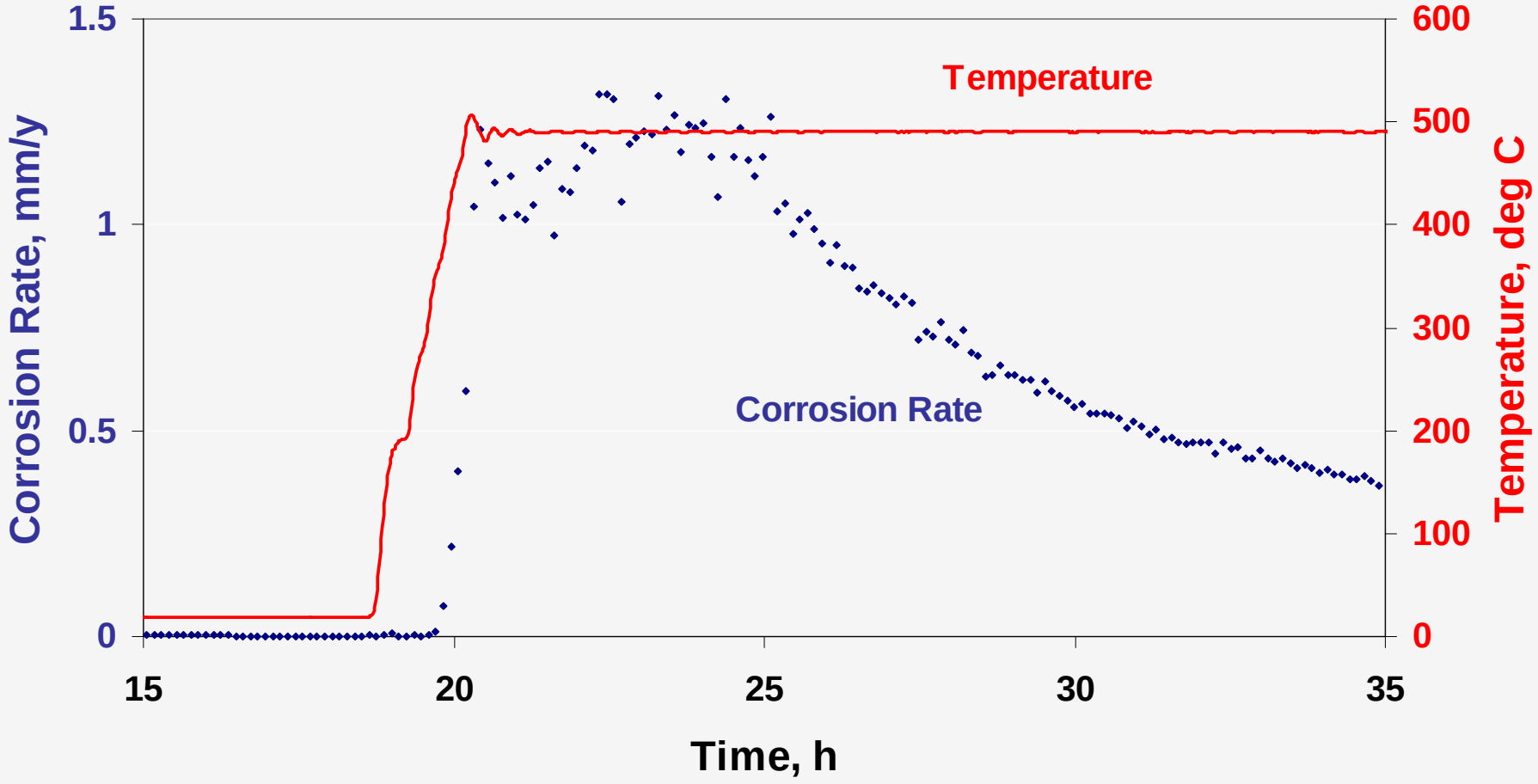

Experiment Plan

Alloys	Gases	Temperatures
Mild Steel	N_2, O_2, CO_2, SO_2	500°C
304 SS	"	"
316 SS	"	"
Ni Alloy	"	"

15 CO_2-3.5 O_2-1 SO_2-10H_2O-bal N_2

Plus (1) Incinerator Ash or (2) Coal Ash

Incinerator Ash / Coal Ash

Incinerator Ash	Coal Ash
Al – 3.63%	Al_2O_3 – 7.6%
Mn – 631 ppm	Mn –
As – 107 ppm	As –
Ca – 9.97%	CaO – 28.3%
K – 3.69%	**K_2O – trace**
Pb – 2.7%	**Pb –**
Ti – 0.514%	TiO_2 – trace
Mg – 0.734%	MgO – 15.6%
Na – 3.53%	**Na_2O – trace**
Cr – 482	Cr –
Ag – < 20	Ag –
P – 0.213%	P_2O_5 – trace
Cd – 883	Cd –
Se – <50	Se –
Cl – 6.71%	**Cl –**
LOI – 26.6%	LOI –
C – 0.135%	C –
N_2 – 0.171%	N_2 –
Fe – 5%	Fe_2O_3 – 6.4
Si – 8%	SiO – 23.7
S – 6.47	**SO_3 – 15%**

Typical Probe Behavior

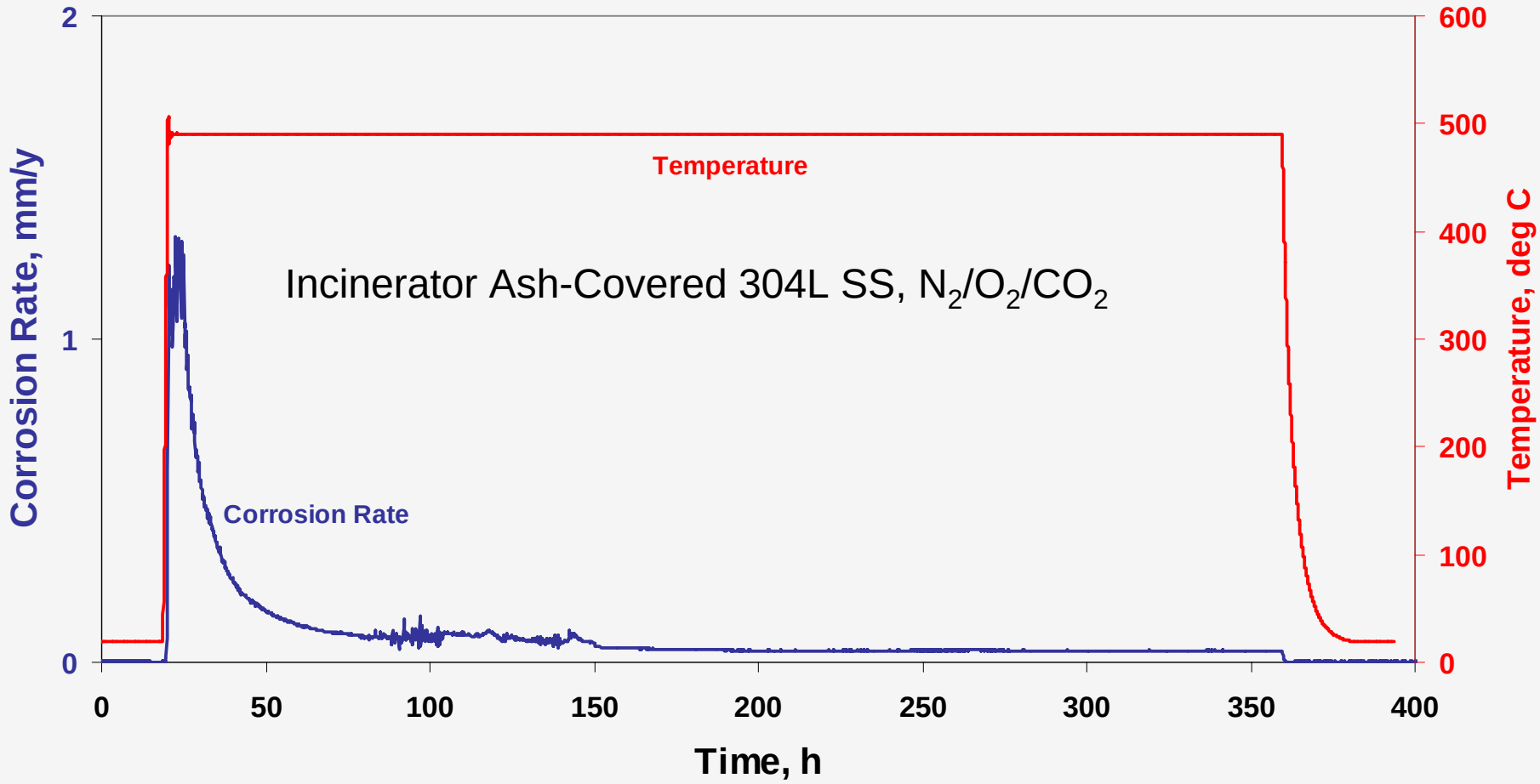

Quantitative Nature

- Electrochemical Corrosion Rates
- Mass Loss Corrosion Rates of coupons
- Volume Loss Corrosion Rates of sensors
  - Profilometry

Mass Loss Coupons

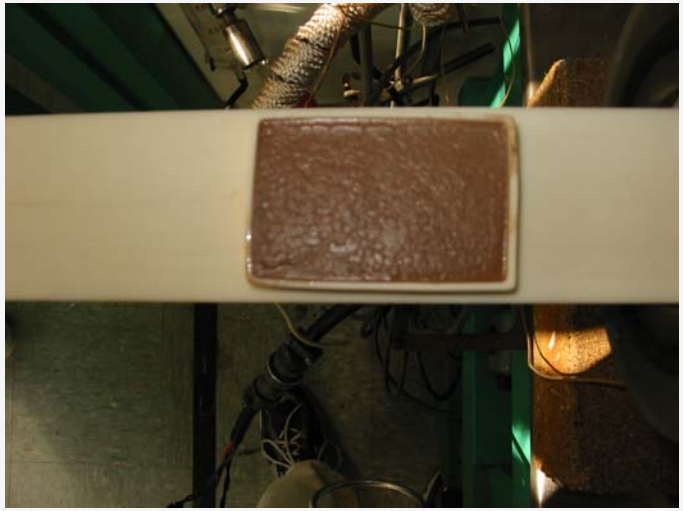

Corrosion Rate Comparison
Different Gases, Temperatures, and Times

Alloy	SmartCET	Mass Loss
304	1.0	2.2
304	1.2	1.3
304	3.3	1.7
316	3.8	3.8
316	1.1	1.3
316	2.8	2.5
Mild Steel	1.6	1.2

Incinerator Ash, mm/y

Optical Profilometry

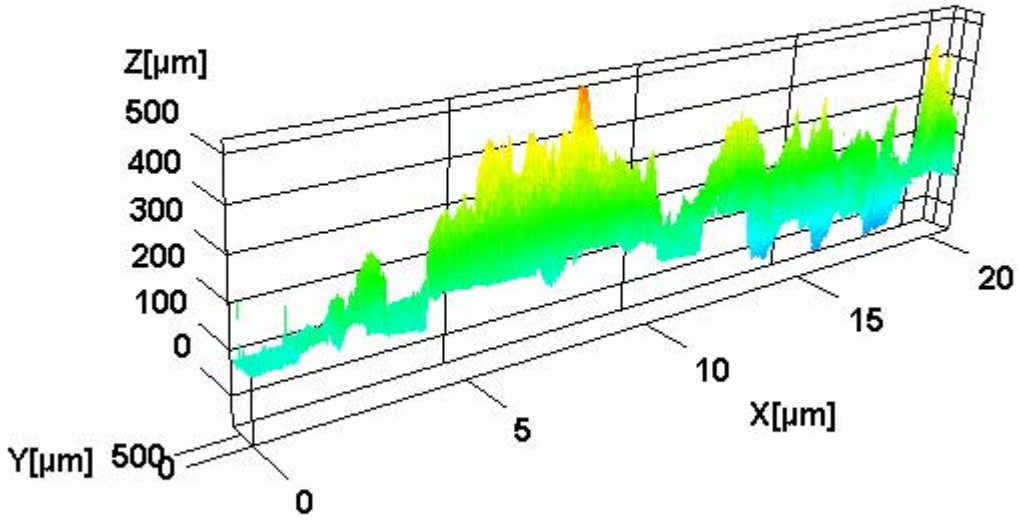

Probe Response

- Effect on Corrosion Rate of Changes in:
  - Temperature
  - Gas Composition
  - Water Content of Gas
  - Ash Composition

Start of Corrosion & Effect of Temperature - Incinerator ash

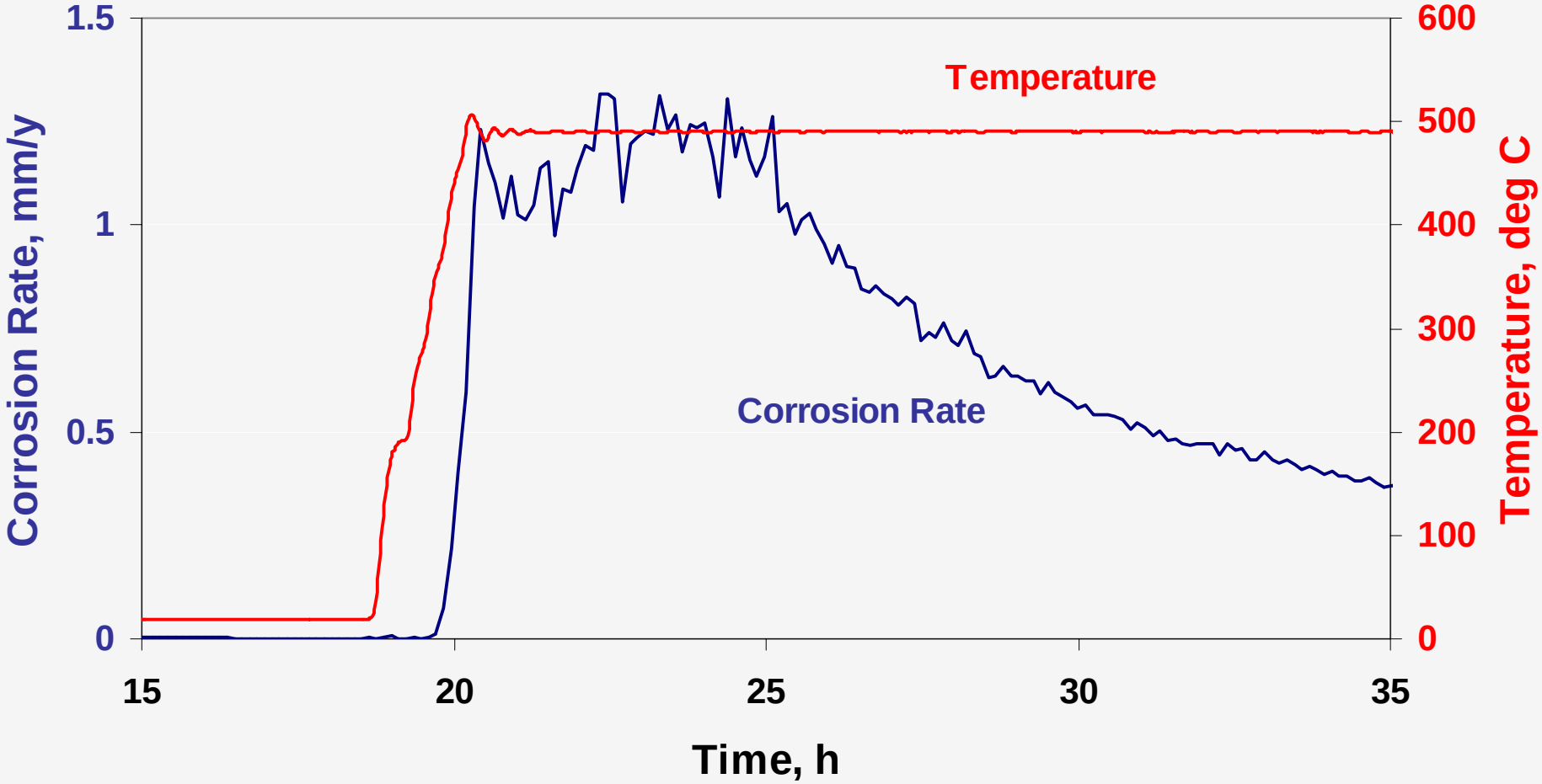

Response to Gas Changes – Incinerator Ash

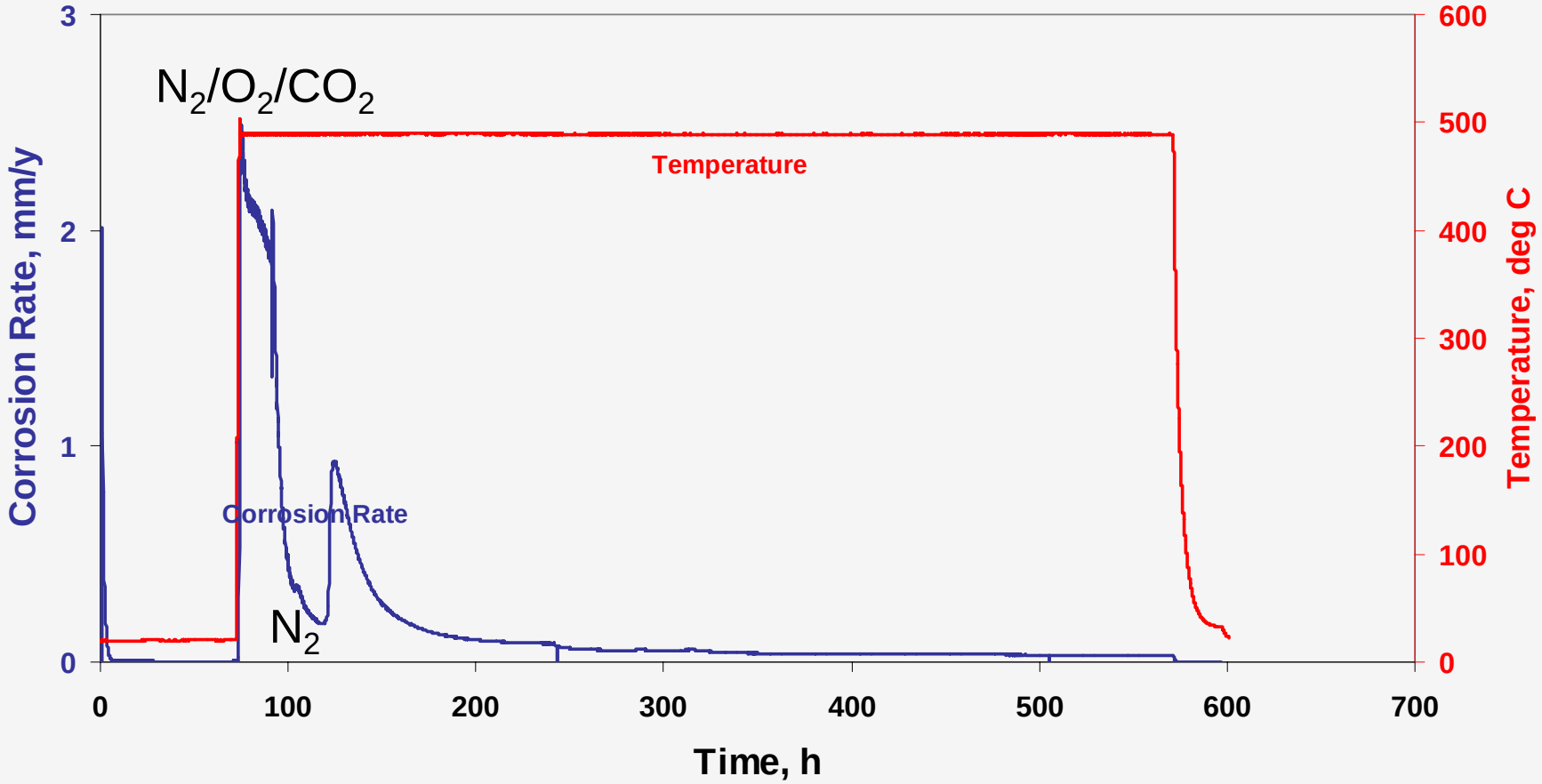

Probe Response to Gas Changes – Incinerator Ash

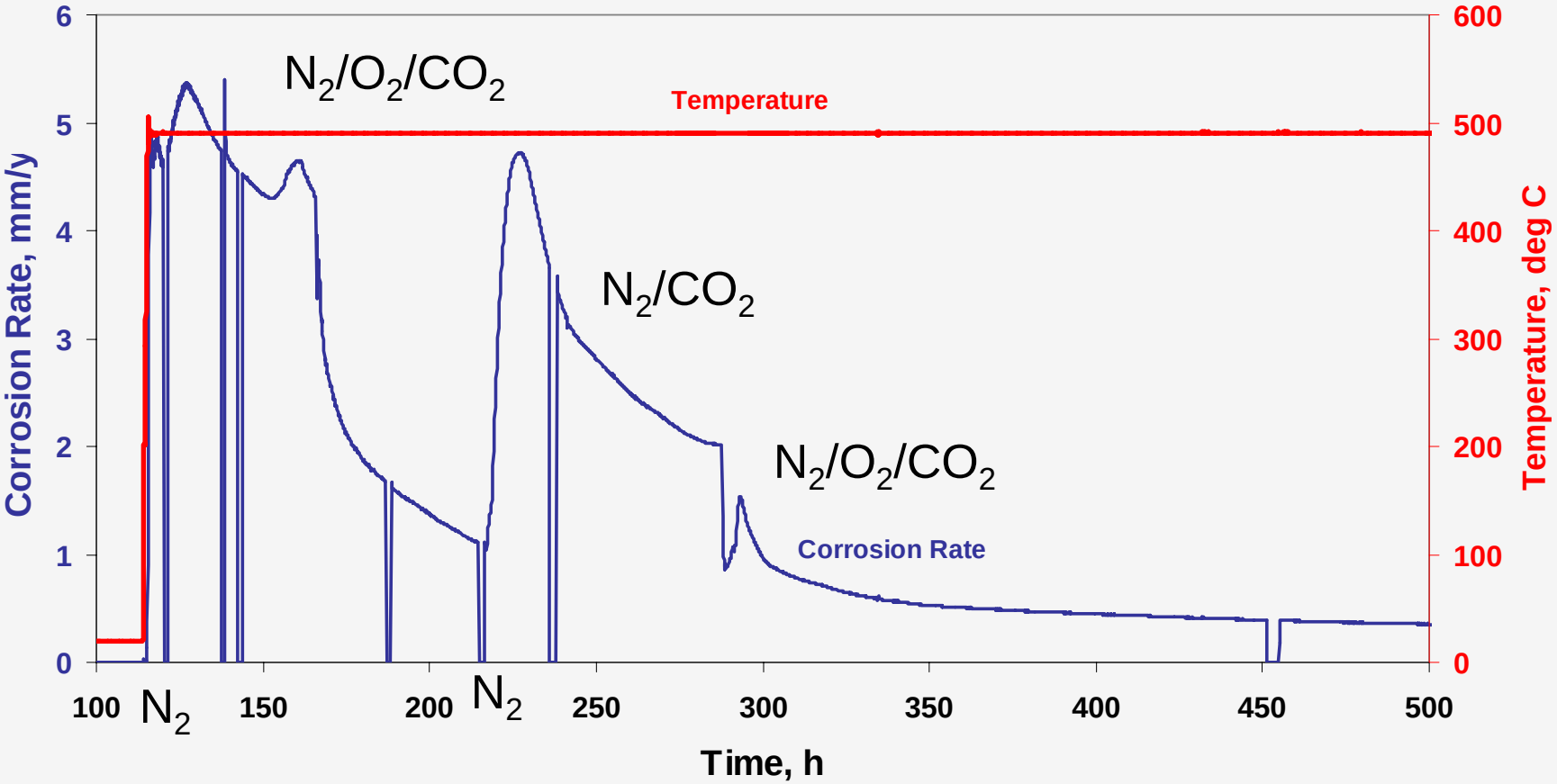

Probe Electrochemistry

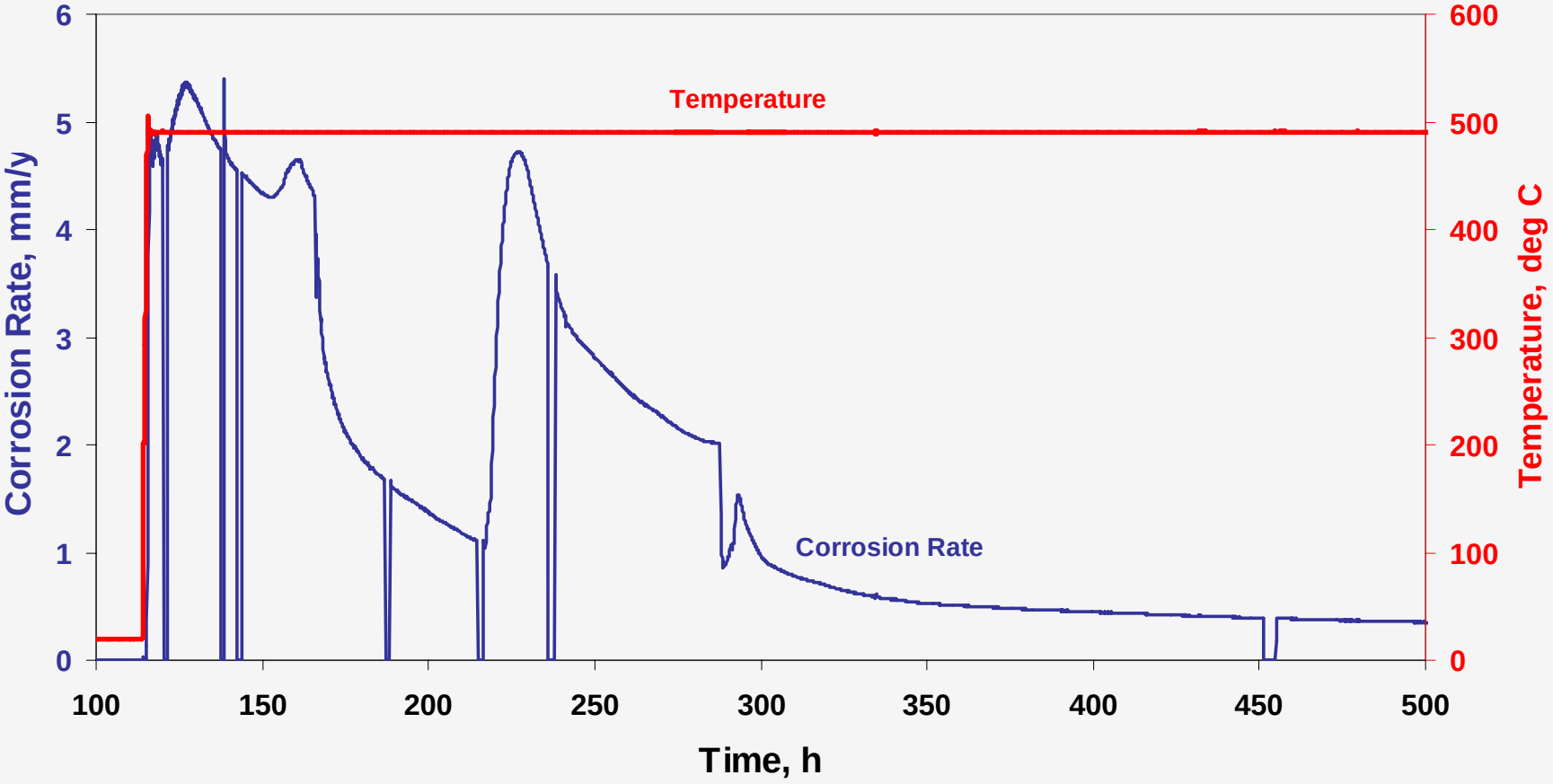

Probe Electrochemistry – Incinerator Ash

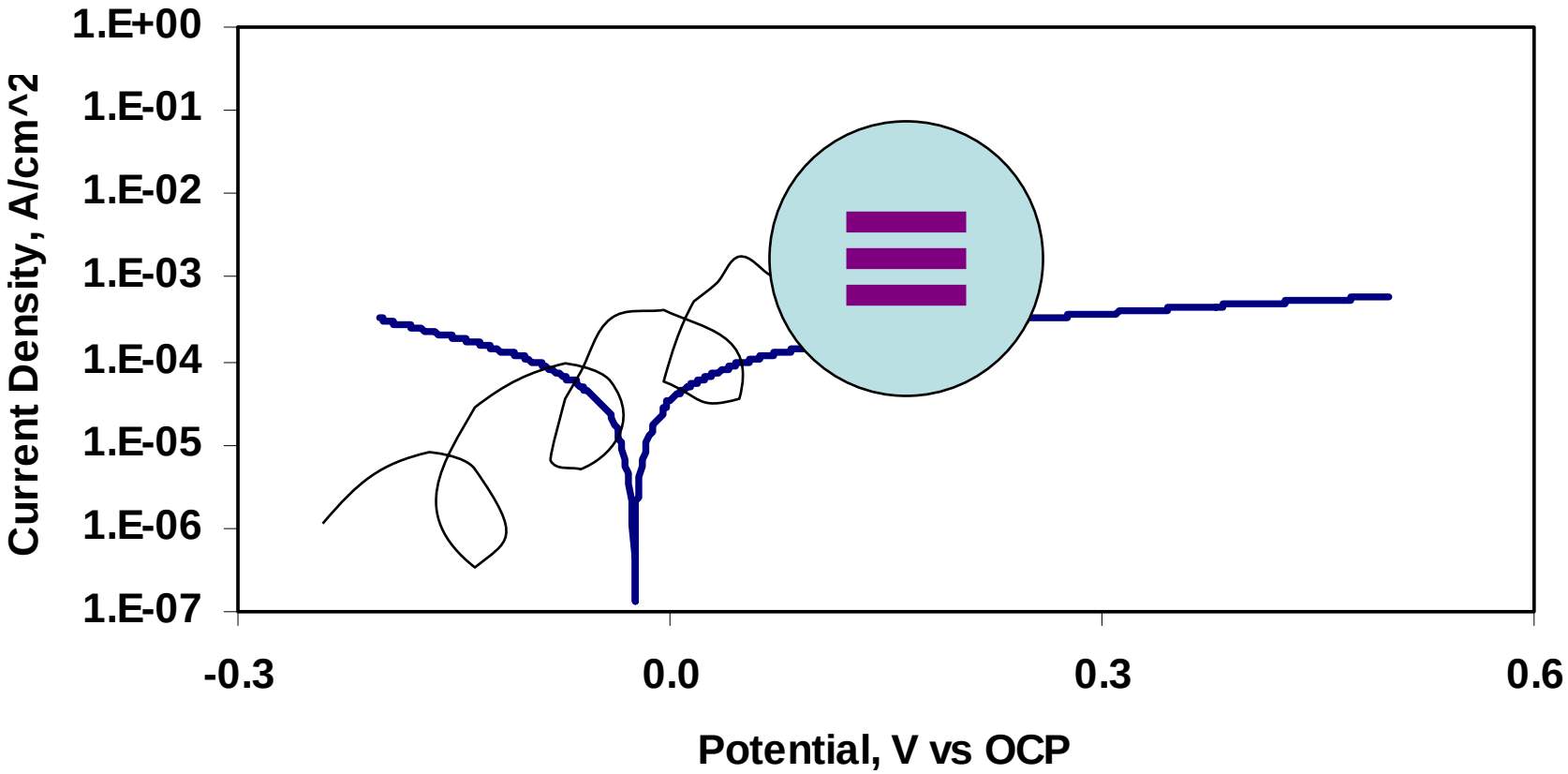

Corrosion Rate Comparisons – mm/y

SmartCET	PAR LPR	PAR PD
0.0028	0.0008	na
1.83	1.63	na
1.79	1.65	1.52
0.66	0.60	0.45
0.44	0.41	0.30
1.44	1.28	0.91
0.15	0.14	0.14

Good Agreement

304 SS in Coal Ash

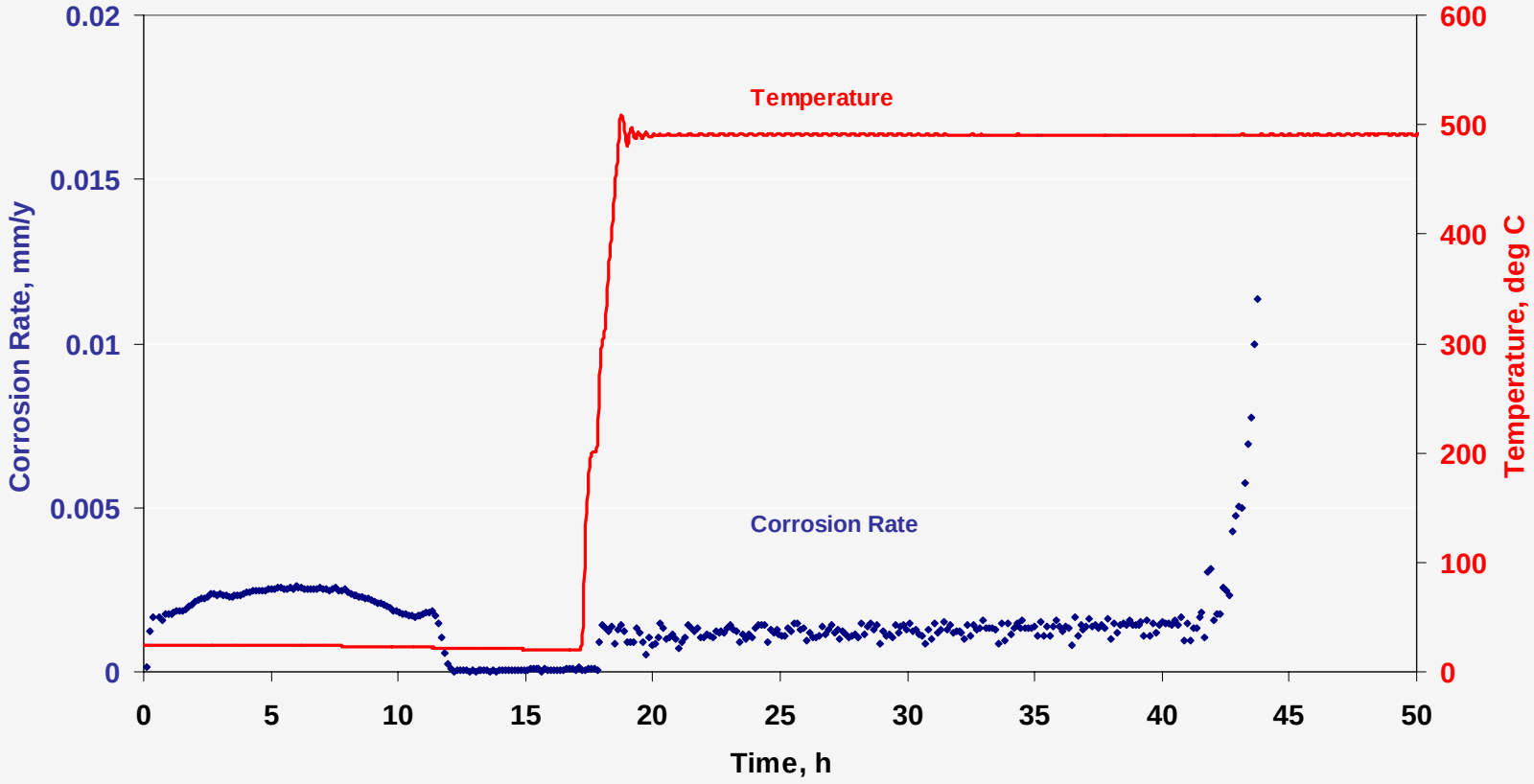

304SS in Coal Ash

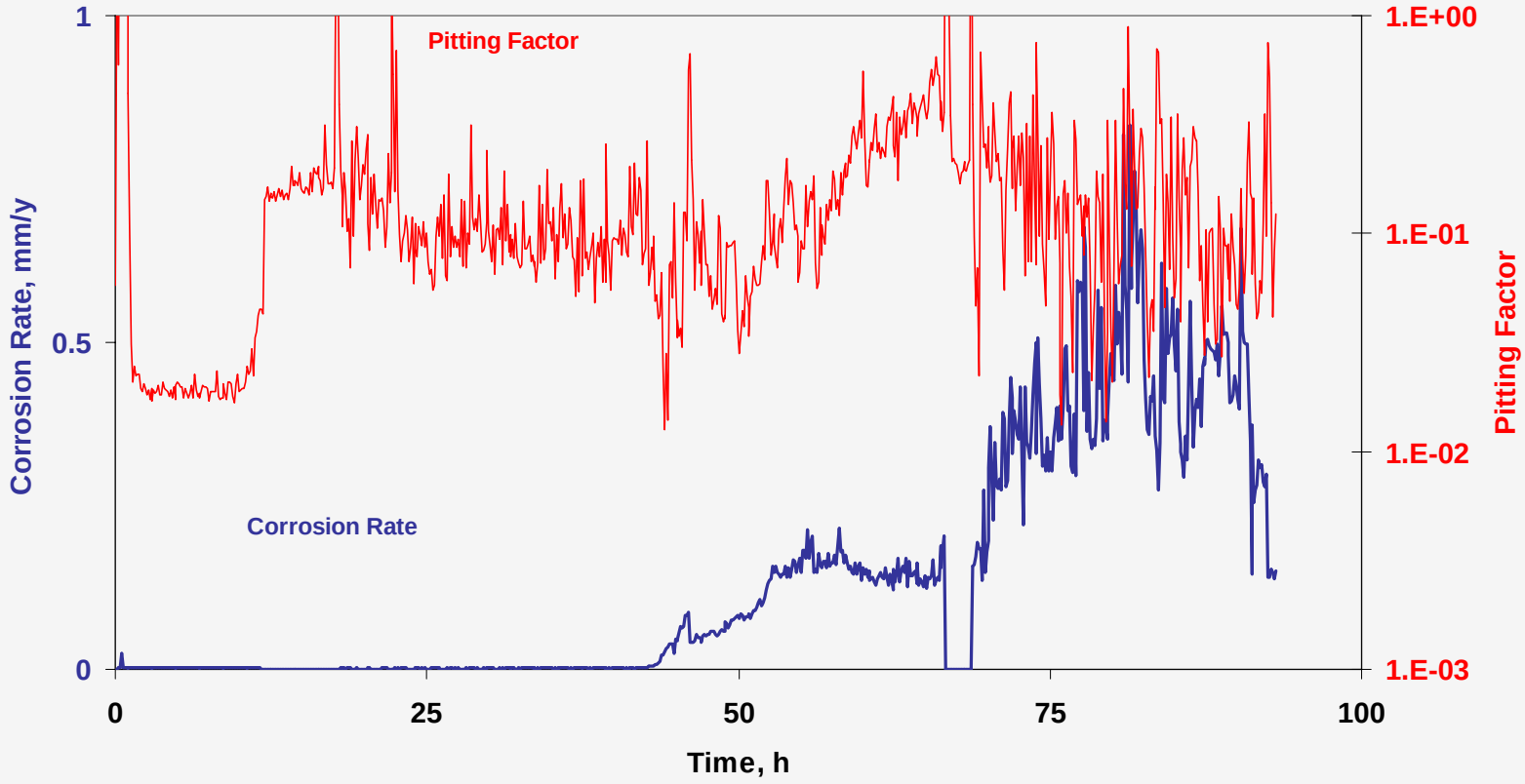

Electrochemistry in Coal Ash

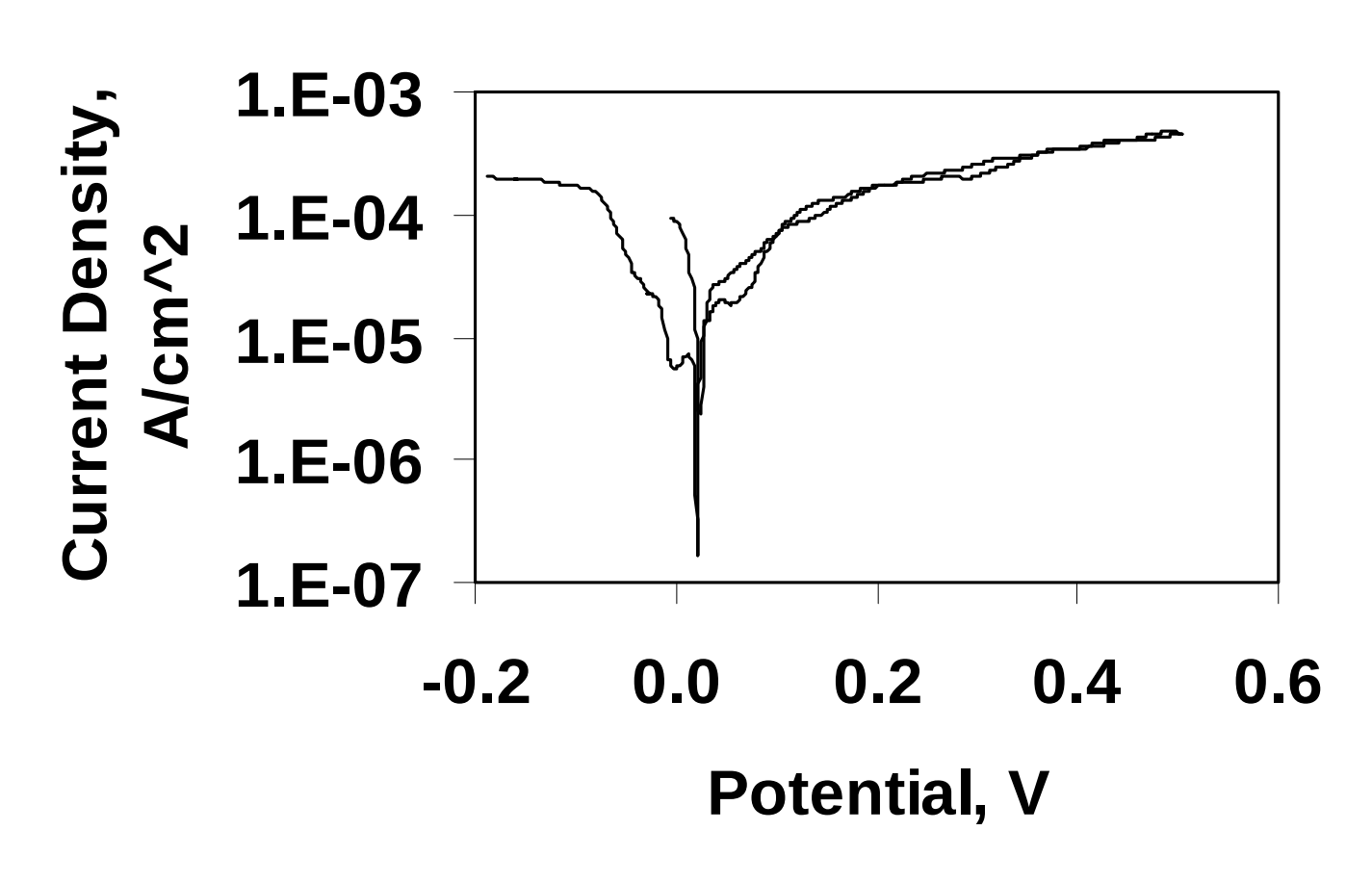

Air-Cooled Probe

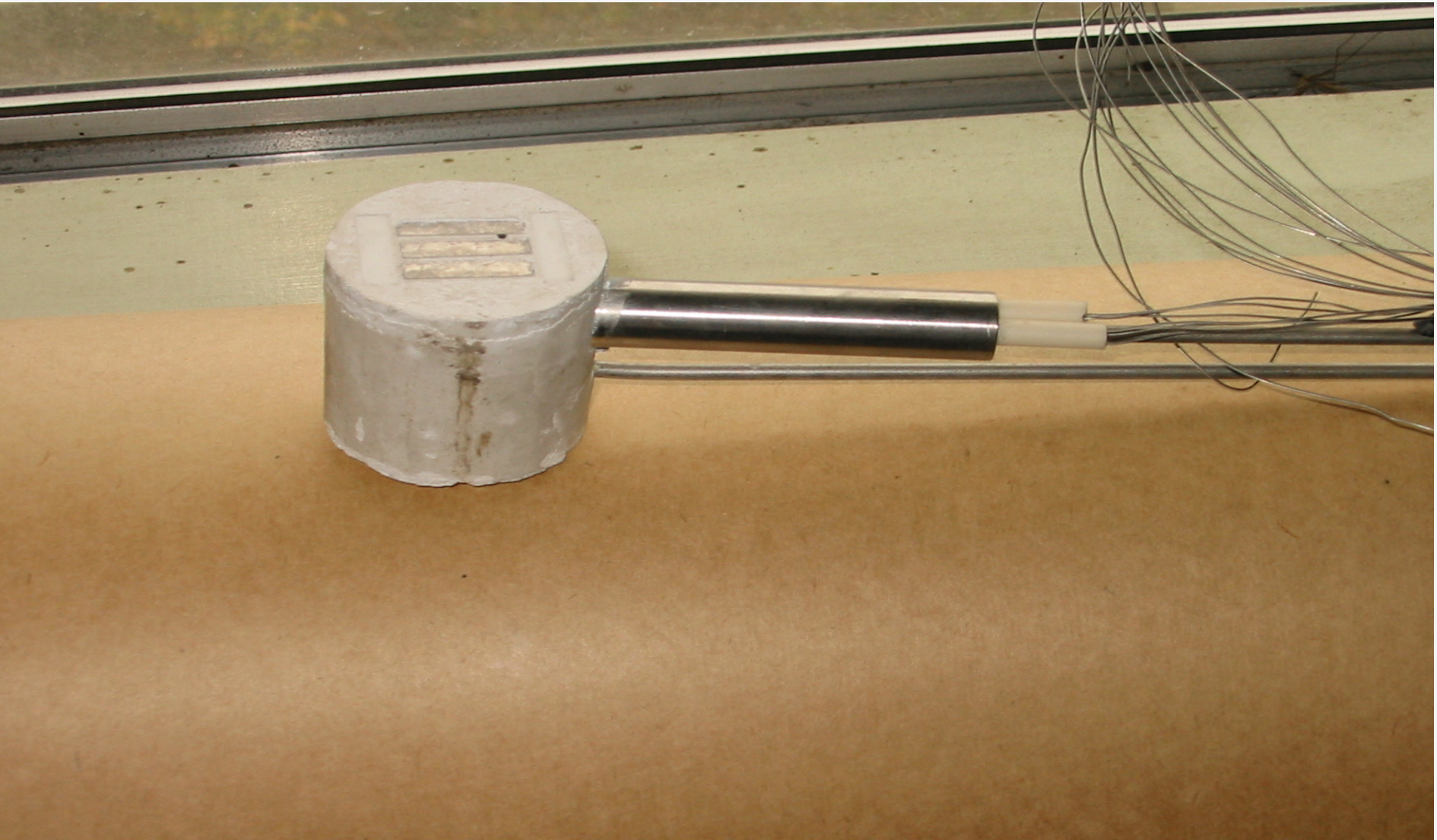

Thermal Gradient Effects

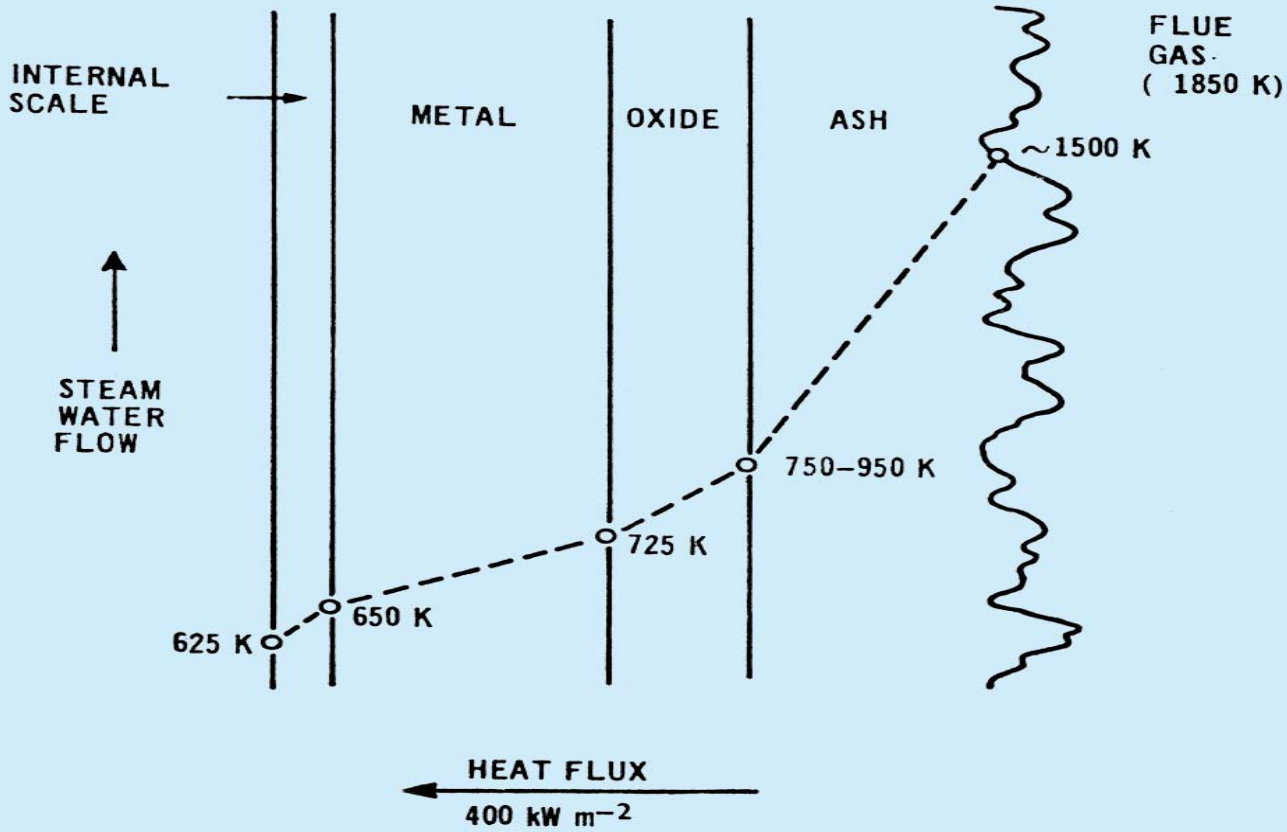

Evaporator Tube Wall

Cutler and Raask (1981)

Multi-Corrosion Probes

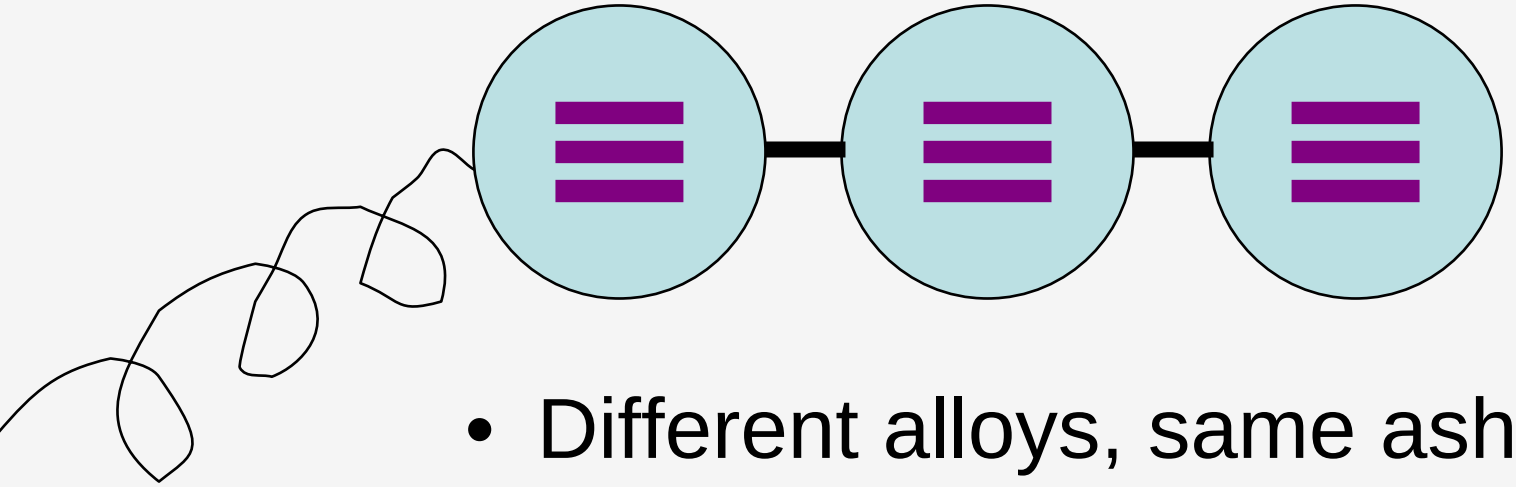

- Different alloys, same ash
- Same alloys, different ash

Conclusions

- The electrochemical corrosion probe appears to quantitatively measure corrosion rates.
- Corrosion reactions in the ash are electrochemical in nature.
- Electrochemical measurements made using common potentiostats agree with SmartCET measurements.
- The electrochemical corrosion probe is responsive to changes in the environment.

Thank You !

DEVELOPMENT OF NONDESTRUCTIVE EVALUATION METHODS FOR CERAMIC COATINGS

W.A. Ellingson, R.J. Visher, R. Lipanovich, H. Jasti. M.D. Shields

ENERGY TECHNOLOGY DIVISION
ARGONNE NATIONAL LABORATORY
ARGONNE, IL

19th Annual Conference on Fossil Energy Materials
Knoxville, TN
May 9-11, 2005

Work supported by US Department of Energy/Office of Fossil Energy/Advanced Research-Materials Program

BACKGROUND

- Any TBC health monitoring tool must be able to monitor *buried* damage evolution.
  - -Optical techniques most amenable to non-contact monitoring.

ARGONNE'S OPTICAL APPROACHES

•Laser-based Elastic Optical Back-scatter has advantages as a TBC health monitoring tool.

- Applicable to EB-PVD
- Applicable to APS

•Optical Coherence Tomography (OCT)

- Applicable to EB-PVD
- Application to APS under investigation

Background – thermal barrier coatings

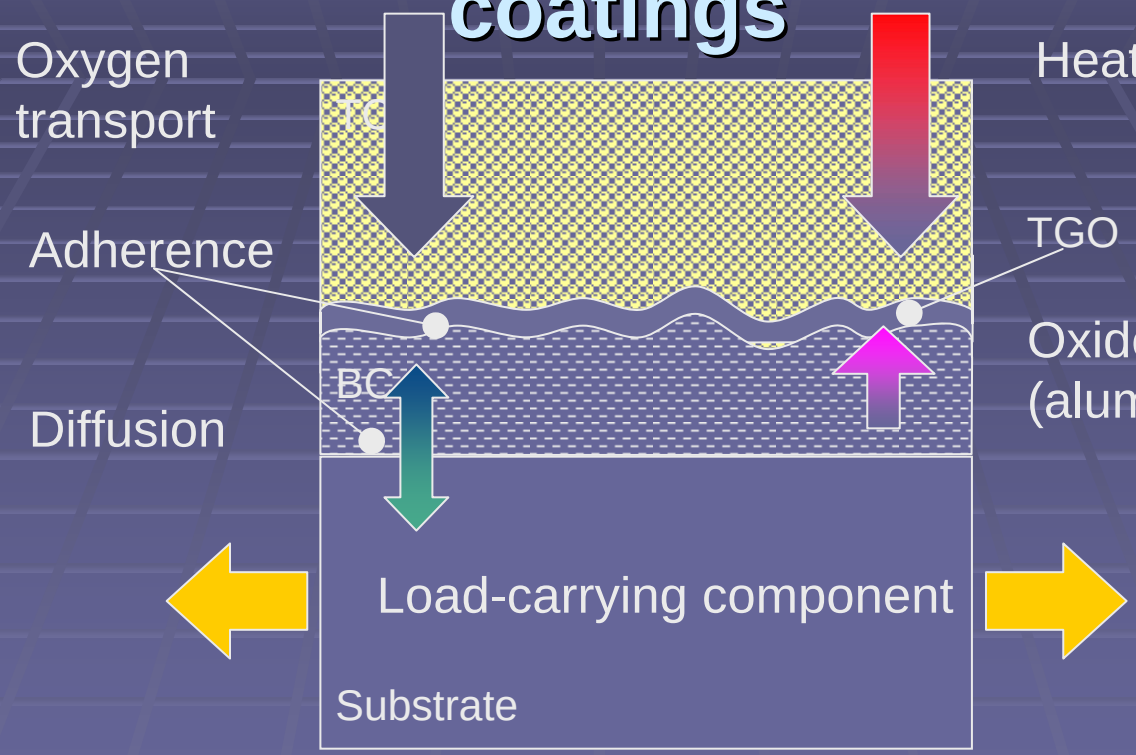

Fatigue testing – failure mechanisms

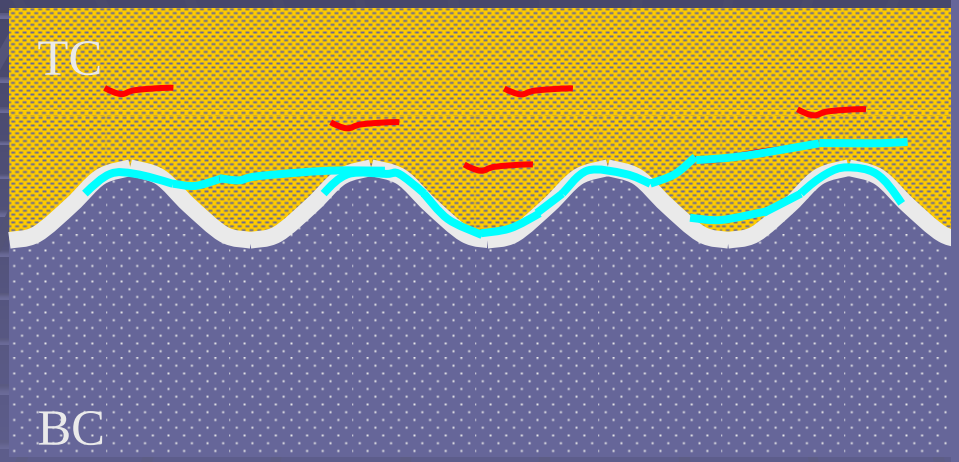

Mechanisms for TBC spallation.

- TC microcracks in virgin material
- Crack initiation at TC / BC interface
- Propagation at interface (black, interface crack)
- Propagation in TC (mixed, kink crack)
- Initiation and growth in TC (white, ceramic crack)

Primary Location of Spallation in Thermal Barrier Coatings on Airfoil Components

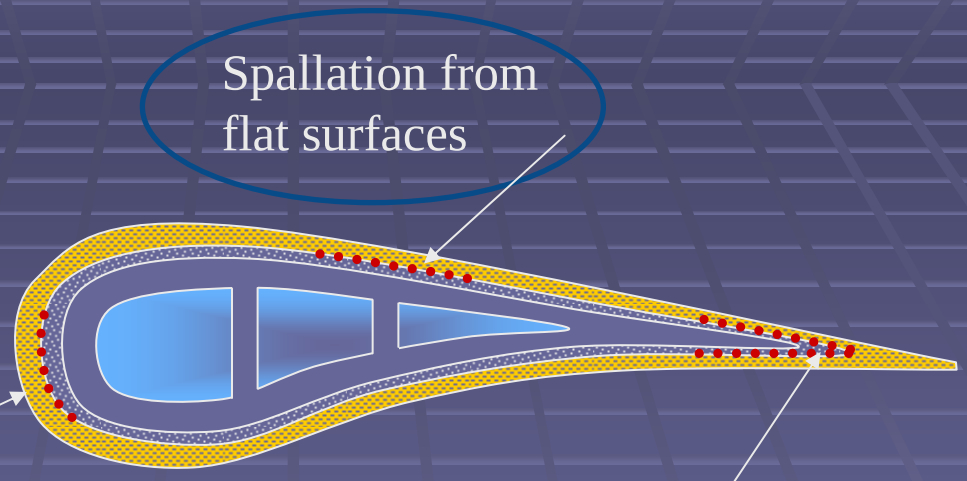

TBC Failure mechanisms.

SCHEMATIC OF ELASTIC OPTICAL BACKSCATTER NDE EXPERIMENTAL TEST SETUP

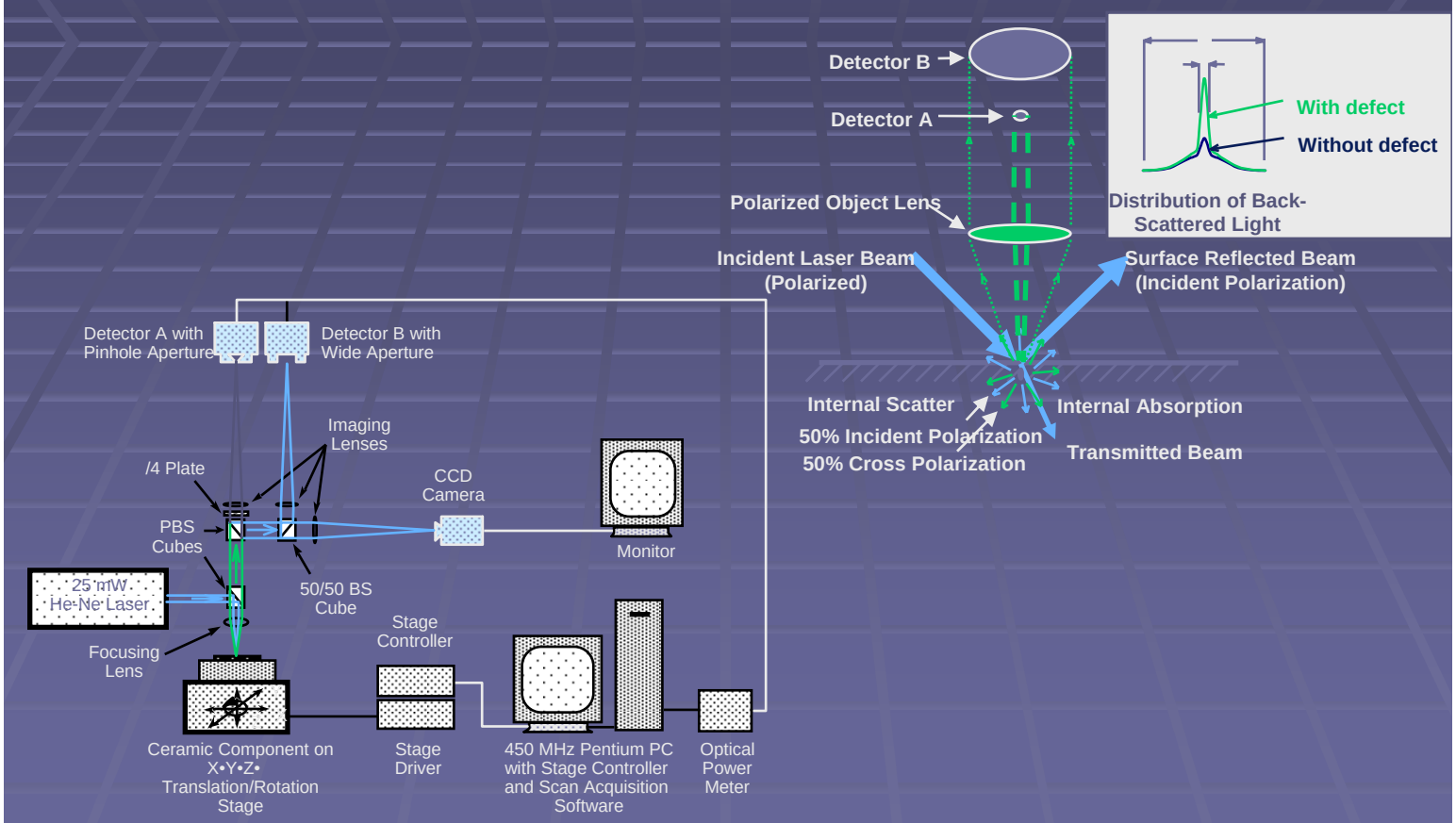

Argonne National Laboratory

EFFECT OF THERMAL CYCLING OF APS TBC ON LASER BACKSCATTER

MCrAlY Bond Coat with APS TBC

Sample Set 3

0 cycles (heat treated) **233 cycles** **326 cycles** **374 cycles**

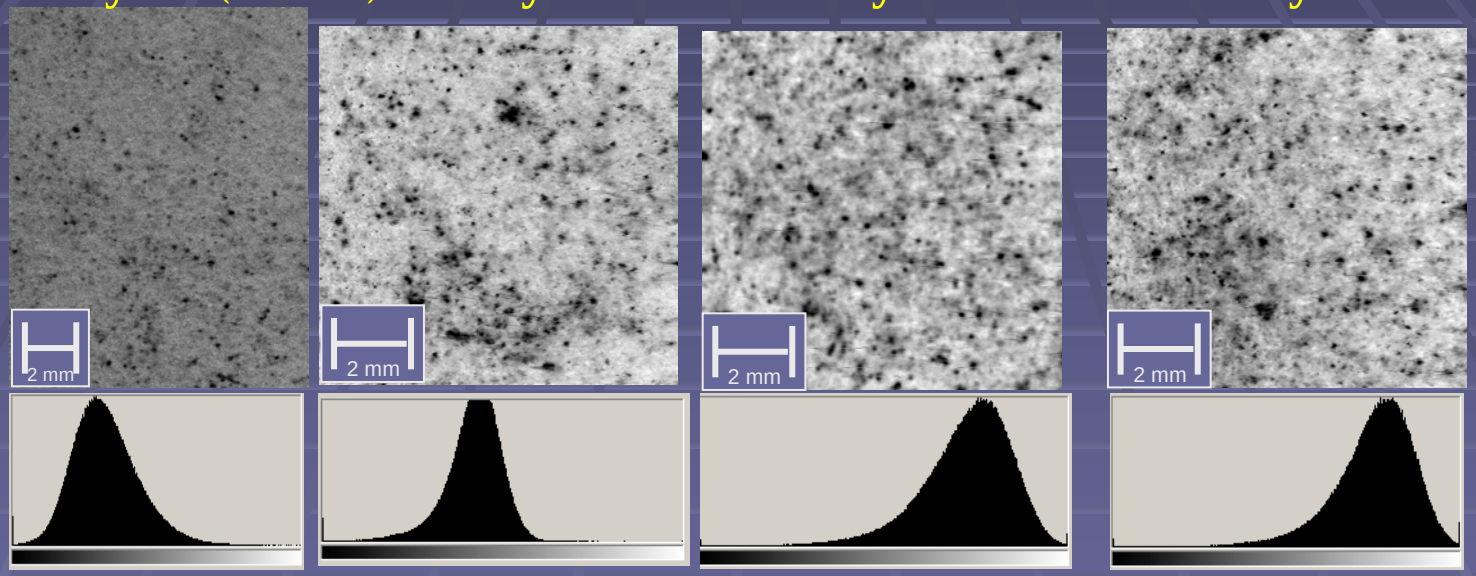

Note: All backscatter data presented as normalized data: meaning all four scans are combined to form one data set.

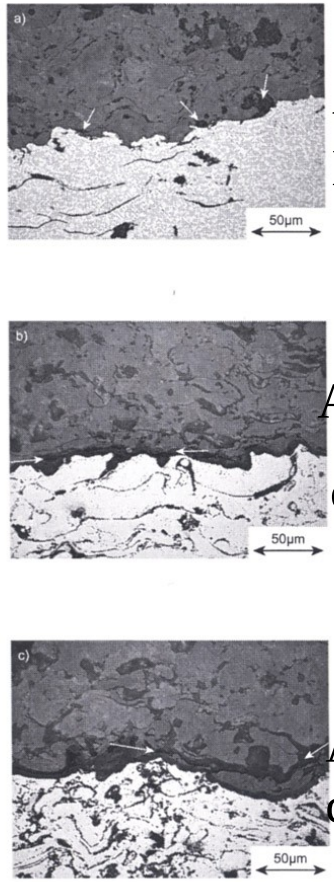

As produced

After 100 cycles

After >200 cycles

50 um

Figure 5: Development of the TBC delamination process. Figure a) shows the as coated state, b) correspond to the microstructure with interface cracks, c) represent the interface with kink crack.

Optical Photomicrographs of APS coating showing development of cracking at the TBC/TGO interface as a function of thermal cycles

From Brodin and Jinnestrand, Univ. Linkoping, Sweden, 2004

GRAY SCALE MEAN VALUE vs THERMAL CYCLES FOR SAMPLE SET 3-APS

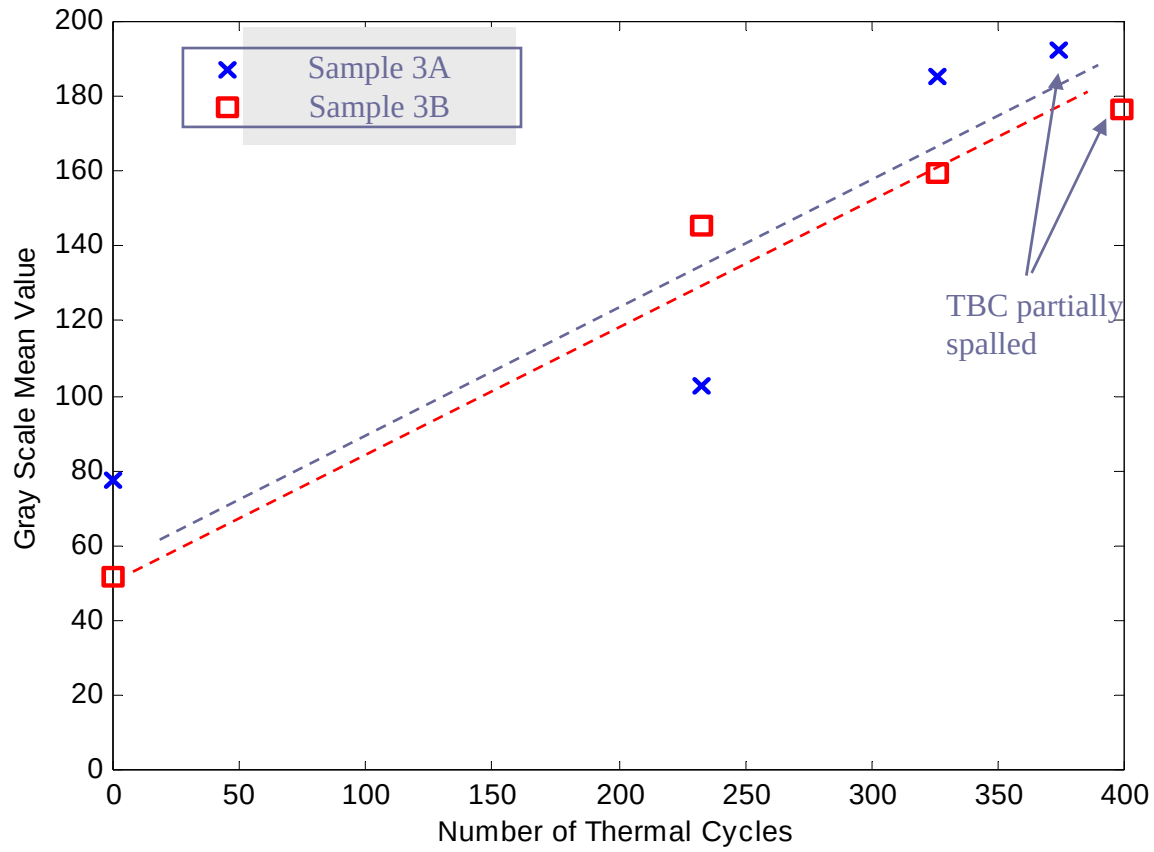

COEFFICIENT OF VARIATION vs THERMAL CYCLES FOR SAMPLE SET 3--APS

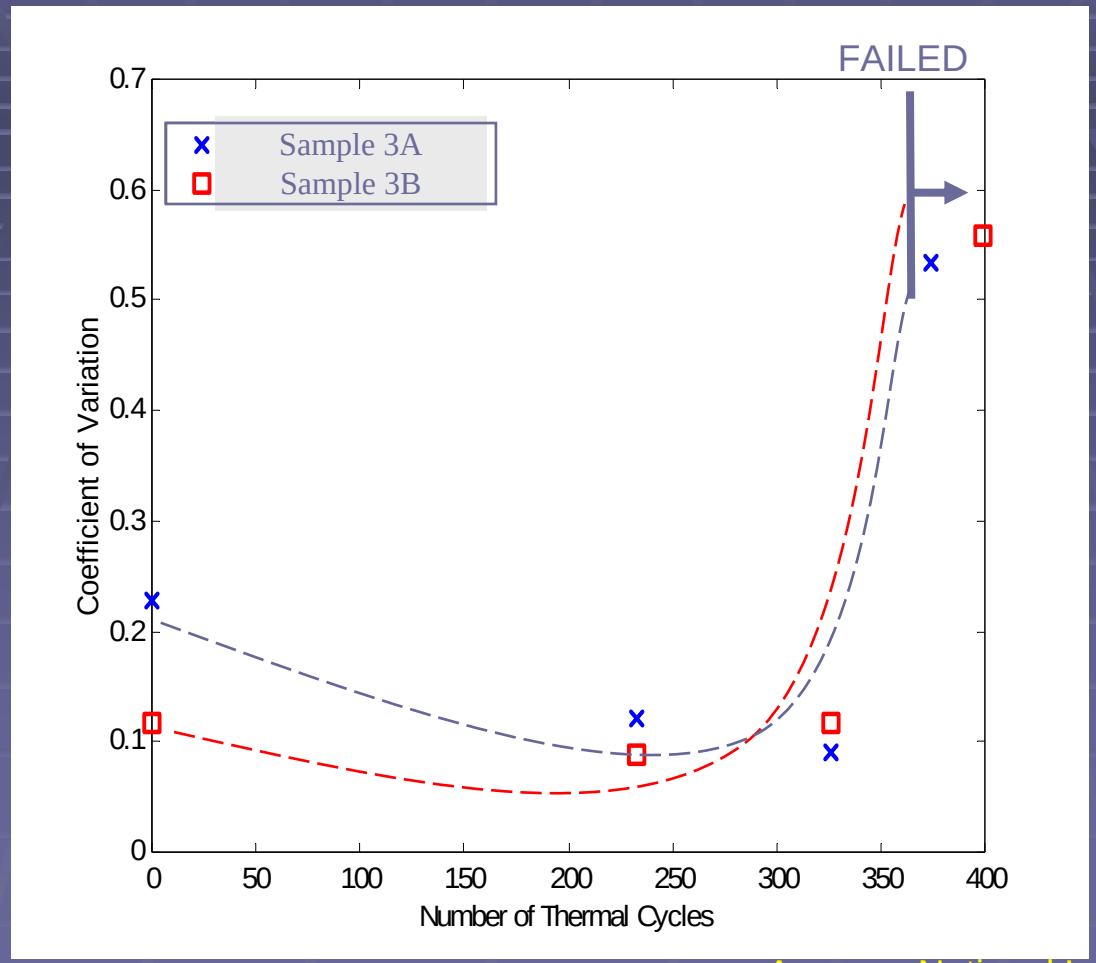

APS/TBC Cv vs THERMAL CYCLES
WAVELENGTH = 700, 750, 800, 850 nm

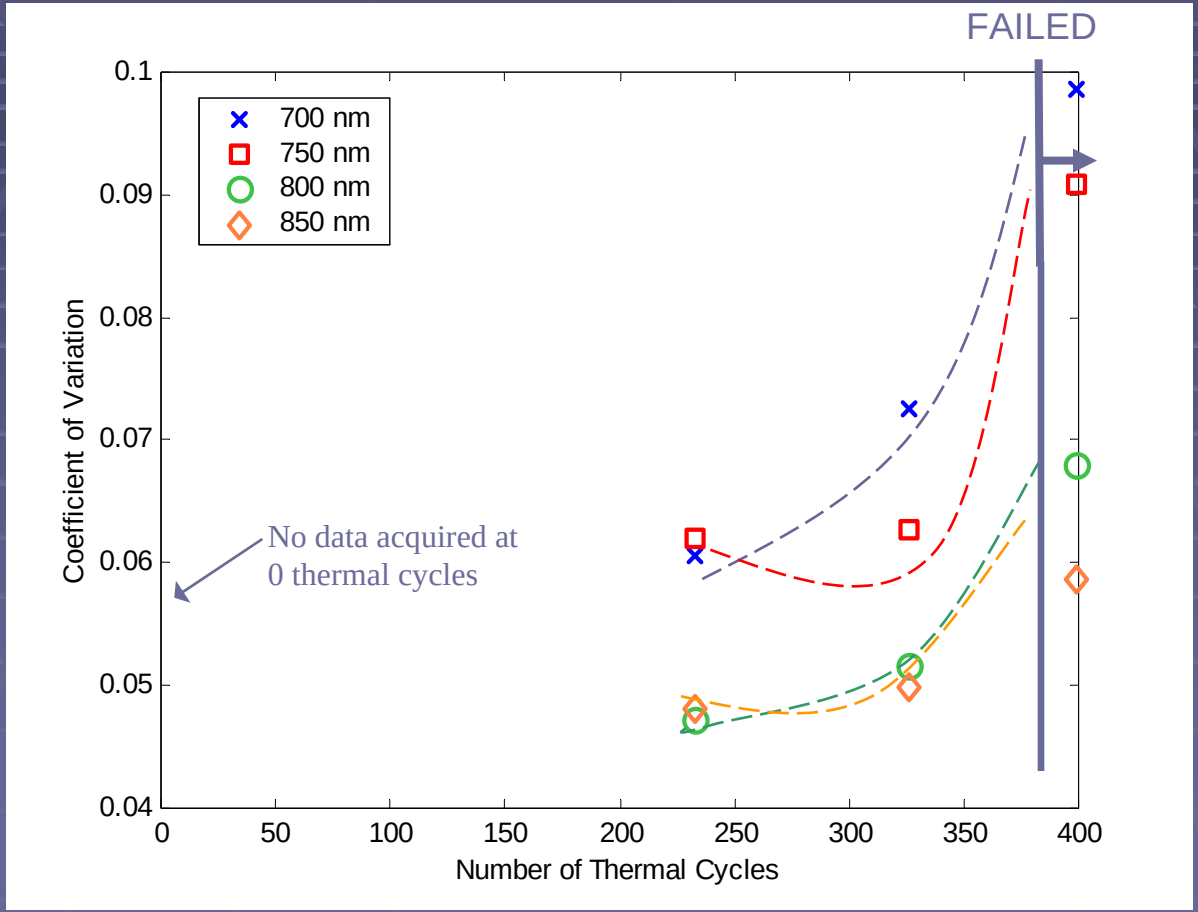

Average Power As A Function of Thermal Cycles (Sample Set 3--APS)

Sample 3A

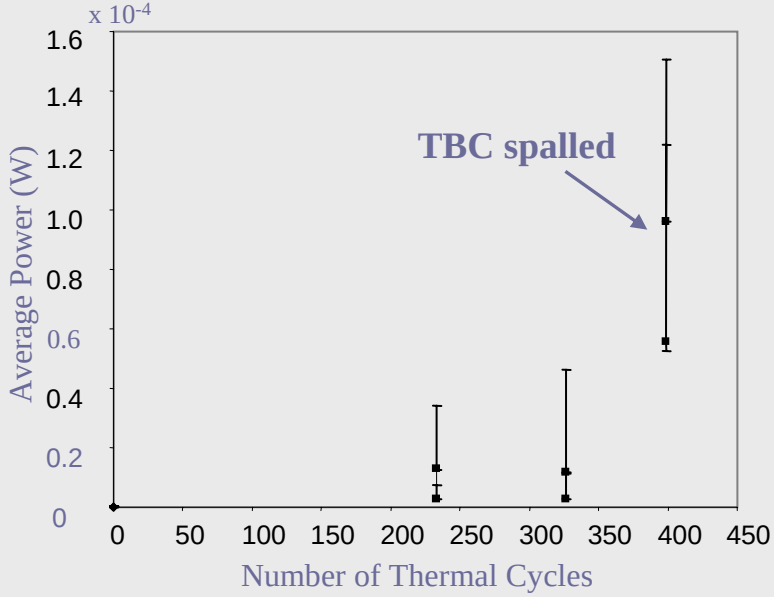

Sample 3B

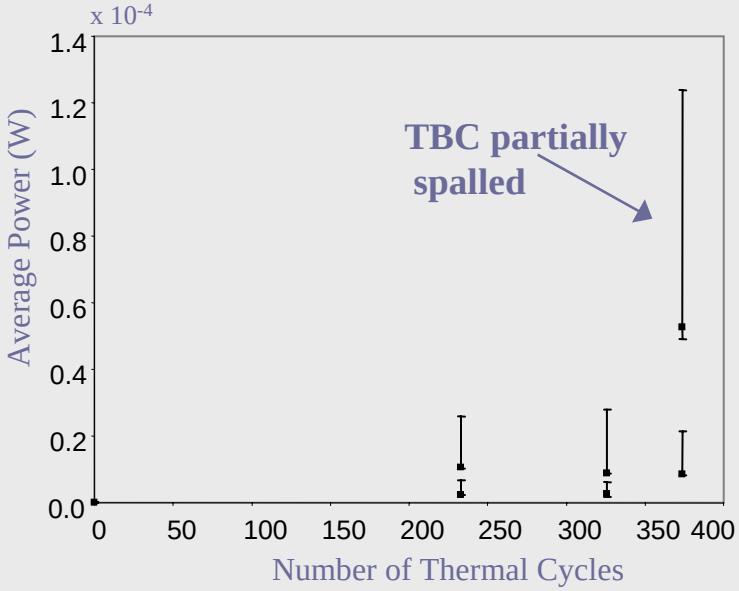

Delamination damage development in thermal barrier coatings

Delamination crack growth, APS

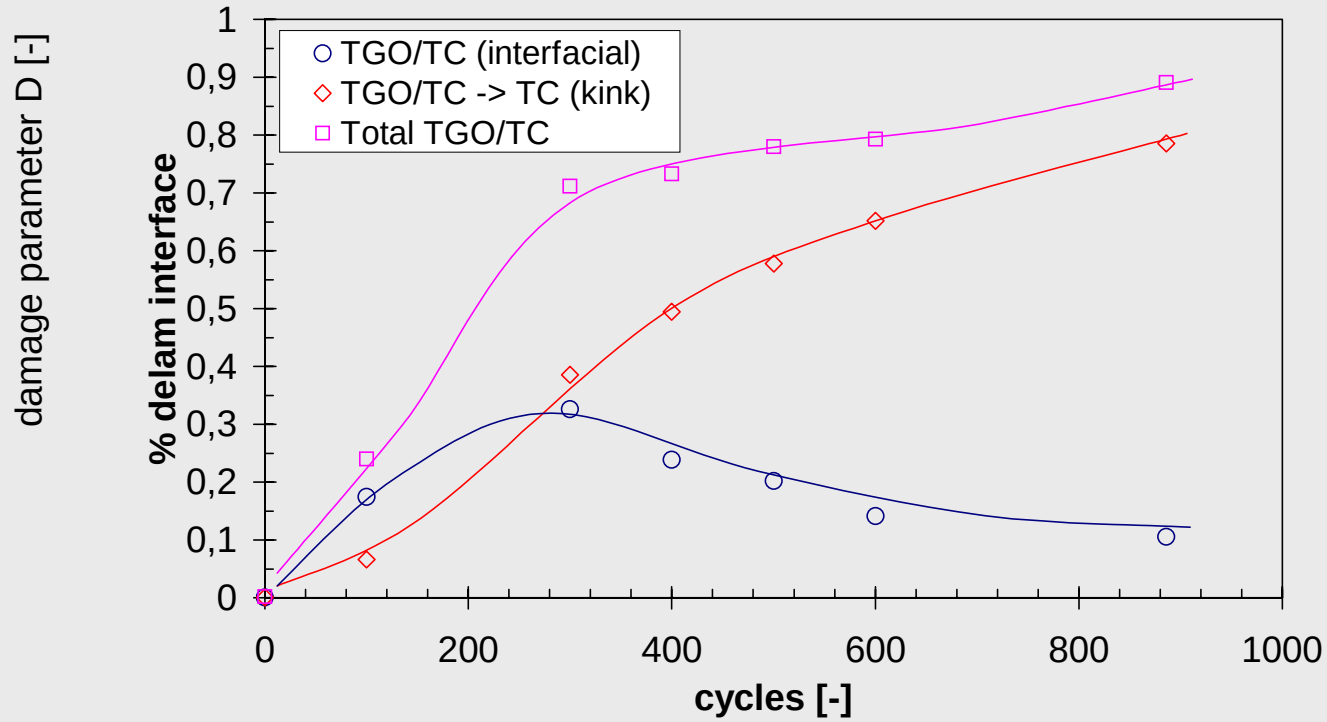

Development of interface damage during TCF testing.

After Bronin and Jinnestrand, Univ. Linkoping, Sweden , 2004

Delamination damage development in thermal barrier coatings

Delamination development

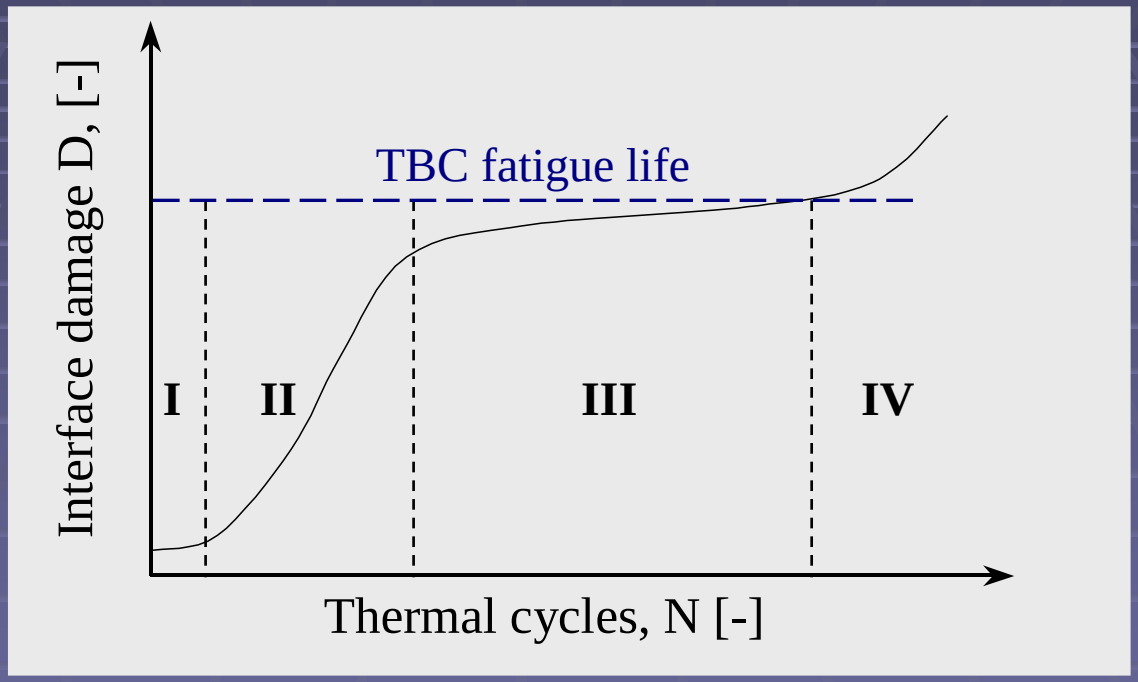

General TBC delamination behaviour.. Region I – initiation, II – fast crack growth, III – slow crack growth and IV – spallation.

After Bronin and Jinnestrand, Univ. Linkoping,Sweden, 2004

OPTICAL TRANSMISSION CHARACTERISTICS OF EB-PVD 7YSZ COATING

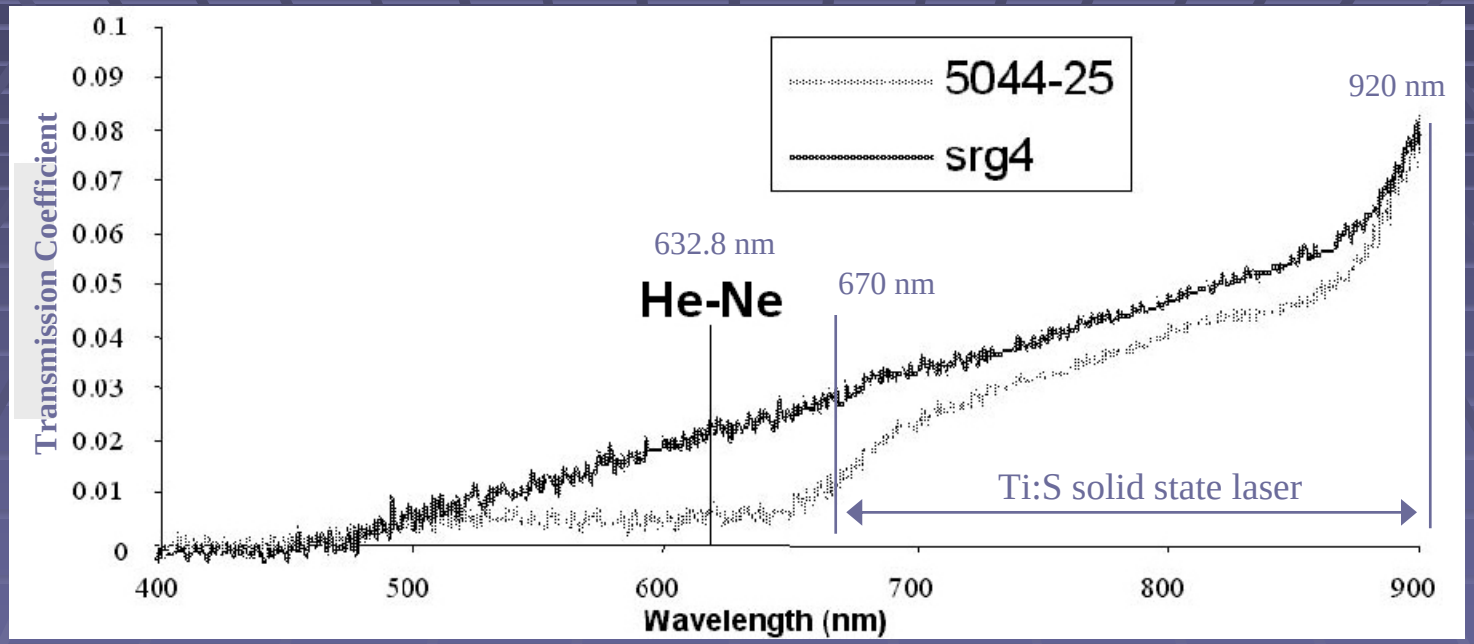

INVESTIGATION OF EB-PVD TBC SAMPLE WITH KNOWN DELAMINATIONS

(sample courtesy of B.Baufeld, German Aerospace Center, Cologne, Germany)

Digital Photograph

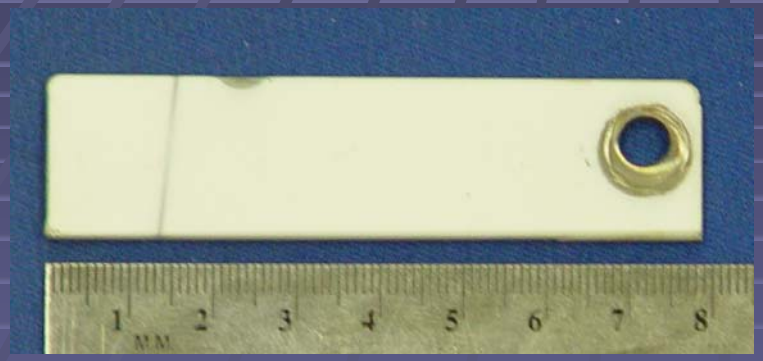

5X Optical Micrograph

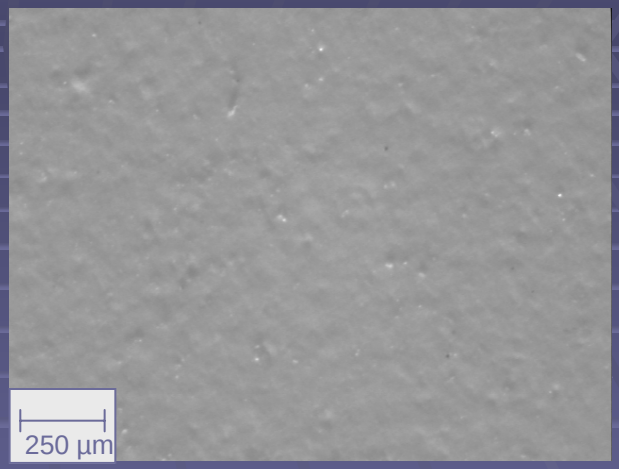

Sample Schematic Showing Intentional Delaminations (not to scale)

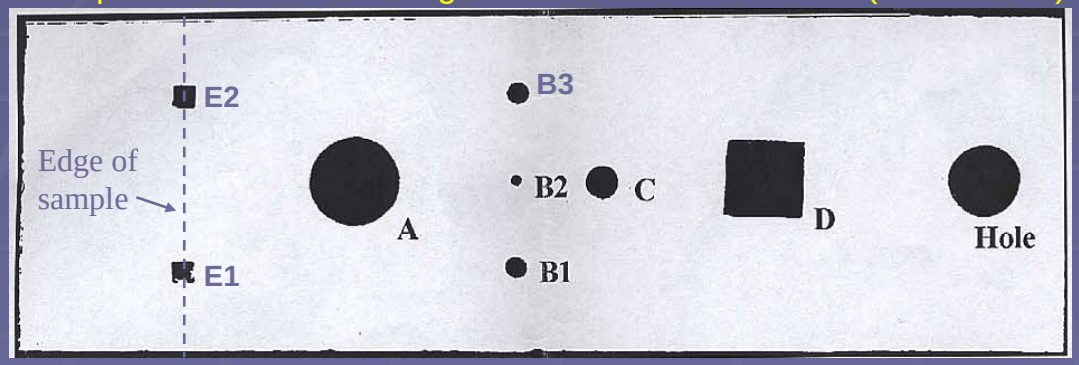

Defects A, B1, B2, C & D were intentionally introduced to the bond coat before applying the TBC to produce known delaminations.

MCrAlY bond coat with EB-PVD YSZ TBC

Comparison of Elastic Optical Scattering Data to Thermal Image Data –EB-PVD

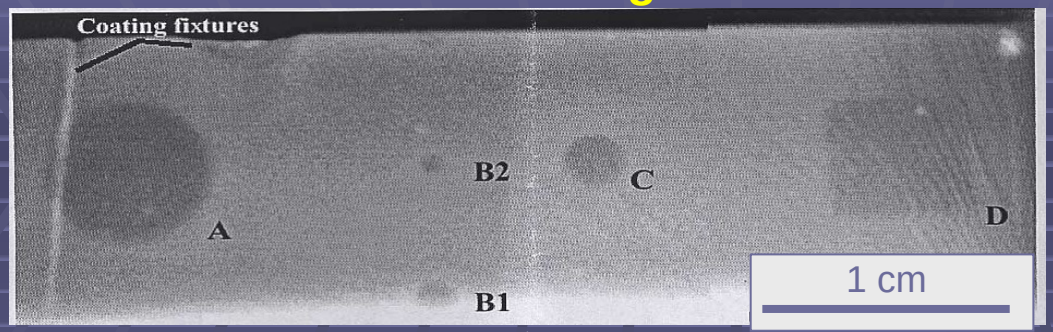

Thermal Image
(provided by B.Baufeld, German Aerospace Center)

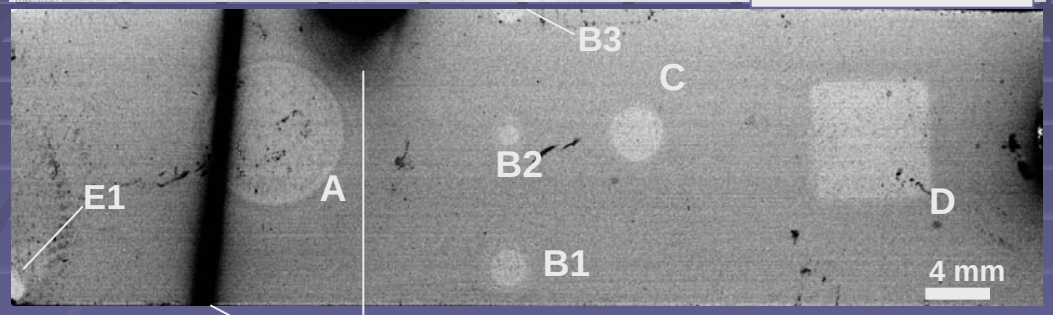

Power Scale
337.9 x 10^{-9} W
8.722 x 10^{-9} W

EOS Image

Approximate Defect Sizes

A → 8 mm	B3 → 2 mm
B1 → 2.5 mm	C → 3.5 mm
B2 → 1 mm	D → 7 mm

Average Power Values of "Defect" Regions (x10^{-9} W)

Region	Mean	% Diff	Region	Mean	% Diff
A	253.7	8.10	B3	309.2	31.75
B1	268.8	14.53	C	293.1	24.88
B2	287.9	22.67	D	282.4	20.29
Intact Coatin	234.69	n/a			

Advanced Signal Processing For Enhancement of Laser Backscatter Features

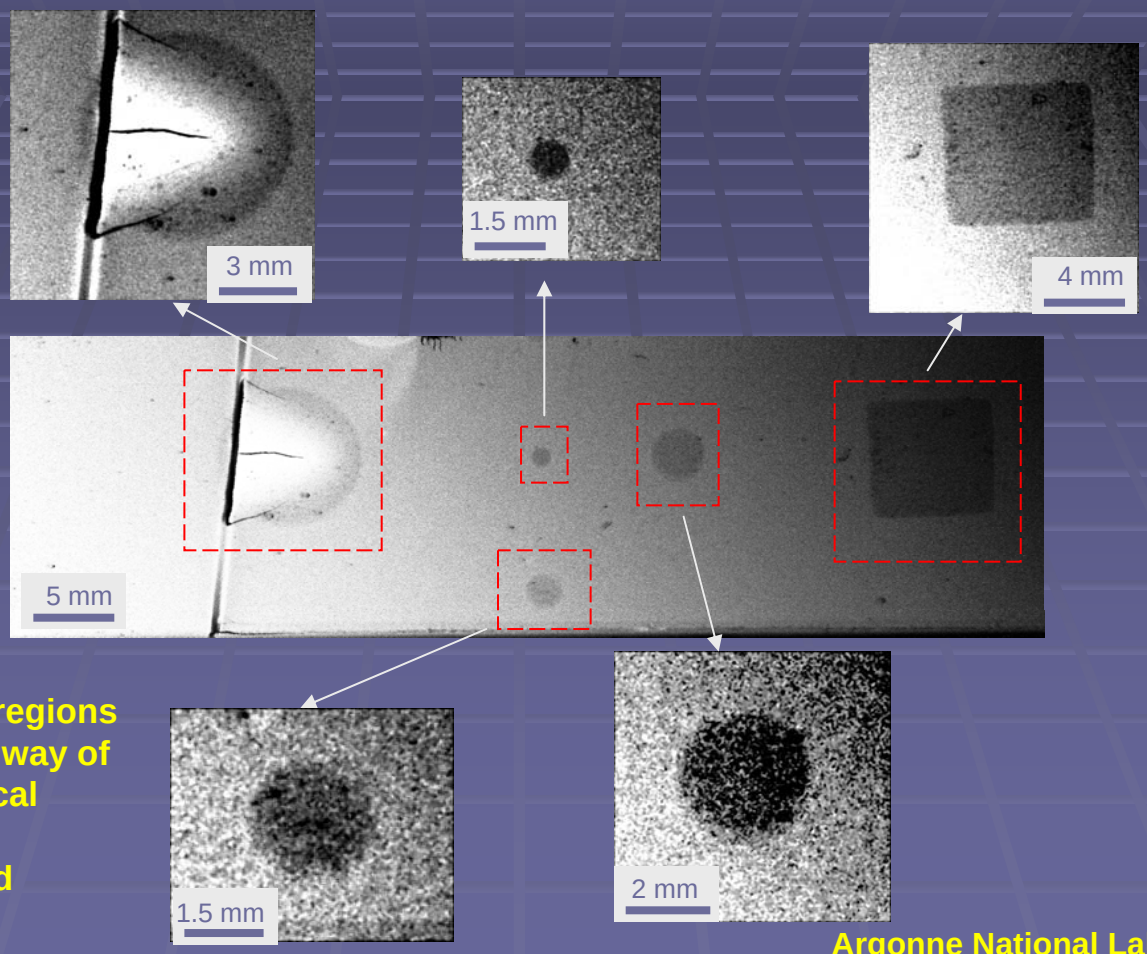

Local defect regions enhanced by way of order statistical filtering and neighborhood equalization.

Comparison Between Elastic Optical Scattering and Thermal Imaging of Known Defect—EB-PVD

Sample courtesy of B. Baufield, German Aerospace Center, Cologne, Germany

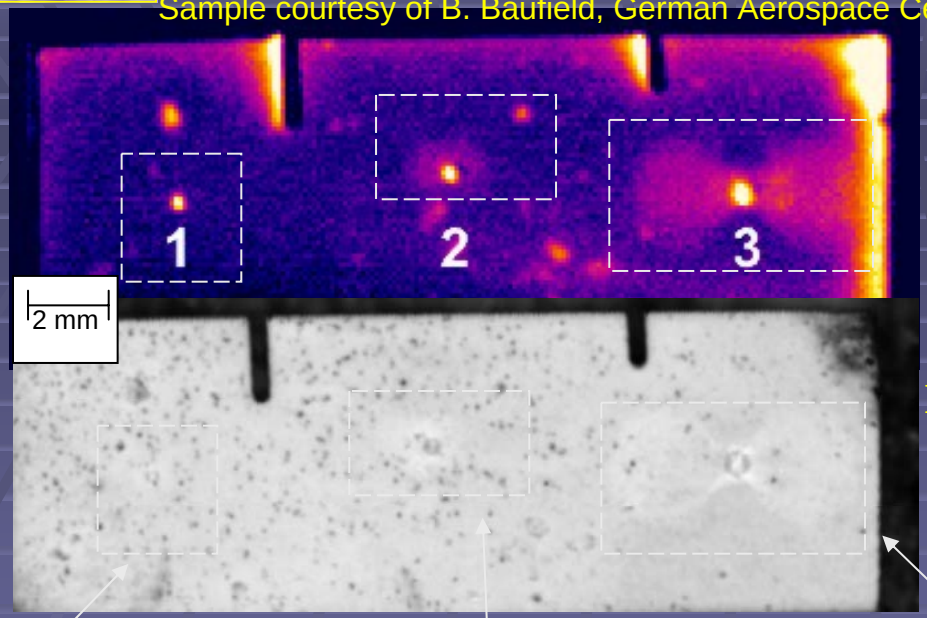

Thermal Image

EOS Image

Indent 1: 62.5 kg load
Indent 2: 125 kg load
Indent 3: 250 kg load

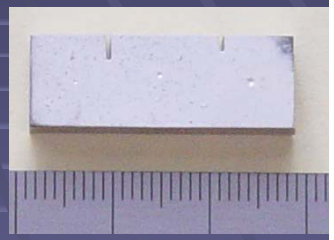

Power Scale

267.6×10^{-9} W

5.204×10^{-9} W

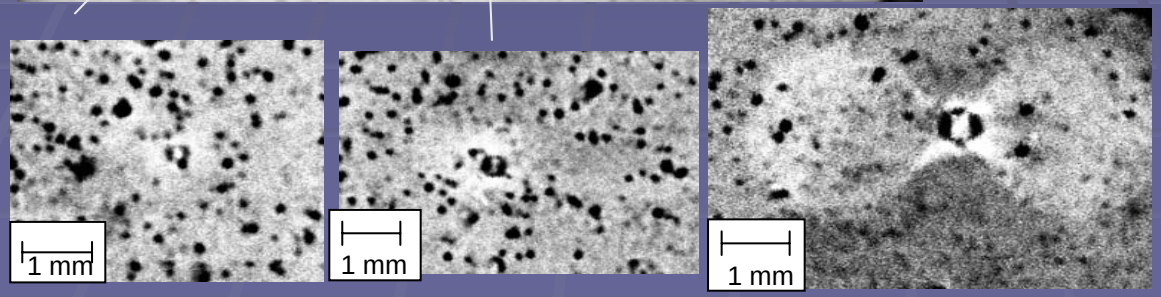

Note: Each sub-region has been normalized using only the detected power values within that region.

Effect of Thermal Cycling of EB-PVD TBC on Elastic Optical Scattering

MCrAlY Bond Coat with EB-PVD YSZ TBC

Sample Set 1

48 Cycles

96 Cycles

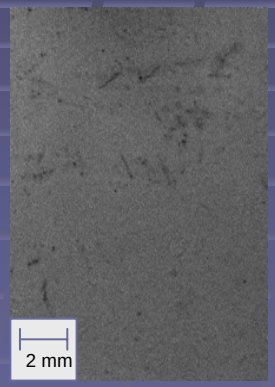

146 Cycles

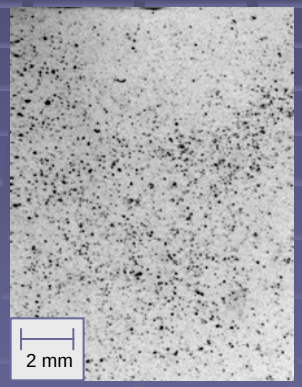

171 Cycles

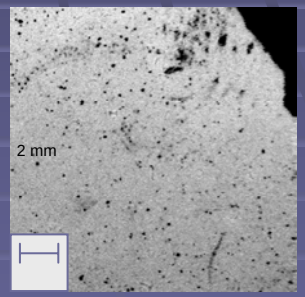

191 Cycles

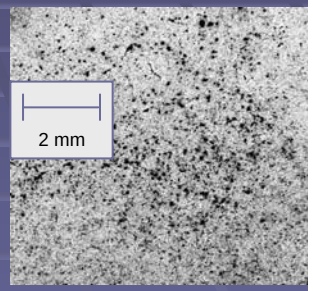

Note: All backscatter data presented as normalized data: meaning all four scans are combined to form one data set.

Average Power As A Function of Thermal Cycles (Sample Set 1—EB-PVD)

Sample 1A

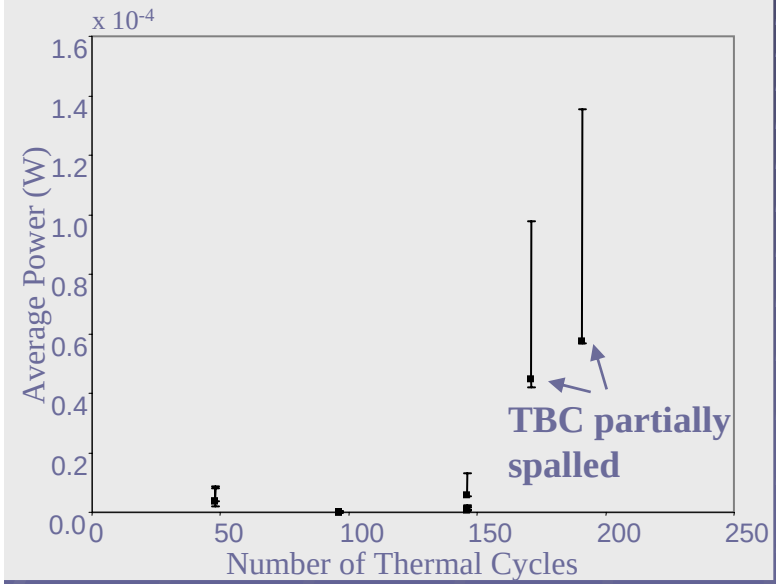

Sample 1B

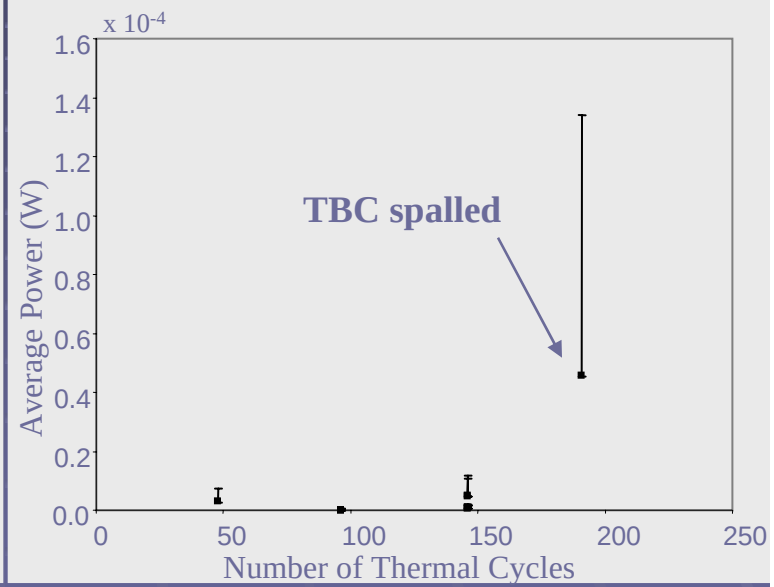

Average Power As A Function of Thermal Cycles (Sample Set 2—EB-PVD)

Sample 2A

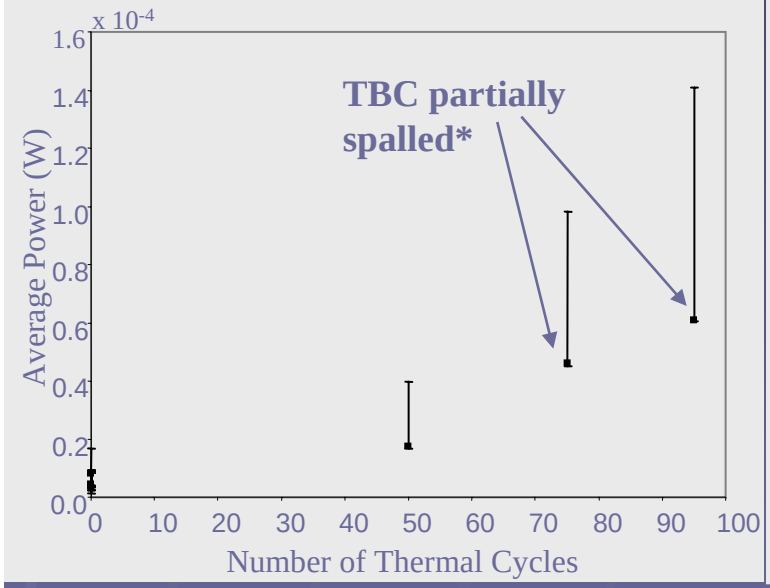

Sample 2B

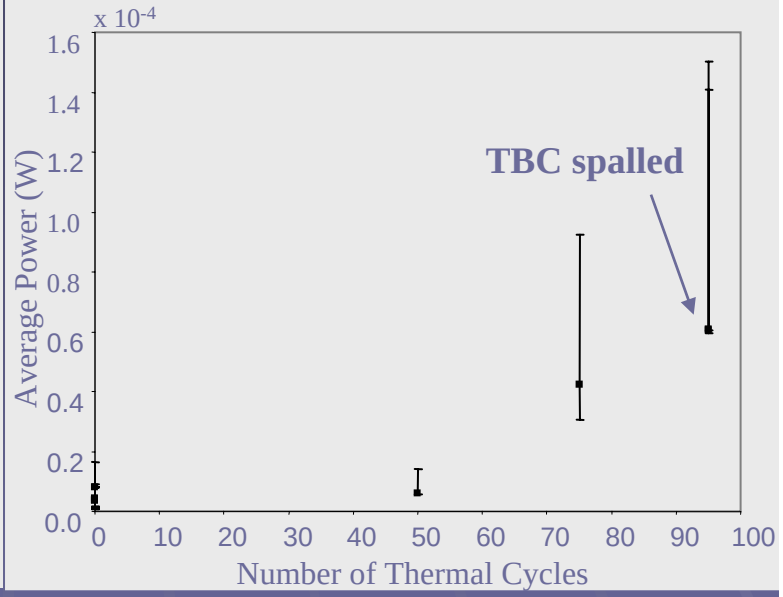

* Note: Sample 2A failed between thermal cycles 95 and 115.

Simulation of Elastic Optical Scattering
TBC Model Geometry

Layered geometry
- Base Case

5μm V-notch on Conductor

Layers (base case)

- 2μ Alumina
- 10μ Zirconia
- Vacuum on top

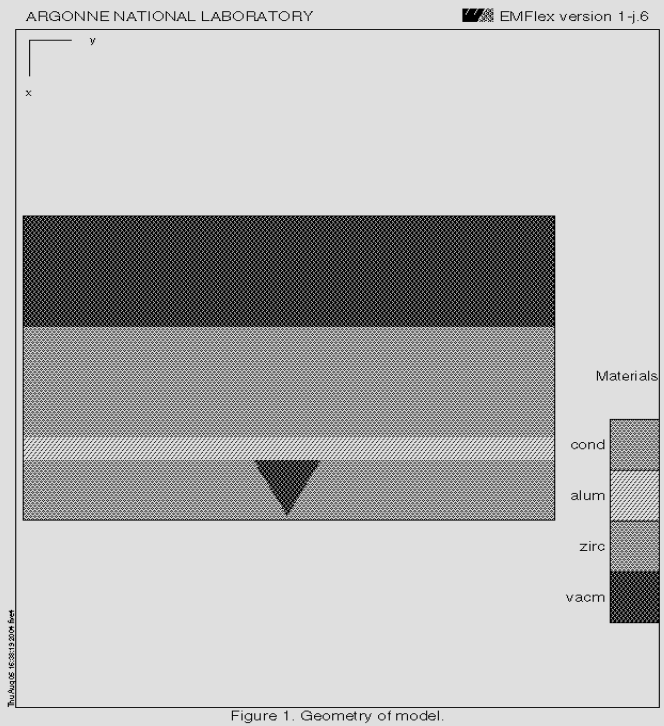

Figure 1. Geometry of model.
(5mu Geometry)

Finite Element Model Simulation of Elastic Optical Scattering TBC Layered Model Scattered Electric Field

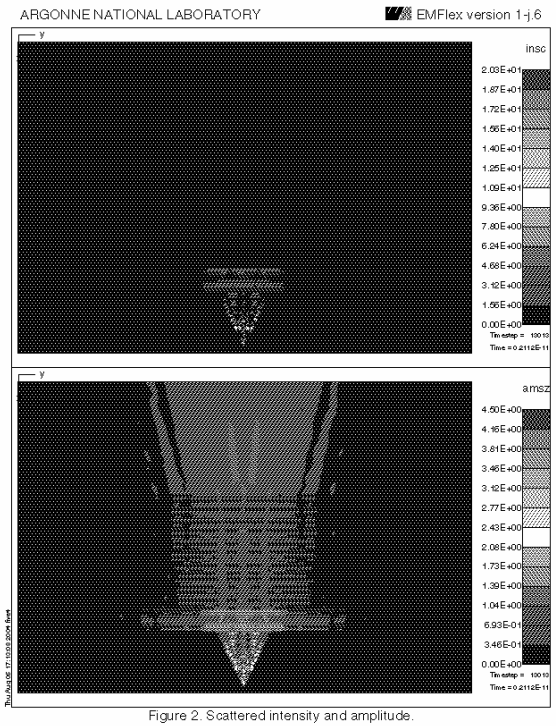

Figure 2. Scattered intensity and amplitude.
(5mu Geometry)

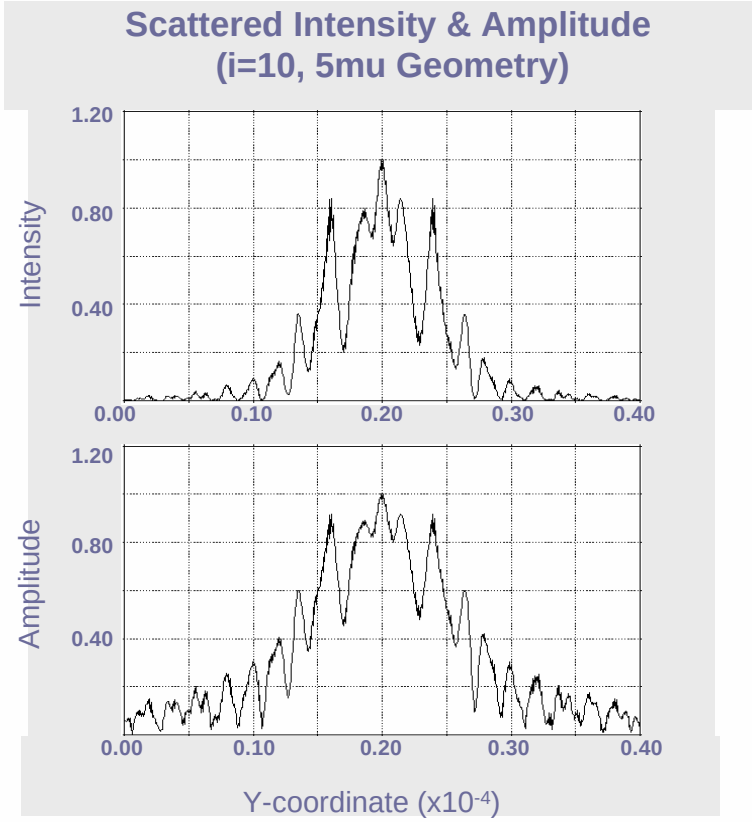

Comparison Between Model Predication and Elastic Optical Scattering Results

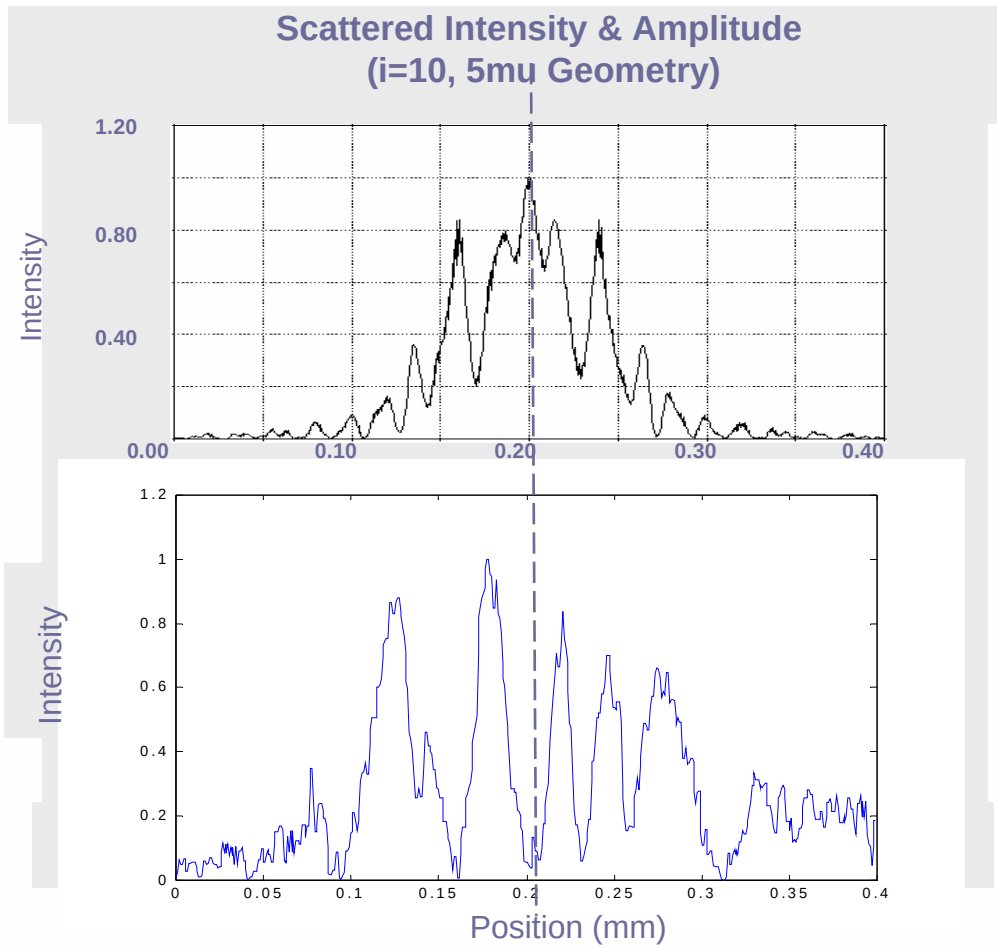

Theoretical Prediction

Experimental Result

Comparison Between Model Predication and Laser Backscatter Results

Theoretical prediction

3D representation of Scattered Amplitude

Experimental result

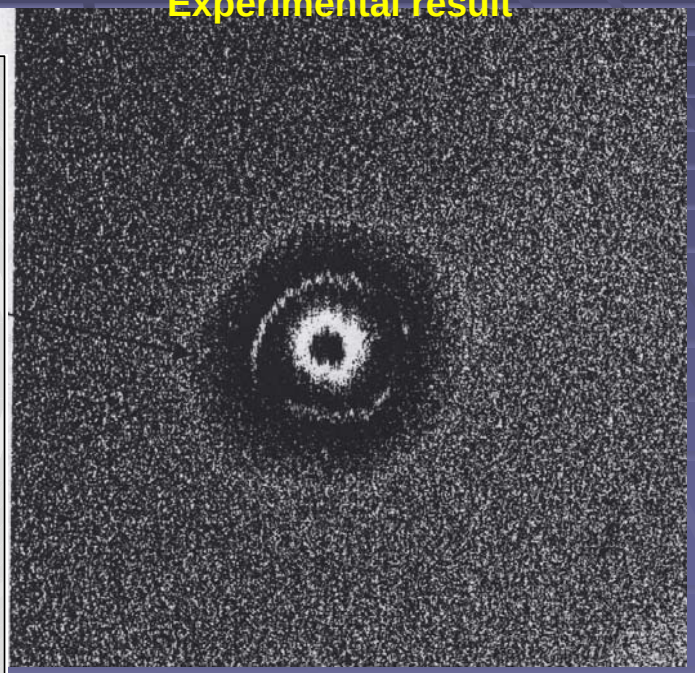

EB-PVD TBC Sample Courtesy of University of Pittsburgh

OPTICAL COHERENCE TOMOGRAPHY

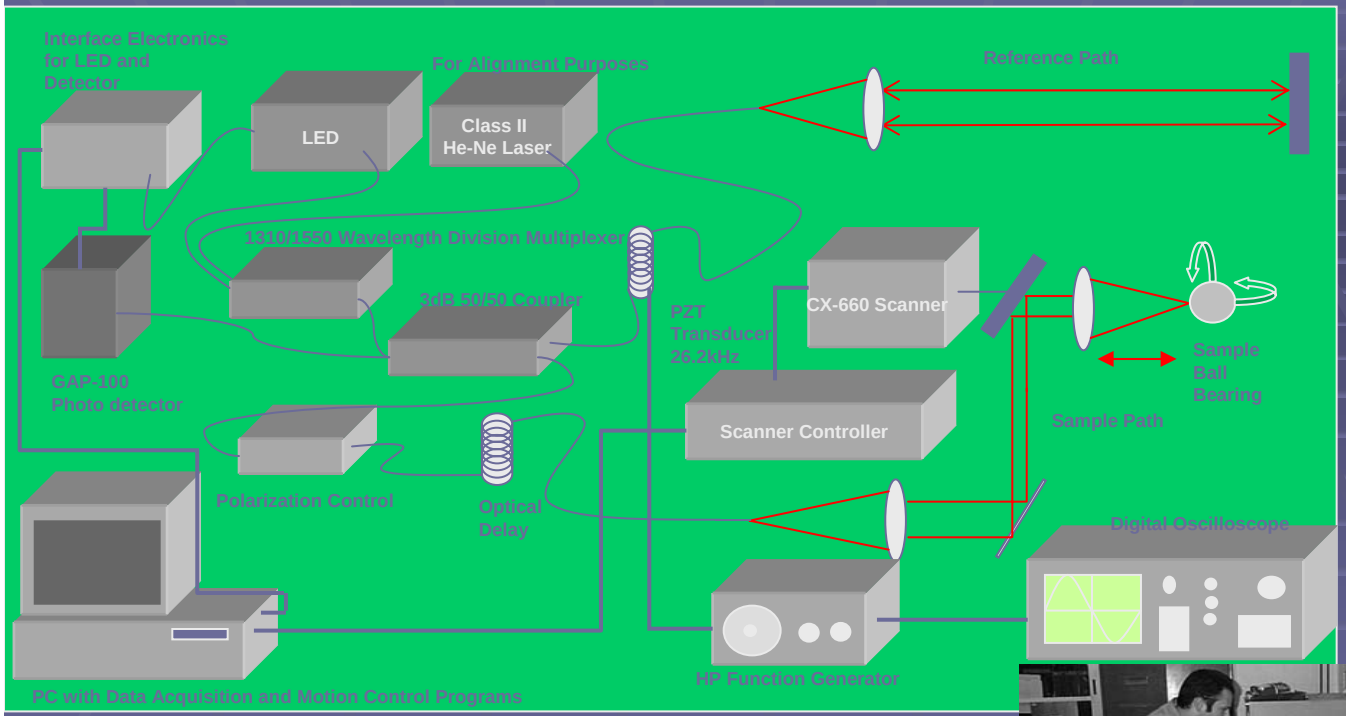

ARGONNE'S OPTICAL COHERENCE TOMOGRAPHY SYSTEM

Provided by Saint Gobain Ceramics and Plastics

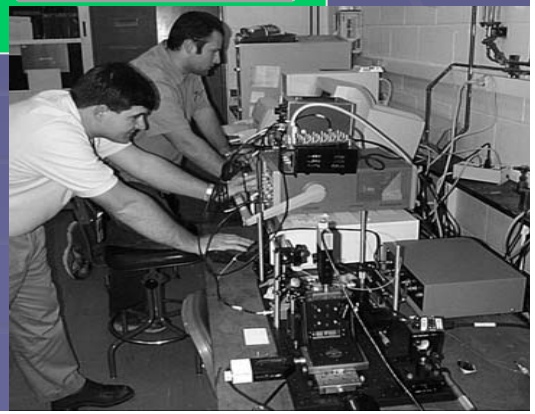

APPLICATION OF OCT TO EB-PVD YSZ TBC

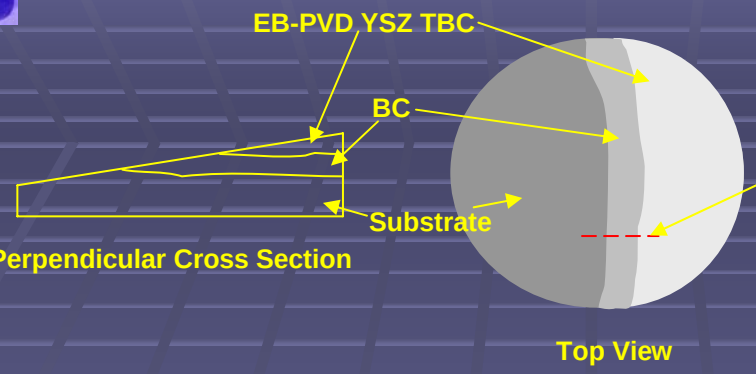

OCT Vertical Cross-Section

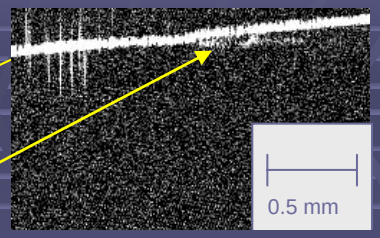

TBC/BC interface

25 mm diameter sample polished to expose bond coat and substrate (MCrAlY Bond coat with EB-PVD YSZ TBC)

OCT Vertical Cross-Section

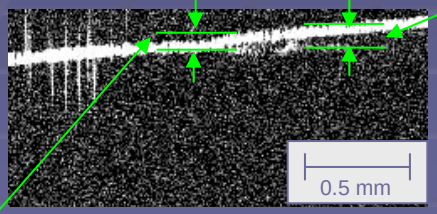

Dimension B

Dimension A

Optical Micrograph (5X)

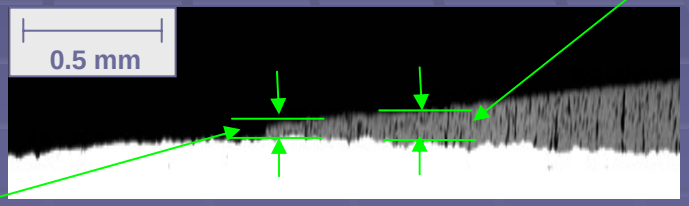

Dimension B

Dimension A

TBC Thickness Measurements	Dim. A	Dim. B
Micrograph	25 µm	44 µm
OCT	20 µm	50 µm

OCT measurements taken from middle of white line

SUMMARY

- INITIAL CORRELATIONS ESTABLISHED BETWEEEN EOS DATA AND DAMAGE LEVELS IN TBCs FROM THERMAL CYCLING FOR BOTH APS AND EB-PVD TBCs.

- RECENT EUROPEAN WORK ON APS TBCs SUGGESTS THAT THE Argonne EOS DATA TRACKS WITH THERMAL CYCLING DAMAGE LEVELS BOTH PREDICTED AND EXPERIMENTALLY OBTAINED

- LASER-BASED ELASTIC OPTICAL BACKSCATTER (EOS) TECHNOLOGY HAS BEEN DEMONSTRATED TO DETECT DISBOND REGIONS OF EB-PVD TBCs.

SUMMARY-2

OPTICAL COHERENCE TOMOGRAPHY HAS BEEN DEMONSTRATED TO MEASURE COATING THICKNESS OF EB-PVD WITHOUT DESTRUCTION OF THE SAMPLE

THEORETICAL FINITE ELEMENT MODEL HAS BEEN DEMONSTRATED TO CORRELATE TO EXPERIMENTAL EOS DATA WHICH MAY ENHANCE FAILURE PREDICTION CAPABILITIES

PLANNED FUTURE EFFORTS

- EXPAND THE LASER BACK SCATTER EXPERIMENTAL EFFORTS ON THICK APS THERMAL BARRIER COATINGS (THICK, >500um-1MM)
- ESTABLISH THE LASER BACK SCATTER COMPUTER MODEL TO INCLUDE THICK APS TBCS
- FURTHER VALIDATE THE LASER BACK SCATTER DATA WITH A WIDER VARIETY OF SUBSTRATE MATERIALS, BOND COAT SYSTEMS AND COMPOSITIONS OF TBCS(Including new material using nanophase powders)
- FURTHER DEVELOP THE OPTICAL COHERENCE TOMOGRAPHY SYSTEM THROUGH INSTALLATION OF FEMTO-SECOND LASER (Higher power and larger bandwidth)
- EXPAND INTERACTIONS WITH EUROPEAN, UK AND JAPANESE PARTNERS
- BEGIN INITIAL EFFORTS TO LOOK AT COUPLING TO FIBER OPTIC ARRAYS FOR “ON-ENGINE” INSPECTION CAPABILITY

U.S. Department of Energy
Energy Efficiency and Renewable Energy

industrial technologies program

DOE-EERE Industrial Technologies Program (ITP)

Fossil Energy Materials
Knoxville, TN
May 9-11, 2005

Sara Dillich
Industrial Technologies Program
Energy Efficiency and Renewable Energy
U.S. Department of Energy

DOE- EERE Programs

- Biomass
- Building Technologies
- Distributed Energy
- Federal Energy Management
- Freedom CAR & Vehicle Technologies
- Geothermal Technologies
- Hydrogen, Fuel Cells, & Infrastructure Technologies
- Industrial Technologies (ITP)
- Solar Energy Technologies
- Weatherization & Intergovernmental
- Wind & Hydropower Technologies

ITP Program Areas

Industry Specific

- Aluminum
- Chemicals
- Forest Products
- Glass
- Metal Casting
- Mining
- Petroleum
- Steel

Crosscutting Technologies

- Combustion
- Sensors & Automation
- Materials
- Supporting Industries

Best Practices

MISSION

Improve the energy efficiency of U.S. industry through coordinated research and development, validation, and dissemination of innovative technologies and practices.

Energy Use By Industry

Total 2001 End Use: 32.3 Quads

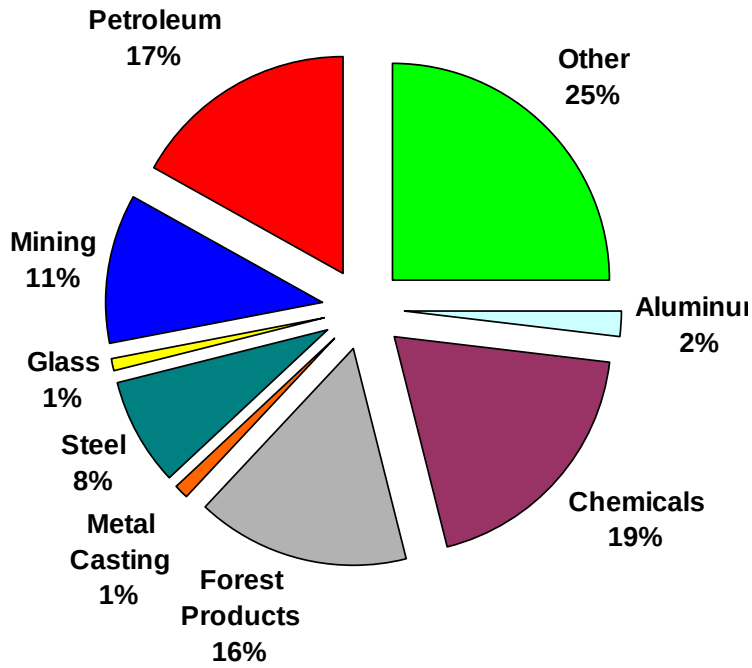

- David Rodgers, Acting Program Manager

Technology Manager:

Sara Dillich	Materials

Golden Field Office:

Mahesh Jha	Materials
Brad Ring	Aluminum

ITP's Total Budget

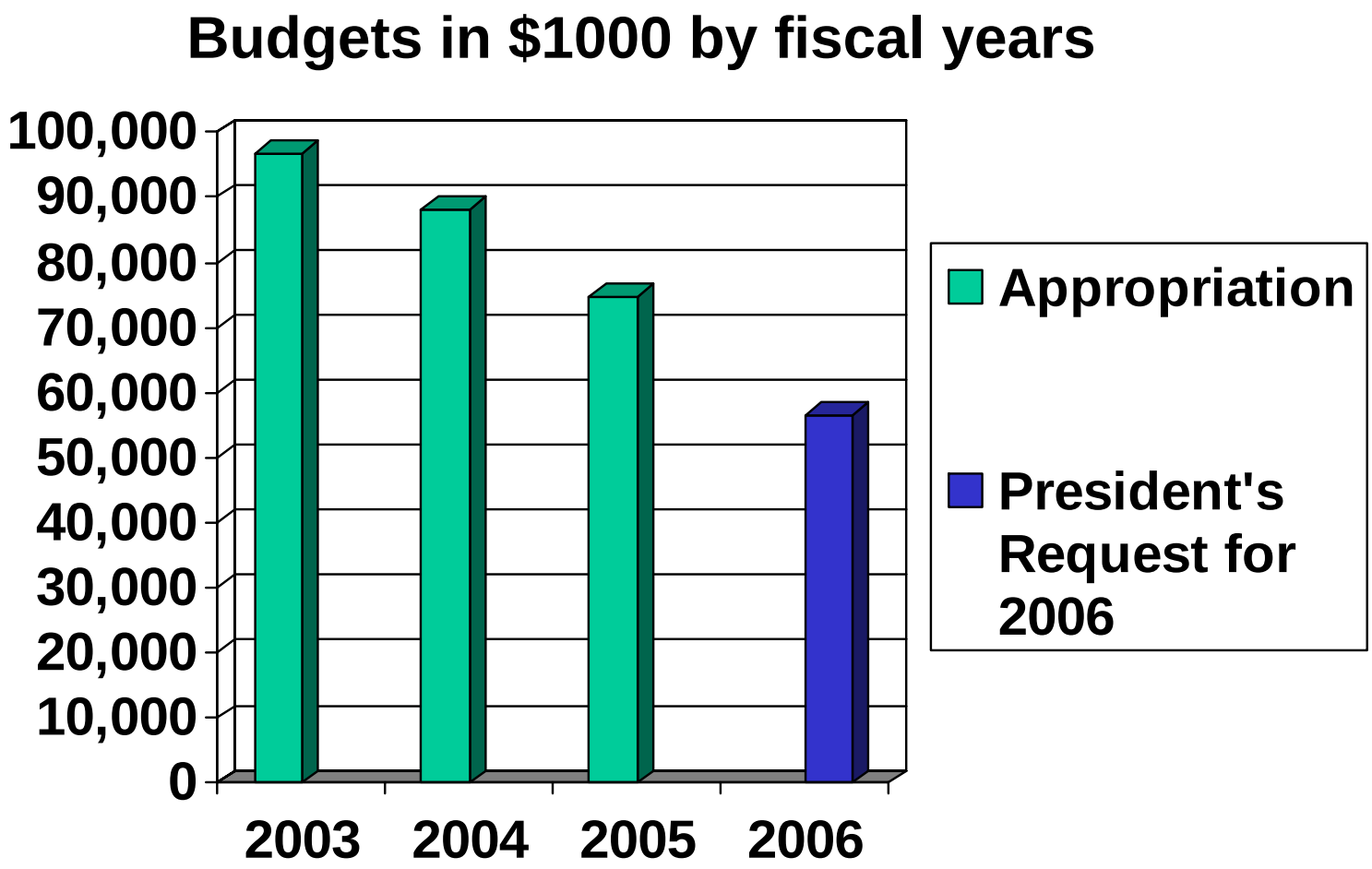

ITP partners with industry to manage risk in development of new technologies

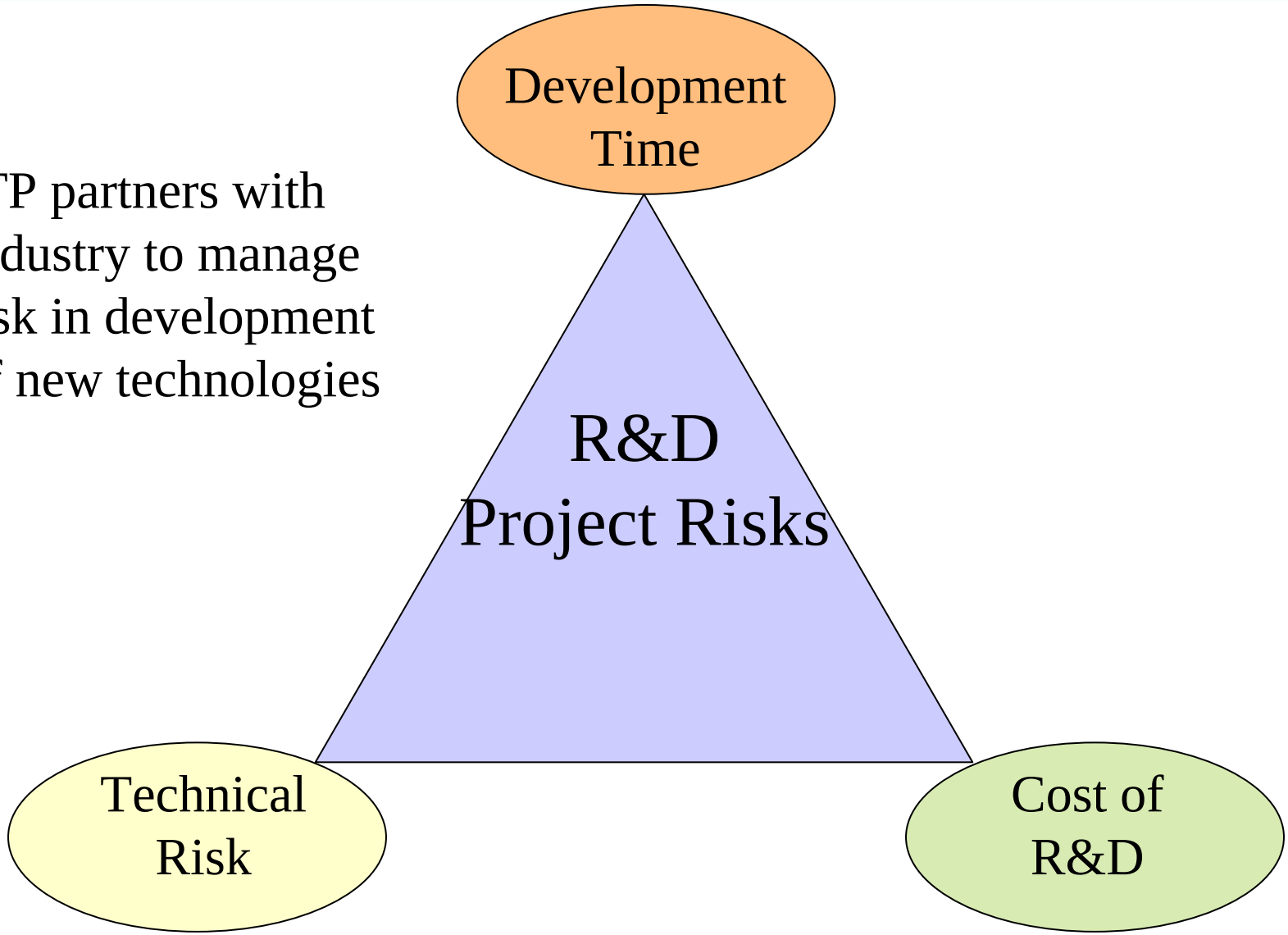

R&D Investment Strategy

Investment Strategy based on

- **Analysis** of energy savings opportunities

- Portfolio balance: want **transformational technologies** as well as shorter term

- Emphasis on **high risk, high potential impact** R&D will continue to grow

Life-path of a project

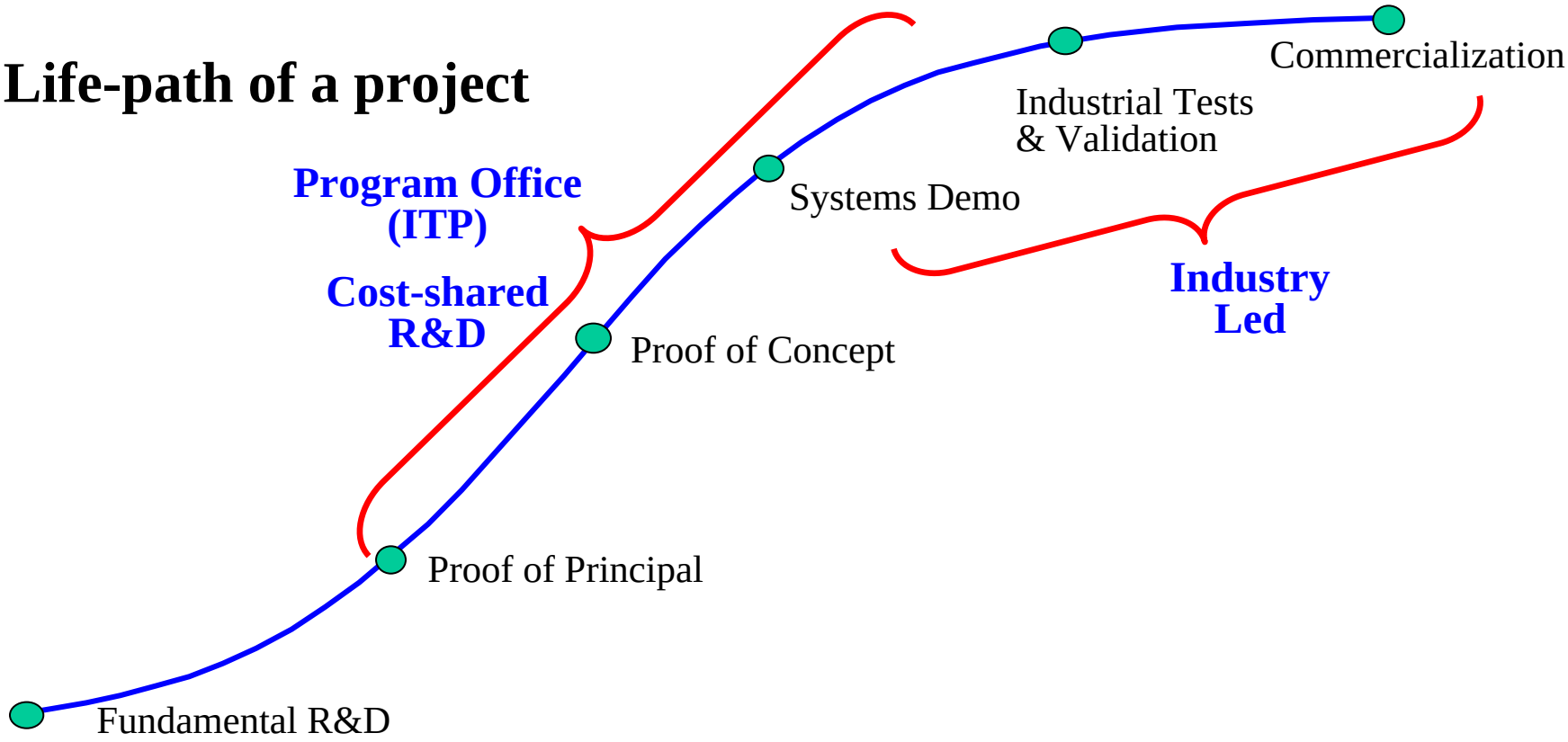

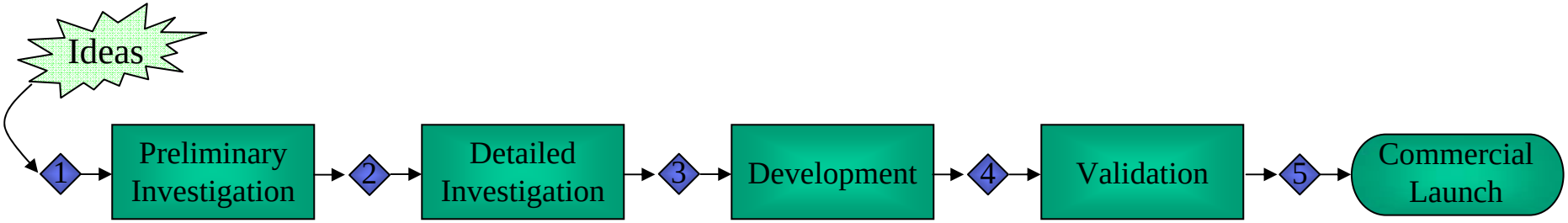

EERE Stage-Gate Process

Materials: A Cornerstone of ITP and EERE

Geothermal: Advanced drill bit materials can lead to 15% lower drilling costs.

Chemicals: If catalytic processes for the top 50 chemicals were raised to maximum yields, energy savings would exceed 0.47 quads per year.

Aluminum: Melters typically exhaust flue gases at 2,200°F, wasting over 50% of thermal input; recuperators cannot survive the corrosive flue gases to capture this energy.

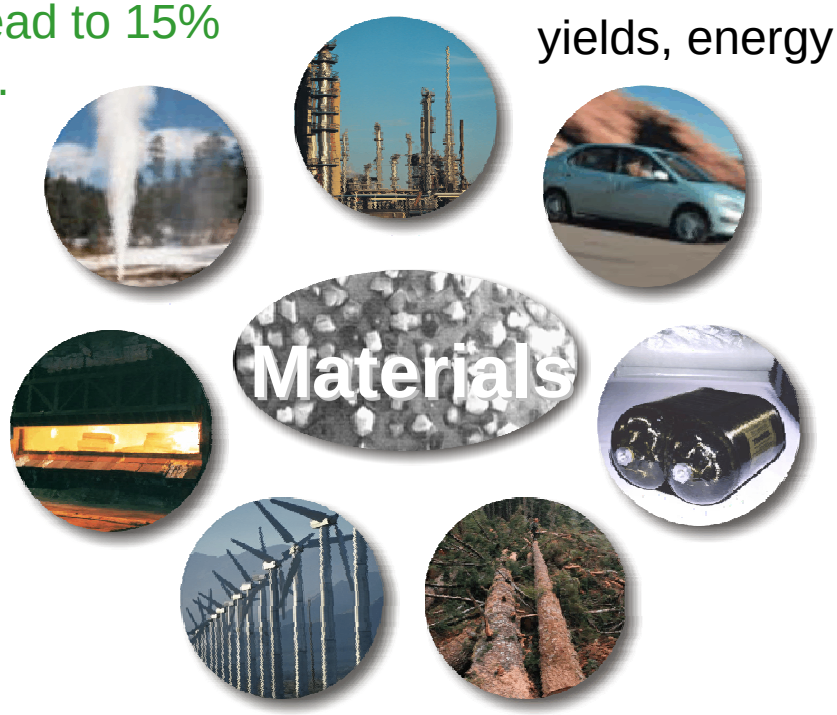

FreedomCAR: 1% vehicle weight reduction yields 0.6-0.8% higher energy efficiency.

Hydrogen Storage: Materials for pressure tanks, metal hydrides, carbon nanotubes.

Wind: Advanced tower materials can extend tower heights from today's 100 ft. to 230 ft., accessing higher-speed wind.

Forest Products: Corroding Kraft recovery boiler tube materials can force unscheduled shutdowns costing mills $300-$1,000k per day.

EERE-ITP Materials Portfolio

Mission - Lead a national effort to research, design, develop, engineer, and test new and improved materials, as well as more profitable uses of existing materials, for U.S. manufacturing and processing industries

$11 M for 2005

Materials, Aluminum, Steel, Research Budgets

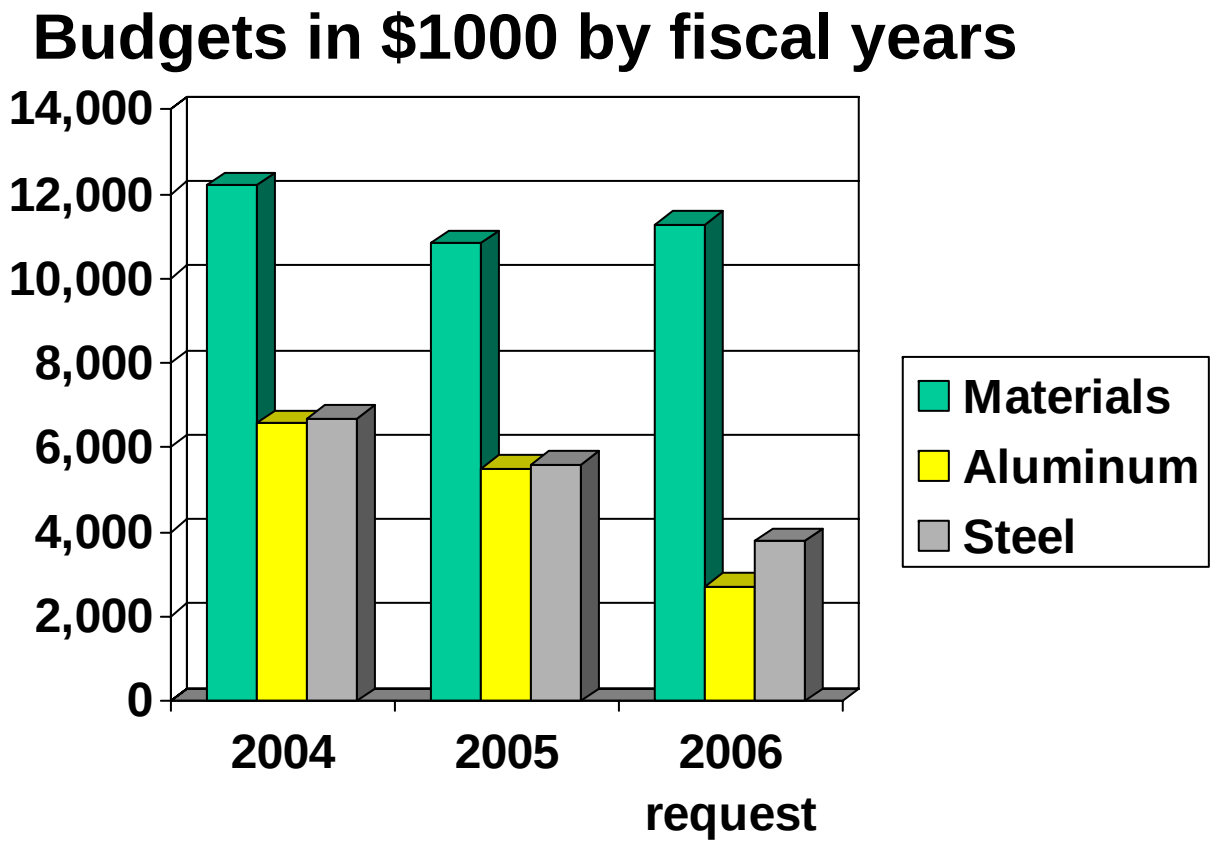

Portfolio Focus Areas

- **Degradation Resistant Materials**
  - Advanced Processing and Coatings
  - Ultra-Hard Materials
  - Metal Dusting Prevention
- **Materials for Energy Systems**
  - Refractories
  - Materials for Energy Recovery
- **Materials for Separations**
  - Membranes, Zeolites, Filters
- **Thermophysical Databases & Modeling**
  - Degradation Prediction, Transformations & Kinetics Modeling and Simulations

Materials FY 2005 Portfolio

- 30 active projects, Over 140 partners

Projects by Focus Area

Degradation Resistant Materials (18)

Materials for Energy Systems (8)

Materials for Separations (1)

Thermophysical Databases and Modeling (3)

DOE Dollars by Partner Type FY05

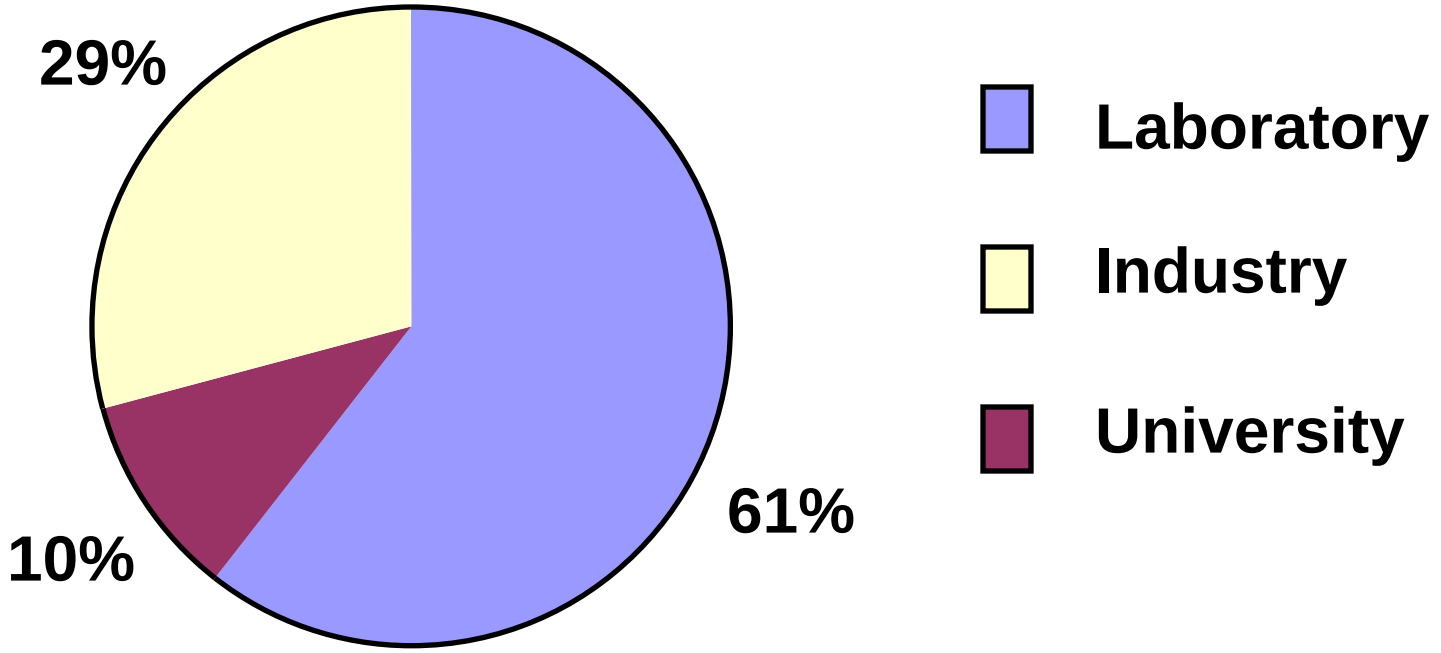

Analytic Basis for Portfolio Priorities

- Set focus areas based on areas of greatest need among manufacturing industries (Roadmaps, etc)
- Quantify potential energy savings in each focus area via Opportunity Analyses
- Issue solicitations to realize Opportunities

Focus Areas → **Opportunities Analysis** → **Projects**

1. Degradation-Resistant Materials
2. Materials for Energy Systems
3. Materials for Separation
4. Thermophysical Databases and Modeling

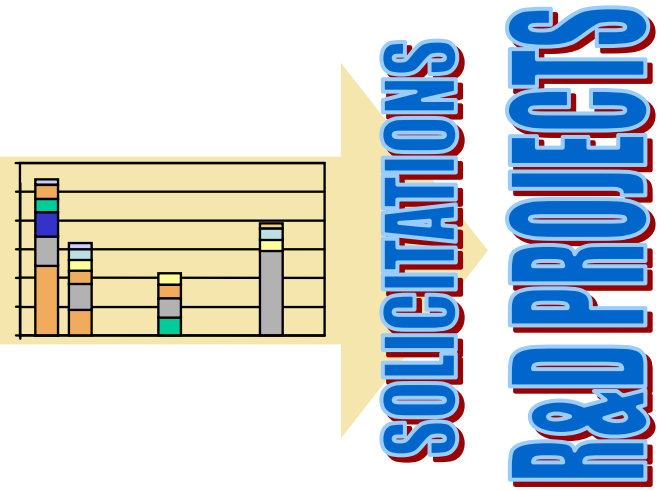

Recent Materials Analyses

Recent Reports :

- Materials for Separations
- Refractories
- Energy Use, Loss and Opportunities Analysis

In preparation:

- Materials for Waste Heat Recovery
- Nanorobotics – opportunity analysis for manufacturing industries

Analysis Report - Materials for Separation Technologies

U.S. Department of Energy
Energy Efficiency and Renewable Energy

Separation technology crosscuts manufacturing industries

- accounts for ~4,500 TBtu/yr, or about 22% of all in-plant energy use in the US;
- four largest energy consuming industries include (chemicals, petroleum refining, forest products and mining); and
- more than 240 TBtu/yr could be saved by developing new or advanced materials for low energy separations.

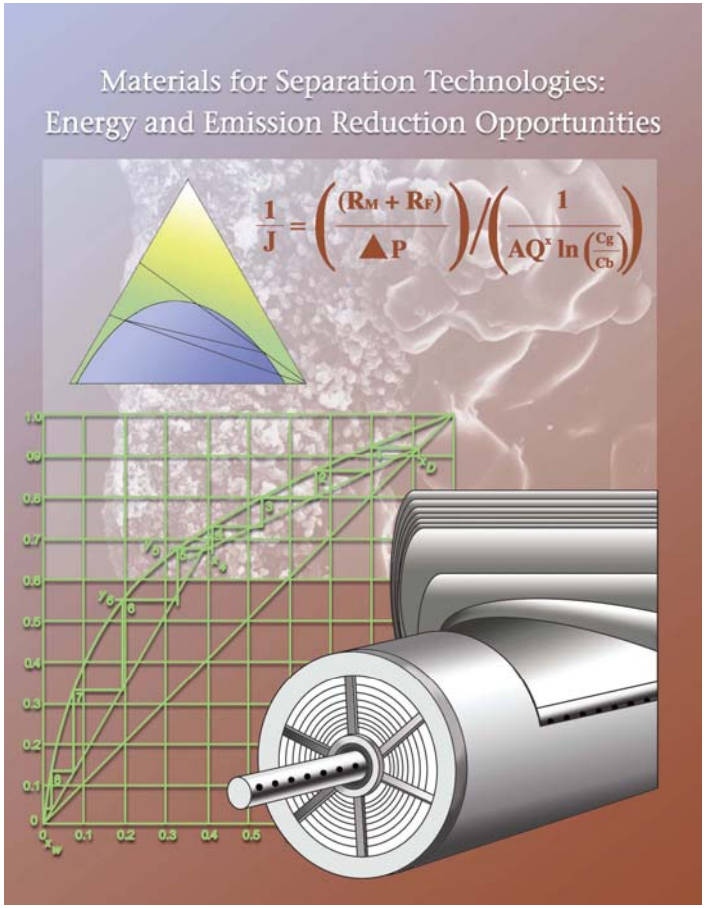

www.eere.energy.gov/industry/imf/pdfs/separations_report.pdf

Opportunity Analysis: Refractories for Industrial Processing

Refractories affect large amounts of energy used by U.S. industrial processes

Up to 400 TBtu/yr potential energy savings from refractory improvements in just 4 furnace types:

Boilers and reaction systems

Reverbatory furnaces

Gasifiers

Kilns/Calciners

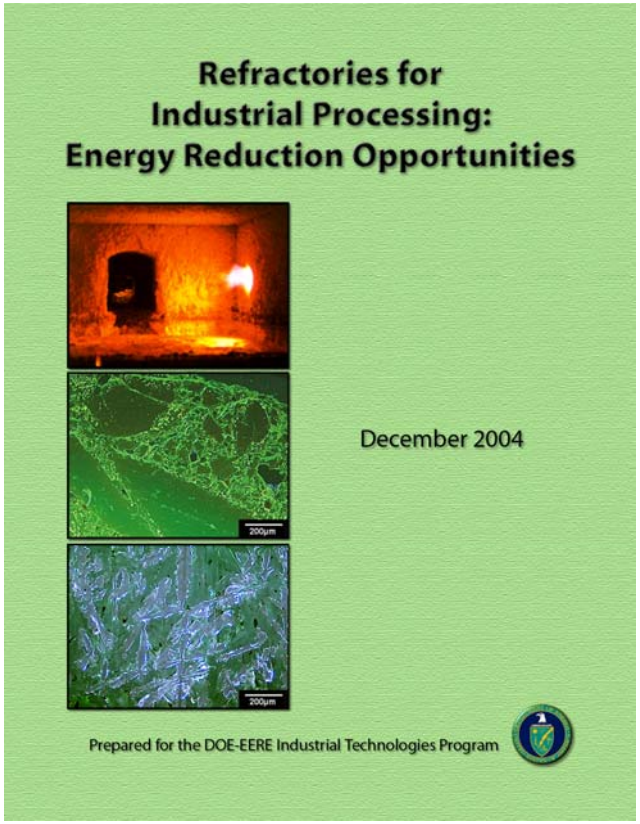

- Energy savings goals based on the needs and estimates of 15 furnace types used throughout the various manufacturing industries.
  www.eere.energy.gov/industry/imf/pdfs/refractoriesreportfinal.pdf

EERE-ITP Materials

Recent Successes

Enhanced Properties of Nickel Aluminide for Rolls in Reheat Furnaces

ORNL R&D on welding of Ni_3AL is successfully applied in industrial trial

- **Development of manufacturing procedures enabled production of 115 rolls for installation and testing**
-
- **Materials successfully reached 26 month milestone – more than 215,000 tons of steel processed**
- **Eliminated over 70 furnace shut downs**
- **Higher yield and increased product quality due to *no roll-related downgrading* of steel; and**
- **35% increase in furnace energy efficiency.**

Rapid Infrared Heating of Aluminum Billets Increases Energy Efficiency of Forging Process

U.S. Department of Energy
Energy Efficiency and Renewable Energy

- Decreases energy consumption by factor of three *(~2TBtu/yr)*
- Reduces heating times by an order of magnitude *(reduces from 10hr to new 1hr)*
- Produces high-performance forgings with significantly improved tensile and fatigue properties *(2.5X to 3X better)*
- Improves product yield and throughput *(4x better)*

- **2004 R&D 100 award**

Project Funded by US DOE, EERE, Industrial Technologies Program, Supporting Industries, Industrial Materials for the Future, and Aluminum

Degradation-Resistant Materials Example: Refractories for Black Liquor Gasification

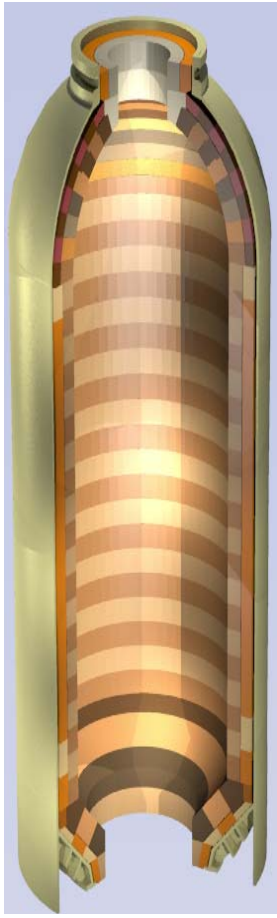

Goal: Develop gasification unit to replace Kraft black liquor recovery boilers.

Challenge: *Development of degradation resistant refractory material* - High alkali concentrations (Na2SO4, Na2SO3, *etc.*) and high temperature result in 40% refractory material loss per year, creating structural and safety issues, thermal efficiency losses, and unacceptable maintenance cost and downtime.

Benefits: Greater energy output per unit input
14 % energy savings
18 % reduction in CO_2 emissions
Reduction in NOx, SO_2, and PM
Renewable energy net electricity export

Status: New, corrosion resistant, spinel refractory panels inserted in gasifier unit in September 05.

Participants:

R&D Organizations
- Oak Ridge National Laboratory
- University of Missouri – Rolla
- PSL
- Simulent

Forest Products Industry
- Weyerhaeuser

Refractory Suppliers
- Monofrax
- Harbison-Walker

Development and Demonstration of Advanced Tooling Alloys for Molds and Dies

Goal: Increase die life by a minimum of 20%; reduce energy consumption associated with the manufacture of heat treatment of dies by a minimum of 25%.

Challenge: Utilize spray forming and rapid solidification processing to simplify mold making and tailor properties of ferritic mold and die tool steels.

Benefits: Reductions in cost and delivery time for tooling, reduced energy consumption, and potential to improve die performance

FY05 Activities: Complete sample die preparation and in-service evaluation of dies. Continue commercialization effort through licensing partner.

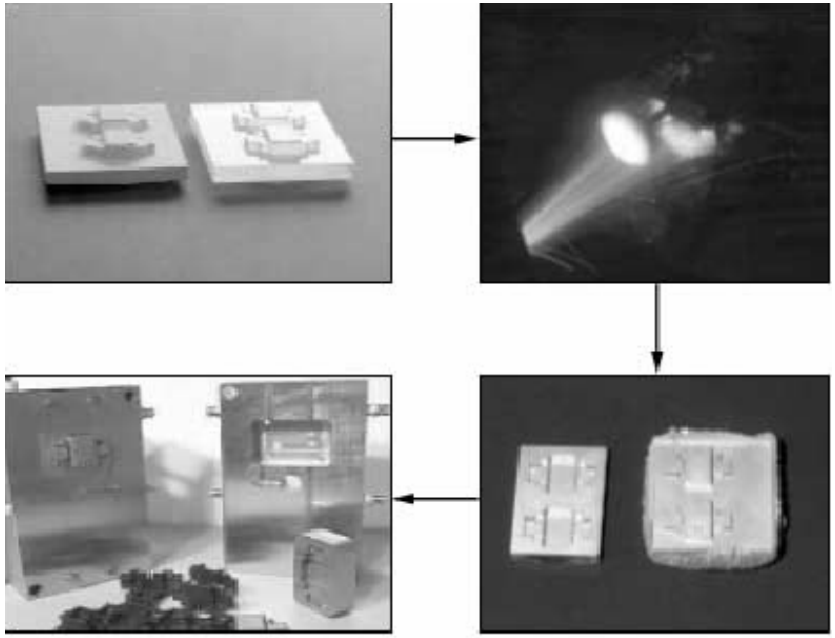

RSP Tooling™ processing steps

R&D 100

2004

Participants: Idaho National Engineering & Environmental Laboratory, Univ. of California-Davis, RSP Tooling LLC, Glass Manufacturing Industry Council, and General Aluminum Manufacturing Co.

Alloys for Ethylene Production (Chemicals IOF)

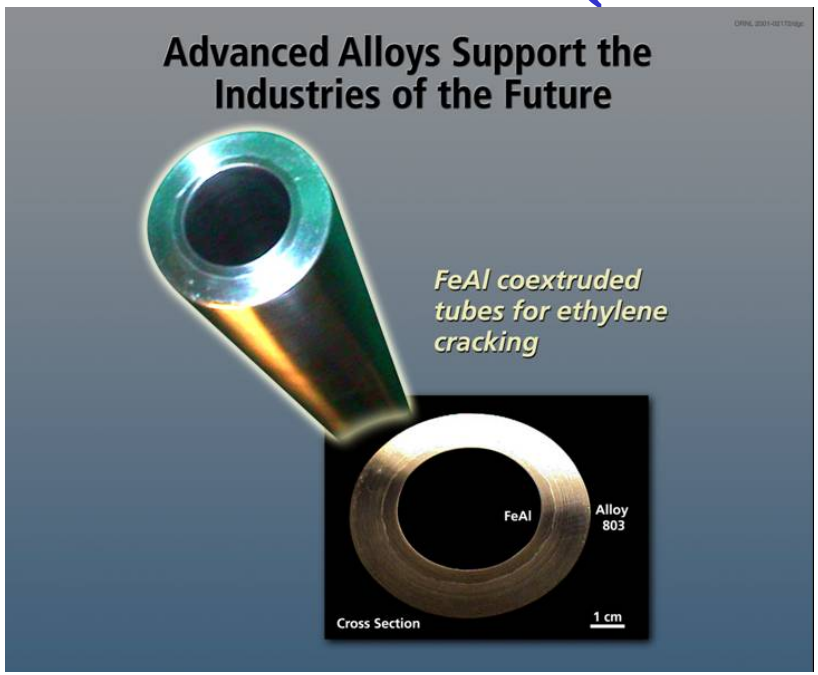

Goal: Develop and commercialize furnace tubes based on iron and nickel aluminides and advanced metallic alloys.

Challenge: Current ethylene furnace tubes are susceptible to coking, reducing mass flow and heat transfer. Carburization along the tube wall further limits the furnace tube's structural life.

Benefits: Al_2O_3 forming alloys have potential to minimize coking and carburization.

FY05 Activities: Initiate in-plant testing of bimetallic tubes made of coking resistant, alumina-forming, alloys such as those high in Al (e.g., FeAl) or those low in Al with high Cr such as Fe-20Cr-4.5-6.5Al

Participants: Exxon, Equistar, Shell, BP Amoco, Air Products, Akzo Nobel, Sandvik Steel, Special Metals, Duraloy, Nooter Industries, the Materials Technology Institute, and Oak Ridge National Laboratory

Transformational Technologies

Ultra-Hard Materials →

- Ultrananocrystalline diamond
- Boron-aluminum-magnesium
- Nanocrystalline tungsten carbide

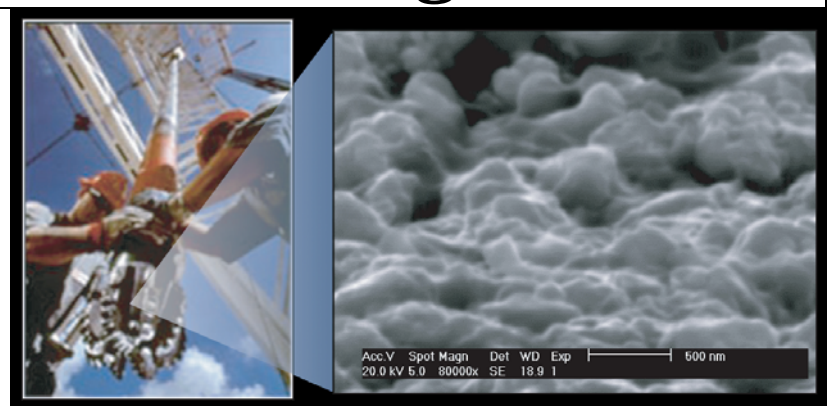

← **Materials for Separations**

- Design Systems
- Membranes
- Sorbants
- Filters

Materials for Energy Systems →

- Waste heat recovery - thermoelectrics
- Emissions conversion – molecular sieves
- Improved efficiency - refractories

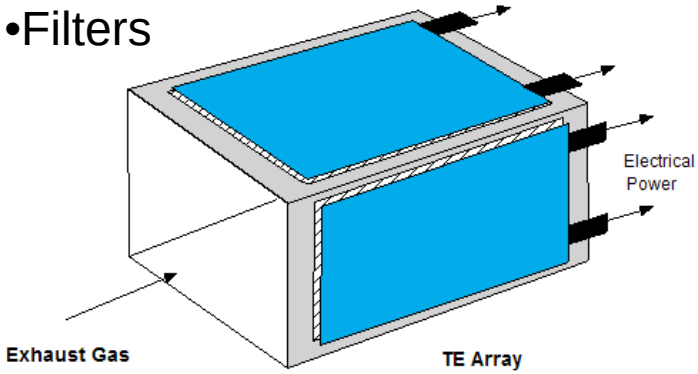

Materials for Energy Loss Recovery

Transformational

Waste to Electricity

Current Technologies

e.g. Heat Exchangers / Recuperator

Materials and design pathways for efficiency gains

•Improved structural materials*

•Improved refractories*)

•High efficiency heat transfer - Microchannel heat exchangers

Future Technologies

Thin film thermoelectrics for waste heat recovery*) Potential savings 18 TBtu/yr by 2020

Other possible pathways

• Piezoelectric

•Thermophotovoltaic

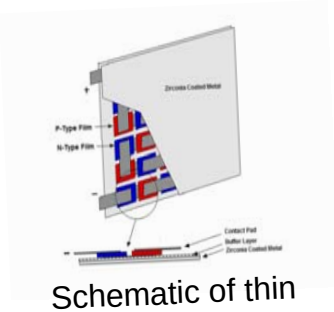

Schematic of thin film material configuration

*ongoing R&D

Thermoelectric Materials for Waste Heat

Goal: Integrate advanced thermoelectric materials into thermoelectric device with efficiency >20%.

Challenge: Multi-layered, thin-film materials show promise for thermoelectric performance but lack sufficient robustness and economical scalability for industrial application.

Benefits: Recovery of energy from industrial waste heat stacks; conversion of waste heat into electrical power; energy savings of 18 trillion Btu/year in 2020.

FY05 Activities: incorporate materials into prototype power generating device; fabricate and demonstrate 5 kW device. Demonstrate Z=2 for thin films

FY06: Initial in-plant evaluations

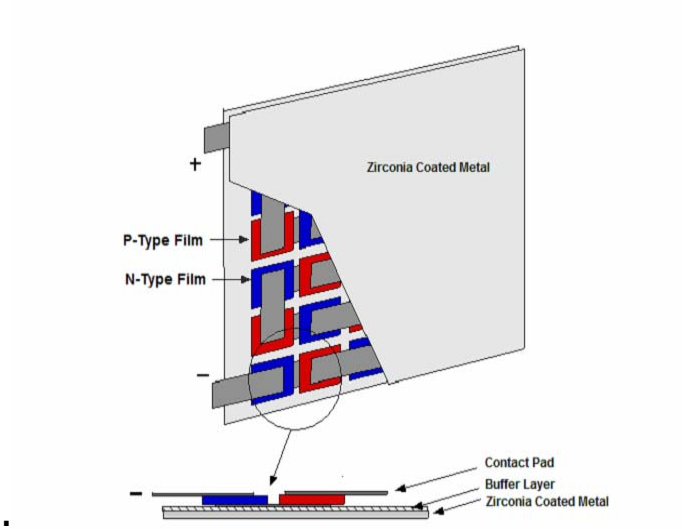

Schematic of thin film material configuration

Participants: Pacific Northwest National Laboratory, Pittsburgh Plate Glass, Michigan Technical University, Ledbetter & Sons, Alcoa

2005
Separations Facility
distillation dominates

2010-2012
Hybrid Systems –
low-energy separation technologies (e.g., membranes) augment distillation

2020
Separations dominated by low-energy intensity systems (new plant footprint)

Examples:

Mixed Hydrocarbon feedstock streams for separations

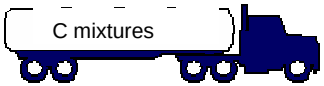

Ethylene 160 TBtu/yr

Propylene 53 TBtu/yr

p_ Xylene* 10 TBtu/yr

Butadiene 4 TBtu/yr

Isoprene* 1 TBtu/yr

Use of Hybrid systems will result in 10-20% Energy Intensity Reduction

Increases in

Material

selectivity

throughput

robustness

Processes domination by low-energy system could result in 30-60% Energy Intensity Reduction

* Ongoing ITP investigations of separations using modified zeolite membranes

Ultra-Hard Materials

low wear, low friction materials to reduce processing energy

BAM - changing the paradigm
from simple structures
to multiphase, multicomponent
materials for cutting, wear and
friction surfaces

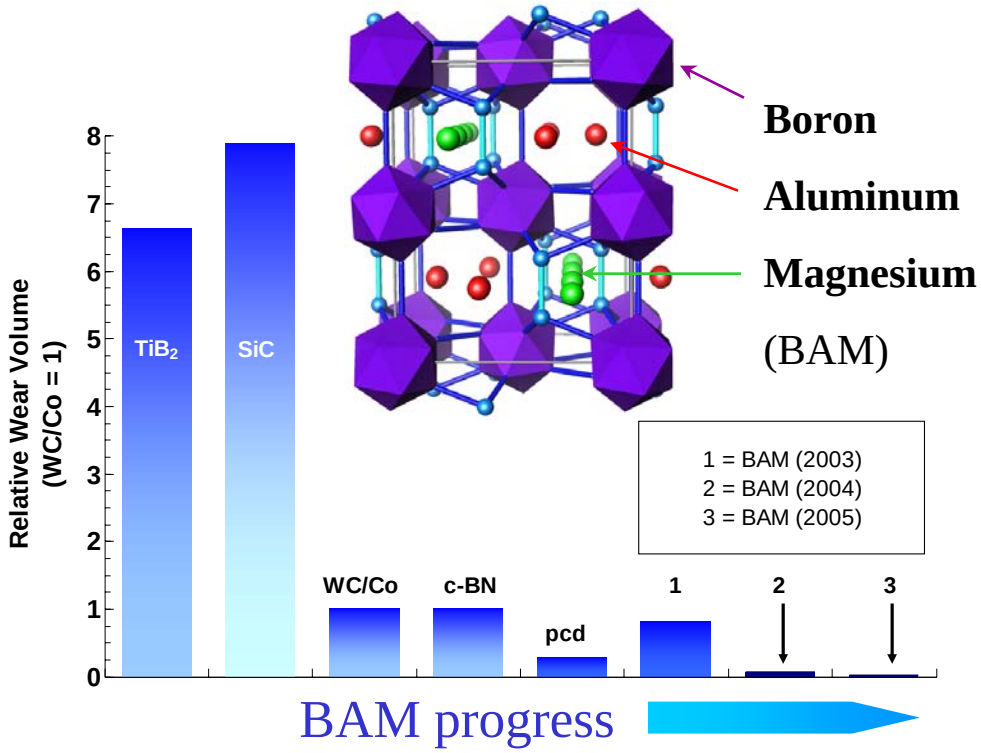

Ultra Nano-Crystaline Diamond
(UNCD) coatings for mechanical
pump seals

significant reductions in
friction and wear

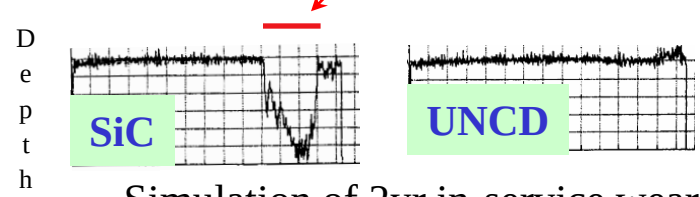

Simulation of 2yr in-service wear

ITP Solicitations

See ITP Solicitations calendar on web:

www.eere.energy.gov/industry/financial/solicitations.html

Materials Solicitation: end of June for FY 2007 funds

- Lab Call
- Industry Call

Priorities

- Novel Structures/Materials e.g. Ultra-Hard Materials
- Materials for Sensors
- Advanced Refractories
- Materials for Waste Heat Recovery
- Novel Separations Systems for Low Energy Industrial Separations
- Transformations & Kinetics Modeling and Simulations

ITP Materials Project and Portfolio Review Meeting

June 1-3, 2005
Wyndham Chicago

For more info and to register:

http://www.energetics.com/imfreview05.html

Contact Information

Sara Dillich

202-586-7925

sara.dillich@ee.doe.gov

Web: **http://www.eere.energy.gov/industry/**

- End of Presentation

Extended Alloy Lifetimes Through Improved Coating Performance and Reactive Element Optimization

B. A. Pint, J. A. Haynes and I. G. Wright
Metals and Ceramics Division
Oak Ridge National Laboratory
Oak Ridge, TN 37831-6156

Y. Zhang
Center for Manufacturing Research
Tennessee Technological University
Cookeville, TN 38505-0001

Research sponsored by DOE, Fossil Energy Advanced Research Materials Program

High Temperature Oxidation

What we like:

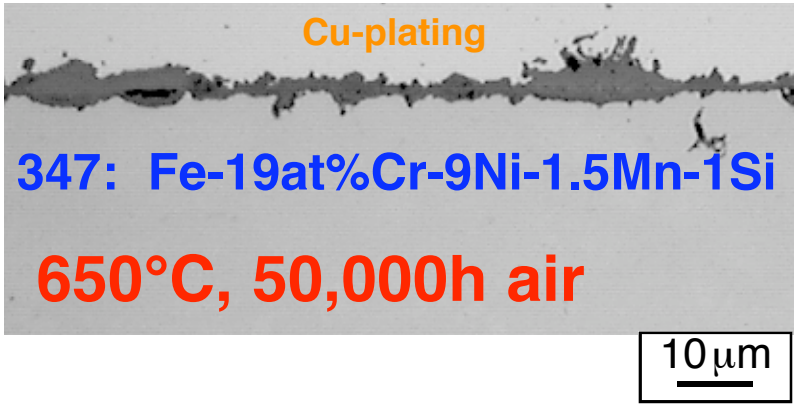

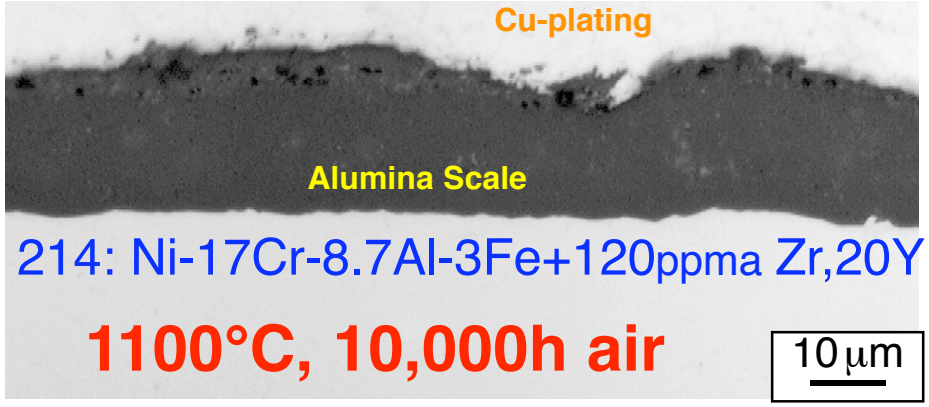

Sometimes, what we get:

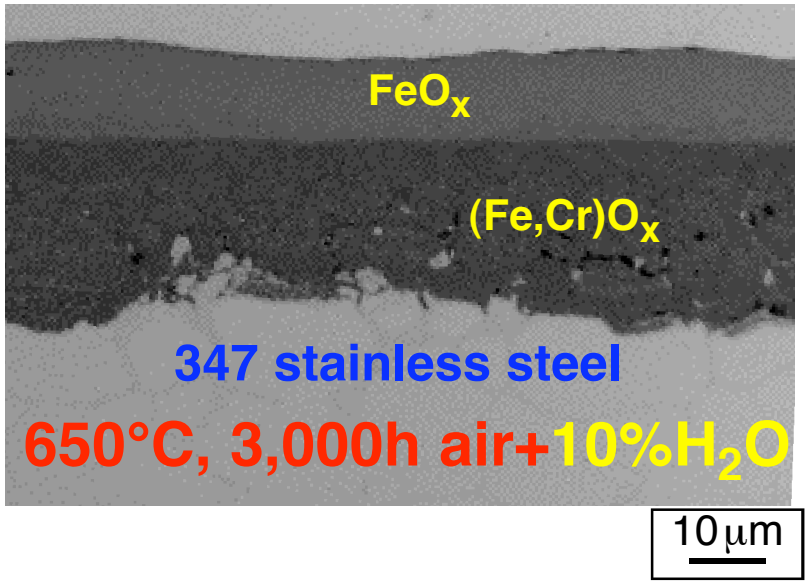

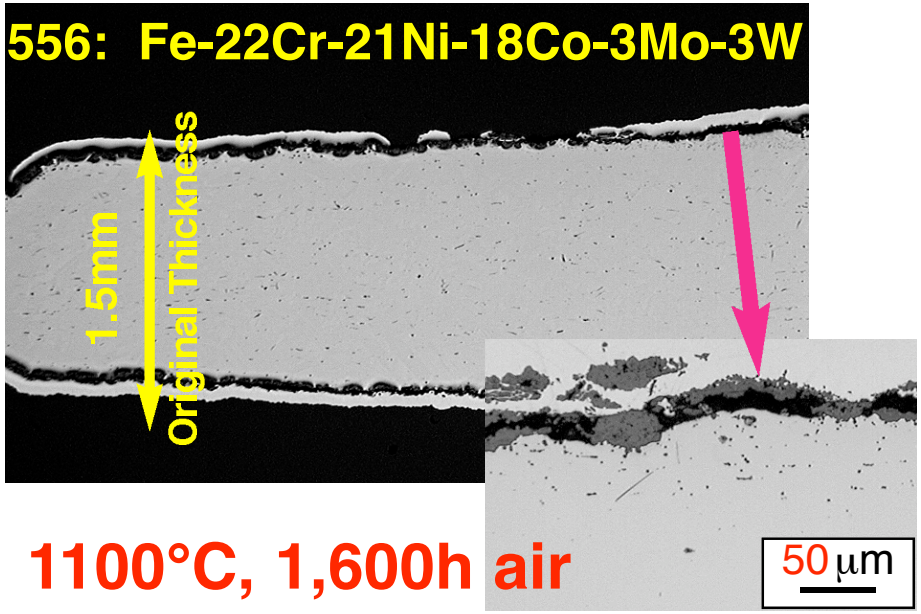

One Solution: Coatings

Ex: high activity CVD aluminide coating on Fe-9Cr-1Mo

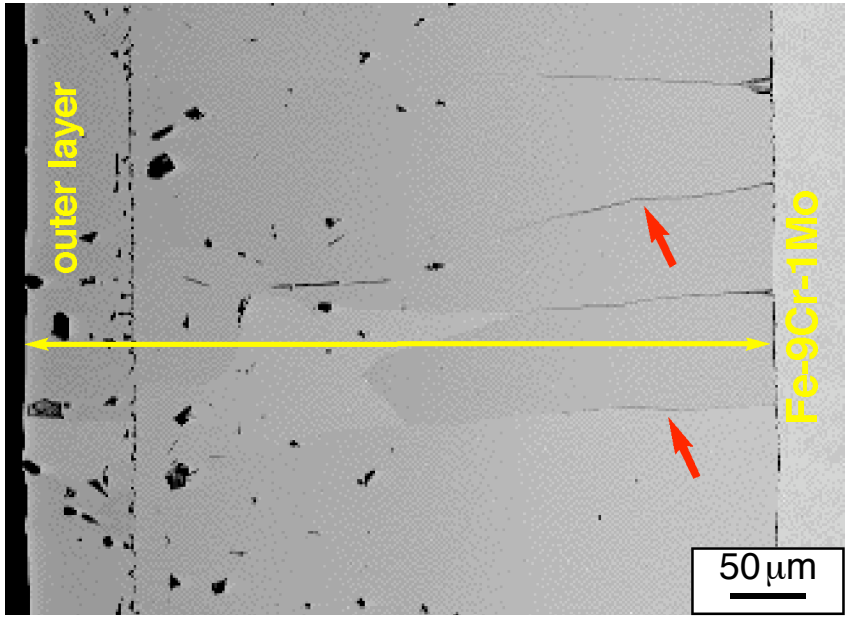

As-deposited coating by chemical vapor deposition (CVD), 6h at 1050°C showing:
- outer Al-rich layer
- inner lower Al layer
- defects: voids and cracks (red arrows) observed for both ferritic and austenitic substrates

Microprobe (EPMA) composition profiles:
Lines - thinner low activity coating
Symbols - thicker high activity coating

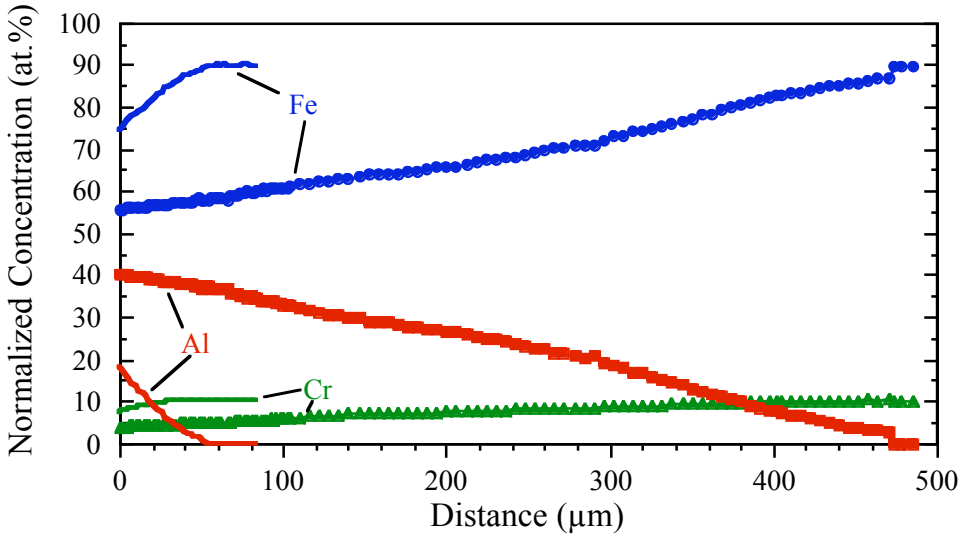

Aluminized Fe-9Cr-1Mo

Characterized after 2000 x 1h at 700°C in humid air

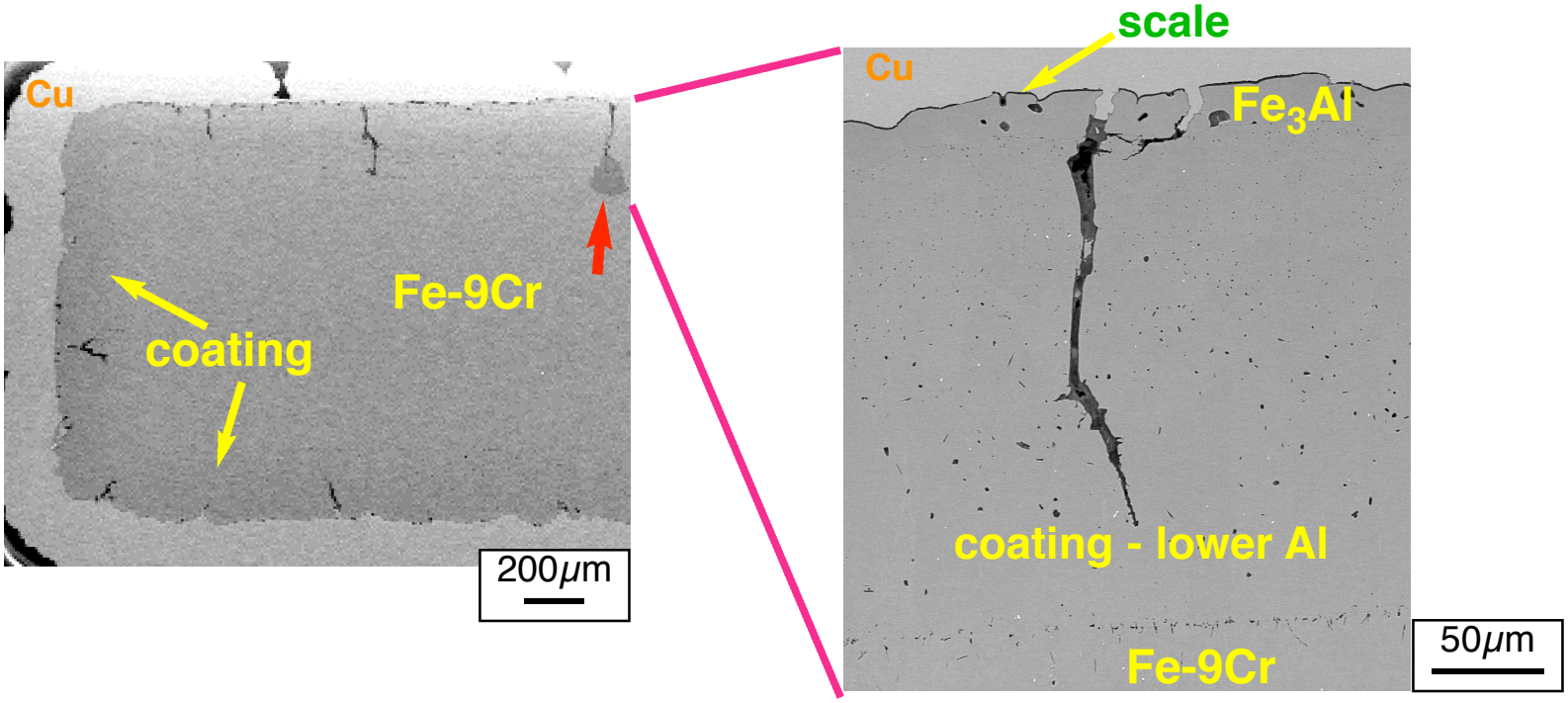

Thin, protective scale formed, BUT

Deep cracks observed through coating

Coating breached in one location (red arrow)

Similar or worse problem for austenitic 304L substrate

Cause: thermal expansion mismatch - Fe_3Al/substrate

Why do the coatings crack?

Likely explanation is the thermal expansion mismatch

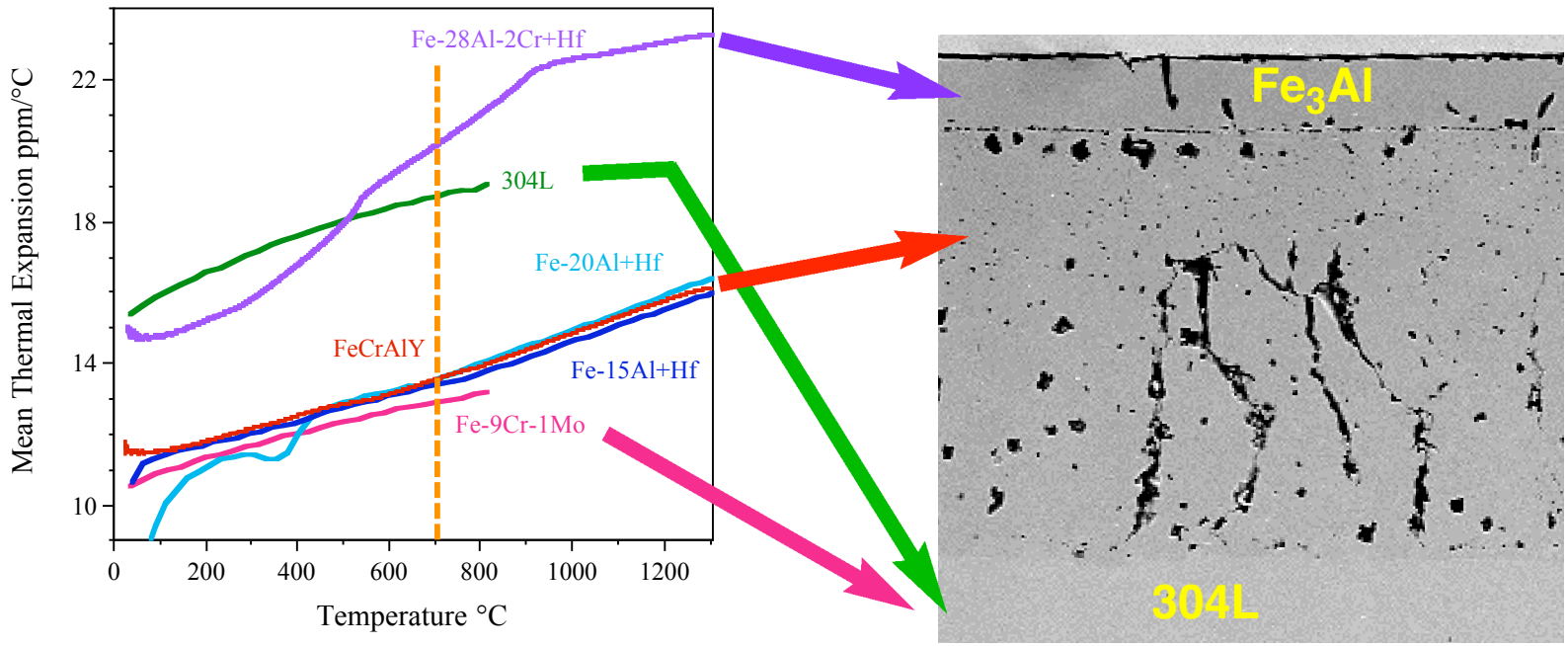

For coated 304L,

- Al addition likely created a ferritic inner layer
- Three layers have distinct thermal expansion behavior (hi/low/hi)
- Mismatch may have resulted in stress sufficient to crack coating

For coated Fe-9Cr-1Mo:

- Outer Fe_3Al layer different, inner coating & substrate are ferritic
- Crack started in outer layer may have propagated through inner layer

If CTE mismatch is problem, does coating thickness affect performance?

Thin & thick CVD coatings, 1h cycles, 700°C, humid air

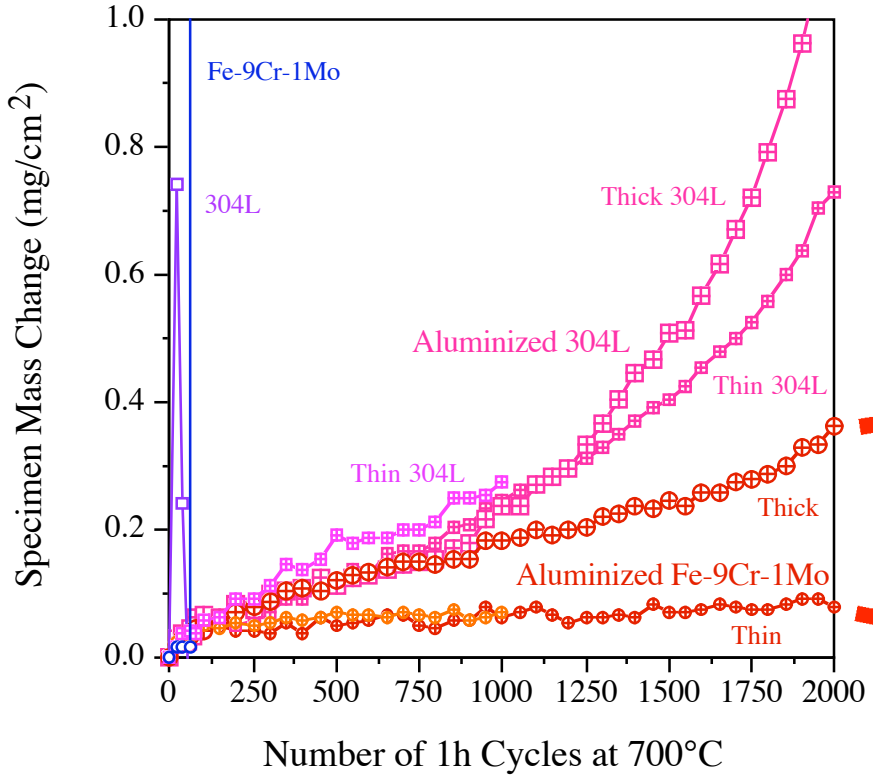

$$\sigma_{coating} = f(\Delta\alpha_{coat\text{-}sub})$$

$$\varepsilon_{coating} = f(\delta_{coating})$$

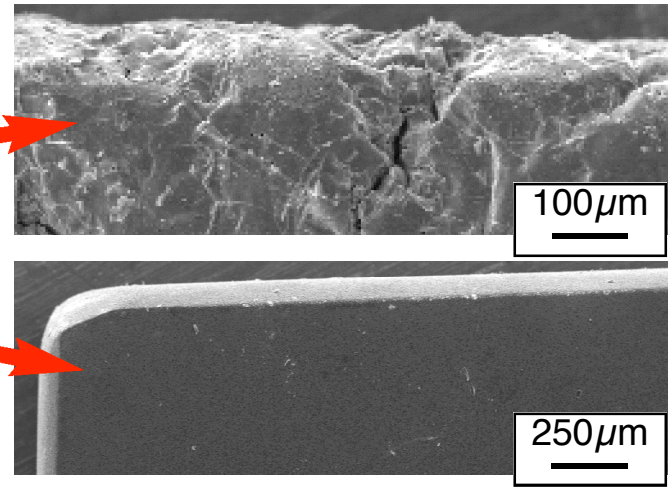

For Fe-9Cr-1Mo, thinner coating not showing signs of degradation after 2000 cycles at 700°C, similar to 2001 result (stop at 1000h)

For 304L, thin and thick coatings showing similar performance possibly less cracking in thinner coating but still penetrated

Effect of cycle frequency at 700°C

In 100h cycles, coatings have reached >10,000h

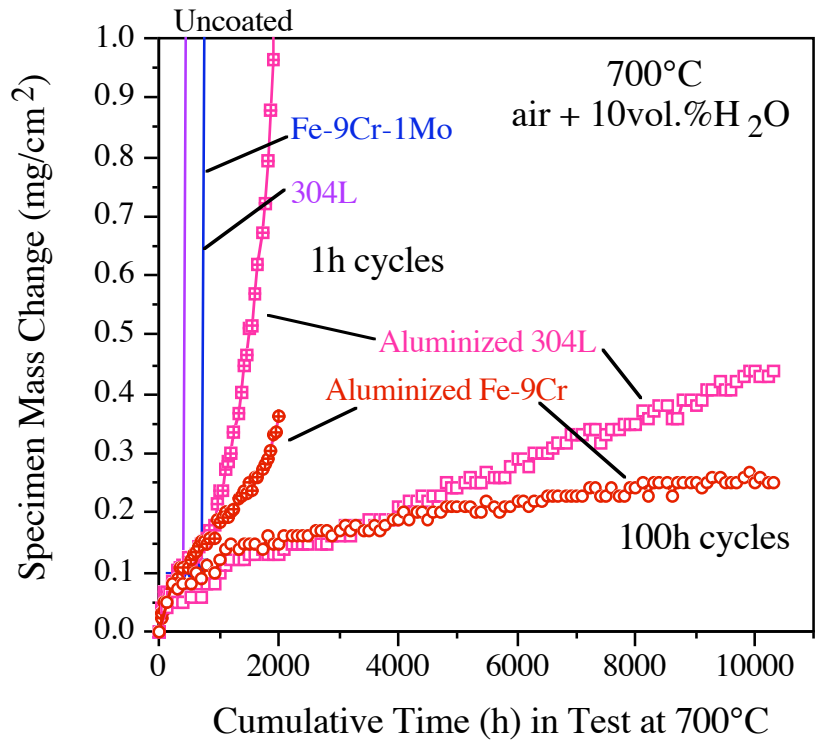

700°C, 1292°F

100h cycle before cooling to room temperature

Higher mass gain for austenitic 304L substrate

No signs of accelerated attack due to H_2O

Lower mass gain than observed for 1h cycles

(Details in Zhang et al., Surf. Coat. Tech. 188-189 (2004) 35)

Surface plan view after cycling

slightly increased damage between 6,000h and 10,000h

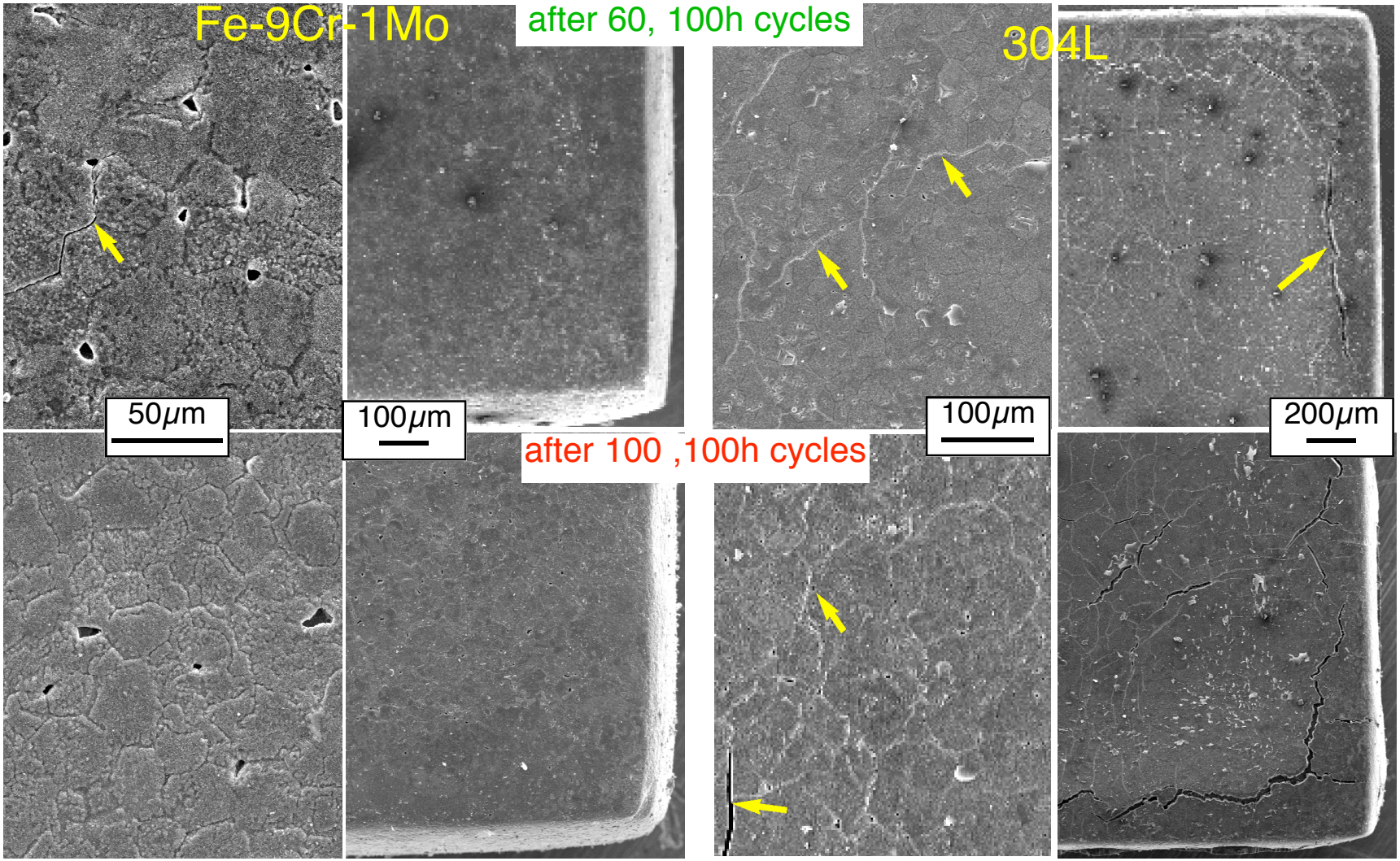

Fe-9Cr-1Mo: cracks in specimen face but no edge cracking

304L: scale spallation and macro-cracking on face and at coating edge

Accelerated testing: 800°C

100h cycles, air+10%H_2O

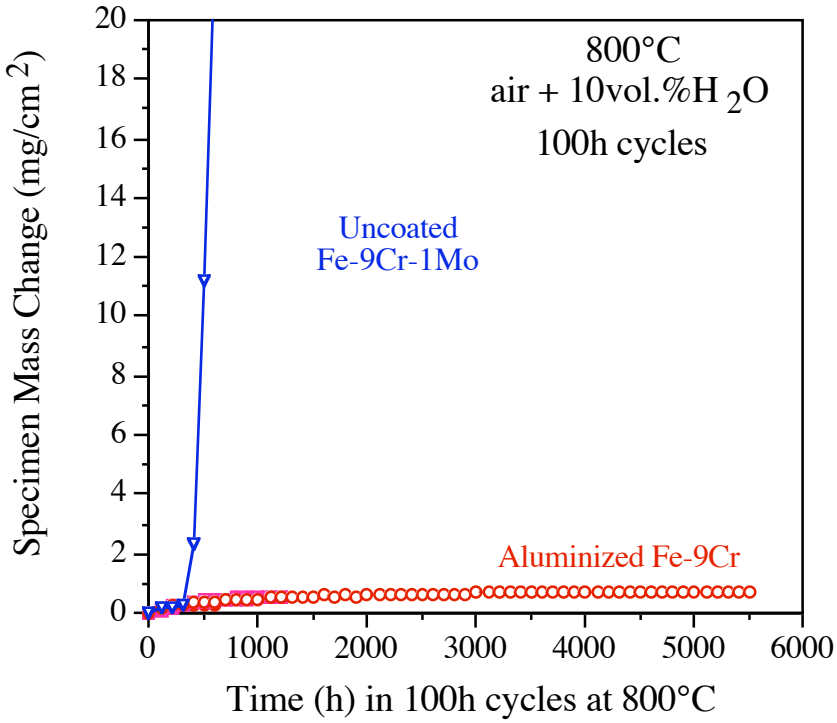

800°C, 1472°F

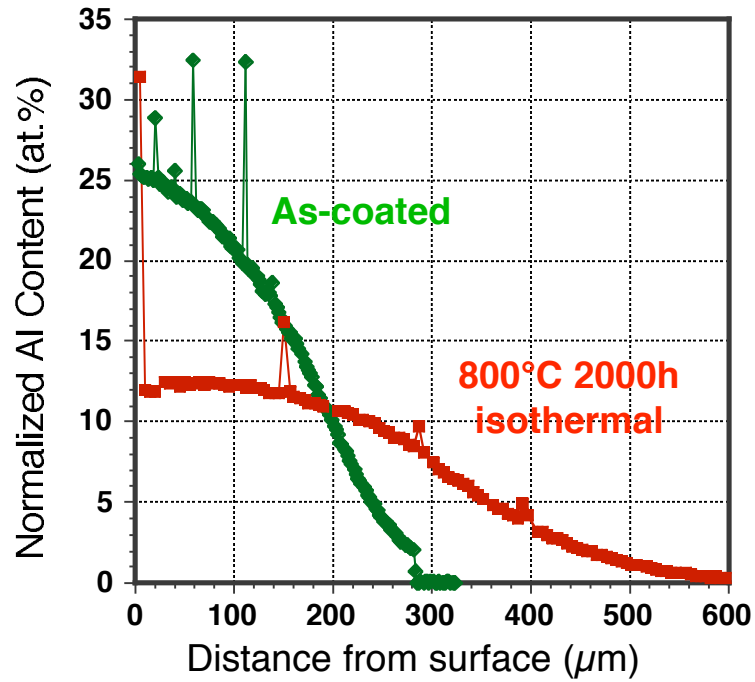

Aluminized Fe-9Cr-1Mo specimen recently reached 5,500h

Diffusion test (isothermal, air) showed coating had dropped to 12 at.%Al at surface after 2,000h at 800°C

Calculation shows Al down to 9at.%Al and Al tail to specimen center!

Coating Program Update

Model developed based on diffusion-oxidation data

- Missing is critical Al content C_b at coating failure
- Based on cast Fe-Al alloys: ≈10at.%
  - ≥9%Cr in coating lowers C_b below Fe-Al value
  - Finer grain size in coating should lower C_b

Determining C_b:

- At 700°C, coating at 10,300h and counting
  - duplicate coating to be stopped at 10,000h
  - testing "thin" coating, lower Al reservoir
- At 800°C, (accelerated test) coating at 5,500h
  - diffusion model suggests Al diffused to center
  - duplicate coating to be stopped at 5,000h
  - making coating on thicker (3mm) substrate

Lower as-coated defects by reducing alloy N content

- Currently showing no life increase in 1h cycles

Modeling Oxidation-Limited Alloy Life

Lifetime model developed by Quadakkers, Bennett, et al. for ODS FeCrAl tubes with 1-3 mm cross-sections

Premise: Calculate time to breakaway (FeO_x formation) by knowing total Al reservoir available and rate of Al consumption

Model inputs:

- initial Al content (**C_o**)
- the critical Al content where Al_2O_3 will no longer form: (**C_b**)
- the thickness of the specimen (**d**) and density (ρ)
- Al consumption rate (e.g. **kt^n**), **t** is time (**n**=0.5 for parabolic)
  consumption rate is higher when scales spall, **n** -> **1!**

$$(C_o - C_b)/100 \cdot d/2 \cdot \rho = k \cdot t^n \cdot \frac{\text{(mole Al)}}{\text{mole O in } Al_2O_3}$$

Assuming: (1) Al concentration profile is flat in alloy
(2) oxidation can be described by constants **k** and **n**

How extend life? Reduce consumption or increase reservoir

Affect **k** and **n**(?) by slowing scale growth & reducing spallation

Thicker components or new alloys with higher C_o-C_b value

Alloy Development Program

Better alumina-forming alloy(?) and feedback for coatings

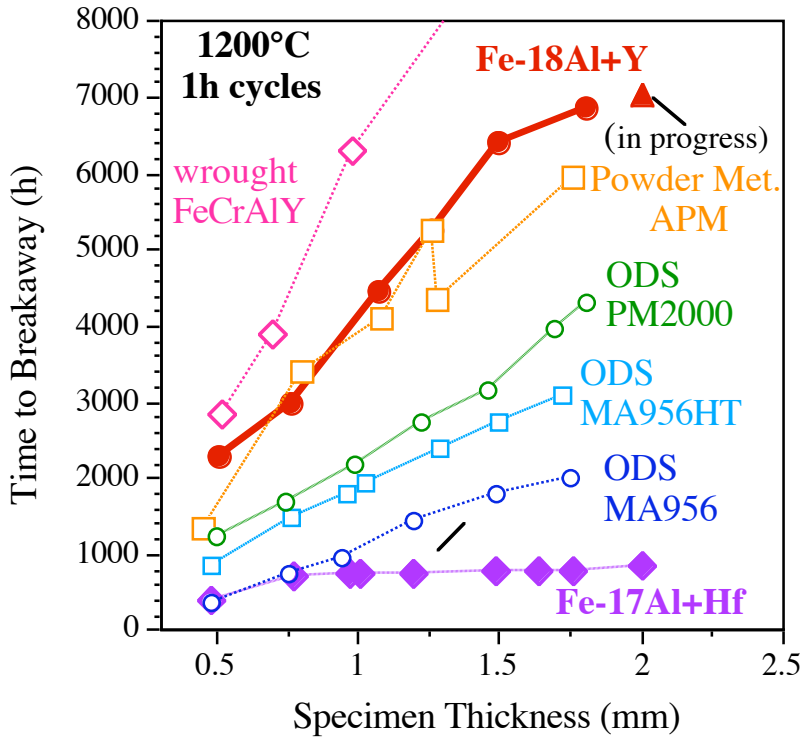

Y

Hf

Real life:

n≈1 for FeCrAl

Fe-17Al+Hf

Al gradients

lower life

Looking for Fe-base alloys with longer life than FeCrAlY

Y/Hf co-doped increase 37% (J. Am. Ceram. Soc. 2003)

Fe-Al alloys with higher Al contents (C_o) than FeCrAl

Intermetallic Fe-Al spalls too much

Ferritic Fe-Al have more potential - optimized with Y

Problems with Fe-Al+Y

Long-term at 1200°C & 1250°C showed accelerated attack

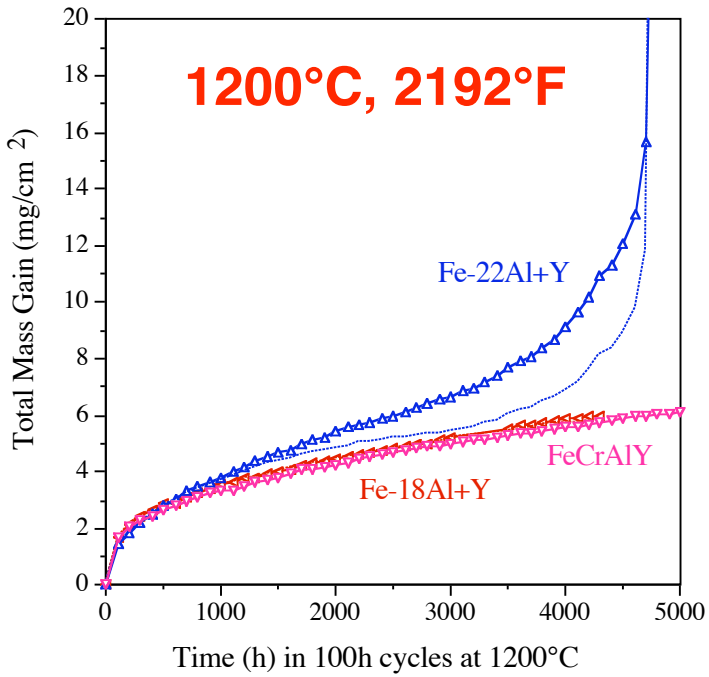

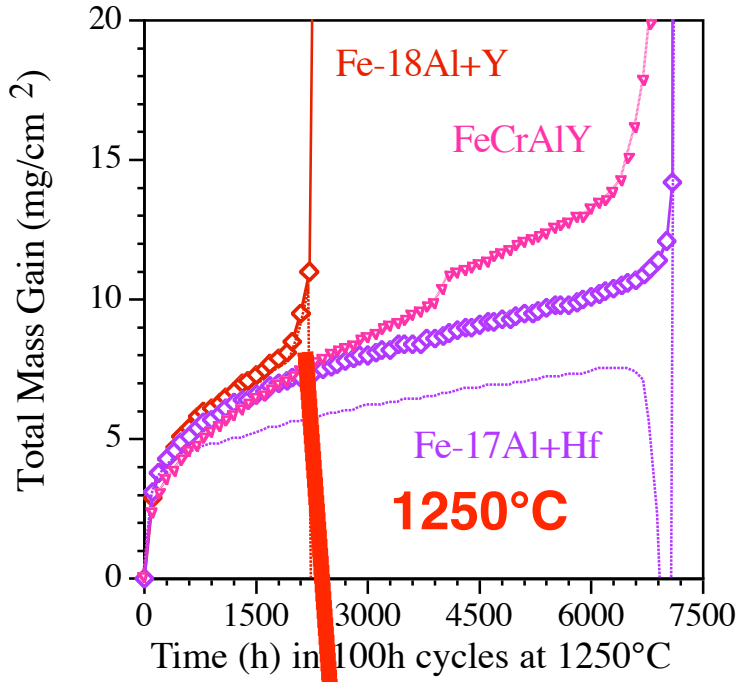

Accelerated attack at alloy grain boundaries: Quadakkers' "broccoli"

Associated with internal attack of carbides in alloy

No strong carbide-formers with Y

May occur at long times at low T

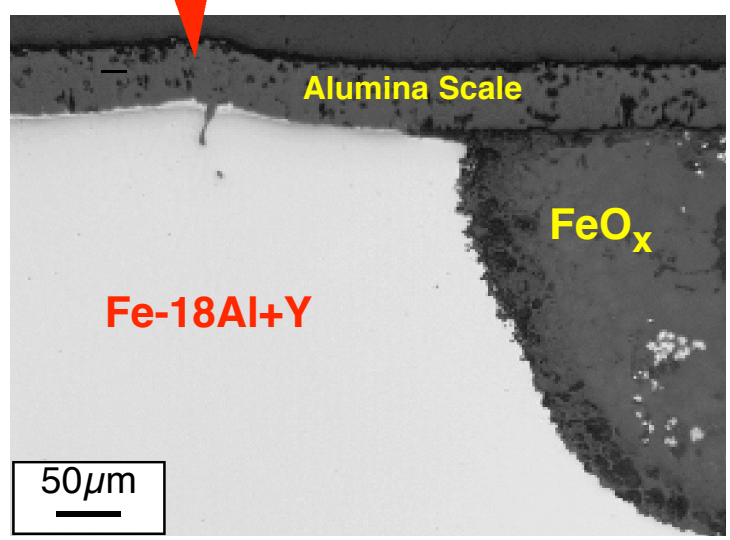

Cures for “broccoli”

Quadakkers: alloys need low C or strong carbide-formers

Fe-17Al **1250°C, 2282°F** **Fe-22Al**

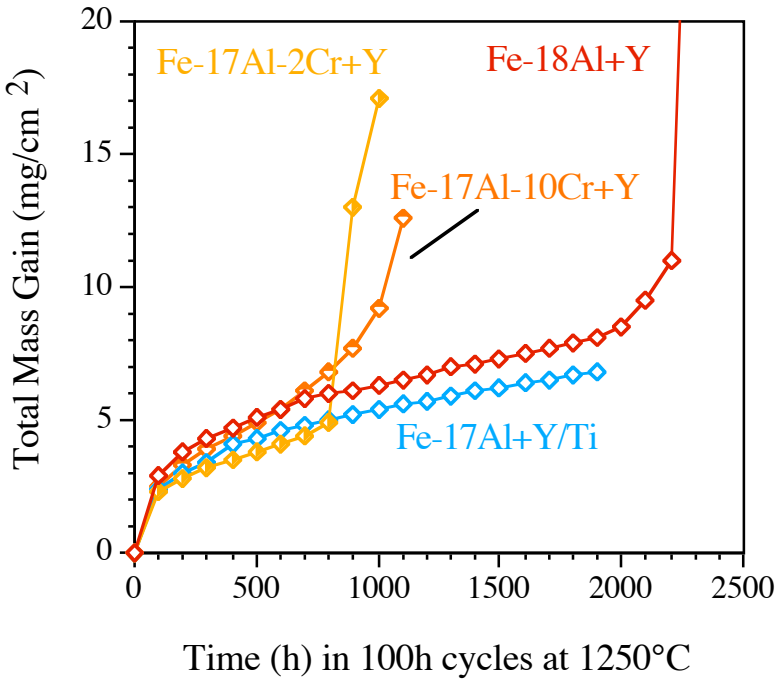

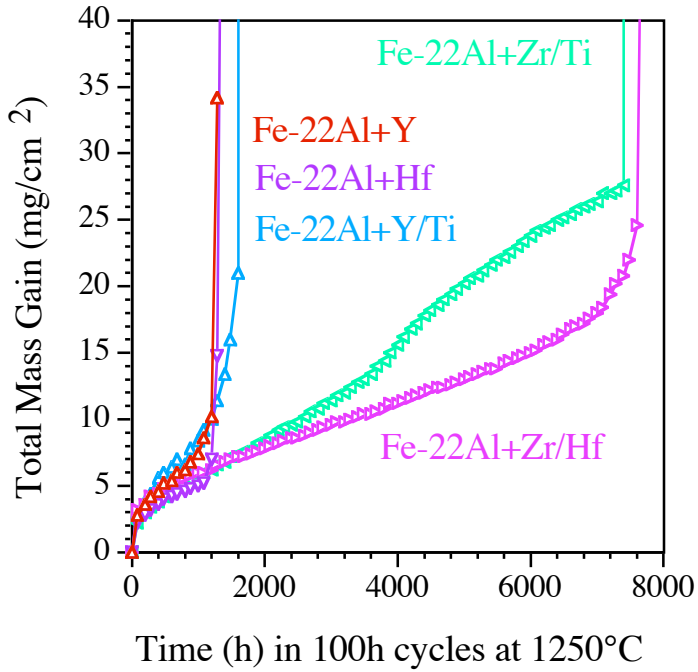

Fe-17Al: lower life with Cr additions

Trying Y/Ti and Y/Hf (new alloy); Y/Zr another choice

Fe-22Al: Problems with Y, Hf, Y/Ti

Alloys with Zr additions showed long life

Optimization of RE dopants still not complete for Fe-Al

Case study: RE/C effect in FeAl

Relationship between RE dopant and interstitials (C, S, etc.)

ORNL base alloy: Fe-40Al-0.2Mo-0.05Zr-0.4C Zr/C=0.12

200h at 1200°C

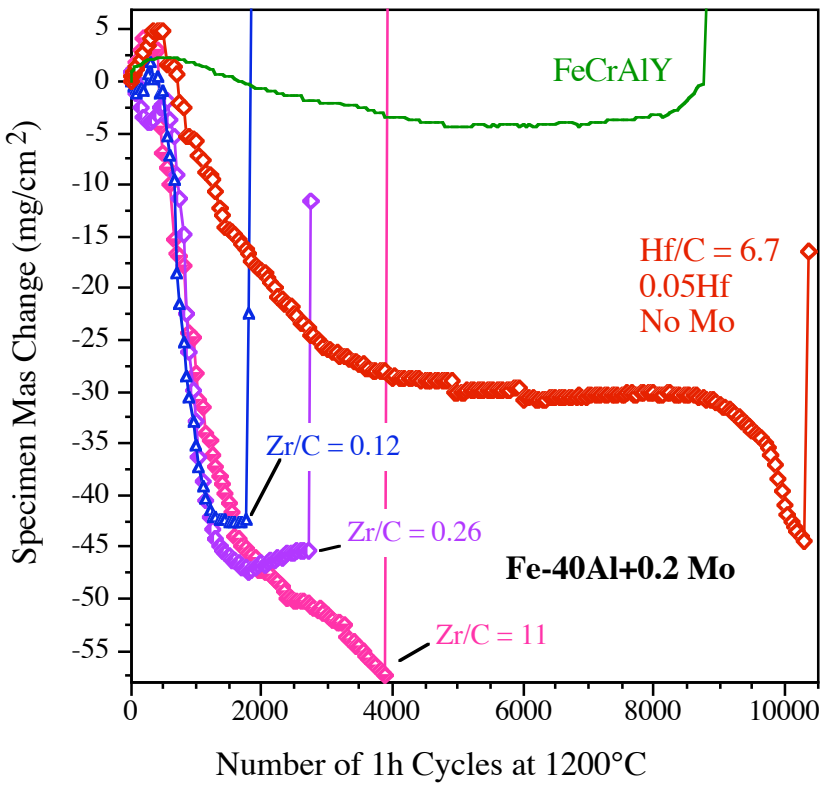

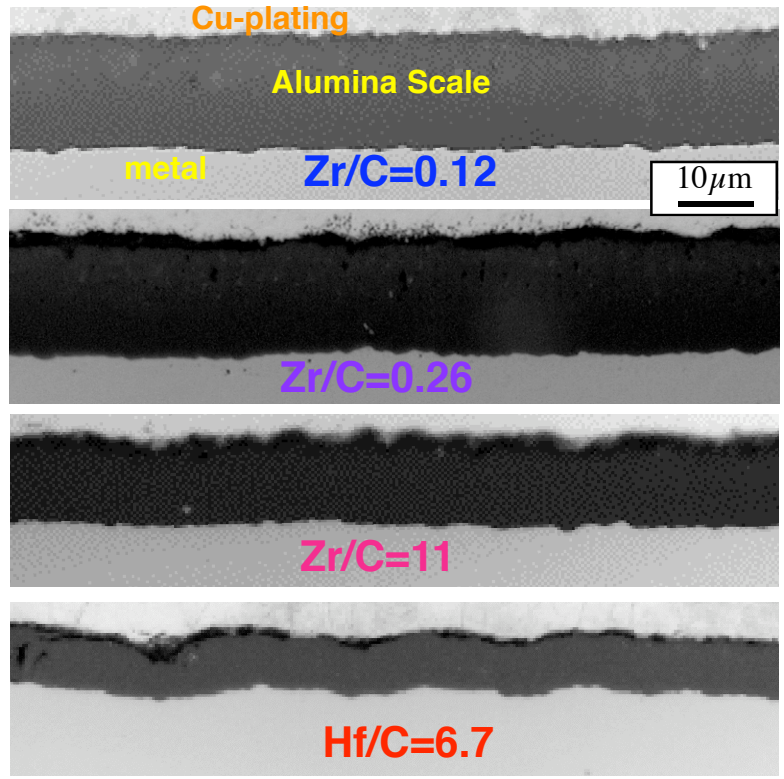

Prior work showed RE/C≥1 preferable

Remove C - increased normalized lifetime by 2X

Change Zr to Hf - increased normalized lifetime by 6X

Changes reduce growth rate but not significantly

Chemical vs. Mechanical effect?

H. E. Evans et al. view - softer materials have longer life

compressive yield at 1000°C

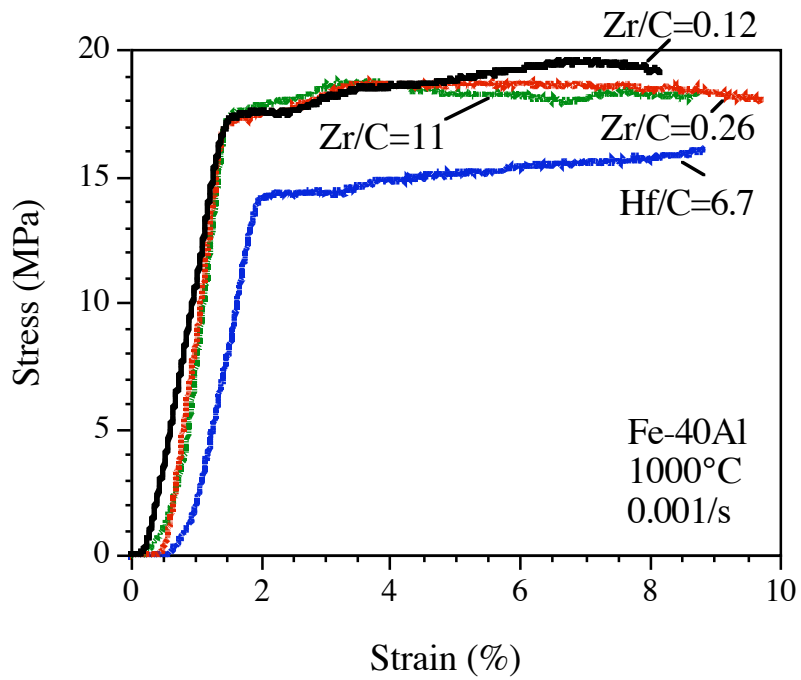

10 x 500h at 1000°C

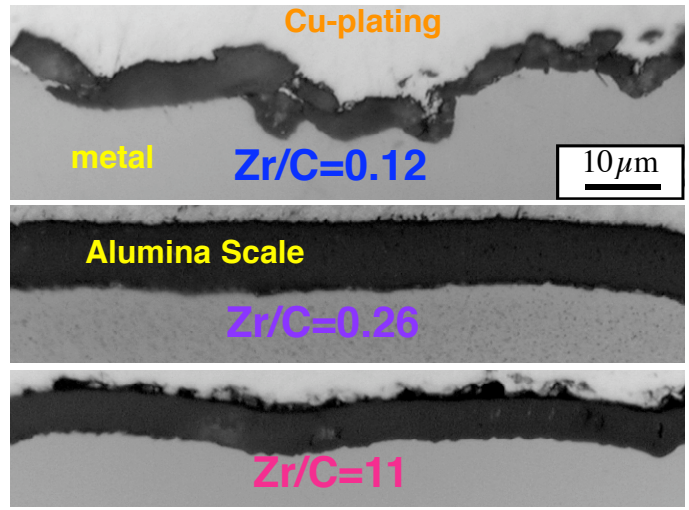

Did removing C soften the material? No more ZrC

Compressive yield at 1000°C showed no effect of C

20% lower yield stress for Hf without 0.2Mo

Lifetime would need to be very sensitive to strength

Does not explain surface deformation observed at 1000°C

(Details in Pint and Schneibel, Scripta Mater. 52 (2005) 1199)

General routes for improvement

Increased oxidation lifetime by slower Al consumption and increased Al reservoir (C_o-C_b)

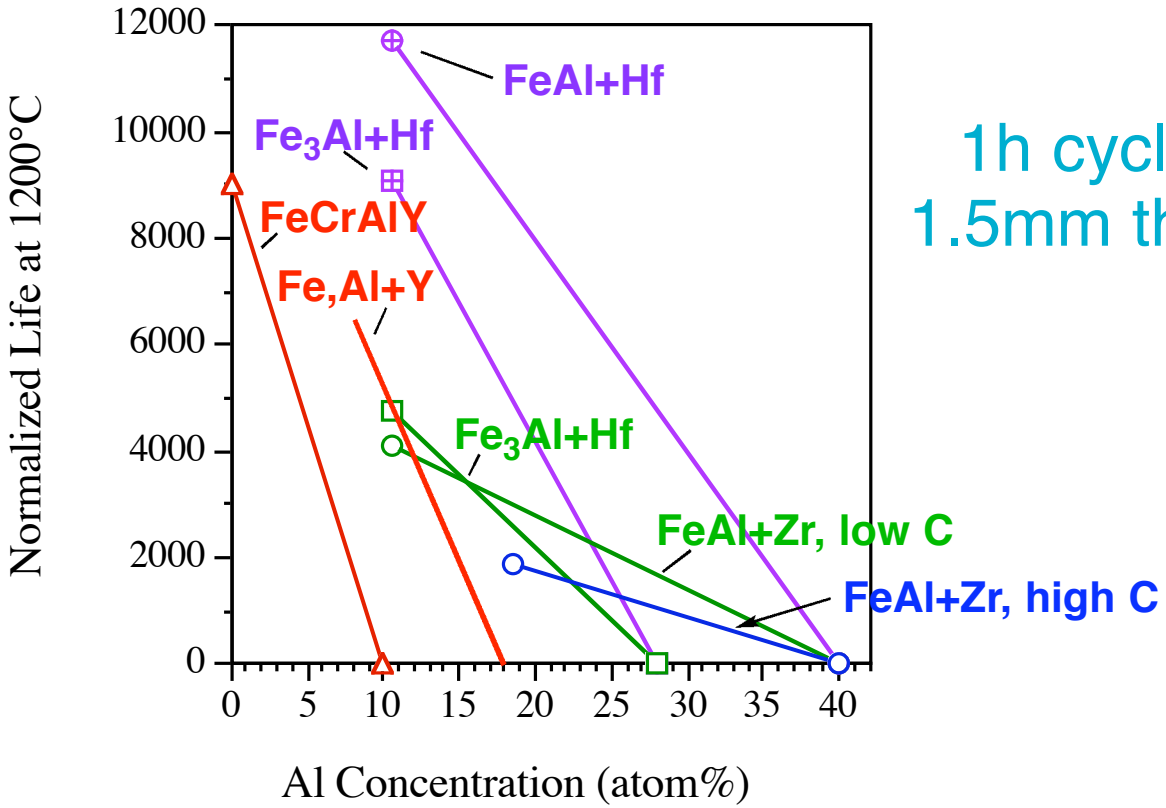

1h cycles at 1200°C
1.5mm thick specimens

FeCrAlY consumption baseline - low reservoir, high life

Fe-Al materials - need slower consumption and lower C_b

Some limitations due to observation of Al gradients

Internal nitridation of Fe-Al in air

Observed at 900°C, similar to work on Fe_3Al and FeAl

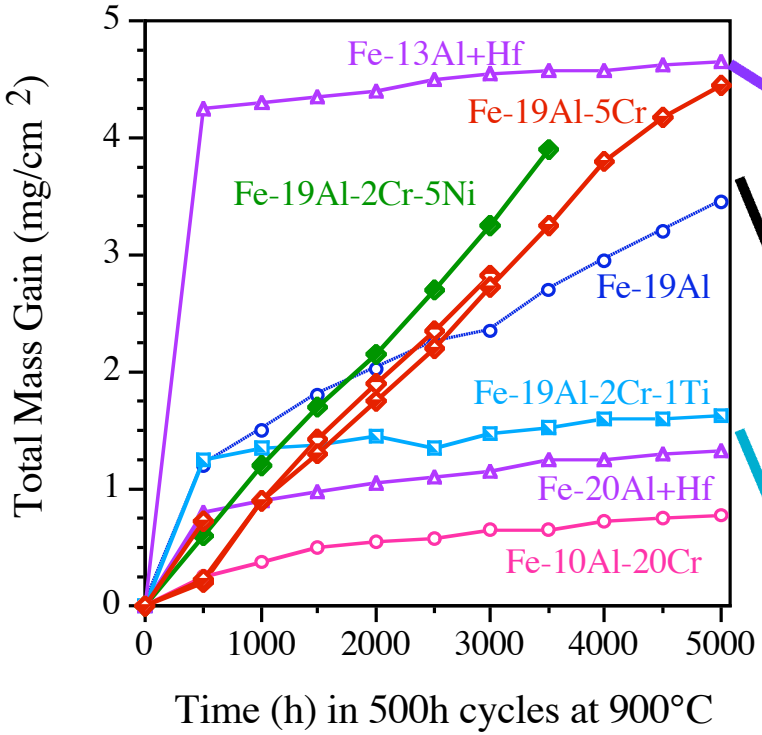

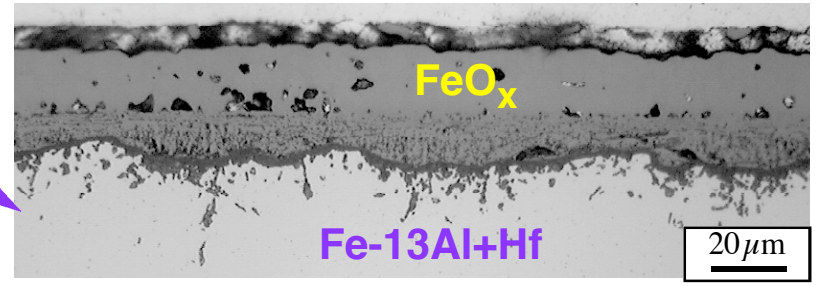

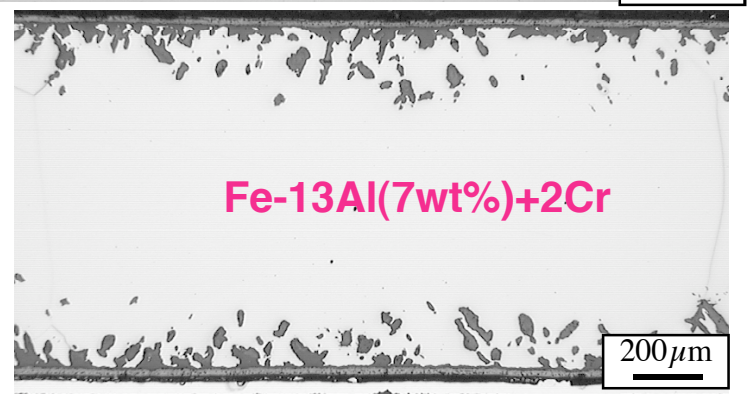

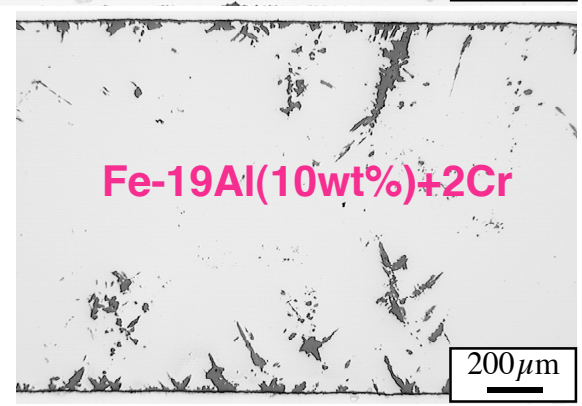

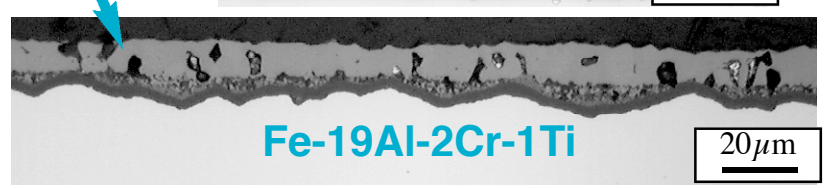

Low Al - form FeO_x at 900°C
Fe-Al±Cr±Ti alloys (Lehigh prog.)
EPMA confirmed AlN
Hf, Ti, Zr prevent it, not Ni, Cr
Not seen in undoped FeCrAl

Followup on Fe-Al Nitridation

Is nitridation a potential problem for coatings?

Summer 2004 project of Ryan Deacon, Lehigh Univ.

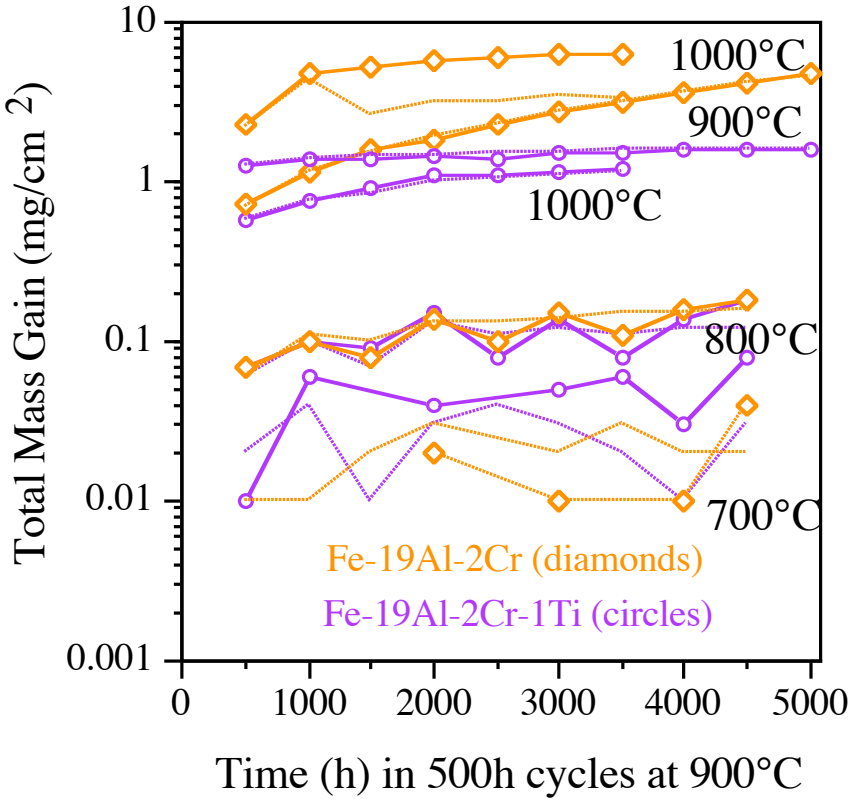

Fe-19Al(10wt%)+2Cr

Fe-19Al-2Cr-1Ti

Alumina crucibles in lab. air

Solid line - total mass
Dashed line - specimen mass

Major effect at 900° and 1000°C with and without Ti

No difference observed at 700° and 800°C

Still looking for a mechanistic explanation for nitriding

Future Work

Coatings

- longer times at 700° and 800°C to failure
- duplicates running to 10,000h at 700°C, 5,000h at 800°C
- coat thicker specimens for 800°C exposure
- coat Fe-9Cr miniature tensile specimens for creep test
- TN Tech: developing pack process
  larger parts for creep and potential pilot plant testing

Alloy Development

- characterize C_b as f(Al content, temperature, time, etc.)
- lower C_b by Cr or Mn additions
- reduce Al use by lowering CTE (Mo) & optimizing RE

Modeling

Have oxidation data and Al back-diffusion data

Need failure criteria: ≈18 at.%Al needed in sulfidation

<10%Al needed for steam/H_2O, depending on C_{Cr}

Summary

Program focus on CVD coatings for laboratory test
- reduced cracking problem with 100h cycles
- protective coating for >10,000h at 700°C
- protective coating with <10at.%Al at 800°C

For lifetime model need critical Al (C_b) at failure
- to estimate lifetime or determine T_{max} at 40kh

Alloy development looking at ferritic Fe-Al
- no CTE problem like Fe-Al intermetallics
- limited by higher C_b (≈10%) than FeCrAl
- improvement in life with Y doping
- solutions for “broccoli” problem
- studying internal nitridation issue

Acknowledgments

K. Cooley - CVD coating fabrication

G. Garner, L. D. Chitwood, J. Moser - oxidation experiments

H. Longmire - metallography

K. S. Reeves - SEM

L. Walker - EPMA

This research was sponsored by the U. S. Department of Energy, Fossil Energy Advanced Materials Research Program under contract DE-AC05-00OR22725 with UT-Battelle, LLC.

Substrate chemistry control - low N

Less cracking, fewer defects in coatings

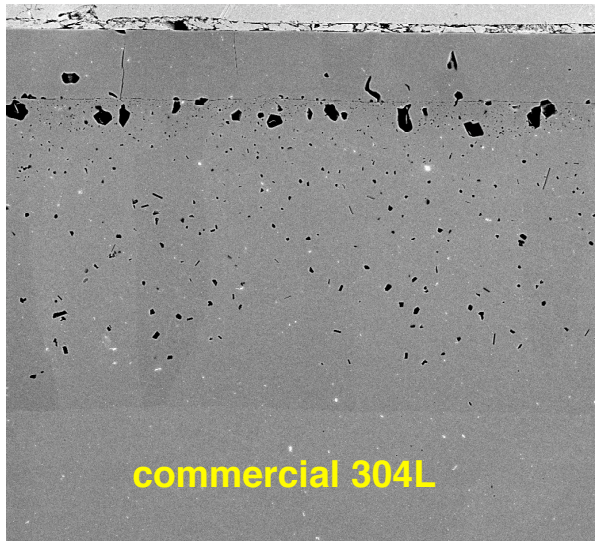

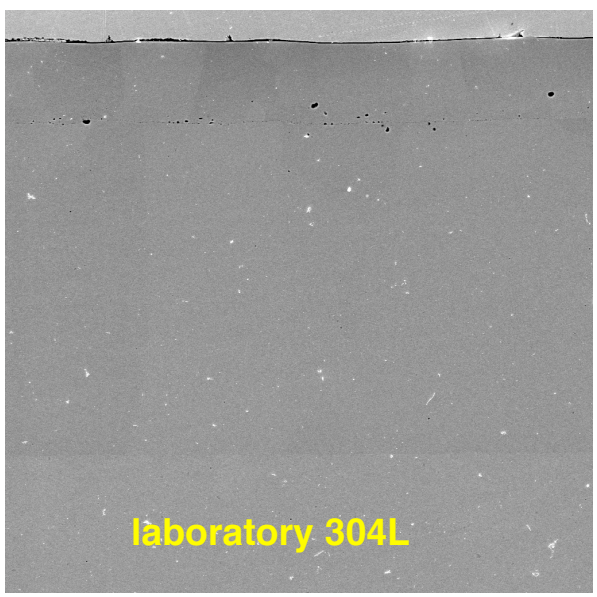

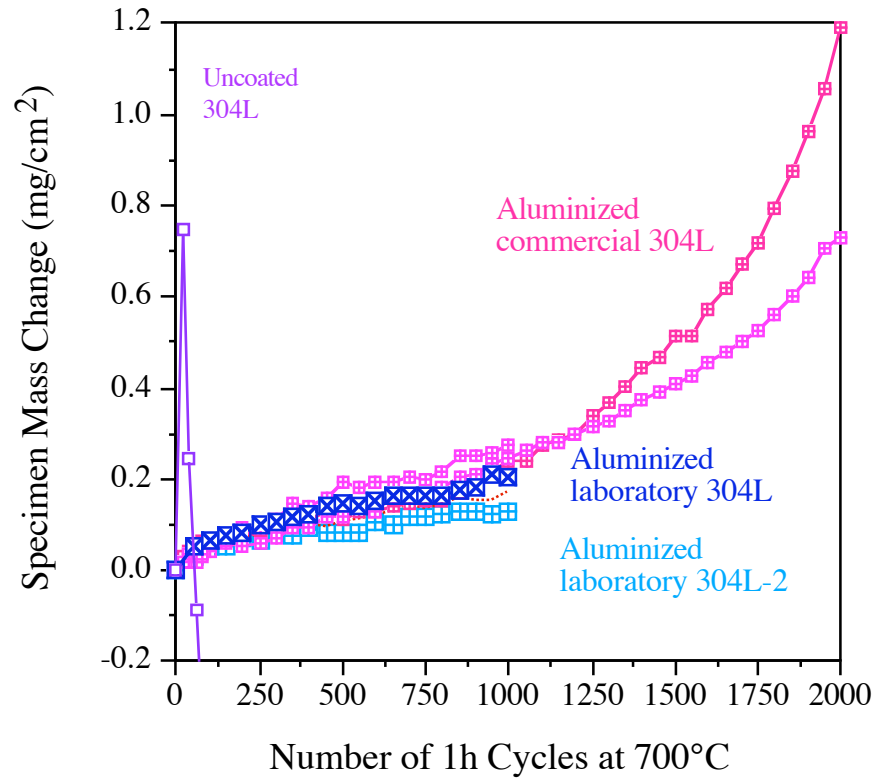

Preliminary results:

- similar mass change as before
- 1000h, 2000h behavior?

Model Fe-Al-Cr alloy performance

after 100, 1h cycles at 700°C in humid air

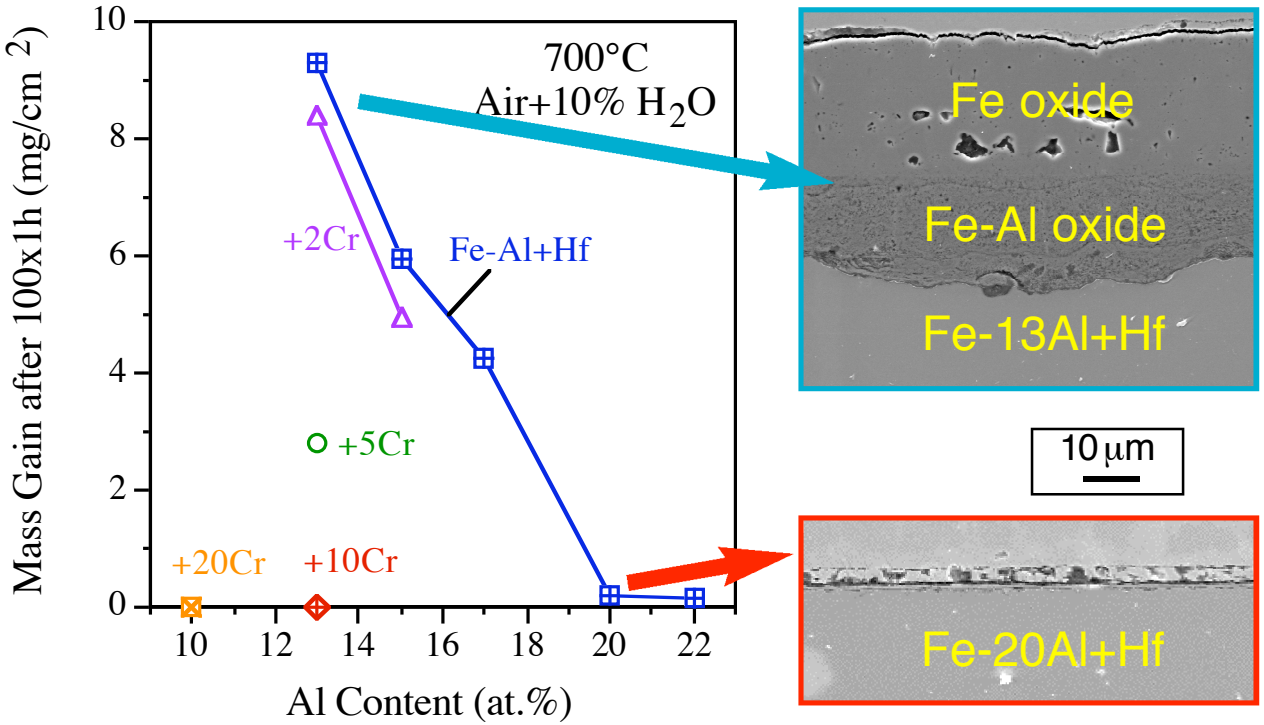

Model alloys indicate with binary Fe-Al, need 20 at.%Al to avoid FeO_x formation

However, when Cr present, critical Al content drops with 10%Cr (≈Fe-9Cr-1Mo), protective with 13%Al with 20%Cr (≈304L) protective with 10%Al (FeCrAl)

Aluminized 304L

Characterized after 2000 x 1h at 700°C in humid air

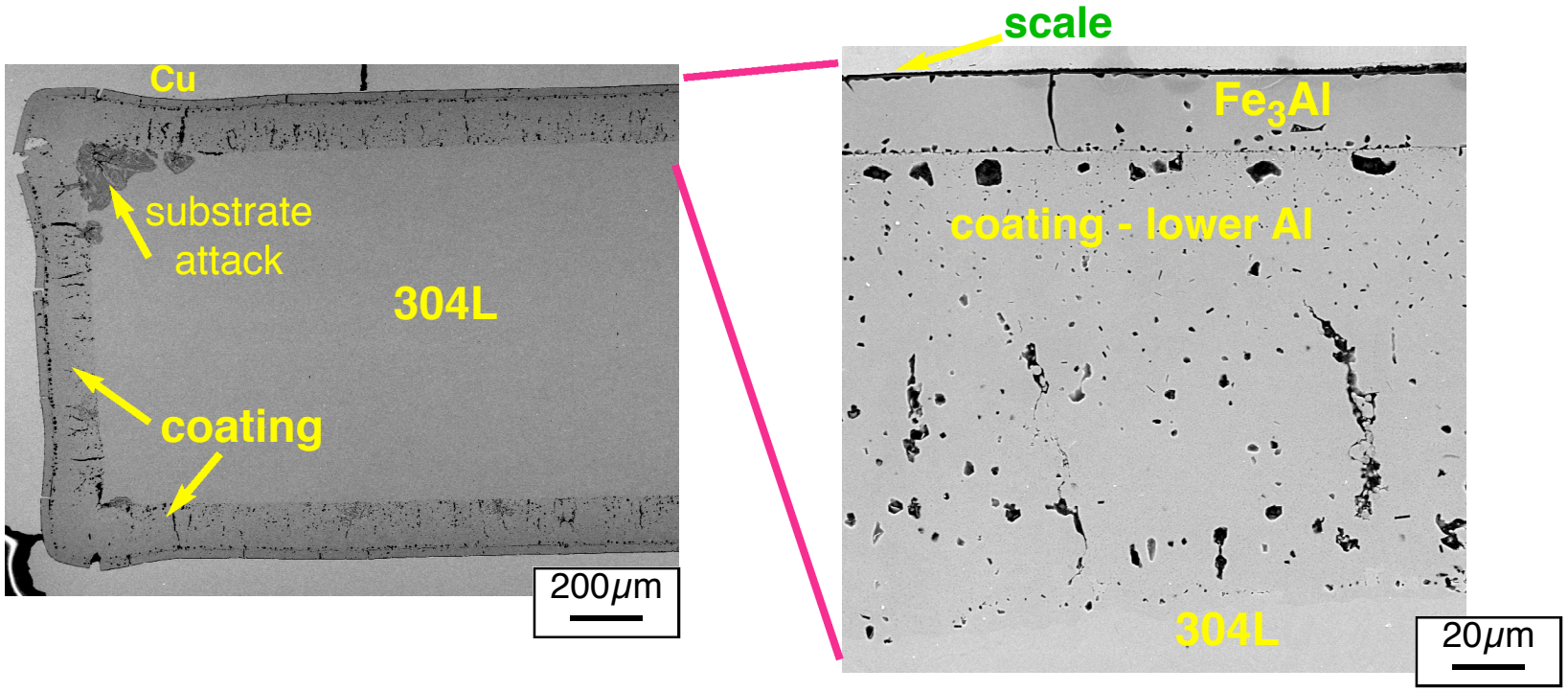

Cracks mainly observed in outer Al-rich layer

Coating breached in corner

Observed mass gain due to attack of the substrate

Thin surface scale where coating intact

27-30at.%Al remained in outer layer (using EPMA)

Coatings exposed without cycling

Characterized after 2000h at 700°C in laboratory air

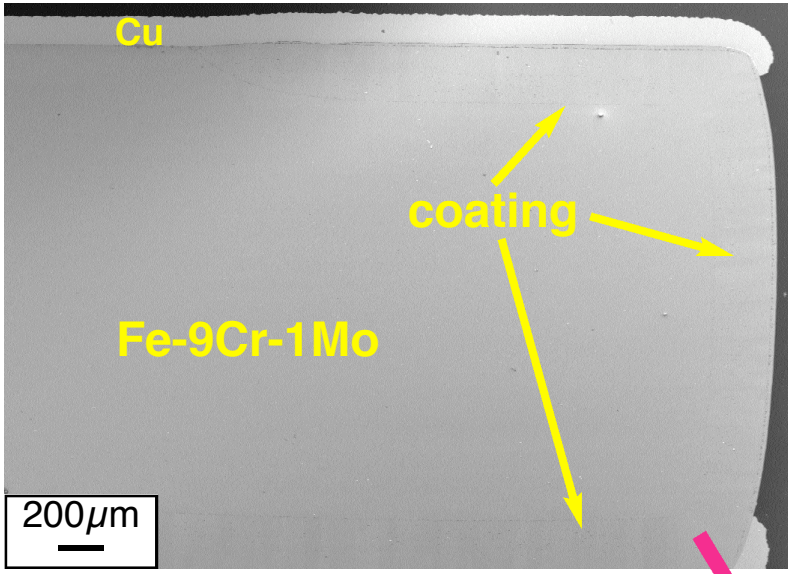

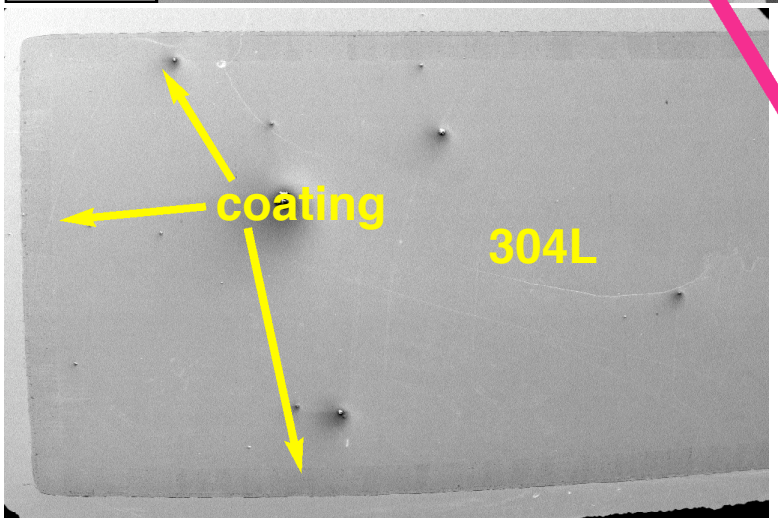

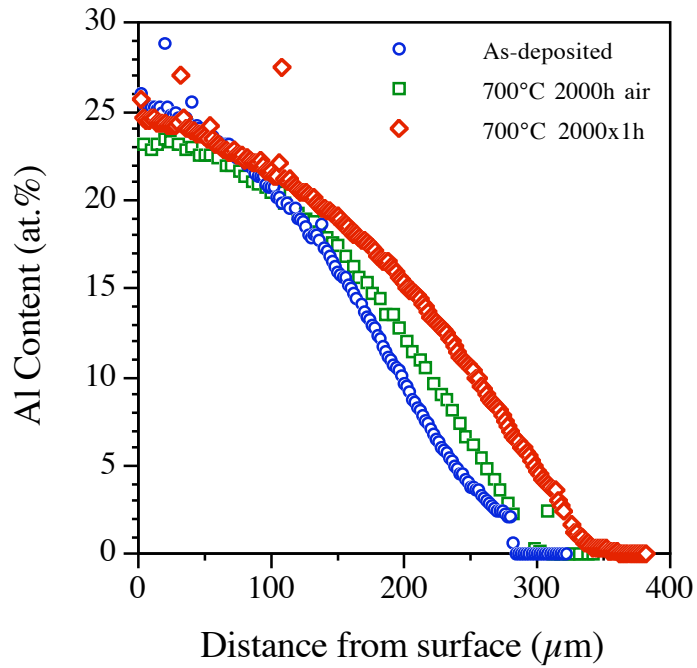

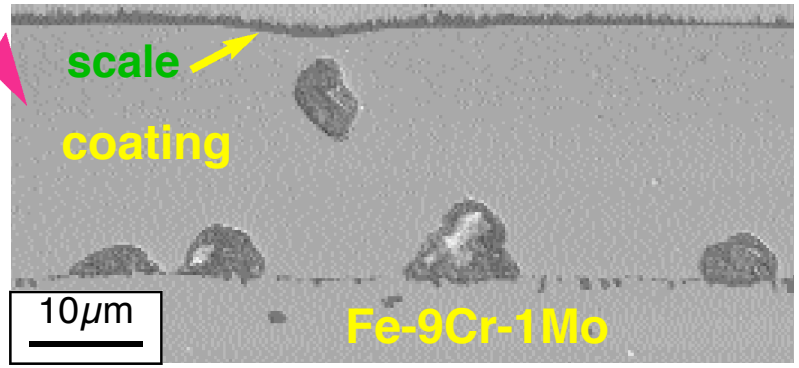

Damage observed after 2000 cycles not due to Al loss

Experimental Procedure

Chemical vapor deposition (CVD) process

selected for controlled laboratory studies, not commercialization

similar to a well-controlled above-pack process

1-2mm x ≈12 x 20 specimens, 2 per run

ORNL laboratory scale reactor

flowing H_2-$AlCl_3$, 100 Torr, 6h, 1050°-1100°C

increase Al activity by adding Cr-Al alloy inside reactor

"Thick" coatings ≈40μm Al-rich outer layer, "Thin" ≈5μm Al-rich outer layer

Environmental testing:

800°C, 20h cycles, H_2-H_2S-H_2O-Ar ($P_{S_2}=10^{-6}$atm; $P_{O_2}=10^{-22}$atm)

800°C, 1h cycles, air+10%H_2O

700°C, 1h cycles, air+10%H_2O

700°C, 100h cycles, air+10%H_2O

800°C, 100h cycles, air+10%H_2O

Lesson learned with Fe_3Al

High CTE alloys spall despite reactive elements!

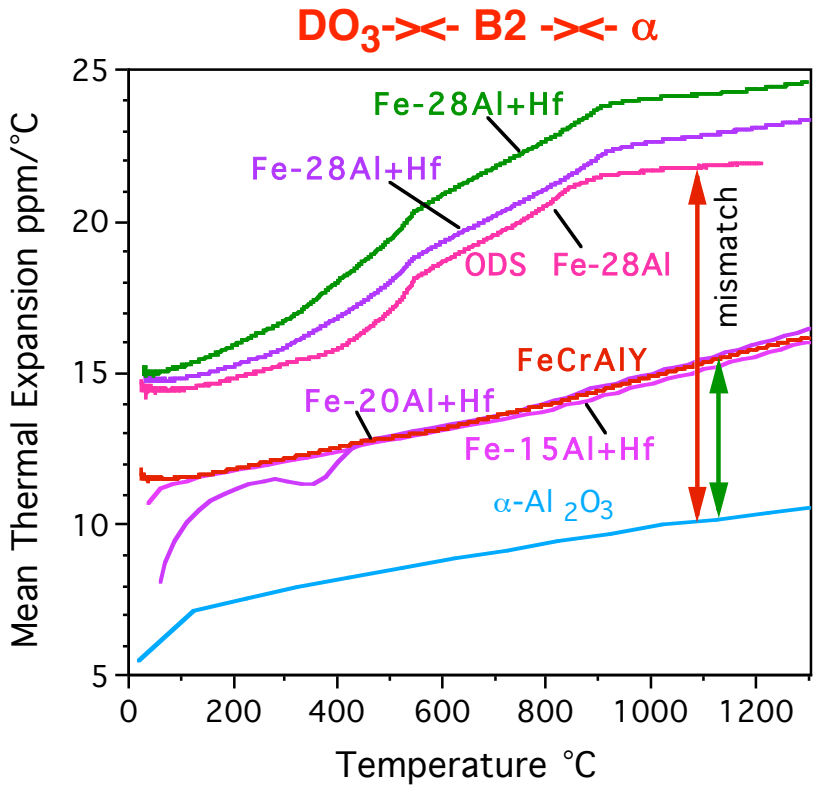

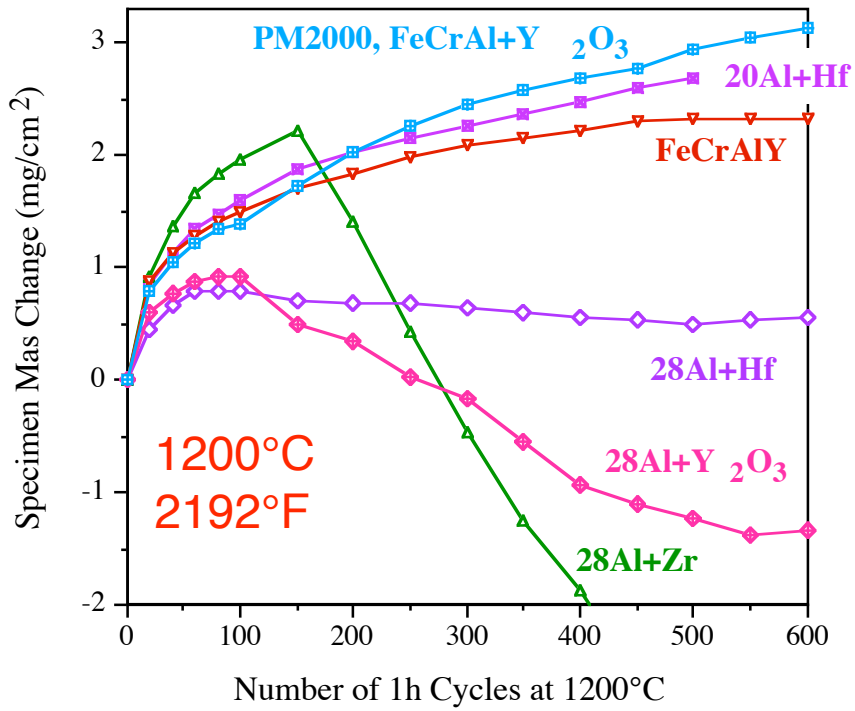

Additions of Zr, Hf and Y_2O_3 to Fe-28Al alloy don't prevent spallation

- Removing S from ODS Fe_3Al showed no improvement

Lowering the Al content in Fe-Al alloys:

- Avoids the DO_3 phase and related transformations to B2 and α
- Improves scale adhesion similar to FeCrAl alloys

Smialek and Doychak first suggested CTE problem for Fe-40Al in 1990

Coating degradation with time

defining the failure criteria

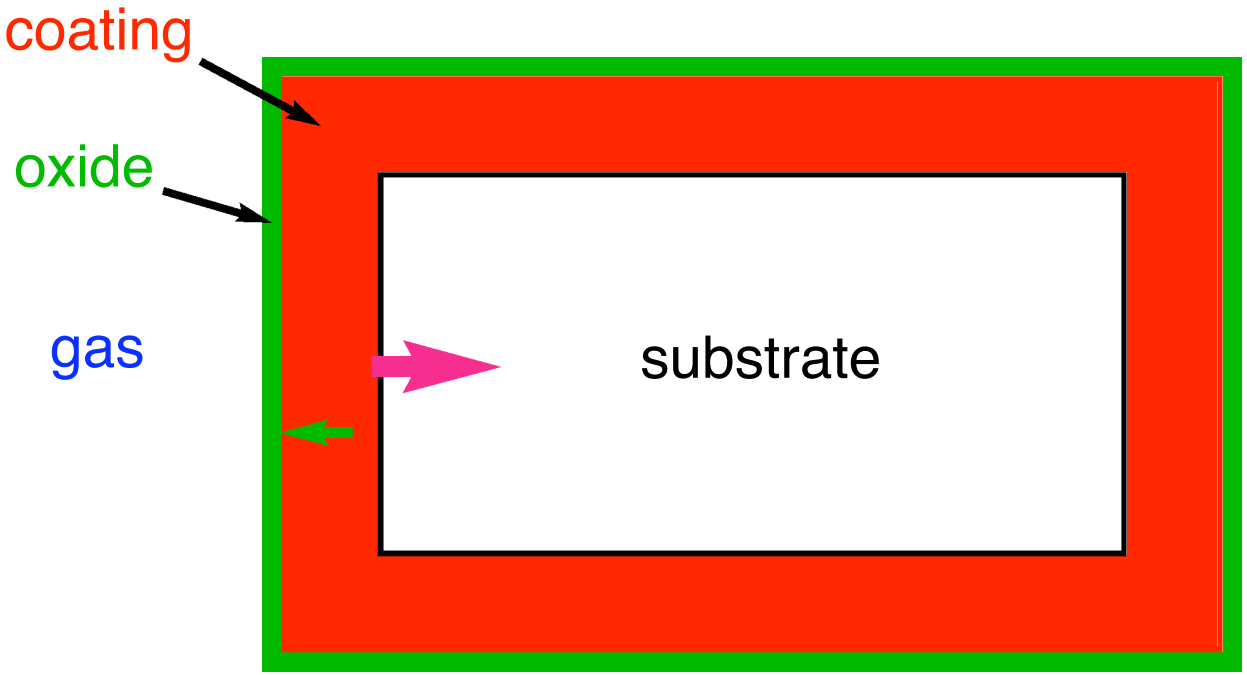

Al supply: coating thickness and starting Al concentration

Coating thickness loss or Al content drop due to:

(1) oxidation/sulfidation: selective formation of reaction product

(2) diffusion into substrate

At low temperatures 650-700°C expect loss by (1) << loss by (2)

How low can coating thickness or Al content drop before coating is no longer effective?

Coating Microstructure-Property-Performance Issues

Terry C. Totemeier
Richard N. Wright

Material Sciences
Idaho National Laboratory

19th Annual Conference on Fossil Energy Materials
May 9-11, 2005, Knoxville, TN

Idaho National Laboratory

Overview

- Introduction: coating performance testing objectives
- TGA corrosion testing of free-standing coatings
- Coating-substrate thermal cycling tests
- Coating fracture testing
- Conclusions and future test plans

Introduction

- **Research goal: understand relationships between *coating processes*, *coating characteristics*, and *coating performance***
- **Coating types:**
  - **HVOF Fe_3Al, FeAl, (alumina formers)**
  - **HVOF Ni-Cr (chromia former)**
  - **APS Mo-Si-B (silica former)**
- **Substrates:**
  - **Low-alloy ferritic steels**
  - **Advanced ferritic-martensitic steels**
  - **Austenitic stainless steels**
  - **Ni-base alloys**

Coating Performance Testing

- **Purpose:**
  - **Establish baseline properties and characteristics**
    - **Relative confidence in coating service performance**
  - **Screening of coating types and coating-substrate combinations**
    - **Down-select for service tests**
  - **Determine contributions of coating system parameters to critical properties**
    - **Select best parameters, understand variations**
  - **Understand failure modes and strategies to mitigate**
- **<u>Service testing is ultimately required</u>**

Critical Coating Characteristics

1. Environmental resistance
   - Coating vs. feedstock alloy → TGA, furnace exposure
   - Isothermal vs. thermal cycled → TGA, furnace exposure
   - Influence of imposed stresses/strains → Coated substrates
2. Adherence
   - Critical for thermal spray coatings
   - How to characterize meaningfully? → ASTM C633?
   - Influence of service exposure → Post-corrosion tests
3. Resistance to cracking prior to and in service
   - Thermal fatigue due to CTE mismatch → Cyclic exposure of coated substrates
4. Post-defect behavior of coated system → Corrosion test of cracked coatings

TGA Testing

- Intrinsic coating resistance to simulated coal combustion gas
- Free-standing coatings:
  - Fe_3Al (560 and 620 m/s spray particle velocity)
  - FeAl (540 and 700 m/s)
- Baseline materials for comparison:
  - 9Cr-1Mo-VNb (grade 91 steel)
  - Type 316 SS
  - Fe_3Al sheet (2%Cr)
- Gas composition:
  - N_2 – 9%CO – 4.5%CO_2 – 1.8%H_2O – 0.12%H_2S (Lehigh)
- Temperatures: 500, 600, 700, 800°C
- Duration: 25 and 100 hr (scoping tests)
- Rates characterized by linear fit near end of test

TGA Results - Steels

- 9Cr-1Mo-V: expected peak in rate at 700°C
- 316 SS: variable behavior, high attack or very little

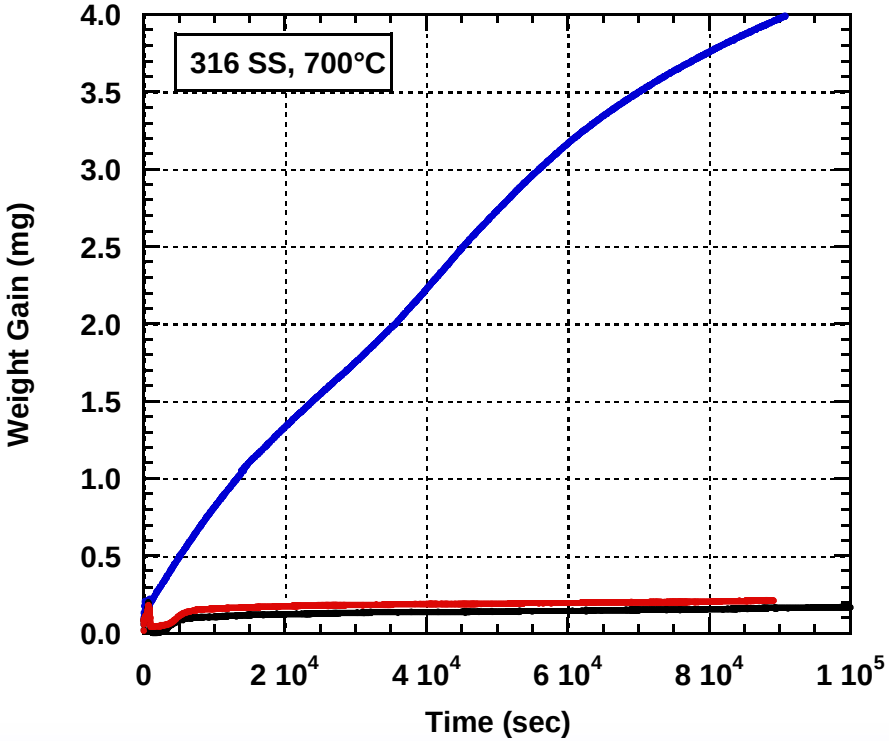

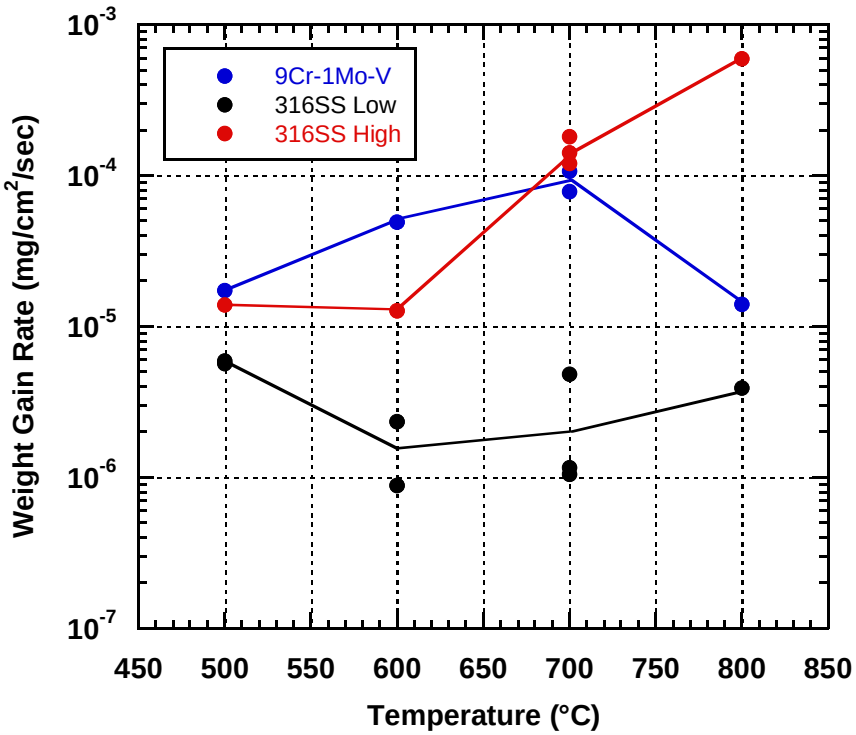

Idaho National Laboratory

TGA Results - Steels

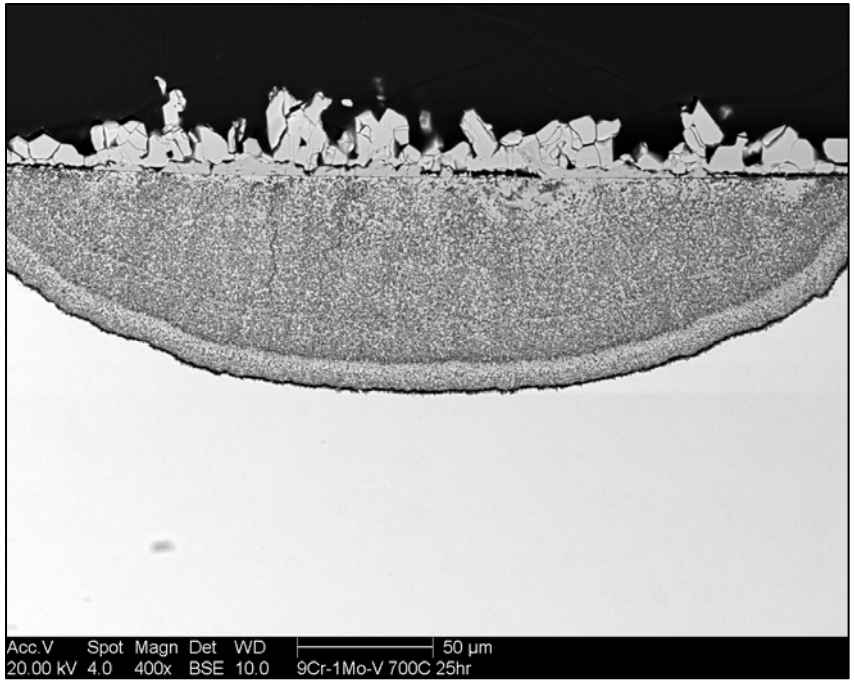

Localized corrosion in 9Cr-1Mo-V after 25 hrs at 700°C

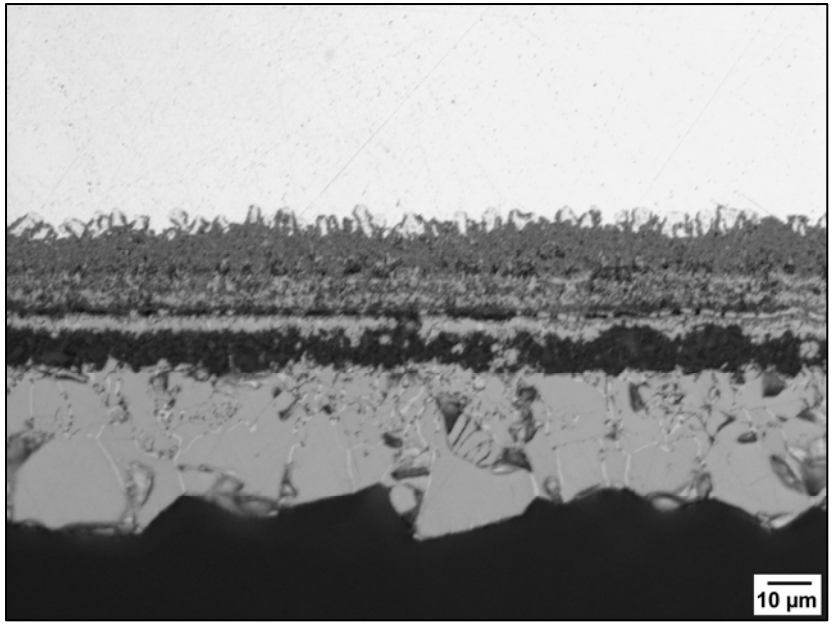

General corrosion in "high gain" 316 SS after 25 hrs at 700°C

TGA Results – Material Comparison

- Relative rates of attack for 700°C, 100 hr test
- Coatings much more resistant than 9Cr or "high" 316 SS
- Fe_3Al sheet shows essentially no attack
- "Low" 316 SS comparable to coatings

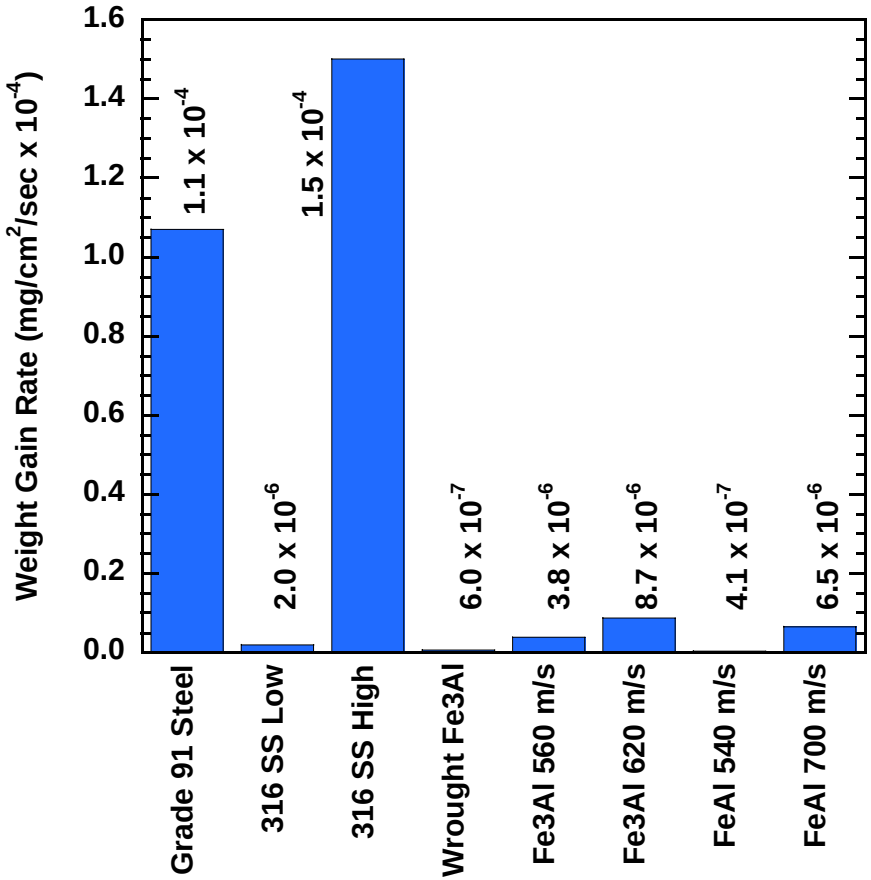

TGA Results - Coatings

- Coatings show initially decreasing rates which become linear
- Relatively low weight gains
- Inconsistent rates vs. temperature

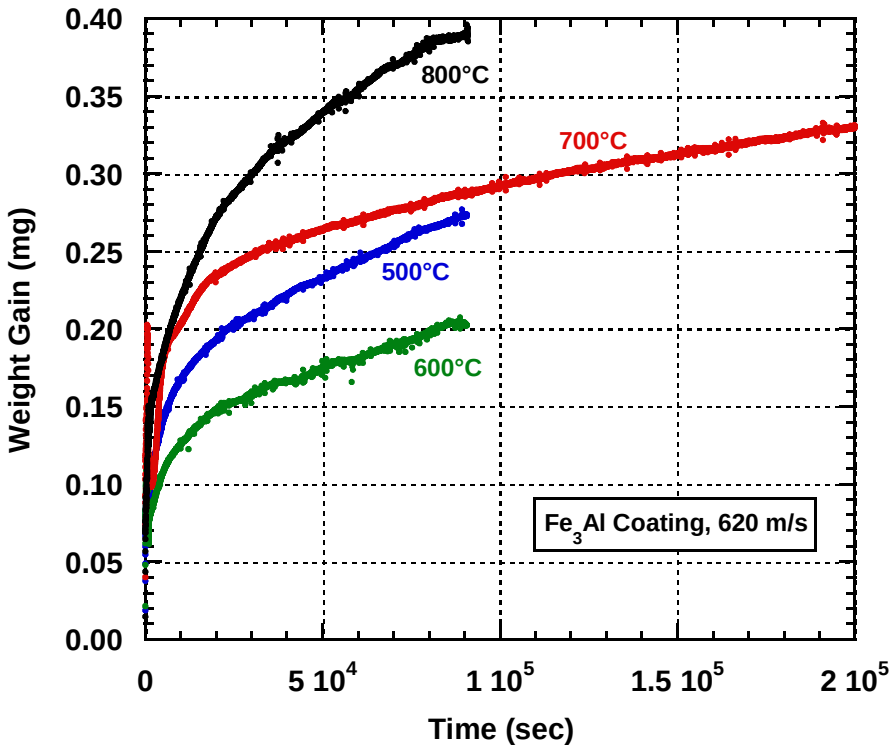

Idaho National Laboratory

TGA Results - Coatings

- No clear difference between coatings
- Coating rate slightly higher than wrought Fe_3Al
- Rates are roughly 10X lower than recently reported by Corvino, et al for similar HVOF Fe_3Al coatings

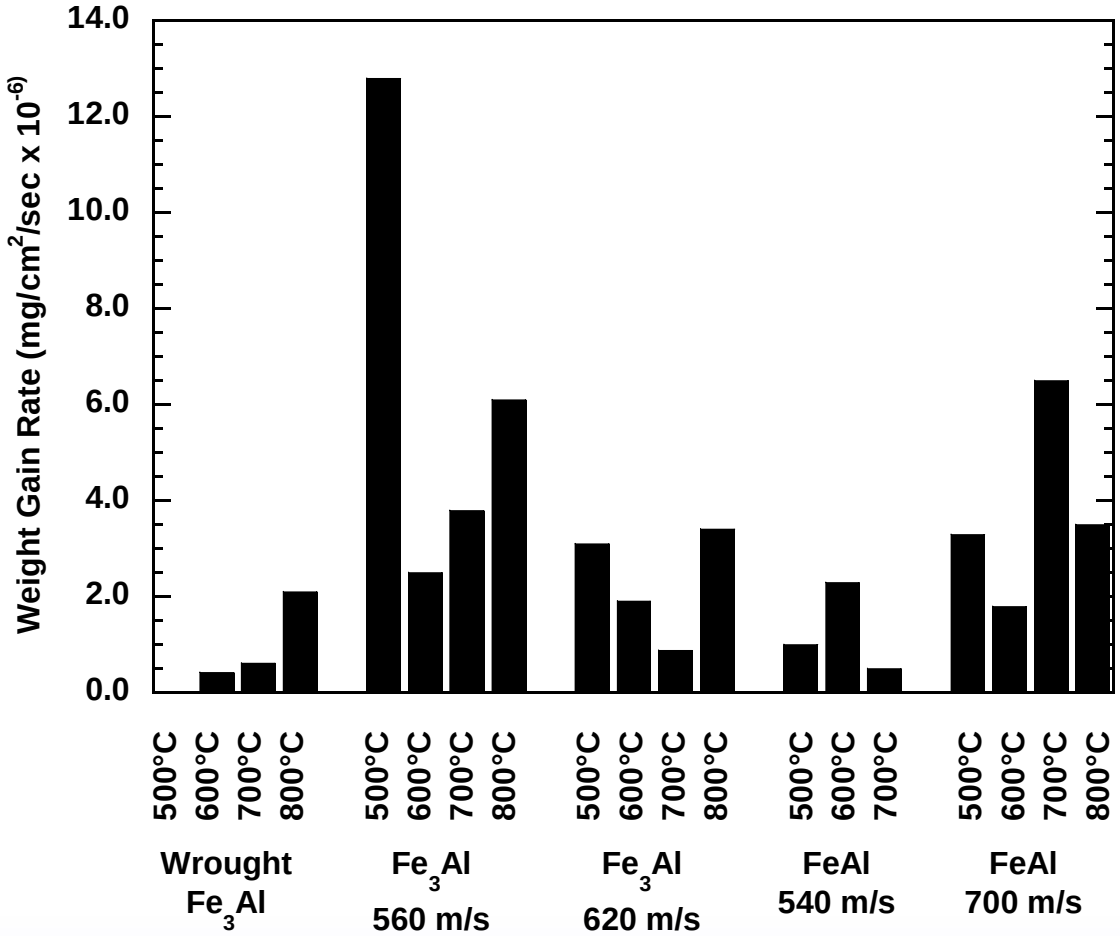

Idaho National Laboratory

TGA Results - Coatings

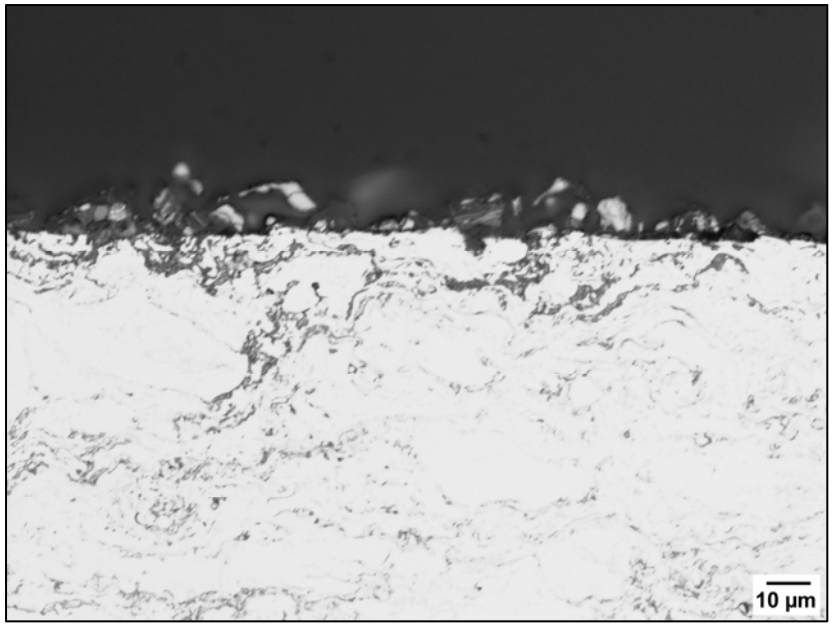

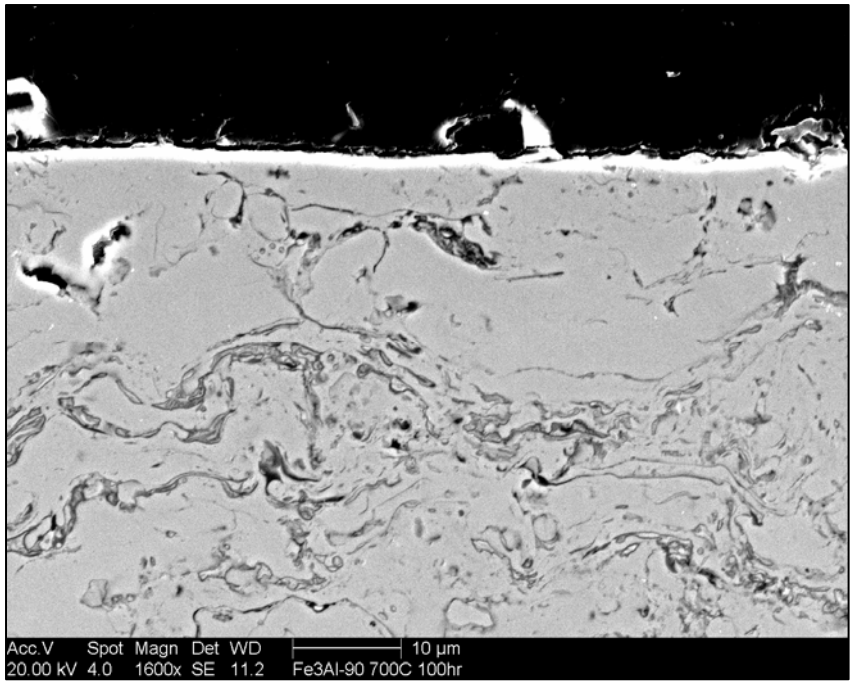

Little indication of attack in examination performed to date

Fe_3Al coating, 620 m/s, 100 hr exposure shown

Coating-Substrate Thermal Cycling

- 500 µm coatings on cylindrical substrates
- Repeated cycles from RT to 800°C in air (1, 15, 30 cycles examined)
- Metallographic examination for cracking
- Results:
  - FeAl:
    - Cracking in higher-velocity coatings on 316 SS
  - Fe_3Al:
    - No cracking on 316 SS
    - Slight cracking on IN600
  - Mo-Si-B:
    - Catastrophic cracking on 316 SS (vacuum exposure)
  - 316 SS coatings
    - No cracking on 316 SS

Coating-Substrate Thermal Cycling

- Cracking behavior agrees with simply-calculated thermal stresses/strains

Case	Initial Residual Stress	CTE Mismatch Thermal Strain Range	Coating Stress at 800°C	Coating Stress at RT (After Relaxation)	Cracking ?
FeAl-540-316SS	–70 MPa	0.27%	–370 MPa	+330 MPa	No
FeAl-660-316SS	–220 MPa		–630 MPa	+407 MPa	30 cycles
FeAl-700-316SS	–390 MPa		–820 MPa	+434 MPa	15 cycles
Fe_3Al-560-316SS	–140 MPa	0.12%	–40 MPa	–100 MPa	No
Fe_3Al-620-316SS	–530 MPa		–370 MPa	–140 MPa	No
Fe_3Al-560-IN600	+10 MPa	0.16%	–130 MPa	+140 MPa	30 cycles
Fe_3Al-600-IN600	– 230 MPa		–420 MPa	+190 MPa	1 cycle
Fe_3Al-620-IN600	–370 MPa		–590 MPa	+220 MPa	30 cycles
Mo-Si-B-316SS	–30 MPa	0.86%	+1400 MPa	–1460 MPa	Yes
316SS-520-316SS	–190 MPa	None	–190 MPa	None	No
316SS-640-316SS	–340 MPa		–340 MPa		

Blue = low stress, Black = moderate stress, Red = severe stress

Coating Fracture Testing

- Coating strain to fracture measured using acoustic emission monitoring
- 500 µm coatings applied to dogbone-shaped tensile specimen substrates
  - Reduced area section
- Two AE sensors attached to each end of substrate near grips
  - Used to locate events within coated gage section
- Coating cracking produces clear AE signals

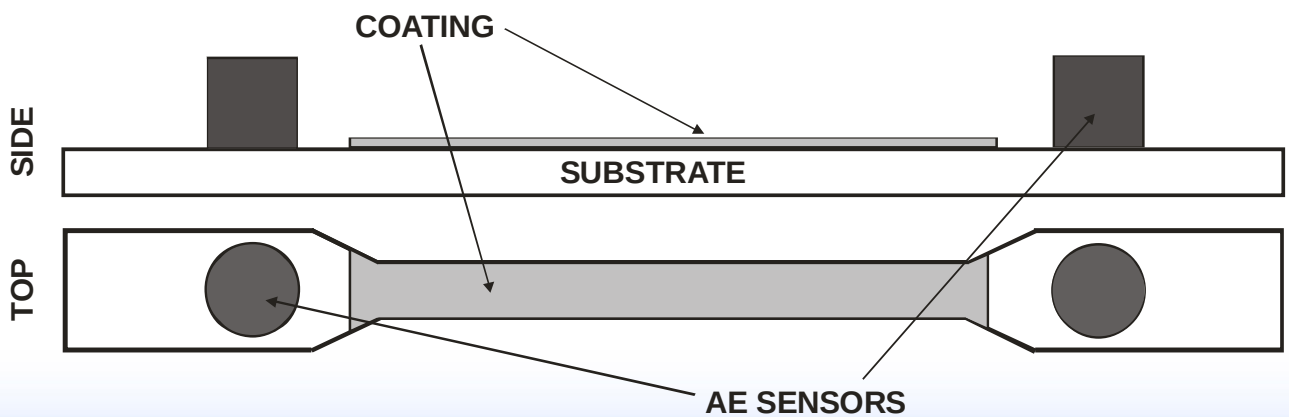

Coating Fracture Strain Results

- Coating fracture stains exceed substrate yield strain
- Behavior consistent with relative ductilities of Fe_3Al and FeAl
- No marked effect of spray particle velocity
- Lower fracture strain on CS substrate may be due to less compressive residual stress
- Coatings failed in a brittle manner
  - Extensive debonding in some cases (not consistent)

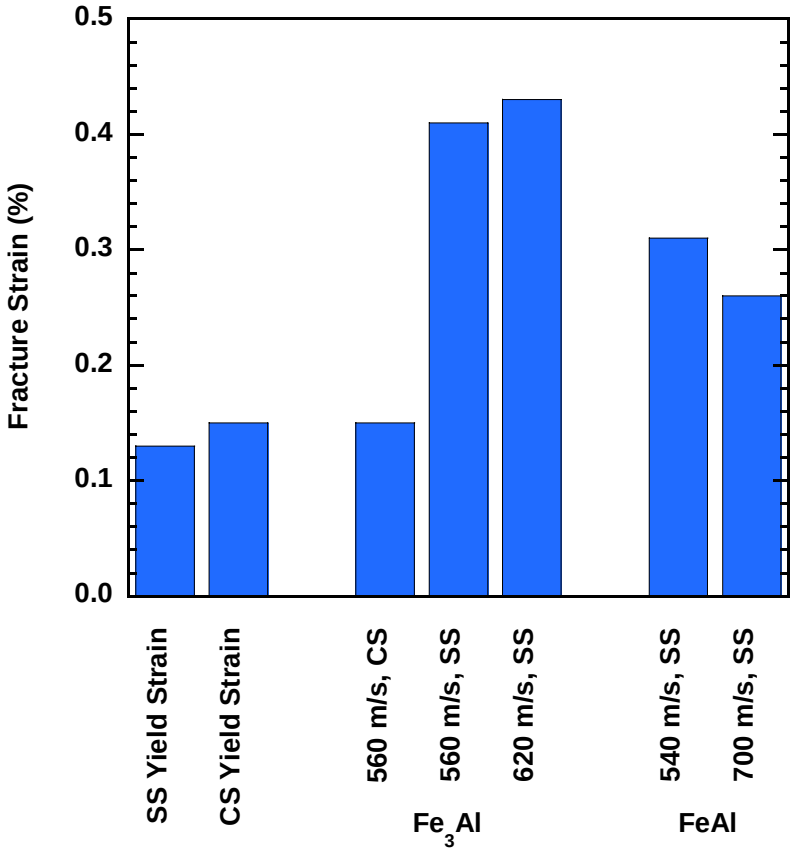

Conclusions – Future Plans

- Iron aluminide coatings show good resistance to gas-phase corrosion
  - Similar to wrought alloy behavior
  - No marked effect of alloy composition or spray parameters
- CTE mismatch is primary determinant of cracking in thermal cycling
  - Residual stress secondary effect
- Coatings show reasonable RT ductility
- Future plans:
  - Gas-slag corrosion tests on free-standing coatings (isothermal and cyclic)
  - Preparation and characterization of Ni-50Cr HVOF coatings
  - TGA tests of Mo-Si-B coatings at high temperatures (>1000°C)
  - Corrosion testing of defected coatings on substrates
  - Further cycling and adhesion testing
    - Better ways to assess thermal fatigue resistance and adhesion?

LEHIGH University

High-Temperature Corrosion Resistance of Candidate Fe-Al-Cr Coatings in Low NOx Environments

J.T. Murphy, J.R. Regina, R.M. Deacon, J.N. DuPont, and A.R. Marder

Lehigh University
Materials Science and Engineering
Bethlehem, PA 18015

Fossil Energy Materials Conference 2005

Overview

- ***Background***
  - *Low NOx furnace environments*
  - *Fe-Al-Cr high-temperature corrosion resistance*
  - *Weldability of Fe-Al-Cr based overlay claddings*
- ***High-Temperature Corrosion Results***
  - *Weldable Fe-Al-Cr compositions*
  - *Identification of candidate Fe-Al-Cr weld coatings*
- ***Target Low NOx Combustion Environments***
  - *Coal-Ash Corrosion*
  - *Investigation of Fe-Al-Cr as weld overlays*
- ***Summary and Conclusions***

Low NOx Environments

- *Clean Air Acts require reduction in harmful NOx compounds*
- *Fuel rich environment utilized to reduce emission of NOx compounds*
- *Change in combustion parameters increases the amount of corrosive sulfur compounds present in the gas*
- *Rapid corrosion of furnace components due to sulfidation*

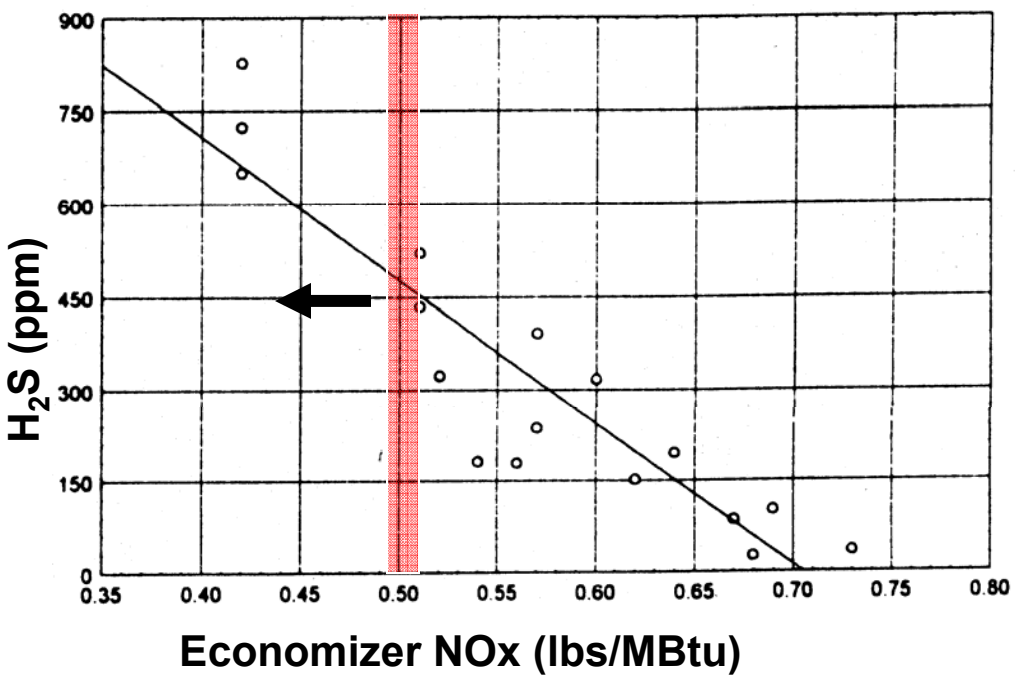

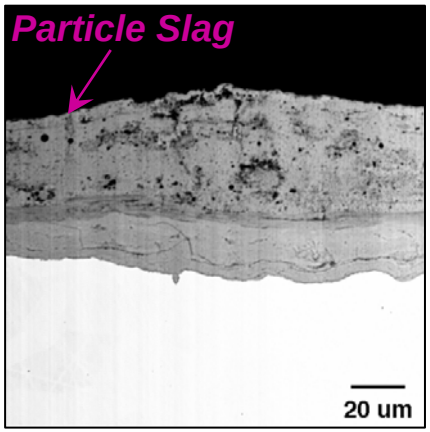

Boiler Tube Surface

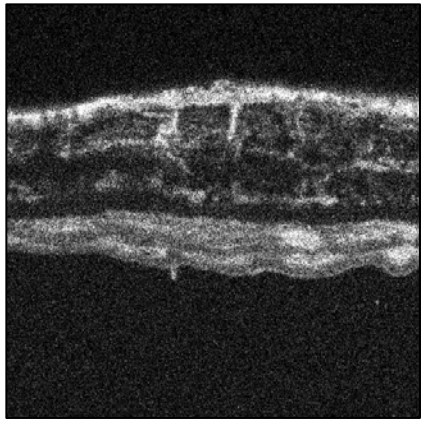

Sulfur X-Ray Map

***Gabrielson and Kramer**, Joint Power Generation Conference (1996)*

Fe-Al Based Weld Overlay Coatings

Advantages of Fe-Al Weld Overlays:

- Low cost: ~ $5/lb (Ni-based alloys ~$20/lb)
- No microsegregation of Al in weld
- Superior corrosion resistance to Ni-based superalloy and stainless steel weld coatings

Simulated low NOx Environment

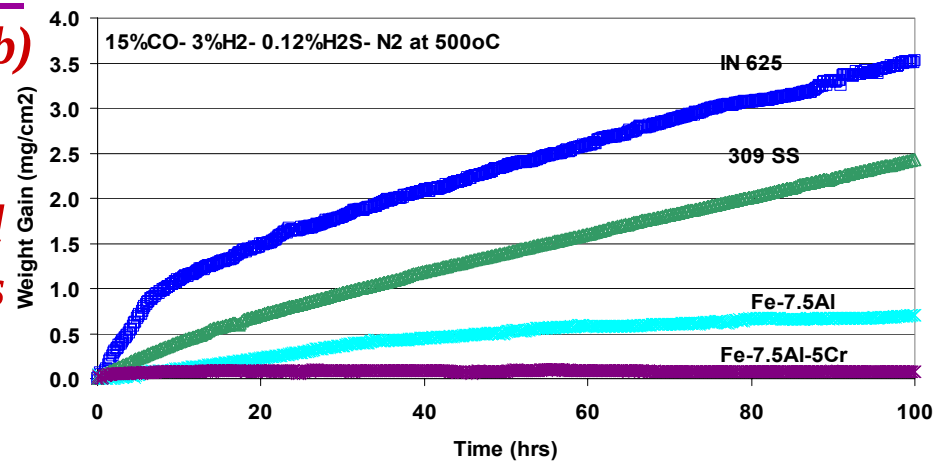

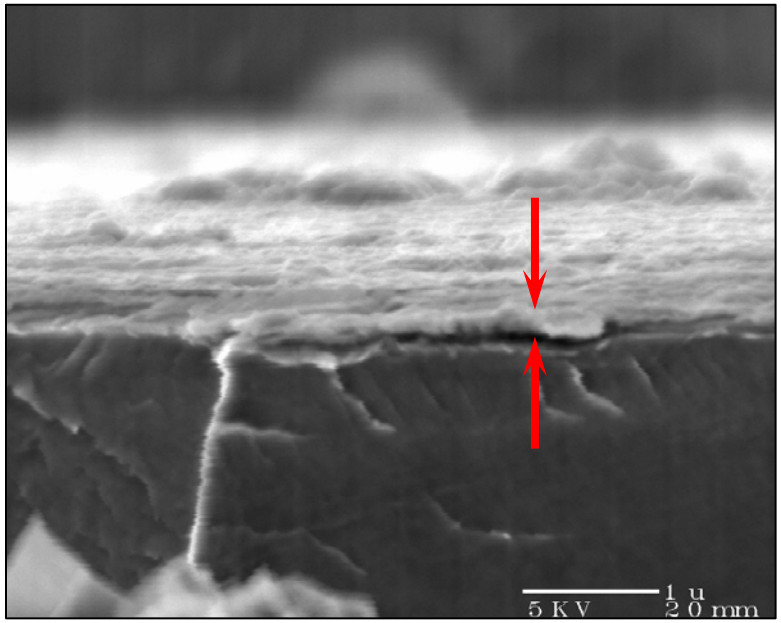

Passive Oxide Layer on FeAlCr Alloy

Passive Oxide Layer Formation:

- Alloys rely on passive layer formation and maintenance for corrosion resistance
- Fe-Al-Cr based alloys form passive oxide layer even in environments containing low Po_2
- Binary Fe-Al alloys are suceptible to hydrogen cracking at high Al concentrations

Experimental Procedure

GTAW Weldability Study

- *Simultaneously deposit two filler metal wires to control the aluminum and chromium contents independently*
  - *Commercially Pure Al wire (1100)*
  - *430SS (Fe-16wt%Cr)*
- *Treat two wires as if one filler metal wire was fed into weld pool*

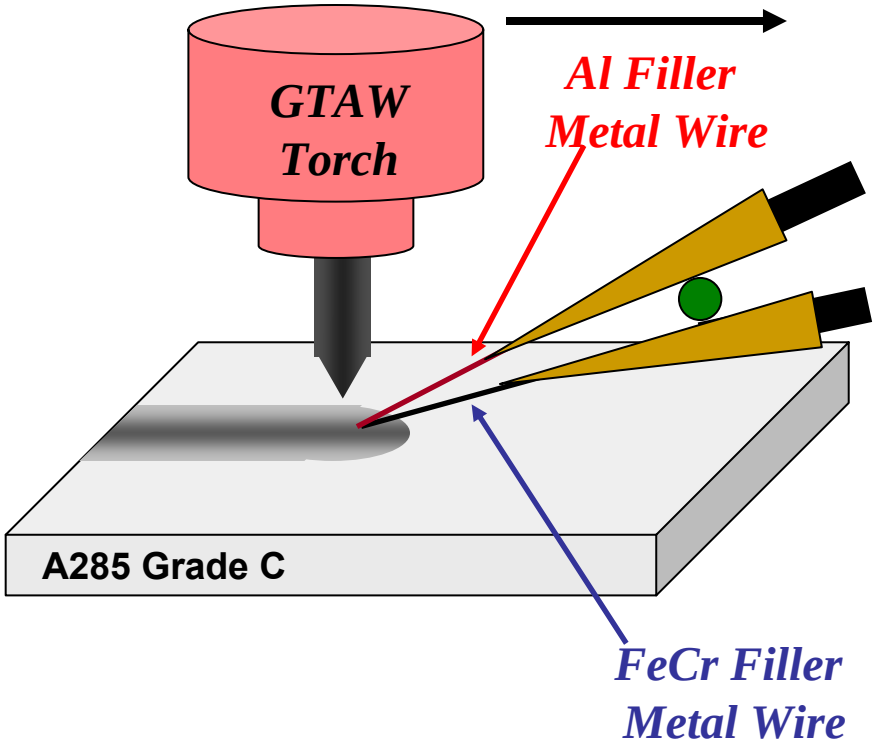

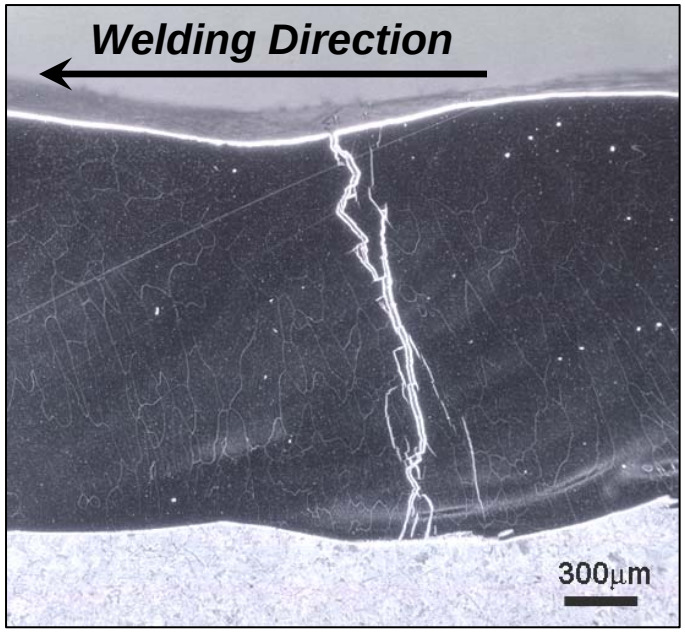

- *Cover a wide range of aluminum and chromium compositions*
- *Dye Penetration Testing and LOM to examine for cracking*

FeAlCr Weldability Results

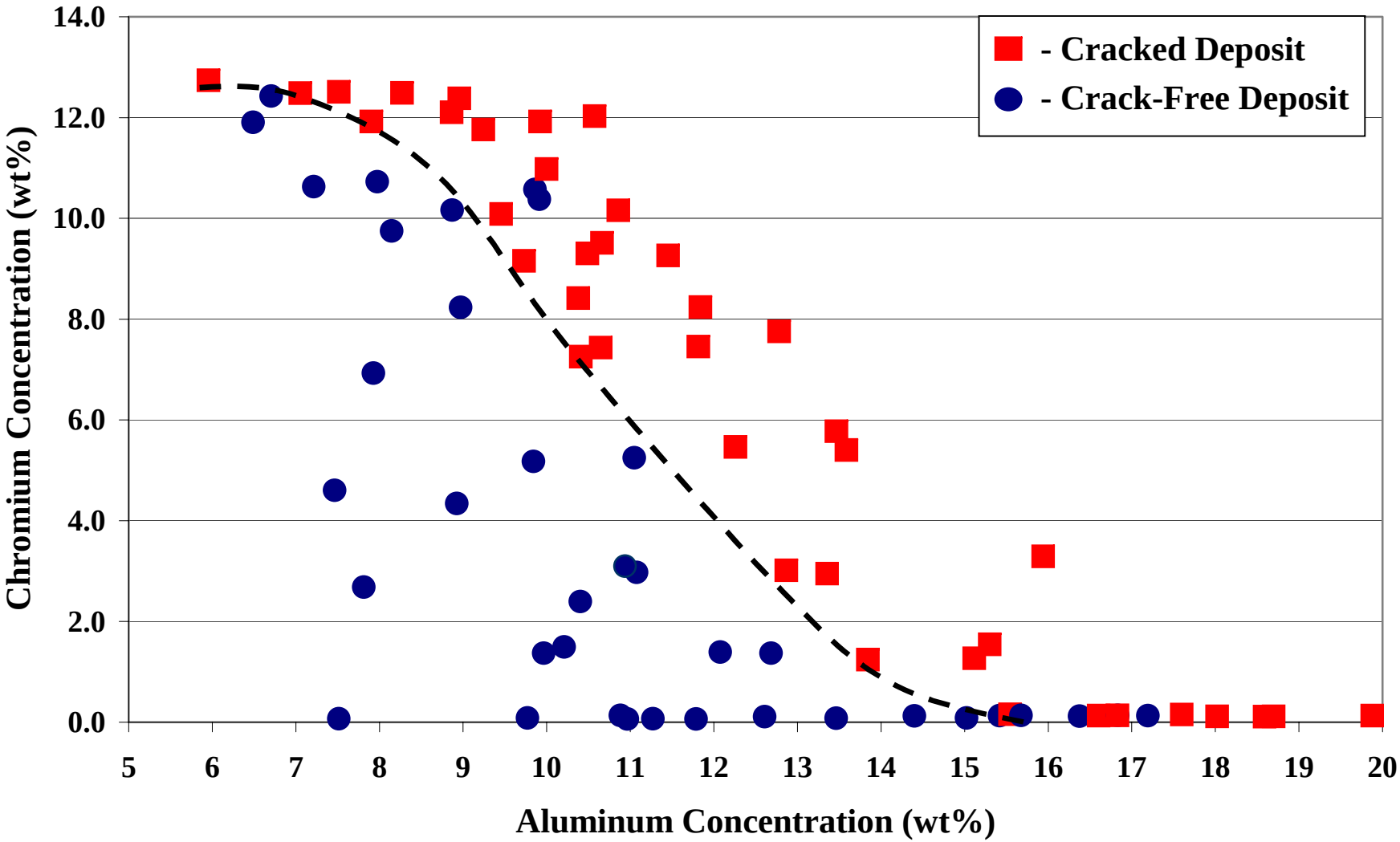

Weld compositions determined using Electron Probe Microanalysis (EPMA)

Low NOx Corrosion Testing

Experimental Procedure

- *Crack-free weld compositions used for gaseous corrosion testing*
- *Samples exposed to a mixed oxidizing/sulfidizing gas at 500°C*
  - *10%CO- 5%CO_2- 2%H_2O- 0.12%H_2S- N_2*
- *Weight measurements were used to quantify the corrosion behavior*

Exposed Alloys

- Fe- 12.5*wt*%Al
- Fe- 10*wt*%Al- 5*wt*%Cr
- Fe- 7.5*wt*%Al- 10*wt*%Cr
- Ni- 622 (currently used)

Exposure Times

100, 250, 500, 1000 and 2000 hours

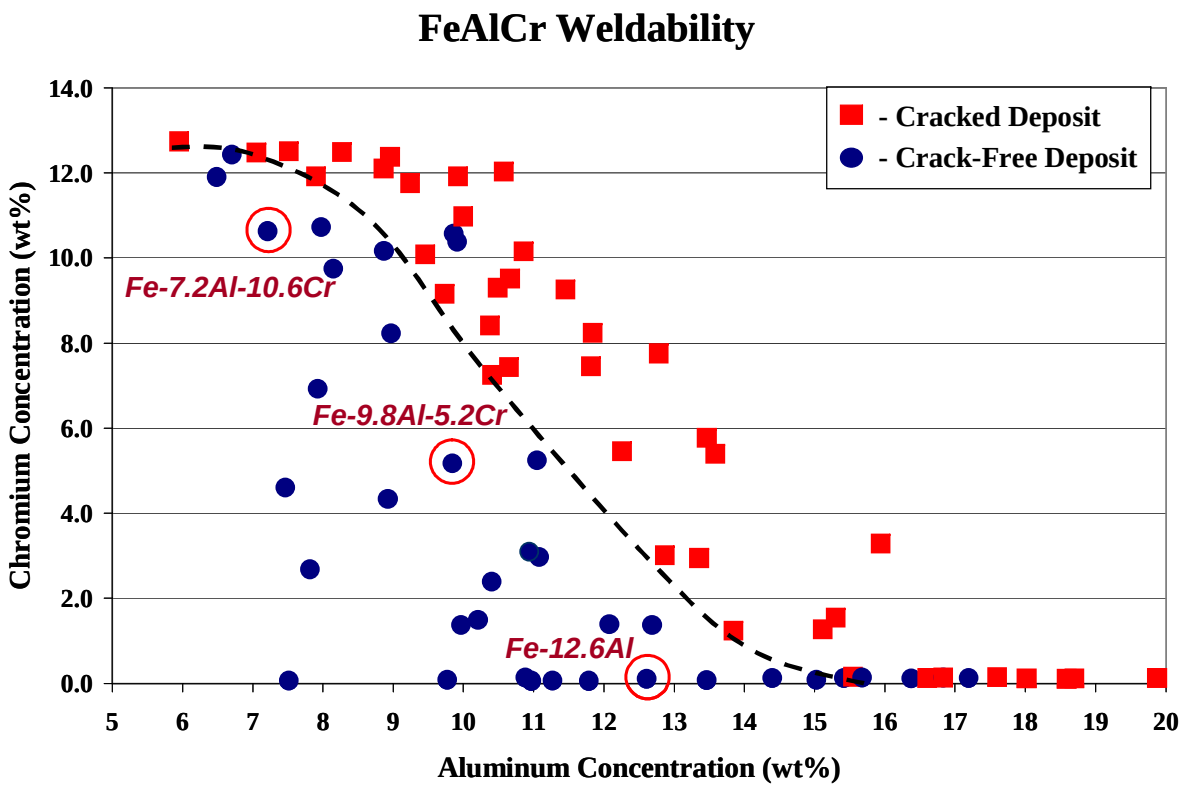

Low NOx Corrosion Results

Mixed Oxidizing/Sulfidizing Environment

10%CO- 5%CO_2- 2%H_2O- 0.12%H_2S- N_2

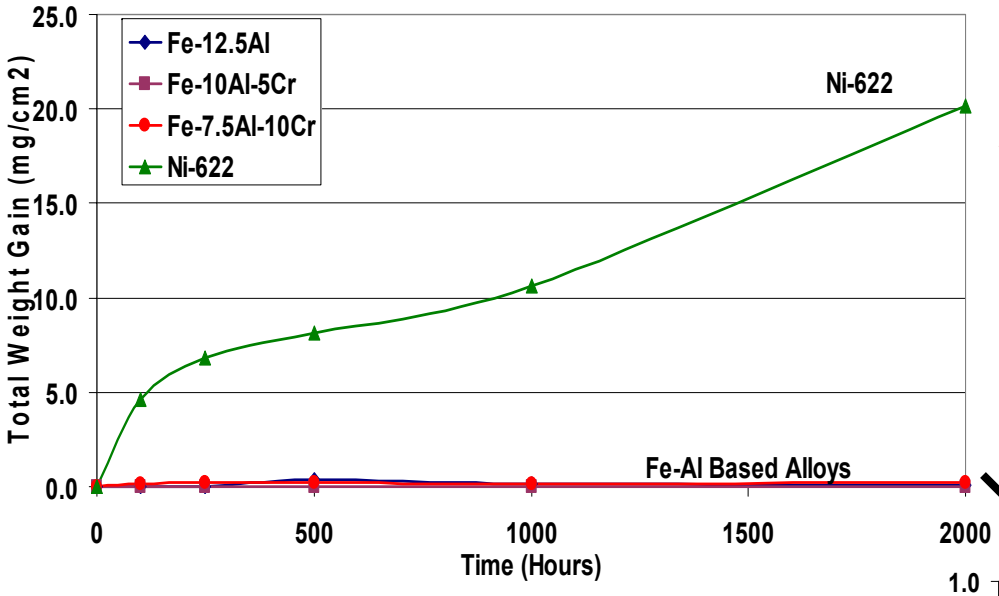

Fe-Al Based Alloys demonstrated superior corrosion resistance when compared to the currently used Ni-based superalloy (Ni-622)

The Fe-10Al-5Cr Alloy out-performed all Fe-Al Based Alloys and gained no weight during 2000 hours of exposure

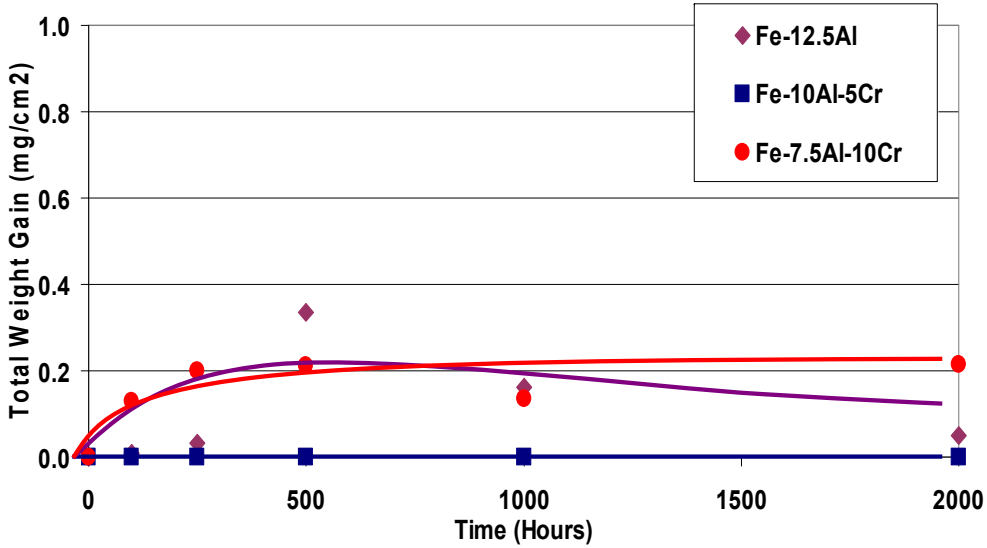

Corrosion Scale Morphology

Ni-based Superalloy (622)

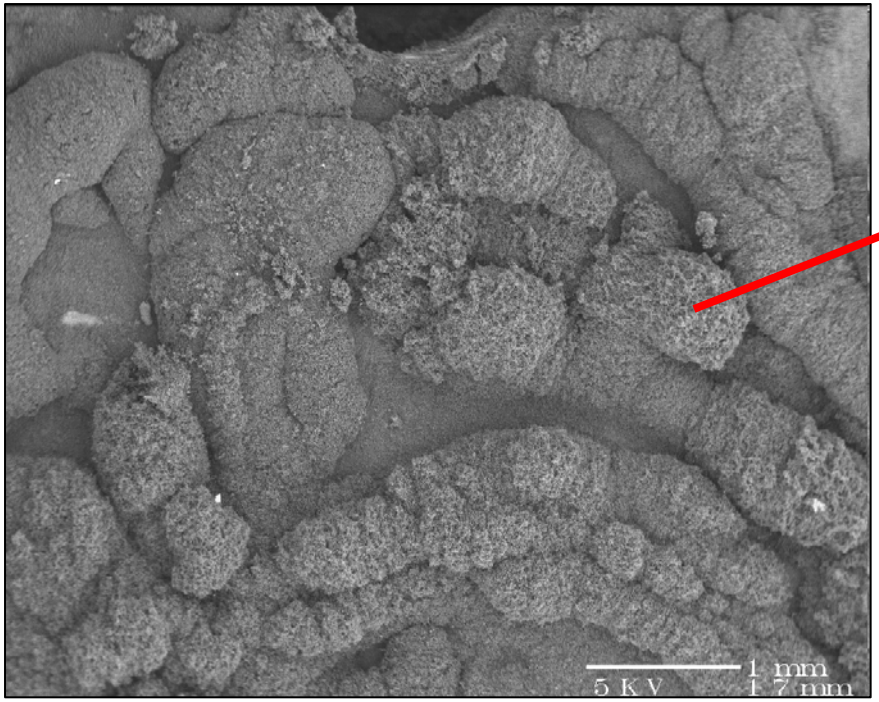

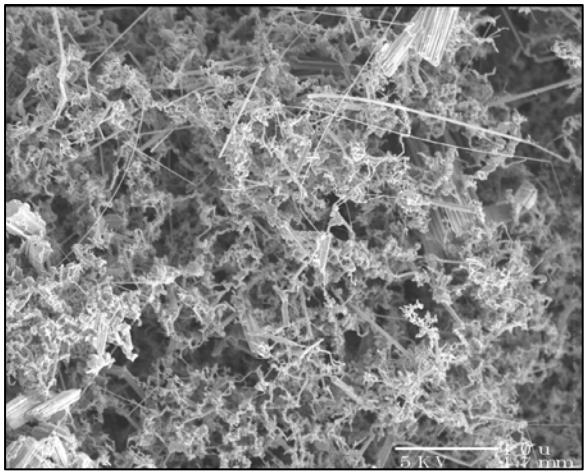

Iron-nickel sulfide scale

Ni-622 formed thick porous corrosion scale identified by EDS as iron-nickel sulfide

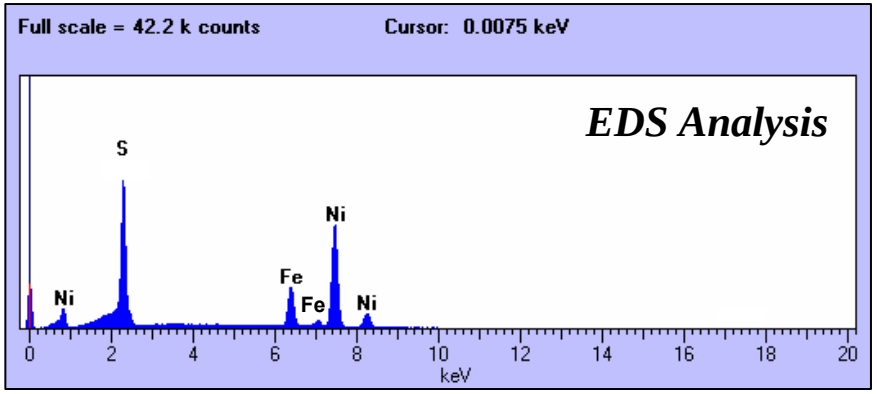

2000 Hour Exposure

Corrosion Scale Morphology

2000 Hour Exposure

Fe-7.5Al-10Cr

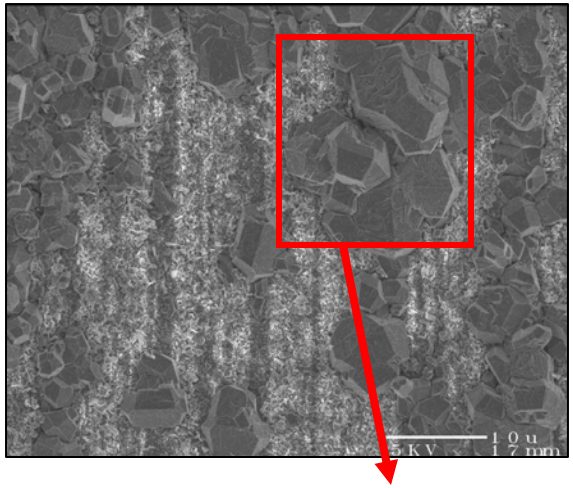

Fe-12.5Al

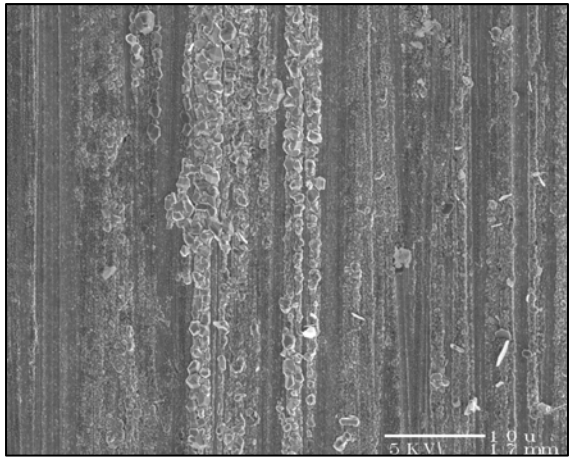

Fe-10Al-5Cr

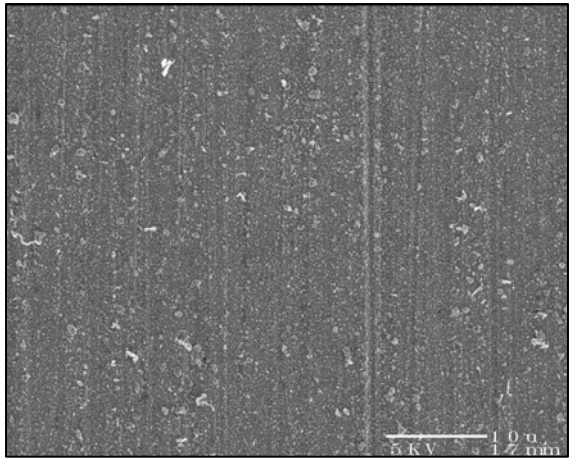

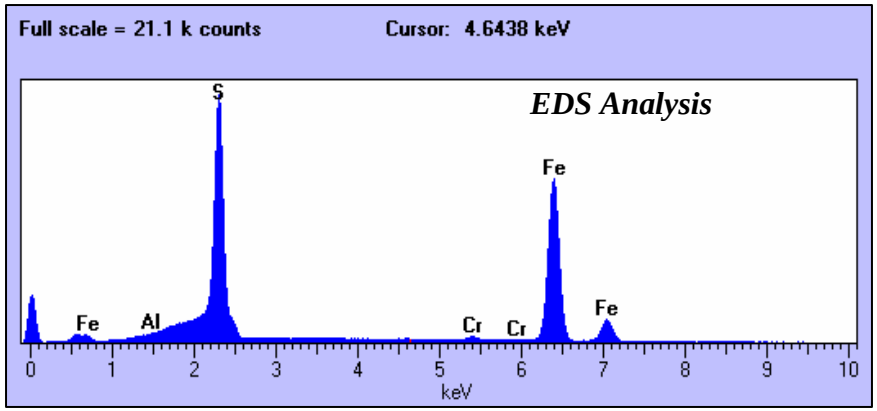

Block-like corrosion products identified as iron-sulfides

Fe-10Al-5Cr demonstrated best corrosion resistance of all alloys tested for 2000 hours in the simulated low NOx environment

Confirmed that a minimum of 10wt%Al and 5wt%Cr was required for extended corrosion resistance

Low NOx Environments

	Typical Low NOx Environments	*Target Low NOx Environments*
Temperature	*500ºC*	*> 600ºC*
Corrosive Gas	H_2S, SO_2, CO, H_2O, CO_2	H_2S, SO_2, CO, H_2O, CO_2
Slag Components	FeS_x, Fe_xO_y, C	FeS_x, Fe_xO_y, C Na_2SO_4, K_2So_4

- ***Candidate Fe-Al-Cr weld overlay coatings provide excellent corrosion in current burning conditions up to 2000 hours***
- ***The performance of these weld overlays make them strong candidates for use in new Target Low NOx Conditions***

Boiler Tube Corrosion in the Target Condition

- *Waterwall tubes will see temperatures that gives rise to corrosion by alkali-iron trisulfates (AIT)*
- *Promotes much higher metal degradation rates than oxidation or sulfidation alone*
- *Coal-ash corrosion is prevalent in an oxidizing environments*
- *Conditions of the low NOx environment at the higher temperatures are not currently known.*

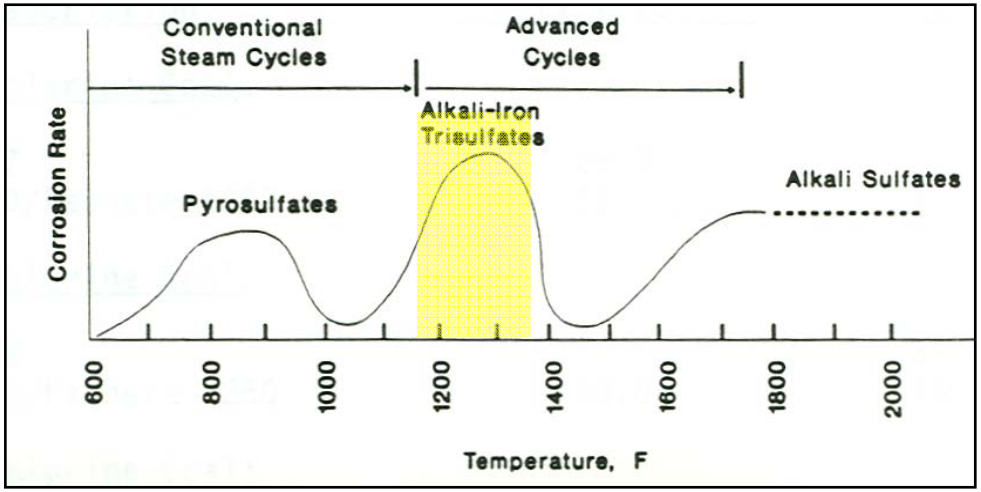

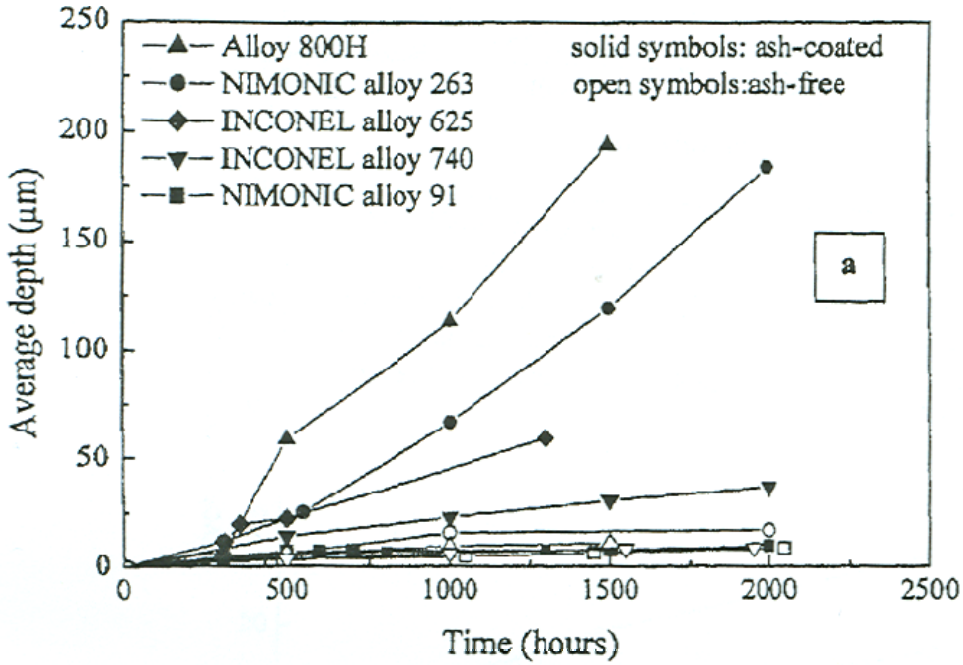

--- ***Van Wheele & Blough,*** *Foster Wheeler Report 1990*

Corrosion Behavior of AIT's

- *Corrosion rates follow 'bell-shape' dependence to temperature*
- *Three regions of behavior*
  - *Low Temperature (600°C)*
  - *Mid-Range Temperature (675°C - 725°C)*
  - *High Temperature (>750°C)*
- *Exact location of max corrosion varies alloy to alloy*
- *Corrosion rates show strong dependence on chromium content*
  - *Increase in Cr lowers the temperature of max corrosion and decreases the total amount of corrosion*
  - *Literature shows corrosion rates decrease with Cr additions up to 20-25wt%*

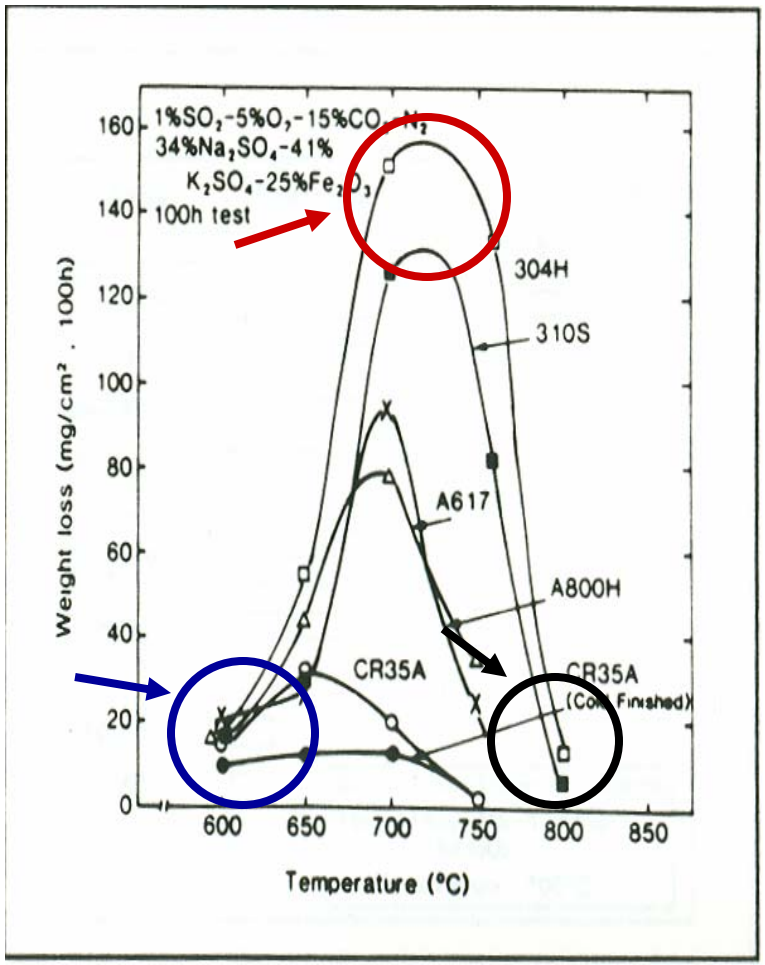

Van Wheele & Blough,
Foster Wheeler Report 1990

Project Outlines

- ***Literature has shown the suggested waterwall alloys in the New temperature conditions are ASTM – 213/213M Grades 92 (9.5wt%Cr) and 23 (2.5wt%Cr)***
  - ***ALSTOM & Foster Wheeler***

- ***Both alloys provide high temperature strength necessary to operate In higher temperature regimes***

- ***However, they are limited by corrosion resistance (<625°C) and therefore require protective weld overlays to operate at higher temperatures***

- ***Research and testing will be performed to determine the weldabilty of Fe-Al-Cr overlays on the new alloy substrates***

- ***Fe-Al-Cr weld overlays will be evaluated in both gaseous and synthetic coal ash corrosion conditions for the new projected temperature ranges***

Weldability Study of New Substrates

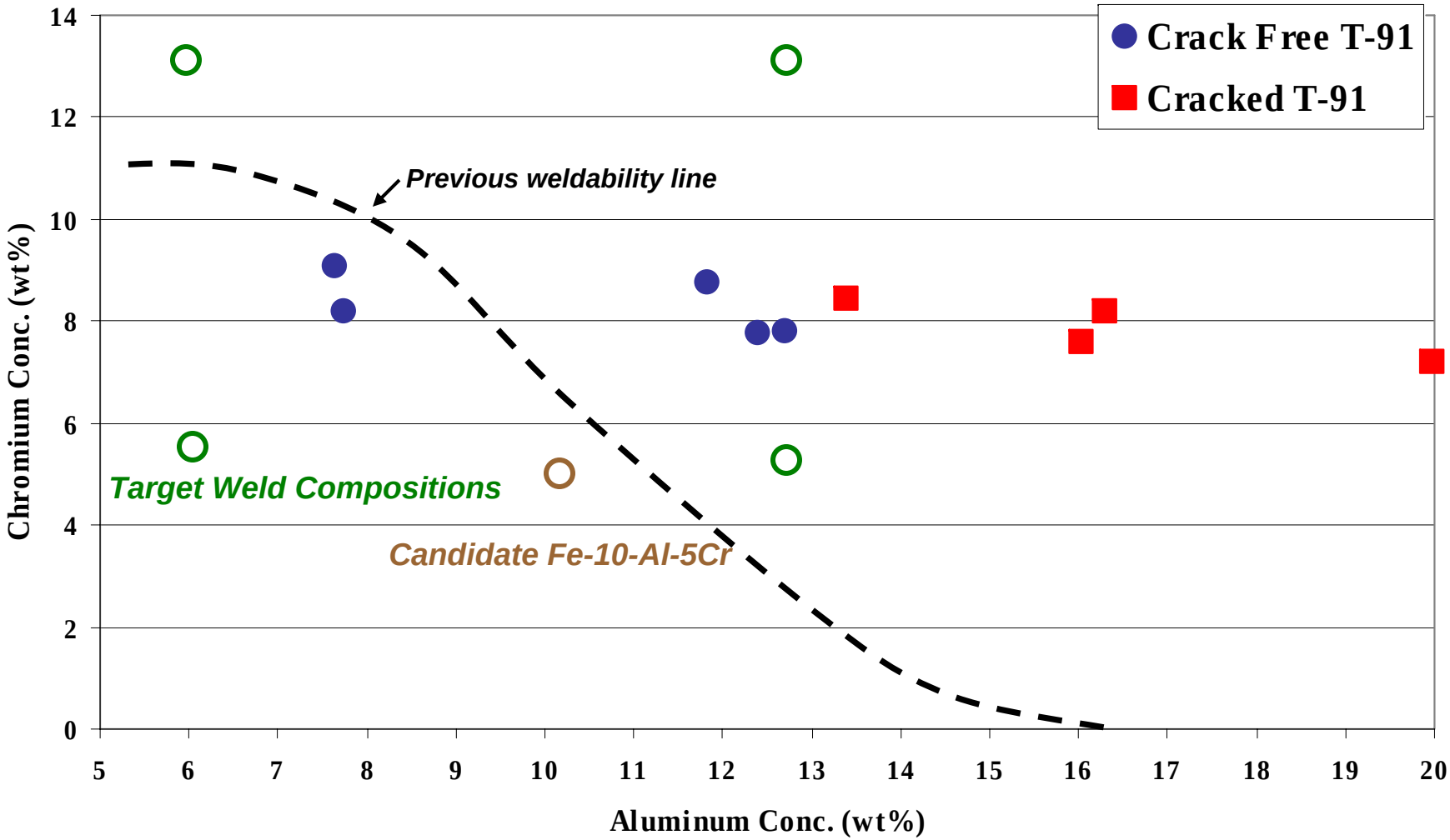

Weld compositions determined by wet chemical analysis

Initial welding study shows an increase of the weldable Fe-Al-Cr compositions

Experimental Procedure

- ***Total of seven alloys to be tested:***
  - ***T-92 and T-23 bare substrates***
  - ***4 weld alloys of indicated compositions***
  - ***Fe-10%Al-5%Cr weld alloy (candidate comp. from previous study)***
- ***Gaseous Corrosion Environment***
  - ***Simulated low NOx gas environment***
  - ***Testing Temperatures: 600ºC, 675ºC, and 750ºC***
  - ***Testing Times: 100hrs***
- ***Synthetic Coal Ash Corrosion***
  - ***Simulated low NOx gas environment***
  - ***Synthetic sulfate ash composition:***
    - ***Fe_2O_3: 25 wt%***
    - ***Na_2SO_4: 37.5 wt%***
    - ***K_2SO_4: 37.5 wt%***
  - ***Testing Temperatures: 600ºC, 675ºC, and 750ºC***
  - ***Testing Time: 100hrs***

Summary and Conclusions

Previous Research on Weldable Fe-Al-Cr Alloys

- Three weldable Fe-Al-Cr alloys demonstrated superior corrosion resistance compared to Ni-based superalloy (622) during exposure in a simulated low NOx environment at 500℃
  - Best candidate weld overlay coating was Fe-10wt%Al-5wt%Cr

Target Low NOx Corrosion Environments

- Determine the weldability of Fe-Al-Cr alloys on T-92 and T-23
  - Possibility of increasing Al and Cr concentration
- Fe-Al-Cr weld overlay claddings to be evaluated in corrosive gas and potential coal ash environments at the new temperature regimes
- Target temperatures (>600℃) have been shown to promote formation of liquid AIT's
  - Potential for coal ash corrosion

Acknowledgements

- ***US Department of Energy (DOE)***
  - ***Fossil Energy Advance Research and Technology Development (AR&TD) Materials Program***
- ***Oak Ridge National Laboratory (ORNL)***
  - ***V. Sikka and B. Pint***
  - ***P. Tortorelli and I. Wright***
- ***Technical Support***
  - ***J. Blough – FENOC***
  - ***G. Stenko – Foster Wheeler***
  - ***S. Goodstine – ALSTOM***

Ultra-Supercritical Condition

- *Over the past few decades efforts have been made to increase the efficiency of conventional boiler/steam turbine fossil power plants*
- *Directed at increasing steam pressure and temperature*
- *Increase in temperature improves efficiency as well as decreases the total amount of SO_2, NO_2, CO_2 emissions*
- *USC is generally defined as a combustion condition above 24MPa/593°C*

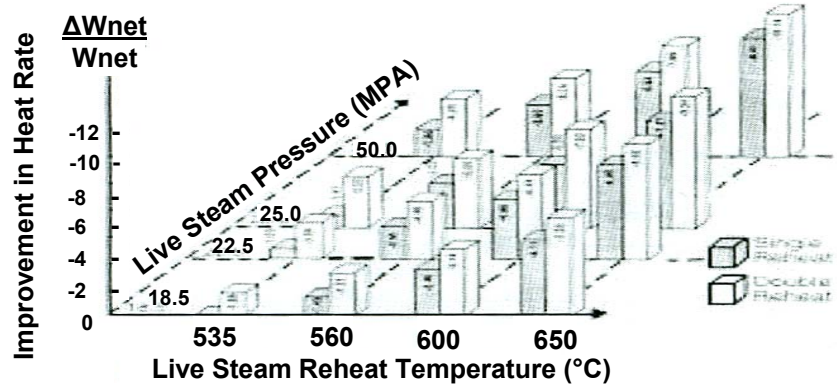

Viswanathan and Bakker, *JMPEG (2001)*

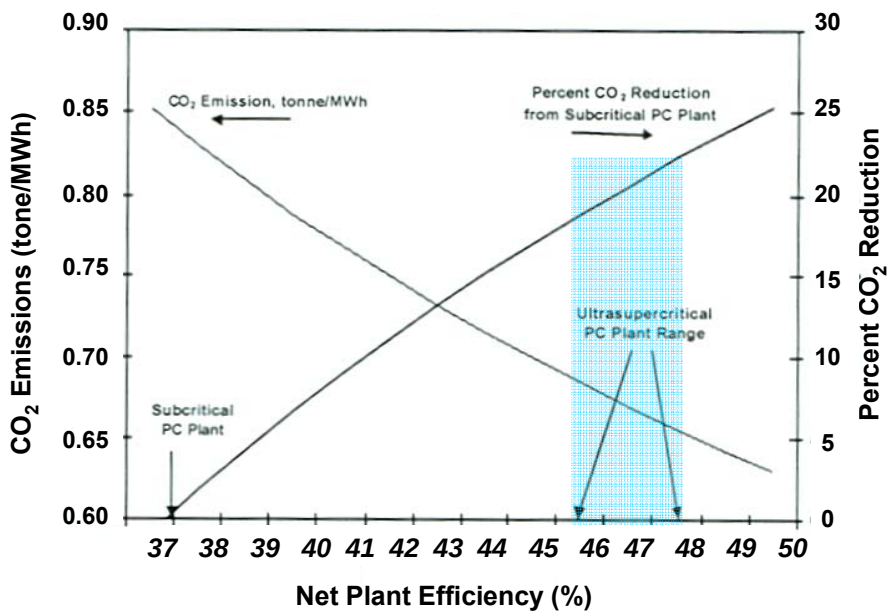

Henry et. al, *Coal Utilization and Fuel Systems Conference 2004*

Coal-Ash Corrosion

- *Reaction occurs between gas environment, slag deposits, and metal surface to form low melting temperature phase:*

$$3(Na,K)_2SO_4 + Fe_2O_3 + 3SO_3 = 2(Na,K)_3Fe(SO_4)_3$$

- *This phase when molten can dissolve oxides which prevents the formation of protective passive layer.*
- *The molten AIT's will attack the bare metal surface by fluxing away the top layer of the tube and exposing the lower surface to oxidation and sulfidation*

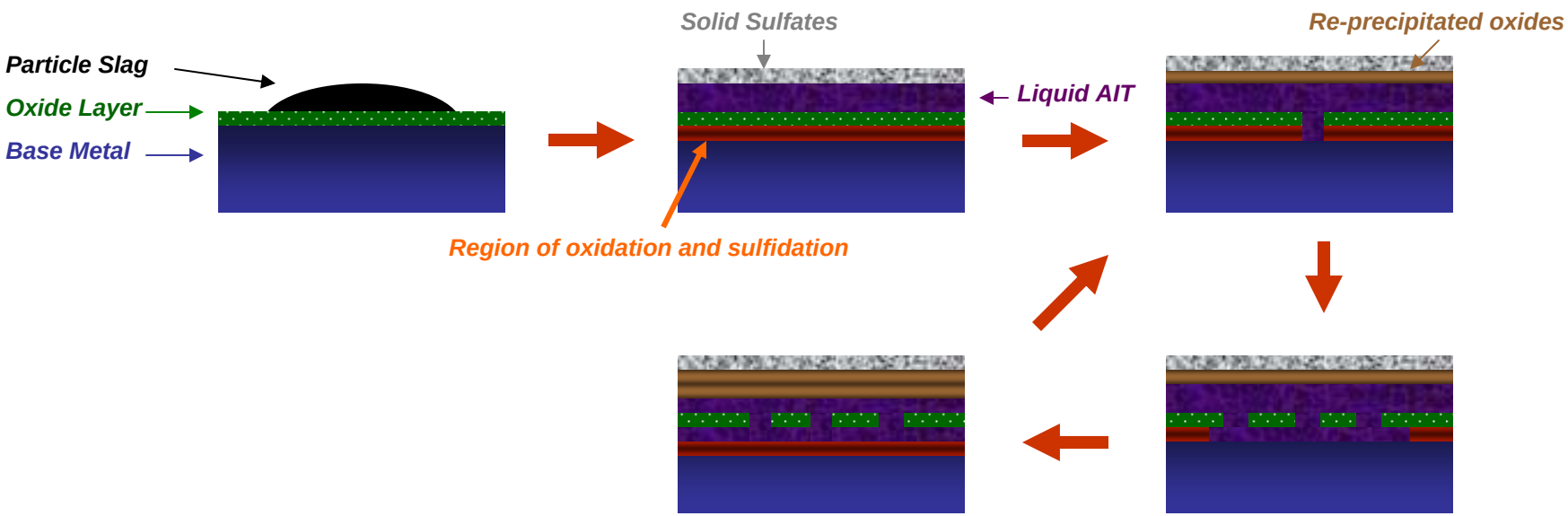

MOCVD of Thermal Barrier YSZ Coatings

T.M. Besmann, J. J. Henry, Jr., and B. A. Pint
Oak Ridge National Laboratory

S. Qui and T.L. Starr
University of Louisville

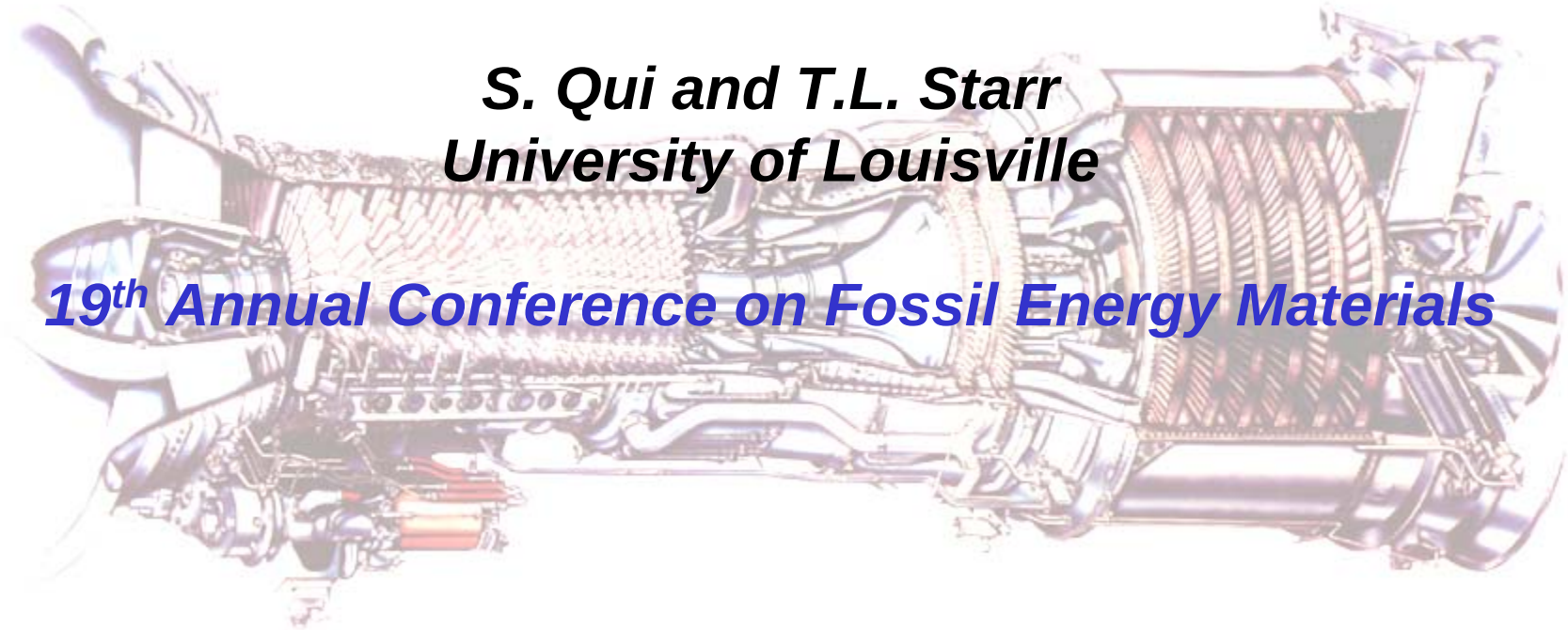

19th Annual Conference on Fossil Energy Materials

Research supported by Advanced Research, Materials,Office of Fossil Energy, National Energy Technology Laboratory, and the Distributed Energy Resources Program, Office of Power Technology, U.S.DOE

Goals and Issues

- **Objectives:**
  - **Lower cost of coating turbine components (blades) with thermal barrier coating (TBC)**
  - **Coat non-line-of-sight surfaces with TBC**
  - **Deposit TBC with adequate durability and thickness**
- **Current Barriers:**
  - **High capital and operating cost of coating processes**
  - **Difficult/impossible to coat hidden surfaces**
  - **Complex shapes avoided because of the difficulty in coating**
- **Path Forward:**
  - **Use metal-organic chemical vapor deposition (MOCVD) to reduce cost and coat hidden surfaces**
  - **Understand coating process to allow scale-up**
  - **Understand interface behavior to assure adequate adherence/durability**

Gas Turbine Research Driven by Interest in Increasing Engine Performance

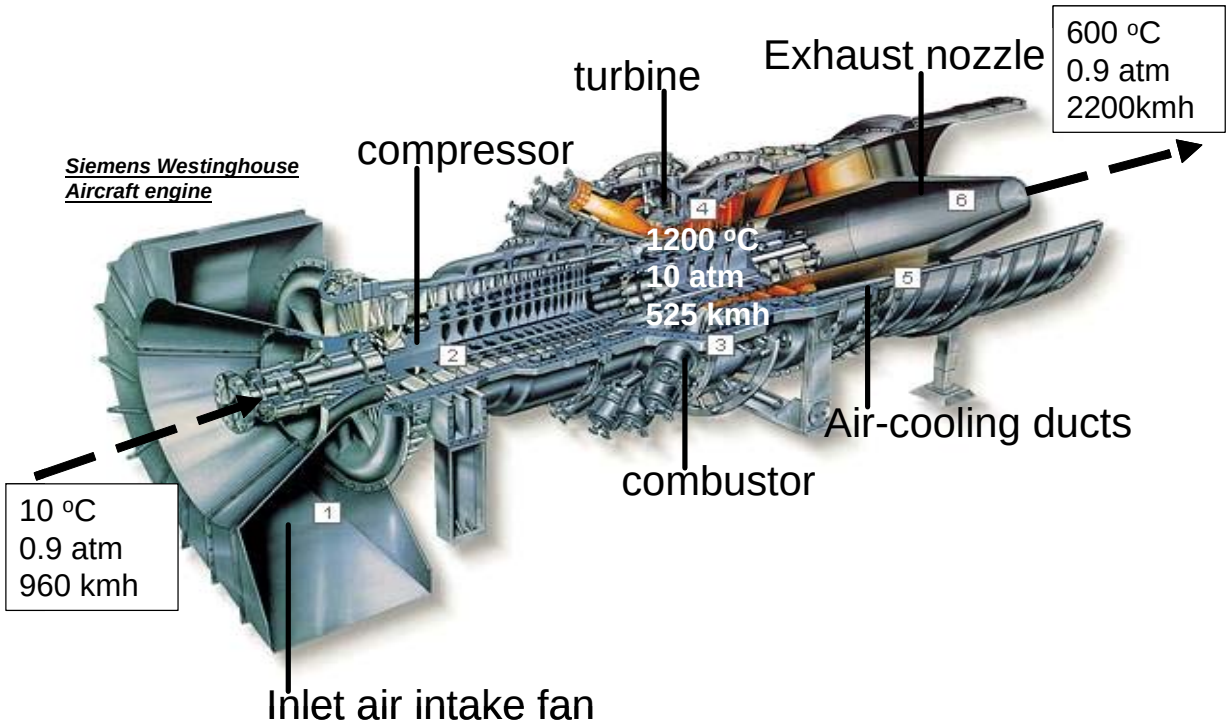

Super-alloy blade melting temperatures: 1230-1315°C

Current turbine inlet gas temperatures: ➢1200°C

Super-alloy operating temperatures (air-cooled): ~850 – 1100°C

- **Higher turbine inlet temperatures = increased efficiency and/or power**
- **Reduced air cooling of components = improved efficiency**
- **Lower component temperatures = improved engine durability**

YSZ TBCs Provide Increased Engine Protection/Performance

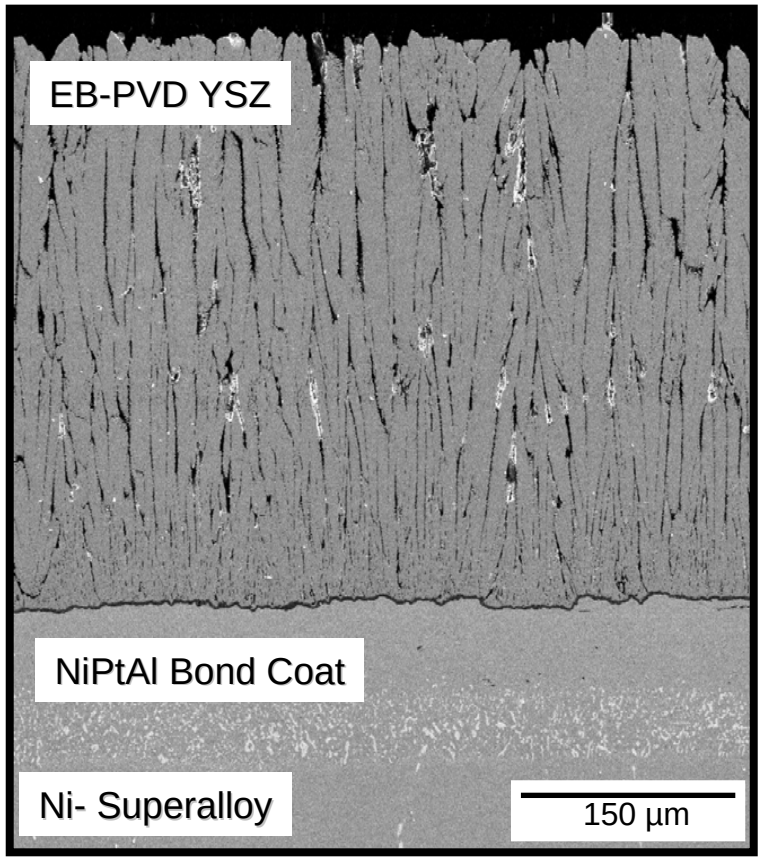

Ceramic top coat

- **tetragonal (6-8 wt.%)Y_2O_3-ZrO_2 (YSZ)**
- **Low thermal conductivity at engine temperature**
- **Phase stable during engine operation**
- **ΔT= –200°C thus lowering metal temp.**

Increased engine performance

- **Engine efficiency +1-3%**
- **Inlet gas temperatures = +5-10%**
- **air cooling = –2-3%**
- **Fuel efficiency = +1%**

TBC Failure Occurs by Decohesion at the Alumina Layer During Engine Service

Turbine blades courtesy of G.E. Aircraft Engines

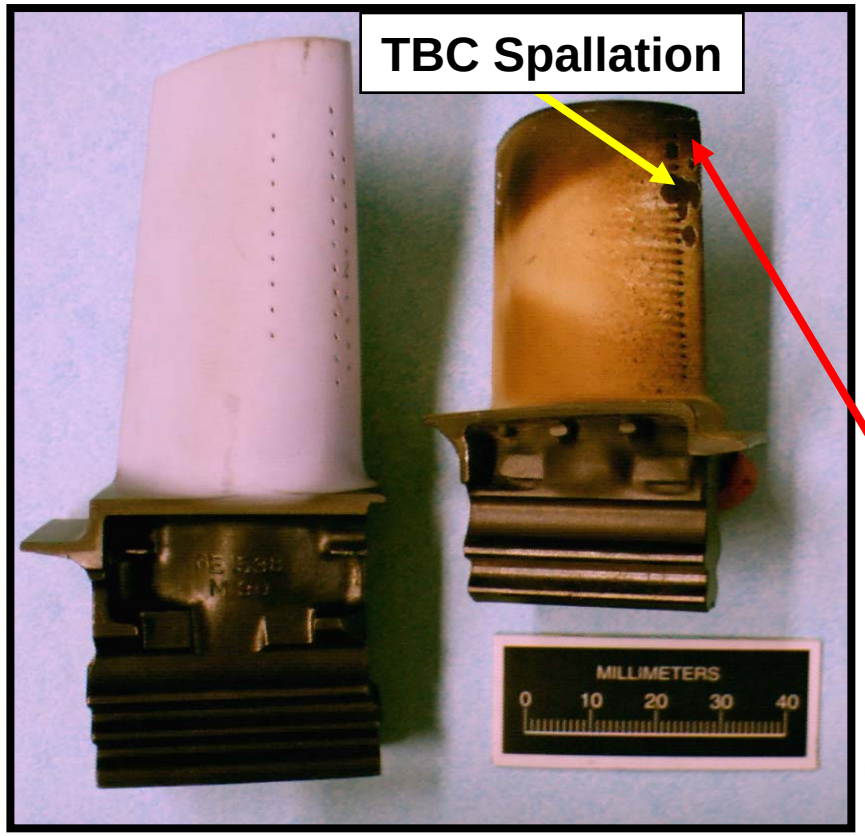

As Deposited **Engine Exposed**

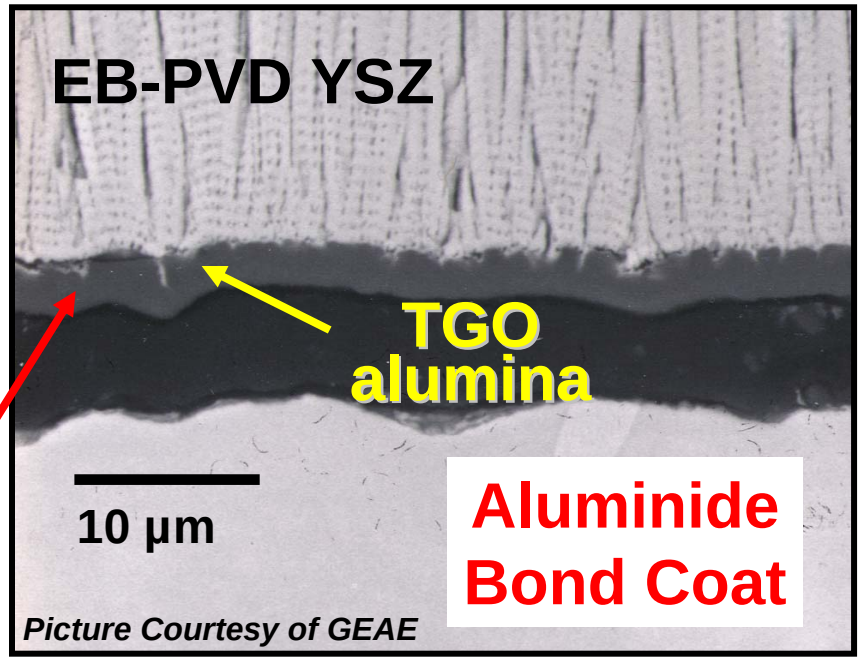

400 1-h thermal cycles

TBC failure influenced by CTE mismatch between ceramic and metallic components

- **Improved materials fabrication may help reduce cost and increase lifetime of the exposed engine materials**

CVD Offers Several Advantages Over EB-PVD

Comparison is with EB-PVD coatings as they are closer in microstructure to MOCVD than are plasma sprayed coatings

EB-PVD

- **Capital intensive**
  - **Evaporation-condensation process**
  - **Intricate robotics, high voltage, and High vacuum equipment**
- **"Line-of-sight"**
  - **~ 4 to 10 μm min^{-1} over 1 mm^2 surface**
  - **Cannot effectively coat high curvature or internal surfaces**
- **Microstructure allows**
  - **Alloy exposure to hot, combustible gases**
  - **Ingress of contaminants or salt**

CVD

- **Lower-cost**
  - **Metal precursors easily delivered**
  - **Eliminates need for intricate robotic, high-voltage, or high vacuum equipment**
- **"Non-line-of-sight"**
  - **Deposition conforms to complex and internal blade surfaces**
  - **Flexible reactor geometries for internal surface coating**
- **Can have EB-PVD advantages**
  - **Strongly adherent**
  - **High deposition rates**
  - **Columnar microstructures**
  - **Graded/layered composition**

Issues For MOCVD of YSZ TBCs

- Deposition of controlled composition
  - Yttria content
  - Purity
  - Uniformity
- Control of thickness
  - Spatial uniformity over large components
  - Protection of cooling channels
- Coating strength/cohesion
  - Internal stresses versus coating material strength
  - Adhesion to substrate surface
  - Stress states at interfaces
- Chemical stability
  - Resistance to corrosive fuel/contaminants
  - Advisability of a seal coat to protect substrate

Current Approach Is to Use Solely Metalorganic Precursors

Parallel deposition reactions produce YSZ from metal butoxides

– $Zr(OBut^{n})_{4\ 4(g)} + xsO_{2(g)} \rightarrow ZrO_{2(s)}$ + react. prod.

– $Y(OBut^{n})_{3(g)} + xsO_{2(g)} \rightarrow Y_2O_{3(s)}$ + react. prod.

Initial Thermochemial Assessment of ZrO_2-$YO_{1.5}$ Based On Models of Du et al

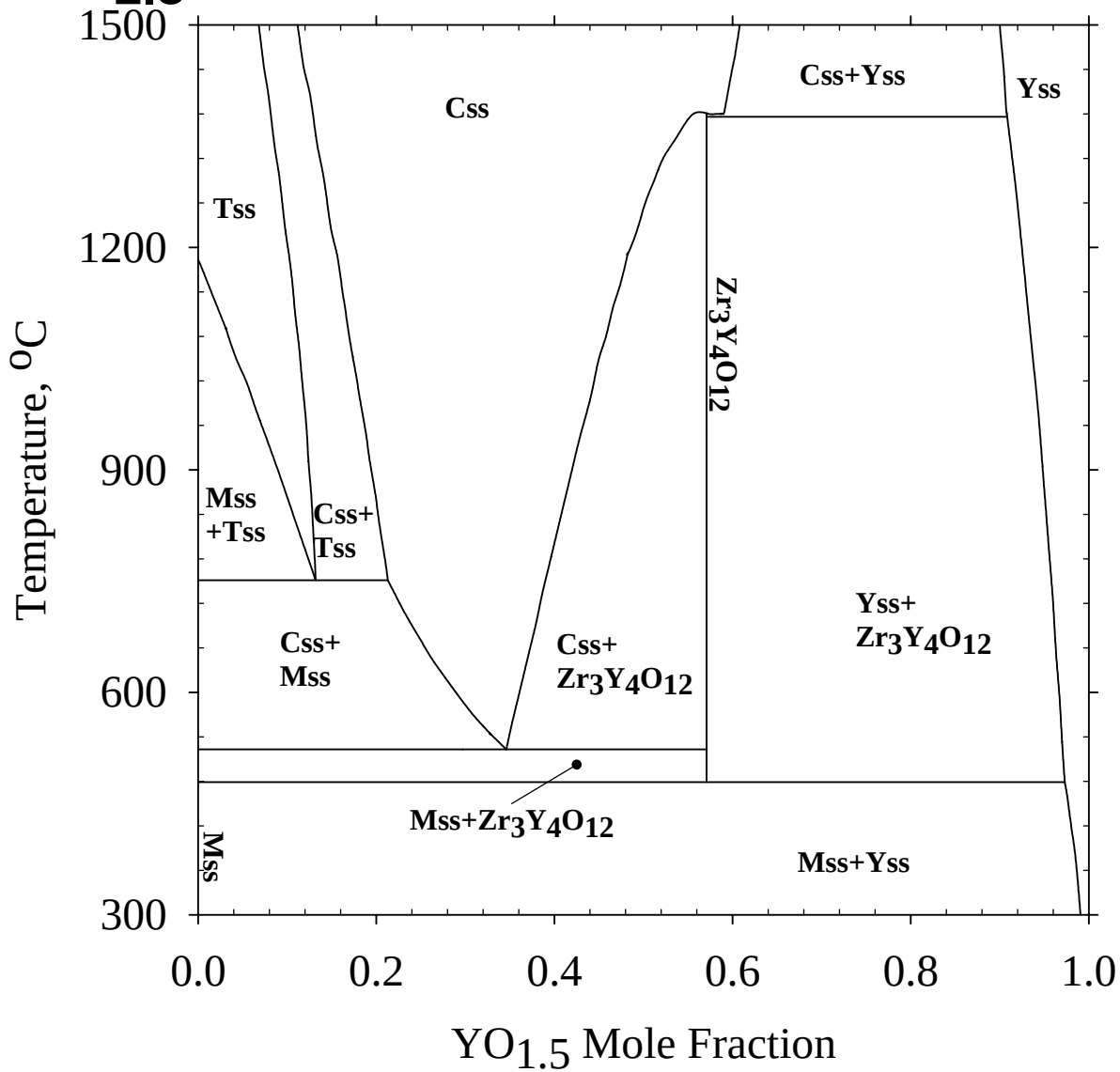

Thermodynamic Modeling Identified CVD Conditions for Tetragonal YSZ Deposition

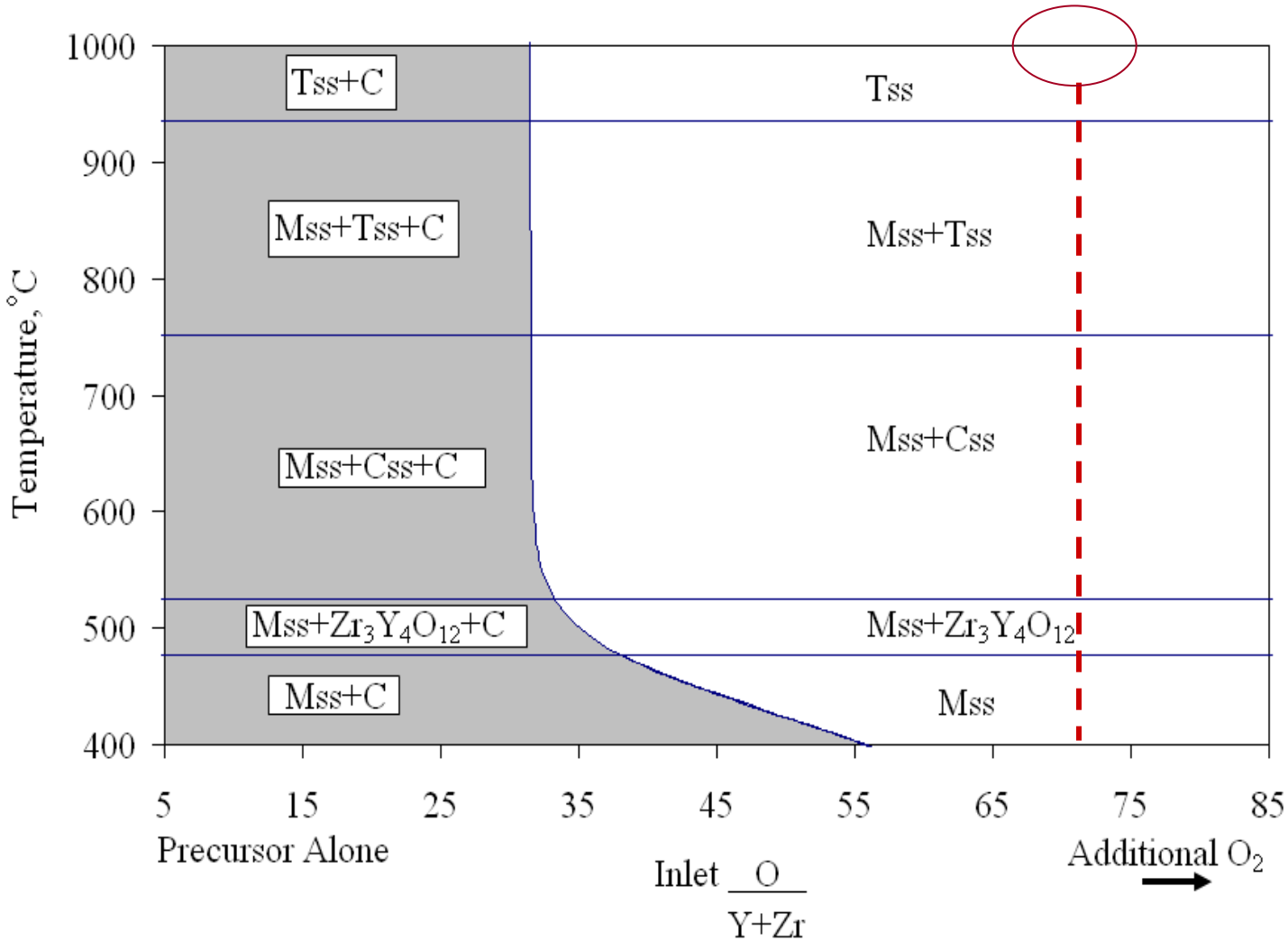

C - carbon

Css - face-centered cubic solid solution

Mss - monoclinic solid solution

Tss - tetragonal solid solution

$Zr_3Y_4O_{12}$ - 3:4 perovskite

Y/(Y+Zr)=0.08, C/(Y+Zr)=30, H/(Y+Zr)=60, $x_Y+x_{Zr}=10^{-3}$, P=10^4 Pa

ORNL Bench-Scale YSZ MOCVD Reactor

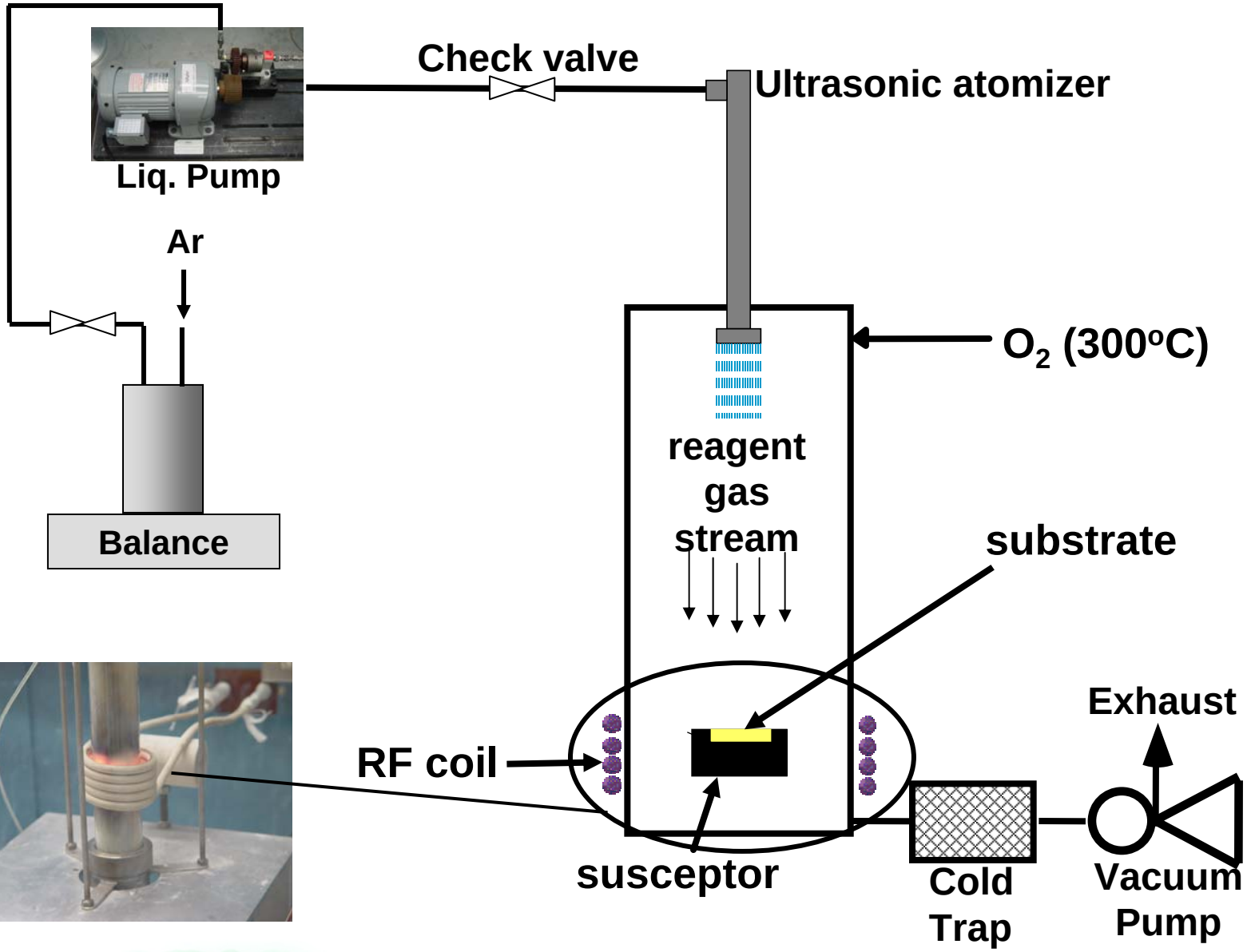

Thermodynamically Derived Experimental Conditions for High Temperature Deposition

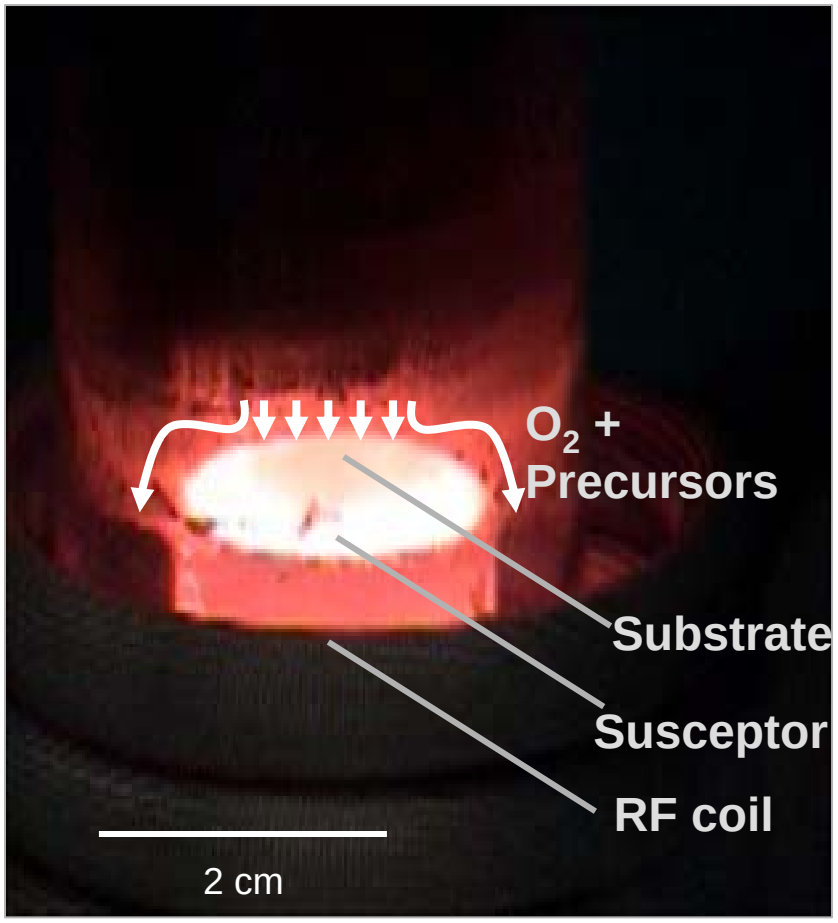

Deposition Conditions

- Pressure = 10^4 Pa
- O/(Y+Zr) = 72 (1200 sccm O_2 flow)
- Substrate = 770-1012°C
- Susceptor = 900-1200°C
- Liq. flow rate = 1 ml/min
- Y/(Y+Zr) = 0.08
  - 25 ml Y-butoxide/toluene
  - 63 ml Zr-butoxide/n-butanol
  - Diluted to 40% in butanol
  - Y+Zr = 0.0015 moles/min

Installation of a Non-Pulsating (Gear) Pump Now Allows Continuous Precursor Feed

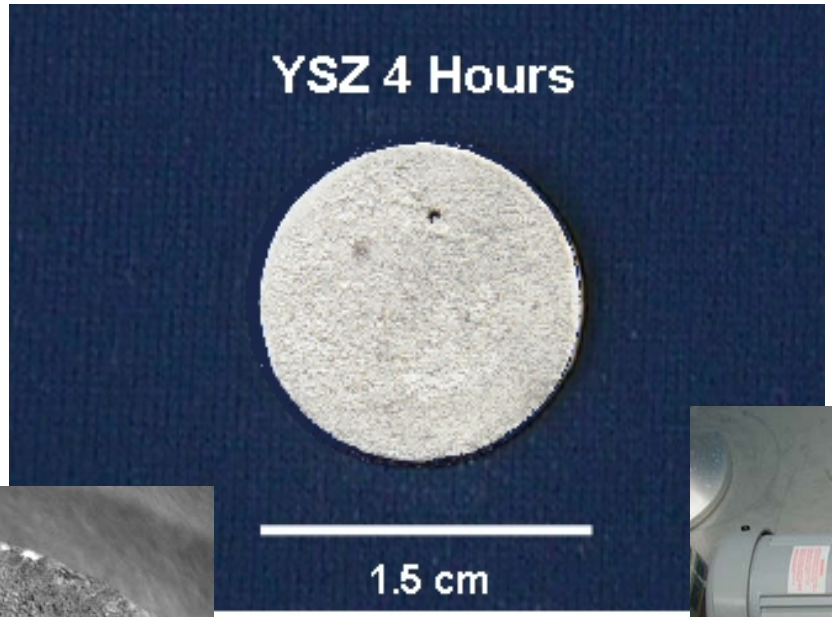

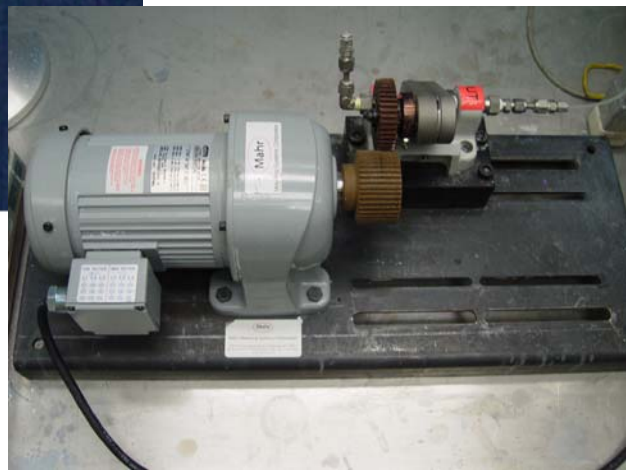

Four-hour deposition run resulted in substantial coating thickness and demonstrated long time deposition at controllable flow rates.

XRD Results Indicate Single-Phase *t*-YSZ

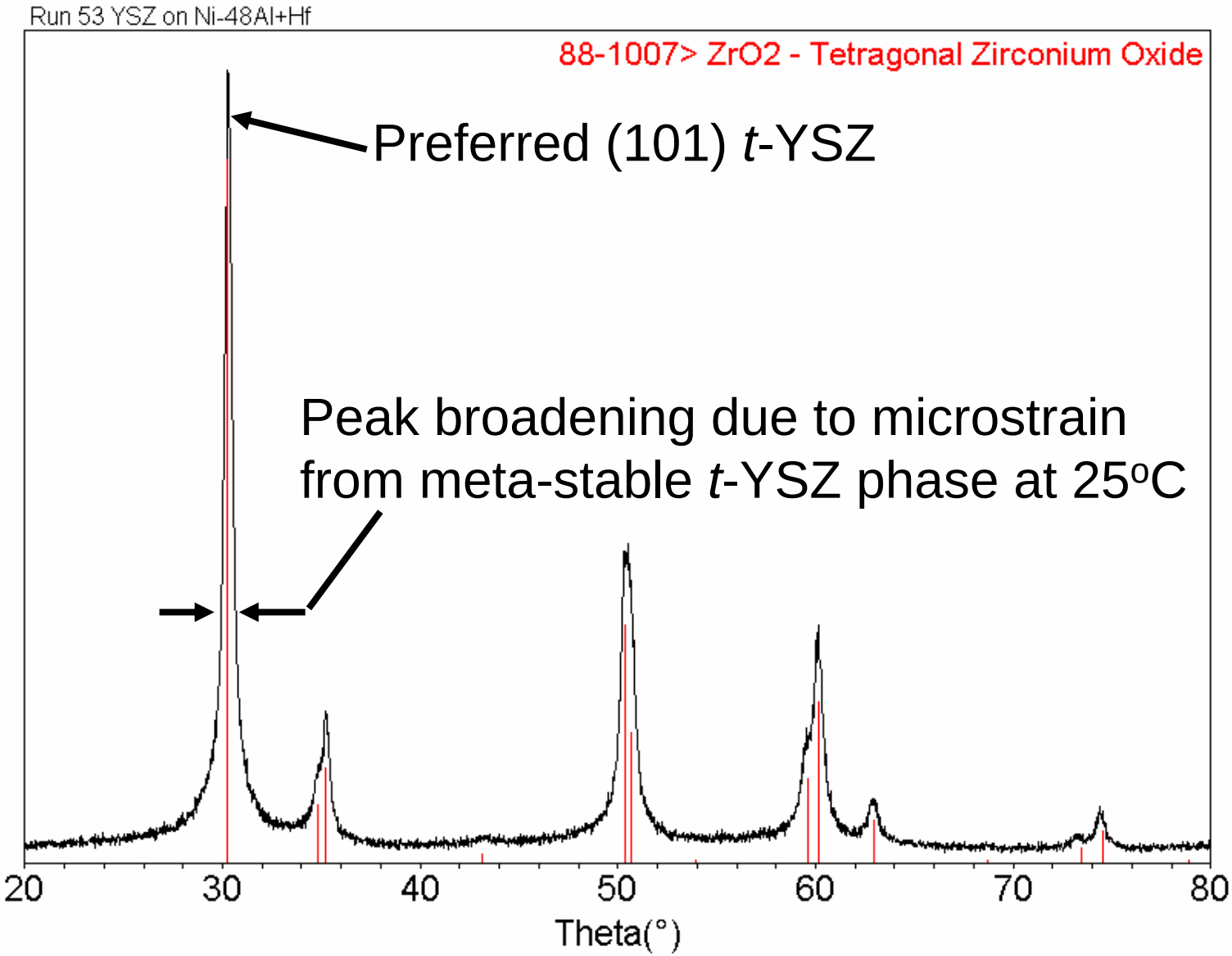

Substrate Surface Treated to Improve Coating Lifetime and Subjected to Thermal Cycling

- **Final 600-grit polish and cleaning**
- **30-minute preoxidation at 1060°C in reduced pressure oxygen**
- **Deposition rate increase observed, potentially due to better adherence (~120 μm total or ~65 μm/h growth rate from wt. gain)**

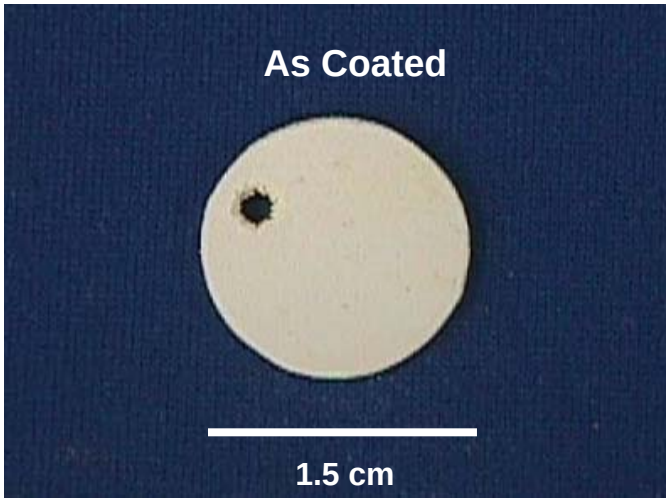

Thermal Cycling of YSZ On Pretreated FeCrAlY Demonstrates Long Life

Mass change under thermal cycling for uncoated, coated without pretreatment, and pretreated, coated samples

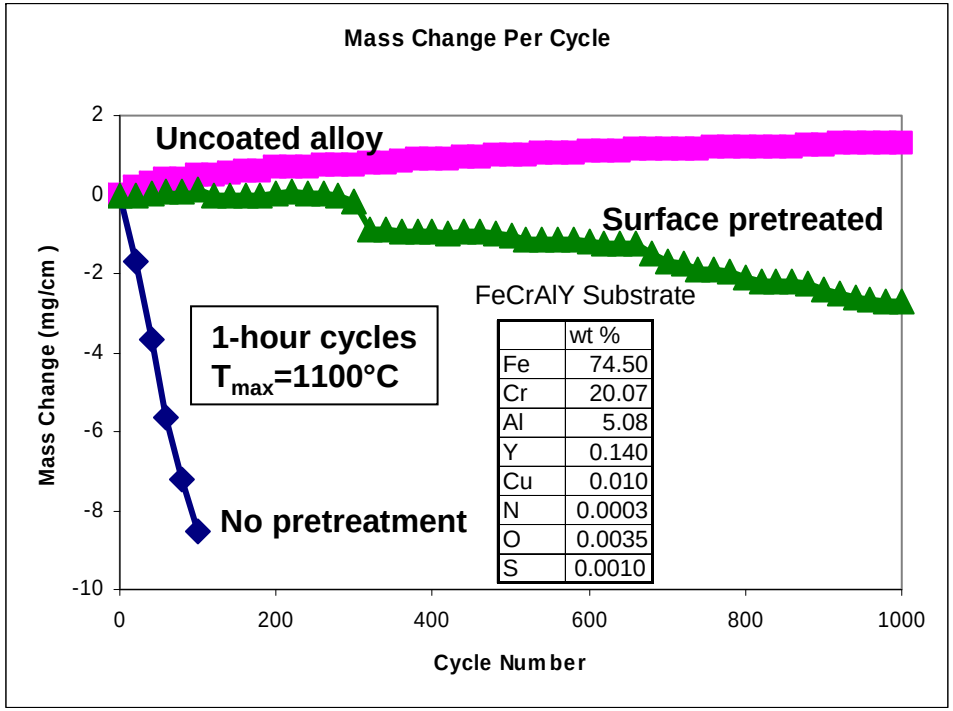

The Surface of the Uncoated Alloy and YSZ Coating After 1000 Thermal Cycles

Uncoated Alloy

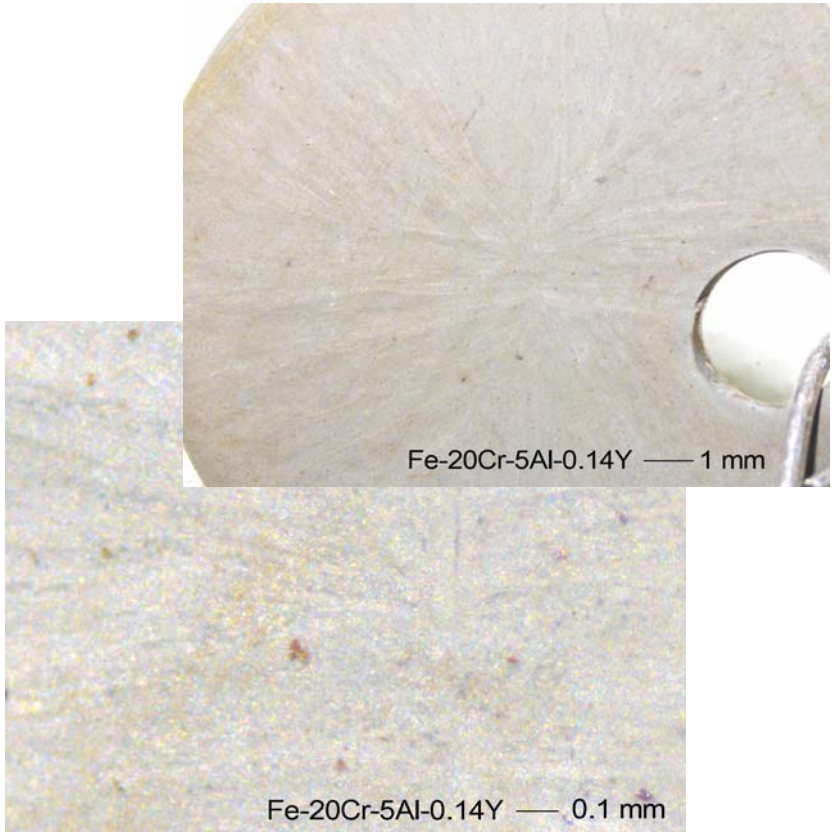

YSZ-Coated Alloy

The uncoated FeCrAlY showed minor corrosion during thermal cycling and the YSZ-coated substrate macroscopically appeared unaffected

MOCVD YSZ Retains Its Microstructure After 1000 Thermal Cycles

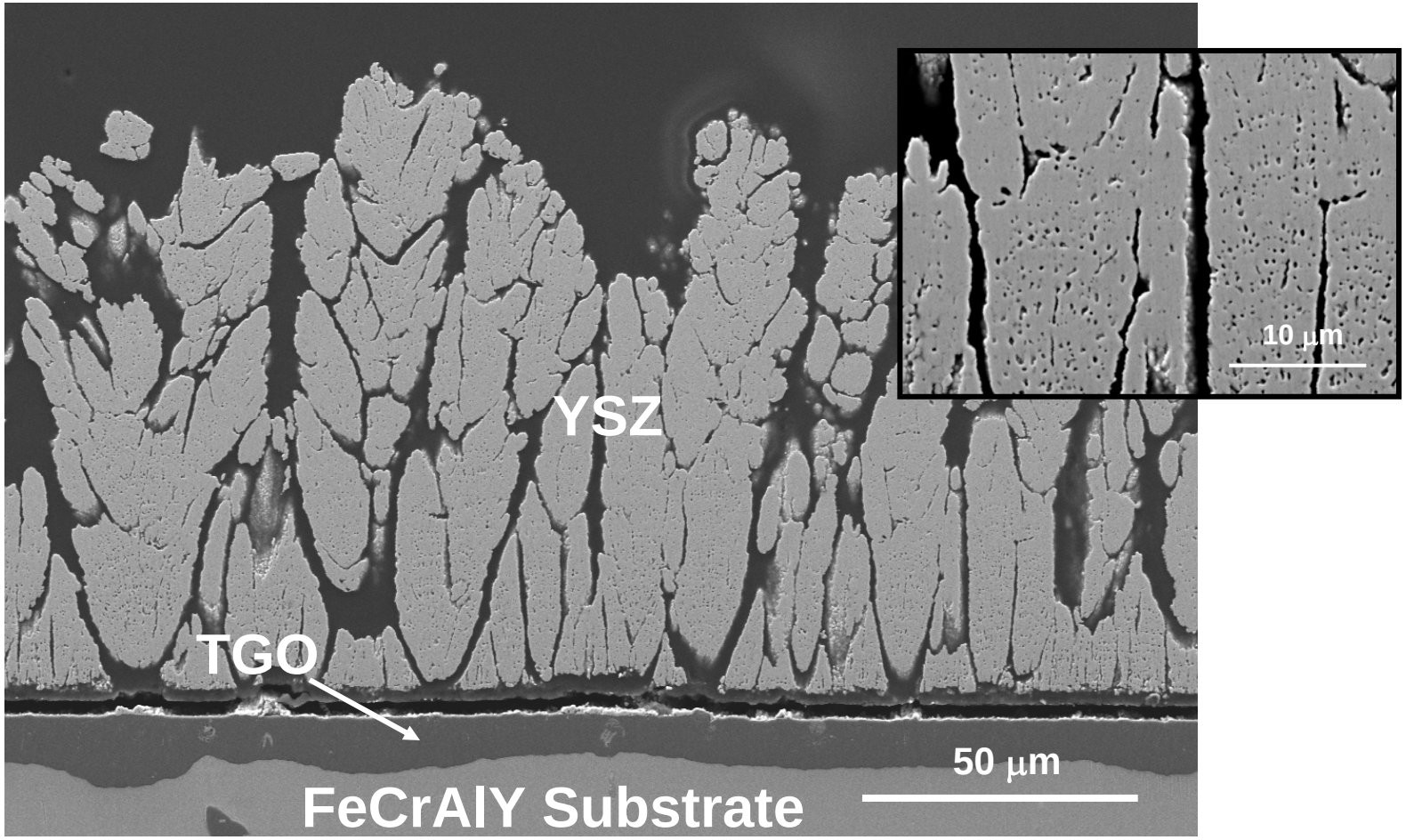

After 1000 Cycles the TGO Interface Is Stable

Wrinkling in the TGO under thermal cycling that typically promotes failure appears to be absent in the MOCVD YSZ system

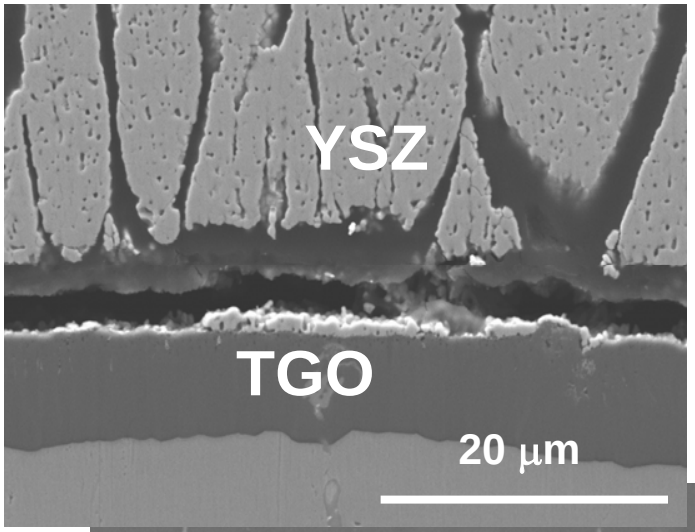

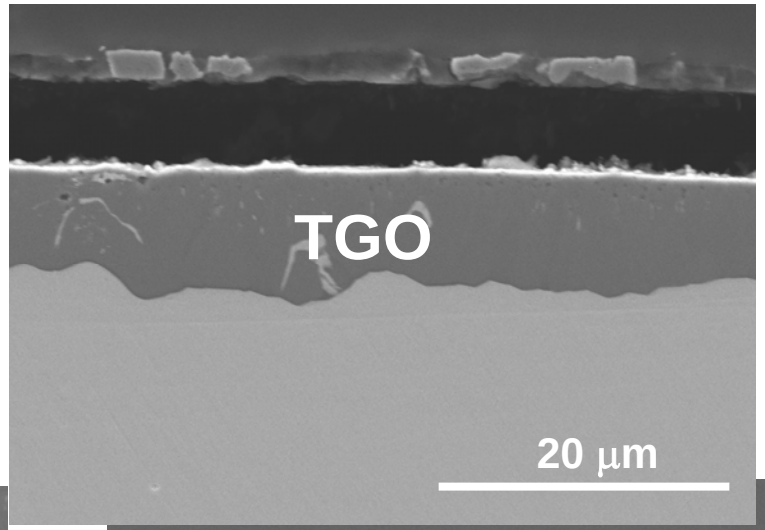

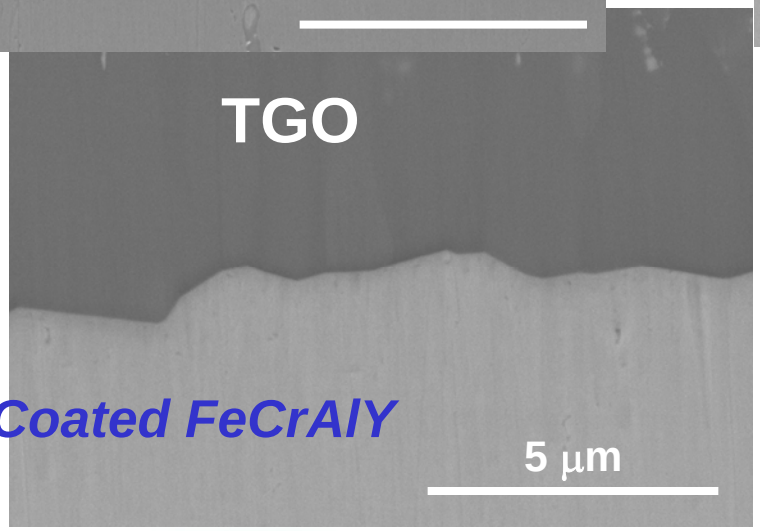

YSZ Coated FeCrAlY

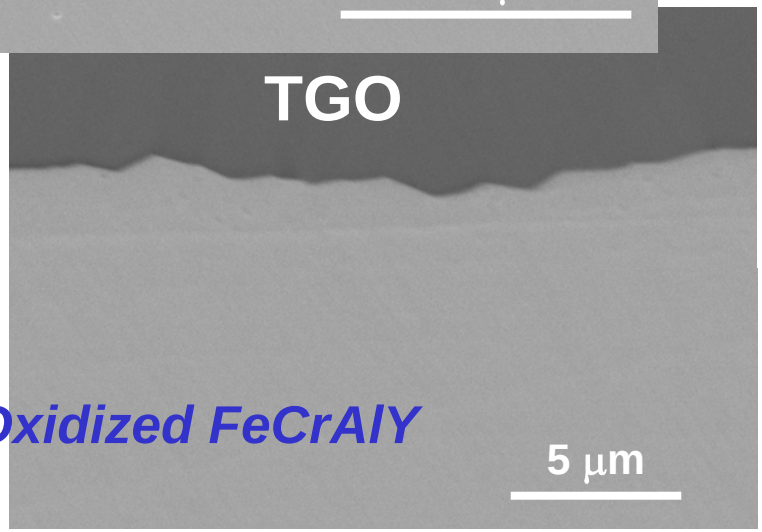

Oxidized FeCrAlY

MOCVD YSZ Coating Also Exhibits Stability

The buckling in EB-PVD YSZ coating caused by compression in the TGO under thermal cycling appears to be absent in the MOCVD YSZ system

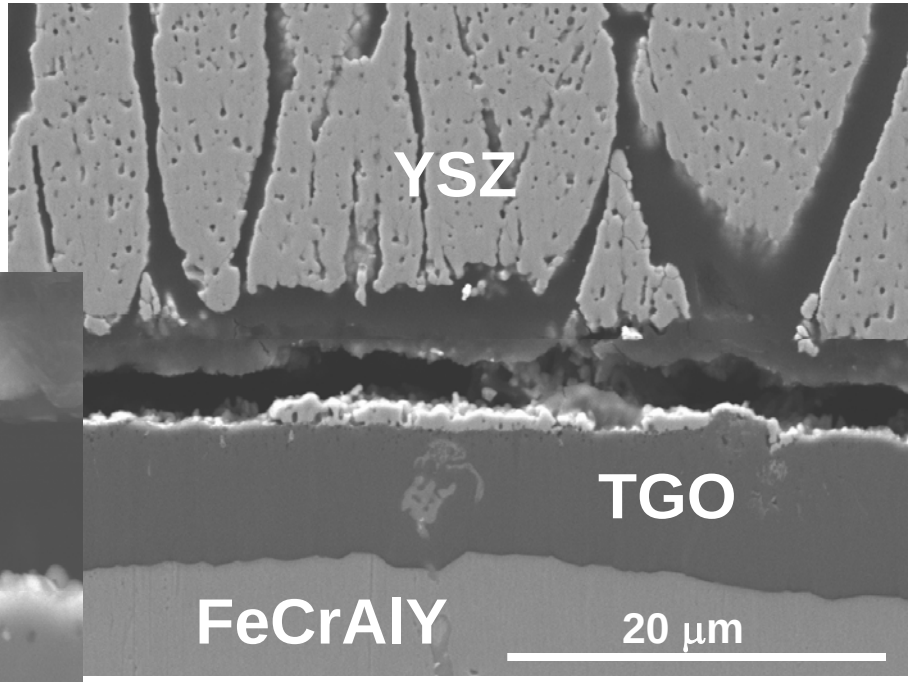

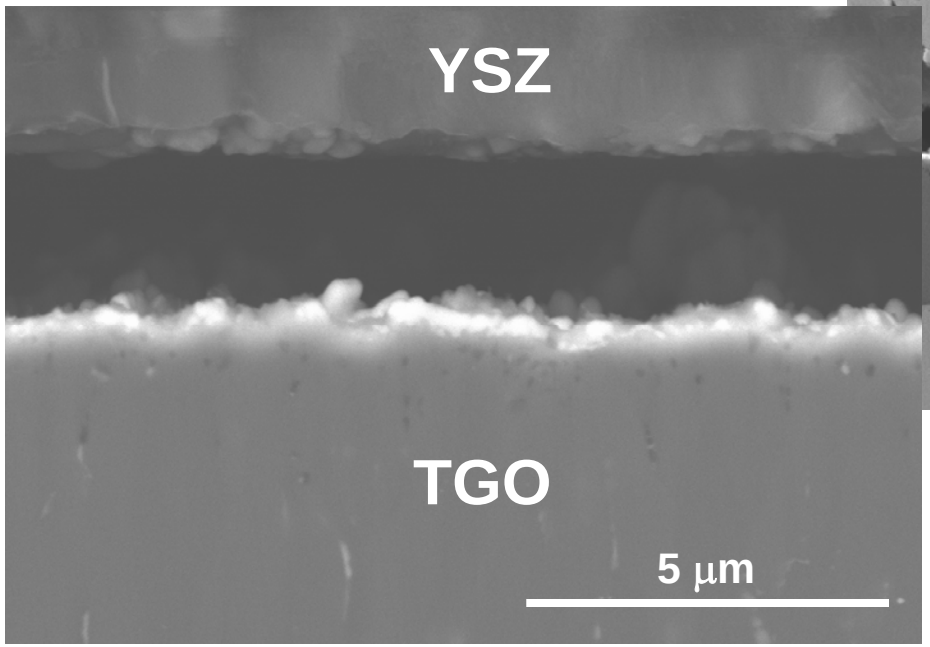

Metallographic cross-sections of sample that underwent 1000 thermal cyles

Vaporization Behavior of Zirconia Precursors

- Ambient pressure TGA measurements
- Precursors from specialty chemical suppliers
- Alkoxides – lower vaporization temperature than tmhd
- n-butoxide solution – multi-stage solvent-precursor vaporization

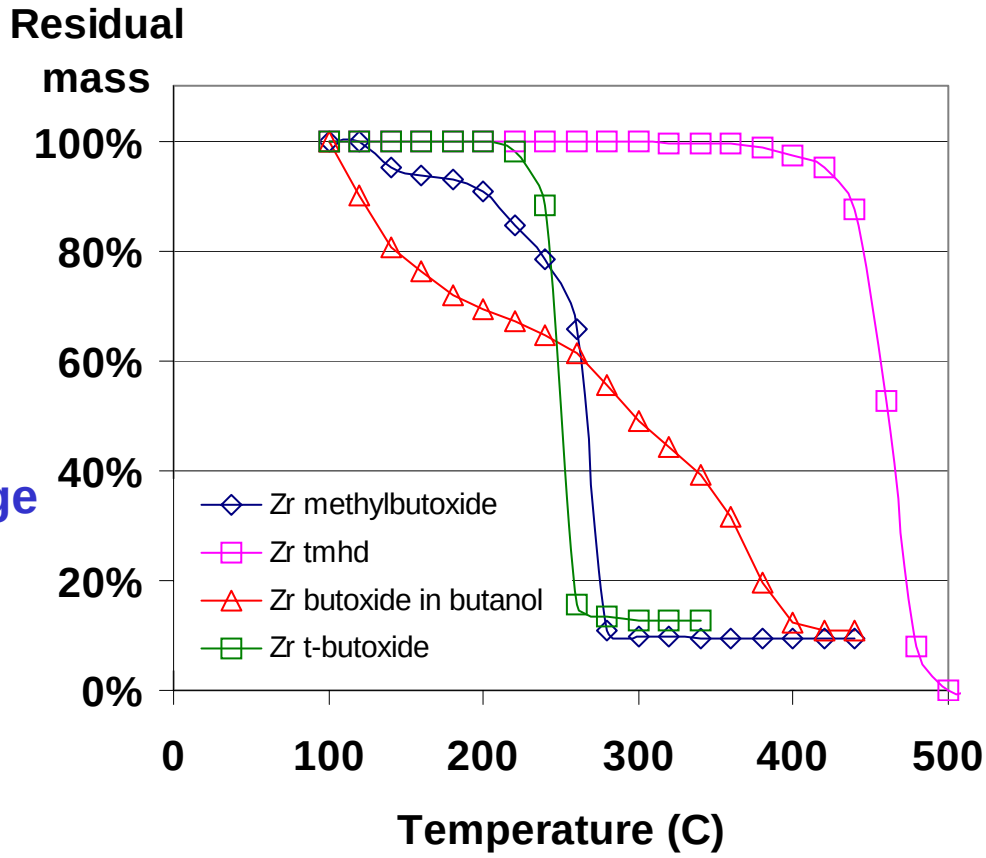

Lower Cost Zirconia Precursor Solutions Have Been Evaluated

- Commercial-scale solutions from DuPont
- Used in coatings, catalysis, polymer manufacturing
- All show multi-stage solvent-precursor vaporization
- NBZ identical to n-butoxide from specialty chemical supplier
- NPZ (n-propoxide) vaporization temperature lower than NBZ

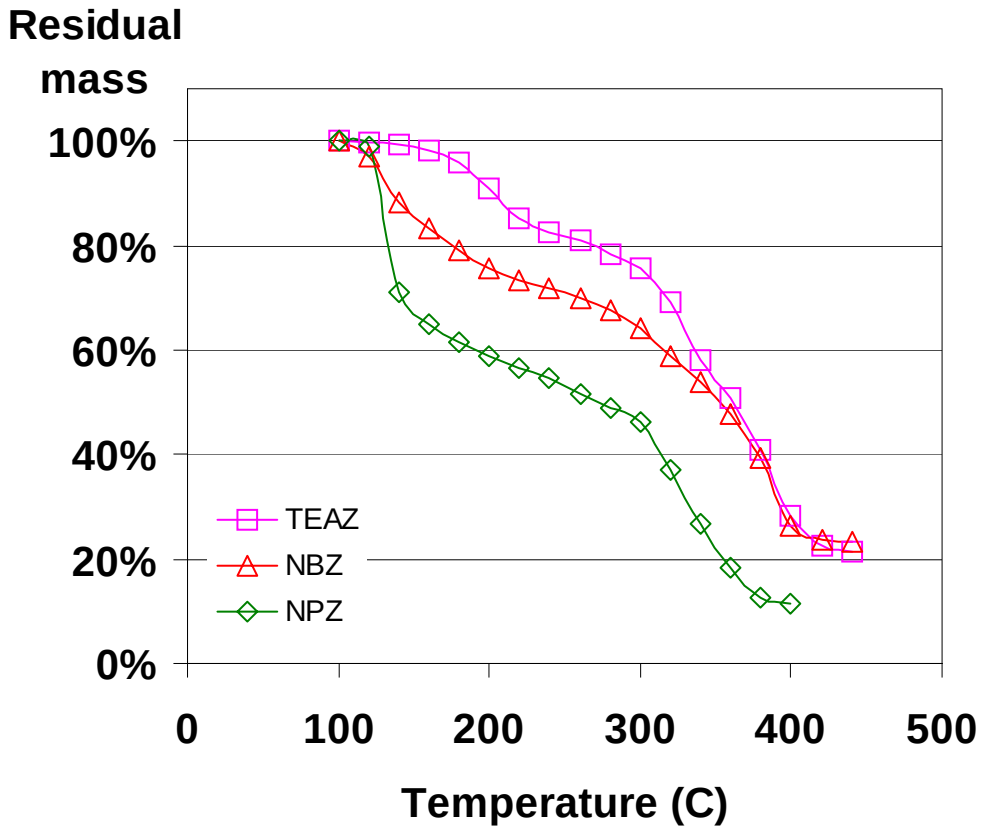

TEAZ = triethanolamine zirconate
NBZ = zirconium n-butoxide in n-butanol
NPZ =zirconium n-proxide in n-propanol

Yttria Precursors: Preliminary Results

- Precursors from specialty chemical suppliers
- Isopropoxide oxide – lower vaporization temperature than tmhd
- Also available:
  - Methoxyethoxide solution
  - Butoxide solution

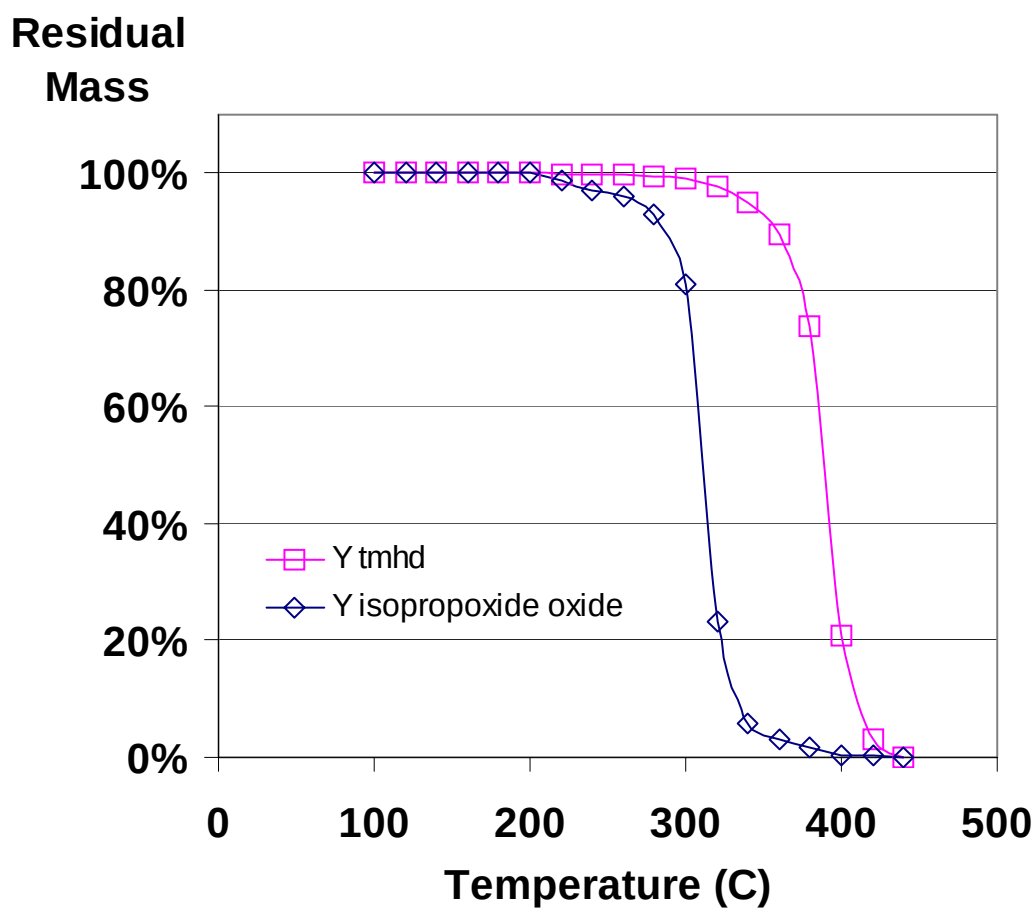

Modeling Has Been Used to Develop Sub-Scale Reactor Layout and Geometry

- Cylindrical reactor
- Top or bottom outlet
- Left and right side inlets
- Vertical orientation
- RF heating

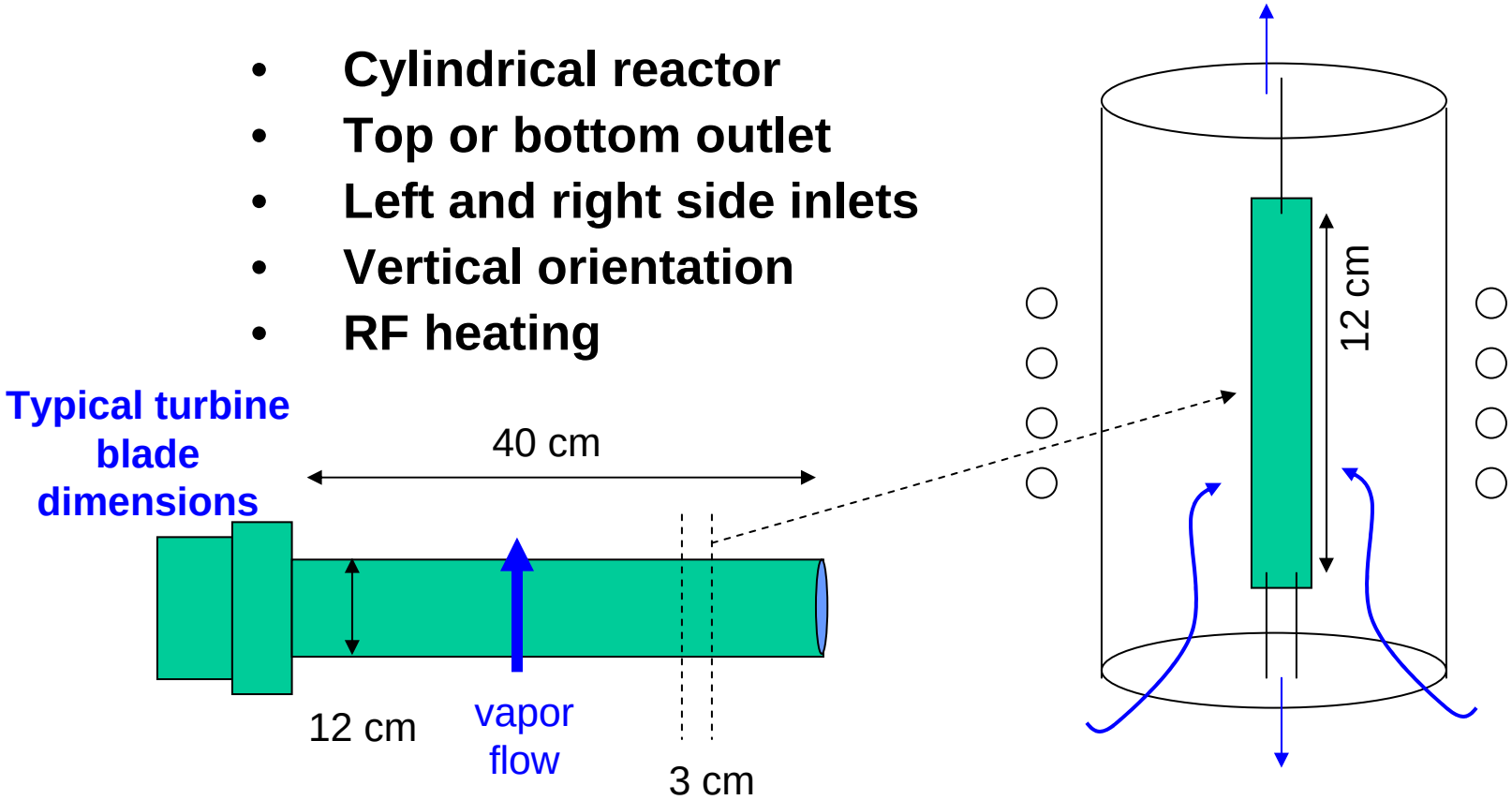

Need to Demonstrate Uniform Deposition Along 10-12 cm Length

Scale-Up Reactor Design Based on Modeling Results for Coating Prototypical Blade Width

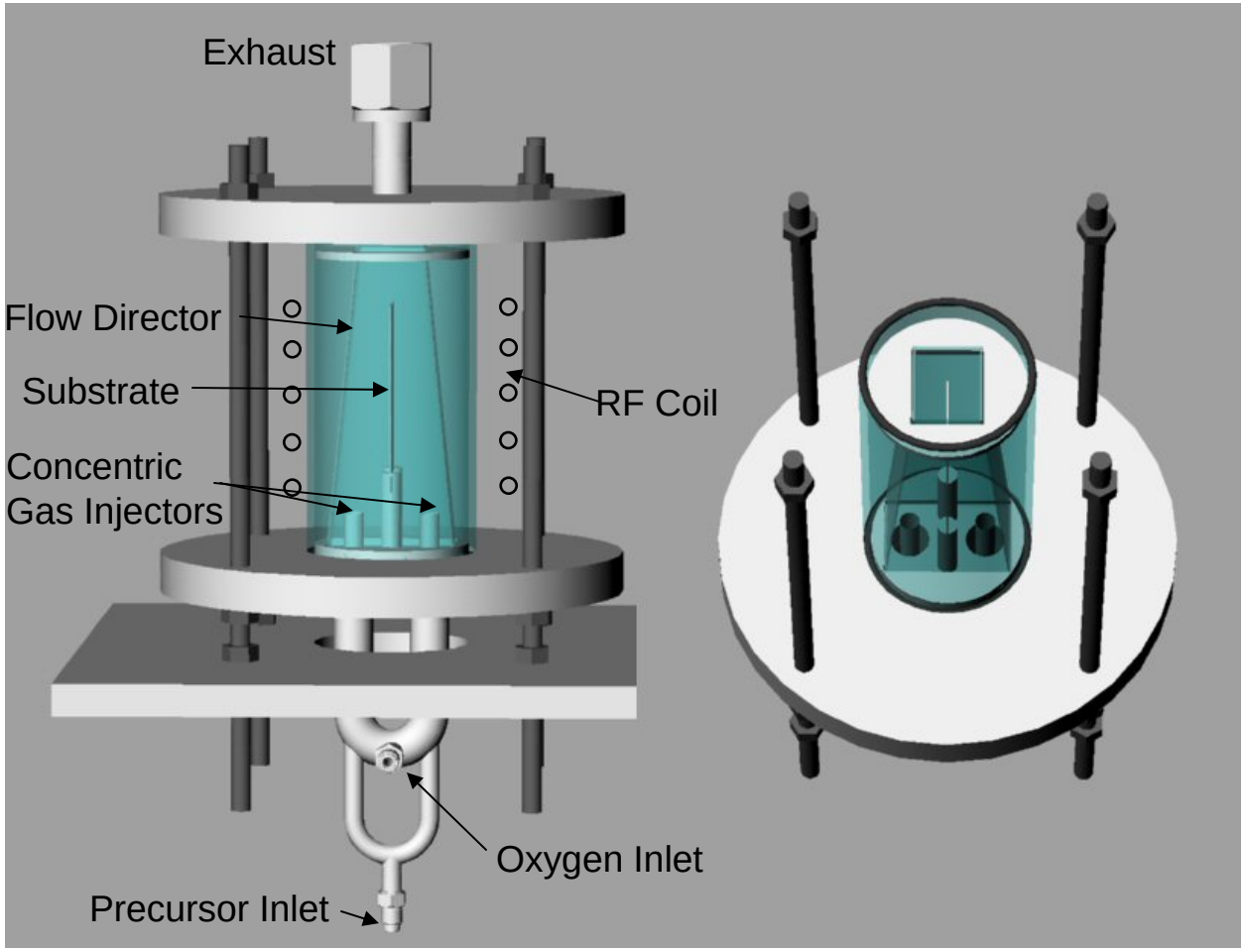

Scale-Up System Is Currently Being Installed

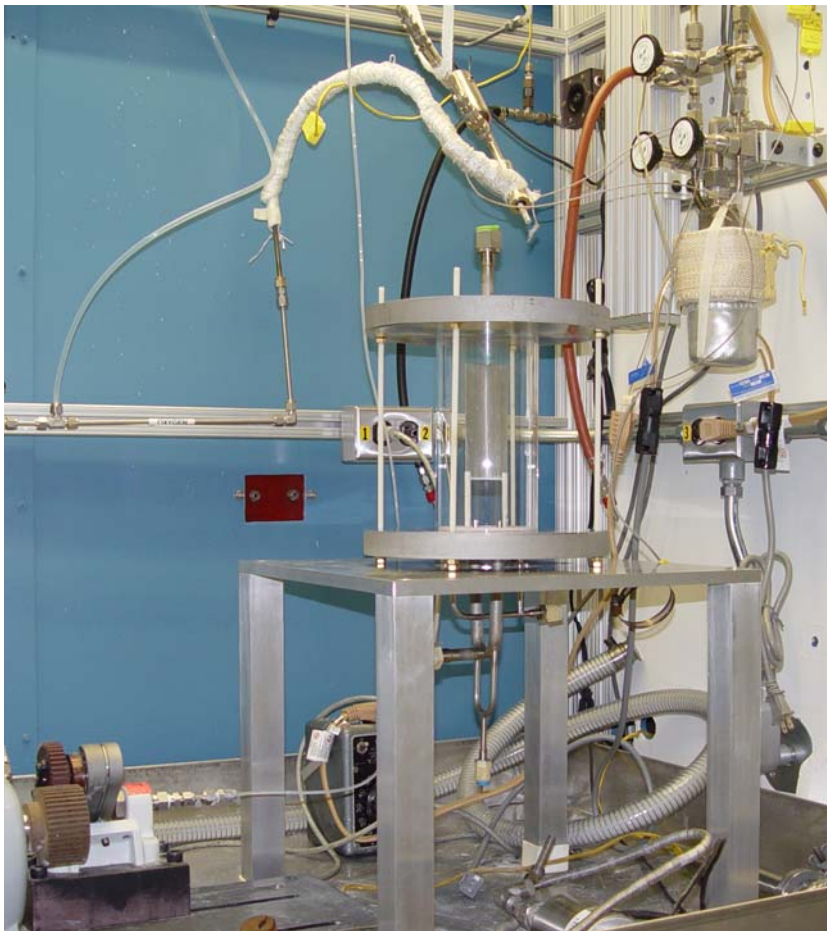

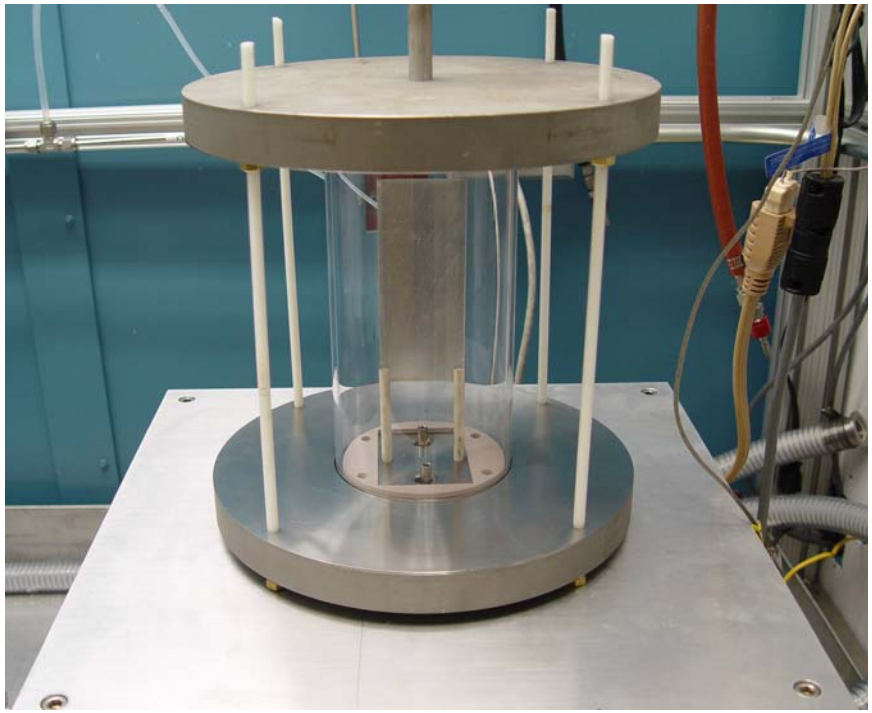

Scale-Up System for MOCVD With Pulsed Deposition Capability

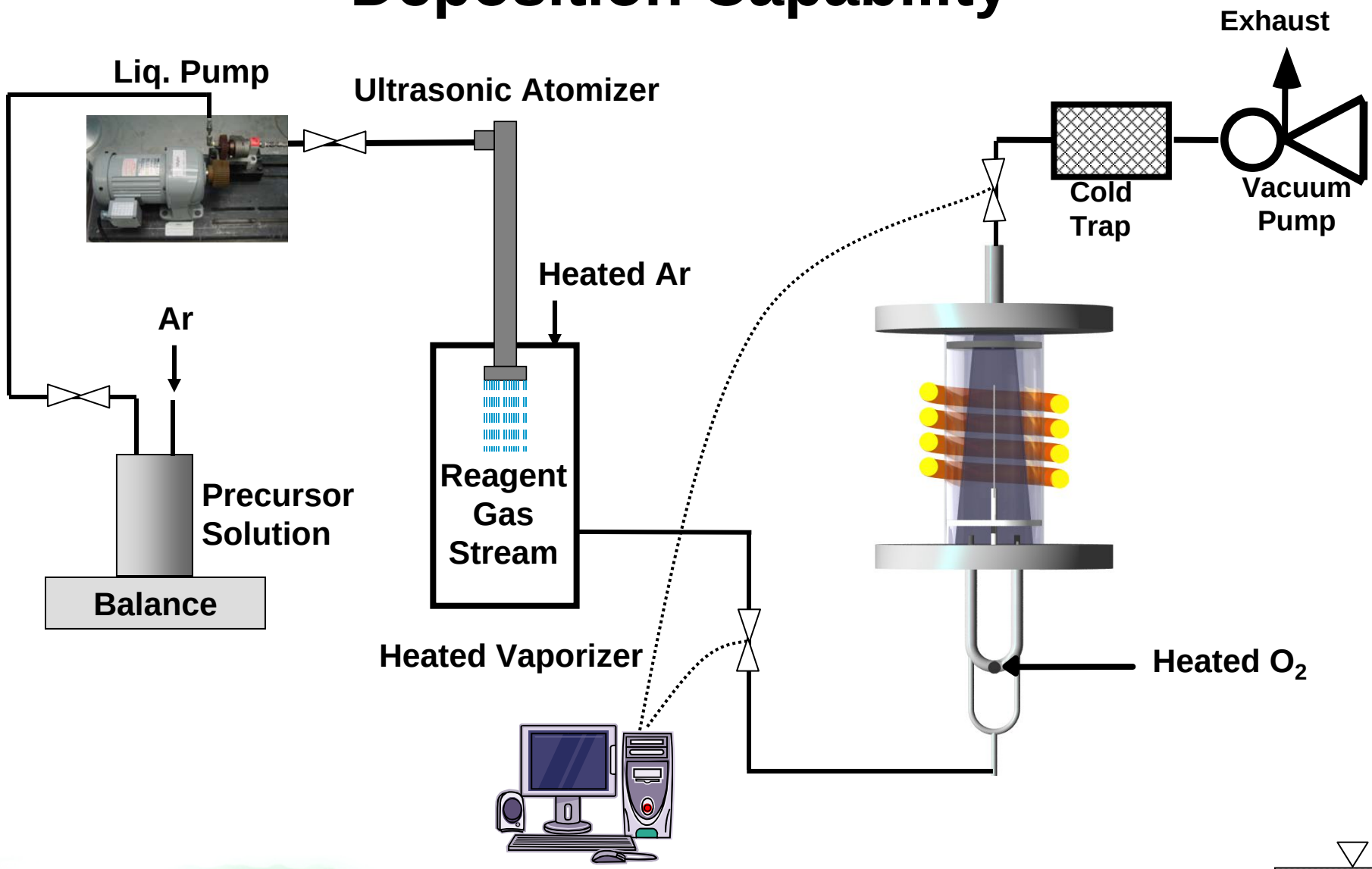

Pratt & Whitney Will Test Coated Specimens in Their Ducted Burner Rig

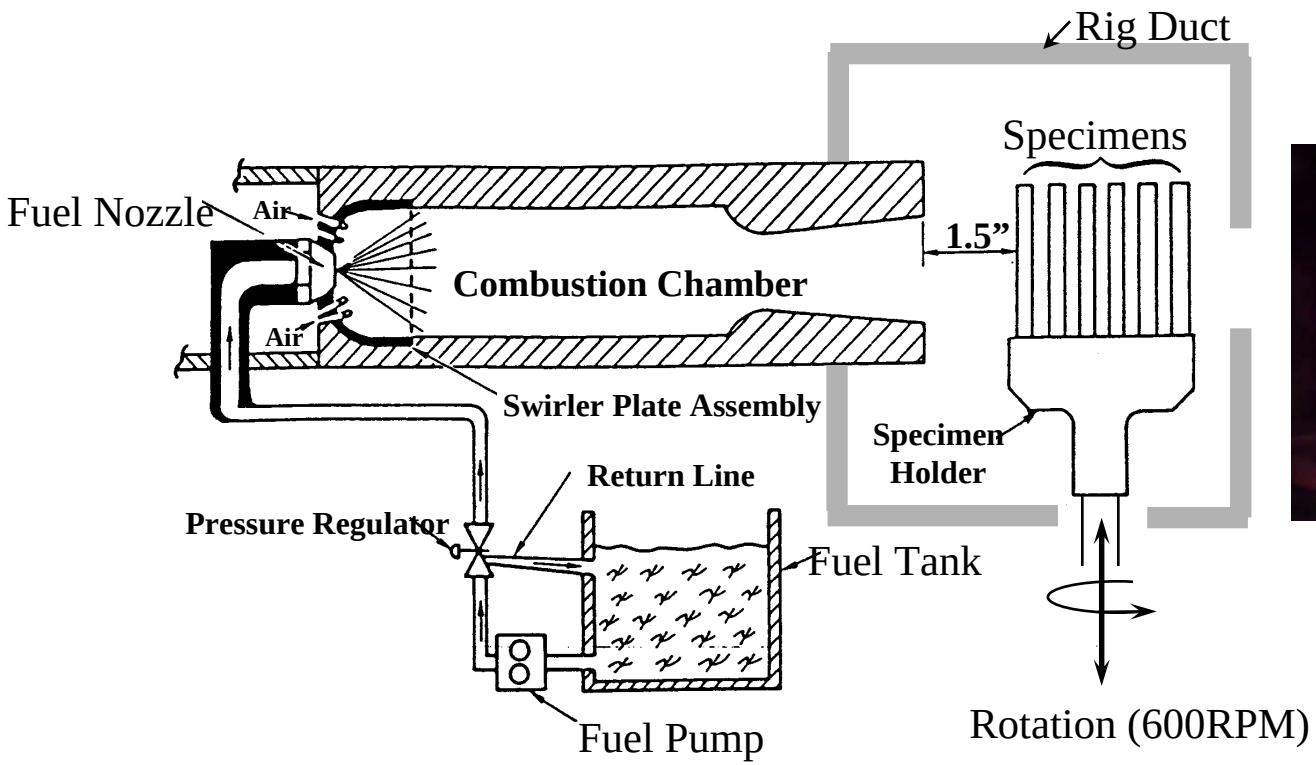

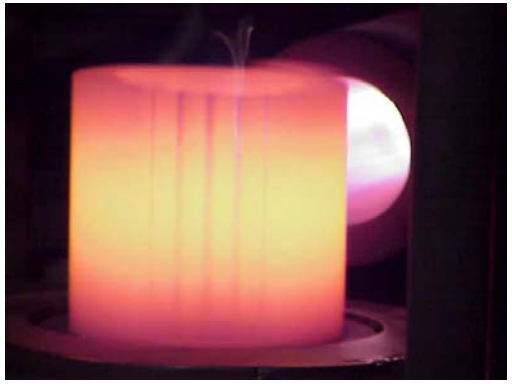

Mike Maloney of Pratt & Whitney has expressed a strong interest in the MOCVD of turbine components as potentially less costly and having a non-line-of-sight ability to coat surfaces. Pratt & Whitney will supply substrate specimens for coating.

Summary/Accomplishments

- Coatings with columnar microstructures can be achieved with high growth rates/uniformity and continuous deposition
- Single-phase tetragonal YSZ relatively easy to deposit
- Preoxidized surface improves adherence
- Adherence to FeCrAlY substrates demonstrated through 1000 thermal cycles
- Interface microstructural changes during thermal cycling that cause EB-PVD and APS YSZ coatings to fail appear to be absent in the current system
- Parallel efforts to find even less costly and more convenient metalorganic precursors show promise for a number of options
- Process modeling has been used to design a scale-up system
- Pulse deposition is being evaluated as a means to improve deposition uniformity for larger/multiple substrates and that capability is being included in the scale-up system
- Pratt & Whitney will supply substrates for coating and will perform burner rig testing

Problems/Needs

- **Industry evaluation**
  - **Scale to sample size appropriate for greater industry evaluation**
  - **Demonstrate possibility of industrial scale coating system**
  - **Demonstrate thermal properties as a function of lifetime**

- **Substrate/coating exploration**
  - **Review alternative substrate systems that are "cutting edge"**
  - **Explore ability to modify coatings to increase capability, for example,**
    - **Doping to produce color centers to increase emissivity**
    - **Interrupted/layered coatings that increase thermomechanical stability at larger thicknesses**

Modeling of Chemical Vapor Deposited Zirconia for Thermal Barrier and Environmental Barrier Coatings

Thomas L. Starr and Shenghong Qiu
Chemical Engineering Department
University of Louisville, Louisville, KY

In collaboration with
Theodore M. Besmann and John Henry
Oak Ridge National Laboratory

Presented at the 19th Annual Conference on Fossil Energy Materials, Knoxville, TN, May 9-11, 2005

Introduction

- YSZ is an effective thermal barrier coating for high temperature energy systems
- CVD process offers advantages over current application methods
- Computer modeling provides
  - Understanding of deposition process
  - Tool for reactor design and optimization

Computer Model Developed from Stagnation Flow Reactor

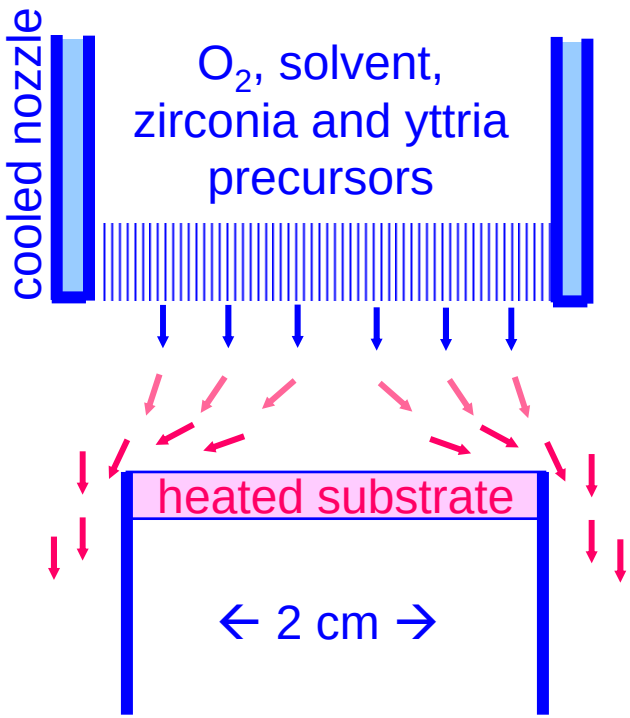

Computer model yields detailed view of transport and reaction phenomena

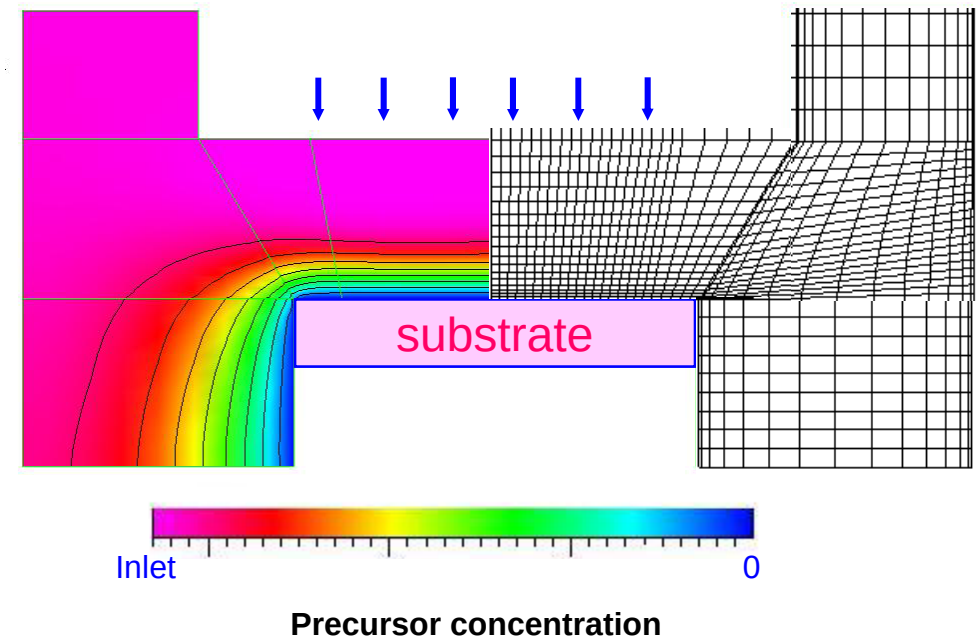

High Deposition Rate

- Zirconium and Yttrium alkoxide precursors in solvent
- Deposition is " transport-limited" at high coating rate

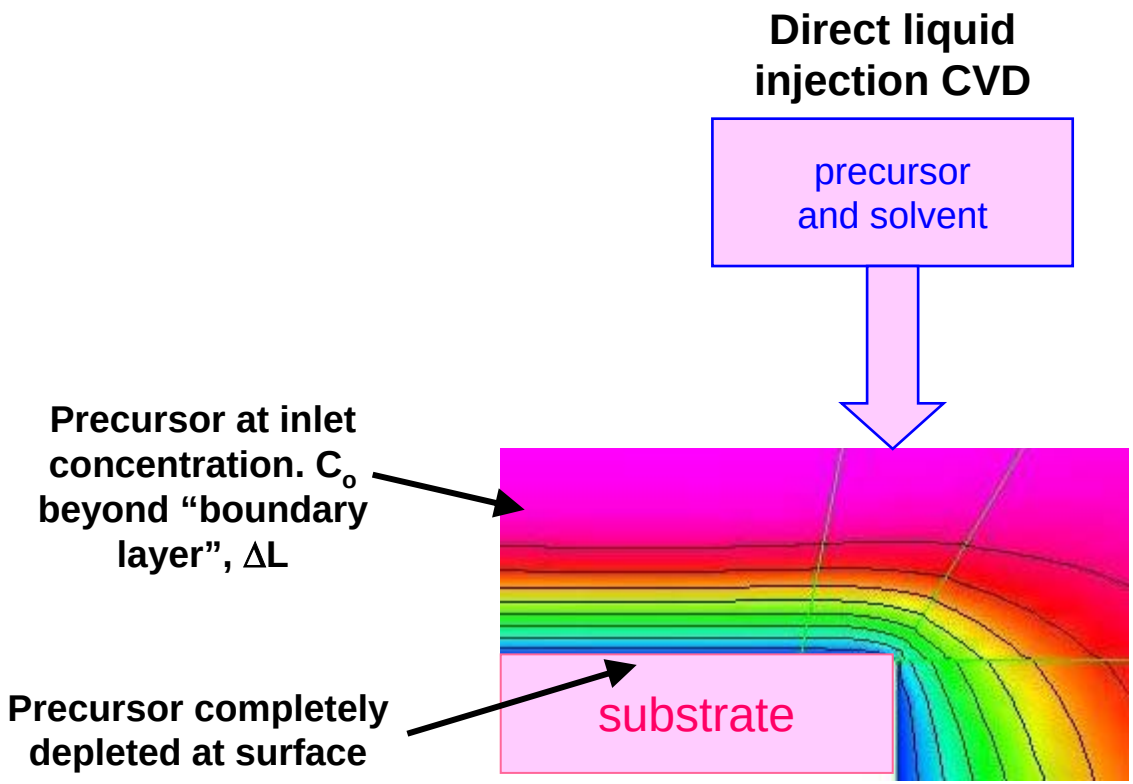

Deposition rate = diffusion rate ~ $C_o \Delta L$

Industrial Gas Turbine Blade

Process Requirements

- High deposition rate to reduce processing time
- Good crystallinity and columnar microstructure requires high temperature
- Uniform coating over blade surface
- Scalable process

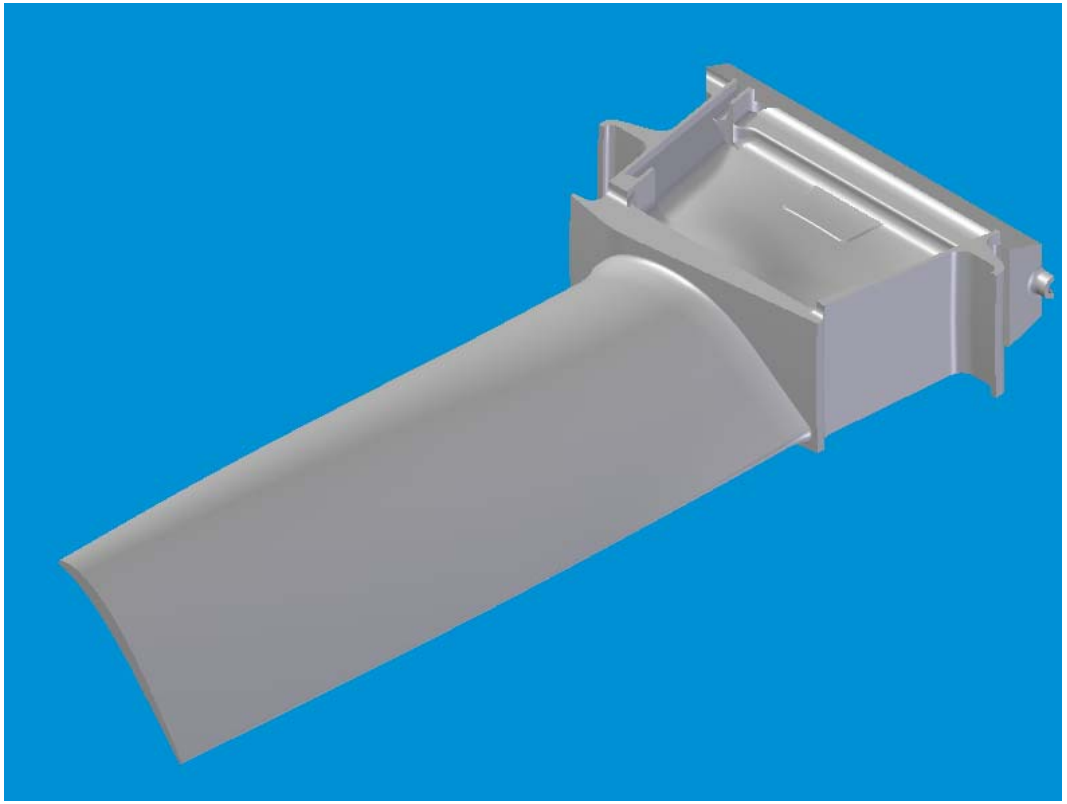

Subscale Reactor Design

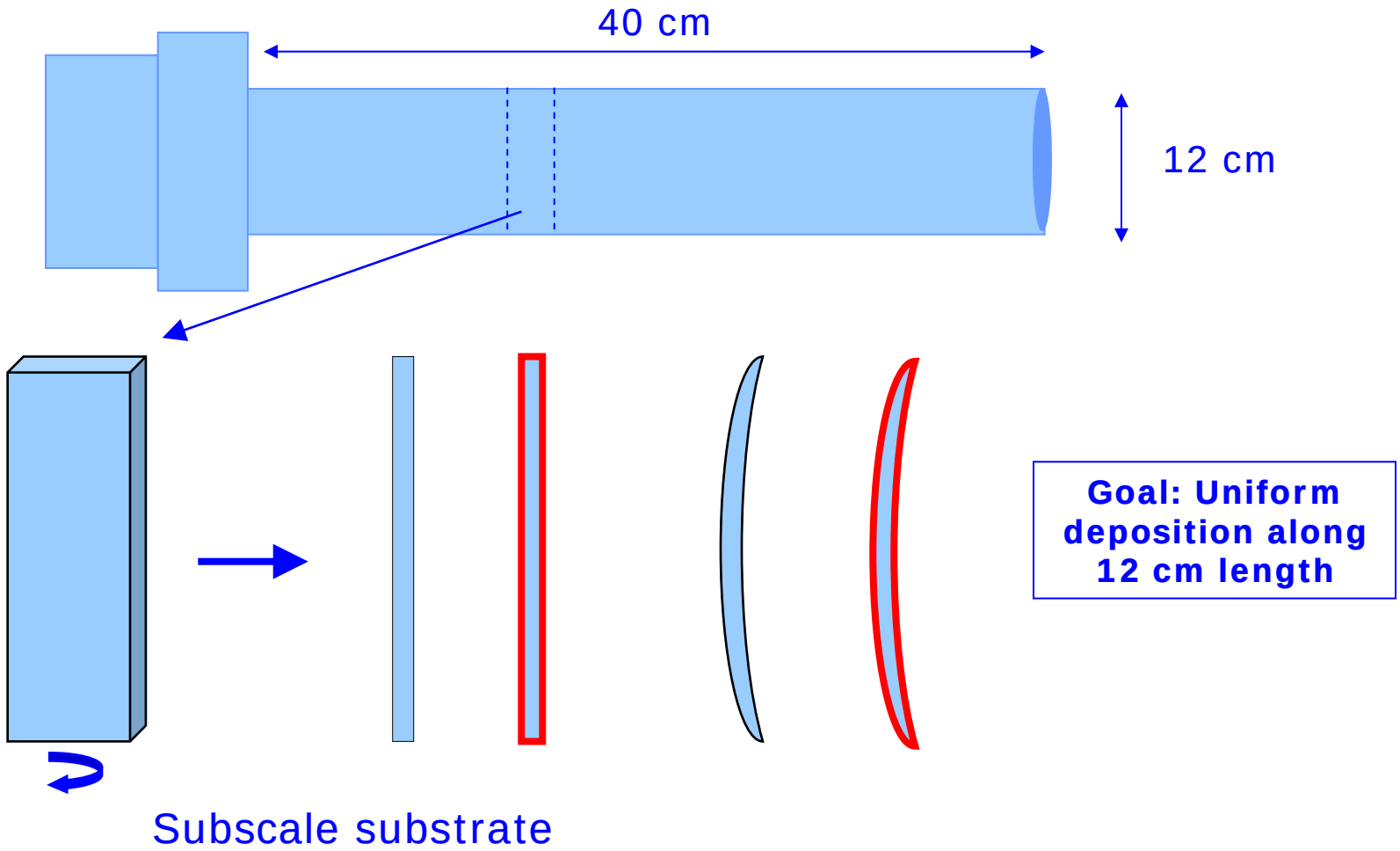

Subscale Reactor Design

- Reactant delivery methods
  - Impinging flow
  - Parallel flow
  - Pulsed
- Computer model for evaluation of design
- Concept for full-scale, multi-blade system

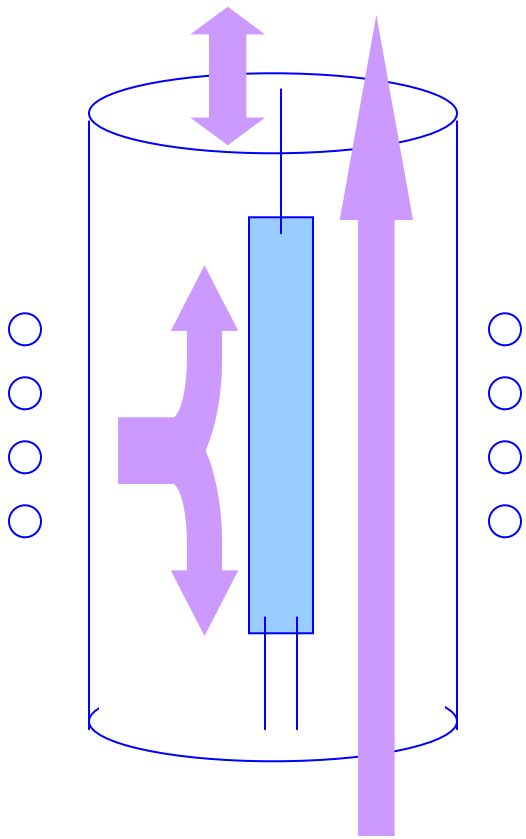

Impinging Flow Design

- Flow pattern similar to coupon-scale experiments
- Significant non-uniformity along length
- Increased deposition rate at edges
- Scale-up to full, multiple blade system is difficult

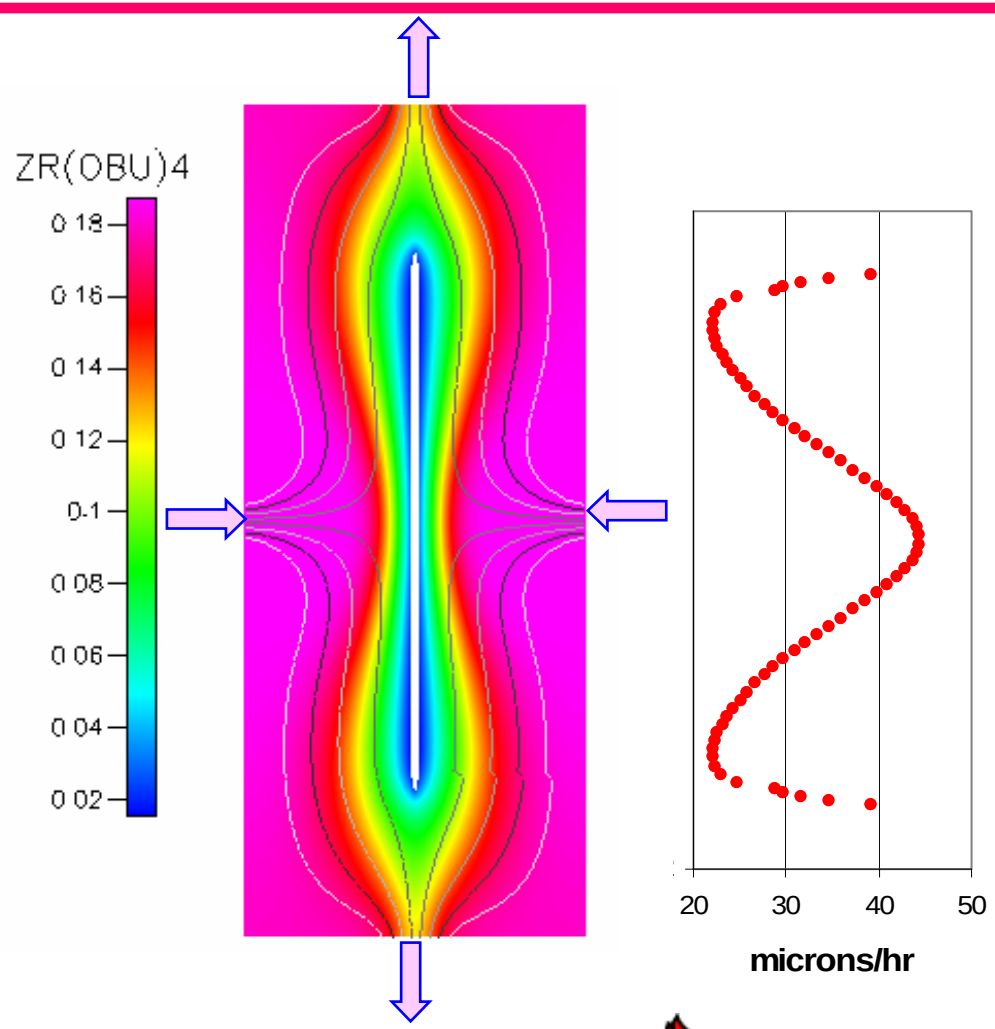

Parallel Flow Design

- Improved uniformity through central length
- Increased deposition rate at edges
- Simpler scale-up to full, multiple blade system

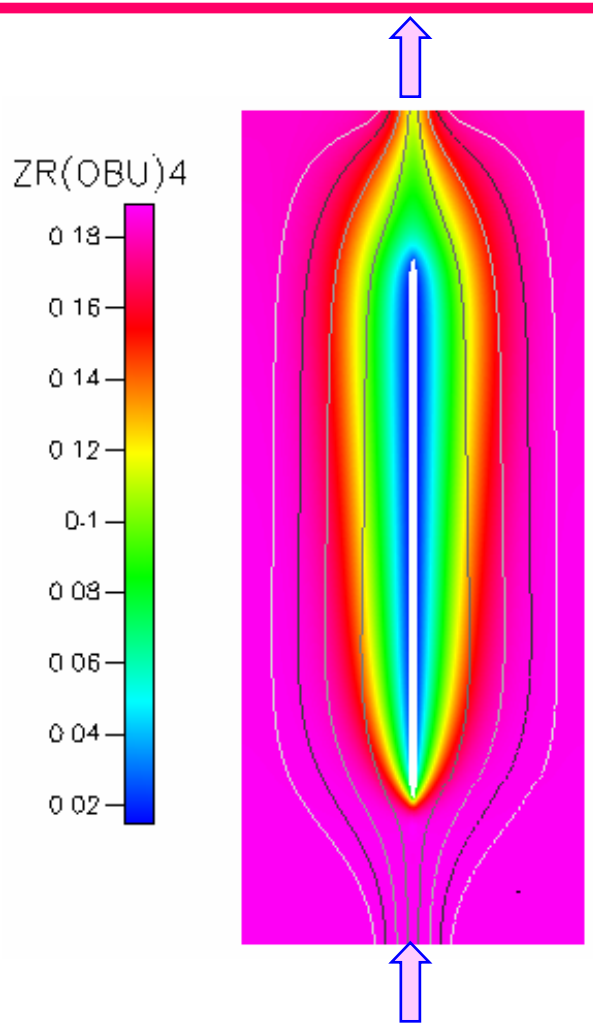

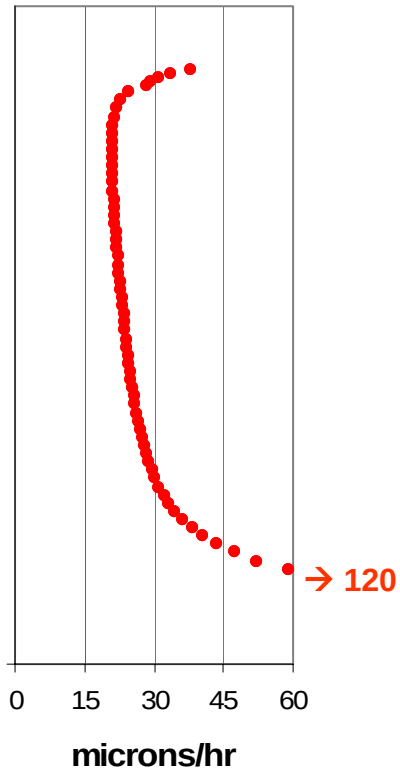

Reduce Leading Edge Deposition

- Two inlets on opposite sides
- Decreased deposition rate at leading edge
- Little improvement in central length

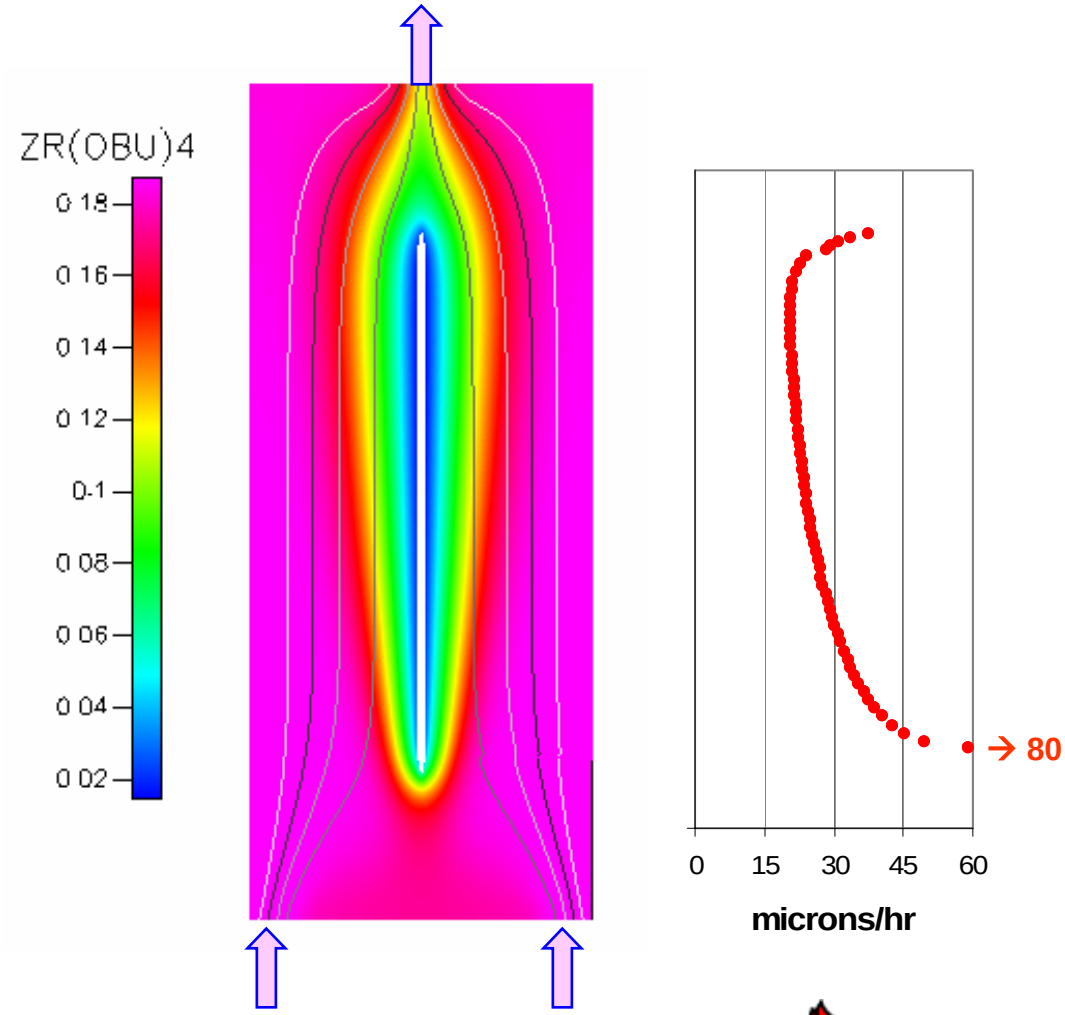

Improve uniformity in central length

- Reduce reactor width near outlet
- Nearly uniform deposition in central length

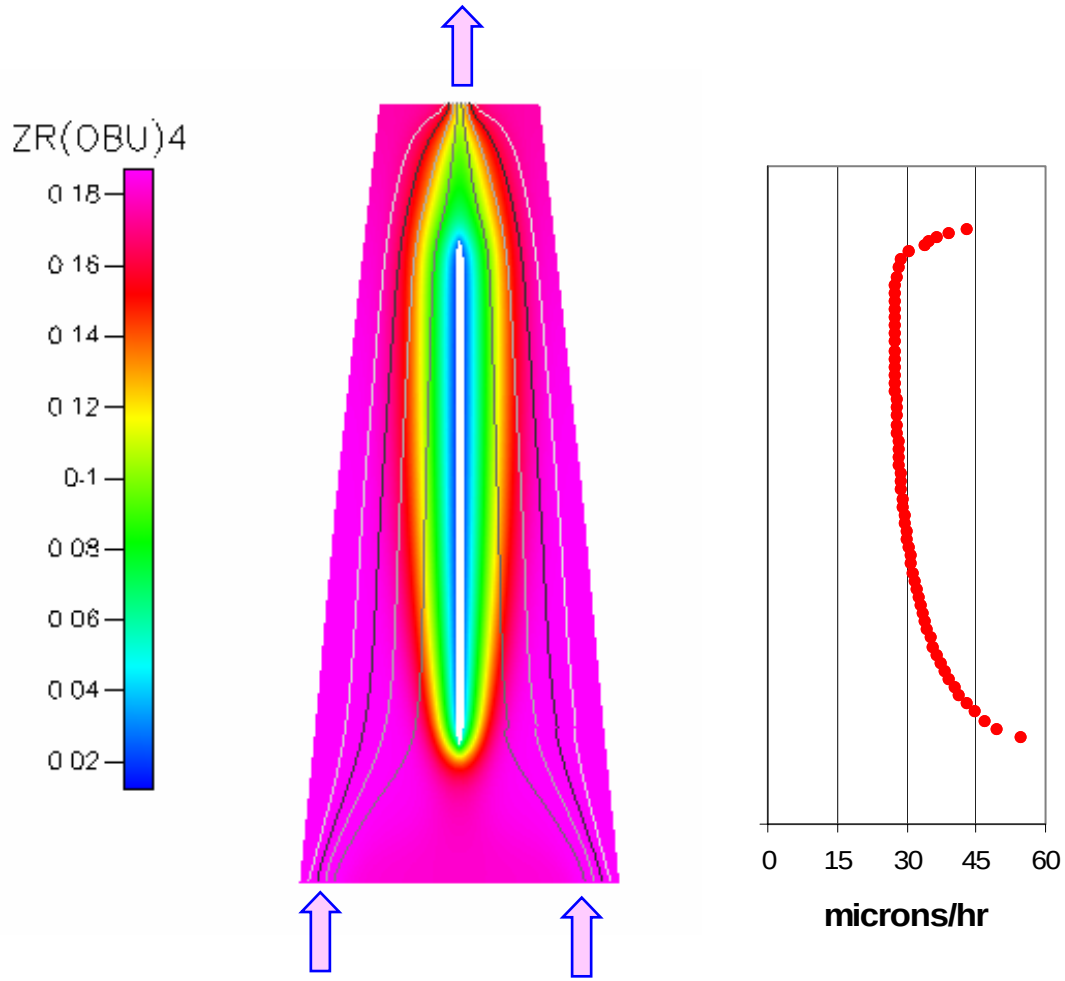

Reduce Deposition on Leading and Trailing Edges

- Add baffles at inlet and outlet
- Nearly uniform deposition along whole length

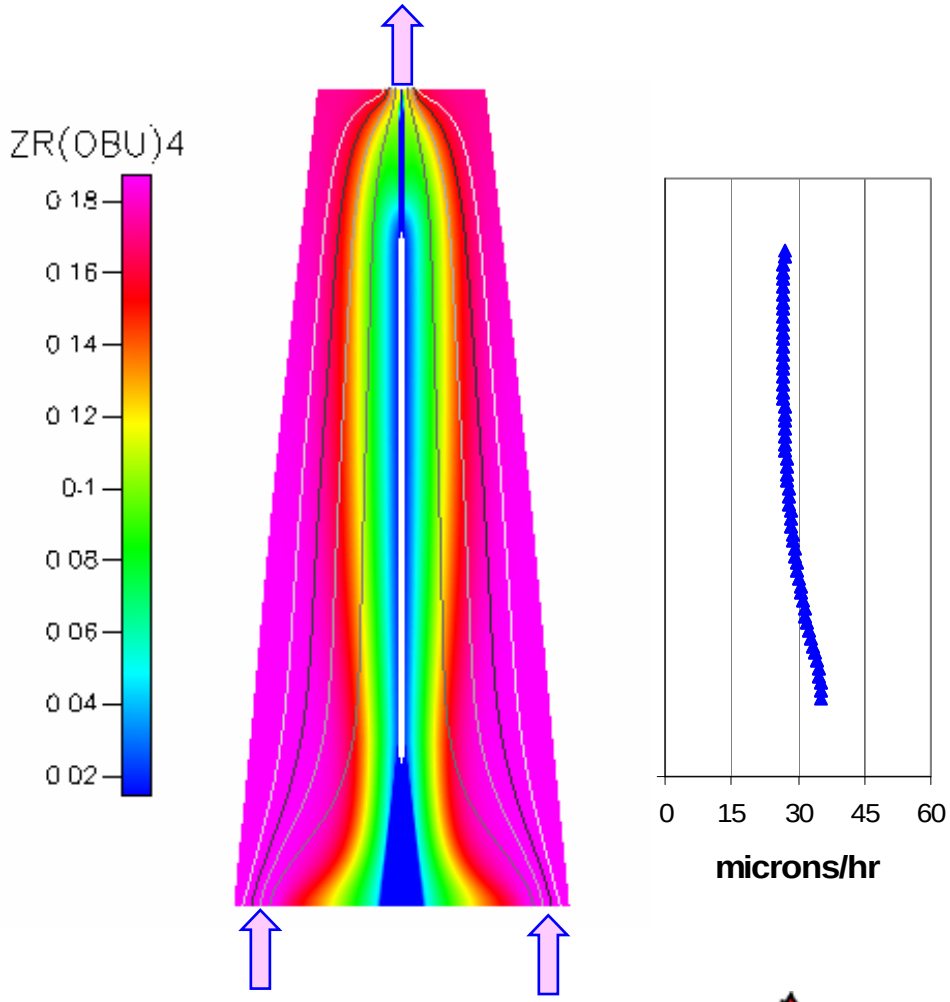

Scale-Up Coating System: Conceptual Design

- Multi-blade, batch reactor
- Outlet-to-inlet “ gang” arrangement
- Fixturing to constrain flow

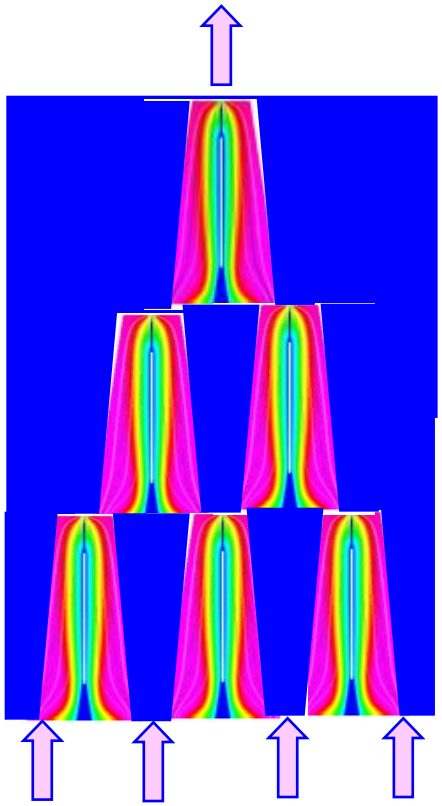

Pulse Process: Cyclic Evacuation and Fill

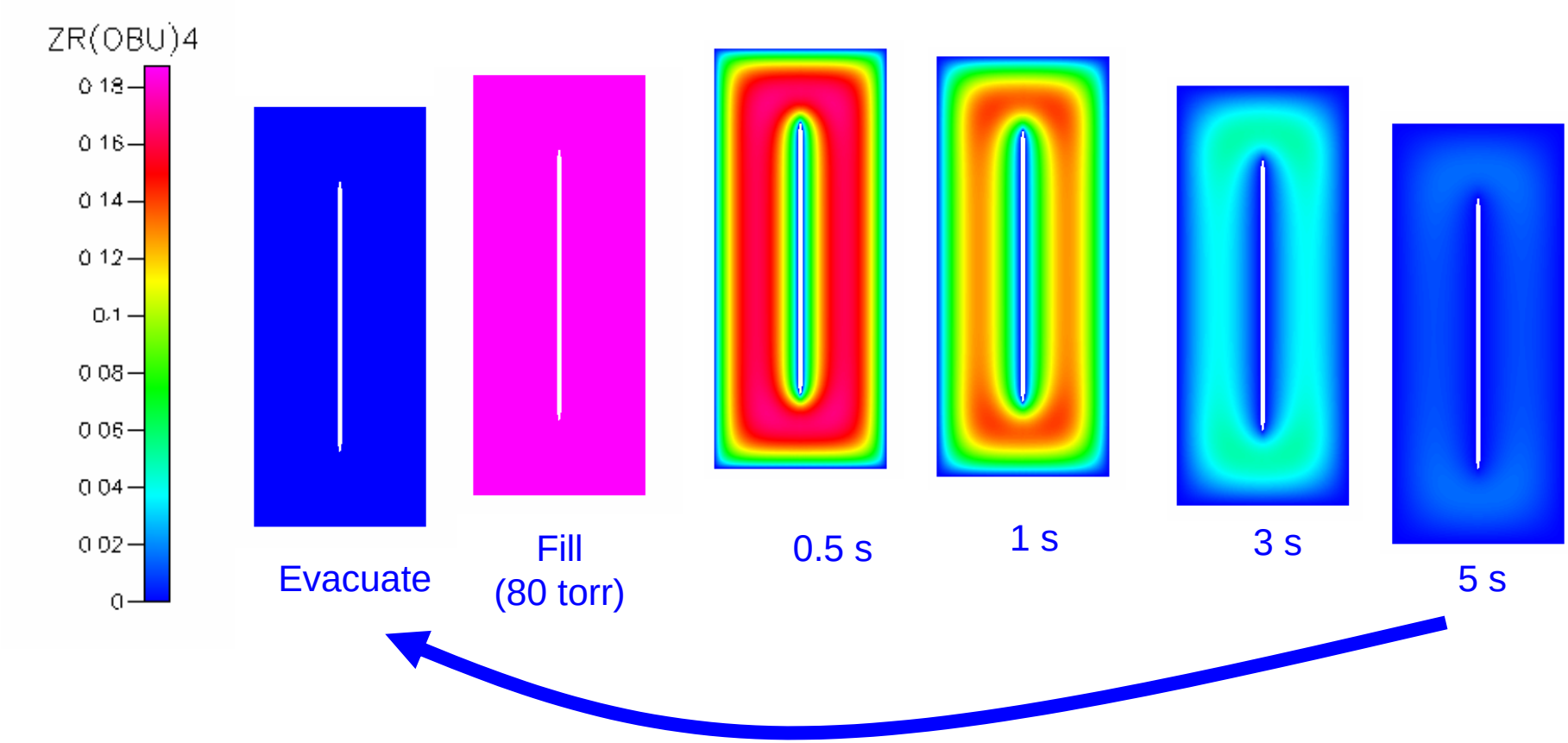

Deposition Rate Drops Sharply with Time

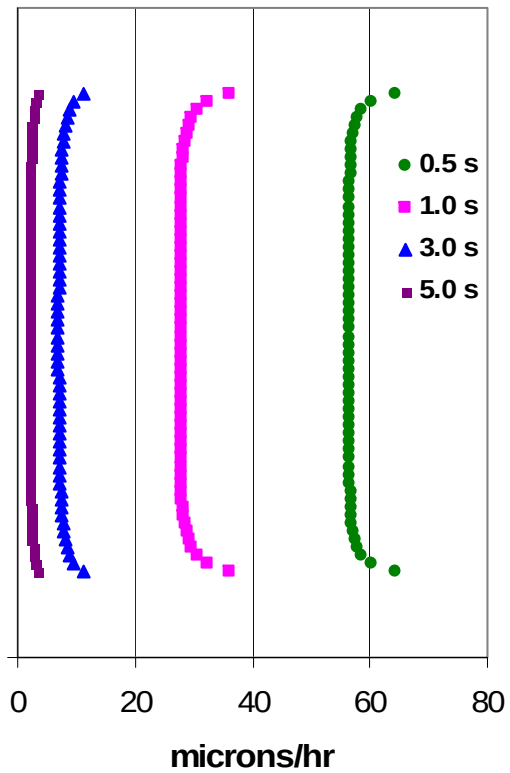

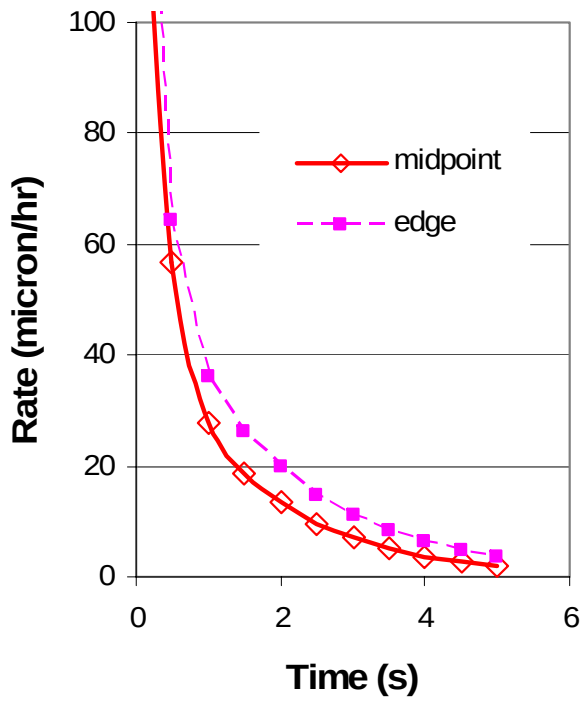

- Instantaneous rate decreases as precursor is depleted
- Deposition is nearly uniform along length

Cycle Deposition Rate Is Greater

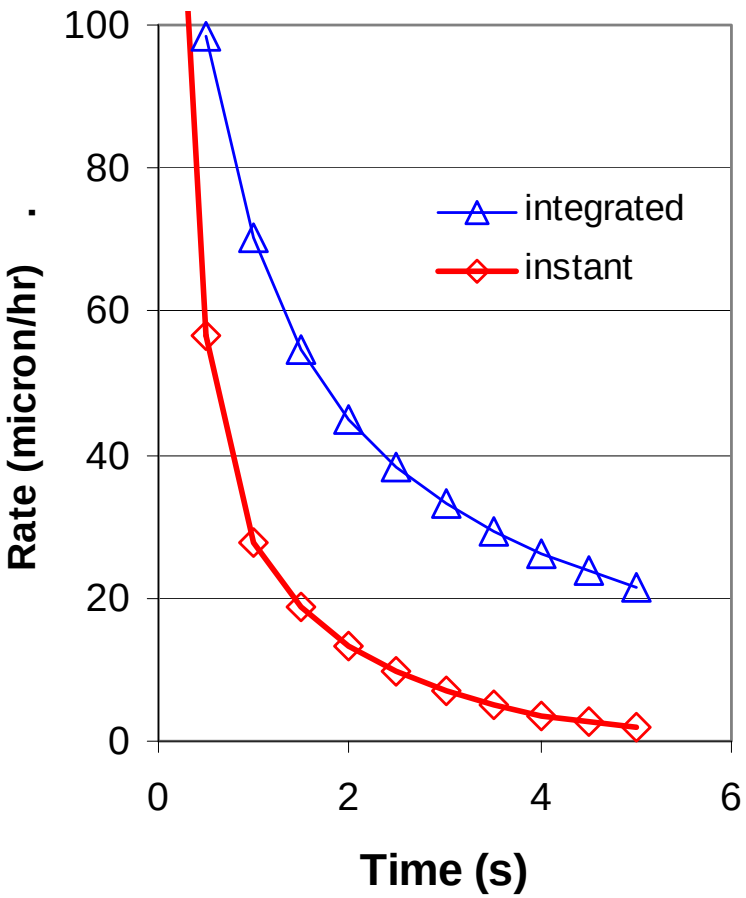

- Integrated rate is average over cycle
- Overall rate depends on practical evacuation-refill time, i.e cycles/hr
- Pressure effect:
  80 → 400 torr = 5x rate increase

Conclusions

- Uniform coating over 12 cm can be achieved through control of gas flow pattern
- Pulse process shows potential for good uniformity
- Scale-up is possible with both approaches